AUGUST 1966

ANALYTICAL CHEMISTRY

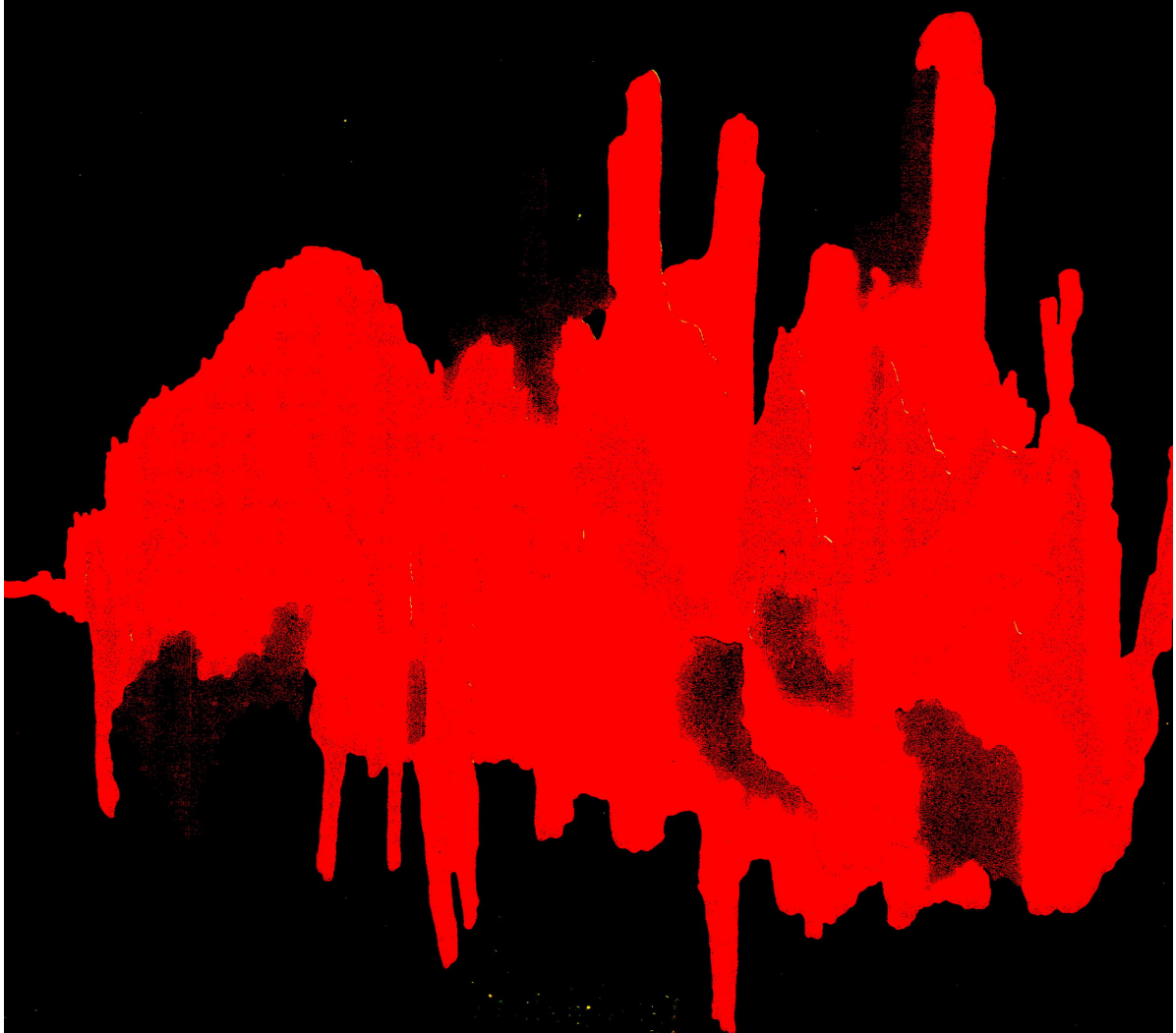

SPECIFICATIONS FOR EVALUATION OF INFRARED REFERENCE SPECTRA 27A

NEW budget saving fiberglass fume hoods

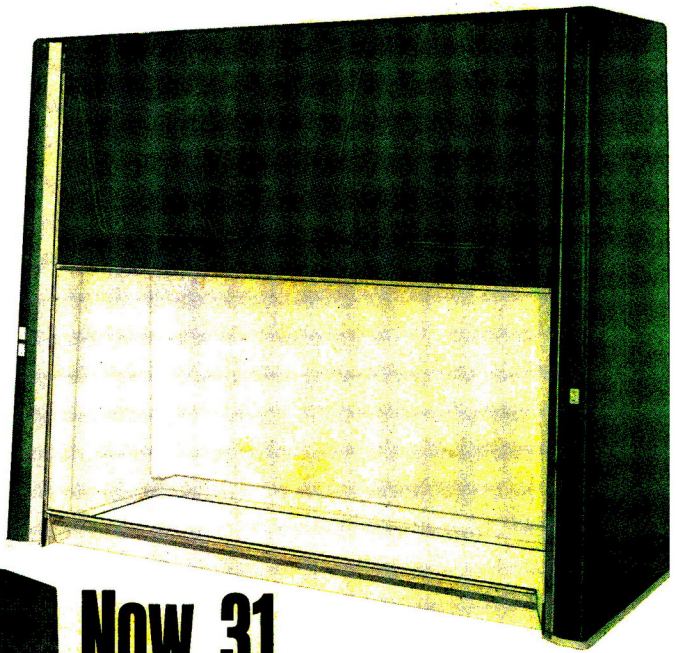

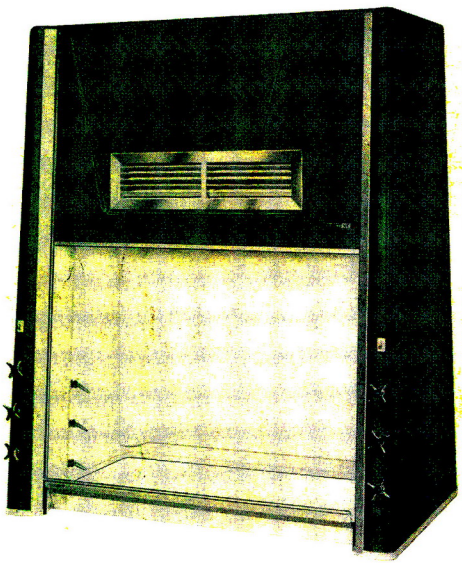

Now 31 models available from Labconco

Six years ago Labconco introduced the first fiberglass fume hood. Since that time thousands have been put to hard use in all kinds of laboratories all over the world...for two good reasons: **They outperformed old-fashioned hoods and cost a lot less.**

Now Labconco has improved and expanded its fume hood line. Standard models have been redesigned, new models added. There is now a money-saving Labconco Fiberglass Fume Hood for every purpose, for every budget, for every lab.

For the complete, money-saving story contact your laboratory supply dealer or write to **Labconco Corporation,** 8815 Prospect, Kansas City, Mo. 64132

SUMMARY OF FEATURES

- **Sizes from 28″ to 70″ wide.**
- **Prices from $270. Biggest, most advanced only $1284.**
- **Hoods shipped complete, ready to plug in and use.**
- **Standard models; induced-air models; explosion-proof models; models for radioactive work.**
- **Fire retardant, corrosion resistant, rugged.**
- **Available with sidewall or cabinet mounted fixtures.**
- **No paint to peel, transite to sag, metal to corrode.**
- **One-piece, coved corners inside and out. Easy to clean.**
- **Lightweight, install them yourself.**

LAB CON CO®

Circle No. 46 on Readers' Service Card

Questions about centrifugation?

Try these answers.

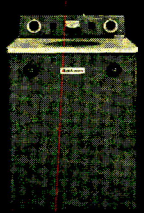

Model L

The lowest cost preparative ultracentrifuge available—and the most widely used. More than 3000 units in use throughout the world. The Model L gives you 50,000 rpm and 274,000 *g*, yet it costs less than many instruments offering lesser speeds. An unbeatable combination of high force and low cost for basic sedimentation work.

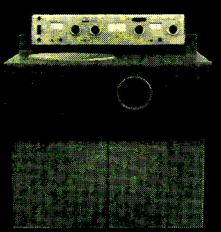

Model L2-65

65,000 rpm and forces to 420,000 g —the highest force in the field reduces sedimentation times, separates smaller particles, and improves resolution in density gradient studies. With its big chamber and large capacity rotors, the Model L2-65 is the outstanding general-purpose preparative ultracentrifuge.

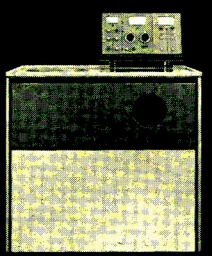

Model L4

Continuous Flow, Zonal, and 65,000 rpm capabilities — the largest volume, most versatile preparative ultracentrifuge ever built. As a Zonal Ultracentrifuge, the L4 spins 1725 ml and permits recovery of fractions during rotation. As a Continuous Flow Ultracentrifuge, the L4 accepts sample at rates to 10 liters per hour. For additional utility, it also uses most rotors in the broad Beckman line.

Some things you should also know if you've never used a Beckman ultracentrifuge: Beckman has a nationwide network of field service engineers, factory-trained to keep your instrument in choice condition . . . central locations throughout the U.S. for fast delivery of accessories and parts . . . the largest line of fixed angle and swinging bucket rotors, with the widest range of capacities, speeds, forces . . . the widest range of accessories and centrifuge tubes, all made by Beckman or for Beckman to stringent specifications . . . and Beckman has experience; Spinco Division of Beckman has been making preparative ultracentrifuges for more than 15 years. For more information on our preparative ultracentrifuges, a review of density gradient techniques, and a comprehensive applications bibliography, write for Data File L-7.

Beckman® INSTRUMENTS, INC.
SPINCO DIVISION
PALO ALTO, CALIFORNIA • 94304

INTERNATIONAL SUBSIDIARIES: GENEVA; MUNICH; GLENROTHES, SCOTLAND; TOKYO; PARIS; CAPETOWN; LONDON; MEXICO CITY

Circle No. 87 on Readers' Service Card

VOLUME 38, NO. 9 AUGUST 1966

ANALYTICAL CHEMISTRY

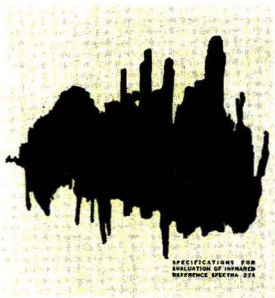

A colorful, artistic presentation of infrared spectra is depicted on the cover. For the Coblentz Society's Report on Specifications for Evaluation of Infrared Reference Spectra, see page 27 A.

© Copyright 1966
by the American Chemical Society
Issued July 22, 1966

MANUSCRIPT REQUIREMENTS published in December 1965 issue, page 1815, outlines scope and copy requirements to be observed in preparing manuscripts for consideration. Manuscript (3 copies) should be submitted to ANALYTICAL CHEMISTRY, 1155 Sixteenth St., N.W., Washington, D. C. 20036.

The American Chemical Society assumes no responsibility for the statements and opinions advanced by contributors to its publications. Views expressed in the editorials are those of the editors and do not necessarily represent the official position of the American Chemical Society.

1966 Subscription Rates

	1 yr.	2 yr.	3 yr.
Members, domestic and foreign	$ 4.00	$ 7.00	$10.00
Nonmembers, domestic and Canada	5.00	9.00	12.00
Nonmembers, foreign except Canada	15.00	27.50	40.00

Postage: Canada and Pan-American Union, $2.50; foreign, $3.50. Single copies: current, $1.50. Postage: Canada and Pan-American Union, $0.15; foreign, $0.20. Rates for back issues and volumes are available from Special Issues Sales Dept., 1155 Sixteenth St., N.W., Washington, D. C. 20036. Claims for missing numbers will not be allowed if received more than 60 days from date of mailing plus time normally required for postal delivery of journal and claim. No claims allowed because of failure to notify the Subscription Service Department of a change of address, or because copy is "missing from files."

Published monthly with review issue added in April by the American Chemical Society, from 20th and Northampton Sts., Easton, Pa. 18042; Executive offices, Editorial Headquarters, and Subscription Service Department, 1155 Sixteenth St., N.W., Washington, D. C. 20036; Advertising Office, 430 Park Ave., New York, N. Y. 10022; News Bureaus: 733 Third Ave., New York, N. Y. 10017; Philadelphia National Bank Bldg., Broad & Chestnut Sts., Philadelphia, Pa. 10103; 530 William Penn Place, Pittsburgh, Pa. 15230; 36 South Wabash Ave., Chicago, Ill. 60603; 1367 East Sixth St., Cleveland, Ohio 44114; 57 Post St., San Francisco, Calif. 94104; 422 South Western Ave., Los Angeles, Calif. 90005; 1121 Walker St., Houston, Tex. 77002; 1155 Sixteenth St., N.W., Washington, D. C. 20036; Grosse Bockenheimerstrasse 32, Frankfort/Main, West Germany; Apt. 306, 47 Dai-machi, Akasaka, Minato-ku, Tokyo, Japan; 27 John Adam St., London W.C. 2, England.

Second class postage paid at Easton, Pa.

CHANGE OF ADDRESS: Notify Subscription Service Department, American Chemical Society, 1155 Sixteenth St., N.W., Washington, D. C. 20036. Such notification should include both old and new addresses, with ZIP code numbers, and be accompanied by mailing label from a recent issue. Allow four weeks for change to become effective.

CONTENTS

REPORT FOR ANALYTICAL CHEMISTS

As a service to the scientific community, ANALYTICAL CHEMISTRY presents the full text of the Coblentz Society's Report on Specifications for the Evaluation of Infrared Reference Spectra...**27 A**

NEWS SECTION

The Analytical Division program for the 152nd ACS Meeting in New York City, Sept. 11 to 16, is given. The National Bureau of Standards Symposium on Trace Characterization—Chemical and Physical program is also presented. Other meetings and courses are scheduled.....**45 A**

EDITORS' COLUMN

The availability to nonprofit institutions of sets of infrared spectral data is noted, and a new Photonuclear Data Center is described.....**79 A**

LABORATORY OF THE MONTH

The Purex Corporation has provided new research facilities to aid in its widely diversified operations.....**87 A**

INSTRUMENTATION

Dr. Müller describes new automatic optical pyrometers used to measure high temperatures.....**93 A**

AUTHOR INDEX...6 A
BOOK REVIEWS AND NEW BOOKS...69 A
BRIEFS...11 A
CALENDAR OF EVENTS...62 A
NEW CHEMICALS...119 A
EDITORIAL...1105
FUTURE ARTICLES...134 A
MANUFACTURERS' LITERATURE...121 A
NEW PRODUCTS...105 A
READERS' INFORMATION SERVICE...102 B

Scientific Communication

Determination of Nickel by Atomic Fluorescence Flame Spectrometry. D. N. ARMENTROUT 1235

Symposium on Electroanalytical Instrumentation

Effect of Uncompensated Resistance on Electrode Kinetic and Adsorption Studies by Chronocoulometry. George Lauer and R. A. Osteryoung . . 1106

Kinetic Current Measurements with Controlled Potential. Application to Uranium(V) Disproportionation Reaction. D. T. Pence and G. L. Booman 1112

Some Investigations on Instrumental Compensation of Nonfaradaic Effects in Voltammetric Techniques. E. R. Brown, T. G. McCord, D. E. Smith, and D. D. DeFord 1119

Instrumentation for Digital Data Acquisition in Voltammetric Techniques. D. C. and A. C. Polarography. E. R. Brown, D. E. Smith, and D. D. DeFord 1130

Use of a Multichannel Analyzer as a Data Acquisition System in Electrochemistry. George Lauer and R. A. Osteryoung 1137

A Digital Data Collection, Waveform Generation, and Timing Instrument for Electrochemical Measurements. G. L. Booman 1141

End of Symposium

Electrode Potential Gradients and Cell Design in Controlled Potential Electrolysis Experiments. J. E. Harrar and Irving Shain 1148

Evaluation of Stationary Electrode Polarography and Cyclic Voltammetry for the Study of Rapid Electrode Processes. S. P. Perone 1158

Automatic Determination of Weak Organic Acids by Means of Partition Column Chromatography and Indicator Titration. Leo Kesner and Edward Muntwyler. 1164

The Nonaqueous Microtitration of Dibenzoylmethane and Other Weak Acids. D. A. Lee 1168

A Rapid and Sensitive Method for the Determination of Iodine-131 in Milk by Ion Exchange on Silver Chloride. W. D. Fairman and Jacob Sedlet 1171

Determination of Strontium-90 from Seawater after Concentration by Manganese Dioxide. W. H. Shipman 1175

Gas Chromatographic Determination of Pyruvic and LacticAcids and Krebs Cycle Components. Esterification and Recovery. Frances L. Estes and R. C. Bachmann 1178

An Improved Method for the Determination of Orthophosphate Suitable for Assay of Adenosine Triphosphatase Activity. S. M. Mozersky, J. D. Pettinati, and S. D. Kolman 1182

Nucleation Rate and Crystal Growth Rate of the Complex as Factors in Microscopical Fusion Analysis of Quinone–Carcinogenic Agent Complexes. D. E. Laskowski 1188

Fast Scan High Resolution Mass Spectrometry. Operating Parameters and Its Tandem Use with Gas Chromatography. W. J. McMurray, B. N. Greene, and S. R. Lipsky 1194

Determination of Nonfiller Magnesium in Polyesters Containing Fillers. John E. Newell 1205

Fast and Sensitive Method for Determination of Nitrogen. Selective Nitrogen Detector for Gas Chromatography. R. L. Martin 1209

Automatic Analyzer with Direct Readout for Determining Carbon in Steel. L. L. Lewis and M. J. Nardozzi 1214

Spectrophotometric Determination of Platinum with 3,4-Diaminobenzoic Acid. L. D. Johnson and G. H. Ayres 1218

Analysis of a High-Molecular-Weight Phenolic Inhibitor. H. S. Knight and Herbert Siegel 1221

Identification of Normal Paraffins, Olefins, Ketones, and Nitriles from Colorado Shale Oil. Takeo Iida, Eiichi Yoshii, and Eitaro Kitatsuji 1224

Absorptiometric Methods in Rapid Silicate Analysis. C. O. Ingamells 1228

Correction. Estimation of Medium Effects for Single Ions and Their Role in the Interpretation of Nonaqueous pH. Orest Popovych 1227

CONTRIBUTED ARTICLES

Correspondence

Application of the Rule of Six to the Separation of Diastereoisomeric Esters by Gas–Liquid Chromatography. An Exchange of Comments. Boris Weinstein, B. L. Karger and R. L. Stern 1238

p-Bis-(o-Methylstyryl)Benzene, Useful Secondary Fluor for Liquid Scintillation Counting. Yutaka Kobayashi 1240

Relative Efficiency of a New Liquid Scintillation Fluor, *p*-Bis-(o-Methylstyryl)Benzene. E. T. Bush . 1241

The Rate of Oxidation of Platinum Electrodes. K. H. Pool, J. G. Smith, and A. L. Crittenden 1242

Quantitative Determination of Individual Tocopherols by Thin Layer Chromatographic Separation and Spectrophotometry. P. A. Sturm, R. M. Parkhurst, and W. A. Skinner 1244

Gas Chromatographic Study of the Separation of Resin Acid Methyl Esters on a QF-1 Column. C. W. J. Chang and S. W. Pelletier 1247

Determination of Chloride in Glass by Pyrohydrolysis. V. E. Caldwell 1249

Determination of Long-Chain Alkyl Sulfates as Chloroform-Soluble Azure A Salts. J. van Steveninck and J. C. Riemersma 1250

On the Interpretation of Solute Vaporization Interference in Flame Photometry. C. Th. J. Alkemade . 1252

Radiochemical Determination of Cesium Using Permanganate as a Precipitant. W. H. Shipman and David Mueller 1253

Determination of Deuterium Ion Concentration in Dilute Unbuffered Deuterium Oxide Solutions. E. W. Baumann 1255

Determination of Dissolved Ammonia by Gas Chromatography. R. W. Jenkins, Jr., C. H. Cheek, and V. J. Linnenbom 1257

Derivation of Expression for Integrated Luminescence Intensity When Using Pulsing Techniques in Luminescence Spectrometry. T. C. O'Haver and J. D. Winefordner 1258

Analysis of Cesium-134–Cesium-137 Mixtures by Gamma-Ray Spectrometric Methods. Sachio Yamamoto 1261

The Effect of Water on Saponification of Organic Esters. W. H. Greive, K. F. Sporek, and M. K. Stinson . 1264

Application of Radiometric Techniques to the Quantitative Paper Chromatography of Iron, Copper, Manganese, and Cobalt. A. R. Landgrebe, T. E. Gills, and J. R. DeVoe 1265

Semiquantitative Estimation of Nitrogen in Ammonium Faujasite by Differential Thermal Analysis. P. B. Venuto, E. L. Wu, and John Cattanach . 1266

Fluorometric Determination of Zinc. R. E. Jensen and R. T. Pflaum 1268

Spectrophotometric Determination of Sulfur Dioxide Using *p*-Aminoazobenzene. S. J. Kniseley and L. J. Throop 1270

Voltammetric Determination of 2,6-Di-*tert*-Butyl-*p*-Cresol in Hydrocarbons. J. C. Suatoni 1271

Kinetics of Polymerization by Infrared Spectrometry. Arthur Hirsch and B. E. Bridgland 1272

Aids for Analytical Chemists

Calibration Heater for Thermometric Titrations. M. J. Stern, R. Withnell, and R. J. Raffa 1275

An Electronic Coulostat. George Lauer 1277

A Precision Method for Generation of Solvent Gradients. F. R. Blattner and J. N. Abelson 1279

A Nomogram for Calculating the Results of an Automatic Amino Acid Analysis. W. A. Schroeder, W. R. Holmquist, and J. R. Shelton 1281

Cryoscopic Molecular Weight Determinations Using Dimethyl Sulfoxide as the Solvent. R. S. George and R. K. Rohwer 1285

Selective Removal of Aldehydes from Complex Mixtures during Gas Chromatography. R. R. Allen 1287

Near-Infrared Determination of Deuterium Oxide in Water. W. E. Keder and D. R. Kalkwarf 1288

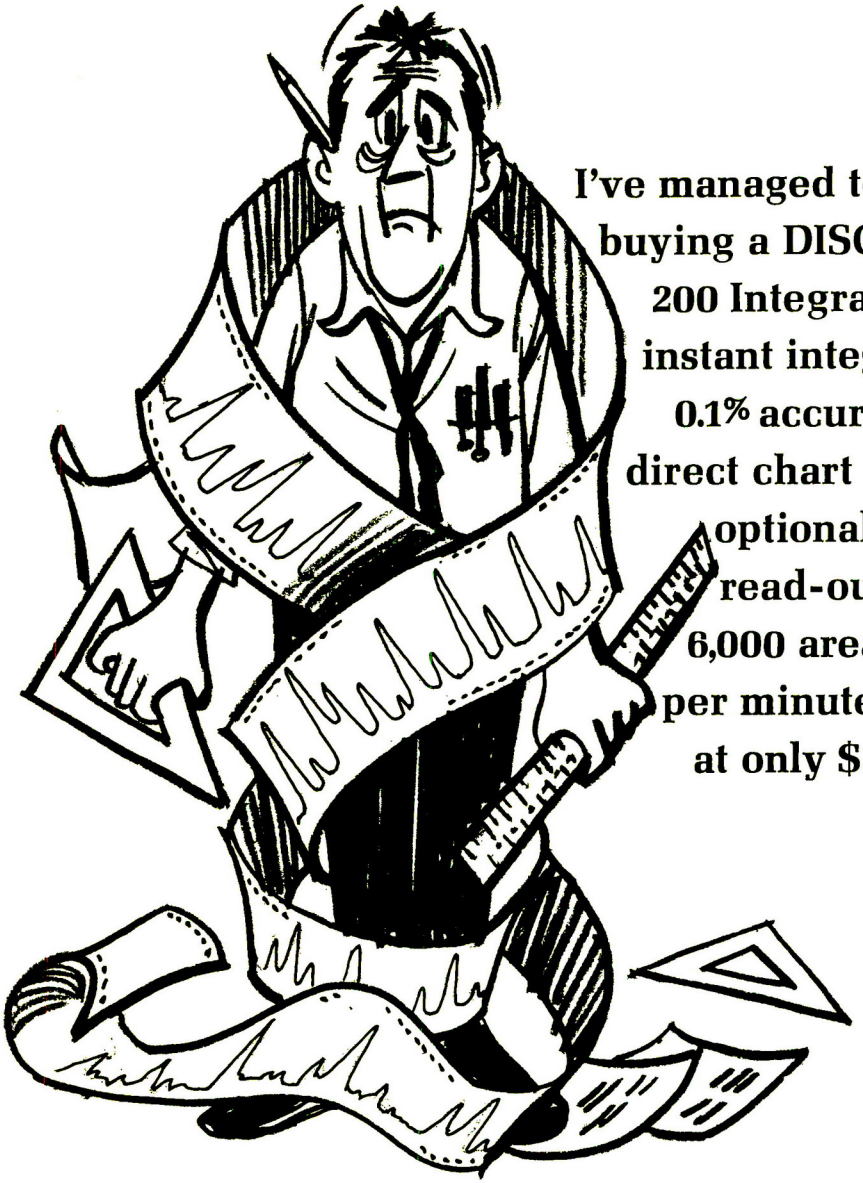

I've managed to resist buying a DISC® Series 200 Integrator...with instant integration, 0.1% accuracy, direct chart or optional digital* read-out, and 6,000 area counts per minute – at only $585.00

If **you** want to eliminate the boredom, inaccuracy and repetitiousness associated with triangulation or hand planimeter methods of peak area analysis, don't resist. Disc® Series 200 Integrators are available as standard equipment from all chromatograph or recorder manufacturers, or can be installed on existing recorders in a few hours by your own laboratory personnel. Insist on one . . . or two . . . or three . . .

**Duo-Digital Counter additional.*

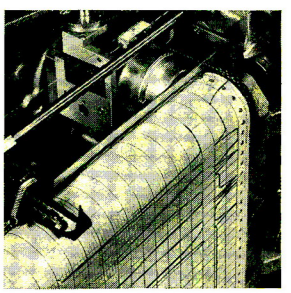

DISC INSTRUMENTS, INC.
2701 S. Halladay St. • Santa Ana • California 92705
Telephone: (714) 549-0345 • TWX: 714-546-0434

DISC

Circle No. 27 on Readers' Service Card

THE FLOW SHEET

One of a series devoted to

enriching the Art of conveying & controlling fluids

Working With GAS CHROMATOGRAPHY?

Let HOKE Help You . . .

Reduce carrier gas pressure. This pressure balanced regulator provides 2-stage regulation accuracy with single stage cost and design.

Protect your system against impurities. Sintered filtering element traps contaminants before they damage your costly equipment.

Meter minute quantities of process media. Extremely accurate and reproducible flow settings are easy to come by with this fine metering valve. Low internal volume, 3° angle stem, 3/64" orifice.

Control the on-off flow of your sample. A flick of the finger opens or closes this toggle valve instantly.

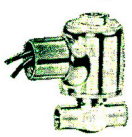

Sample your process fluid automatically. Normally open, normally closed or universal flow solenoid valves are available.

And don't forget to hook-up the entire system with New, Hoke Gyrolok Tube Fittings. A catalog is available.

For complete information on how these Hoke products can help you, contact your local Hoke distributor or write to us directly.

HOKE

Hoke Incorporated • 1 Tenakill Park • Cresskill, N.J.

Circle No. 105 on Readers' Service Card

AUTHOR INDEX

Abelson, J. N., 1279
Alkemade, C. Th. J., 1252
Allen, R. R., 1287
Armentrout, D. N., 1235
Ayres, G. H., 1218

Bachmann, R. C., 1178
Baumann, E. W., 1255
Blattner, F. R., 1279
Booman, G. L., 1112, 1141
Bridgland, B. E., 1272
Brown, E. R., 1119, 1130
Bush, E. T., 1241

Caldwell, V. E., 1249
Cattanach, J., 1266
Chang, C. W. J., 1247
Cheek, C. H., 1257
Crittenden, A. L., 1242

DeFord, D. D., 1119, 1130
DeVoe, J. R., 1265

Estes, F. L., 1178

Fairman, W. D., 1171

George, R. S., 1285
Gills, T. E., 1265
Greene, B. N., 1194
Greive, W. H., 1264

Harrar, J. E., 1148
Hirsch, A., 1272
Holmquist, W. R., 1281

Iida, T., 1224
Ingamells, C. O., 1228

Jenkins, R. W., Jr., 1257
Jensen, R. E., 1268
Johnson, L. D., 1218

Kalkwarf, D. R., 1288
Karger, B. L., 1238
Keder, W. E., 1288
Kesner, L., 1164
Kitatsuji, E., 1224
Knight, H. S., 1221
Kniseley, S. J., 1270
Kobayashi, Y., 1240
Kolman, S. D., 1182

Landgrebe, A. R., 1265
Laskowski, D. E., 1188
Lauer, G., 1106, 1137, 1277
Lee, D. A., 1168
Lewis, L. L., 1214
Linnenbom, V. J., 1257
Lipsky, S. R., 1194

Martin R. L., 1209
McCord, T. G., 1119
McMurray, W. J., 1194
Mozersky, S. M., 1182
Mueller, D., 1253
Muntwyler, E., 1164

Nardozzi, M. J., 1214
Newell, J. E., 1205

O'Haver, T. C., 1258
Osteryoung, R. A., 1106, 1137

Parkhurst, R. M., 1244
Pelletier, S. W., 1247
Pence, D. T., 1112
Perone, S. P., 1158
Pettinati, J. D., 1182
Pflaum, R. T., 1268
Pool, K. H., 1242

Raffa, R. J., 1275
Riemersma, J. C., 1250
Rohwer, R. K., 1285

Schroeder, W. A., 1281
Sedlet, J., 1171
Shain, I., 1148
Shelton, J. R., 1281
Shipman, W. H., 1175, 1253
Siegel, H., 1221
Skinner, W. A., 1244
Smith, D. E., 1119, 1130
Smith, J. G., 1242
Sporek, K. F., 1264
Stern, M. J., 1275
Stern, R. L., 1238
Steveninck, J. van, 1250
Stinson, M. K., 1264
Sturm, P. A., 1244
Suatoni, J. C., 1271

Throop, L. J., 1270

Venuto, P. B., 1266

Weinstein, B., 1238
Winefordner, J. D., 1258
Withnell, R., 1275
Wu, E. L., 1266

Yamamoto, S., 1261
Yoshii, E., 1224

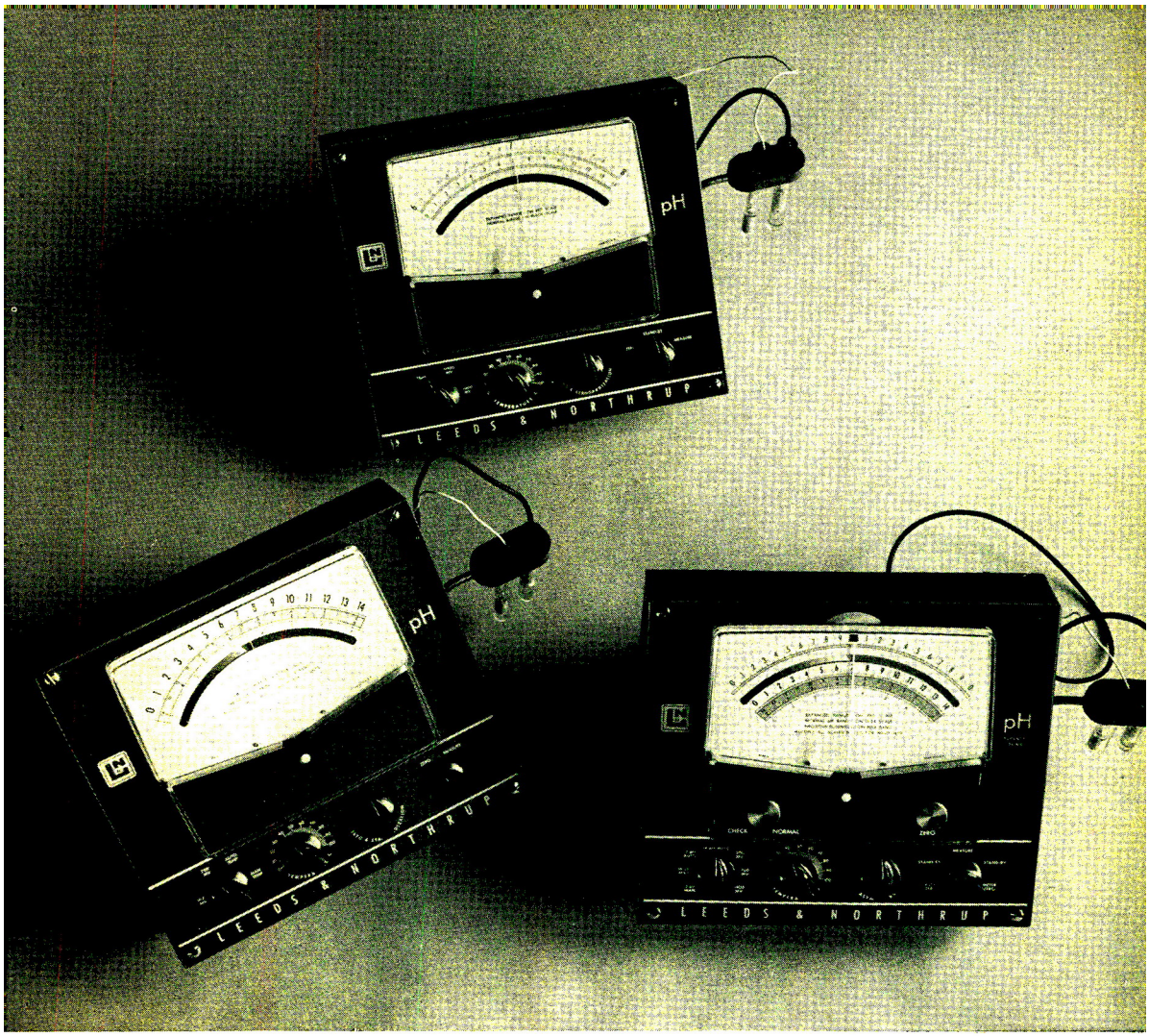

± 1/20, ± 1/100, ± 1/200 of a pH.
If the first isn't accurate enough, pick one of the other two.

We've designed a whole new family of pH meters—the A2 Series. They give you a choice of relative accuracies: ± 0.05, ± 0.01 and ± 0.005 pH.

But that's not all by a long shot. We've modernized and perfected the meters in every significant detail.

For instance, we've changed to photoconductive choppers which are inherently more stable and trouble-free. They avoid the self-generated stray signals of mechanical converters.

We've adopted the glass-electrode connections now popular in U. S. practice.

We've given the meters a new look. Increased their stability, reliability, reproducibility.

But we still rely on our feedback-stabilized amplifier whose basic concept has been so widely imitated.

And hand wiring.

And a highly responsive meter with the practical scale length of 7". (Not for us the unstable zero of oversized meters!)

And taut-band suspension. Eliminating the dead band you get with pivot systems.

And a rugged housing. Epoxy-coated case. Melamine-coated front panel.

And our own pH electrodes manufactured to perfectionist standards.

All the new meters are line-operated. All have a 10 microamp polarizing current for measurements by the Karl Fischer method and output terminals for recorder display.

Choose the one you need. General Purpose — good for routine measurements in lab and plant. Expanded Scale —for the more exacting requirements of research or quality control. Precision — for highest practical accuracy in research, medicine or industry.

You'll get a great deal that's new... at the same old price.

For details on each and for the name of the L&N laboratory pH dealer nearest you, write to: Leeds & Northrup, 4906 Stenton Ave., Philadelphia, Pa. 19144.

LEEDS & NORTHRUP
Philadelphia 44 • Pioneers in Precision

Circle No. 117 on Readers' Service Card

Every Bausch & Lomb constant

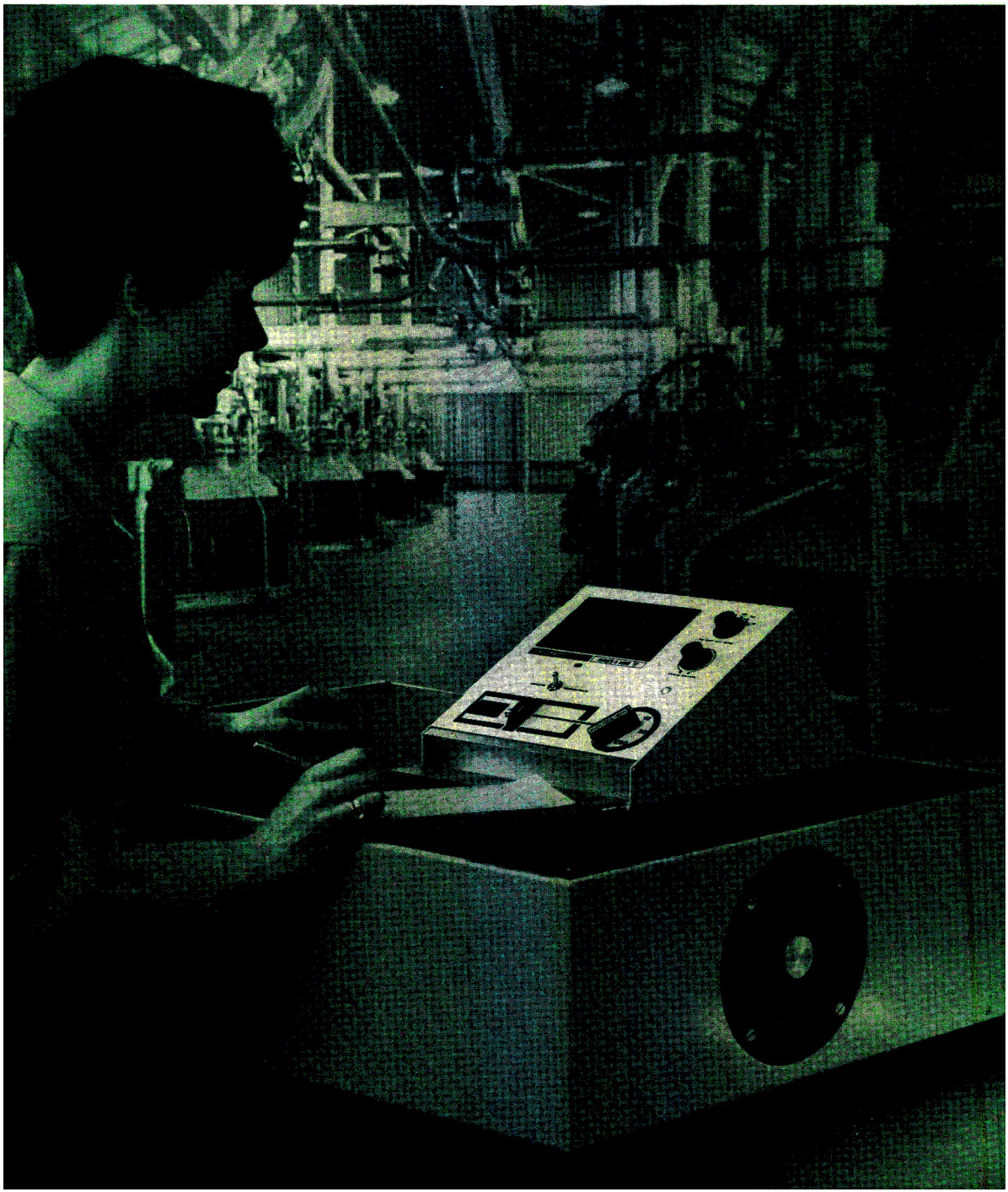

bandpass SPECTROPHOTOMETER is best in its class!

BEST IN CLASS

The SPECTRONIC 600...for SPEED, SENSITIVITY, SIMPLICITY

. . . double-beam, double-grating, ratio-indicating. UV-visible range, 200mμ-650mμ. Best for concentrating on a few selected wave lengths. Best for high stability and reliability requirements. Best for getting many determinations in a short time.

EXTRA SPEED. 3 scanning speeds—10, 50, 250 mμ/minute. 2 slewing speeds—forward and reverse. Automatic zero adjustment. Quick-set 100% line. All operating controls are grouped, readily accessible.

EXTRA SENSITIVITY. Two 1200 groove/mm Certified-Precision gratings in series—assure top performance. Wavelength accuracy and bandpass are constant—5A over the entire range.

EXTRA CONVENIENCE AND EASE OF OPERATION. Two built-in light sources. Large, 103mm long, sample compartment—takes all sizes and shapes of adsorption cells and 10mm square cuvettes. Emission or transmittance measurements with a flick of a switch. Built-in utility receptacle, V.O.M. Recorder jack and wavelength marker. Large, 3 square feet, working surface. Modular, circuit-board design for rapid, simple servicing.

SPECTRONIC 505

. . . double-beam, double-grating, ratio-recording. UV-visible range, 200mμ-650mμ. 6 built-in scanning speeds, combination light source; built-in wavelength calibration. Wavelength accuracy—.5A. Narrow, constant bandpass—5A and 50A standard.

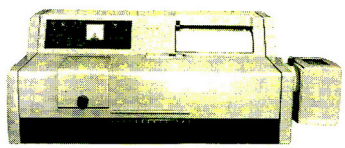

PRECISION SPECTROPHOTOMETER

. . . single-beam, double-grating. UV-visible range, 190mμ-700mμ. Large sample compartment (6″ x 6″ x 8 1/16″). Choice of collimating or focusing optics. Wavelength accuracy—.5A. Wavelength graduations—.2mμ. Combination light source. Constant bandpass—2A, 5A and 20A.

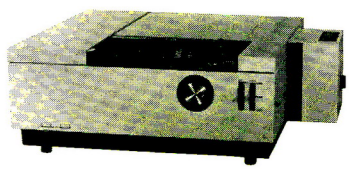

SPECTRONIC 20

. . . extended range from 340mμ-950mμ. Low stray light, high sensitivity at all wavelengths. Direct scale readings, fast warmup, remarkable stability, easy interchangeability of parts. A Spectrophotometer as well as a Colorimeter.

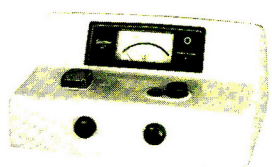

AND TO GIVE YOU TOTAL FLEXIBILITY . . . THESE BEST OF CLASS ACCESSORIES:

- UV Reflectance Attachment
- Fluorescence Accessory
- Flame Attachment
- End-on Photomultiplier Housing
- Flow-thru Cell
- Constant Temperature Cell Holder
- V.O.M. Strip Chart Recorders
- Microcell Cuvettes
- Time Rate Accessory
- Trichromatic Chart Paper
- Transmittance Chart Paper
- Absorbance Chart Paper
- Tri-Stimulus Integrator
- DT-20 Digital Readout
- AT-20 Digital Readout
- Automatic 100% Adjust
- Specular Reflectance Attachment
- Thermoelectric Heater-Cooler
- Thermindicator
- Gear-Shifter Accessory
- Scale and Pointer Accessory
- Wavelength Reversing Gear Accessory
- Temperature Coefficient Meter

ASK FOR A DEMONSTRATION TODAY!

For complete information on all 4 instruments write for Brochure 33-2184, Bausch & Lomb, 60932 Bausch St., Rochester, N.Y. 14602. Or let us arrange a demonstration at your convenience.

BAUSCH & LOMB

Visit our Booth No. 707 at the 1966 Chemical Exposition Show; N.Y.C., Sept. 13–1

"See Laboratory Guide for all Products/Sales Offices"

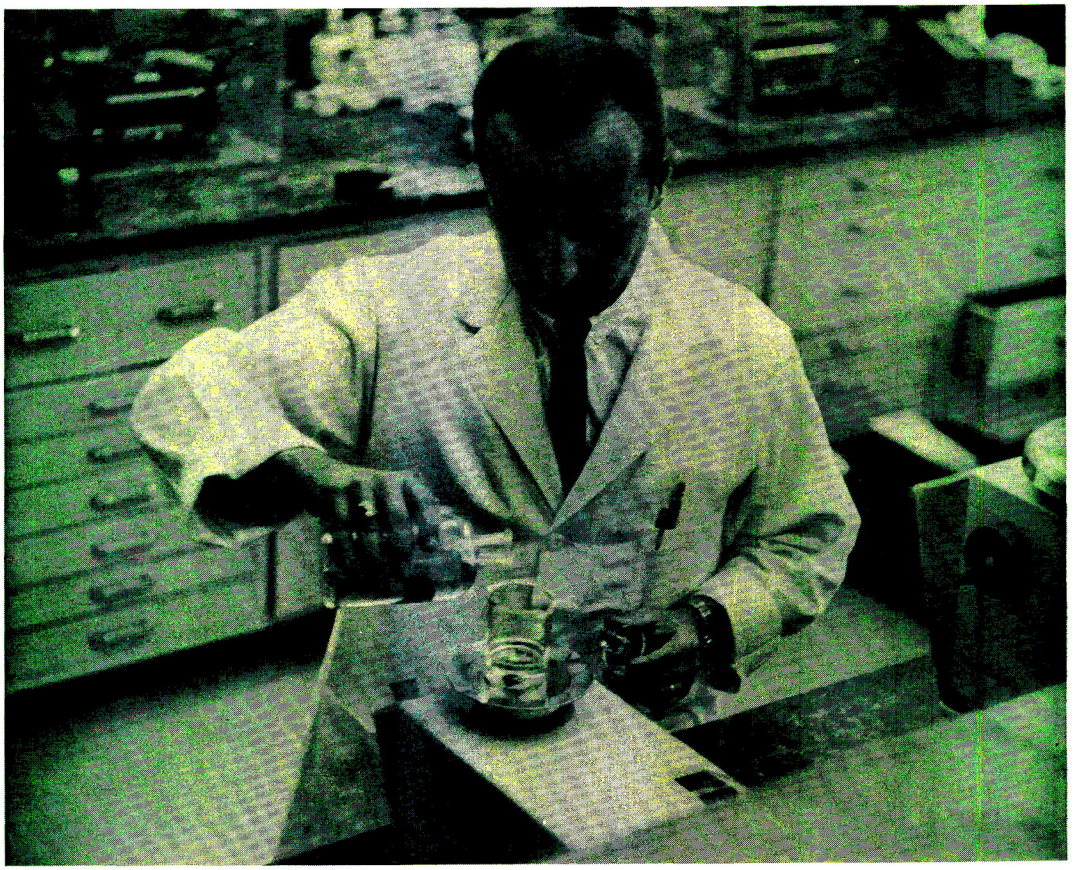

AT COLGATE-PALMOLIVE RESEARCH CENTER...

"Our Mettler top-loaders let us test our ideas on the spot"

"We usually make formulations of our prototype materials right on our Mettler P-1200 top-loading balance," says Dr. Richard Turse, Senior Research Chemist at the Colgate-Palmolive Research Center.

"The speed and convenience of the Mettler is important to us. By cutting down on the mechanics of putting a test material together, we have more time for theoretical work. With quick, convenient and accurate formulation, we can try out our ideas right on the spot."

Dr. Turse's laboratory at Colgate-Palmolive works with proprietary pharmaceutical products – cough syrups, aerosols, effervescent preparations.

"Because much of our work calls for making up experimental formulations, the Mettler top-loader is in almost continuous use. We tare the beaker weight, add successive components, and fill to target weight ...usually 100 or 200 grams. The P-1200 also has plenty of capacity when we make up kilogram quantities."

The New Brunswick, New Jersey facility is the primary research arm of the Colgate-Palmolive Company, the world's largest manufacturer of toilet articles and one of the largest producers of soaps and detergents. It uses more than 40 Mettler balances in analytical research and product preparation.

Find out how the new Mettler top-loaders combine the precision of analytical balances with top-loading convenience. Let us lend you a balance to try in your own laboratory. Write Mettler Instrument Corporation, 20 Nassau Street, Princeton, New Jersey.

Mettler®

Circle No. 48 on Readers' Service Card

AC BRIEFS

HIGHLIGHTS OF THE SCIENTIFIC AND TECHNICAL ARTICLES IN THIS ISSUE

Effect of Uncompensated Resistance on Electrode Kinetic and Absorption Studies by Chronocoulometry

A positive feedback potentiostatic circuit is described which permits compensation of the potential drop across the uncompensated resistance. The circuit was tested by applying potential steps to an electrical analog of an electrode–solution interface and by determining heterogeneous rate constants of Cd(II) and Tl(I) reduction by chronocoulometry at a hanging mercury drop electrode.

GEORGE LAUER and ROBERT A. OSTERYOUNG, North American Aviation Science Center, Thousand Oaks, Calif. 91360

Anal. Chem. 38, 1106 (1966)

Kinetic Current Measurements with Controlled Potential. Application to the Uranium(V) Disproportionation Reaction

The collection and interpretation of kinetic current data taken at short times by use of controlled potential polarography are discussed. The application of transfer function measurements to test the design and to determine system response time is demonstrated.

DALLAS T. PENCE and GLENN L. BOOMAN, Phillips Petroleum Co., Atomic Energy Division, Idaho Falls, Idaho

Anal. Chem. 38, 1112 (1966)

Some Investigations on Instrumental Compensation of Nonfaradaic Effects in Voltammetric Techniques

Application was made to cyclic voltammetry and to fundamental harmonic and higher harmonic a.c. polarography. Readout of the faradaic component was highly accurate for moderately demanding conditions.

ERIC R. BROWN, THOMAS G. McCORD, DONALD E. SMITH, and DONALD D. DeFORD, Department of Chemistry, Northwestern University, Evanston, Ill.

Anal. Chem. 38, 1119 (1966)

Instrumentation for Digital Data Acquisition in Voltammetric Techniques. D.C. and A.C. Polarography

The instrument incorporates a combination of known electrochemical control and signal conditioning procedures with a commercial digital data acquisition system. It was designed for digital readout of current and potential signals on an IBM card for voltammetric techniques involving relatively long experiment times.

ERIC R. BROWN, DONALD E. SMITH, and DONALD D. DeFORD, Department of Chemistry, Northwestern University, Evanston, Ill.

Anal. Chem. 38, 1130 (1966)

Use of a Multichannel Analyzer as a Data Acquisition System in Electrochemistry

The system is described with particular reference to its use in chronocoulometric studies. This system increases the rapidity and accuracy with which data may be acquired compared to photographing an oscilloscope face.

GEORGE LAUER and R. A. OSTERYOUNG, North American Aviation Science Center, Thousand Oaks, Calif. 91360

Anal. Chem. 38, 1137 (1966)

A Digital Data Collection, Waveform Generation, and Timing Instrument for Electrochemical Measurements

With this instrument, functions such as pulse, square-wave, linear scan, linear-scan-and-hold, stair-step, and bidirectional linear-scan waveforms are obtained easily by changing prewired patchboards.

GLENN L. BOOMAN, Phillips Petroleum Company, Atomic Energy Division, Idaho Falls, Idaho

Anal. Chem. 38, 1141 (1966)

Electrode Potential Gradients and Cell Design in Controlled Potential Electrolysis Experiments

The effect of potential distribution in electrolysis cells used for large-scale, controlled-potential electroanalytical experiments was investigated and the conditions and geometric arrangements where the working electrode potential exceeds the control potential were evaluated.

J. E. HARRAR, Chemistry Department, Lawrence Radiation Laboratory, University of California, Livermore, Calif., and IRVING SHAIN, Chemistry Department, University of Wisconsin, Madison, Wis.

Anal. Chem. 38, 1148 (1966)

Evaluation of Stationary Electrode Polarography and Cyclic Voltammetry for the Study of Rapid Electrode Processes

It is concluded that scan rates as fast as 2000 volts/second may be used with confidence in fast sweep experiments where the response characteristics of the potentiostat and electrolysis cell have been optimized. It is also indicated that chemical rate processes coupled to the charge transfer step may be studied with time resolution of the order of 1 to 100 μsec. using linear sweep techniques.

S. P. PERONE, Department of Chemistry, Purdue University, Lafayette, Ind.

Anal. Chem. 38, 1158 (1966)

Automatic Determination of Weak Organic Acids by Partition Column Chromatography and Indicator Titration

Quantitative determination of organic acids in the range 0.05 to 3 μequiv. per acid has been performed rapidly and automatically by partition chromatography on a silica gel column followed by indicator titration. Complex mixtures from physiological sources may be analyzed with no preliminary extraction in about 5 hours; less complex mixtures, within an hour.

LEO KESNER and EDWARD MUNTWYLER, Department of Biochemistry, State University of New York Downstate Medical Center, Brooklyn, N. Y. 11203

Anal. Chem. 38, 1164 (1966)

The Nonaqueous Microtitration of Dibenzoylmethane and Other Weak Acids

A potentiometric technique using polarized bimetallic electrodes for determining dibenzoylmethane and other weak acids in anhydrous ethylenediamine or pyridine is described. A solution of tetrabutylammonium methylate is used as the titrant.

D. A. LEE, Chemistry Division, Oak Ridge National Laboratory, Oak Ridge, Tenn.

Anal. Chem. 38, 1168 (1966)

NEW MODEL 3375 TRI-CARB®
LIQUID SCINTILLATION SPECTROMETER...

with these exclusive features:

- Push-button channel selection for single, double or triple label experiments; front panel adjustment permits normalization as required to retain factory-optimized counting conditions
- Patented, volume-independent Automatic External Standardization using a *compound source* of Americium-241 and Radium-226; choice of Ratio or Count methods of standardization
- Patented, "3+2" counting channel configuration; three completely independent channels of pulse-height analysis, each with precision gain control and continuously adjustable discriminators . . . *two additional* channels exclusively for Automatic External Standardization
- "On-line" electronic computation with continuous display of count rate and percent standard deviation; push-button selection of desired display, and full print control; complete selection of all possible Channel Ratios
- IBM Selectric Typewriter data presentation on continuous pre-printed forms . . . easy to read, organize and file

Model 3375 gives you these exclusive features and the latest, reliable integrated circuitry, plus the outstanding performance that is typical of all new Tri-Carb Spectrometer Systems. For complete information see your Packard Sales Engineer or write for Bulletin 1057B to Packard Instrument Company, Inc., 2200 Warrenville Road, Downers Grove, Illinois 60515.

Packard

A Rapid and Sensitive Method for the Determination of Iodine-131 in Milk by Ion Exchange on Silver Chloride

After elution of iodine-131 as iodic acid from the silver chloride column, the eluate can be directly analyzed by gamma counting. If beta counting or increased sensitivity is required, the iodine is subjected to two oxidation–reduction solvent-extraction cycles. With the complete procedure, less than 2 picocuries can be detected in 1 liter.

WILLIAM D. FAIRMAN and JACOB SEDLET, Argonne National Laboratory, 9700 South Cass Ave., Argonne, Ill. 60439

Anal. Chem. 38, 1171 (1966)

Determination of Strontium-90 in Seawater after Concentration by Manganese Dioxide

The adsorption of strontium by hydrous manganese dioxide was used to concentrate strontium in seawater. A complete radiochemical procedure for Sr^{90} in seawater is presented.

WILLIAM H. SHIPMAN, U. S. Naval Radiological Defense Laboratory, San Francisco, Calif. 94135

Anal. Chem. 38, 1175 (1966)

Gas Chromatographic Determination of Pyruvic and Lactic Acids and Krebs Cycle Components. Esterification and Recovery

The components of the tricarboxylic acid cycle, lactic acid, and pyruvic acid were esterified with diazomethane. The chromatographic factors affecting the quantification of the esters were examined.

FRANCES L. ESTES and RICHARD C. BACHMANN, Surgical Research Laboratory, The University of Texas Medical Branch, Galveston, Texas

Anal. Chem. 38, 1178 (1966)

An Improved Method for the Determination of Orthophosphate Suitable for Assay of Adenosine Triphosphatase Activity

The optimal conditions for the determination of orthophosphate in the presence of adenosine-5'-triphosphate, proteins, and various salts were investigated. The precipitate, the removal of the precipitated protein, the form of phosphomolybdate, pH, and molybdate concentration were studied.

SAMUEL M. MOZERSKY, JULIO D. PETTINATI, and STANLEY D. KOLMAN, Eastern Regional Research Laboratory, U. S. Department of Agriculture, Philadelphia, Pa. 19118

Anal. Chem. 38, 1182 (1966)

Nucleation Rate and Crystal Growth Rate of the Complex as Factors in Microscopical Fusion Analysis of Quinone–Carcinogenic Agent Complexes

Methods are described for rapidly determining conditions favorable for nucleation and growth, so that fusion methods may be used to determine if a complex forms in a given binary system and the melting characteristics of that complex.

DONALD E. LASKOWSKI, Department of Pathology, Western Reserve University, Metropolitan General Hospital, Cleveland, Ohio

Anal. Chem. 38, 1188 (1966)

←—"See Laboratory Guide for all Products/Sales Offices"
←—Circle No. 52 on Readers' Service Card

Fast Scan High Resolution Mass Spectrometry. Operating Parameters and Its Tandem Use with Gas Chromatography

An electrical scan system whereby gas chromatographic effluents containing 1 μg. or less can be rapidly monitored by recording spectra on analog magnetic tape at a resolving power of 1 in 10,000 or more at scan speeds down to 8 seconds for a decade in mass is described. Average accuracy is better than 10 p.p.m.

W. J. McMURRAY, B. N. GREENE, and S. R. LIPSKY, Department of Medicine, Yale University School of Medicine, New Haven, Conn.

Anal. Chem. 38, 1194 (1966)

Determination of Nonfiller Magnesium in Polyesters

Low temperature pyrolysis of the cured sample followed by leaching of the residue with a buffered solution separates the nonfiller magnesium from that in the filler. For uncured samples, the acetone solubility of the organically-bound magnesium permits its separation from the filler. The magnesium is determined titrimetrically with EDTA.

JOHN E. NEWELL, Chemical Division, United States Rubber Co., Naugatuck, Conn.

Anal. Chem. 38, 1205 (1966)

Fast and Sensitive Method for Determination of Nitrogen. Selective Nitrogen Detector for Gas Chromatography

The method is applicable to total nitrogen determinations and to selective detection of nitrogen compounds with gas chromatography. Nitrogen quantities as low as 10^{-9} gram can be determined. Samples as high boiling as gas oils containing as little as 0.2 p.p.m. of nitrogen can be analyzed in less than 10 minutes.

RONALD L. MARTIN, Research and Development Department, American Oil Co., Whiting, Ind.

Anal. Chem. 38, 1209 (1966)

Automatic Analyzer with Direct Readout for Determining Carbon in Steel

The steel sample is burned in oxygen and the carbon dioxide formed is collected and measured for a total analysis time of 80 seconds. The linear operating range is from 0.01 to 1.2% carbon, which can be extended down to 0.001 and up to 3.0%.

L. L. LEWIS and M. J. NARDOZZI, Applied Research Laboratory, United States Steel Corp., Monroeville, Pa.

Anal. Chem. 38, 1214 (1966)

Spectrophotometric Determination of Platinum with 3,4-Diaminobenzoic Acid

3,4-Diaminobenzoic acid reacts with platinum to form a blue-green 2:1 complex which has a maximum absorption at 715 mμ. The only ions which interfere enough to require separation are those of palladium, osmium, and ruthenium.

LARRY D. JOHNSON and GILBERT H. AYRES, The University of Texas, Austin, Texas

Anal. Chem. 38, 1218 (1966)

WHY YOU SHOULD INVESTIGATE SADTLER RESEARCH . . .

"Sadtler is a research laboratory that speeds the growth of other companies"

The above quotation is how one of Sadtler's many satisfied customers recently described the company's unique experience and facilities.

The Sadtler record is impressive. It has made important contributions to the sciences, helped spur the growth of many industrial giants, and materially furthered innumerable Government and university research projects.

The basic phenomenon of pH was introduced to industry by Sadtler. Its studies of air pollution was instrumental in establishing industrial pollution controls. Industry and the peoples throughout the world have benefited from its work on tobacco, cigarette filters, petroleum refining, asphalt, minerals, ores, paper making, food, chemicals and other processes.

The modern and highly sophisticated research and chemical analysis facilities of Sadtler Research offer you laboratory equipment and an experienced research group that is difficult to match anywhere.

Following are some of the many Sadtler services:

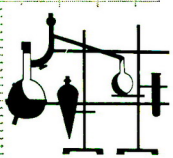

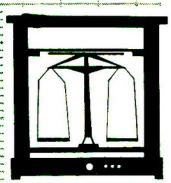

SADTLER STANDARD SPECTRA — A comprehensive collection of 29,000 reference infrared prism spectrograms of pure organic materials. Additions are made annually to keep up with new compounds of both research and industry.

SADTLER STANDARD ULTRAVIOLET SPECTRA — Those chemical compounds, included in the infrared collection, that absorb in the ultraviolet region have been selected for this useful compendium of 16,000 ultraviolet spectra. Indices and the unique Locator are part of the collection.

COMMERCIAL INFRARED SPECTRA — A collection of 12,000 infrared spectra of commercially available compounds — agricultural chemicals; polyols; surface active agents; natural resins and gums; monomers and polymers; pyrolyzates; plasticizers; perfumes and flavors; fats, waxes and derivatives; lubricants; rubber chemicals; fibers; solvents; intermediates; petroleum chemicals; textiles chemicals; dyes, pigments and stains.

NMR — Spectra determined on a Varian A-60A instrument are included in this collection with integration of the curves and spectral assignments. All compound information is found with the spectra and locating them is made easy by use of complete Indices, by name, molecular formula, chemical class and chemical shift.

DTA — Thermograms of both commercially available and research materials are included with interpretation of the graphs. Materials such as monomers, polymers, agricultural chemicals and pharmaceuticals are present.

INORGANICS — Grating spectra covering the region of 2.5 to 40 microns of classical inorganics and coordination compounds make up this collection.

PHARMACEUTICALS—Infrared and ultra violet spectra, when applicable, of commercially available pharmaceutical products listed in the leading drug books comprise this group. Additions are made.

BIOCHEMICALS — Infrared and ultraviolet spectra of compounds of interest to the biochemist are included in this group of 2,000 infrared and over 650 ultra violet spectra.

STEROIDS — A publication containing 250 prism spectra from 2 to 15 microns and 250 grating spectra from 2.5 to 40 microns of steroids. Additions are made to this group employing the grating instrument.

MULTIPLE INDEXING:

Alphabetical—Chemical Abstracts nomenclature classified by parent compounds and substituent derivatives.

Molecular Formula—Compounds listed by increasing order of carbon, hydrogen and other atoms.

Chemical Classes — Location of any single spectrum or group of spectra by functional group.

Numerical — Quickly identifies spectra where Sadtler Serial Number is known but name is not.

Spec Finder—A Sadtler technical reference book method for Standard IR and Commercial IR.

UV Locator—A Sadtler technical reference book method for identification of unknown Ultra Violet Spectra.

LABORATORY SERVICES — Thermoanalysis • Infrared Spectroscopy • N.M.R. Spectroscopy • Food & Drug Analysis • Gas Chromatography • Organic Analysis • Analytical Testing • Polymer Research • Ultra Violet Analysis • Analysis of Commercial Products • Consultation.

IR COMPUTER SERVICE — Unknown samples searched and results reported within 72 hours.

TAPE RENTAL SERVICE—For searching IR and UV spectra. Available to laboratories equipped with or having access to computer installations.

SADTLER COURSES — Unique five-day courses to qualified personnel in the latest techniques in laboratory instrumentation.

Write for brochures including sample spectras

3330 Spring Garden Street PHILADELPHIA, PA. 19104

Agents in principal countries of the world

SADTLER RESEARCH LABORATORIES, INC.

Circle No. 64 on Readers' Service Card

Analysis of a High-Molecular-Weight Phenolic Inhibitor

Gas chromatography and phase solubility analysis were combined. Phase solubility analysis showed that the material was about 99% pure, and about 1% of a related phenol was found by gas chromatography.

H. S. KNIGHT and HERBERT SIEGEL, Shell Development Co., Emeryville, Calif.

Anal. Chem. 38, 1221 (1966)

Identification of Normal Paraffins, Olefins, Ketones, and Nitriles from Colorado Shale Oil

The shale oil was found to be a mixture of paraffins (C_{13-18}), olefins (C_{13-18}) with predominantly 1-alkenes, nitriles (C_{12-13}), and ketones ($_{13-16}$) in which 2-alkanones were predominant. A chromatographic method for the separation of hydrocarbon components using silica gel–silver nitrate mixture is presented.

TAKEO IIDA, EIICHI YOSHII, and EITARO KITATSUJI, Faculty of Pharmaceutical Sciences, Toyama University, Toyama, Japan

Anal. Chem. 38, 1224 (1966)

Absorptiometric Methods in Rapid Silicate Analysis

Spectrometric (or spectrographic), flame photometric, and colorimetric methods are applied to the same sample solution to determine all major elemental constituents of silicates except carbon, hydrogen, and oxygen. A lithium metaborate–nitric acid solution technique is used. A complete analysis is possible with 50 mg. of sample.

C. O. INGAMELLS, College of Mineral Industries, The Pennsylvania State University, University Park, Pa.

Anal. Chem. 38, 1228 (1966)

Scientific Communication

Determination of Nickel by Atomic Fluorescence Flame Spectrometry

D. N. ARMENTROUT, Abteilung fur Med. Physik, Univ.-Hautklinik, 63 Giessen, Germany

Anal. Chem. 38, 1235 (1966)

Correspondence

Application of the Rule of Six to the Separation of Diastereoisomeric Esters by Gas—Liquid Chromatography. An Exchange of Comments

BORIS WEINSTEIN, Department of Chemistry, Stanford University, Stanford, Calif. 94305; and BARRY L. KARGER and ROBERT L. STERN, Department of Chemistry, Northeastern University, Boston, Mass. 02115

Anal. Chem. 38, 1238 (1966)

p-Bis-(o-Methylstyryl) Benzene, Useful Secondary Fluor for Liquid Scintillation Counting

YUTAKA KOBAYASHI, Worcester Foundation for Experimental Biology, 222 Maple Ave., Shrewsbury, Mass. 01545

Anal. Chem. 38, 1240 (1966)

Relative Efficiency of a New Liquid Scintillation Fluor, *p*-Bis-(o-Methylstyryl) Benzene

ELIZABETH T. BUSH, Nuclear-Chicago Corp., 333 E. Howard Ave., Des Plaines, Ill.

Anal. Chem. 38, 1241 (1966)

The Rate of Oxidation of Platinum Electrodes

KARL H. POOL, JAMES G. SMITH, and A. L. CRITTENDEN, Department of Chemistry, University of Washington, Seattle, Washington 98105

Anal. Chem. 38, 1242 (1966)

Quantitative Determination of Individual Tocopherols by Thin Layer Chromatographic Separation and Spectrophotometry

PRISCILLA A. STURM, R. M. PARKHURST, and W. A. SKINNER, Department of Pharmaceutical Chemistry, Stanford Research Institute, Menlo Park, Calif.

Anal. Chem. 38, 1244 (1966)

Gas Chromatographic Study of the Separation of Resin Acid Methyl Esters on a QF-1 Column

CLIFFORD W. J. CHANG and S. W. PELLETIER, Department of Chemistry, The University of Georgia, Athens, Ga. 30601

Anal. Chem. 38, 1247 (1966)

Determination of Chloride in Glass by Pyrohydrolysis

V. E. CALDWELL, Pittsburgh Plate Glass Co., Box 11472, Pittsburgh, Pa. 15238

Anal. Chem. 38, 1249 (1966)

Determination of Long-Chain Alkyl Sulfates as Chloroform-Soluble Azure A Salts

JOHNNY VAN STEVENINCK and J. C. RIEMERSMA, Laboratory of Medical Chemistry, University of Leiden, Holland

Anal. Chem. 38, 1250 (1966)

On the Interpretation of Solute Vaporization Interference in Flame Photometry

C. TH. J. ALKEMADE, Physical Laboratory, State University, Utrecht, The Netherlands

Anal. Chem. 38, 1252 (1966)

VERSATILE 3-MODE ONE METER

MONOCHROMATOR SPECTROGRAPH-DIRECT READER

The Model 216 — a 3 in 1 instrument — is ideal for special problems in spectral analysis because of its:

- Fast f/9 optical system with half-width resolution better than 0.2A.
- Direct reading wavelength scale accurate to within 1A throughout the wavelength range.
- Wavelength reproducible to ±0.1A.
- Stigmatic optical system to allow full use of Hartman diaphragm, sectors and neutral density step filters.

MODES OF OPERATION

Mode 1 — AS A SCANNING MONOCHROMATOR to provide: immediate records of wavelength and intensity — for the wavelength range from 2000A to 40,000A.

Mode 2 — AS A SPECTROGRAPH where: sources are faint or fleeting, wavelength determinations require the accuracy of comparators, there is need for permanent photographic records — 1700A per exposure on 35 mm film.

Mode 3 — AS AN 18-CHANNEL DIRECT READER for the study of: plasmas, combustion dynamics rate coefficients, time-resolved spectra.

Modes 2 and 3 are instantly interchangeable without disruption of any optical alignment, i.e., each mode has its own focal curve which may be racked into position without disturbing other mode.

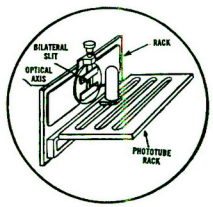

MODE 1

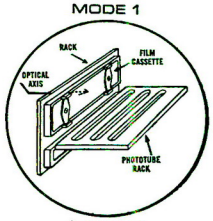

MODE 2

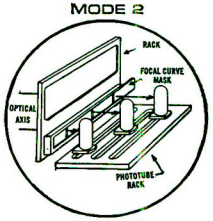

MODE 3

Complete technical data available on request.

McPHERSON INSTRUMENT CORPORATION
530 MAIN STREET, ACTON, MASSACHUSETTS 01720 · TEL: 617 263-7733

Technical Sales and Service Offices in La Canada, California; Cleveland, Ohio; Acton, Massachusetts; London: Germany-Switzerland-Austria; Melbourne; Paris; Tel Aviv; Tokyo.

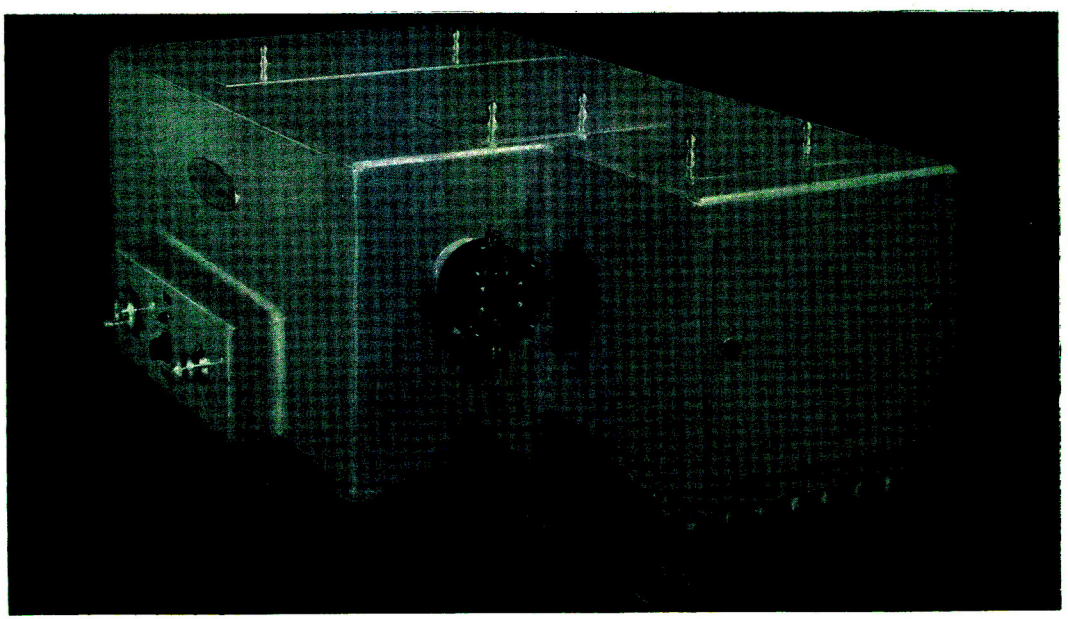

"See Laboratory Guide for all Products/Sales Offices"
Circle No. 135 on Readers' Service Card

Radiochemical Determination of Cesium Using Permanganate as a Precipitant

WILLIAM H. SHIPMAN and DAVID MUELLER, Applied Research Branch, U. S. Naval Radiological Defense Laboratory, San Francisco, Calif. 94135

Anal. Chem. 38, 1253 (1966)

Determination of Deuterium Ion Concentration in Dilute Unbuffered Deuterium Oxide Solutions

ELIZABETH W. BAUMANN, Savannah River Laboratory, E. I. du Pont de Nemours and Co., Aiken, S. C.

Anal. Chem. 38, 1255 (1966)

Determination of Dissolved Ammonia by Gas Chromatography

R. W. JENKINS, JR., C. H. CHEEK, and V. J. LINNENBOM, U. S. Naval Research Laboratory, Ocean Sciences and Engineering Division, Washington, D. C. 20390

Anal. Chem. 38, 1257 (1966)

Derivation of Expression for Integrated Luminescence Intensity When Using Pulsing Techniques in Luminescence Spectrometry

T. C. O'HAVER and J. D. WINEFORDNER, Department of Chemistry, University of Florida, Gainesville, Fla. 32601

Anal. Chem. 38, 1258 (1966)

Analysis of Cesium-134–Cesium-137 Mixtures by Gamma-Ray Spectrometric Methods

SACHIO YAMAMOTO, U. S. Naval Radiological Defense Laboratory, San Francisco, California 94135

Anal. Chem. 38, 1261 (1966)

The Effect of Water on Saponification of Organic Esters

W. H. GREIVE, K. F. SPOREK, and M. K. STINSON, Owens-Illinois, Inc., Corporate Research Technical Center, 1700 N. Westwood Ave., Toledo, Ohio 43607

Anal. Chem. 38, 1264 (1966)

Application of Radiometric Techniques to the Quantitative Paper Chromatography of Iron, Copper, Manganese, and Cobalt

A. R. LANDGREBE, T. E. GILLS, and J. R. DeVOE, Radiochemical Analysis Section, Analytical Chemistry Division, Institute for Materials Research, National Bureau of Standards, Washington, D. C. 20234

Anal. Chem. 38, 1265 (1966)

Semiquantitative Estimation of Nitrogen in Ammonium Faujasite by Differential Thermal Analysis

P. B. VENUTO, E. L. WU, and JOHN CATTANACH, Applied Research and Development Division, Mobile Oil Corp., Paulsboro, N. J.

Anal. Chem. 38, 1266 (1966)

Fluorometric Determination of Zinc

RICHARD E. JENSEN and RONALD T. PFLAUM, Department of Chemistry, University of Iowa, Iowa City, Iowa

Anal. Chem. 38, 1268 (1966)

p-Aminoazobenzene for the Spectrophotometric Determination of Sulfur Dioxide

SHARON J. KNISELEY and LEWIS J. THROOP, Mead Johnson and Co., Evansville, Ind. 47721

Anal. Chem. 38, 1270 (1966)

Voltammetric Determination of 2,6-Di-*tert*-Butyl-*p*-Cresol in Hydrocarbons

JOSEPH C. SUATONI, Physical Sciences Division, Gulf Research & Development Co., Pittsburgh, Pa.

Anal. Chem. 38, 1271 (1966)

Kinetics of Polymerization by Infrared Spectrometry

ARTHUR HIRSCH and B. E. BRIDGLAND, Canadian Technical Tape Ltd., Montreal, Canada

Anal. Chem. 38, 1272 (1966)

Where $\beta = 1.2$...

See this and other QRA apparatus at the "Chemical Exposition, USA, 1966"; QRA Booth No. 720.

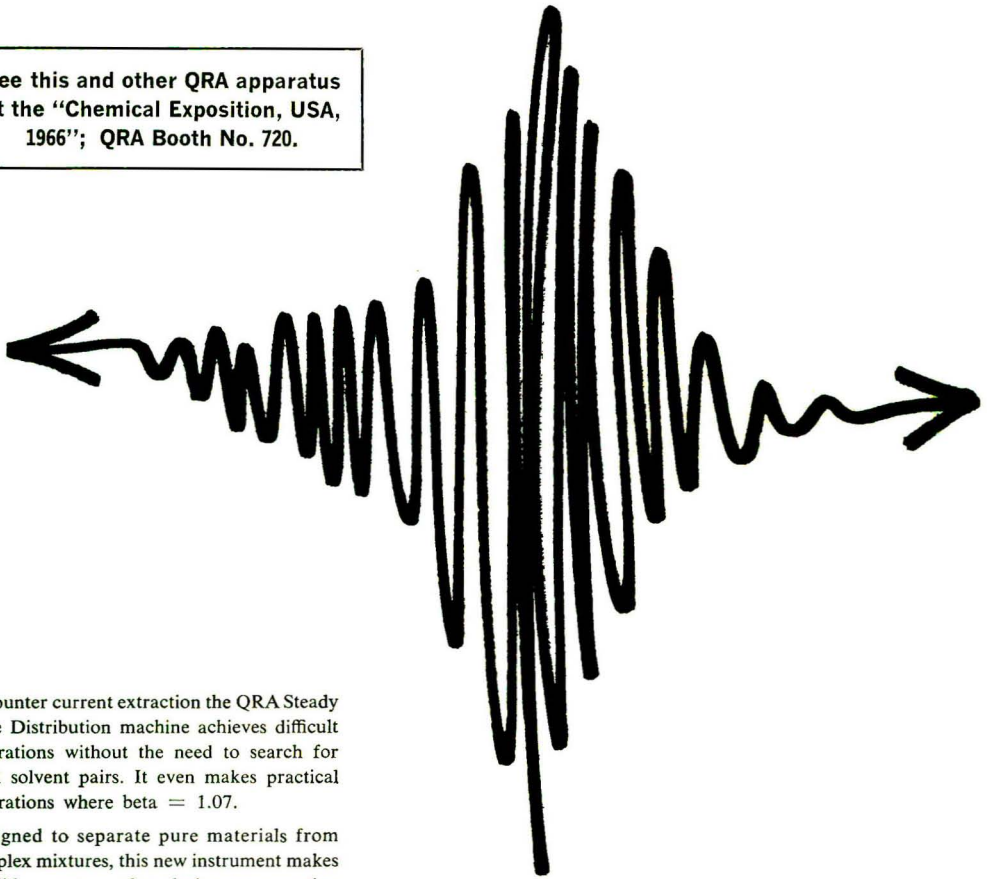

In counter current extraction the QRA Steady State Distribution machine achieves difficult separations without the need to search for ideal solvent pairs. It even makes practical separations where beta = 1.07.

Designed to separate pure materials from complex mixtures, this new instrument makes possible a system of analysis or preparation predicted in theory several decades ago.

Unlike single phase systems, the QRA SSDM moves both solvents in opposite directions, enabling you to separate complex mixtures using relatively few tubes. The key to the flexibility, speed and simplicity of operation of the machine is its program controller. This carries out any sequence of upper to lower transfers. The easy alteration of the ratio of upper to lower phase transfers minimizes the preliminary conditions required to achieve separation. Large numbers of different consecutive separations can be made without changing the solvent system phase volume.

For further information about the Steady State Distribution system and the SSD machine, call or write for our free SSDM booklet.

QUICKFIT REEVE ANGEL STEADY STATE DISTRIBUTION MACHINE

for analysis/concentration and isolation of a minor constituent/continuous preparation

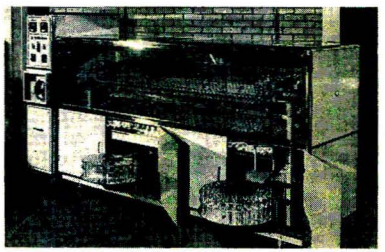

Features:

- Every instrument wet tested with over 1000 transfers.
- Handblown precision glassware.
- Automatic filling and emptying.
- Leak free.
- Precision ball and socket joint.
- No gear train or clutch.
- Available with fraction collectors.

QUICKFIT REEVE ANGEL
1 BRIDEWELL PLACE, CLIFTON, NEW JERSEY 07014.
PHONE 201-667-6767

Circle No. 80 on Readers' Service Card

AC BRIEFS

Aids for Analytical Chemists

Calibration Heater for Thermometric Titrations

MARVIN J. STERN, R. WITHNELL, and RICHARD J. RAFFA, College of Pharmacy, Columbia University, New York, N. Y. 10023 and Chemistry Department, Brookhaven National Laboratory, Upton, L. I., N. Y. 11973

Anal. Chem. 38, 1275 (1966)

An Electronic Coulostat

GEORGE LAUER, North American Aviation Science Center, Thousand Oaks, Calif. 91360, and California Institute of Technology, Pasadena, Calif. 91109

Anall. Chem. 38, 1277 (1966)

A Precision Method for Generation of Solvent Gradients

FREDERICK R. BLATTNER and JOHN N. ABELSON, Department of Biophysics, Johns Hopkins University, Baltimore, Md. 21218

Anal. Chem. 38, 1279 (1966)

A Nomogram for Calculating the Results of an Automatic Amino Acid Analysis

W. A. SCHROEDER, W. R. HOLMQUIST, and J. ROGER SHELTON, Division of Chemistry and Chemical Engineering, California Institute of Technology, Pasadena, Calif. 91109

Anal. Chem. 38, 1281 (1966)

Cryoscopic Molecular Weight Determinations Using Dimethyl Sulfoxide as the Solvent

R. S. GEORGE and R. K. ROHWER, University of California, Los Alamos Scientific Laboratory, P. O. Box 1663, Los Alamos, N. M.

Anal. Chem. 38, 1285 (1966)

Selective Removal of Aldehydes from Complex Mixtures during Gas Chromatography

R. R. ALLEN, Anderson, Clayton & Co., Foods Division, Sherman, Texas

Anal. Chem. 38, 1287 (1966)

Near-Infrared Determination of Deuterium Oxide in Water

W. E. KEDER and D. R. KALKWARF, Battelle-Northwest, Richland, Wash.

Anal. Chem. 38, 1288 (1966)

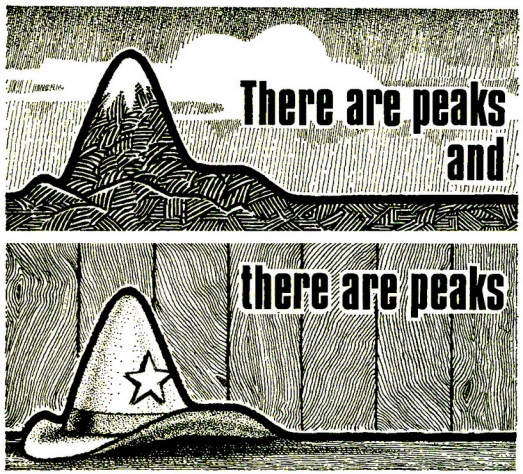

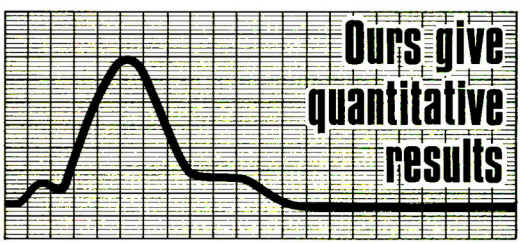

The quantitative peaks we refer to are those recorded by our ultraviolet flow stream monitors. ISCO's monochromatic Model UA-2 and Model 222 are the only low cost UV monitors which conform rigorously to Beer's absorption law. Other analyzers are sensitive to adjacent mercury vapor spectral lines but with ISCO analyzers precise quantitative results will be obtained if the flow stream absorbs *any* light at 254 mμ, regardless of the wavelength of maximum absorption.

The Model UA-2 has a built-in recorder which monitors true linear absorbance (not percent transmittance) at 254 mμ in two ranges; 0 to 0.5 and 0 to 2.5. An interchangeable dual-beam optical unit operates at both 254 and 280 mμ. The Model UA-2 will also actuate an associated fraction collector at the beginning and end of each UV-absorbance peak, depositing each UV-absorbing fraction in a separate collecting tube.

Prices for a complete ISCO absorbance monitoring, narrow bandwidth analyzer start at $650.00.

For complete information and prices send for brochure UA21H.

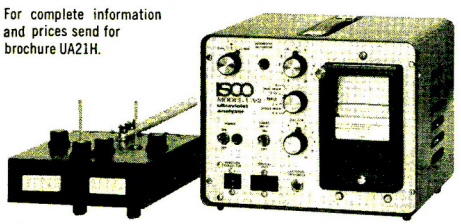

ISCO INSTRUMENTATION SPECIALTIES COMPANY, INC.

5624 SEWARD AVE. PHONE (402) 434-8265
LINCOLN, NEBRASKA 68507, U.S.A. CABLE ADDRESS: ISCOLAB LINCOLN

Circle No. 40 on Readers' Service Card

Miss Knibbs

(Miss) Mary Knibbs enjoys running the British end of the EASTMAN Organic Chemicals business. She is very good at it. She insists that no matter how many laboratories inquire in any given hour for urgently wanted compounds, each must get the impression that the staff had been sitting idle since breakfast, waiting for the phone to ring. She maintains quite a correspondence on the deployment of new organic compounds in attacking scientific problems. It was at her insistence that we have just added *5,5-Dimethyl-2,4-oxazolidinedione* (EASTMAN 9950), a subject of lively debate in the pages of *Science* (150:1294, Dec. 3, 1965; 151: 1564, Mar. 25, 1966; and 152:798, May 6, 1966) concerning efficacy in the estimation of intracellular pH.

EASTMAN 9950 5g., $ 6.95
25g., $29.60

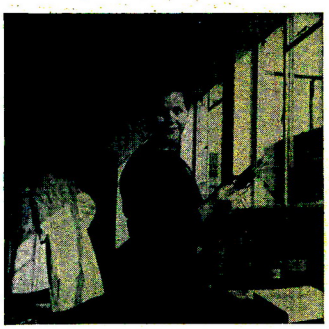

Miss Knibbs' address is Kodak Limited, Kirkby Industrial Estate, Liverpool. It would have been quite justifiable to raid the ranks of British science for one chemist the better to serve the remainder, but this proved unnecessary. Instead, our affiliate won the loyalty of the Personal Assistant to the British Chief of Staff to the Allied Commission for Austria and set her up as secretary to the manager of their very small chemical factory at Liverpool. Soon it was growing fast with Miss Knibbs binding up cut fingers, dispensing aspirin tablets, paying the wages and salaries, and running the cafeteria. Things went so well that when her boss was promoted there was no question about who could best manage the Research Chemical Sales Division. Enough time has elapsed since 1959 for the figures to prove it was a good appointment.

Allen's idea updated

3,4,5,6-Tetrachlorophthalimide (EASTMAN 3698) has been restored to our list. It didn't catch on when we offered it years ago for identification of aliphatic halogen compounds by long heating in sealed tubes to form N-substituted tetrachlorophthalimides. It's back because nowadays these reference derivatives can be conveniently prepared in modern ionizing solvents like N,N-Dimethylformamide (EASTMAN 5870) and Methyl Sulfoxide (EASTMAN P7108) by Gabriel synthesis. The paper that tells about the newer technique (*Anal. Chem.*, 37:158 (1965)) applies it also to identification of alkylsulfonates, including bismethanesulfonates, a class of compounds invented by C.F.H. Allen and a collaborator. Allen, senior author of the 1965 paper as well as of the original method of 1934, has retired from the Kodak Research Laboratories to teach at Rochester Institute of Technology. One career is too few for some guys.

EASTMAN 3698 10g., $ 7.45
25g., $16.70
EASTMAN 5870 500g., $ 2.75
3kg., $ 8.60
EASTMAN P7108 500g., $ 3.00
3kg., $10.15

The family esterification catalyst

Methanedisulfonic Acid (EASTMAN 7746) is preferable to sulfuric acid or toluenesulfonic acid as a catalyst for esterifying carboxylic acids because it drastically cuts esterification time from hours to minutes and even from days to hours in many cases. Tennessee Eastman Company, our division at Kingsport that indulges in very-large-scale synthesis, sees no reason not to share this helpful hint which has served it well. You will recall learning that sulfuric acid catalyzes esterification of acetic acid by methanol only up to a certain point, beyond which there takes over a competitive reaction that forms inert methyloxonium ion.

EASTMAN 7746 5g., $ 3.30
25g., $11.55

NOTE:

If you are reading this after August 30, 1966 and have not yet received EASTMAN Organic Chemicals List No. 44, please so inform **Distillation Products Industries, Rochester, N. Y. 14603** (Division of Eastman Kodak Company). Same address to place orders for any of the random sampling of EASTMAN Organic Chemicals advertised on this page. Prices subject to change without notice, minimum order $10. Our telephone number is (716) 458-4080.

Ferroelectric organic

Glycine Sulfate $(NH_3^+CH_2COO^-)\cdot(NH_3^+CH_2COOH)_2\cdot SO_4^=$ (EASTMAN 9921) may interest some chemists simply because physicists have been investigating the daylights out of it for ten years, ever since it was found to be ferroelectric. Precious little about the crystallographic, electrical, thermal, and mechanical properties of the material has escaped thorough investigation. For a hint as to why the interest, one may note that it has found employment in several types of ferroelectric memory and switching devices. Ferroelectric materials are electrically analogous to ferromagnetic materials. This one has a pretty set of hysteresis loops that one can look at by courtesy of the Institute of Crystallography of the U.S.S.R. Academy of Sciences (*Kristallografiya*, 4: 117, No. 1, 1959).

EASTMAN 9921 25g., $ 4.65
100g., $15.15

For purposes of comparison

Hydroxycinnamic acids are present in most higher plants, occur in bound form, are liberated by hydrolysis with acid or alkali, and have aroused interest lately in their natural distribution, biological function, and biosynthesis. This has led to studies such as reported in *Biochem. J.*, 81:242 (1961), where naturally occurring sugar derivatives of cinnamic acid are examined. We are therefore prompted to offer *p-Hydroxycinnamic Acid* (EASTMAN 9844), prepared by a less interesting route than the one that gets it into potato berries. An interesting comparison of our product with the potato's might be done by thin-layer chromatography with the EASTMAN® CHROMAGRAM® System. We sell the materials and equipment for that, too. It's great.

EASTMAN 9844 5g., $ 5.25
25g., $21.45

Quenched by –SH or –SS–

2',7'-Bis(acetoxymercuri)fluorescein (EASTMAN 9963), or fluorescein mercuric acetate (FMA), as it is called by the sensible people who discovered that its fluorescence is quenched by a thiol group or at high pH by a disulfide group, has become the reagent for detecting 10^{-10} mole of disulfide by spraying as alkaline solution on a paper chromatogram. Their paper (*Anal. Biochem.*, 9:100 (1964)) slightly predated the advent of the EASTMAN CHROMAGRAM System of thin-layer chromatography, which may well turn out to yield faster and better resolved separations for this visualization technique. They also describe a procedure with a solution of the reagent for the continuous assay of cystine-containing peptides in column effluents. Interest runs high in such peptides. Disulfide links are important in giving proteins their immunologically significant shapes.

EASTMAN 9963 5g., $ 3.45
25g., $12.40

EASTMAN Organic Chemicals from Kodak

what are your needs in a recording spectro-photometer?

CHECK THE BENEFITS YOU GET WITH A CARY MODEL 14

DEPENDABILITY
The first CARY 14 was purchased 13 years ago. It's still performing. So is every other one made since then.

SIMPLICITY
Easy to operate. Switch at will to eight different scan speeds. Read wavelength and absorbance data more easily through direct linear recording. There's no need to change paper to study a wide variety of spectra.

VERSATILITY
Accessories make the CARY 14 adaptable for a wide variety of studies. Accessories include dewars, fluorescence, reflectance, and both sample handling and digitizing devices.

ECONOMY
Low-cost operation and maintenance. Depreciate the CARY 14 in five years—appreciate it for many more.

ACCURACY
Outstanding for a recording spectrophotometer. 0.002 absorbance near zero and 0.0005 with expanded scale. Wavelength: better than 4Å. Resolution: 1Å in Visible and UV; 3Å in Near-Infrared.

REPRODUCIBILITY
Excellent for repeatable, linear wavelength and photometric readings. Records data with minimum of correcting or reprocessing.

QUALITY
Sound engineering practices demand care in the design and selection of components. Tough tests and extensive calibration also provide more reasons why CARY makes the world's finest research instruments.

Need additional information? Then send today for the CARY 14 brochure A604-86

CARY® INSTRUMENTS
APPLIED PHYSICS CORPORATION
2724 S. PECK RD., MONROVIA, CALIF.

UV/VIS/IR/Raman Recording Spectrophotometers
Manual Spectrophotometers • Spectropolarimeters
Vibrating Reed Electrometers & Amplifiers

Circle No. 141 on Readers' Service Card

Do you need new glasses... or Mallinckrodt thin layer sorbents?

A change to Mallinckrodt SilicAR® sorbents is like getting a new set of eyes. Spots sharpen. Clarity improves. Uniform results become a matter of course.

The uniformity of Mallinckrodt silicic acid is legend. Our purity specifications excel the standards of comparably priced sorbents. And, further, we provide tight control of organic contaminants—the source of greyness on charred plates, contamination at the solvent front and other TLC troubles. Few sorbents offer this control.

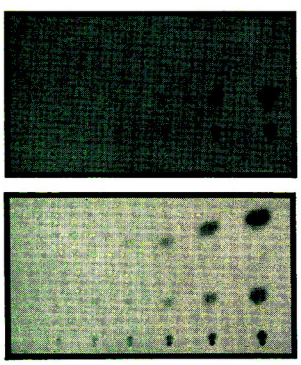

There's an additional advantage in our fluorescent sorbents. The phosphors emit white light instead of green, resulting in superior uv visualization. The photos at left compare the same sample on a green plate (top) and our white plate (bottom) under uv.

If you haven't been seeing spots like you should, don't blame your glasses. Blame your "specs." Order a supply of SilicAR sorbents from your Mallinckrodt distributor.

Mallinckrodt®

Visit Booth 140 at the A.C.S. Show

MALLINCKRODT CHEMICAL WORKS

St. Louis, Missouri 63160

Circle No. 154 on Readers' Service Card

Circle No. 145 on Readers' Service Card →

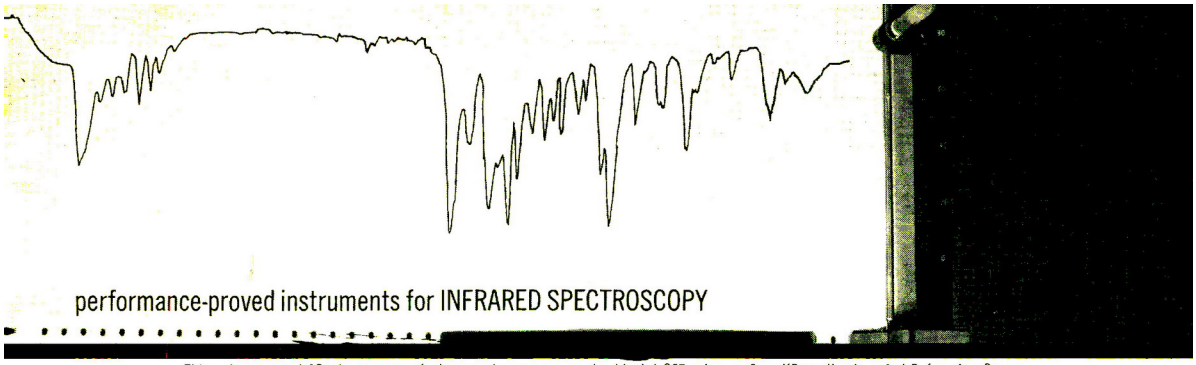

This uninterrupted 12-minute scan of phenacetin was run on the Model 257 using a .5mm KBr pellet in a 1x4 Refracting Beam Condenser. Sample volume was 1 microgram. A Refracting Beam Condenser was also placed in the Reference Beam.

FLEXIBILITY AT THE TOUCH OF A BUTTON— THE MODEL 257

Here is a high-resolution double-grating infrared spectrophotometer that gives you flow-chart recording and automatic control features not found in any other instrument in its moderate price range. The Model 257 offers·

- A wider range of scan speeds: 5, 12, and 48 minutes per run.
- Automatic reset—at the end of the run, monochromator automatically returns to 4000 cm^{-1}.
- Abscissa expansion, by factors of 2.5 and 10X, to spread out the close, sharp bands typical of grating spectra—particularly in the analysis of gases.
- Time drive, to permit the quantitative determination of kinetic changes in a sample, at one significant frequency, over a period of time.
- Variable slit control, allowing very narrow slits for high resolution, as well as the wide openings required for energy-limited analyses such as by ATR and micro-sampling.
- Visual mode and frequency indicators: you always have a positive indication of mode of operation and frequency position.

The Model 257's large f/5 aperture enables you to obtain accurate spectra even with very small samples. You can vary the slit program to suit the requirements of the analysis. Or you can keep the frequency fixed and record the changes in transmittance as a function of time.

You have a choice of three recording speeds—plus an extra-fast speed control that lets you move quickly from one spectral region to another.

You read your results on a flow chart recording system (linear transmittance vs. linear frequency) which is continuous in presentation. The chart is synchronized with the monochromator drive, and both start with a single pushbutton.

At the end of the run the monochromator setting automatically returns to the start position while the operator tears off the completed chart prior to recording the next spectrum. The chart is pre-calibrated; no alignment is necessary to start a new recording. You can make forty complete recordings on a single roll of chart paper. Because of the unique positive sprocket drive, abscissa accuracy is unaffected by humidity or temperature fluctuations.

For full details and sample spectra, write The Perkin-Elmer Corporation, 702 Main Avenue, Norwalk, Connecticut.

TPC

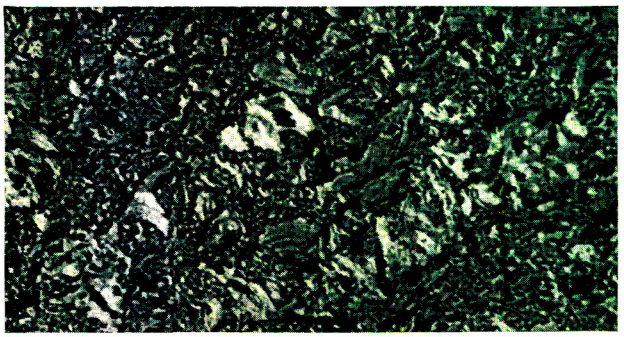

'Total Product Control'—exclusive with NATIONAL spectroscopic electrodes—provides today's finest STRUCTURE.

Union Carbide Corporation is the only manufacturer equipped for "Total Product Control" of spectroscopic electrodes—from selection of raw materials to final package.

Only through this unique capability is it possible to maintain the finest *structure*—a must for reliable reproducibility *every time*.

The above photomicrograph shows the superior uniformity of pore and particle size of a NATIONAL spectroscopic electrode. This unsurpassed structure is maintained throughout the rod—and from batch to batch.

Why gamble with hundreds of dollars worth of product when electrode costs are just pennies per analysis?

Get maximum confidence by calling your dealer for NATIONAL spectroscopic electrodes—the electrodes with today's finest structure.

"National" is a registered trademark of
UNION CARBIDE CORPORATION
CARBON PRODUCTS DIVISION

UNION CARBIDE

270 Park Avenue · New York, N. Y. 10017
In Canada: Union Carbide Canada Limited, Toronto

Circle No. 73 on Readers' Service Card

NATIONAL Spectroscopic Dealers

ANGSTROM, INC.
APPLIED RESEARCH LABORATORIES
BAIRD-ATOMIC, INC.
di SAR INDUSTRIES
FISHER SCIENTIFIC COMPANY
JARRELL-ASH COMPANY
LaPINE SCIENTIFIC COMPANY
LUCIUS-PITKIN, INC.
NATIONAL SPECTROGRAPHIC LABORATORIES
SPEX INDUSTRIES, INC.

The facts have changed!

Three new pre-coated systems for Thin Layer Chromatography have lowered cost, raised quality, widened its application.

New facts about pre-coated glass

The new E. Merck, A. G. (Darmstadt) Pre-Coated Glass Plate is the finest, most versatile pre-coated TLC system ever developed. Yet a 20 x 20 cm. plate costs as little as 68¢ (in quantity) — about half as much as previously available glass systems. And it offers 5 notable advantages:

- glass only 1 mm. thick —easier to store, easier to cut into strips
- a sorbent layer (Silica Gel F 254) 250 microns in thickness—the same as you get with your own coating apparatus—offering higher capacity than thinner pre-coated systems currently available
- the hardest coating yet developed—meaning plates that are abrasion-proof under normal conditions—guaranteed to arrive in good condition—may be stacked one on top of another
- the best separating characteristics of any pre-coated system now available—equivalent to the plate you make yourself
- unique organic binder—may be used with corrosive sprays (including sulphuric and perchloric acids) and charring techniques —cannot be eluted by organic solvents— does not interfere with stains

New facts about plastic foils

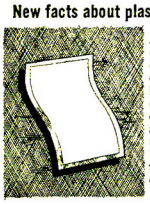

Although it is the most elegant TLC system in existence, use of the pre-coated plastic foil has been extremely limited due to its relatively high cost and narrow range of applications. Now Brinkmann introduces the MN Polygram pre-coated foil, far more versatile but costing about 30% less.

The MN Polygram foil features a dry layer with significantly higher capacity than that of previously available coated foils.

Four different types of coating are available: silica gel with starch binder, silica gel with starch binder and fluorescent indicator, cellulose powder without binder, and cellulose powder without binder but with fluorescent indicator. Each type comes in both 20 x 20 and 5 x 20 cm sizes.

Where a binder is used, starch has been selected because previously used binders (such as polyvinyl alcohol) have a substantial negative effect on the adsorption characteristics, especially when non-polar solvents are employed. Starch, however, is normally satisfactory except with highly aqueous systems, in which case the foils must be handled with care.

The Chromatotube—a new fact in itself

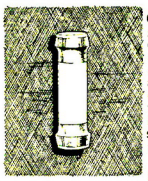

Chromatotubes are round glass tubes (12.5 x 2.5 cm) coated with sorbent on the inside. Since one end is closed, they are also self-contained developing tanks. After spotting, the open end is immersed in an auxiliary solvent tube sealed to the side by a plastic ring.

Special binders are not required and all conventional solvents and staining reagents may be employed. After separation, the tube can be eluted overnight and reused after activation.

Providing the most reliable, reproducible Rf values, Chromatotubes are probably the best TLC system for maintenance of uniform standards. The developing distance of 10 cm is marked so that the Rf is read at a glance. Thus the Chromatotube is ideal for mass analyses as in production control, clinical testing, and teaching procedures involving numerous students. At a relatively low cost each student has a complete chromatographic assembly.

Two types are available: Series AT tubes have been activated for 30 minutes at 110°C and subsequently sealed against external moisture; Series IT tubes are air dried and can be activated according to individual requirements.

Become up to date.

Please send me the following literature:

1. Pre-Coated Systems for TLC. 2. Catalog on apparatus, sorbents and ion exchangers for TLC. 3. I have the following problem:

_____

Name:_____

Institution:_____

Street:_____

City:_____ State:_____

BRINKMANN INSTRUMENTS

CANTIAGUE ROAD, WESTBURY, N.Y. 11590/ED 4-7500

Circle No. 19 on Readers' Service Card

Would you be interested in a completely functional x-ray diffraction laboratory if the cost was well under $10,000?

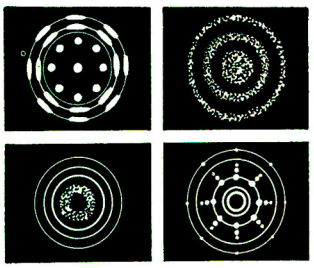

And if you knew that this included a full wave x-ray diffraction unit *plus* a single crystal or powder diffraction camera?

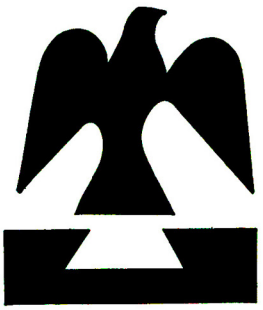

And if we told you that this x-ray diffraction unit has ACA-accepted dovetail camera track and fittings at no extra cost?

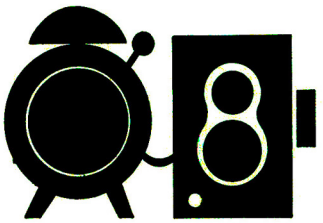

And if we explained that the diffraction unit also has timer-controlled electromagnetic shutters for simultaneous and independent exposure timing—at no extra cost?

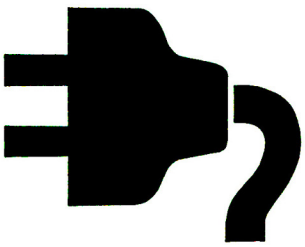

And if we installed the equipment at no extra cost?

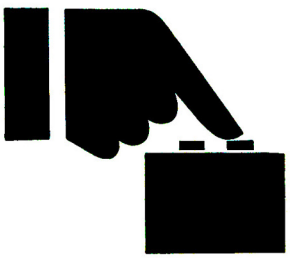

And if we showed you how to use it at no extra cost?

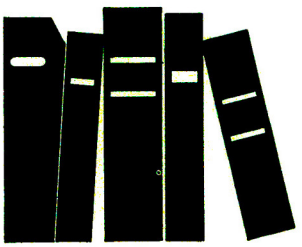

And if we provided valuable background literature at no extra cost?

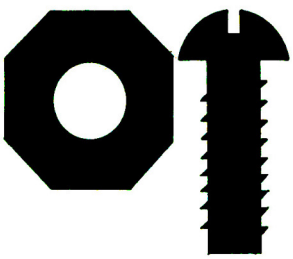

And if we gave you a complete parts warranty at no extra cost?

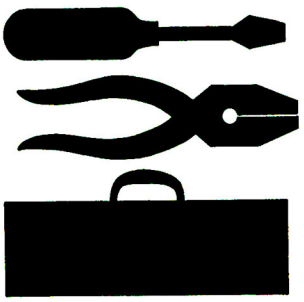

And if we included a labor warranty at no extra cost?

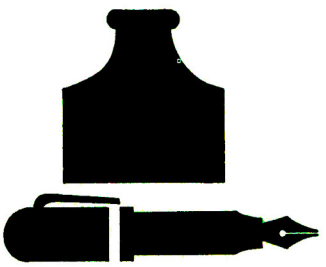

And if we promised to send you complete and explicit information about this equipment—also at no extra cost? Please request file CX-AC8.

Picker Nuclear: 1275 Mamaroneck Avenue, White Plains, New York 10605

PICKER nuclear

"See Laboratory Guide for all Products/Sales Offices"
Circle No. 57 on Readers' Service Card

Specifications for Evaluation of Infrared Reference Spectra

By
The Coblentz Society Board of Managers

In spite of the large number of infrared spectra now available through commercial and literature sources, a great need exists for additional reference spectra. To help meet this need, the National Standard Reference Data System at the National Bureau of Standards, together with the American Society for Testing and Materials, is exploring the feasibility of making generally available a number of spectra from government and private collections. Such spectra must be evaluated and selected before they are published. The Coblentz Society has been commissioned to define the specifications for publishable spectra, and the following report is the result of that effort. Although these specifications were set up for the purpose of guiding the evaluators who will screen spectra submitted for consideration in the Bureau of Standards program, it is anticipated that they will also prove useful to other spectroscopists in setting standards for their own laboratories.

ANY COMPLETE COLLECTION of reference data on pure materials must include their absorption properties in the electromagnetic spectrum, of which the infrared spectrum is an important part.

For purposes of evaluation, infrared spectra can be classified into three categories: Class I, standard spectra; Classes II and III, reference spectra.

CLASS I spectra are designated as "standard spectra" because they are of a sufficiently high quality to be acceptable as physical constants of the substances, under precisely defined conditions of measurement, and further refinements in spectrophotometric technique will not be expected to change them significantly. Few, if any, spectra of this quality have as yet been produced but they may be obtainable for condensed phase systems within two to five years. It is the unanimous opinion of the Board of Management of the Coblentz Society that the specifications and format of such Standard Spectra should be defined by international agreement and it is noted that the Commission on Molecular Structure and Spectroscopy of I.U.P.A.C. is now studying this problem.

CLASS II spectra are reference spectra obtained on the best currently available commercial infrared grating spectrophotometers, operated at maximum efficiency under conditions consistent with acceptable laboratory practice. The purity of the compounds must be rigidly specified with respect to the type and quantity of any spectroscopically detectable impurity present.

Class II spectra differ from Class I spectra because all currently available spectrophotometers distort the spectra to some extent, especially when operated under con-

ditions acceptable in routine use. The specifications for Class II spectra given in this report apply only to the absorption spectra of condensed phase systems, and it is not considered practical to write specifications for vapor phase spectra or for reflectance spectra at this time. It may be desirable to upgrade Class II specifications from time to time as instrumental techniques improve, but too frequent changes are to be discouraged and it is not contemplated that any major change should be necessary in the next few years.

CLASS III are the absorption spectra of individual compounds, polymers, and resins of known composition that have been obtained with sufficient accuracy to be useful in the identification of unknown materials. Only spectra that are superior to other spectra of the same compounds already in available catalogs should be published. Spectra that fail to meet Class III specifications should not be published (but may be useful to evaluators as comparison spectra). In the future, laboratories submitting spectra to this collection should be encouraged to meet Class II specifications; Class III is to be regarded primarily as a repository for usable data recorded prior to the general availability of high resolution grating spectrophotometers.

It must be made emphatically clear that the panel of spectroscopists established to evaluate these spectra (subsequently referred to as "the evaluators") cannot be expected to establish in all cases the correctness of the reputed chemical structures simply from the infrared spectra alone. Their prime responsibility is to rule on the technical quality of the spectra and check for gross incompatability with the assigned structure. In some cases it may be desirable to refer the spectrum, after spectroscopic evaluation, to a chemist with special knowledge of the compound type; a panel of chemical specialists should be assembled for this purpose. Users of Class III spectra, in particular, must be informed that many of these spectra will have been drawn from large collections that were not compiled with this kind of definitive documentation in mind, so that some incorrectly assigned spectra will, in all likelihood, pass through the screening process.

The Board of Management of the Coblentz Society recommends that spectra in Classes II and III be called "reference spectra" and that they be so designated in the published charts and in associated literature. It strongly recommends that the use of the word "standard" be reserved solely for spectra of Class I.

Specifications pertinent to spectrometer operation, presentation of data, sample preparation, and sample purity for Class II and Class III spectra are presented below.

Class II Spectra

I. *Spectrometer Operation*

A. Resolution. The spectral slit width should not exceed 2 $cm.^{-1}$ through at least 80% of the wavenumber range. Because there is difficulty in this measurement, evaluation will be based on a spectrum of indene, run under the same conditions as were used to produce the submitted spectrum (Appendix).

B. Wavenumber Accuracy. Wavenumbers, as read from the chart, should be accurate to $\pm$ 5 $cm.^{-1}$ above 200 $cm.^{-1}$ and $\pm$ 3 $cm.^{-1}$ below 2000 $cm.^{-1}$. Calibration corrections within these limits are to be encouraged and should be indicated on the chart.

Proof of wavenumber accuracy will be an appended spectrum of indene run under the same conditions as the sample (Appendix). On each chart a small fiduciary mark should be recorded at a selected and designated wavenumber (most conveniently the starting wavenumber) to establish the correct alignment of the chart wavenumber grid. It is recommended, to ensure against errors from paper shrinkage or chart-spectrometer mismatch, that a second fiduciary mark be inserted at the end of the scan at a designated wavenumber.

C. Noise Level. The noise level must not exceed 1% average peak-to-peak (or 0.25% R.M.S.). The evaluator's judgment is permissible.

D. Energy. The spectrophotometer must be purged with dry gas or evacuated to ensure that at least 50% of the source energy is available at all wavenumbers (except at the 2350 $cm.^{-1}$ CO_2 absorption).

If the control system of the spectrophotometer permits, it is desirable that adequate purging or evacuation be illustrated by a single beam run, or a run against a constant test signal, measured under the normal scanning conditions, with no sample in the beam.

E. Other Performance Criteria. (Established by reference to the indene spectrum. See Appendix.)

1. Scattered light. Apparent stray radiation should be less than 1% above 500 $cm.^{-1}$

2. Servo system. Any spectrum showing evidence of dead spots or excessive overshoot will be rejected. The spectrometer time constant must be compatible with the scan time (Appendix, Section B).

3. Photometric accuracy. These spectra are not intended to have absolute quantitative significance, and at present it is not feasible to set specifications for photometric accuracy. Such a test might be added later, but for the time being it must suffice that the indene bands be in reasonable agreement in shape and relative intensity with an acceptable indene curve.

II. *Presentation*

A. Information to Appear on Chart. Both the structural and the molecular formulas of the compound must appear on the chart. It is also recommended that the compound name be included, and preferably this should conform with the nomenclature used by *Chemical Abstracts*. The make and model of the spectrophotometer must be recorded as well as the date on which the spectrum was obtained. All changes of gratings, filters, and cells must be specified, including the wavenumbers at which they occur. No mechanical attenuator is to be placed in the reference beam. The name and address of the laboratory contributing the spectrum will normally be given on the chart (see Section *III*-A).

The physical condition of the sample must be stated (e.g., solution, pure liquid, Nujol mull, etc.). For measurements on solutions the solvent used in each region of the spectrum must be recorded. The

concentration and nominal path length should be given both for solutions and for alkali halide pellets. The nominal path length of pure liquid samples should be included. Very thin layers may be described as "capillary film."

B. SPECTRAL RANGE. The chart must cover 3800 to 400 cm.$^{-1}$, without gaps; extensions above or below this range are acceptable.

C. INTENSITY. It is preferred that the intensity ordinate values be expressed in absorbance units and that the charts be plotted on paper having a logarithmic ordinate grid so that intensity in absorbance can be interpolated directly from linear transmittance measurements. Spectra plotted on a linear absorbance scale, or in linear transmittance presented on a linear percent transmission ordinate grid, are also acceptable.

Any band over 1.5 absorbance units must be reproduced on a less absorbing sample. A significant fraction of the useful bands should have absorbance greater than 0.2. At least one band in the spectrum must have absorbance not less than 0.7. When multiple traces are required their number should be kept to a minimum.

D. WAVENUMBER READABILITY. Sharp band peaks should be readable to 4 cm.$^{-1}$ above 2000 cm.$^{-1}$ and 2 cm.$^{-1}$ below 2000 cm.$^{-1}$ Only spectra recorded with the abcissa linear in wavenumber are acceptable.

E. RECORDING. Recording should be continuous with no gaps in wavenumber, but it is permissible for spectra to extend over more than one chart. Discontinuities in ordinate (absorbance), if present, should not exceed 0.01 absorbance unit. Hand retraced spectra are not acceptable.

F. ATMOSPHERIC ABSORPTION. None should be detectable (note also Section *I*-D).

III. *Sample Identification*

A. COMPOUND IDENTITY AND PURITY. No spectrum will be published unless:

1. Two curves derived from samples obtained from different sources are available; these spectra must be in reasonable agreement.

or

2. The evaluator is supplied with a reasonably detailed description of the chemical preparation and purification history of the measured sample, together with other physical and chemical evidence for the correctness of the assigned structure. This evidence must be sufficient to satisfy an expert in the field.

Spectra should show no inconsistencies with the postulated structure; any spectrum exhibiting an obvious impurity band will be rejected. Because the prime responsibility for correctness of the structure lies with the contributing laboratory, its name and address should be recorded on the chart. In exceptional cases spectra contributed anonymously may be published, but such spectra will be prominently labelled "Chemical Structure Not Authenticated."

Polymers and resins are not ordinarily considered to be pure materials; only essentially crystalline polymers of known structure can be included as pure materials.

B. SAMPLE PREPARATION.

1. Liquid State

a. For analytical purposes it is desirable that the sample be run in liquid solution, normally at concentrations in the range of 5 to 10% weight (g.) per volume (ml.). Where practicable, the solvent should be carbon tetrachloride (or other solvent of equivalent transparency) in the range 4000 to 1335 cm.$^{-1}$, and carbon disulfide in the approximate range 1350 to 400 cm.$^{-1}$, at path lengths in the range 0.05 to 0.3 mm. Where the measurements extend below 400 cm.$^{-1}$ carbon tetrachloride is the preferred solvent from 450 cm.$^{-1}$ to the lowest recorded wavenumber. Solvent bands should be compensated, but not more than 75% of the energy should be removed from the beam by such compensation, and then only over a very short region. Any solvent bands resulting from incomplete compensation must be clearly indicated on the chart.

b. For documentation purposes it is desirable that the spectrum of the pure liquid be recorded. Solution spectra and pure liquid spectra are to be regarded as complementary and not as substitutes for one another.

2 new

S&S
FILTER PAPER
GRADES
of interest to
every chemist

COUPON BELOW BRINGS
FREE SAMPLES

These two completely new S&S grades were created according to the requirements of a large number of chemists and technicians in the fields of analytical chemistry, as well as chromatography and electrophoresis.

S&S No. 591

For analytical use, request S&S No. 591-A. Pure cotton fibers. Basic paper for general filtration—medium filtration speed. High in quality, but inexpensive. Standard circle sizes and sheets.

For chromatography and electrophoresis, request S&S No. 591-C. Specially selected. Uniform surface. Medium absorption. Suitable for both one and two dimensional chromatography. Standard size sheets, also in strips.

S&S No. 593

For analytical use, request S&S No. 593-A. Pure cotton fibers. Thick paper of medium filtration speed. Increased retention without loss in speed. Standard circle sizes and sheets.

For chromatography and electrophoresis, request S&S No. 593-C. Specially selected. Thick, medium flow rate. Smooth surface. For separation of larger quantities, especially amino acids, peptides, etc. Standard size sheets, also in strips.

FREE DATA & SAMPLES

So that you may quickly become familiar with these new filter papers, we will be pleased to send samples for you to try in your own laboratory, as well as a new folder giving complete data and specifications.

MAIL COUPON BELOW

Carl Schleicher & Schuell Co.
Keene, New Hampshire—Dept. AC68

Without obligation please send samples and free literature on the following:

S&S 591-A ☐ 11 cm circles ☐ 23″ x 23″ sheets
S&S 593-A ☐ 11 cm circles ☐ 23″ x 23″ sheets
S&S 591-C ☐ 23″ x 23″ sheets
S&S 593-C ☐ 23″ x 23″ sheets

Name_____
Company_____
Address_____
City_____ State_____ Zip Code_____

Circle No. 67 on Readers' Service Card

If the heating system you want hasn't been built yet... build it!

It's simple—with Lindberg Hevi-Duty building blocks of heat. These flexible, low-cost elements can be assembled in countless ways.

They're perfect to heat piping systems where liquids must be kept at constant temperature. Or for special lab requirements that don't justify a furnace. Or where there isn't a furnace to do the job.

They have excellent capacity. High watt density. 1000° or 1200° C. Control them manually, or automatically.

They're available from leading lab dealers in sizes, shapes, and lengths to fit your projects.

Write for bulletin 50910, Lindberg Hevi-Duty, Watertown, Wis. 53094.

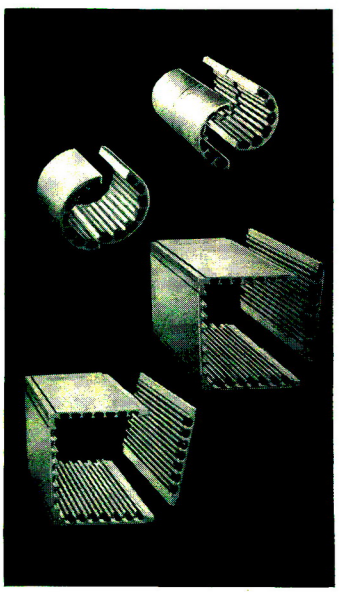

LINDBERG HEVI-DUTY SB

DIVISION OF SOLA BASIC INDUSTRIES

See Buyers' Guide for all products/sales offices.
Circle No. 129 on Readers' Service Card

c. Liquids not soluble in transparent solvents are to be run as capillary films (see Section *II*-C).

2. Solid State

a. Solution spectra in the most transparent solvents are preferred, provided the solvents and path lengths are chosen to leave no significant gaps due to solvent obscuration (see 1-a above).

b. For insoluble compounds, mulls are preferred to pressed pellets, unless it is known that the pellet gives an undistorted spectrum. Solid state spectra must meet the following criteria:

In regions of no absorption band, the I_0 (background) absorbance must be less than 0.20 at 400 cm.$^{-1}$ (transmission greater than 60%) and less than 0.10 at 2000 cm.$^{-1}$ (transmission greater than 80%). No gross abnormalities should be evident in the background. Compensation in the reference beam by a blank pellet or mull must be indicated and in no case should it reduce the reference radiation intensity by more than 50%. The Christiansen effect should not be apparent, but minor distortions resulting from this effect may be permitted at the evaluator's discretion. Interference fringes should not be apparent. Pellets must exhibit no water absorption bands greater than 0.03 absorbance unit. Mulls should be made with perhalogenated oils (or equivalent) for the range 4000 to 1335 cm.$^{-1}$ and the intensity of the overtone band near 2300 cm.$^{-1}$ should not exceed 0.02 absorbance unit. Nujol (or equivalent) should be used below 1335 cm.$^{-1}$, and intensity of the band near 720 cm.$^{-1}$ should not exceed 0.05 absorbance unit.

The above specifications apply to isomorphous solid materials. Spectra of non-isomorphous samples, such as single crystals or crystalline polymers, must also be accompanied by a statement describing the orientation of the sample with respect to the radiation beam.

IV. *Appendix. Spectrophotometer Performance Checks*

A. Wavenumber Calibration. For the range 4000 to 700 cm.$^{-1}$ the wavenumber calibration is checked on a sample of indene containing 0.8% (by weight) of cyclohexanone and 0.8% (by weight) of camphor. This solution, prepared from freshly distilled materials, should be stored in sealed glass ampoules which are freshly opened before use. The spectrum is published in "Tables of Wavenumbers for the Calibration of Infrared Spectrometers," prepared by the Commission on Molecular Structure and Spectroscopy of I.U.P.A.C. (Butterworths, London, 1961, reprinted from *Pure and Applied Chemistry*, Vol. 1, 1961, pp. 679–83. See also Jones, R. N., Nadeau, A., *Spectrochim. Acta* **20,** 1175 (1964).

Below 700 cm.$^{-1}$ a solution prepared from equal parts (by weight) of indene, cyclohexanone and camphor is used. [See Jones, R. N., Faure, P. K., Zaharias, W., *Rev. Universelle Mines* **15, 417** (1959).]

Each set of spectra must be accompanied by a set of indene spectra run significantly close in time to the submitted spectra, and measured at the same slit width, noise level, scanning speed, and recorder time constant. A nominal cell thickness of 0.2 mm. is recommended for the range 4000 to 1580 cm.$^{-1}$ and 0.03 mm. for the range 1600 to 700 cm.$^{-1}$ A cell thickness of 0.1 mm. is recommended for the 1:1:1 mixture below 700 cm.$^{-1}$

Recommended calibration points (cm.$^{-1}$ in vacuum) are the absorption maxima shown in Table I.

These proposals are tentative; other secondary standards calibrated over the entire spectral range may also be accepted, subject to compatability with sections B and C below.

Table I. Absorption Maxima

3927.2	3798.9	3660.6	3297.8	3139.5	2770.9	2598.4
2305.1	2090.2	1915.3	1797.7	1741.9	1713.4	1661.8
1587.5	1361.1	1312.4	1288.0	1226.2	1205.1	1122.4
1067.7	1018.5	914.7	830.5	730.3	693	647.5
551.5	489	381.5				

B. Dynamic Error. The indene spectrum should be rerun from 1250 to 900 cm.$^{-1}$ at one fourth of the scanning rate used for the reference spectra, with other operating conditions unchanged. The heights from the base line of the bands at 1288.0, 1226.2, 1205.1, 1018.5, and 914.7 cm.$^{-1}$ are measured in absorbance units on both the fast and slow scanned charts. The peak height ratios $\nu_{1288.0}/\nu_{1226.2}$, $\nu_{1205.1}/\nu_{1226.2}$, and $\nu_{1018.5}/\nu_{914.7}$ should not differ by more than $\pm$ 0.02 between the slow and fast runs.

C. Spectral Slit-Width. This can be evaluated approximately in the neighborhood of 1200 cm.$^{-1}$ from the ratio $\nu_{1205.1}/\nu_{1226.2}$ computed in the dynamic error test, namely:

$\nu_{1205.1}/\nu_{1226.2}$	Approximate Spectral Slit-Width, cm.$^{-1}$
0.80	4.0–5.0
0.85	3.0–3.5
9.90	2.0–2.5
9.95	1.0–1.5
0.97	<1.0

More exact data should be available later.

D. Scattered Light. The indene spectrum should show total absorption at 3050, 1609.6, and 765.4 cm.$^{-1}$, if measured at the designated thicknesses. A 0.4 mm. layer of indene is totally absorbing at 392, 420, and 551 cm.$^{-1}$.

E. Photometric Accuracy. See Section *I*. E. 3.

F. Check of I_0. Each set of spectra must be accompanied by an I_0 check, obtained by scanning the wavenumber range of the submitted spectra with no cell in either beam at the same slit width, noise level, scanning speed, and recorder time constant. The I_0 trace should be nominally flat, i.e., lie between $\pm$0.01 nominal absorbance units (at the discretion of the evaluator).

G. Cell Blank Check. Each set of solution spectra must be accompanied by a trace obtained at the same slit width, noise level, scanning speed, and recorder time constant, with solvent in both cells. The same cells must be used as in the submitted spectra. No extraneous bands should appear. It is recognized that solvent bands may

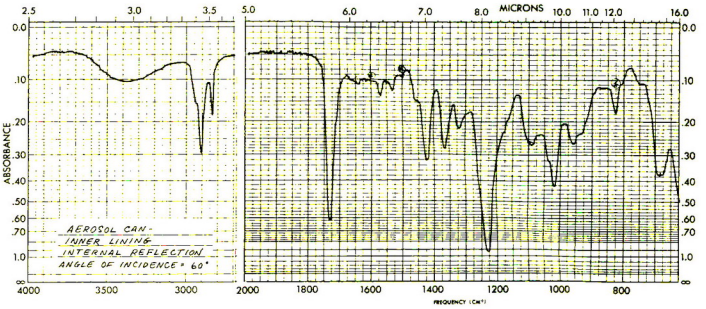

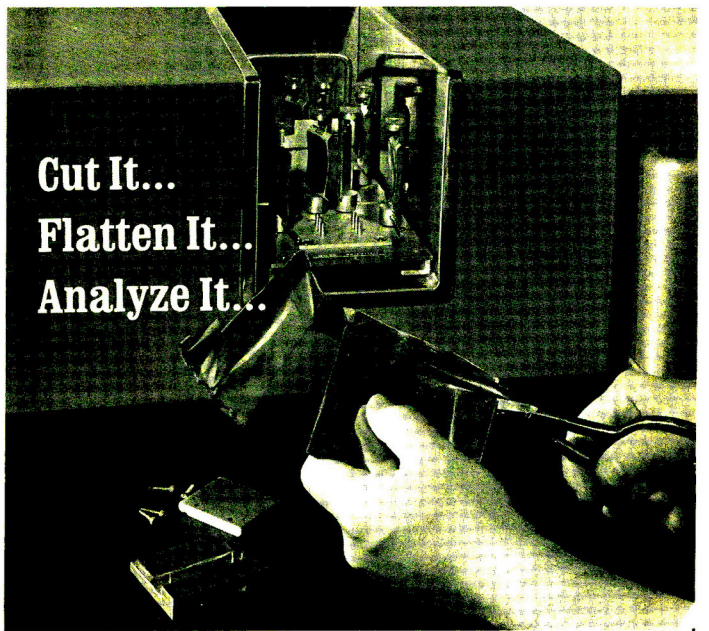

. . . with coatings on metal food containers, for example, it's as simple as that!

But Wilks Scientific internal reflection (ATR) attachments are not limited to coatings on tin cans. Practically any coating you can think of will yield its secrets to the versatile Wilks' MIR Attachments—paper coatings, coatings on fabrics, even surface degradation effects. The two standard models available from Wilks Scientific will fit directly into the sampling area of practically all infrared spectrophotometers, offer three angles of incidence, up to 50 internal reflections, and are surprisingly easy to work with.

Descriptive literature, specifications, and prices for a complete product line of internal reflection accessories available upon request.

"Techniques" . . . a new technical bulletin about internal reflection spectroscopy, published bi-monthly by Wilks Scientific — available upon request, too.

WILKS SCIENTIFIC CORPORATION
SOUTH NORWALK • CONNECTICUT 06854
TELEPHONE • (203) 838-4537

Circle No. 163 on Readers' Service Card

MAGNA
CHEMICALS ■ INSTRUMENTS ■ SERVICE

Only The ANOTROL™ Potentiostat Gives You:

HIGH CURRENT CAPACITY—10 amps anodic, 5 amps cathodic at 10 volts. (An auxiliary power supply boosts anodic and cathodic current to 25 amps at 20 volts, 10 amps at 50 volts.)

FAST RISE TIME—For typical potential step changes, output of the 4700 reaches 90% of new potential value in approximately one microsecond.

STABILITY—The 4700 Research Potentiostat maintains a potential of ± 0.5 millivolt per 24 hours throughout 0 to ± 6 volt range.

DUAL CHANNEL POTENTIAL CONTROL—Allows selective scanning from one potential to another with Model 4510 Linear Scan Unit. The Model 4700 Potentiostat can also be switched instantaneously from one potential value to another. The Linear Scan Unit can also be used with the 4100 Potentiostat.

TM-Trademark of Continental Oil Company

MAGNA CORPORATION
11808 S. Bloomfield Ave.,
Santa Fe Springs, Cal. 90670
Telephone: (213) 863-4781

MAGNA

AC8

Please send information on:

☐ MODEL 4700 RESEARCH POTENTIOSTAT
☐ MODEL 4510 LINEAR SCAN UNIT

Name_____
Title_____
Company_____
Telephone_____
Address_____
City_____ State_____
A Subsidiary of TRW Zip Code_____

Circle No. 165 on Readers' Service Card

not be completely compensated in the cell blank spectrum.

H. Energy Check. See Section *I*-D.

Class III Spectra

I. *Spectrometer Operation.*

A. Resolution. The make and model of the spectrometer must be reported on the published chart, and the dispersing element must be identified (e.g., NaCl prism; grating). The resolution should be consistent with the operating specifications for the spectrometer. The minimum acceptable performance is that obtainable from a sodium chloride prism spectrometer in good operating condition.

B. Wavenumber Accuracy. Charts showing evidence of wavenumber calibration error in excess of ± 30 $cm.^{-1}$ at 3000 $cm.^{-1}$ or ± 5 $cm.^{-1}$ below 2000 $cm.^{-1}$ will be rejected. For spectra recorded on a linear wavelength scale the permitted tolerance is ± 0.04 micron in all ranges.

C. Noise Level. Charts exhibiting more than 2% average peak-to-peak noise should be rejected.

D. Energy. It is recommended that the spectrometer be purged with dry air to ensure that at least 50% of the source energy is available throughout the spectrum (except at the 2350 $cm.^{-1}$ CO_2 absorption).

E. Other Performance Criteria.

1. Charts exhibiting evidence of more than 5% stray radiation in any region of the spectrum, or excursions of any absorption band beyond the nominal zero transmission region are not acceptable.

2. Charts exhibiting evidence of a dead servo-system or of excessive overshoot will be rejected.

II. *Presentation.*

A. Information to Appear on the Chart. Both the structural and the molecular formulas of the compound must appear on the chart. It is also recommended that the compound name be included, and preferably this should conform with the nomenclature used by *Chemical Abstracts*. The make and model of the spectrophotometer must be recorded as well as the date on which the spectrum was obtained.

The physical condition of the sample must be stated (e.g., Nujol mull, solution, pure liquid, etc.). For measurements on solutions the solvent used in each region of the spectrum must be recorded on the published chart. The path length and concentration should also be given, but spectra lacking this information may be accepted at the discretion of the evaluator. The path length of pure liquid samples and concentrations in pelleted disk spectra should be given if possible.

B. Spectral Range. The chart must cover 3700 to 700 $cm.^{-1}$. Gaps caused by solvent interference or by obscuration from mulling agents may be permitted at the discretion of the evaluator, but must be designated as such on the published chart.

C. Intensity. It is anticipated that many spectra will be recorded on a linear transmittance ordinate grid, but spectra recorded on paper having a logarithmic ordinate grid are preferable, since this permits the direct interpolation of absorbance intervals.

The absorption bands must be strong enough to be useful in characterizing the material. Spectra are generally unacceptable if they show:

1. No bands more intense than 0.6 absorbance unit
2. Many bands exhibiting total absorption
3. An average I_0 less than 60 to 75% T.

D. Wavenumber Readability. Band peak positions must be readable on the published chart to ± 15 $cm.^{-1}$ at 3000 $cm.^{-1}$ and ± 2.5 $cm.^{-1}$ below 2000 $cm.^{-1}$. Spectra recorded on a linear wavelength scale in microns are acceptable, but in selecting among alternative spectra for a given compound preference should be given to the linear wavenumber presentation unless there are strong reasons to decide otherwise. The peak positions for linear wavelength charts must be readable to 0.02 micron.

E. Recording. It is preferred that the spectrum exhibit no gaps in wavenumber (evaluator's discretion).

Hand retraced spectra are undesirable, but if they are so designated

There are a lot of pH meters for sale...

but only the Zeromatic® II keeps on selling you after you buy it

The Zeromatic II is more than just the pH meter with the large, 8.2-inch, easy-to-read scale—the convenient push-button controls—the high accuracy (±0.05 pH) and repeatability (±0.015 pH)—the rugged, chemical-resistant case.

When you buy a Zeromatic II pH Meter—or for that matter, any Beckman pH meter—you buy: Sales Engineers to assist you on instrument operation and the selection of accessories and electrodes... Application Engineers to advise you on difficult or unusual applications... Service Engineers to provide you with periodic maintenance or on-the-spot repair... plus, 30 years of experience behind every Beckman pH meter.

Why not call your local Beckman Sales Office and ask for a demonstration of the Zeromatic II? Or request Data File LpH-466.

The Zeromatic II offers more—because it *is* more instrument—with more to back it up. Let it sell you.

Beckman® INSTRUMENTS, INC.
SCIENTIFIC AND PROCESS INSTRUMENTS DIVISION
FULLERTON, CALIFORNIA • 92634

INTERNATIONAL SUBSIDIARIES: GENEVA; MUNICH; GLENROTHES, SCOTLAND; TOKYO; PARIS; CAPETOWN; LONDON; MEXICO CITY

Circle No. 158 on Readers' Service Card

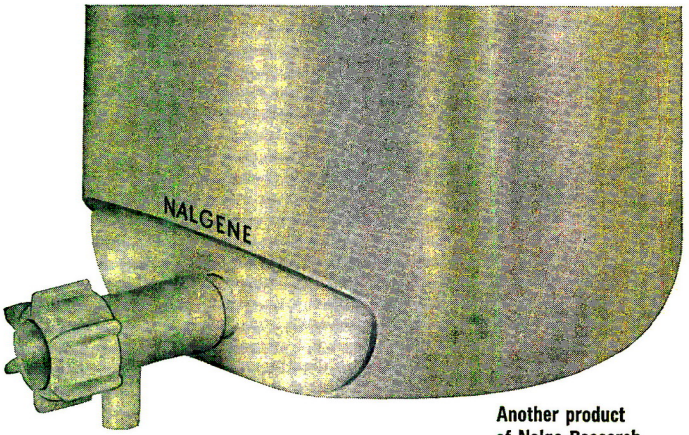

Another product
of Nalge Research

A NEW CONCEPT IN CARBOY DESIGN

It's the new Nalgene® Aspirator Carboy with Spigot! This unique, new design incorporates the threaded boss as an integral part of the carboy. Greater strength is assured... possibility of leakage is eliminated! This sophisticated new blow molding technique is a result of Nalge's advanced molding skills. The Nalgene Aspirator Carboy provides the safest and most efficient tool for handling, storing and dispensing corrosive liquids, as well as distilled water.

Available in 1, 2, 5, 6½ and 13 gallon sizes. Recessed handgrips or shoulder-mounted carrying handles on three largest sizes. Assortable with other Nalgene Labware for maximum discounts. Order from your lab supply dealer or write for our new 1966 Nalgene Labware Catalog. Department 1132, The Nalge Co., Inc., Rochester, New York 14602.

NALGENE LABWARE
Leader in quality plastic labware since 1949

Circle No. 1 on Readers' Service Card

on the published chart, they may be accepted at the discretion of the evaluator.

F. Atmospheric Absorption. Bands resulting from atmospheric absorption should ordinarily be no greater than 2% T. (Discretion of the evaluator.)

III. *Sample Identification.*

A. Compound Identity and Purity.

1. Identity. Spectra should not show any obvious inconsistencies with the postulated structure, but the consistence is not, by itself, acceptable as proof of the correctness of the postulated structure.

Purchase of a material from a reputable chemical supply house, or preparation according to an accepted procedure, are not, in themselves, acceptable as proof of structure. Additional physical and chemical evidence, sufficient to satisfy an expert in the field should be supplied to the evaluator. Preferably this evidence should come from measurements on the same batch as was used for the infrared spectrum. The names and addresses of laboratories contributing spectra will normally appear on the published charts, and also literature references to the preparation of the compound, where such are available. Spectra may be published without the name and address of the supply laboratory, but such charts will be prominently labelled "Chemical Structure Not Authenticated."

The infrared spectrum itself may be acceptable as supporting proof of structure when it is in substantial agreement with the spectrum of another sample from an independent source.

2. Purity. The purity of the samples should be such that only bands of minor intensity due to impurities are present and these bands should all be identified on the published chart. (The permitted intensity of the impurity band is at the discretion of the evaluator but should not normally exceed 10% of the absorbance of the major band of established structural significance.) Not more than three impurity bands should appear. Allowance will be made for compounds that are readily hydrolyzed,

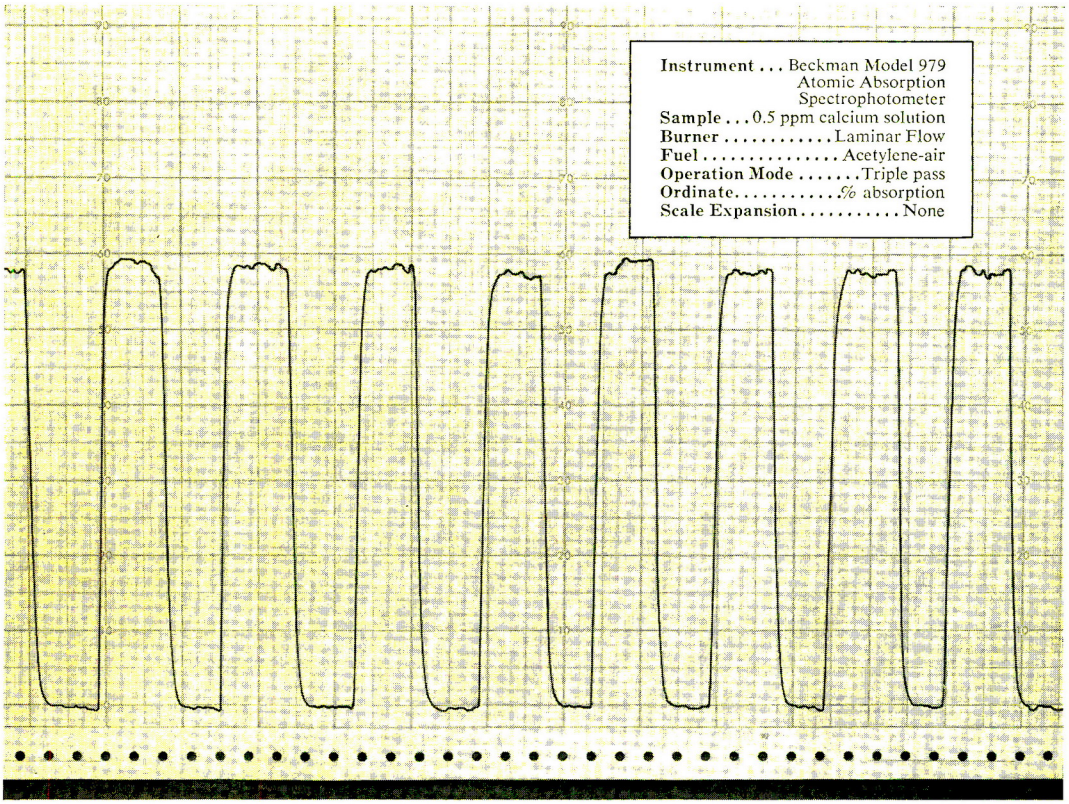

This atomic absorption analysis is 16 times better than you've seen before

This record-setting, highly reproducible curve represents a percentual concentration limit of 6 parts per billion calcium. It was run on an unaltered stock Atomic Absorption Spectrophotometer – Beckman's Model 979. And, it's merely typical –with other elements, measurements as low as one part per billion are frequently achieved. The unmatched performance of this instrument stems primarily from (1) a Laminar Flow Burner* that delivers 5 to 20 times greater analysis-sensitivity than any other burner. It eliminates the solvent, concentrates the sample *before* it reaches the extremely stable flame. Only solid sample is burned. No solvent dilutes it or cools the flame. (2) Multi-Path Optics that permit passing the beam through the flame 3 times, in many cases increasing the sensitivity two to threefold.

Model 979 is also operational in seconds for flame emission photometry and a gamut of spectrophotometric studies – a versatility unmatched among grating-type instruments.

You get this step-ahead versatility and performance for less than $6,600 including the Laminar Flow Burner and Linear Log 5" Recorder – about the same cost as most single-purpose AA instruments. For additional information, write for Data File LUV-566-SP.

Circle No. 159 on Readers' Service Card

*Patent pending

Price is stated in U. S. funds and is subject to change without notice.

Beckman® INSTRUMENTS, INC.
SCIENTIFIC AND PROCESS INSTRUMENTS DIVISION
FULLERTON, CALIFORNIA • 92634

INTERNATIONAL SUBSIDIARIES: GENEVA; MUNICH; GLENROTHES, SCOTLAND; TOKYO; PARIS; CAPETOWN; LONDON; MEXICO CITY

It'll never be a best seller because it's free from Fisher Scientific. A concise, thorough description and bibliographical guide to FLORISIL®— a highly selective adsorbent for chromatography.

You will discover many uses for Florisil in preparative and analytical chromatography. Among its principal applications are: detection and isolation of pesticide residues; isolation and separation of steroids; purification of pharmaceuticals. Florisil is an extremely white, hard granular or powdered magnesia-silica gel. This free Florisil booklet, supplied by Fisher Scientific, will suggest other applications that can fulfill your particular needs. **To get your Florisil booklet,** please write Fisher Scientific Company, 100 Fisher Building, Pittsburgh, Pa. 15219. J-547

FISHER SCIENTIFIC CO.

Instruments, Apparatus, Furniture and Chemicals for Laboratories

Complete stocks in all these locations: Atlanta • Boston • Chicago • Cleveland • Houston • New York Philadelphia • Pittsburgh • St. Louis • Union, N. J. • Washington • Edmonton • Montreal • Toronto • Vancouver

"See Laboratory Guide for all Products/Sales Offices"

Circle No. 31 on Readers' Service Card

oxidized, or isomerized. It should be noted that the presence of correctly identified impurity bands in the spectra of unstable materials is not necessarily a detriment, since one of the uses of the published spectra is for the detection and identification of such common impurities. It may be helpful to supply the evaluator with copies of spectra containing higher amounts of the designated impurities, where these are available, but such spectra should not be published. No spectrum containing known impurity bands should be published where acceptable curves of samples of higher purity are available. Cases may arise where it is desirable to publish spectra that fail to meet these criteria for proof of structure. If this is done the published chart must be prominently marked "Chemical Structure Not Authenticated (see also Section *III*-A).

B. Sample Preparation.

1. Liquid State

a. Solution spectra should satisfy the requirement that the solvents and path lengths in different regions of the spectrum are selected to leave no significant gaps due to solvent obscuration (note also Section *II*-C).

b. Thin layers of the pure liquids are acceptable.

2. Solid State

a. Solution spectra in the most transparent solvents are preferred provided the solvents and path lengths leave no significant gaps due to solvent obscuration.

b. For insoluble compounds mulls are preferred to pellets, unless it is known that the pellet gives an undistorted spectrum. Such solid state spectra must meet the following criteria:

There must be at least 25% nominal transmission at 3700 $cm.^{-1}$ and at least 40% nominal transmission at 2000 $cm.^{-1}$ in the absence of specific compound absorption. There must be no gross abnormalities or discontinuities. Spectra should not exhibit appreciable pseudo-structure attributable to interference fringes, and any such fringe patterns should be identified on the published chart. The Christiansen effect should not be great enough to distort the band contours signifi-

The shortest time between 2 points is a curve!

We can prove it with the DK®-2A Automatic Recording Spectrophotometer.

By scanning the entire wavelength range automatically, you save up to 95% of the time required in plotting a qualitative curve. And this recording spectrophotometer also: Performs quantitative, conjugation, purity and kinetic studies in both research and quality control. Assures correct wavelength selection, because the entire range is recorded. Readily detects interfering substances and impurities. Simplifies identification and qualitative analyses. And provides a permanent record of every analysis.

No manual spectrophotometer does all that. *All* makes of automatics *do*. But *only* Beckman's DK-2A Recording Spectrophotometer offers these added advantages: A 185 $m\mu$-3500$m\mu$ wavelength range. A flatbed XY recorder for viewing the entire record at all times. The lowest price in its class (as low as $8,990). A flat 100% line without need for adjustment. Immediate delivery from your local Beckman Sales Office—member of the most extensive sales and service network in the industry. And you can extend its usefulness with precision-matched reflectance, flame and fluorescence accessories.

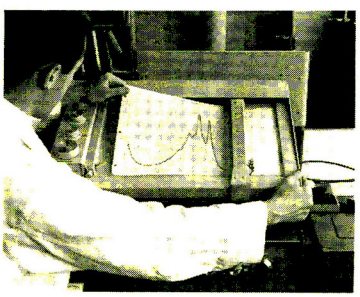

Efficiency is more than its own reward when you operate the high-performance, lowest-priced, double beam DK-2A—case histories show its payout time often is 6 months or less. After that, it's like getting an annual budget increase—automatically. For more information, contact your Beckman Sales Representative, or write for Data File LUV 167-2.

Beckman® INSTRUMENTS, INC.

SCIENTIFIC AND PROCESS INSTRUMENTS DIVISION

FULLERTON, CALIFORNIA • 92634

INTERNATIONAL SUBSIDIARIES: GENEVA; MUNICH; GLENROTHES, SCOTLAND; TOKYO; PARIS; CAPETOWN; LONDON; MEXICO CITY

Price is stated in U.S. funds and is subject to change without notice.

Dependability Uniformity Availability

3 reasons why the support for gas/liquid chromatography for over 10 years has been:

Chromosorb*

J-M Celite Division

Why settle for less? From the very beginnings of gas/liquid chromatography, Johns-Manville Chromosorb products have set the pace for performance, and have established product standards for chromatographers. Over ten years of a world-wide reputation for proven dependability, uniformity and availability are behind Chromosorb.

Dependability—Every order tested and inspected in the J-M chromatographic laboratory to assure positive results.

Uniformity—Bottle to bottle, package to package, order to order, you get quality assurance and reproducible results.

Availability—Around the world, from leading equipment manufacturers, laboratory supply houses, and their overseas subsidiaries.

The Johns-Manville laboratory devoted to chromatography combines basic and applied research with product development. In this way we continue to generate new and improved products to make *your* results optimum every time.

Chromosorb is available in the following grades:

P, W, G } Acid washed, non-acid washed, and HMDS or DMCS treated.

T

A

High Performance G&W, acid washed DMCS treated.

"Prep Scale" P&W.

Wide selection of mesh ranges.

Literature available. To be put on our special mailing list of chromatographers to receive technical data on gas/liquid chromatography and new product information, write Johns-Manville, Box 325, New York, N. Y. 10016. Or cable Johnmanvil. J-M Chromosorb also available in Canada.

JM

Johns-Manville

*Chromosorb is a Johns-Manville registered trademark for its brand of products developed for use as support material or absorbents for gas chromatography.

Circle No. 43 on Readers' Service Card

cantly. In spectra of alkali halide pellets, the water absorption bands must not exceed 0.1 absorbance unit.

3. Gas and Vapor State

The pressure of the absorbing gas should be selected so as to display the significant features in the spectrum, while showing a minimum number of bands so strong that structure is lost (note also Section *II*-C). Very intense absorptions should be rescanned at lower pressure, but the number of additional tracings should be kept to a minimum. It is desirable that the pressure of the absorbing gas be stated; and if an inert diluent gas is used, it should be identified and the total pressure given also. The path length of the cell should be preferably 5 to 10 cm., and should be stated.

Users of gas and vapor spectra must recognize that such spectra are strictly qualitative, since the intensity of an absorption may depend strongly on the total pressure as well as on the partial pressure of the absorbing species. (Intensities may change by a factor of 5 or more upon pressurizing a gas from zero to one atmosphere with an inert diluent.) Furthermore, the intensities of different bands do not respond equally to pressurization.

On the other hand, the exact frequency of sharp spikes is likely to be important for qualitative analysis. Thus, it is especially important for gas and vapor spectra that wavenumber calibration accuracy be established and maintained.

This Report was prepared by the members of the Coblentz Society Board of Managers: *N. Fuson,* Fisk University; *R. N. Jones,* National Research Council, Canada; *H. B. Kessler,* The Perkin-Elmer Corp.; *L. E. Kuentzel,* Wyandotte Chemical Co.; *R. S. McDonald,* General Electric Research and Development Center; *F. S. Mortimer,* Shell Development Co.; *J. Overend,* University of Minnesota; *W. J. Potts, Jr.,* Dow Chemical Co.; *A. Lee Smith,* Dow Corning Corp.; *Clara D. Smith,* Cranbury, N. J.; and *J. E. Stewart,* Beckman Instruments Co.

Show-Stoppers!

The new Beckman CPM-100™ and DPM-100™ Liquid Scintillation Systems literally stopped the show at a recent scientific meeting. And for good reason. These new systems electronically compute data and provide readout in CPM, DPM, or quench-corrected DPM with 2 sigma % error. And of equal significance, they now make it possible to achieve uncompromised performance and data quality from a room-temperature system with 100-sample capacity.

These three-channel systems attain an E^2/B of better than 100 with no refrigeration. The degree of quenching is accurately determined by external-ratio standardization, and the entire system is easily calibrated with the adjustment of only one control. They also feature a Command Tower Programmer™ which allows the personal selection of samples and channels of interest. The CPM-100 and DPM-100 Spectrometers represent a major advancement in the field of liquid scintillation analysis. Yet, the CPM-100 is priced at $7,995.00† and the DPM-100 is only $8,995.00†.

For more information on these advanced liquid scintillation counters, contact your Beckman Sales Representative today about a demonstration, or write for Data File LLS-266-Sp.

†Prices are stated in U.S. funds and are subject to change without notice.

Beckman® INSTRUMENTS, INC.
SCIENTIFIC AND PROCESS INSTRUMENTS DIVISION
FULLERTON, CALIFORNIA • 92634

INTERNATIONAL SUBSIDIARIES: GENEVA; MUNICH; GLENROTHES, SCOTLAND; TOKYO; PARIS; CAPETOWN; LONDON; MEXICO CITY

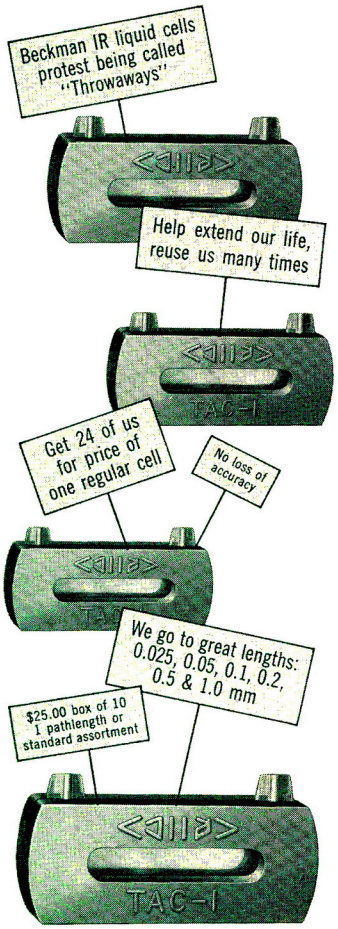

Let us demonstrate all the advantages and abilities of our so-called "Throwaways": These AgCl cells are usable for aqueous and most non-aqueous samples in IR analysis up to 22 micron wavelength. Wider selection of pathlengths for less money. Reusable *many* times. And if cells get too dirty to clean easily, you can afford to throw them away at only $2.50 a throw. (Special holders adapt them to all IR spectrophotometers.) Write for Data File LIR-466-14* on cells and accessories — the finest, most complete line in the field.

**Includes products manufactured by the Research and Industrial Instrument Company of London, England; formerly marketed by the Limit Research Corporation. Both RIIC and Limit are now a part of Beckman Instruments, Inc.*

Price is stated in U. S. funds and is subject to change without notice.

Beckman INSTRUMENTS, INC.
SCIENTIFIC AND PROCESS INSTRUMENTS DIVISION
FULLERTON, CALIFORNIA • 92634

INTERNATIONAL SUBSIDIARIES: GENEVA; MUNICH; GLENROTHES, SCOTLAND; TOKYO; PARIS; CAPETOWN; LONDON; MEXICO CITY

Circle No. 162 on Readers' Service Card

We're being two-faced about our graduates

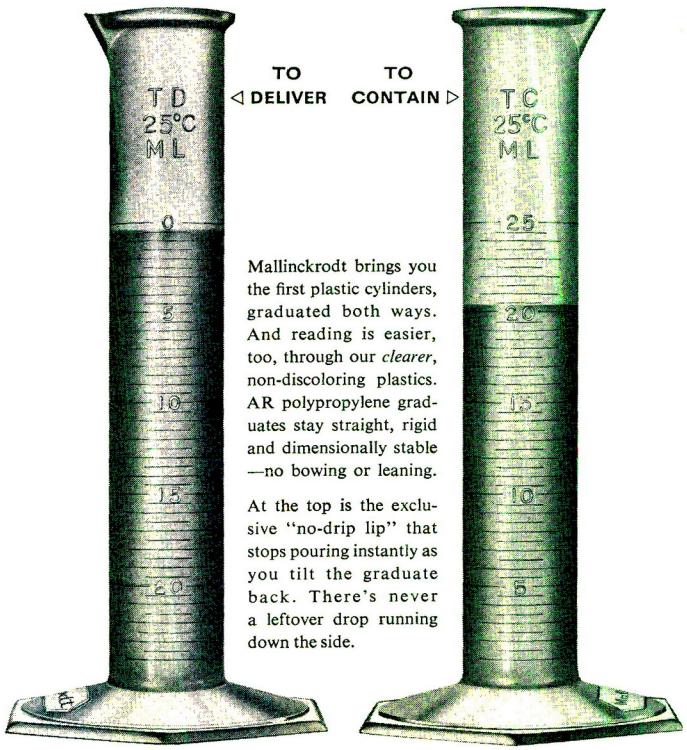

Mallinckrodt brings you the first plastic cylinders, graduated both ways. And reading is easier, too, through our *clearer*, non-discoloring plastics. AR polypropylene graduates stay straight, rigid and dimensionally stable —no bowing or leaning.

At the top is the exclusive "no-drip lip" that stops pouring instantly as you tilt the graduate back. There's never a leftover drop running down the side.

Down here at the bottom, there's a base that's more than twice as big as you'll find on most other graduates. That makes AR graduates more stable; and, if you drop an AR graduate, you pick it up with your hand—not with a broom.

Another new idea in labware from the people who think past the product. Stocked in several sizes for immediate shipment by your lab supplier.

Capacity tolerance conforms to Class A specifications given in NBS Circular 602

Mallinckrodt® AR® Plastics

MALLINCKRODT CHEMICAL WORKS
St. Louis • New York • Los Angeles

Circle No. 157 on Readers' Service Card

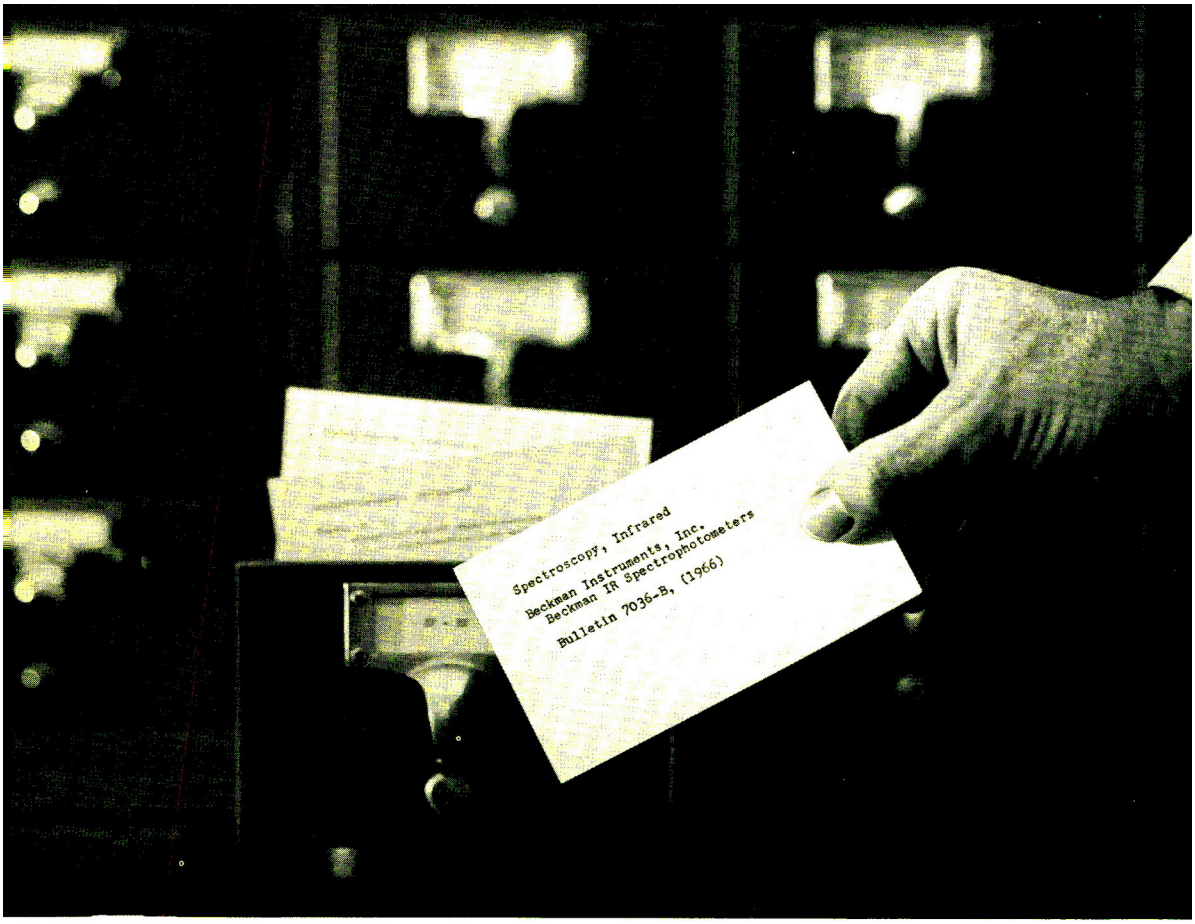

Another prime reference for the spectroscopy laboratory

It's new Bulletin 7036-B...40 pages that cover the subject of infrared instrumentation...including absorption spectra, optical diagrams, and specifications for 11 of the finest infrared spectrophotometers available.

The spectrophotometers described cover every possible application in the infrared field from 0.27 to 300+ μ. Whatever research or quality control application you have—whatever caliber of performance you require—whatever your budget—there is a Beckman spectrophotometer for your laboratory.

Also in Bulletin 7036-B you'll find ...the addresses of over 40 local offices and 4 regional application engineering labs...a list of reference literature available without charge... as well as a description of accessories to broaden the versatility of your infrared instrument.

For your copy of Bulletin 7036-B, write for Data File LIR-666-11. You will find that when it comes to infrared instrumentation, it thoroughly covers the subject.

Beckman® INSTRUMENTS, INC.
SCIENTIFIC AND PROCESS INSTRUMENTS DIVISION
FULLERTON, CALIFORNIA • 92634

INTERNATIONAL SUBSIDIARIES: GENEVA; MUNICH; GLENROTHES, SCOTLAND; TOKYO; PARIS; CAPETOWN; LONDON; MEXICO CITY

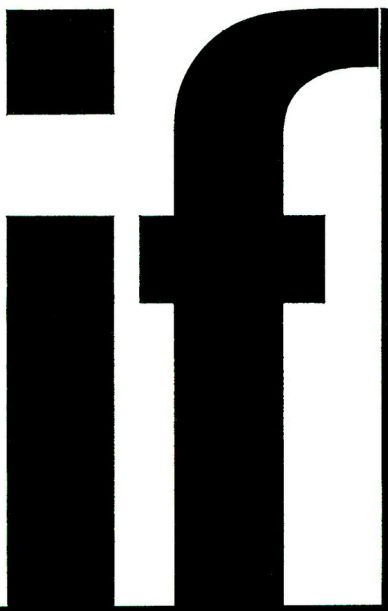

YOU WANT

to add another mode to your counting system...

to increase your counting capacity...

to automate your manual counting system...

you can save up to 35% with Tracerlab System Modules

That's right. In nuclear counting systems, the Tracerlab Systems Module Concept can give you exceptional flexibility and versatility by making the most of your present equipment.

Tracerlab System Modules enable you to buy just one additional instrument for major gains in capability — instead of starting all over again.

Result: You can switch from one type of analysis to another, from single to multiple counting modes, from manual to fully automatic operation — simply by buying an additional unit each time.

Or buy one type of system and add on any type of sample changer at a future date — and you get total system versatility at lowest cost.

All Tracerlab nuclear counting System Modules are based on the Systems Module Concept, and are fully compatible with each other as well as other makes of instruments now in use.

So: Take one instrument, add another, plug them together — and you've got a system. Add another instrument—and you've got still another system.

Call your Tracerlab sales representatives for a complete preview on all the permutations possible (8758 so far!) with Tracerlab System Modules. He'll help you pick the one you need — and soon you'll be counting your money as well as your samples!

LFE | TRACERLAB

A Division of Laboratory For Electronics, Inc.
WALTHAM, MASSACHUSETTS 02154

Richmond, California • Malines, Belgium • Sales Offices in Principal Cities

Film Badge Service • Health Physics • Bioassays • Sources • Nuclear Instrumentation • Radiochemicals
Radioactive Waste Disposal • Radiation Monitoring Instrumentation • Isotope Applications

Circle No. 3 on Readers' Service Card

when you want

- Fully Modularized Liquid Scintillation Counting
- Fully or semi-automatic operation
- To choose from 25 or 100 sample capacity modules
- To operate with your existing electronics
- To operate at room or controlled temperatures
- Better than 80% efficiency for C-14
- Better than 45% efficiency for H-3
- Latest technology with dual phototubes
- Pulse summation for improved isotope separation
- Selectable coincident resolving times
- External standardization for quench determination
- High performance and budget savings

Freedom to adapt to your changing needs:

- Simply add our 25 or 100 sample module to your present nuclear equipment or
- Specify a complete system for single or dual labelled compounds
- Expand your nuclear lab to include scintillation well and planchet counting

Call your Tracerlab Instrument Representative

LFE | TRACERLAB
A Division of Laboratory For Electronics, Inc.
WALTHAM, MASSACHUSETTS 02154

Richmond, California • Malines, Belgium • Sales Offices in Principal Cities

Circle No. 4 on Readers' Service Card

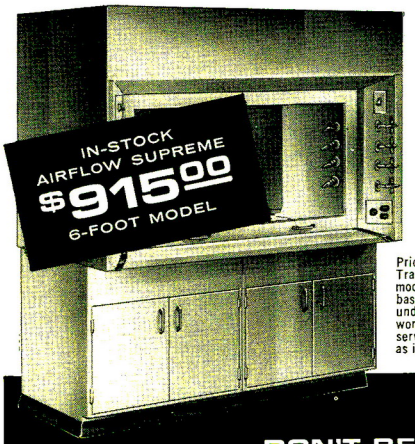

Price is for Transite lined model and includes base cabinet understructure, work top and service fixtures as illustrated.

DON'T BE
"HOOD WINKED"
YOU CAN GET THE FINEST
FUME HOODS
FOR THESE LOW PRICES!

Price includes base cabinet understructure, work top and service fixtures as illustrated.

All types and sizes of quality Kewaunee Laboratory Fume Hoods are readily available from stock at surprisingly low prices. Both the Airflow Supreme and Improved Conventional Fume Hoods are available from stock in 4-ft., 5-ft. and 6-ft. lengths. Improved Conventional Fume Hoods are available with a fire-resistant Transite lining, but Airflow Supreme Fume Hoods are available with both Transite and stainless steel linings. Airflow Supreme Perchloric Acid Fume Hoods (with Type 316 stainless steel lining and work surface) are also available from stock.

Send for Complete Information:

KEMMETAL
KEWAUNEE MFG. CO., ADRIAN, MICHIGAN
5090 S. Center St.

Circle No. 142 on Readers' Service Card

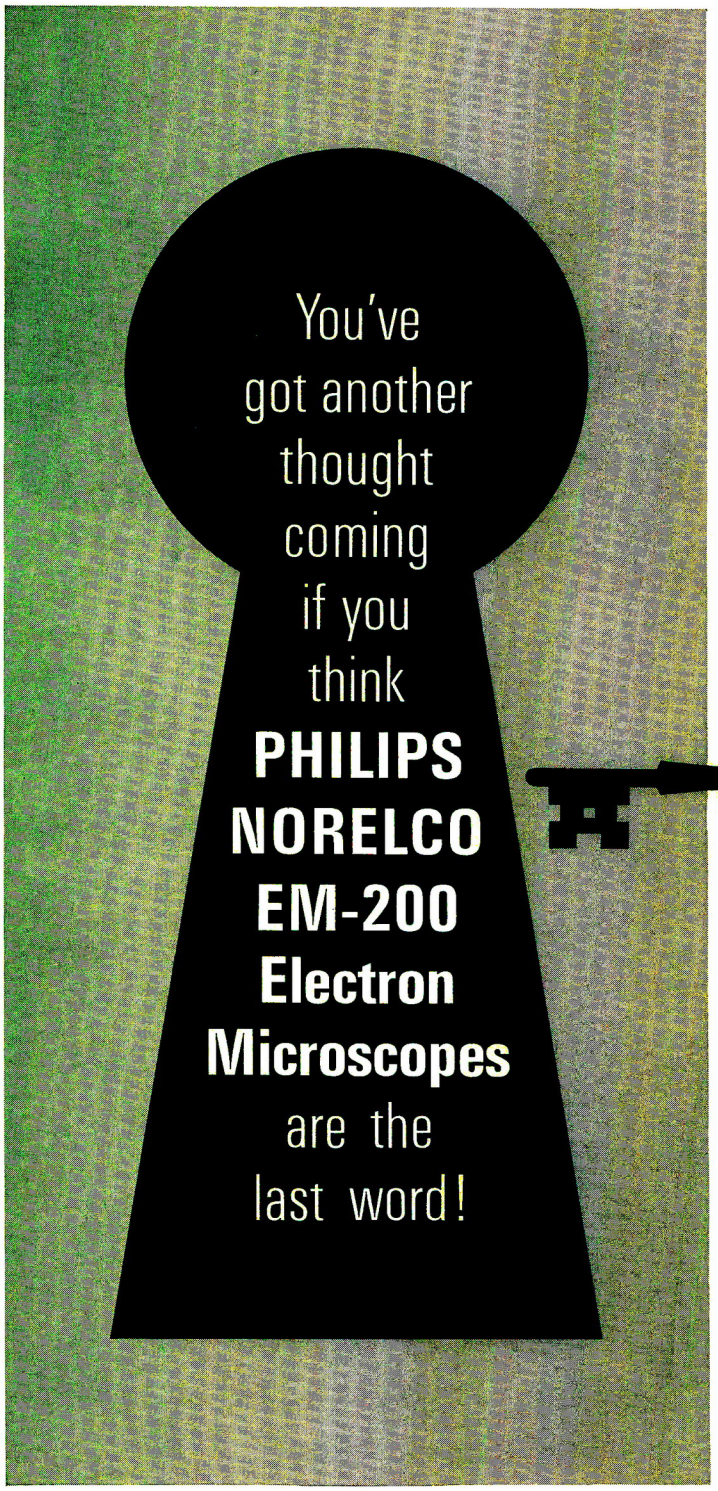

Listen and watch
for the
latest news
from the
**Sixth
International Congress
for Electron Microscopy**
Kyoto, Japan

World's Highest Standards in Quality Instrumentation

Norelco® PHILIPS ELECTRONIC INSTRUMENTS

Division of Philips Electronics and Pharmaceutical Industries Corp.
750 South Fulton Avenue, Mount Vernon, New York 10550

"See Laboratory Guide for all Products/Sales Offices"
Circle No. 55 on Readers' Service Card

ANALYTICAL CHEMISTRY NEWS

152nd National ACS Meeting, New York City

THE PROGRAM of the 152nd National ACS Meeting to be held in New York City, September 11 to 16, is the largest ever. General and preliminary information on the meeting are given in *Chem. Eng. News*, June 27, pp. 70 to 81.

Headquarters for the Analytical Division sessions is the Waldorf Astoria Hotel. The chemical exposition with more than 140 exhibits will be held at the New York Hilton, Second Floor. A symposium sponsored by the Division of Fuel Chemistry on "Current Analytical Methods for Fuels" will be held Monday morning at the Warwick Hotel. The Analytical Division has planned the following special symposia in addition to general sessions: Inorganic Ion Exchange Separations, Instrumental Techniques as Aids in the Determination of Structure of Complex Ions, Trends in Pharmaceutical Analysis, N. Howell Furman Memorial Symposium, Spark Source Mass Spectrometry, and Teaching of Analytical Chemistry (joint with the Division of Chemical Education). The latter symposium will be held at the Park-Sheraton Hotel.

The Monday afternoon symposium on Inorganic Ion Exchange Separations will feature presentation of the ACS Award in Chromatography and Electrophoresis, sponsored by Labline, Inc., to Kurt A. Kraus of the Oak Ridge National Laboratory. His Award Address is entitled "Ion Exchange as a Tool in Inorganic and Analytical Chemistry."

The Analytical Division dinner will be held at 7:00 Thursday evening and will be highlighted by an illustrated talk by Z. Lewin of New York University on "Analytical Chemistry in Art and Archeology."

The detailed program of the Analytical Division sessions and the special symposium of the Division of Fuel Chemistry are given below.

ANALYTICAL DIVISION PROGRAM

W. D. Cooke, Chairman — C. V. Banks, Secretary

Monday Morning, Sept. 12

INORGANIC ION EXCHANGE SEPARATIONS

F. Nelson, Presiding

9:10 Ion Exchange Resins–Versatile Separation Tools. R. E. Anderson, Physical Research Laboratory, Dow Chemical Co., Midland, Mich. 48640

9:40 Comparative Chromatography of the Chloroplast Pigments. H. H. Strain, Chemistry Division, Argonne National Laboratory, Argonne, Ill. 60439

10:15 Separation of Niobium, Tantalum, Molybdenum, and Tungsten by Reversed-Phase Chromatography. J. S. Fritz, L. H. Dahmer, Department of Chemistry, Iowa State University, Ames, Iowa 50010

10:45 Cation Exchange in Concentrated Mineral Acids and Mineral Acid Mixtures; Group Separations of Elements. Frederick Nelson, Oak Ridge National Laboratory, P. O. Box X, Oak Ridge, Tenn. 37831

11:15 Reversed-Phase Partition Chromatography in Inorganic Chemistry. A Survey on Results Obtained at CISE. Enrico Cerrai, c/o CISE, Casella Postale 3986, Milano, Italy

DIVISION OF FUEL CHEMISTRY

J. D. Clendenin, Chairman — Frank Rusinko, Jr., Secretary-Treasurer

Monday Morning, Sept. 12

SYMPOSIUM ON CURRENT ANALYTICAL METHODS FOR FUELS

Edward A. Zawadzki, Presiding

9:10 Inorganic and Organic Analysis by Infrared Spectrometry in Coal Problems. R. A. Friedel, J. A. Queiser, Bureau of Mines, 4800 Forbes Ave., Pittsburgh, Pa. 15213

9:35 Measurement of the Surface Areas of Coals from the Dynamic Sorption of Carbon Dioxide. Josephus Thomas, Jr., G. S. Benson, Illinois State Geological Survey, 221 Natural Resources Bldg., Urbana, Ill., G. M. Hieftje, Department of Chemistry, University of Illinois, Urbana, Ill.

10:00 Gas Chromatographic Separations of Benzene Carboxylic Acids Derived from Coal. M. L. Kaufman, Sidney Friedman, Irving Wender, Pittsburgh Coal Research Center, U. S. Bureau of Mines, 4800 Forbes Ave., Pittsburgh, Pa. 15213

10:25 Quantitative Ultraviolet Analysis of C_{10}–C_{15} Naphthalenes in Hydrocarbon Oils. Patricia A. Estep, Edward E. Childers, John J. Kovach, Clarence Karr, Jr., Bureau of Mines, U. S. Dept. of Interior, P. O. Box 880, Morgantown, W. Va.

10:50 Analysis of Sulfur in Coals by X-Ray Fluorescence. Martin Berman, Sabri Ergun, Solid State Physics Group, Pittsburgh Coal Research Center, U. S. Bureau of Mines, 4800 Forbes Ave., Pittsburgh, Pa. 15213

11:15 A Micromethod for Total Sulfur Determination in Nonleaded Light Hydrocarbon Feedstocks. A. Attari, Institute of Gas Technology, 3424 South State St., Chicago, Ill. 60616

ANALYTICAL DIVISION PROGRAM (CONT.)

Monday Afternoon

INORGANIC ION EXCHANGE SEPARATIONS

F. Nelson, Presiding

2:00 Introduction of K. A. Kraus, G. Scatchard

2:10 Ion Exchange as a Tool in Inorganic and Analytical Chemistry. (Award Address—ACS Award in Chromatography and Electrophoresis for 1966, sponsored by Labline, Inc.). K. A. Kraus, Oak Ridge National Laboratory, P. O. Box X, Oak Ridge, Tenn. 37831

3:00 Analytical Applications of Liquid Ion Exchangers. J. C. White, Analytical Chemistry Division, Oak Ridge National Laboratory, Oak Ridge, Tenn. 37830

3:35 Self-Diffusion of Ions in the Colloid Na-Cs-Montmorillonite-Water. Adrien Cremers, H. C. Thomas, Department of Chemistry, University of North Carolina, Chapel Hill, N. C. 27514

4:15 Hyperfiltration with Ion-Exchange Membranes. J. S. Johnson, Jr., Chemistry Division, Oak Ridge National Laboratory, P. O. Box X, Oak Ridge, Tenn. 37830

Section B

INSTRUMENTAL TECHNIQUES AS AIDS IN THE DETERMINATION OF STRUCTURE OF COMPLEX IONS

S. Kirschner, Presiding

2:05 Diffraction Studies of Coordination Compounds. J.

A. Ibers, Department of Chemistry, Northwestern University, Evanston, Ill. 60201

2:45 The Application of Nuclear Magnetic Resonance Techniques to Coordination Compounds. R. S. Drago, University of Illinois, Urbana, Ill.

3:25 The Application of Electron Spin Resonance Techniques to the Determination of Structure of Coordination Compounds. H. B. Gray, Gates and Crellin Laboratories of Chemistry, California Institute of Technology, Pasadena, Calif., James Preer, Columbia University, New York, N. Y.

4:05 The Application of Nuclear Quadrupole Resonance to the Determination of the Electronic and Molecular Structure of Coordination Compounds. F. A. Cotton, C. B. Harris, Department of Chemistry, Massachusetts Institute of Technology, Cambridge, Mass. 02139

Tuesday Morning, Sept. 13

Section A

INSTRUMENTAL TECHNIQUES AS AIDS IN THE DETERMINATION OF STRUCTURE OF COMPLEX IONS

D. B. Rorabacher, Presiding

9:00 The Application of Mass Spectrometric Techniques to the Determination of Structure of Coordination Compounds. T. L. Brown, G. E. Hartwell, Noyes Chemical Laboratory, University of Illinois, Urbana, Ill.

9:30 The Application of Chromatographic Techniques to the Determination of Structure of Coordination Compounds. E. L. King, Department of Chemistry, University of Colorado, Boulder, Colo.

10:00 The Application of Optical Rotatory Dispersion Techniques to the Determination of Structure of Coordination Compounds. Stanley Kirschner, Department of Chemistry, Wayne State University, Detroit, Mich. 48202

10:30 The Application of Circular Dichroism Techniques to the Determination of Structure of Coordination Compounds. B. E. Douglas, Department of Chemistry, University of Pittsburgh, Pittsburgh, Pa. 15213

11:00 The Application of Magnetic Circular Dichroism and Magnetic O.R.D. to the Determination of Structure of Coordination Compounds. R. N. Schatz, A. J. McCaffery, Department of Chemistry, University of Virginia, Charlottesville, Va., P. J. Stephens, Institute for the Study of Metals, University of Chicago, Chicago, Ill.

11:30 Polarized Crystal Spectra: Application and Interpretation with Coordination Compounds. R. A. D. Wentworth, Department of Chemistry, Indiana University, Bloomington, Ind. 47401

Section B

GENERAL

R. W. Murray, Presiding

9:05 Determination of pK_a Values of Some Substituted Nitroaliphatic Acids by Potentiometric Titration. Mae I. Fauth, Annie C. Richardson, G. W. Nauflett, Research & Development Department, U. S. Naval Propellant Plant, Indian Head, Md. 20640

9:20 Determination of Ionization Constants of Monobasic Acids in Ethanol–Water by Direct Potentiometry. J. W. Frohliger, Hildred Irwin, Richard Gartska, Omar Steward, Department of Chemistry, Duquesne University, Pittsburgh, Pa. 15219

9:35 Ionization Constants of Substituted Benzoic Acid in Ethanol–Water. G. M. Brauer, George Durany, Harold Argentar, Dental Research Section, National Bureau of Standards, Washington, D. C. 20234

10:00 Nature of the Solvent Effect of Methanol on the Dissociation of Protonated Tris (Hydroxymethyl) Aminomethane. P. W. Schindler, University of Bern, Bern, Switzerland, R. A. Robinson, R. G. Bates, National Bureau of Standards, Washington, D. C. 20234

10:20 The Electrochemical Measurement of Adsorption by Current Reversal Chronopotentiometry. H. B. Herman, H. N. Blount, Department of Chemistry, University of Georgia, Athens, Ga.

10:35 Spherical, Shielding, and Streaming Effects in Current-Reversal Chronopotentiometry at the Hanging Mercury Drop Electrode. R. W. Murray, Department of Chemistry, University of North Carolina, Chapel Hill, N. C. 27514, D. J. Gross, U. S. Army Nuclear Defense Laboratory, Edgewood Arsenal, Md. 21010

10:55 Electrochemical Studies on Metal Acetylacetonates in Acetonitrile Solvent. R. W. Murray, Department of Chemistry, University of North Carolina, Chapel Hill, N. C. 27514, L. K. Hiller, Jr., Procter & Gamble Co., Miami Valley Laboratories, Cincinnati, Ohio

11:10 Anodic Polarographic Acetylacetonate Waves—A Bis-Lithium Acetylacetonate Complex. R. W. Murray, Department of Chemistry, University of North Carolina, Chapel Hill, N. C. 27514, L. K. Hiller, Jr., Procter & Gamble Co., Miami Valley Laboratories, Cincinnati, Ohio

11:25 Polarography of Aquodiethyltin(IV) in Aqueous Solution. M. D. Morris, Department of Chemistry, Pennsylvania State University, University Park, Pa. 16802

11:40 Voltammetry and Related Studies of Uranium in Molten LiF-BeF_2-ZrF_4. Gleb Mamantov, Department of Chemistry, University of Tennessee, Knoxville, Tenn. 37916, D. L. Manning, Analytical Chemistry Division, Oak Ridge National Laboratory, Oak Ridge, Tenn.

Section C

TEACHING OF ANALYTICAL CHEMISTRY

(Joint with Division of Chemical Education)

L. B. Rogers, Presiding

9:00 Introduction. L. B. Rogers

9:15 Methods of Separation—The Sophomore Course in Analytical Chemistry. R. V. Dilts, Department of Chemistry, Box 1590, Station B, Vanderbilt University, Nashville, Tenn. 37203

9:30 Modern Analytical Chemistry for Sophomores. R. L. Pecsok, Department of Chemistry, University of California, Los Angeles, Calif. 90024

10:15 A Junior-Year Analytical/Organic Laboratory Course. R. L. Grob, Chemistry Department, Villanova University, Villanova, Pa. 19085

10:30 A Novel Senior Analytical/Physical Chemistry Course. A. J. Diefenderfer, Jerome Daen, Chemistry Department, Lehigh University, Bethlehem, Pa. 18015

10:45 Analytical Chemistry from the Kinetic Viewpoint: A New Approach to Undergraduate Instruction. G. A. Rechnitz, Department of Chemistry, State University of New York, Buffalo, N. Y. 14214

11:00 The Use of a Modular System for the Teaching of Instrumental Analysis. L. P. Morgenthaler, Department of Chemistry, Georgetown University, Washington, D. C. 20008

Tuesday Afternoon

Section A

INSTRUMENTAL TECHNIQUES AS AIDS IN THE DETERMINATION OF STRUCTURE OF COMPLEX IONS

P. Oliver, Presiding

2:00 Raman Spectroscopic Determination of Structures of Mixed Complexes in Solution. R. A. Plane, Department of Chemistry, Cornell University, Ithaca, N. Y.

2:30 The Application of Infrared Techniques to the Determination of Structure of Coordination Compounds. Kazuo Nakamoto, Department of Chemistry, Illinois Institute of Technology, Chicago, Ill. 60616.

3:00 The Application of Visible–UV Spectroscopic Techniques to the Determination of Structure of Coordination Compounds. R. L. Carlin, Department of Chemistry, Brown University, Providence, R. I. 02912

3:30 The Application of Electrochemical Methods to Structure Studies of Coordination Compounds. D. T. Sawyer, F. A. Schultz, Department of Chemistry, University of California, Riverside, Calif.

4:00 Applications of Magnetic Susceptibility Techniques to Coordination Chemistry. L. N. Mulay, Materials Research Center, Pennsylvania State University, University Park, Pa.

4:30 The Application of Thermoanalytical Techniques to the Determination of the Structure of Coordination Compounds. W. W. Wendlandt, Department of Chemistry, University of Houston, Houston, Texas 77004

Section B

GENERAL

B. McDuffie, Presiding

2:05 Theory and Application of Derivative Voltammetry with Kinetic Systems. S. P. Perone, C. V. Evins, Department of Chemistry, Purdue University, Lafayette, Ind. 47907

From INSTRUMENTS, INC., of Tulsa SINCE 1947

IN-VAL-CO. Instruments Valves Controls CRAFTSMANSHIP ASSURES QUALITY

What Is The C-40 Chromatograph "Closed Door" Policy?

C-40 Chromatograph Offers:

VERSATILITY — Handles either liquids or gases on a choice of columns simply by rotating a valve knob.

LARGE OVEN SPACE — 920 sq. inches working space permits easy access to multiple columns.

INCREASED SPEED & ACCURACY — smaller detector volume allows smaller sample size/column length with less sample time and increased sensitivity.

SEPARATE TEMPERATURE COLUMNS — on oven, detector, and injection port with separate read-out for finer control of operating conditions.

COMPLETE PLUG-IN WIRING — for fast and easy connection between components.

CHOICE OF THERMISTOR — (both 10K & 100K), hot wire and hydrogen flame detectors.

BOTH GAS & LIQUID SAMPLING VALVES AND INJECTION PORT for convenient handling.

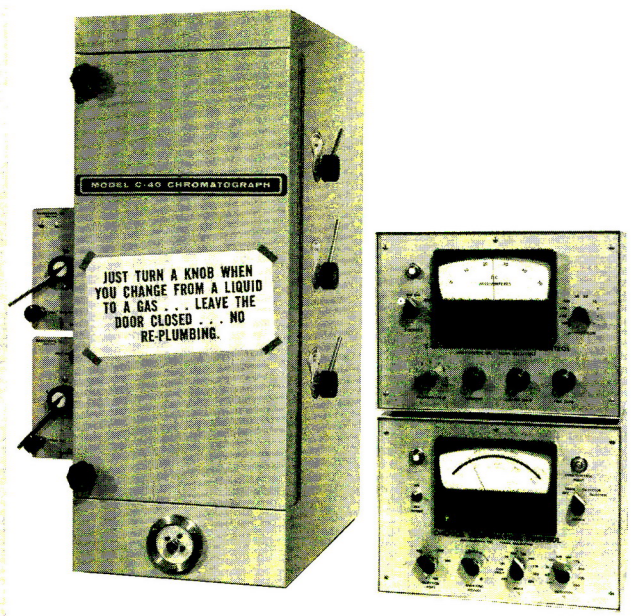

IN-VAL-CO. Instruments Valves Controls CRAFTSMANSHIP ASSURES QUALITY

INSTRUMENTS, INC.
of Tulsa, Oklahoma
Box 556 Tulsa, Oklahoma 74101

Circle No. 152 on Readers' Service Card

2:25 Application of Controlled Potential Techniques to the Study of Rapid Coupled Chemical Reactions. Electro-Oxidation of Ascorbic Acid. S. P. Perone, W. J. Kretlow, Department of Chemistry, Purdue University, Lafayette, Ind. 47907

2:45 Coulometric Titration of Hypochlorite Ion. A. F. Krivis, E. S. Gazda, Chemicals Division Research, Olin Mathieson Chemical Corp., New Haven, Conn.

3:00 Evaluation of Thin Mercury Film Electrodes for Anodic Stripping Voltammetry. R. J. Joyce, C. C. Wescott, Beckman Instruments, 2500 Harbor Blvd., Fullerton, Calif.

3:25 The Diffusion of Amino Acids in Paper Chromatography. Sr. Ellen M. Duffy, R.S.M., Mercy College, 555 Broadway, Dobbs Ferry, N. Y. 10522, G. N. Kowkabany, Catholic University, Washington, D. C. 20017

3:35 Solute Retention in Liquid–Liquid Chromatography. D. C. Locke, Esso Research & Engineering Co., P. O. Box 121, Linden, N. J. 07036

3:55 Thin Layer Chromatography of the Brominated Salicylanilides on DEAE Cellulose. N. E. Skelly, Dow Chemical Co., 574 Bldg., Midland, Mich. 48640, K. A. Kamke, Pitman-Moore Division, Dow Chemical Co., Indianapolis, Ind.

4:10 Quantitative Analysis of Chlorpromazine Metabolites by Thin Layer Chromatography. C. F. Rodriguez, D. E. Johnson, 8500 Culebra Rd., Southwest Research Institute, San Antonio, Texas 78206

4:20 The Application of Radioactive Isotopes to the Quantitative Analysis of Trace Amounts of Inorganic Substances on Paper and Thin Layer Chromatograms. A. R. Landgrebe, T. E. Gills, J. R. DeVoe, National Bureau of Standards, A361 Bldg. 222, Washington, D. C. 20234

Wednesday Morning, Sept. 14

Section A

TRENDS IN PHARMACEUTICAL ANALYSIS

J. Bomstein, Presiding

9:10 Some Recent Developments in the Analysis of Pharmaceuticals by NMR Spectroscopy. T. G. Alexander, S. A. Koch. Food and Drug Administration, 200 C St., S. W., Washington, D. C. 20204

9:45 Radioisotopes as Analytical Tools in Pharmaceutical Analysis. Ross Crabtree, Eli Lilly and Co., Indianapolis, Ind. 46206

10:30 Differential Thermal Analysis and Thermogravimetric Analysis—an Analytical Approach to Pharmaceutical Problems. R. N. Boos, Merck Sharp & Dohme, Rahway, N. J. 07065

11:10 Phosphorimetric Analyses in Pharmaceutical Chemistry—Theory and Application. W. J. McCarthy, J. D. Winefordner, Department of Chemistry, University of Florida, Gainesville, Fla.

Section B

N. HOWELL FURMAN MEMORIAL SYMPOSIUM

J. F. Flagg, Presiding

9:10 Electron Transfer Processes with Coupled Chemical Reactions. R. N. Adams, Department of Chemistry, University of Kansas, Lawrence, Kan. 66044

9:35 Redox Processes Involving Oxy-Ions. G. P. Haight, Jr., Chemistry Department, University of Illinois, Urbana, Ill.

10:05 Determination of Some Typical and Unusual Impurities in Metallurgical Products by Atomic Absorption Spectroscopy. W. C. Cooper, Noranda Research Centre, Pointe Claire, Quebec, Canada, S. Barabas, Technicon Instruments, Ardsley, N. Y.

10:20 The Mechanism of the Karman–Giuffrida Detector. J. J. Saturno, W. D. Cooke, Department of Chemistry, Cornell University, Ithaca, N. Y. 14850

11:00 Some Challenges in Analytical Biochemistry. W. B. Mason, School of Medicine and Dentistry, University of Rochester, Rochester, N. Y. 14620

11:25 Determination of Oxygen in Gases by Photochemically Generated Reducing Agent. P. B. Sweetser, Central Research Dept., E. I. du Pont de Nemours & Co., Wilmington, Del. 19898

11:40 Photochemical Oxidation of Methanol to Formaldehyde. Nora L. Ford, C. E. Bricker, Department of Chemistry, University of Kansas, Lawrence, Kan.

Section C

GENERAL

L. M. Chambers, Presiding

9:05 The Measurement of Infrared Spectra of Gas Chromatography Fractions by Multiple-Scan Interferometry. M. J. D. Low, School of Chemistry, Rutgers, The State University, New Brunswick, N. J., S. K. Freeman, International Flavors and Fragrances (US), 800 Rose Lane, Union Beach, N. J.

9:25 Selected Copper-Amine Complexes as Stationary Phases. A. G. Altenau, Firestone Tire & Rubber Co., 1200 Firestone Parkway, Akron, Ohio 44317, Charles Merritt, Jr., U. S. Army Natick Laboratories, Natick, Mass. 01762.

9:45 Quantitative Gas Chromatography. Normal Paraffins as a Diagnostic Aid. Frederick Baumann, Frank Tao, Jack Gill, Varian–Aerograph, P. O. Box 313, Walnut Creek, Calif.

10:05 Apparatus and Method of Locating Double Bonds by Ozonolysis and Gas Chromatography at the Milligram and Microgram Level. Morton Beroza, Barbara A. Bierl, U. S. Department of Agriculture, Beltsville, Md. 20705

10:40 Physicochemical Measurements of Metal Chelates by Gas–Liquid Partition Chromatography. R. W. Moshier, D. R. Gere, Chemistry Research Laboratory, Wright–Patterson AFB, Ohio

11:00 Use of a Nitrogen Detector for the Gas Chromatographic Analysis of Amino Acids. D. E. Johnson, Theron Goodson, J. W. Rhoades, Southwest Research Institute, 8500 Culebra Rd., San Antonio, Texas 78206

11:10 Gas Chromatography and Structural Correlation of Substituted Aziridines. W. L. Zielinski, Jr., Lawrence Fishbein, Bionetics Research Laboratories, Inc., P. O. Box 26, Falls Church, Va. 22046

11:25 Calculation of Essential Parameters in Programmed Temperature Gas Chromatography from Programmed Temperature Data Alone. Robert Rowan, Jr., New Mexico State University, Box C, University Park, N. M.

11:40 Gas–Liquid Interface and Solid Support Effects of Polar Solute–Nonpolar Solvent Systems in Gas Chromatography. R. L. Pecsok, B. H. Gump, University of California, 405 Hilgard Ave., Los Angeles, Calif.

Wednesday Afternoon

Section A

TRENDS IN PHARMACEUTICAL ANALYSIS

J. Bomstein, Presiding

2:00 Applications of Ion-Pair Extraction to the Partition Chromatographic Separation of Pharmaceutical Amines. T. D. Doyle, Joseph Levine, Food and Drug Administration, 200 C St., S. W., Washington, D. C. 20204

2:30 New Thermochemical Approaches to Organic Functional Group Analysis. Joseph Jordan, R. A. Henry, 212 Whitmore Laboratory, Pennsylvania State University, University Park, Pa.

3:40 Enzymic Methods for the Analysis of Pharmaceutical Compounds. G. G. Guilbault, Louisiana State University, New Orleans, La.

Section B

N. HOWELL FURMAN MEMORIAL SYMPOSIUM

J. F. Flagg, Presiding

2:00 N. H. Furman and His Contributions to Science. I. M. Kolthoff, University of Minnesota, Minneapolis, Minn.

2:15 Isotopic Ion Exchange in Activation Analysis. G. H. Morrison, Fouad Tera, Department of Chemistry, Cornell University, Ithaca, N. Y.

2:55 Determination of Carbonate, Trititanate, and Orthotitanate in Barium Metatitanate. D. R. Norton, Sprague Electric Co., North Adams, Mass. 01248

3:10 Polarography in Biochemistry and Allied Areas. P. J. Elving, Department of Chemistry, University of Michigan, Ann Arbor, Mich.

3:40 Catalysis in Organic Electrode Reactions. J. D. Voorhies, Stamford Research Laboratories, American Cyanamid Co., Stamford, Conn. 06904

Newest member of the Spectroscopy Family

SO NEW

NSEC

MÖSSBAUER EFFECT ANALYZERS

...ALL THE APPLICATIONS HAVEN'T BEEN EXPLORED!

MODEL B

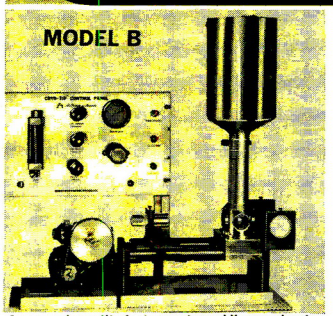

A research quality instrument, providing semi-automatic data collection, for use in routine laboratory experiments or non-routine research.

Constant velocity, 0 to 15mm/sec.

Optional source or absorber cooling variable 16° to 70° K also available.

MODEL AM-1

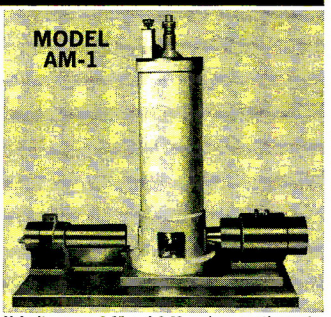

Velocity range 0-15 and 0-60 cm/sec, continuously variable.

Source and/or absorber cooling to liquid helium temperature.

Automatic data collection. Full spectrum display. ±1% system linearity over 95% of the half period of the velocity waveform.

Write for our free Applications Bulletin on Mossbauer Spectroscopy

NSEC

Nuclear Science & Engineering Corporation

P.O. Box 10901 • Pittsburgh, Pa. 15236 Area Code 412 462-4000

LEARN MORE at the NSEC SYMPOSIUM

"The Mossbauer Effect and its Applications in Chemistry"

•

September 12, 1966
at the
152nd National Meeting
of the
AMERICAN CHEMICAL SOCIETY
Hotel Americana
New York City

•

Dr. R. H. Herber, Rutgers University will be Chairman of the Symposium.

- Lectures by prominent authorities in the field of Mossbauer Spectroscopy.
- Panel discussion on Applications.
- Demonstrations of Analyzers.

WRITE IMMEDIATELY FOR A PROGRAM:

Nuclear Science & Engineering Corp.

Dept. A P.O. Box 10901 Pittsburgh, Pa. 15236

Circle No. 169 on Readers' Service Card

SCIENTIFIC GLASS APPARATUS CO. INC. BLOOMFIELD, NEW JERSEY

LABORATORY...
♦ APPARATUS
♦ INSTRUMENTS
♦ CHEMICALS
♦ GLASSWARE

Branches: Boston 16 Mass. • Danbury Conn. • Elk Grove Village Ill. • Fullerton Calif. • Philadelphia 2 Penna. • Silver Spring Md. • Syracuse 2 N.Y.

"See Laboratory Guide for all Products/Sales Offices"

Circle No. 41 on Readers' Service Card

4:00 Twin-Electrode Thin-Layer Electrochemistry: Kinetics of Second-Order Disproportionation of Uranium(V) by Decay of Steady-State Current. C. N. Reilley, Department of Chemistry, University of North Carolina, Chapel Hill, N. C. 27514, Bruce McDuffie, Department of Chemistry, State University of New York, Binghamton, N. Y.

4:20 Cobalt(III) Catalyzed Deuterium Exchanges on Ligands with Glycinate Rings. C. N. Reilley, J. B. Terrill, Department of Chemistry, University of North Carolina, Chapel Hill, N. C. 27514

Section C

GENERAL

D. J. Macero, Presiding

2:05 A Rapid Method for the Carrier-Free Determination of Individual Rare Earths by Ion Exchange at Room Temperature. S. C. Foti, L. Wish, U. S. Naval Radiological Defense Laboratory, San Francisco, Calif. 94135

2:20 Counter Double Current Distribution: Effects of Varying Number of Stages. R. O. Butterfield, Constance K. Tjarks, H. J. Dutton, Northern Utilization Research and Development Division, 1815 North University, Peoria, Ill. 61604

2:40 Radiochemical Separation of Copper by Amalgam-Exchange. R. R. Ruch, J. R. DeVoe, National Bureau of Standards, Washington, D. C. 20234

3:00 The Dissolution of Some Inert Metals in Gamma Irradiated Hydrochloric Acid. Hisashi Kubota, Oak Ridge National Laboratory, P. O. Box X, Oak Ridge, Tenn. 37831

3:20 Depolarized Light and Differential Thermal Analysis of Some Polyolefin Transitions. E. M. Barrall II, E. J. Gallegos, Chevron Research Co., P. O. Box 1627, Richmond, Calif. 94802

3:40 Protonation of L-Cysteine and Some of Its Derivatives. D. E. Leyden, D. B. Walters, Department of Chemistry, University of Georgia, Athens, Ga. 30601

3:55 Base-Catalyzed Isotopic Exchange in Bivalent Metal–EDTA Chelates. C. N. Reilley, J. B. Terrill, Department of Chemistry, University of North Carolina, Chapel Hill, N. C. 27514

4:10 Kinetics and Mechanisms of Ligand Exchange in the Strontium–EDTA Systems. R. J. Kula, D. L. Rabenstein, University of Wisconsin, Madison, Wis.

4:25 Statistical Analysis of Variations in Complex Mixtures. S. J. Hawkes, Chemistry Department, Brigham Young University, Provo, Utah 84601

6:00 DIVISION SOCIAL HOUR

7:00 DIVISION DINNER.

Speaker: Z. Lewin, New York University.
Subject: Analytical Chemistry in Art and Archeology (illustrated)

Thursday Morning, Sept. 15

Section A

SPARK SOURCE MASS SPECTROMETRY

G. H. Morrison, Presiding

9:05 Production and Analysis of Ions: Fundamentals and Instrumentation. R. E. Honig, RCA Laboratories, Princeton, N. J.

9:45 Quantitation. A. J. Ahearn, Bell Telephone Laboratories, Murray Hill, N. J. 07971

10:40 Photographic Detection. J. Franzen, K. D. Schuy, Max-Planck-Institut fur Chemie, Mainz, Germany

11:20 Electrical Detection. H. J. Svec, R. J. Conzemius, Iowa State University, Ames, Iowa

Section B

GENERAL

E. C. Dunlop, Presiding

9:05 Decomposition of Organic Fluorine Compounds Using Sodium–Biphenyl Reagents. Phyllis P. Wheeler, Mae I. Fauth, Research and Development Department, U. S. Naval Propellant Plant, Indian Head, Md. 20640

9:15 Glyoximes as Reagents for the Determination of Bismuth. L. D. Wiersma, P. F. Lott, Chemistry Department, University of Missouri at Kansas City, Kansas City, Mo. 64110

9:30 Spectrophotometric Determination of Aluminum in Nickel- and Iron-Base Alloys. K. E. Burke, International Nickel Co., Inc., Paul D. Merica Research Laboratory, Suffern, N. Y. 10901

9:45 Some Alkylated 8-Mercaptoquinolines as Analytical Reagents. Akira Kawase, Henry Freiser, Department of Chemistry, University of Arizona, Tucson, Ariz. 85721

10:05 Microanalysis by Selective Chromate Reactions. D. A. Abdo, Boeing Co., P. O. Box 3985, Seattle, Wash.

10:35 Quantitative Chemical Analysis of Small Surface Areas of Tungsten Metal for Zirconium and Titanium. K. F. Sugawara, AFML (MAYA), Wright Patterson AFB, Ohio 45433

10:50 Determination of Parts per Billion Iron in High Temperature Hydrocarbon Jet Fuels. F. R. Short, W. G. Scribner, H. C. Eyster, Monsanto Research Corp., Dayton Laboratory, Dayton, Ohio 45407

11:05 Determination of Trace Elements in High Purity Zinc by Atomic Absorption and Flame Emission Spectrophotometry. T. C. Rains, Oscar Menis, National Bureau of Standards, Washington, D. C. 20234

11:25 Characterization of the Blank Correction in the Determination of Oxygen in Sodium by the Amalgamation Method. J. M. Scarborough, P. F. DeVries, Atomics International, P. O. Box 309, Canoga Park, Calif. 91304

Thursday Afternoon

Section A

SPARK SOURCE MASS SPECTROMETRY

G. H. Morrison, Presiding

2:05 Data Processing. P. R. Kennicott, G. E. Research and Development Center, Schenectady, N. Y.

2:35 Determination of Carbon, Oxygen, and Nitrogen in Solids. R. K. Skogerboe, W. L. Harrington, G. H. Morrison, Department of Chemistry, Cornell University, Ithaca, N. Y.

3:20 Microprobe Techniques. W. M. Hickam, Westinghouse Research Laboratories, Pittsburgh, Pa. 15235

4:00 Role in Analysis. E. B. Owens, Lincoln Laboratory, M.I.T., Lexington, Mass. 02173

Section B

GENERAL

J. C. White, Presiding

2:05 Diffusion Coefficient of Oxygen in Neutral and Basic Solutions. S. L. Phillips, I.B.M. Corp., Box 390, Dept. C27, Poughkeepsie, N. Y.

2:25 The Polarographic Determination of Aminocaproic Acid in Nylon Polymer. T. A. Robinson, Fibers Division, Allied Chemical Corp., P. O. Box 31, Petersburg, Va.

2:45 A Rapid Instrumental Method for Carbonate Determination. C. E. Van Hall, V. A. Stenger, Bldg. 574, Dow Chemical Co., Midland, Mich. 48640

3:05 A Rapid Method for Determination of Chemical Oxygen Demand. V. A. Stenger, C. E. Van Hall, Bldg. 574, Dow Chemical Co., Midland, Mich. 48640

3:30 New Technique for Determination of Impurities in Flowing Gases. D. C. Myers, F. Schmidt-Bleek, Department of Chemistry, Purdue University, W. Lafayette, Ind.

3:40 X-Ray Spectrographic Determination of Rare Earths in Catalysts. I. C. Stone, Jr., K. A. Rayburn, W. R. Grace & Co., Washington Research Center, Clarksville, Md. 21232

3:55 Oxidation of Some Aryl Amines by Copper(II) in Acetonitrile. Byron Kratochvil, D. A. Zatko, Department of Chemistry, University of Wisconsin, Madison, Wis.

4:10 A Kinetic Study of the Osmium-Catalyzed Ce(IV)–As(III) Reaction. R. L. Habig, Department of Biochemistry, Duke University Medical Center, Durham, N. C. 27706, H. L. Pardue, Department of Chemistry, Purdue University, Lafayette, Ind. 47907

4:25 Determination of the Abundances of the Platinum Metals in Iron and Stony Meteorites. J. G. Sen Gupta, Geological Survey of Canada, 601 Booth St., Ottawa, Ontario, Canada

4:45 Arsenazo III as a Sensitive and Selective Reagent for Palladium and Its Application to the Determination of Palladium and Thorium in Iron and Stony Meteorites. J. G. Sen Gupta, Geological Survey of Canada, 601 Booth St., Ottawa, Ontario, Canada

Name one company that offers this many planchet counting systems.

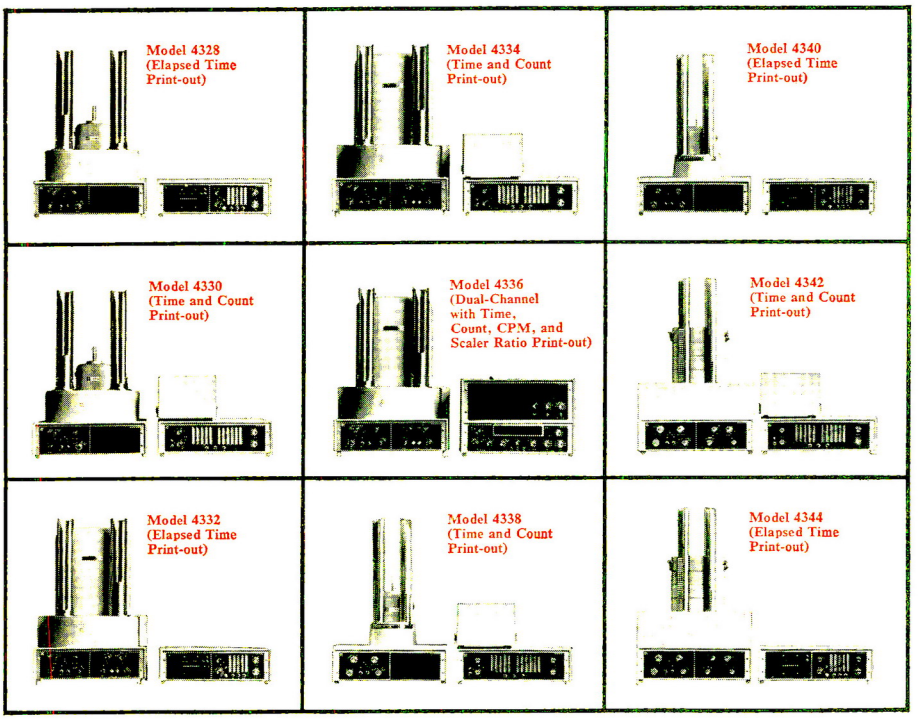

Name two.

Only Nuclear-Chicago gives you a total of nine different automatic planchet counting systems to choose from. There are systems for normal counting (Models 4328 and 4330) or low-background counting (Models 4332, 4334, and 4336) of 2-inch-diameter planchets. And there are systems for 1¼-inch diameter planchets for normal counting (Models 4338 and 4340) or low-background counting (Models 4342 and 4344).

That's nine unique combinations of planchet size, background shielding, sample capacity, and data readout. One of these systems is sure to match your application—exactly. And each system uses an efficient gas-flow detector that's uniformly sensitive up to the edge of the window. Plus a heavy-duty, solid-state-logic sample changer that has extra capacity when add-on sample magazine extensions are used.

Besides this complete array of planchet counting systems, we can also supply a full range of accessories—such as sample pans and carriers, detector windows, and counting gas.

To get detailed information on these systems and accessories, consult your Nuclear-Chicago sales engineer or write to us. NUC-8-6-738

NUCLEAR-CHICAGO CORPORATION

351 East Howard Avenue, Des Plaines, Illinois 60018, U.S.A. / Donker Curtiusstraat 7, Amsterdam W, The Netherlands.

Circle No. 51 on Readers' Service Card

Buchler Gives You a Choice

VERTICAL GEL ELECTROPHORESIS APPARATUS

POLYACRYLAMIDE

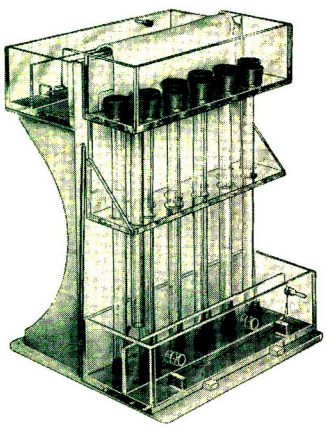

- *Large Sample Capacity*
- *Easy Gel Removal*
- *Wider Separations*

Designed to fill needs for larger Gel Column Electrophoresis. Eleven 5.050 ml samples may be run at one time. Acrylic plastic walls of tube and special molded plugs, along with the Buchler column extractor, provide for easy removal of gel column. Wide band spreads—up to six inches—are sharply defined and spaced for easy identification and separation.

Write for Bulletin AC3-1071

STARCH GEL

- *Direct Insertion of Liquid Samples Without Paper or Starch Granules*
- *10 Samples of 0.040 to 0.045 ml Can Be Processed Simultaneously or 1.6 ml in a Single Slot*

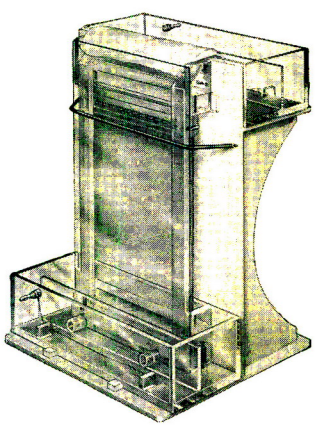

Provides samples which can be resolved into more zones than with paper electrophoresis . . . without overlapping of components. Insertion of sample from underside permits use of glass plate for covering gel thus assuring 2 co-planar surfaces. Removable multiple slot former fixes the depth of slots in molten gel. Gel remains undisturbed until electrophoresis is completed.

Conversion Kits Available for Either Method

Write for Bulletin AC3-1070

SEE YOU IN NEW YORK AT THE ACS MEETING, BOOTH #636

BUCHLER INSTRUMENTS

LABORATORY APPARATUS • PRECISION INSTRUMENTS

BUCHLER INSTRUMENTS, INC.

1327 16TH STREET, FORT LEE, NEW JERSEY 07024

"See Laboratory Guide for all Products/Sales Offices"

Circle No. 92 on Readers' Service Card

Trace Characterization Symposium Program

Program plans are now complete for the first Materials Research Symposium to be held at the National Bureau of Standards' new site in Gaithersburg, Md., from October 3 through October 7, 1966. The Symposium, presented by the NBS Institute for Materials Research (U. S. Department of Commerce), will be on Trace Characterization—Chemical and Physical.

The purpose of the Symposium is to improve the effectiveness of materials research by summarizing the present capabilities and the future potentials of the more useful tools for trace characterization of materials, and by promoting with international participation the exchange of knowledge among the various disciplines upon which a complete and meaningful trace characterization depends.

The program offers a coherent full-week symposium, consisting of invited lectures followed by discussion sessions on the same topics. Rapporteurs will summarize the salient points of contributed papers and lead the general discussion. No simultaneous sessions will be held, and it is intended that registrants will participate in all sessions. The invited lecturers and rapporteurs are listed in the Outline of Program below.

Advance registration forms are being sent six weeks prior to the Symposium to those expressing interest in attending. As attendance will be limited by the capacity of the Bureau's large auditorium, those wishing to attend should return the forms promptly.

The registration fee of $35 will cover transportation between NBS and the Sheraton Park Hotel, a "mixer" at the hotel, a reception and buffet dinner at the Museum of History and Technology, a book of preprints of contributed papers, and a hard-bound edition of the proceedings of the Symposium containing the invited papers and discussions.

Those who have not previously indicated their interest in the Symposium may write to Dr. Roger G. Bates, Institute for Materials Research, National Bureau of Standards, Washington, D. C. 20234.

PROGRAM

Sunday, Oct. 2

Registration. Sheraton Park Hotel, Washington, D. C.

Monday Morning, Oct. 3

Opening of Symposium. A. V. Astin, Director, National Bureau of Standards, Washington, D. C.

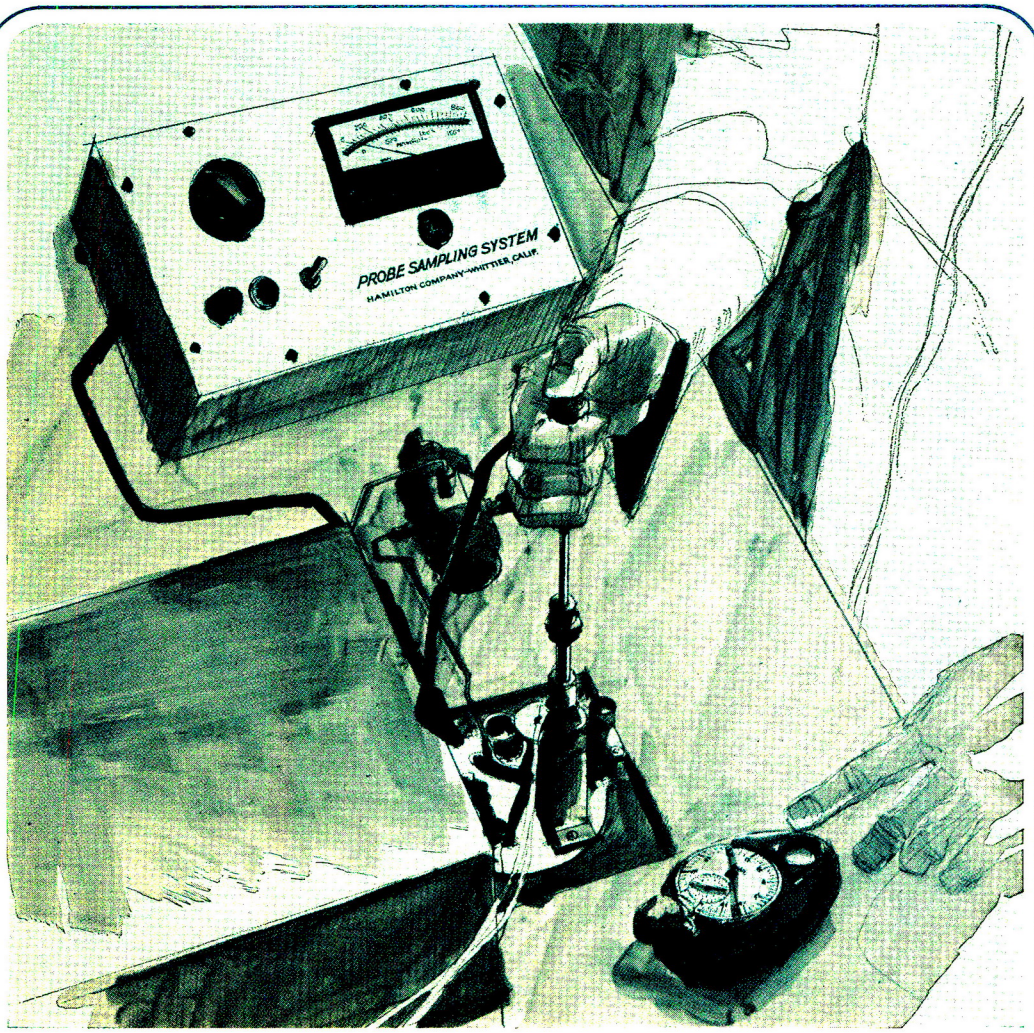

An economical answer for analytical pyrolysis

Here is an easy, economical approach to vaporization of solids, pyrolysis, and extraction of volatiles. It is ideal for plastics, rubber, and other low volatility solids. You can obtain the precise weight of the sample before introduction and all the sample vapor is flushed into the column. Vaporization or pyrolyzation takes place in an inert glass chamber. This unique Probe Sampling System was designed for Hamilton's Inlet, which converts easily for normal syringe sampling. ***Write today for catalog and prices.***

HAMILTON

For a copy of our catalog, simply clip the coupon, attach to company letterhead, and mail.

To: HAMILTON COMPANY • P.O. Box 307-B • Whittier, Calif.
Exclusive European Agent: Micromesure N.V., P.O. Box 205, The Hague

Name_____ Title_____

Circle No. 37 on Readers' Service Card

mini-pet™

BIOLOGISTS, CHEMISTS, LAB TECHNICIANS:
Dispense, dilute or pipet, acids, solvents or chemicals repeatedly with the MINI-PET. Quick, simple, safe, with *one-handed ease.*
MINI-PET'S exclusive (pat. pend.) hollow *NON-STICK Teflon plunger:*

- ELIMINATES FREEZING ■ SLIDES EASILY
- SELF-LUBRICATING (ELIMINATES GREASE CONTAMINATION)
- SIMPLE TO CLEAN
- AUTOCLAVABLE (ENTIRE UNIT)

Unlimited uses in the laboratory and industry where equal amounts of liquid have to be dispensed.

MINI-PETS are easily adjustable to any volume within their capacity. **Repetitive accuracy ± 0.5%.** Sizes 1 ml, 2 ml and 10 ml.

Prices from $21.50 complete.

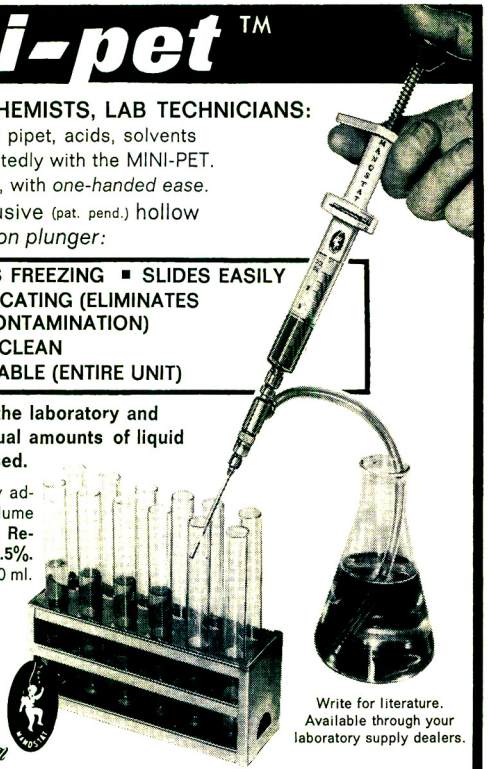

MANOSTAT *Corporation*

Write for literature. Available through your laboratory supply dealers.

20-22 N. Moore St., Dept. 521, N.Y.C. 10013

Circle No. 104 on Readers' Service Card

We're Specialists: Are You?

GLASS LATHES
GAS/OXY BURNERS
ACCESSORIES
MERCURY
HEATHWAY

CATALOG? YES

BETHLEHEM APPARATUS CO., Inc.
FRONT AND DEPOT STS. ● HELLERTOWN, PA. 18055
Telephone (215) 838-3691

Circle No. 5 on Readers' Service Card

NEWS

General Lecture. N. Bruce Hannay, Lecturer, Bell Telephone Laboratories, Murray Hill, N. J.
Electrical Measurements. Leonard Weisberg, Lecturer, RCA Research Laboratories, Princeton, N. J.

Monday Afternoon, Oct. 3

Electrochemical Methods. Herbert A. Laitinen, Lecturer, University of Illinois, Urbana, Ill.
Electrochemical Methods—Discussion. Robert A. Osteryoung, Rapporteur, North American Aviation Science Center, Thousand Oaks, Calif.
Electrical Measurements—Discussion. Robert L. Powell, Rapporteur, National Bureau of Standards, Boulder, Colo.

Monday Evening, Oct. 3

Mixer. Sheraton Park Hotel

Tuesday Morning, Oct. 4

Optical and X-Ray Spectroscopy. N. W. H. Addink, Lecturer, Philips Research Laboratories, Eindhoven, Netherlands.
X-Ray Diffraction. Jun-ichi Chikawa, John B. Newkirk, Lecturers, Denver Research Institute, University of Denver, Denver, Colo.

Tuesday Afternoon, Oct. 4

Optical and X-Ray Spectroscopy—Discussion. Heinrich Kaiser, Rapporteur, Institut für Spektrochemie und Angewandte Spektroskopie, Dortmund, Germany.
X-Ray Diffraction—Discussion. H. Steffen Peiser, Rapporteur, National Bureau of Standards, Washington, D. C.

Wednesday Morning, Oct. 5

Optical Methods. Eugene Wong, Lecturer, University of California, at Los Angeles, Los Angeles, Calif.
Optical Methods—Discussion.
Chemical Spectrophotometry. T. S. West, Lecturer, Imperial College of Science and Technology, London, England.
Chemical Spectrophotometry—Discussion

Wednesday Afternoon, Oct. 5

Tours of Washington Area

Wednesday Evening, Oct. 5

Reception. Museum of History and Technology, Smithsonian Institution, Buffet Dinner at Museum.

Thursday Morning, Oct. 6

Nuclear Methods. A. A. Smales, Lecturer, Atomic Energy Research Establishment, Harwell, Berks, England.
Mass Spectroscopy. Arthur J. Ahearn, Lecturer, Bell Telephone Laboratories, Murray Hill, N. J.

Thursday Afternoon, Oct. 6

Nuclear Methods—Discussion. Vincent P. Guinn, Rapporteur, General Atomic Division, General Dynamics Corp., La Jolla, Calif.

DUAL BEAMS DOUBLE SCOPE VERSATILITY!

Two Completely Independent Traces In One Display Make Comparisons Easier!

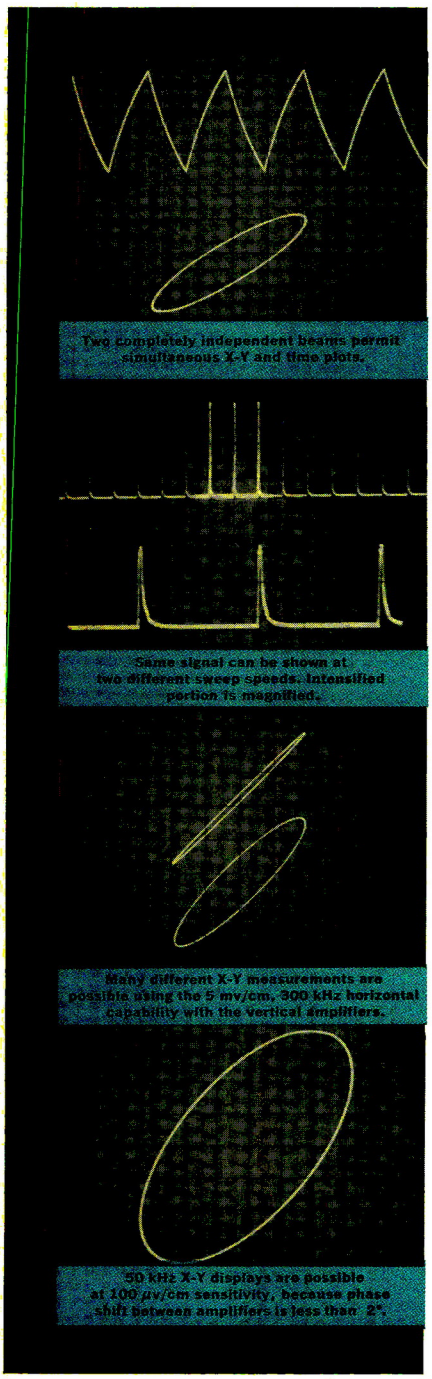

Capability of many different displays through two independent CRT beams easily doubles versatility of the hp Model 132A Dual Beam Oscilloscope. This two-in-one scope allows simultaneous comparisons of two different traces—quantitatively and qualitatively!

Waveforms look the same from range to range with the Model 132A because the high sensitivity, stable vertical amplifiers retain full bandwidth of 500 kHz at all sensitivities from 1 mv/cm through 20 v/cm. At the most sensitive range, 100 μv/cm, bandwidth becomes 200 kHz.

Stability of the two vertical amplifiers is provided through use of Nuvistor tubes in an aluminum shock-mounted block. This heat sink keeps Nuvistor temperatures identical, which gives the scope excellent DC drift stability. When DC coupling is not needed, drift can be eliminated entirely by using the AC amplifier coupling switch.

Internal time base may be applied through one or both horizontal amplifiers, thereby allowing two different sweep speeds or a simultaneous X-Y and Y vs. time display.

Compare these and additional features such as outputs from each vertical amplifier for monitoring and recording; front panel beam finder to facilitate location of off-screen traces; non-glare, parallax-free internal graticule CRT; plug-in circuit boards for easy servicing. Get the double versatility of the hp 132A for the low price of $1275. Call your hp field representative for a demonstration. Or, write Hewlett-Packard, Palo Alto, California 94304, Tel (415) 326-7000; Europe: 54 Route des Acacias, Geneva.

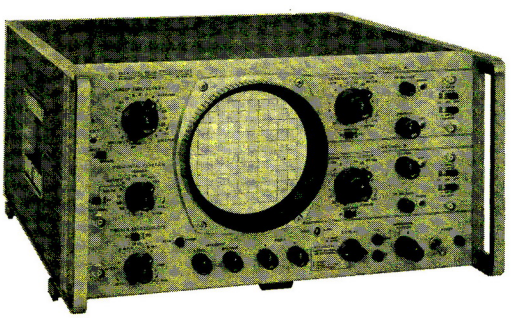

HEWLETT hp PACKARD

An extra measure of quality

Circle No. 146 on Readers' Service Card

NEWS

neld of weights and

New Producer throws hat into phenolic ring...

Clairton, Pa. – A new supplier of phenolic resins has entered the field according to informed sources at Pennsylvania Industrial Chemical Corporation, the new supplier. Users of this type of resin now have a choice of new grades with desirable properties not available in other grades of phenolic resins on the market today, according to this new producer. Technical data and physical properties of these new resins are now available, including those on non-reactive, rosin-free phenol formaldehyde resins, and terpene phenolic resins. These resins have particular application in coatings and adhesives.

The election of officers members of the Associat

DATA

Pennsylvania Industrial Chemical Corporation
149 State St./Clairton, Pennsylvania

Please send me technical data bulletin PPN-078 which summarizes general properties and applications of this new series of phenolic resins.

Name_____

Position_____

Company_____

Type of Business_____

Address_____

City_____ State_____ Zip_____

8/66 AC

Circle No. 171 on Readers' Service Card

NEWS

Mass Spectroscopy—Discussion. Edward B. Owens, Rapporteur, Lincoln Laboratory, M.I.T., Lexington, Mass.

Friday Morning, Oct. 7

Pre-Concentration Methods. J. Minczewski, Lecturer, Technical University of Warsaw, Warsaw, Poland.

Electron and Optical Microscopy. S. Amelinckx, Lecturer, Belgium Atomic Energy Center, Mol, Belgium.

Pre-Concentration Methods.—Discussion. George H. Morrison, Rapporteur, Cornell University, Ithaca, N. Y.

Friday Afternoon, Oct. 7

Electron and Optical Microscopy—Discussion. Heinz G. F. Wilsdorf, Rapporteur, University of Virginia, Charlottesville, Va.

Closing Remarks, W. W. Meinke, National Bureau of Standards, Washington, D. C.

Materials Research Journal

An international journal, the Materials Research Bulletin, reporting research on crystal growth and materials preparation and characterization is going to be published by Pergamon Press, 122 East 55th St., New York, N. Y. 10022. Joint Editors-in-Chief are Heinz K. Henisch and Rustum Roy from the Pennsylvania State University, Materials Research Laboratory, University Park, Pa. 16802. The first issue of this new monthly is expected in September. The annual subscription rates are $50 for libraries, University departments, government laboratories, industrial, and other multiple-reader institutions and $15 for personal subscriptions.

Scope of the journal includes crystal growth (theory of crystal growth, nucleation and transport; new methods of growing single crystals; application of known methods to new materials; growth of special form, e.g., whiskers and thin films). Materials preparation and materials characterization research papers will also be included. The journal promises fast publication (aiming at 6 weeks) by the use of direct photographic reproduction of authors' typescripts and offset printing. Authors will be permitted to submit their papers to any of the Associate Editors, who will personally communicate accepted papers to the Bulletin. Conventional reviewing is offered to those who prefer it. More information on this journal is available by writing to the publishers.

Symposium on Electrode Processes

A symposium on Electrode Processes is being sponsored by the University Grants Commission and organized by

laboratory refrigeration

our specialty

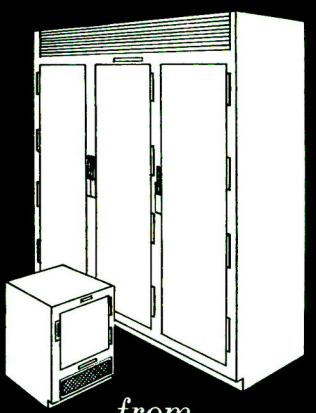

from 4 cubic feet to 69 cubic feet . . .

- REFRIGERATORS
- FREEZERS
- EXPLOSION SAFE
- BLOOD BANK
- INCUBATORS

CHOOSE FROM 29 MODELS . . . for temperature control storage of materials in your laboratories.

Name of your local representative available upon request.

PUFFER-HUBBARD
REFRIGERATOR DIVISION
Challenge Stamping & Porcelain Co.
GRAND HAVEN, MICHIGAN
TELEPHONE 616/842-2080

Circle No. 61 on Readers' Service Card

(ADVERTISEMENT)

ANALOG MONOLOGUE

On Means for Modelling, Measuring, Manipulating, & Much Else

ANALOG ELECTRONICS & OPERATIONAL AMPLIFIERS

Surely we are at least thirty years too late to justify the use of electronics — in *measuring* almost any physical or chemical parameter; in *manipulating* the measured data; or in *computing, simulating,* or otherwise *predicting* the behavior of a physical system. After three decades, however, the outlines of any discipline become blurred — hence this refresher.

One process is at the root of every contribution electronics ever made to its sister sciences: *Amplification.* There are many ways to characterize this effect, but perhaps the most general is to say that electronic circuits raise the energy level of data — that they are inherently very *sensitive* — and can be made to respond, with *reliability* (stability) and fidelity (accuracy) to very small changes in the input parameter. If the input is not already an electrical signal, it must be converted to an equivalent electrical parameter, by a "transducer."

The need for amplification — for high sensitivity — is apparent from first principles. For example, we may restate Heisenberg's Exclusion Principle as follows: *"The accuracy of a measurement is a direct function of the observer's ability to make it with a minimum of disturbance to the system observed."* If we read "loading", or "burden" for "disturbance", the need for sensitive circuits is apparent. Unfortunately, electronic amplifiers are not ideal. Left to itself, the sensitivity of a simple electronic amplifier circuit will vary so much (in response to both external influences and the instability of its own component parts) as to render it useless for all but the crudest of applications. For this reason, among others, we have had to invent ways of stabilizing amplifier gain. The most convenient, powerful, and successful of these ways is called *Feedback.*

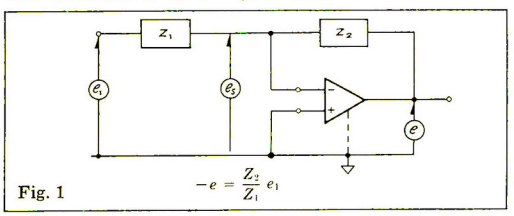

Fig. 1 $\quad -e = \frac{Z_2}{Z_1} e_1$

There are many ways to describe feedback. We shall use a simple example. To obtain a particular value of amplification, with a specific degree of stability and fidelity, one first designs an unstabilized amplifier having much higher "raw" amplification than is required; then one interconnects the output and input circuits of the amplifier by means of a more-readily-stabilized electrical circuit, called a feedback loop, or feedback network (see Figure 1) in such a way that this feeding back of output energy *reduces the apparent amplification, but gives to that modified amplification characteristic the inherently-higher stability of the feedback network.* Thus, we can trade excess amplification for superior stability — *and* superior fidelity, by the way. Because this kind of feedback *reduces* the apparent amplification, it is called "negative" feedback.

The feedback "network" may be as simple as a pair of resistors. The cost of such a circuit is modest, and its data-measurement and data-manipulation capabilities are impressive. . . but it is only the beginning.

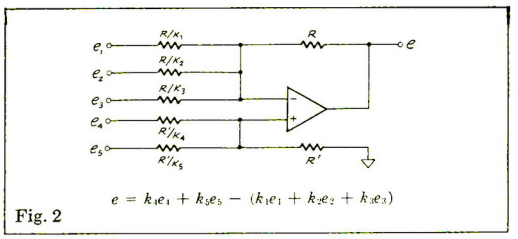

Fig. 2 $\quad e = k_4e_4 + k_5e_5 - (k_1e_1 + k_2e_2 + k_3e_3)$

By modifying the feedback network, so as to include *reactances* (capacitors or inductors) as well as resistances, you may create circuits that perform important and useful *mathematical operations* on a signal; for example one can differentiate or integrate it. Differentiation will convert velocity signals into acceleration, or position into velocity; or, with two differentiators, in cascade, position into acceleration. By integrating, one may reverse the process.

There is almost no limit to the ingenious behavioral variations one may create and control, merely by choosing appropriate feedback network configurations. Nowadays, using inexpensive standard "hardware", one may quickly assemble circuits that respond logarithmically, exponentially, or trigonometrically and circuits that multiply and divide too — almost as faithfully as the circuit of Figure 2 adds and subtracts.

Remember — all of this is done with equipments that cost, generally, hundreds of dollars or less, and not the thousands or more one might expect, from their capabilities and potential usefulness.

The kind of amplifier required for performing these operations with accuracy and fidelity is a very special beast, called (naturally) an Operational Amplifier, and we have devoted much of our time and energy over more than 20 years to its development and refinement.

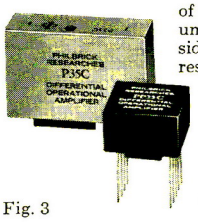

Fig. 3

We manufacture several "generations" of this very special device in large volume at surprisingly low cost . . . considering the care we take and the resultant state-of-the-art performance and reliability. Several sell for less than $20.00. Each year, we send many tens of thousands of them into service, to do thousands of different jobs, in hundreds of different applications across the entire spectrum of Science and Engineering. Figure 3 shows two of the 107 standard Philbrick Operational Amplifiers.

If you should want to begin serious study of this subject on your own, we suggest that you write for the following items, as a "Starter Set". They are free.

• *Applications Manual for Computing Amplifiers* (112 pages — normally $3.00 per copy) • *Generalized Instrumentation for Research and Teaching* (104 pages) • Bulletin 6000 *Philbrick in Brief*

For faster action, please note that we maintain the busiest, best-equipped Applications-Engineering service in the field. For further information write: Philbrick Researches, 45-G Allied Drive at Route 128, Dedham, Massachusetts, Phone (617) 329-1600.

PHILBRICK

Visit us at WESCON — Booths 130-131.

"See Laboratory Guide for all Products/Sales Offices"

Circle No. 54 on Readers' Service Card

Tonic for sluggish circulation ...The Temptrol Line

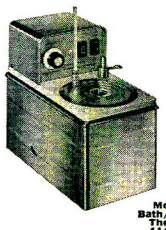

Model 150 Bath/Circulator, Thermostat, 1¼ gallons

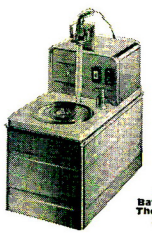

Model 151 Bath/Circulator, Thermoregulator, 1¼ gallons

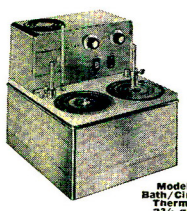

Model 152 Bath/Circulator, Thermostat, 2¾ gallons

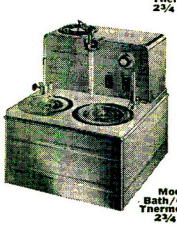

Model 153 Bath/Circulator, Thermoregulator 2¾ gallons

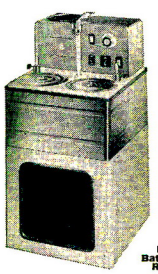

Model 154 Bath/Circulator, Refrigerated

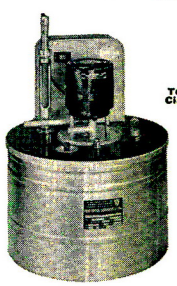

Temptrol Circulator

Your lab circulators running hot and cold? Level out with Temptrols. These constant temperature combination baths and circulating systems are made in a wide variety of models that allow you to:

- select the level of precision temperature control you need.
- select the capacity you need.
- select the temperature range you need.

Modestly priced models equipped with a hydraulic thermostat achieve a uniformity of ±0.5°C or better; those with a thermoregulator give you a uniformity of ±0.07°C or better. And you can choose the temperature range that best meets your specific needs—from −10°C to 100°C. Pumping capacities range from 42.5 to 300 gal/hr at zero head.

Temptrol baths may be used simultaneously with circulation or alone. You are assured of precise temperature control both within their built-in-baths and in separate instruments or baths through which the liquid is circulated.

The Temptrol line also includes the Lo-Temptrol, a large capacity unit that cools down to −30°C, and two versatile, budget-minded portable units, the Stir-Pump and the Porta-Temp.

In order to make the right choice, you'll want to have complete performance data on individual Temptrol units. Ask your Precision Scientific Distributor or write us, requesting Bulletin 629A.

Since 1920 • The Finest in Quality Laboratory Apparatus

PRECISION SCIENTIFIC CO. SUBSIDIARY OF GCA CORPORATION

3737 W. Cortland Street, Chicago, Illinois 60647
Local Offices in New York • Chicago • Los Angeles

Circle No. 59 on Readers' Service Card

NEWS

the University of Jodhpur, India. It will be held at the university from Nov. 1 to 6, 1966. All those research workers interested in electrochemistry are invited.

Those wishing to present papers should send a short summary to Prof. R. C. Kapoor, Director of the Symposium on Electrode Processes, Faculty of Science, University of Jodhpur, Jodhpur, India, before Sept. 30, 1966.

4th International Symposium on Advances in Gas Chromatography

The Fourth International Symposium on Advances in Gas Chromatography will be held at the Waldorf Astoria Hotel in New York City, April 3 to 6, 1967. The previous three symposia were held in Houston, Texas. The program will include lectures by internationally known leaders in the field. New developments in detectors and columns for liquid chromatography will be included. There will also be an exhibition of new gas chromatographic equipment.

Participation in the symposium will be on the basis of invited papers as well as solicited contributions. Those who wish to contribute are requested to submit an abstract of about 500 words by December 1, 1966. Complete manuscripts will be required by January 15, 1967. Financial assistance for travel will be available for authors of papers accepted from abroad.

Abstracts and inquiries concerning this meeting should be directed to Professor A. Zlatkis, Department of Chemistry, University of Houston, Houston, Texas.

XIII Colloquium Spectroscopicum Internationale

The Canadian Association for Applied Spectroscopy is sponsoring the XIII Colloquium Spectroscopicum Internationale to be held at Carleton University from June 19 to 23, 1967, in Ottawa.

Technical sessions are being planned in the following fields:

Information Storage and Retrieval; Education
Optical Emission, Flame Photometry, Atomic Absorption
Astrophysical and Solar Spectroscopy
Spectroscopic Applications in Geochemistry and Biogeochemistry
Ultraviolet Absorption and Fluorescence
X-Ray Diffraction, Fluorescence, Electron Probe
Infrared Absorption Spectroscopy
Metals Analysis

Those wishing to contribute papers should submit three copies of an abstract 400 to 500 words in length. The

(Continued on page 64 A)

Circle No. 144 on Readers' Service Card

UNIMODULAR 4000 SERIES GAS CHROMATOGRAPHS FOR CHEMICAL, BIOMEDICAL, PESTICIDE ANALYSIS

EXCLUSIVE FEATURES – All Standard

Most advanced 4-column oven – allows unparalleled column-detector combinations. All-glass or metal columns. ■ **4 universal injection ports.** For use with 1/16 to 3/4" columns. ■ **Up to 4 detector ovens,** each individually temperature controlled on standby for immediate operation. ■ **Vibrating reed electrometer.** All solid-state design. Drift less than 1% per month. Sensitivity 3×10^{-13} amps. ■ **Digital Log Electrometer.** 1000-fold range increase. No switching or attenuation. For use with standard recorder. ■ **Priced from $2095.** Nowhere else can you obtain the combination of desirable features – plus exclusive Victoreen features – found in GC4000 Series instruments. For versatility... accuracy... stability... economy Victoreen Gas Chromatographs lead the entire field.

6960-A

VICTOREEN

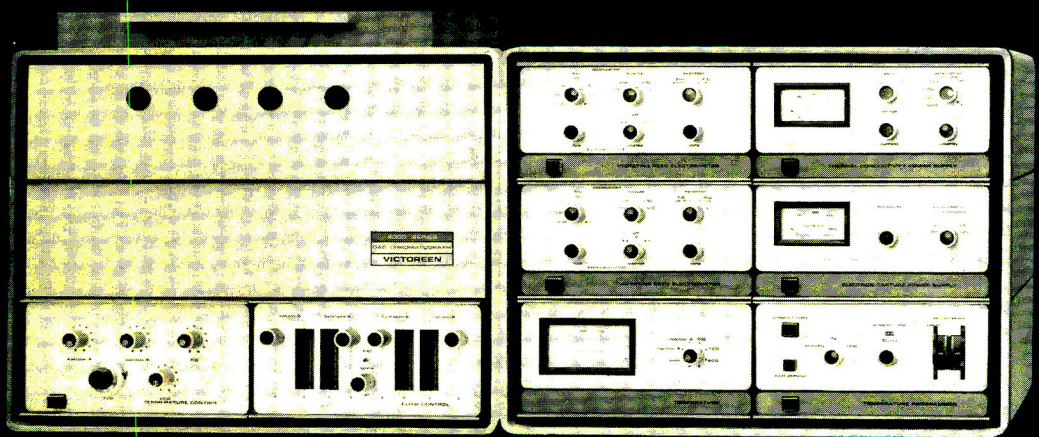

Research 4000 Series Instrument System

Analytical Instrumentation Division
THE VICTOREEN INSTRUMENT COMPANY
10101 WOODLAND AVENUE • CLEVELAND, OHIO 44104
EUROPEAN SALES OFFICE GROVE HOUSE, LONDON RD., ISLEWORTH, MIDDLESEX, ENGLAND

VICTOREEN

Is there

SO_2

in your air?

Measure and Record it . . .
Accurately and Continuously
with the S/I Model 65-8
SO_2 ANALYZER/RECORDER

A direct, quantitative and specific method for measuring sulfur dioxide, by volume, in the air.

HIGH ACCURACY...
Concentrations of SO_2 as small as 1 pphm, by volume, can be measured and recorded.

WIDE OPERATING RANGE...
Four pre-set ranges — (0—.04, 0—.1,0—.4,0—1 ppm) — with built-in inter-range calibrations.

AUTOMATIC CYCLING...
Automatic flushing and cycling capability from 2 to 30 minutes for full scale deflection.

PORTABLE...
Weighs only 30 pounds net.
Measures only 10" x 14" x 14".
Operates on 110v., 60cy.

INEXPENSIVE...
Cost is substantially less than any comparable unit.
Only $1,775.00 fob factory.

Call or write for detailed literature.

S/i Scientific Industries, Inc.

15 Park Street,
Springfield, Massachusetts, 01103
(413) 732-6233

"See Laboratory Guide for all Products/Sales Offices"
Circle No. 128 on Readers' Service Card

Scheduled Courses in Analytical Techniques

Aug. 1 to 5—Infrared and Ultraviolet Absorption Spectroscopy. Arizona State University. *Contact:* Jacob Fuchs, Department of Chemistry, Arizona State University, Tempe, Ariz.

Aug. 1 to 5—Photographic Emission Spectroscopy Course. Waltham, Mass. *Contact:* Director, Jarrell-Ash Training Institute, 590 Lincoln St., Waltham, Mass. 02154.

Aug. 1 to 5 and 8 to 12—Direct Reading Spectroscopy Course. Waltham, Mass. *Contact:* Director, Jarrell-Ash Training Institute, 590 Lincoln St., Waltham, Mass. 02154.

Aug. 8 to 12—Measurements of the Appearance Properties of Materials. Park Arlington Motel, Arlington, Va. *Contact:* Hunter Associates Laboratory, Inc., 9529 Lee Highway, Fairfax, Va. 22030.

Aug. 8 to 12—Technique of Infrared Spectroscopy. MIT. *Contact:* Dr. J. M. Austin, Director of the Summer Session, Room E19-356, Massachusetts Institute of Technology, Cambridge, Mass. 02139.

Aug. 8 to 12—Short Course on Gas Chromatography for Practicing Chromatographers. Colorado Woman's College, Denver, Colo. *Contact:* Dr. C. E. Borchers, ISA Gas Chromatography Short Course Coordinator, Instrument Society of America, 530 William Penn Place, Pittsburgh, Pa. 15219.

Aug. 15 to 18—Atomic Absorption Spectrometry Course. Waltham, Mass. *Contact:* Director, Jarrell-Ash Training Institute, 590 Lincoln St., Waltham, Mass. 02154.

Aug. 15 to 19—Applications of Infrared Spectroscopy. MIT. *Contact:* Dr. J. M. Austin, Director of the Summer Session, Room E19-356, Massachusetts Institute of Technology, Cambridge, Mass. 02139.

Aug. 15 to 26—Modern Industrial Spectroscopy. Arizona State University. *Contact:* Jacob Fuchs, Department of Chemistry, Arizona State University, Tempe, Ariz.

Aug. 22 to 26—Nuclear Magnetic Resonance Workshops. Rutgers, The State University. Aug. 22 to 24, Introductory Workshop; Aug. 25 to 26, Advanced Workshop. *Contact:* Mr. Frank Dee, Bldg. 1440, Kilmer Area, Rutgers, The State University, New Brunswick, N. J.

Aug. 22 to 27—Course in Modern X-Ray Spectroscopic Research. State University of New York at Albany. *Contact:* Dr. Henry Chessin, Physics Dept., State University of New York at Albany, 135 Western Ave., Albany, N. Y. 12203.

Aug. 22 to 26—Infrared Course. Philadelphia, Pa. *Contact:* Sadtler Research Laboratories, Inc., 3314 Spring Garden St., Philadelphia, Pa. 19104.

Aug. 22 to 26—Gas Chromatography Course. Philadelphia, Pa. *Contact:* Sadtler Research Laboratories, Inc., 3314 Spring Garden St., Philadelphia, Pa. 19104.

Aug. 23 to 27—First Infrared Spectroscopy Session of the 17th Annual Fisk University Schedule. *Contact:* Director, Fisk Infrared Institute, Box 8, Fisk University, Nashville, Tenn. 37203.

Aug. 23 to 27—Gas Chromatography Session of the 17th Annual Fisk University Schedule. *Contact:* Director, Fisk Infrared Institute, Box 8, Fisk University, Nashville, Tenn. 37203.

Aug. 27 to 28—ACS Short Course on Computer Programs in Chemical Research. University of Maryland Computer Science Center, College Park, Md. *Contact:* Dr. Moses Passer, American Chemical Society, 1155 Sixteenth St., N. W., Washington, D. C. 20036.

Aug. 29 to Sept. 2—Second Infrared Spectroscopy Session of the 17th Annual Fisk University Schedule. *Contact:* Director, Fisk Infrared Institute, Box 8, Fisk University, Nashville, Tenn. 37203.

Aug. 29 to Sept. 2—Infrared Spectroscopy. Canisius College. Four simultaneous 5-day sessions. *Contact:* Dr. Herman A. Szymanski, Canisius College, 2001 Main St., Buffalo, N. Y. 14208.

Sept. 4 to 10—Summer School in Spectroscopy: Organic (Infrared and NMR) and Inorganic (Emphasis on Infrared). School of Pharmacy, Brunswick Square, London, W.C.1. and Royal Free Hospital Medical School. *Contact:* Royal Institute of Chemistry, Summer School 1966, 30, Russell Square, London, W.C.1, England.

Sept. 7 to 8—Workshop on Internal Reflection Spectroscopy. Norwalk, Conn. *Contact:* Wilks Scientific Corp., 140 Water St., South Norwalk, Conn. 06856.

Sept. 9 to 16—ACS Short Course on Thin Layer Chromatography. Three sessions, one and one-half days each: Sept. 9 to 10; Sept. 12 to 13; Sept. 15 to 16. St. John's University. *Contact:* Dr. Moses Passer, American Chemical Society, 1155 16th St., N. W., Washington, D. C. 20036.

Sept. 10 to 11—ACS Short Course on Interpretation of Infrared Spectra. Brooklyn College of the City University of New York. *Contact:* Dr. Moses Passer, American Chemical Society, 1155 16th St., N. W., Washington, D. C. 20036.

Sept. 10 to 11—ACS Short Course on Mass Spectrometry. Columbia University. *Contact:* Dr. Moses Passer, American Chemical Society, 1155 16th St., N. W., Washington, D. C. 20036.

Sept. 12 to 16—Activation Analysis Course. San Diego, Calif. *Contact:* Robert M. Watkins, General Atomic Div., General Dynamics Corp., P. O. Box 608, San Diego, Calif. 92112.

Sept. 12 to 17—Course on the Photographic Process as a Scientific Instrument. Rochester Institute of Technology. *Contact:* A. Robert Maurice, Extended Services Division, Rochester Institute of Technology, Rochester, N. Y. 14608.

Sept. 12 to Oct. 7—Uses of Radioisotopes in Research. Oak Ridge, Tenn. *Contact:* Special Training Division, Oak Ridge Institute of Nuclear Studies, Oak Ridge, Tenn. 37831. Page 57 A, Mar.

Sept. 14 to 17—ACS Short Course on Molecular Characterization of Polymers. New York University. *Contact:* Dr. Moses Passer, American Chemical Society, 1155 16th St., N. W., Washington, D. C. 20036.

Sept. 19 to 23—Infrared Course. Philadelphia, Pa. *Contact:* Sadtler Research Laboratories, Inc., 3314 Spring Garden St., Philadelphia, Pa. 19104.

Sept. 19 to 23—Gas Chromatography Course. Philadelphia, Pa. *Contact:* Sadtler Research Laboratories, Inc., 3314 Spring Garden St., Philadelphia, Pa. 19104.

Sept. 26 to 30—Nuclear Magnetic Resonance Course. Philadelphia, Pa. *Contact:* Sadtler Research Laboratories, Inc., 3314 Spring Garden St., Philadelphia, Pa. 19104.
Sept. 26 to 30—Advanced Infrared Course. Philadelphia, Pa. *Contact:* Sadtler Research Laboratories, Inc., 3314 Spring Garden St., Philadelphia, Pa. 19104.
Sept. 28 to 29—Workshop on Internal Reflection Spectroscopy. San Francisco, Calif. *Contact:* Wilks Scientific Corp., 140 Water St., South Norwalk, Conn. 06856.
Oct. 4 to 5—Workshop on Internal Reflection Spectroscopy. Norwalk, Conn. *Contact:* Wilks Scientific Corp., 140 Water St., South Norwalk, Conn. 06856.
Oct. 6 to 8—Short Course on Gas Chromatography. Holiday Inn, South in Indianapolis, Ind. *Contact:* Dr. R. M. Brooker, Indiana Central College, Indianapolis, Ind. 46227.
Oct. 10 to 14—Infrared Course. Philadelphia, Pa. *Contact:* Sadtler Research Laboratories, Inc., 3314 Spring Garden St., Philadelphia, Pa. 19104.
Oct. 10 to 15—X-Ray Diffraction Course. Waltham, Mass. *Contact:* Director, Jarrell-Ash Training Institute, 590 Lincoln St., Waltham, Mass. 02154.
Oct. 13 to 15—ACS Short Course on Electron Spin Resonance. San Francisco, Calif. *Contact:* Dr. Moses Passer, American Chemical Society, 1155 16th St., N. W., Washington, D. C. 20036.
Oct. 17 to 21—Gas Chromatography Course. Philadelphia, Pa. *Contact:* Sadtler Research Laboratories, Inc., 3314 Spring Garden St., Philadelphia, Pa. 19104.
Oct. 17 to 21—Photographic Emissions Spectroscopy Course. Waltham, Mass. *Contact:* Director, Jarrell-Ash Training Institute, 590 Lincoln St., Waltham, Mass. 02154.
Oct. 17 to 21 and 24 to 28—Direct Reading Spectroscopy Course. Waltham, Mass. *Contact:* Director, Jarrell-Ash Training Institute, 590 Lincoln St., Waltham, Mass. 02154.
Oct. 18 to 19—Workshop on Internal Reflection Spectroscopy. Chicago, Ill. *Contact:* Wilks Scientific Corp., 140 Water St., South Norwalk, Conn. 06856.
Oct. 22 to 23—ACS Short Course on Interpretation of Infrared Spectra. Atlanta, Ga. *Contact:* Dr. Moses Passer, American Chemical Society, 1155 16th St., N. W., Washington, D. C. 20036.
Oct. 25 to 26—ACS Short Course on Interpretation of Infrared Spectra. Tulsa, Okla. *Contact:* Dr. Moses Passer, American Chemical Society, 1155 16th St., N. W., Washington, D. C. 20036.
Oct. 29 to 30—ACS Short Course on Interpretation of Infrared Spectra. Portland, Ore. *Contact:* Dr. Moses Passer, American Chemical Society, 1155 16th St., N. W., Washington, D. C. 20036.
Oct. 31 to Nov. 3—Atomic Absorption Spectrometry Course. Waltham, Mass. *Contact:* Director, Jarrell-Ash Training Institute, 590 Lincoln St., Waltham, Mass. 02154.
Nov. 1 to 2—Workshop on Internal Reflection Spectroscopy. Norwalk, Conn. *Contact:* Wilks Scientific Corp., 140 Water St., South Norwalk, Conn. 06856.
Nov. 7 to 11—Gas Chromatography Course. Philadelphia, Pa. *Contact:* Sadtler Research Laboratories, Inc., 3314 Spring Garden St., Philadelphia, Pa. 19104.
Nov. 28 to Dec. 2—Infrared Course. Philadelphia, Pa. *Contact:* Sadtler Research Laboratories, Inc., 3314 Spring Garden St., Philadelphia, Pa. 19104.
Dec. 6 to 7—Workshop on Internal Reflection Spectroscopy. Norwalk, Conn. *Contact:* Wilks Scientific Corp., 140 Water St., South Norwalk, Conn. 06856.
Dec. 7 to 9—Theory and Application of Gas Chromatography in Industry and Medicine. Philadelphia, Pa. *Contact:* Dr. Henry S. Kroman, Hahnemann Medical College & Hospital, Philadelphia, Pa.

Society for Analytical Chemists of Pittsburgh Supports Analytical Division Summer Fellowship

The Analytical Division of the American Chemical Society has announced that the Division Summer Fellowship held by James R. Birk [ANAL. CHEM. **38**, June, 65 A (1966)] is to be supported by the Society for Analytical Chemists of Pittsburgh. It will be called "The Pittsburgh Analytical Chemists Summer Fellowship."

The Society for Analytical Chemists of Pittsburgh is affiliated with the Pittsburgh Section of the American Chemical Society and together with the Pittsburgh Section of the Society for Applied Spectroscopy sponsors the Annual Pittsburgh Conference for Analytical Chemistry and Applied Spectroscopy.

Undergraduate Curriculum Conference

The Second Annual North Central States Regional Conference on Undergraduate Curriculum will be held Oct. 13 to 15 at North Dakota State University, Fargo, N. D. The general topics and speakers are listed below. Discussion groups will explore problems peculiar to these areas.

Inorganic Chemistry. Fred Basolo, Northwestern University
Physical Chemistry. L. O. Brockway (tentative), University of Michigan
Analytical Chemistry and Total Curriculum. D. N. Hume, M.I.T.
Freshman Chemistry. W. T. Lippincott, Ohio State University
Analytical Chemistry. L. B. Rogers, Purdue University

Further information is available from R. M. Fitch, North Dakota State University, Fargo, N. D.

Circle No. 109 on Readers' Service Card →

TO WORK SAFELY WITH AIR SENSITIVE MATERIALS..

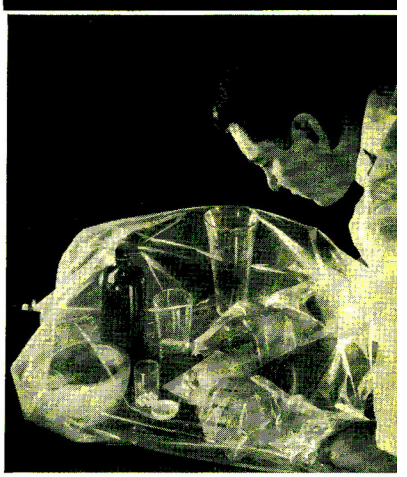

GLOVE BAG is just the thing for safe handling of air sensitive materials. Flexible and easily purged, an inflate GLOVE BAG is 17″ wide × 17″ dee × 11″ high, large enough for most ex periments (larger sizes are available) The gloves are integral—no accesso ies to buy—simply attach a cylinde of nitrogen and in a few seconds yo have that dry, inert atmosphere yo need!

After use, deflate, fold up and sav GLOVE BAG for another experimen or discard it if contaminated. Th price? An economical box of six fo $13.95 (plus postage)—specify GLOV BAG model XX-17-17

I²R

INSTRUMENTS FOR RESEARCH & INDUST
106 Franklin Ave. Cheltenham, I

THERMOLYNE®

Laboratory Apparatus for:
☑ HEAT
☐ LIGHT
☐ MOTION

Dial your temperature

on furnace type 2000

2000°F MODEL
$247.50

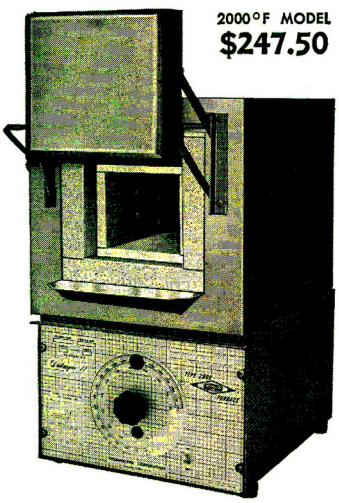

- **FULLY AUTOMATIC** electronic control—sensitive potentiometer type.
- Spot-light dial setting—**HEATS UP** to **AND HOLDS** set **TEMPERATURE.**
- Rugged, "fail-safe" design includes **THERMOCOUPLE BREAK PROTECTION.**
- **EMBEDDED HEATING ELEMENTS**—give uniform heat, protected from damage, and sag.
- **CHAMBER:** 4" Wide x 3¾" High x 9" Deep.

NEW! 40-Page complete line catalog of heat/light/motion items: furnaces, controllers, hot plates, magnetic stirrers, Stir-Plates, constant temp. apparatus, Dri-Baths, culture incubators, PBI Apparatus, lab lights, meters.

Write now for F R E E copy of Catalog 65

THERMOLYNE CORPORATION
2555 KERPER BLVD.
DUBUQUE, IOWA 52003 U.S.A.

Contact Dept. 478H for name of nearest dealer
Circle No. 70 on Readers' Service Card

CALENDAR OF EVENTS

Aug. 1 to 3	**Summer Symposium of the ACS Division of Physical Chemistry.** Michigan State University. Subject: Electron Spin Resonance Spectroscopy. *Contact:* Prof. Max T. Rogers, Dept. of Chemistry, Michigan State University, East Lansing, Mich. 48823.
Aug. 8 to 9	**Eighth Annual Rocky Mountain Spectroscopy Conference.** Albany Hotel, Denver, Colo. *Contact:* R. C. Reinke, Dow Chemical Co., Rocky Flats Division, P. O. Box 888, Golden, Colo. 80402. Page 49 A, Apr.
Aug. 8 to 12	**Gordon Research Conference on Separation and Purification.** Colby Junior College, New London, N. H. *Contact:* W. George Parks, Department of Chemistry, University of Rhode Island, Kingston, R. I. 02881.
Aug. 10 to 12	**Fifteenth Annual Conference on Applications of X-Ray Analysis.** Albany Hotel, Denver, Colo. *Contact:* Dept. of Metallurgy, University of Denver, Denver Research Institute, Denver, Colo. 80210. Page 70 A, Mar.
Aug. 15 to 19	**International Symposium on Microscopy.** Chicago, Ill. *Contact:* Walter C. McCrone, FRMS, The McCrone Research Institute, 451 East 31st St., Chicago, Ill. 60616. Page 70 A, Mar.
Aug. 15 to 19	**18th National Meeting American Association of Clinical Chemists.** Americana Hotel, Bal Harbour (Miami Beach), Fla. *Contact:* George T. Lewis, P. O. Box 359, S. Miami, Fla. 33143.
Aug. 22 to 26	**Gordon Research Conference on Analytical Chemistry.** New Hampton School, New Hampton, N. H. *Contact:* W. George Parks, Department of Chemistry, University of Rhode Island, Kingston, R. I. 02881.
Aug. 22 to 26	**Gordon Research Conference on Infrared Spectroscopy.** Kimball Union Academy, Meriden, N. H. *Contact:* W. George Parks, Department of Chemistry, University of Rhode Island, Kingston, R. I. 02881.
Aug. 28 to Sept. 4	**Sixth International Congress of Electron Microscopy.** Kyoto, Japan. *Contact:* Prof. E. Snito, Secretary General, Institute of Chemical Research, Kyoto University, Kyoto, Japan.

Coming Events

Sept. 5 to 7—Rare Earth Conference. University of Durham, England. *Contact:* Meetings Officer, The Institute of Physics and The Physical Society, 47 Belgrave Square, London S. W. 1., England.

Sept. 5 to 9—**IX International Conference on Coordination Chemistry.** St. Moritz-Bad, Switzerland. Sponsors: Swiss Chemical Society, Swiss Society of Chemical Industries, and IUPAC. *Contact:* Dr. R. Gut, IX I.C.C.C., Anorg. Chemie Eth, Universitaetstr. 6, 8006 Zurich, Switzerland.

Sept. 6 to 10—**20th Annual Molecular Spectroscopy Symposium.** Columbus, Ohio. *Contact:* Prof. Harald H. Nielsen, Ohio State University, Dept. of Physics, 174 West 18th Ave., Columbus, Ohio. 43210. Page 72 A, May.

Sept. 8 to 14—**First International Nuclear Industries Fair.** Nuclex-66, Basle, Switzerland. *Contact:* Swiss Industries Fair, Bale 21, Basle, Switzerland.

Sept. 11 to 16—**National American Chemical Society Meeting.** New York City. Includes Analytical Division Sessions. *Contact:* Program Chairman: Dr. John K. Taylor, National Bureau of Standards, Washington, D. C. 20234 or Division Secretary: Dr. Charles V. Banks, Dept. of Chemistry, Iowa State University, Ames, Iowa 50012. Page 45 A, Aug.

Sept. 12—**Symposium on the Mossbauer Effect and Its Applications in Chemistry.** Americana Hotel, New York City. *Contact:* Nuclear Science and Engineering Corp., P.O. Box 10901, Pittsburgh, Pa. 15236.

Sept. 12 to 16—**Conference on the Measurement of Nuclear Radiation.** Berkeley, Gloucestershire, England. *Contact:* Meetings Officer, The Institute of Physics and The Physical Society, 47 Belgrave Square, London S. W. 1., England. Page 68 A, Mar.

Sept. 12 to 16—**Symposium on Nuclear, Radio-, and X-Ray Chemistry.** Julich, West Germany. *Contact:* Gesellschaft Deutscher Chemiker, Geschaftsstelle, 6 Frankfurt am Main 9, Postfach 9075 Germany.

Sept. 14 to 16—**Particle Size Analysis Conference.** Loughborough, England. *Contact:* Society for Analytical Chemistry, 14 Belgrave Square, London S.W. 1, England.

Sept. 15 to 16—**Symposium on Pyrolysis-Gas Chromatography.** École Polytechnique, Paris, France. *Contact:* Dr. G. Guiochon, École Polytechnique, 17, rue Descartes, F 75, Paris, 5, France. Page 67 A, Mar.

Sept. 19 to 21—**Conference on Instrumental Optics and Optical Design.** Chelsea College of Science and Technology. *Contact:* Meetings Officer, The Institute of Physics and The Physical Society, 47 Belgrave Square, London, S. W. 1., England. Page 50 A, Apr.

Sept. 20 to 23—Sixth International Symposium on Gas Chromatography. Catholic University, Rome, Italy. Sponsor: Gas Chromatography Group of the Institute of Petroleum. *Contact:* Dr. A. B. Littlewood, School of Chemistry, The University, Newcastle upon Tyne 1, England. Page 68 A, Sept.

Sept. 24—Symposium on Gel Filtration. Istituto Superiore di Sanita, Rome, Italy. *Contact:* Dr. F. Dentice, Istituto Superiore di Sanita, viale Regina Elena, 299, Roma, Italy.

Sept. 27 to 29—Tenth Conference on Analytical Chemistry in Nuclear Technology. Mountain View Hotel, Gatlinburg, Tenn. *Contact:* Mr. L. J. Brady, Oak Ridge National Laboratory, P. O. Box X, Oak Ridge, Tenn. 37831. Page 70 A, June.

Sept. 28 to Oct. 4—International Symposium on Macromolecular Chemistry. Tokyo and Kyoto, Japan. *Contact:* Organizing Committee, International Symposium on Macromolecular Chemistry, C.P.O. Box 1966, Tokyo, Japan.

Oct. 3 to 6—National Institutes of Health Annual Research Equipment Exhibit and Instrument Symposium. National Institutes of Health, Bethesda, Md. *Contact:* Mr. James B. Davis, National Institutes of Health, Bethesda, Md. 20014. Page 65 A, June.

Oct. 3 to 7—Conference on Trace Characterization, Chemical and Physical. Washington, D. C. *Contact:* Dr. W. W. Meinke, Analytical Chemistry Division, National Bureau of Standards, Washington, D.C. 20234. Page 52 A, Aug.

Oct. 8 to 16—Second International Chemical Exhibition and the Seventeenth International Congress "Chemistry Days." Milan, Italy. Includes instruments and apparatus. *Contact:* General Secretary, Piazzale Rodolfo Morandi 2, Milano, Italy.

Oct. 10 to 12—Fifth Annual Meeting on the Practice of Gas Chromatography. Dennis Hotel, Atlantic City, N. J. Sponsor: Committee E-10 on Gas Chromatography of the American Society for Testing & Materials. *Contact:* M. G. Bloch, Socony Mobil Oil Co., Inc., Paulsboro, N. J. 08066.

Oct. 10 to 13—Association of Official Analytical Chemists 80th Annual Meeting. Marriott Motor Hotel, Twin Bridges, Washington, D. C. *Contact:* Luther G. Ensminger, Association of Official Analytical Chemists, Box 540, Benjamin Franklin Station, Washington, D. C. 20044. Page 53 A, July.

Oct. 10 to 14—Symposium on the Standardization of Radionuclides. Vienna, Austria. *Contact:* International Atomic Energy Agency, Vienna, Austria.

Oct. 11 to 13—Fourteenth Detroit Anachem Conference. McGregor Memorial Conference Center, Detroit, Mich. *Contact:* Roger E. Marce, Allied Research Products, 400 Midland Ave., Detroit, Mich. Page 73 A, May.

Oct. 11 to 14—Conference on Progress in Raman Spectroscopy. Weimar, Germany. *Contact:* Dr. H. Kriegsmann, Deutsche Akademie der Wissenschaften Zu Berlin, 1199 Berlin-Adlershof, den Rudower Chausskee 5, Berlin, Germany.

Oct. 13 to 14—Eleventh Annual Symposium on Advances in Tracer Methodology. Sheraton Plaza Hotel, Boston, Mass. *Contact:* New England Nuclear Corp., 575 Albany St., Boston, Mass. 02118. Page 70 A, Mar.

Oct. 16 to 19—ACS Western Regional Meeting. Jack Tar Hotel, San Francisco, Calif. *Contact:* R. L. LeTourneau, Chevron Research Co., P. O. Box 1627, Richmond, Calif. 94802. Page 57 A, Mar.

Oct. 17 to 19—1966 Technicon International Symposium on Automation in Analytical Chemistry. Statler-Hilton Hotel, New York City. *Contact:* Technicon Instruments Corp., Chauncey, N. Y. 10502.

Oct. 17 to 21—Joint Meeting and Equipment Exhibit. Sponsors: Calif. Section, ACS; Northern Calif. Section Society for Spectroscopy; Optical Society of America. *Contact:* John Conway, Lawrence Radiation Laboratory, University of California, Berkeley, Calif.

Oct. 17 to 21—International Conference on Electron Nuclear Hyperfine Interactions in Spectroscopy. Wellington, New Zealand. *Contact:* Dr. R. A. Golding, Royal Society of New Zealand, C/-Chemistry Division, DSIR, Private Bag, Petone, Wellington, New Zealand. Page 55 A, July.

Oct. 17 to 22—3rd Exhibition and Congress of Laboratory, Measurement, and Automation Techniques in Chemistry. Basle, Switzerland. *Contact:* Exhibition and Congress Secretariat, CH-4000 Basel 21, Switzerland.

Oct. 18 to 19—Symposium on Liquid Scintillation Counting. National Physical Laboratory, Teddington, Middlesex, England. *Contact:* Meetings Officer, The Institute of Physics and The Physical Society, 47 Belgrave Square, London, S. W. 1., England.

Oct. 18 to 20—IMEKO Symposium on Microwave Measurement. Budapest, Hungary. *Contact:* Organizing Committee of the IMEKO Symposium on Microwave Measurements, Budapest 5, P.O.B. 457, Hungary.

Oct. 19 to 21—Nuclear Science Symposium. Statler-Hilton Hotel, Boston, Mass. *Contact:* Dr. J. A. Coleman, Electron Devices Section, National Bureau of Standards, Washington, D. C. 20234. Page 65 A, May.

Oct. 23 to 25—Sixth Informal Conference on Vacuum Microbalance Techniques. Newporter Inn, Newport Beach, Calif. *Contact:* Sixth Informal Conference on Vacuum Microbalance Techniques, 7500 Jefferson St., Paramount, Calif. 90723. Page 67 A, Mar.

Oct. 24 to 26—1966 Canadian Symposium on Applied Spectroscopy. Holiday Inn Hotel, Montreal, Quebec. *Contact:* Dr. S. Barabas, Noranda Research Centre, 240 Hymus Blvd., Pointe Claire, Quebec, Canada. Page 49 A, Apr.

Oct. 24 to 27—21st Annual ISA Instrument-Automation Conference and Exhibit. New York City. *Contact:* The Instrument Society of America, 530 William Penn Place, Pittsburgh 19, Pa.

Oct. 27 to 28—1966 Midwest Regional ACS Meeting. University of Kansas, Lawrence, Kan. *Contact:* Dr. Norman Rabjohn, Dept. of Chemistry, University of Missouri, Columbia, Mo. Page 53 A, July.

Oct. 27 to 29—Southeastern ACS Regional Meeting. Kentucky Hotel, Louisville, Ky. *Contact:* Thomas H. Crawford, University of Louisville, Louisville, Ky. Page 62 A, Apr.

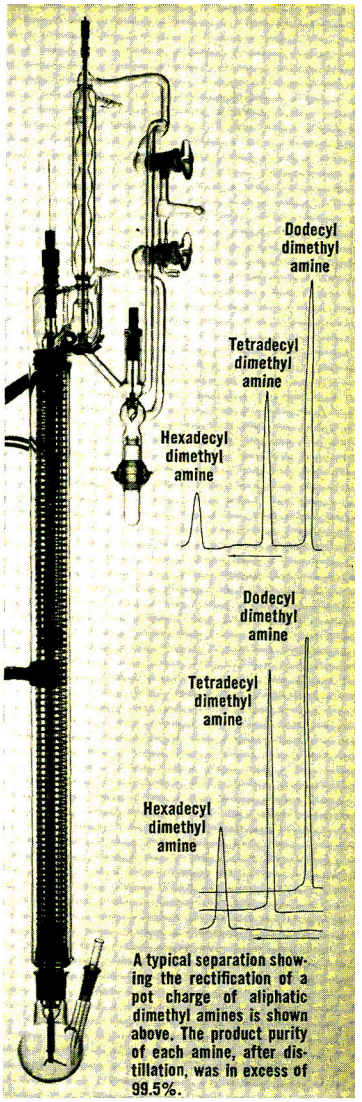

A typical separation showing the rectification of a pot charge of aliphatic dimethyl amines is shown above. The product purity of each amine, after distillation, was in excess of 99.5%.

Annular Spinning Band Distillation Column* for High Purity Separations

Nester/Faust's new Annular Still employs a **Teflon** band in annular configuration for high plate efficiency (in excess of 125 plates), low holdup (0.3 ml) and low pressure drop (3 mmHg at 50 cc boil-up) to produce **previously unattainable rectification.** Complete price is under $900. Specifications and application data are contained in Distillation Brochure PIB-65630.

Nester/Faust Glass Products Division, 2401 Ogletown Road, Newark, Delaware.
*U.S. and foreign patents pending.

NESTER/FAUST

"See Laboratory Guide for all Products/Sales Offices"
Circle No. 166 on Readers' Service Card

the versatile LOOMIS laboratory press

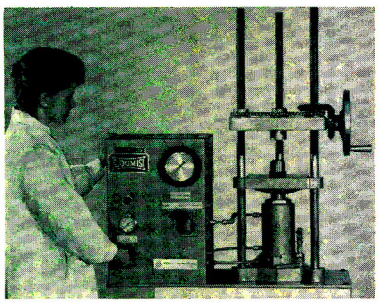

Loomis 20 ton press with compact power unit. 30 and 50 ton models also available.

- Designed and engineered for multiple laboratory use.
- Forms KBr pellets and X-ray pellets.
- Plastic molding and forming operation.
- Adapts to extrusion and isostatic pressing.
- Quick changeover with handwheel for accurate change of opening.
- Sturdy design and construction protects expensive dies. Does all kinds of testing.

Call or write:

MIDVALE-HEPPENSTALL
PRESSURE EQUIPMENT DIVISION
Nicetown, Philadelphia, Pa. 19140 Area Code 215 225-5000
Subsidiary of HEPPENSTALL COMPANY, Pittsburgh, Pa.

Circle No. 124 on Readers' Service Card

RUGGED

YET *FAST-ACTING*—THE NEW PHOTOVOLT ELECTRODES

Always ready for immediate use. Adaptable for all makes and models of pH meters. Manufactured in Photovolt's own U.S.A. plant. Choose from more than 20 different types.

Ask your Laboratory Supply Dealer, or write to:

PHOTOVOLT

1115 Broadway, New York, N.Y. 10010

Circle No. 125 on Readers' Service Card

(*Continued from page 58 A*)

abstract may be in English, French, or German but must be received before October 1, 1966.

Residential accommodations will be available at Carleton University and multilingual guides will be on hand to assist visitors. Exhibitions of instruments and books and tours of scientific establishments will be arranged. A full social program is also being planned. Further information is available from The Secretary, XIII Colloquium Spectroscopicum Internationale, National Research Council, Ottawa 7, Canada.

Industry Items

Fisher Scientific is moving from Manhattan in New York City to a new site in Springfield, N. J., early in 1967. A new building, to be erected on a 9-acre site in Union County Industrial Park, will feature automated order-handling equipment, computerized inventories, and excellent access to N. Y., N. J., and Conn. laboratories.

Operation **GRASP**, a gas chromatography review and applications study program, is designed to fit the company's gas chromatography instrumentation to the needs of the customer. The program includes 5 days of training in applied biomedical analysis by gas chromatography in **Warner-Chilcott's** modern well-equipped training laboratories at Morris Plains, N. J.

Materials testing service to industry is now available from **Harrop Laboratories.** The laboratory, located at 3470 East Fifth Ave., Columbus, Ohio 43219, will undertake sponsored testing assignments directed toward the determination of thermal characteristics of materials under a wide range of temperature and atmospheric conditions.

Honeywell, Inc., has acquired **Electro Instruments, Inc.** Electro Instruments has operations in San Diego, Calif., and Annapolis, Md. Its line of instruments includes digital voltmeters, differential voltmeters and ohmmeters, X-Y plotters, logging systems with digital printout, d.c. amplifiers, monitor oscilloscopes, a.c. potentiometers, and laboratory standards.

JEOLCO (U.S.A.), Inc., has announced that all instruments of the Electron Optics Division will be sold directly from the company which is located at 477 Riverside Ave., Medford, Mass. The instruments were previously marketed by **Fisher Scientific Co.**

The Nalge Co., Inc., has merged with **Ritter Pfaudler** of Rochester, N. Y.

Circle No. 95 on Readers' Service Card ⟶

Look at it this way... and you'll buy Kimax

This cross-sectional view shows why KIMAX® beakers are a cut above the ordinary. Walls that are uniform and heavier . . . rugged rims built to withstand long hard use . . . an improved pour-out design. And note the printed volume scale — another thoughtful improvement you now get at no extra cost. Altogether, quite a change from the beakers on the market just a few years ago.

Kimble now is offering beakers and Erlenmeyer flasks *in lower case quantities,* for convenience and economy.

Shouldn't you look at it this way, for the best value in scientific glassware?

OWENS-ILLINOIS

Maker of Kimble Products
Toledo, Ohio 43601

From Nalge research...

THE NEWEST NALGENE® LABWARE

CAT. NO. 2318

There is an advanced design concept behind this NALGENE ASPIRATOR CARBOY WITH SPIGOT. The threaded boss is molded as an integral part of the carboy... this unitary construction provides greater strength, eliminates leakage.

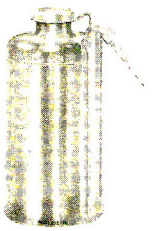

CAT. NO. 2402

This NALGENE UNITARY WASH BOTTLE* is revolutionary in design... better in every way. A unique molding technique incorporates the dispensing tube as an integral part of the polyethylene bottle. Molded of premium-quality conventional polyethylene, it is the first and only seam-free, leakproof wash bottle. *Patent pending

CAT. NO. 3118

This polycarbonate centrifuge tube with screw closure is unexcelled for high speed centrifuging. It can withstand 100,000 x G, and has the clarity of glass. Originally designed for virus vaccine studies. Just one of the full line of unbreakable NALGENE CENTRIFUGE WARE.

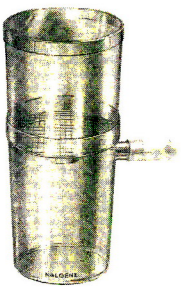

CAT. NOS. 120, 245

For the first time, a disposable membrane filter assembly that's packaged, sterile and complete. The NALGENE FILTER UNIT is always ready for microfiltrations or microanalyses. No wrapping, autoclaving or cooling, no assembly... no danger of cross-contamination.

CAT. NO. 3660

The rugged NALGENE BURETTE has an accurately calibrated column and fitted stopcock precision molded of unbreakable polypropylene. Non-freezing plug of Teflon TFE* requires no lubrication, eliminates any chance of contamination. Unaffected by the strongest caustic titrants—even HF.

*DuPont registered trademark

CAT. NO. 3662

These polypropylene NALGENE GRADUATED CYLINDERS are molded with accuracy well within the limits of Federal Specification Volumetric Apparatus Glass—DD-V-581a. The translucent polypropylene plus no meniscus helps take the guess work out of volume reading. Tipping and rolling are prevented by an octagonal base. The Nalgene 4000 ml size graduate is the largest plastic graduated cylinder available.

NALGENE LABWARE
THE NALGE CO., INC.
a subsidiary of Ritter Pfaudler Corporation

Most Nalgene Labware can be assorted for maximum discount. Order from your lab supply dealer or write for our new Catalog P-166. Dept. 8332, The Nalge Co., Inc., Rochester, N.Y. 14602.

Visit our Booth #108 at the 1966 Chemical Exposition Show, in N.Y.C., Sept. 13–15.

Circle No. 164 on Readers' Service Card

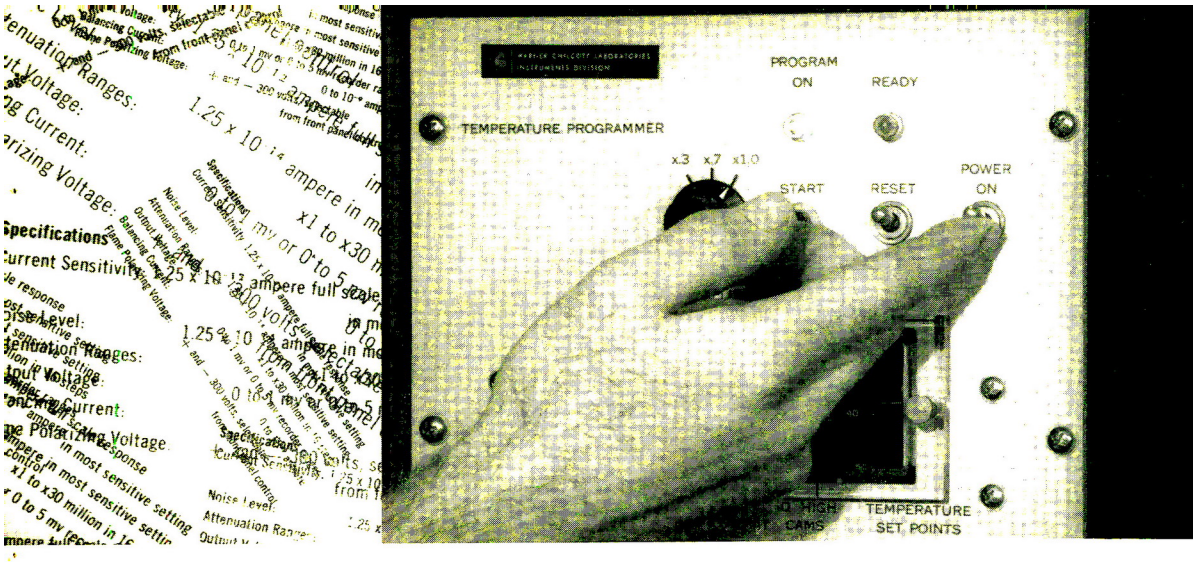

An open question to BIOANALYTICAL GAS CHROMATOGRAPHERS:

DO YOU WANT EQUIPMENT SPECIFICATIONS —OR GUARANTEED RESULTS?

With Warner-Chilcott Gas Chromatography, you get equipment that is *guaranteed* to give the results you need for your specific application. You needn't labor through pages of complex specifications—and then wonder if you've purchased the right system.

We have devised a unique new kind of customer insurance called Operation GRASP. It stands for GAS REVIEW and APPLICATIONS STUDY PROGRAM, and it's a new concept to guarantee that your Warner-Chilcott Gas Chromatograph suits *your* individual needs.

Operation GRASP consists of three major elements:

1. **A Warner-Chilcott Gas Chromatography System**—a versatile, modular system with up to 20 basic building blocks that fit into dozens of configurations depending on your biomedical applications. These include respiratory, anesthetic, and blood gases; blood and tissue volatiles; lipids; fatty acids; glycerides; phospholipids; sterols; steroids; biological toxins and narcotics; barbiturates; tranquilizers; pesticides; and carbohydrates. You get our technical recommendations on how much system capability you need—and what you don't need.

2. **The Warner-Chilcott Training Seminar.** Free to every purchaser of a Warner-Chilcott Gas Chromatography System. In one week, you learn to operate this equipment for your specific application—and you learn in our modern, well-equipped training laboratory at Morris Plains. You learn how simple Warner-Chilcott plumbing and electrical connections are—because you set up the system yourself, step-by-step, using our foolproof set-up method. You even get a certificate of achievement.

3. **You.** You are the reason why Warner-Chilcott has developed the other two elements of Operation GRASP. They're designed to make you a satisfied customer and user, and to give you a good grasp of gas chromatography principles, especially in the practical techniques you need. When you complete the seminar, your equipment will be as familiar to you as your right arm—and just as useful.

A new proficiency for applied chemical analysis by gas chromatography is the result of this combination: the Warner-Chilcott System, and Training Seminar, and You. Send in the handy coupon now and learn more about how Operation GRASP can benefit you.

WARNER-CHILCOTT LABORATORIES
INSTRUMENTS DIVISION
Richmond, Calif. • Morris Plains, N.J.

Warner-Chilcott Laboratories Instruments Division
200 South Garrard B'lvd., Richmond, Calif. 94808

Please tell me more about Operation GRASP.

Name _____ Title/Dept. _____

Company/Institution _____

Address _____ Phone _____

City _____ State _____ Zip _____

"See Laboratory Guide for all Products/Sales Offices"
Circle No. 75 on Readers' Service Card

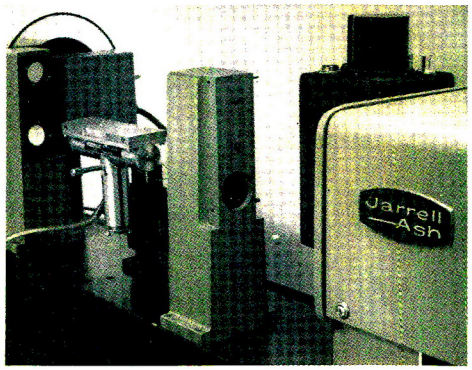

New TRI-FLAME burner delivers optimum versatility in ALL atomic absorption analyses

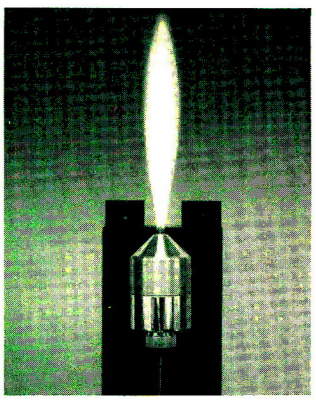

High Efficiency
Total Consumption
(HETCO) Burner

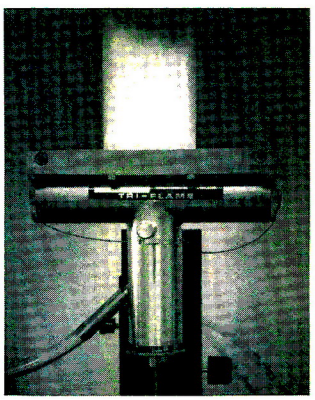

5 cm.
Nitrous Oxide
Burner

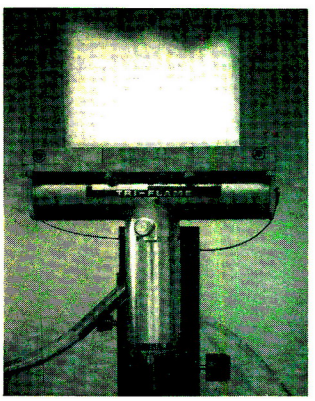

10 cm.
Laminar Flow
Burner

THREE BURNERS ALL IN ONE

A choice of the appropriate burner for any analysis is yours with the new Jarrel-Ash "slip-on" TRI-FLAME Burner. Conversion from one mode to another is done without costly time delay. The accessory is a big money saver in that it eliminates the necessity of purchasing three separate burners. The TRI-FLAME Burner is now exclusive on all Jarrell-Ash Atomic Absorption Instruments. It can be adapted also for use on other commercially-available units. Request our bulletin package containing catalogs on Jarrell-Ash's three Atomic Absorption Instruments and information on the new TRI-FLAME Burner. Jarrell-Ash Company, 510 Lincoln Street, Waltham, Mass. 02154. Telephone: (617) 899-4300. Jarrell-Ash (Europe) S.A., Rue de la Jaluse 6, Le Locle, Switzerland. Nippon Jarrell-Ash Co., Ltd., Kyoto, Japan.

Jarrell Ash

ANALYTICAL INSTRUMENTATION
SPECTROSCOPY · X-RAY DIFFRACTION
Circle No. 42 on Readers' Service Card

Advances in Analytical Chemistry and Instrumentation. Vol. 4. *Charles N. Reilley, editor. viii + 513 pages. John Wiley and Sons, Inc., Interscience Division, 605 Third Ave., New York, 16, N. Y. 1965. $16.*

Reviewed by Robert L. Pecsok, Department of Chemistry, University of California, Los Angeles, Calif. 90024.

This series, under the capable editorial direction of C. N. Reilley, continues to provide a valuable service to all chemists who are concerned with new developments in analytical techniques. Each volume has presented a variety of subjects, each treated by an authority who is active in the field.

In the first chapter (34 pp., 101 refs.) Firsching has reviewed the important contributions to "Precipitation from Homogeneous Solution" which have appeared since Gordon's monograph in 1958. He points out that nearly all precipitations can be achieved by this reproducible technique, and that in most cases, both accuracy and overall speed of analysis are improved.

Craig's chapter on "Differential Dialysis" (40 pp., 37 refs.) is a particularly valuable contribution, because it is a method which is likely to escape the attention of the average analytical chemist. Although the review is short, he summarizes the principles, materials, methodology, and applications.

The chapter by Macdonald on "The Oxygen-Flask Method" (42 pp., 159 refs.) is a review of the literature. Unfortunately, there were very few innovations during the period covered, and the result is an overly detailed catalog of applications, element by element.

Higuchi and Connors discuss a number of techniques under the title "Phase-Solubility Techniques" (96 pp., 63 refs.), including the phase rule itself, precipitation titrations, and Bobtelsky's heterometric titrations. For the most part, the discussion concerns the study of molecular complexes by solubility analysis. An extensive tabulation of stability constants for 535 systems covers over 40 pages. Most of this work was done by Higuchi and coworkers—some of it previously unpublished.

The most comprehensive, and perhaps the most valuable chapter is on "The Electrochemistry of Cation-Sensitive Glass Electrodes," (150 pp., 205 refs.) by Eisenman. This includes a thorough discussion of the two important mechanisms producing the potential across the glass membrane; viz., cation exchange and diffusion. The effect of glass composition is treated in detail and the optimum composition for various cations is given. He concludes that "anionic field strength" largely determines specificity and sensitivity to individual cations, and an empirical equation is proposed which gives the response for a mixture of cations. Many patents, special reports, and literature which is generally unavailable are summarized.

In a rather specialized treatment, Damoth discusses "Recent Advances in Time-of-Flight Mass Spectrometry" (40 pp., 34 refs.). The improved version of the Bendix instrument is described, with a number of unique applications for which this device is particularly suited.

The final chapter on "Organic Analysis with Ultraviolet-Visible Absorption Spectroscopy" by Ferguson (66 pp., 166 refs.) is a reminder that this well-known method has not been superseded by the more glamorous (and more expensive) spectroscopic techniques.

Author, Subject, and Cumulative Indexes are included. It should be noted that all manuscripts were completed within a few months of each other with essentially complete coverage of the literature through 1963 (a few later references as well). Generally, the quality is very high, although the first misprint was spotted in the seventh line of the Editor's "Introduction to the Series." This volume should be in all chemical libraries, and most analytical chemists will want a personal copy for handy reference.

Theory and Principles of Electrode Processes. *B. E. Conway. vii + 303 pages. The Ronald Press Co., 15 East 26th St., New York, N. Y. 1965. $7.*

Reviewed by R. J. Newcombe, Grimsby College of Further Education, Grimsby, Lincs, England.

A book of this type will be welcomed by research students and practicing electrochemists. For the first time a general text book has attempted to present fundamentals of the kinetics and energetics applicable to electrode reactions. The ionic double layer is treated early in this book and is followed by four chapters dealing with the adsorption and kinetic theories involved when ionic and non-ionics are taking part in the electrode reaction. Electrochemists will, I think, find these five chapters particularly useful as it has been difficult to find a modern extensive unified approach in any one textbook of the adsorption work commencing with the original ideas of Frumkin and Grahame—one has had to resort to a combination of text books and various review articles. The chapter on "Applications to Selected Problems" in which electrode processes are described under three main headings (a) gas evolution reactions, (b) ionic redox reactions, and (c) phase growth reactions, will also help to clarify the much discussed topics in electrochemistry as typified by the hydrogen over-voltage phenomena.

One minor criticism of this book might be that the author has attempted an impossible task in writing a book entitled "Theory and Principles of Electrode Processes" as this is a subject which can cover many volumes. Nevertheless Professor Conway has, I think, by careful selection of chapter topics, avoided this pitfall and as stated previously, has managed, in a mere 300 pages (including 319 invaluable references) to present a unified modern approach to the subject.

Polarographic Techniques. 2nd ed. *Louis Meites. xvii + 752 pages. John Wiley & Sons, Inc., 605 Third Ave., New York, N. Y. 10616. 1965. $19.50.*

Reviewed by Michael M. Frodyma, National Science Foundation, Washington, D. C.

The first edition of this book was designed to serve as an introduction to the field of polarography "for students, practical analysts, and research chemists generally." By selecting the topics for discussion judiciously, the author succeeded in providing a concise treatment of the theoretical and practical aspects of the field which complemented the existing polarographic literature.

The second edition is intended for the same readership and, in general, follows the same format as the first. A brief introductory chapter is followed by a chapter on instrumentation and five chapters dealing with polarographic measurements, in that order. A new chapter on voltammetric indicator electrodes other than the dropping-electrode is then introduced, and the text concludes with chapters on amperometric titrations and on such related techniques as coulometry at controlled potential.

As was true with the first edition, the book ends with appendices that contain material of interest to the practicing polarographer. Appendix A concerns

WE BUILD KNIFE-EDGE* BALANCES

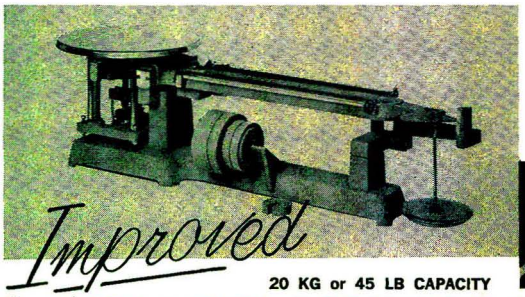

NEW UNIVERSAL END READING DEVICE

20 KG or 45 LB CAPACITY

HEAVY DUTY SOLUTION BALANCE

Now you can load or readout from front or rear with greater accuracy and speed thanks to our newly designed universal indicator.

New improved beam is designed for more rugged use too. Positive load stops prevent overloading.

Long life is assured by hollow ground tool steel knife edges and bearings.

Extensive use of cast aluminum reduces weight without sacrificing strength.

Rear poise rides on notched beam, Front poise has tension spring, and Tare poise can be locked for repetitive weighings.

Illustrated: Model 1119
$110.00

20 Kg capacity
1 gram sensitivity

113

OHAUS SCALE CORPORATION
1050 COMMERCE AVENUE • UNION, NEW JERSEY
dept. HA

Circle No. 126 on Readers' Service Card

take a good look...

at Farrand Grating
MONOCHROMATORS

- Efficient
- Rugged
- Compact
- Versatile
- Precise
- Inexpensive

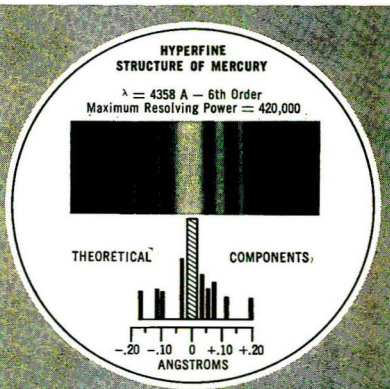

Theoretical resolving power of a Farrand Master Diffraction Grating reflecting the efficiency of Farrand Replicas.

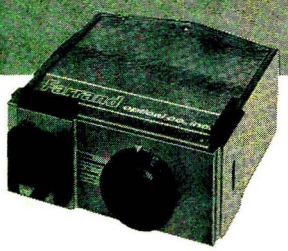

Farrand Grating Monochromators utilize the famous Farrand grating replicas and associated precision optical components . . . resulting in unusually high efficiency, excellent spectral purity and extremely low scatter. A number of models are available to cover various spectral ranges from 200 mμ to 3000 mμ. These Monochromators are ideally suited for a wide range of uses including such applications as microscope illumination, monochromatic projection and spectral measurements.

Write for descriptive literature

Farrand OPTICAL CO., INC.
535-A So. 5th Avenue
Mount Vernon, New York 10550
914-668-9393 / Cable Address: FOCIUS NY

The Pioneers in Fluorometry

Circle No. 30 on Readers' Service Card

NEW BOOKS

itself with trouble-shooting in polarographic circuits and includes several illustrative current-potential curves which should be of assistance in checking the operation of the polarograph and of the dropping-electrode assembly. Appendix B includes a 45-page listing of polarographic data for those inorganic substances deemed by the author to be of most general interest. Appendix C, which is new, presents the polarographic characteristics of approximately 600 organic compounds representative of the important polarographically active functional groups.

Although the general layout of the second edition approximates that of the first, the textual material has been almost completely rewritten and the few deficiencies noted in the first edition have been corrected. For example, whereas the first edition had no description of commercially available polarographs, the second devotes 20 pages to a comparative listing of the characteristics of such polarographs. The literature references which had previously been grouped together at the end of the text are now to be found at the conclusion of the appropriate chapters.

Perhaps the most significant change that has occurred, however, is a shift in the emphasis of the book. The new edition is approximately three times the size of the first, and much of this increase can be attributed to a considerable expansion in the theoretical sections and the inclusion of material that is probably of more interest to the advanced worker in the field than to the tyro. As a result, the second edition is more directly in competition with other monographs in the field than its predecessor. The treatment accorded the operational aspects of polarography is such, however, that the book will doubtlessly find its way into the libraries of most practicing polarographers. At the same time, the above changes plus others, such as the deletion of a series of experiments designed to introduce the beginner to the fundamental polarographic operations, have resulted in leaving the field open for a concise manual more closely approximating the size and scope of the first edition.

Practical Clinical Enzymology. *J. King. viii + 363 pages. D. Van Nostrand Co., Inc., 120 Alexander St., Princeton, N. J. 1965. $12.50.*

Reviewed by Dr. Jacklyn B. Melchior, Chicago College of Osteopathy, Chicago, Ill.

This monograph deals with the heterogeneous group of enzymes which practicing clinicians have found to be of value in establishing diagnosis or in following the results of therapy. The

make us an offer:

Engineering calls it Dave's Bread Box. Management calls it the HSC-101 Spectrophotometer Data Processor.

It all started because Dave used to show up at every staff meeting with a litany of gripes about the length of time and high cost of running spectrophotometer data through a Comp Center for processing. So we added people and bought calculators. Not much help.

Then Dave came up with this Bread Box that compares any specimen against a standard, and processes the graph readings by magnetic tape, readout or printout.

There's also a circuit that corrects the 100% line drawn by the pen graph. You do have to make an initial correction, say, once a day, but after that it's automatic—no matter what the specimen.

Dave's Bread Box is designed so the output can be digitized and punched out, and fed through a computer or standard print-out for further processing. It can even be programmed to give the area under the curve.

Not too long ago, a customer on a plant tour saw it work and wanted it. So we built him one. We didn't give it much thought until somebody else begged for one too. Then another.

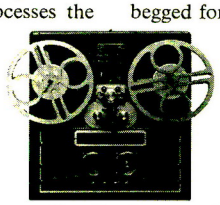

So that's when management got together and named Dave's Bread Box the HSC-101. Not a great name, but we hear, a tremendous Spectrophotometer Data Processor.

If you can use one, make us an offer. I'm interested, especially if it sells between $_____ and $_____. ☐ I'm interested, period.

NAME _____

COMPANY _____ ADDRESS _____

CITY _____ STATE _____ ZIP _____

Hoffman | INDUSTRIAL PRODUCTS

A Division of Hoffman Electronics Corporation / 700 Hoffman Dr., Santa Barbara, Calif. 93105

Circle No. 168 on Readers' Service Card

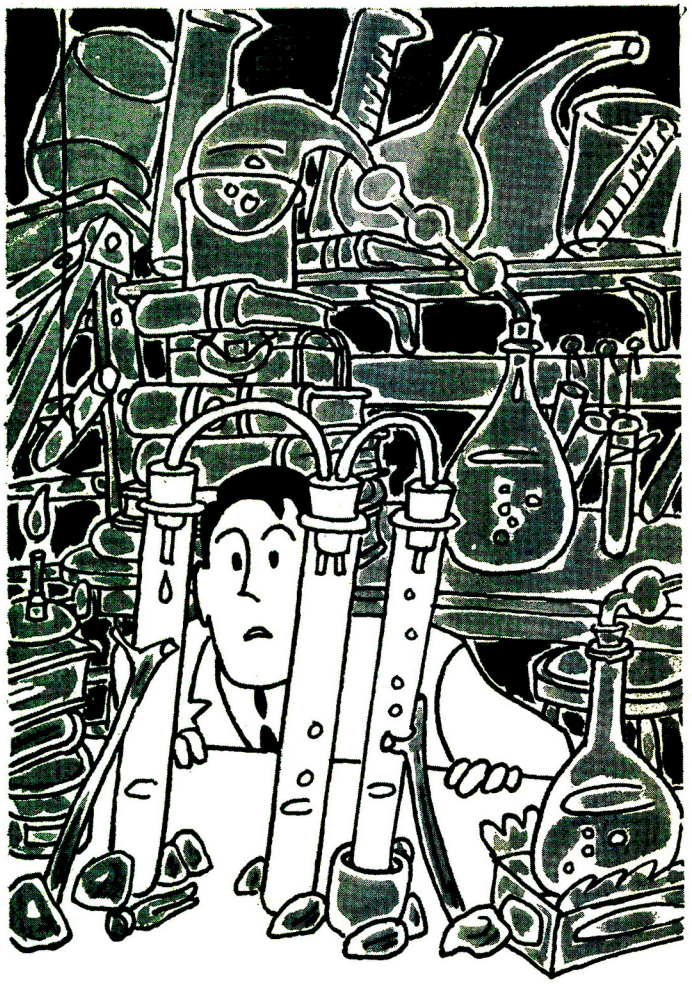

LACKING THE PROPER SUPPORT?

No need to panic. Not if you have Fisher's Castaloy®-R catalog handy. It details the special features, size, uses and price of every Fisher Castaloy-R laboratory clamp, holder and support. You have 42 good chances to find the exact appliance for your job without hunting around. Once you select it, you get it fast . . . from Fisher's nearest branch. And once you've used a Castaloy-R appliance, you'll use it again and again. It lasts almost a lifetime. Fisher's Castaloy-R appliances are versatile, durable, corrosion-resistant, strong, attractive, and about the handiest extra fingers you'll find anywhere. Let Fisher help you solve laboratory support problems. **Send for Bulletin FS-228** today—yours free by writing Fisher Scientific Company, 100 Fisher Building, Pittsburgh, Pa. 15219. J-497

FISHER SCIENTIFIC CO.

Instruments, Apparatus, Furniture and Chemicals for Laboratories

Complete stocks in all these locations: Atlanta • Boston • Chicago • Cleveland • Houston • New York Philadelphia • Pittsburgh • St. Louis • Union, N. J. • Washington • Edmonton • Montreal • Toronto • Vancouver

"See Laboratory Guide for all Products/Sales Offices"

Circle No. 32 on Readers' Service Card

author states that it is intended for hospital biochemists and medical laboratory technicians, and he appears to know his audience well.

The first fifty pages are devoted to a necessarily somewhat oversimplified survey of enzymology. This provides a readable and generally satisfactory introduction to the subject. Unfortunately, a number of statements in this section are misleading; for example, K_m is stated without qualification to be a measure of enzyme–substrate affinity (pp. 27 and 311) and lactate dehydrogenase is said to oxidize pyruvate to L-lactate (p. 2). It is hoped that these and similar errors will be corrected in future editions. The remainder of the book is devoted to a discussion of the properties and assay of specific enzymes. The methods, which are clearly described and should be easy to follow, are selected with knowledge of the instrumentation and skills generally available in a hospital clinical laboratory. Each section concludes with a brief discussion of the clinical implications. Current nomenclature is used throughout, and selected references to other texts and to original articles are generally well chosen.

Those hospital technicians who have not had a course in enzyme chemistry should find their work improved and made more interesting as a result of reading this book. Some will surely find here the stimulus to read further in the subject.

Newer Redox Titrants. *A. Berka, J. Vulterin, and J. J. Zyka. ix + 245 pages. Pergamon Press, Inc., 44-01 21st St., Long Island City, N. Y. 11101. 1965. $10.*

Reviewed by H. S. Swofford, Jr., Department of Chemistry, University of Minnesota, Minneapolis, Minn.

This monograph (200 pages) constitutes a rather exhaustive review of the chemical literature regarding the less commonly encountered redox titrants; more than 1000 references to original work are given in the text. As far as the newness of the reagents presented in the book is concerned, it might be pointed out that most of the materials have been available for years but have not enjoyed wide usage by the analyst. The monograph is well organized by chapter (30 in all), each chapter dealing with a separate redox material. The various chapters are sectionalized according to: 1—a brief discussion, 2—preparation of standard solutions, 3—methods of end point detection, and 4—a review of the determinations dealing with the applications of the particular reagent to analysis. Among the numerous methods outlined in the "Re-

Circle No. 36 on Readers' Service Card→

gilford

SPECTROPHOTOMETERS

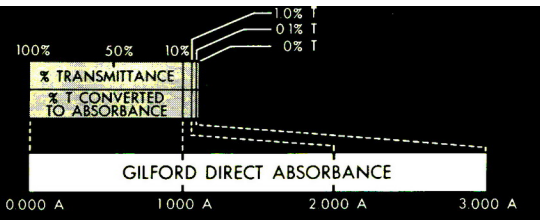

Gilford Spectrophotometers utilize a unique principle to measure Absorbance ***directly.*** The second and third decades, severely compressed in %—transmittance instruments, are fully expanded in Gilford Instruments—for equal accuracy and resolution throughout the complete range. Absorbance is presented digitally to 0.001 **A** —from 0.000 **A** to 3.000 **A** — or it can be readily recorded. Concentration is measurable directly over a 1000:1 range.

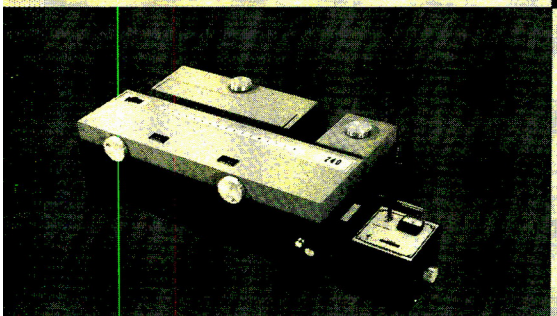

MODEL 240 SPECTROPHOTOMETER

The Model 240 spectrophotometer combines a quality Gilford-designed monochromator with the dependable Gilford photometric system. This combination has produced an instrument of unusual accuracy, range, and versatility—simple to operate and highly productive. The optical system, characterized by low stray light and high UV efficiency, features linear wavelength and slit width controls with numerical indication. A rugged optical-bench accessory mount and clear, uncluttered exit aperture plane promote easy alignment and quick interchange of attachments. The wide range—0.000 to 3.000 A—photometer is a linear absorbance measuring system of high resolution. Stabilizers for the photometer and dual-lamp source are contained in a single solid state supply module. Equipped with a four-position manual cell positioner.

MODEL 2000 AUTOMATIC SPECTROPHOTOMETER

The Model 2000 is a versatile, all-purpose spectrophotometer of superior range, stability, and photometric resolution. It is packaged into two self-contained units: (1) The lamp source, monochromator, automatic cuvette positioner, and photometer/indicator unit. (2) The main console with controls, recorder, power source, photometric circuit, line-voltage regulator, extended cuvette dwell-timer (up to 15 minutes), and circuitry and connections for additional accessories. The Model 2000 is particularly suited for determining time-dependent reaction rates and for automatic, quantitative monitoring of effluents from multiple chromatographic columns or density gradient tubes. Other applications include observation of dissolution and polymerization changes, spectrophotometric titration, precision turbidimetry and colorimetry, large-scale clinical testing, and industrial process and quality control.

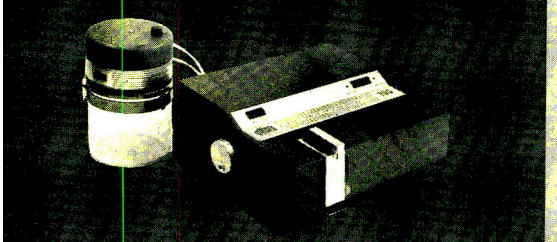

MODEL 300 MICRO-SAMPLE SPECTROPHOTOMETER

The Model 300 is a new concept in precision absorbance spectrophotometry. It is a moderately priced, compact, integrated system whose photometric range and accuracy, combined with a unique rapid sampling system, provide a versatility and simplicity of operation unmatched by complex and costly instruments. The unusual capability of the Model 300 is achieved through the use of three new Gilford elements: a solid-state photometer, an excellent optical system, and a vacuum-driven sampling system coupled to a digital absorbance indicator. Accurately metered samples of 500 microliters or less may be analyzed at a rate of 4 to 6 per minute. The sample cell is filled, the absorbance measured, and the cell flushed by means of a single control lever. Absorbance range extends from 0.000 to 2.000A.

Write or call for specifications and quotation.

GILFORD INSTRUMENT LABORATORIES INCORPORATED

Oberlin, Ohio 44074 • Telephone: (216) 774-1041 • Cable: GILLAB

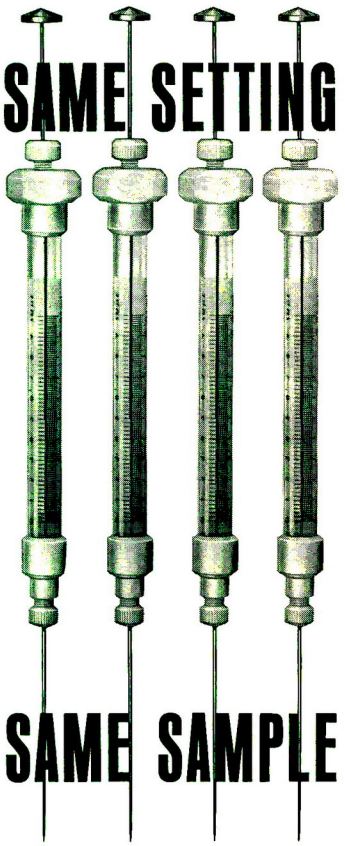

½% reproducibility with Lab-Crest Micro-Syringes*

Accurate chromatograms depend on accurate samples . . . and Lab-Crest Micro-Syringes *double* present accuracy standards. Delivered volume repeats within 0.5% in same syringe; within 1% in *different* syringes. All standard syringes in the Lab-Crest line are gas tight. No need to specify special gas tight syringes.

Du Pont Teflon® assures tight seal *regardless* of plunger position. Needles and other parts are easily interchangeable in your lab . . . and available from stock. Capacities from 10 to 500 microliters available, from stock. Request Catalog 82A780 for complete specifications and prices.

**Patent applied for*

FISCHER & PORTER COMPANY

Lab-Crest® SCIENTIFIC DIVISION

1586 County Line Road
Warminster, Pa. Phone 215-675-6000

Laboratory and Scientific Glassware • Special Glass Fabrication • Glass Process Pipe and Drainline

Circle No. 102 on Readers' Service Card

view of Determinations" sections many involve difficult experimental procedures and it is doubtful in many cases whether such methods would be preferred over well established titrimetric techniques. In summary it might be said that, although the text material is presented in an unstimulating and noncritical fashion, within the narrow limits the authors set forth in the preface the book should prove to be a valuable reference for workers in the field. Its price will limit its acquisition by many analysts.

NEW BOOKS

Electrophoresis. A Practical Laboratory Manual. *S. T. Nerenberg. viii + 264 pages. F. A. Davis Co., 1914 Cherry St., Philadelphia, Pa. 19103. 1966. $9.50.*

Theory and instrumentation including the electrophoretic cell components and power supplies are discussed. Supporting media, methods of quantitative measurement, and application to specific biochemical problems are presented.

Mass Spectrometry. *R. I. Reed, editor. x + 463 pages. Academic Press Inc., 111 Fifth Ave., New York, N. Y. 10003. 1965. 105 s.*

The papers appearing in this volume represent the contributions to the NATO Advanced Study Institute on Mass Spectrometry held at the University, Glasgow, August 1964. Design, operation, and theoretical aspects of mass spectrometry are presented.

Gravimetric Analysis. Part III. *Laszlo Erdey. vii + 301 pages. Pergamon Press Inc., 44-01 21st St., Long Island City, New York, N. Y. 11101. 1965. $7.50.*

The separation and determination of non-metallic elements are covered in this volume. Halogen compounds, sulfur, nitrogen, phosphorus, carbon, silicon, and boron are the elements studied. The appendices include the solubility products of analytical precipitates, stoichiometric factors, logarithm tables, and interpolation diagrams. Author and subject indexes are included.

Progress in the Chemistry of Fats and Other Lipids. Vol. VIII, Part 3 (Chromatography). *Ralph T. Holman, editor. 119 pages. Pergamon Press, Inc., 44-01 21st St., Long Island City, New York 11101. $6.50.*

The thin layer chromatography of methyl esters, triglycerides, sterols, and phospholipides is presented. Apparatus, solid supports, complexing agents and the formation of derivatives are described. Paper chromatographic methods for the analysis of fatty acids and esters, neutral lipids and phospholipids, which are of value comparable to the thin layer methods, are presented. The chapter on column chromatography describes the physical setup, adsorbents, and procedural details. References are included with each section.

Surface Chemistry. *Per Ekwall, Kjell Groth, Vera Runnstrom-Reio, editors. 315 pages. Academic Press, Inc., 111 Fifth Ave., New York, N. Y. 10003. 1966. $15.50.*

This volume contains the Proceedings of the Second Scandinavian Symposium on Surface Activity presented in Stockholm, November 18–19, 1964.

Among the subjects covered are solubilization of steroid hormones, the behavior of micellar solution during gel filtrations, the biological degradation of surfactants, and phase equilibria in aqueous three-component systems of amphilic substances.

Progress in Nuclear Energy. Series IX. Vol. 4, Pt. 3. Analytical Chemistry. *H. A. Elion and D. C. Stewart, editors. 20 pages. Pergamon Press Inc., 44-01 21st St., Long Island City, New York 11101. 1965. $1.75.*

"The Use of Neutron Generators in Activation Analysis" by J. E. Strain is the title of this monograph. Construction, operating conditions, applications, and safety considerations are included.

The Electron Microprobe. *T. D. McKinley, K. F. J. Heinrich, and D. B. Wittry, editors. xvi + 1035 pages. J. D. Wiley & Sons, Inc., 605 Third Ave., New York, N. Y. 10016. 1966. $27.50.*

The proceedings of the symposium sponsored by the Electrothermics and Metallurgy Division of the Electrochemical Society, held in Washington, D. C., October 1964, are presented in this volume.

New techniques and instrumentation, quantitative analysis involving computer programs, intensity corrections, X-ray absorption uncertainty and other concepts, and the applications of the electron microprobe to the study of light elements and metal systems are presented.

If the heating system you want hasn't been built yet... build it!

It's simple—with Lindberg Hevi-Duty building blocks of heat. These flexible, low-cost elements can be assembled in countless ways.

They're perfect to heat piping systems where liquids must be kept at constant temperature. Or for special lab requirements that don't justify a furnace. Or where there isn't a furnace to do the job.

They have excellent capacity. High watt density. 1000° or 1200° C. Control them manually, or automatically.

They're available from leading lab dealers in sizes, shapes, and lengths to fit your projects.

Write for bulletin 50910, Lindberg Hevi-Duty, Watertown, Wis. 53094.

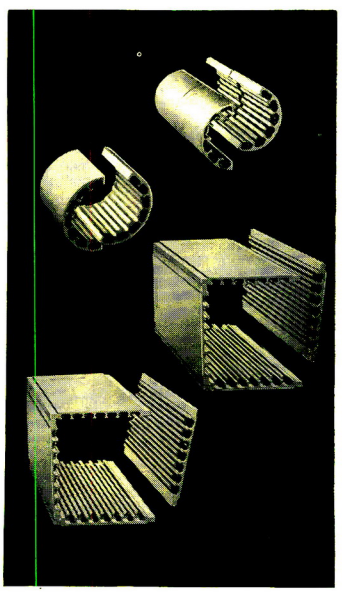

LINDBERG HEVI-DUTY SB

DIVISION OF SOLA BASIC INDUSTRIES

"See Laboratory Guide for all Products/Sales Offices"
Circle No. 130 on Readers' Service Card

NEW BOOKS

Absorption Spectra in the Ultraviolet and Visible Region. Vol. VI. *L. Lang, editor. 412 pages. Academic Press, Inc., 111 Fifth Ave., New York, N. Y. 10003. 1966. $22.*

Data sheets containing the structural formula, spectra, absorbance, solvent, instrument used, and path length are included in this volume. Compounds are indexed by name and formula. Author index and bibliography are also included.

Pesticide Index. *3rd ed. Donald E. H. Frear, editor. 295 pages. College Science Publishers, P. O. Box 798, State College, Pa. 1965. $6.*

The purpose of this volume is to present a glossary of pesticide chemical names. Approximately 4600 pesticides are listed alphabetically by official name. Common names, structural formulae, physical properties, toxicity data, and use are included.

Dictionary of Chemistry and Chemical Technology in Six Languages. *2nd revised edition. Z. Sobecka, W. Choinski, and P. Majorek, editors. 1325 pages. Pergamon Press Inc., 44-01 21st St., Long Island City, N. Y. 11101. 1966. $30.*

This edition, a revision of the "Dictionary of Chemistry and Chemical Technology in Four Languages" edited in 1962, has been expanded by the inclusion of French and Spanish.

Included in the dictionary are approximately 12,000 terms from branches of theoretical and applied chemistry, arranged in alphabetical order of the English terms and numbered consecutively. Indexes of English synonyms for chemical compounds and indexes of the other languages—German, Spanish, French, Polish, and Russian—are arranged alphabetically with reference to the numbers where the corresponding terms in all six languages are given.

Dünnschichtchromatographie in der Aminosäure- und Peptid-chemie. *György Pataki. xx + 250 pages. Walter de Gruyter & Co. Berlin W 30. Genthiner Strasse 13. Germany. 1966. DM 38.*

Apparatus, techniques, and methodology for the analysis of amino acids and peptides derived from protein and peptide hydrolysates and biological materials are described. Illustrations and references are included.

TIRED OF BEING A **PLUMBER?** GET INSTANT RELIEF WITH "CHEMINERT" FITTINGS AND VALVES

designed specifically for liquid chromatography and chemical analysis systems

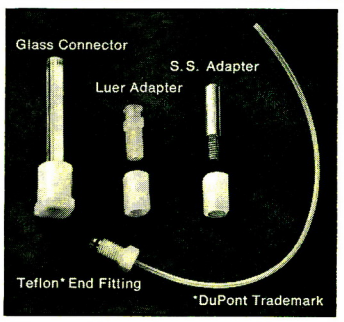

Chemically inert
Zero dead volume
500 psi pressure rating
For 1/16" Teflon* tubing

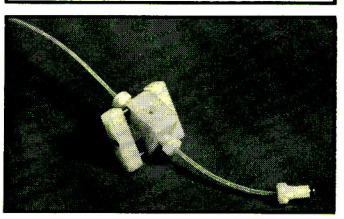

"Cheminert" valves eliminate the problem of dead volume or mixing cavities in flow shut-off and flow switching. Available in 2-way, 3-way and 4-way designs.
Write for literature.

CHROMATRONIX
INCORPORATED
2743 8th St., Berkeley, Calif. 94710
Phone: (415) 841-7221

Circle No. 23 on Readers' Service Card

New Micro Bellows® Metering Pumps

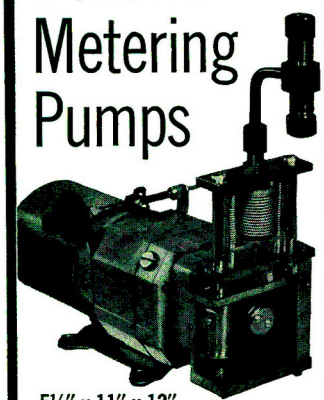

5½" x 11" x 12"

Micro Bellows Pumps, proven for 17 years in major research labs, are ideal for exact metering of contaminant-free materials into your process.

The new SM Model features a variable speed constant torque gear head motor and new micrometer adjustment on the bellows stroke length allowing for a wide range of pumping variations and accurate resetting of flow.

All wetted parts are type 316 stainless—no O rings—gaskets or packing glands to leak or cause contamination.

¾" Bellows Model Shown $345.00. For complete information contact:

RAC

See us at the ACS Show — Booth No. 604

Research Appliance Company
Route 8, Allison Park, Pennsylvania
(Pittsburgh District)
Engineering specialists in research apparatus

Circle No. 83 on Readers' Service Card

U. S. Government Publications

Guide to the Analysis of Pesticide Residues. Vols. I & II. *H. P. Burchfield and Donald E. Johnson. U. S. Department of Health, Education and Welfare. U. S. Government Printing Office, Washington, D. C. 20402. 1965. $12.75 per set.*

This guide is recommended for use in pesticide research and is not intended for regulatory or enforcement purposes. Procedures for the detection of chemical pesticides and their metabolic by-products in human and animal tissues, water, food, soil, and plants are given.

The following publications can be obtained from the Clearinghouse for Federal Scientific and Technical Information, U. S. Department of Commerce, Springfield, Va. 22151.

An Improved Flame Spectrophotometer for Biologic Calcium Analysis. *14 pages. Aerospace Medical Division, Brooks AFB, Texas. 1966. Order AD-628759. $1.*

The calcium content of biological fluids can be determined with an accuracy of plus or minus 1% by the modification of a commercial flame spectrophotometer. Acetylene was substituted for oxygen as the spray gas; a more sensitive adjustment of the wavelength selector, and a change in the photomultiplier circuit to provide increased current amplification with a wider range of control were the effective changes.

The Effect of Chemical Combination on the Soft X-ray K Emission Bands of Nitrogen and Carbon. *D. W. Fischer and W. L. Baun. 20 pages. Wright-Patterson AFB, Ohio. 1965. Order AD-629 103. $1. (Microfiche 50 cents.)*

Results obtained from the use of electron excitation, a lead stearate crystal, and a flow proportional counter, in the study of nitrides and carbon bands from graphite, diamond, lampblack, and some metallic carbides have shown that chemical combination has a marked effect on the shape of the X-ray K emission bands of nitrogen and carbon.

Nonlinear Phase Correction of Interferograms Obtained in Fourier Spectroscopy. *92 pages. Utah State University's Electro-Dynamics Laboratories, Logan, Utah, for the Air Force. July 1965. Order AD-624 086. $3.*

Theory and techniques of Fourier Spectroscopy are presented in this publication.

Research in Activation Analysis. *H. Arino et al. 120 pages. Union Carbide for the AEC. 1964. Order NYO-10175. $4. (microfiche $1.)*

A rapid activation analysis technique for the simultaneous determination of microgram amounts of tantalum and niobium is described. The results of studies show that as many as twelve different neutron-induced radioactive species can be separated from a single neutron-activated sample in a few hours.

Investigation of a New Type Narrow Band X-ray Detector for the Identification of Chemical Elements using Radioisotope X-ray Sources. *J. M. Brinkerhoff and R. Forsyth. 48 pages. Tracerlab, Inc., Waltham, Mass., for the AEC. 1965. Order NYO-3160-1. $3. (microfiche 75 cents.)*

A new narrow band X-ray detection system has been developed for the identification and measurement of chemical elements by means of radioisotope induced X-ray fluorescence. This report discusses an alpha and a beta system and a comparison of narrow band fluorescence and Rayleigh scattering methods.

Experimental Study of Zone Refining of the Binary System Triphenyl Antimony-Naphthalene. *M. S. Brooks and W. R. Hancock. 77 pages. Solid State Sciences Laboratories, Bedford, Mass. 1966. Order AD-630 609. $3.*

The isotope Antimony-124, formed the basis of a method for the nondestructive analysis of this system. Apparent k's were calculated with the aid of computers and the data was compared to that obtained from various mathematical models.

Abstracts of Scientific Papers Presented at the XXth International Congress of Pure and Applied Chemistry. *204 pages. Division of Isotopes Development, AEC, Washington, D. C. 1965. Order CONF-650723. $2. (microfiche $1.25.)*

Abstracts of papers discussing the physical chemistry of surface phenomena and disperse systems, radiation, inorganic, analytical, cosmic chemistry, and chemical technology are presented in this volume.

INSTRUMENTS FOR THE MICROSTRUCTURE DETERMINATION OF POROUS SUBSTANCES

FOR THE AUTOMATIC DETERMINATION OF PORE SIZES AND VOLUME AND OF THE SURFACE AREA OF MATERIALS, SUCH AS:

■ CARBON AND GRAPHITE ■ CATALYSTS ■ CONSTRUCTION MATERIALS ■ FIBROUS MATERIALS
■ FOOD AND PHARMACEUTICALS ■ CERAMICS ■ WOOD AND ROLLED PLASTICS ■ PLASTICS
■ OXIDES AND SALTS ■ SINTERED METALS

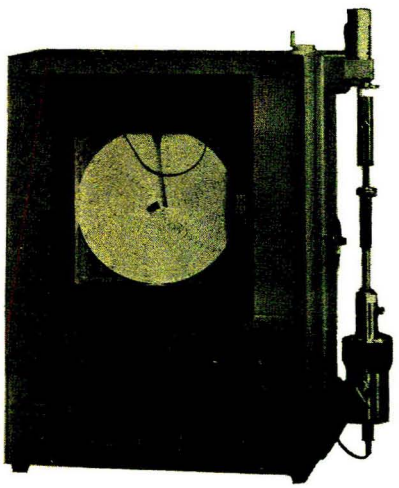

Mercury pressure POROSIMETER

According to the principle of penetration into pores of mercury under pressure (Washburn equation), the porosimeter allows the automatic determination of pores volume and distribution with radius within 75 and 75,000 Å.
A particular device permits also the determination of pores with radius within 75,000 and 750,000 Å.

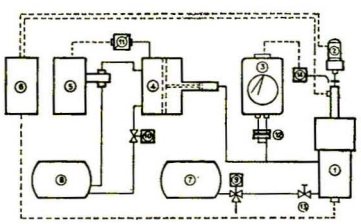

For further information please ask for the issue DT 101.

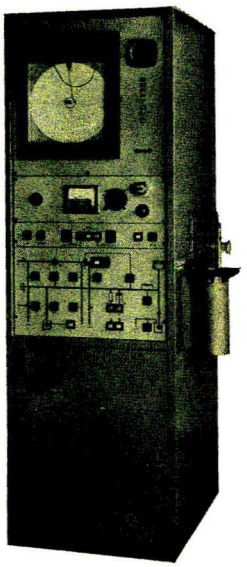

SORPTOMAT

This completely automatic instrument allows the determination of surface areas and of the distribution of pores in materials. Its high accuracy permits the measure of small surface areas (0.5 m^2/g) in accordance with the principle of Nitrogen adsorption isotherms (BET method). The absence of glass parts and mercury makes extremely easy the preliminary operation and limits maintenance to a minimum. Measurable surface areas: from 0.5 m^2/g up to 2,000 m^2/g. Valuable pores radius: from 7.5 to 300 Å.

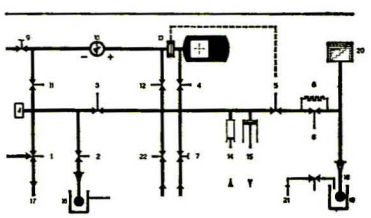

For further information please ask for the issue DT 98.

CARLO ERBA SCIENTIFIC INSTRUMENTS DIVISION
VIA IMBONATI 24 - MILANO (ITALY)

12E - AS

Circle No. 29 on Readers' Service Card

measure four chemical components simultaneously

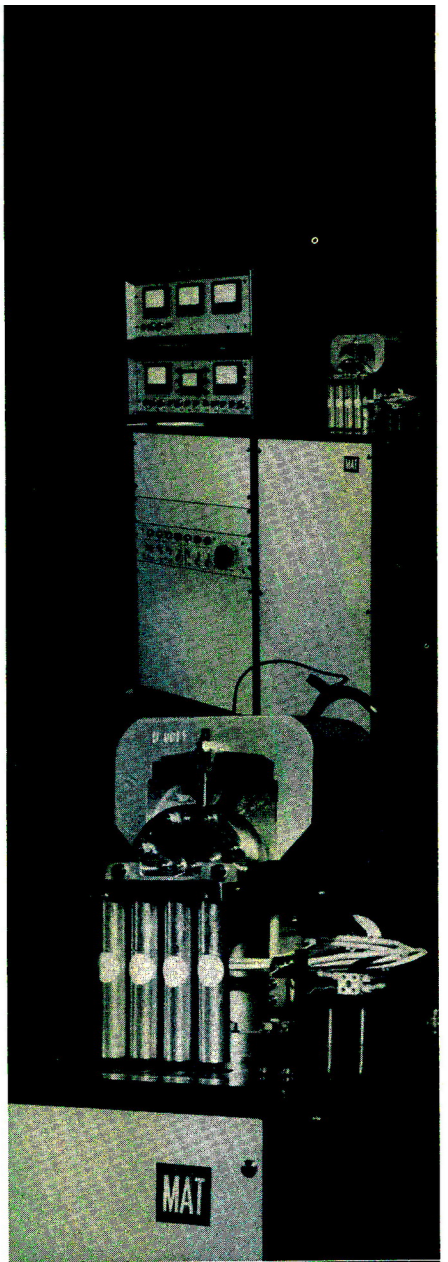

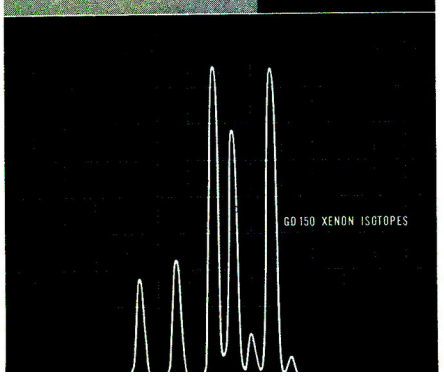

WITH THE NEW ATLAS-MAT GD 150 MASS SPECTROMETER.

The MAT GD 150 features a unique four-collector analyzer that now makes possible simultaneous measurement of almost any four peaks. Each collector can be moved individually for fast, convenient peak selection—even during operation.

The new GD 150 studies a broader range of samples than other comparable instruments. It analyzes any gas and accepts solid samples. And it measures samples as small as 1×10^{-5} cc STP—10,000 times smaller than similar mass spectrometers.

Truly the GD 150 is invaluable to the research chemist. It measures total pressure and mass spectra simultaneously. No other instrument can offer higher resolution (120—10% valley), over a wider mass range (2—300), at a lower cost. ($1500 less than equivalent instruments).

If you're interested in versatility, the GD 150 adapts for: vacuum fusion analysis • process monitoring • mixture analysis • chromatograph effluent identification • trace impurity detection • geological age dating • isotope ratio measurement • residual gas analysis • blood alcohol measurement.

Investigate the advantages of the new GD 150 now. Write for Data File A605-86.

CARY INSTRUMENTS
APPLIED PHYSICS CORPORATION
2724 S. PECK RD., MONROVIA, CALIF.

Atlas-MAT instruments sold and serviced in North America by Applied Physics Corporation
UV/VIS/IR/Raman Recording Spectrophotometers
Manual Spectrophotometers • Spectropolarimeters
Vibrating Reed Electrometers & Amplifiers

Circle No. 81 on Readers' Service Card

THE EDITORS' COLUMN

INFRARED SPECTROSCOPY is one of the most widely used instrumental tools of interest to analytical chemists. Since it is important for studying molecular structure, chemical bond strengths, and related topics, an up-to-date reference collection of reliable infrared spectra of scientific compounds is needed (see Report for Analytical Chemists, page 27 A).

The National Research Council Committee on Spectral Absorption Data and the National Bureau of Standards collaborated, in the years 1952 to 1960, in the publication and distribution of selected infrared spectral data. This collection contains spectra of about 2500 compounds and associated data plus the literature references indicating the sources of the spectra. However, the collection is about six years out of date, and many of the spectra have been superseded by better data obtained from high-precision grating spectrophotometers. These limitations preclude use of the spectra as standard *reference data*, but the information in the files can obviously be put to excellent use.

The collection consists of sets of edge-notched cards, $6^1/_2$ by $7^1/_2$ inches, and sets of $8^1/_2$ by 11 inch sheets.

The Office of Standard Reference Data of the National Bureau of Standards, upon advice of the Coblentz Society Board of Management, has decided to make these remaining sets of spectral data cards and sheets available to colleges, universities, and other nonprofit institutions whose scientific reference sources are limited.

There are approximately 30 sets of cards and 30 sets of sheets available, and the only charge will be for packaging and shipping of the

The Finest Oils, Greases, Waxes...

for High Vacuum Work—also Lubricant for High Vacuum Equipment, Masking of Circuit Boards and Other Scientific Applications

Vacuum pressures of these excellent oils are as low as 10^{-7} torr. Greases as low as 10^{-11} torr at room temperature. Scientists, who try Apiezon oils, prefer them for equipment used in nuclear physics, cyclotrons, electrical equipment, vacuum tubes, etc.; the greases for general laboratory work and gas-liquid chromatography; wax W with suitable solvent as a masking media.

As exclusive distributor in the United States, we offer immediate shipment from stock on the complete range of Apiezon products.

For applications, working characteristics, and list prices, write for new Bulletin 43-AC.

BIDDLE INSTRUMENTS

JAMES G. BIDDLE CO. 614

Electrical and Speed Measuring Instruments
PLYMOUTH MEETING, PENNSYLVANIA 19462
Phone 215/646-9200

"See Laboratory Guide for all Products/Sales Offices"
Circle No. 18 on Readers' Service Card

PHOENIX MICRO-ANALYZER

THE FIRST LOW COST HIGH SPEED Automatic-Recording AMINO-ACID ANALYZER for less than $8,000

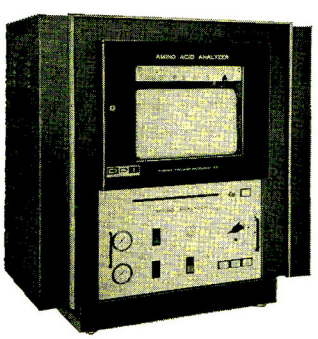

MODEL M-6800

Featuring —

- High speed analyses
- Full automation
- Compact lab bench size
- Moore-Stein or Piez-Morris operation

PHOENIX manufactures the most complete line of Amino Acid Analyzers. For complete information write

PPI

PHOENIX PRECISION INSTRUMENT CO.
A Subsidiary of CENCO INSTRUMENTS CORP.
3803-05 N. FIFTH ST., PHILADELPHIA, PENNA. 19140, U. S. A.
World Wide Sales and Service

"See Laboratory Guide for all Products/Sales Offices"
Circle No. 55 on Readers' Service Card

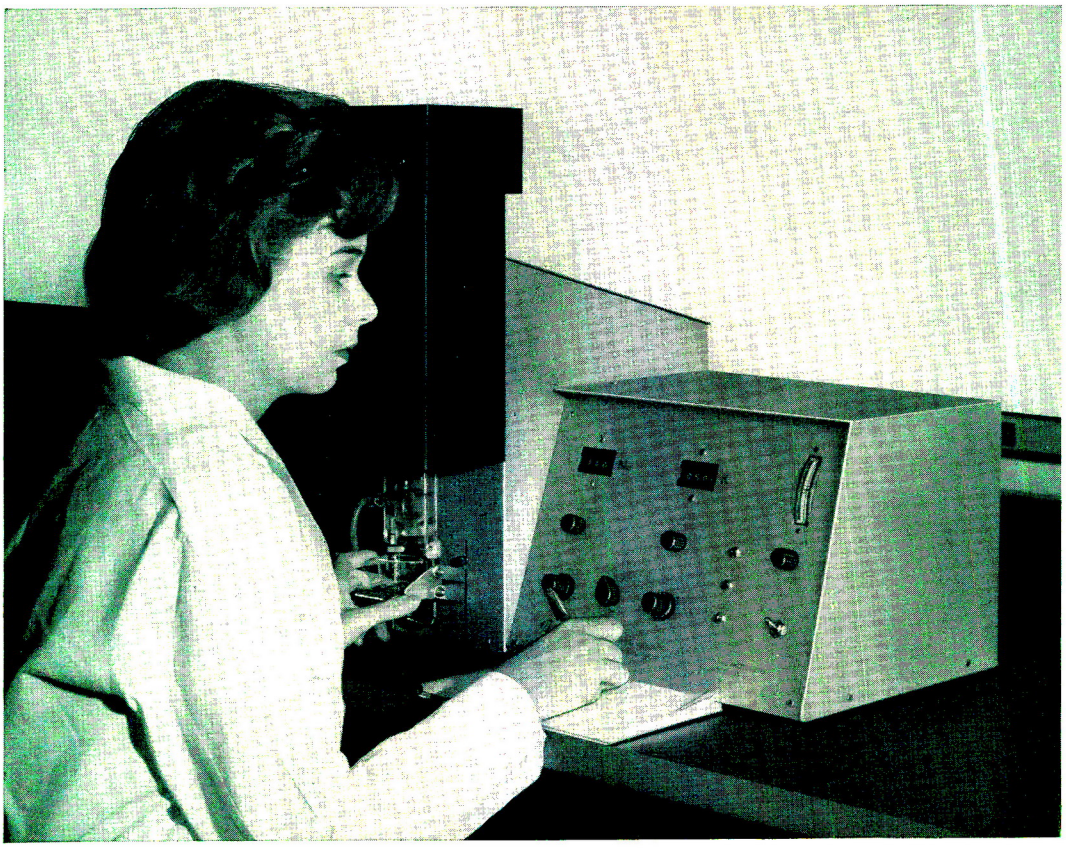

ANALYZE 30 SAMPLES FOR Na+ AND K+ IN TWO MINUTES

The answers are presented simultaneously as large, legible numbers on the new IL Flame Photometer. It is a completely solid state unit. It provides fast response, extreme wide range and a degree of reproducibility unobtainable by even the most expert and painstaking application of conventional flame photometers.

The Model 143 is a new concept in flame photometry. It is well suited for the clinical, research or industrial laboratory. The data collection system is an analog computer and results can be indicated in whatever unit of concentration you select.

One dilution (1:200) covers the entire range of concentrations seen in biological samples, thus providing great convenience when widely ranging samples such as serum and urine are being run together.

For further information call or write your nearest IL authorized dealer and let him show you how fast, accurate and reliable flame photometry has become. Or write for Instrument Data 143 and a list of users in your area.

INSTRUMENTATION LABORATORY INC.

9 GALEN STREET • WATERTOWN, MASS. 02172 • TELEPHONE (617) 926-1700

DISTRIBUTED IN THE U. S. BY ALOE SCIENTIFIC, DIV. OF BRUNSWICK; AND SCIENTIFIC PRODUCTS, DIV. OF AMERICAN HOSPITAL SUPPLY CORP.

"See Laboratory Guide for all Products/Sales Offices"
Circle No. 39 on Readers' Service Card

material. The set of 2500 cards weighs under 100 pounds; the set of sheets weighs considerably more.

Further information on the availability of this material can be obtained by writing to:

Dr. Nelson Fuson, President
The Coblentz Society
P. O. Box 730
Norwalk, Conn.

or

Dr. S. A. Rossmassler
Office of Standard Reference Data
National Bureau of Standards
Washington, D. C. 20234

Since no new data are presented, this activity is essentially an effort to make the best possible use of what would otherwise be discarded as surplus material.

Photonuclear Data Center

Information on the interaction of electromagnetic radiation with nuclei may now be obtained through the Photonuclear Data Center at the National Bureau of Standards. A current file of abstracted data on photonuclear reactions [(γ,n), (γ,p), (γ,γ) etc.], cross sections, ground state capture reactions, and electron scattering cross sections is being maintained, along with a cross-referenced index to the data in the files.

NBS Miscellaneous Publication No. 277 indexes the data in the files abstracted from papers published in the period 1955–64. Regular supplements will be issued to this annotated bibliography that contains quantitative information about the content of each paper and that furnishes a means of readily locating experimental data about a particular nucleus and reaction.

The Photonuclear Data Center is operated by the Photonuclear Physics Section at NBS under the auspices of the Office of Standard Reference Data. Further information on operations, or requests for specific data, can be obtained by telephone (301-921-2625) or by writing to the Center.

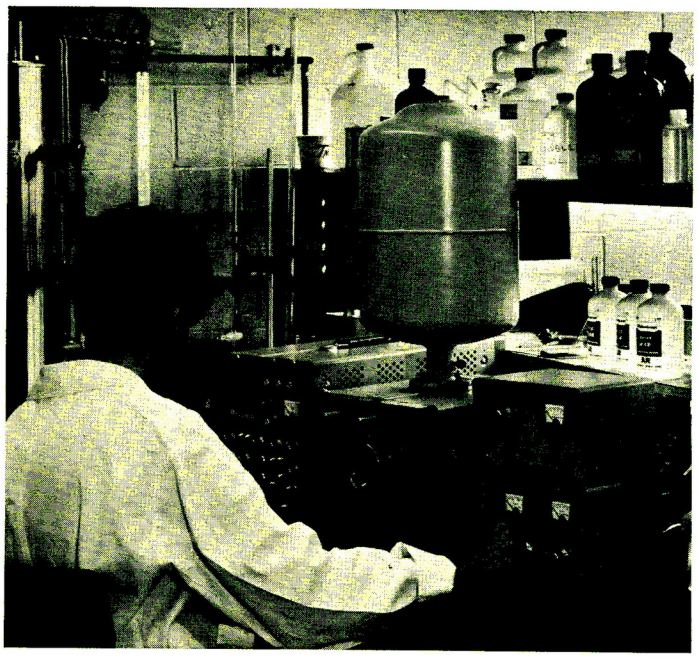

instant chemistry

Here's a new idea in nondestructive chemical analysis: fast, accurate and virtually foolproof. Using a low-level (one millicurie) gamma ray source to excite the sample, TMC's new Photon Spectrometer simultaneously identifies the component elements by measuring the energy and intensity of the secondary X-rays produced.

The entire analytical process is completely automatic from the time a sample is presented to the system until final readout. And speaking of readout, we know of no other spectrometer that offers as wide a range of analog and digital outputs: oscilloscope display, X-Y plotting, printed or punched paper tape and computer-compatible magnetic tape.

If you're interested in a faster, easier, more economical technique for analysis of elements, check these capabilities against your requirements:

- **High speed** — thirty seconds or less for heavy elements.
- **Analyzes solid, granular or liquid samples.**
- **Nondestructive analysis** — no loss or degradation of sample.
- **Simultaneous assay of all elements** heavier than calcium — readily identifies both known and unknown constituents.
- **Low cost per assay** — negligible installation costs (simply plug into 110 volt line), low power consumption, no chemical reagents, no complex sample preparation.
- **Portable** — low power consumption permits battery-powered field operation.
- **Pushbutton operation** — no special training required to operate system or to interpret results.

Typical applications for the Photon Spectrometer include on-line process control, geological surveys, quality control and mining assays. Why not add your application to this list? For complete information contact: Technical Measurement Corporation, 441 Washington Avenue, North Haven, Connecticut 06473.

TMC TECHNICAL MEASUREMENT CORPORATION

Circle No. 137 on Readers' Service Card

"Any CORNING electrode purchased by a user between July 1, 1966, and December 31, 1966, is guaranteed for a period of six months from the date of customer registration. The guarantee applies to any cause which renders the electrode inoperative during six months of normal laboratory use." Conditions:

CORNING announces the six-month guarantee on electrodes

This unprecedented guarantee frees you for six months from the costs of electrode replacement.

And all the while, you'll be using the electrodes that mark a new standard in performance and service. We couldn't guarantee them if they weren't that good.

We couldn't guarantee our CORNING® pH Electrodes with the Triple Purpose Glass Membrane if they weren't so good at giving you general-purpose *and* alkaline region *and* high-temperature performance.

If they weren't all equally good, we couldn't also guarantee our reference, combination, and metallic electrodes, that all come with full options on con-

1. Register his purchase with Corning Glass Works, Medfield, Mass., within one month of purchasing date. 2. Return the inoperative electrode directly to Medfield. Upon receipt of the registered inoperative electrode, Corning Glass Works will promptly send the user a replacement electrode free of charge.

the only electrodes so good they're guaranteed

nectors and lead lengths.

To qualify for coverage, just return a completed registration card to our plant in Medfield. Cards will be available at the time of purchase from your CORNING salesman or your local CORNING Scientific Instruments dealer.

The time is right to survey your electrode needs. Then buy CORNING, and enjoy the confidence of using the only electrodes so good they're guaranteed. Write for our electrode and instrument price list, or ask for it from your CORNING Scientific Instruments dealer.

THE NEW STANDARDS COME FROM CORNING SCIENTIFIC INSTRUMENTS

analyze formaldehyde and acetaldehyde to less than 0.1 ppm...

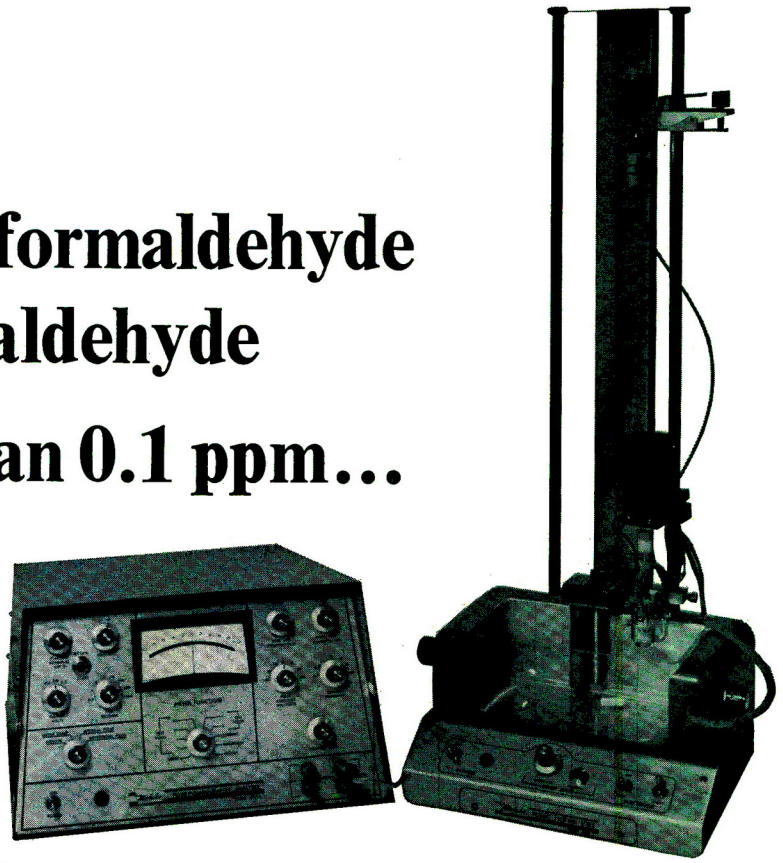

...and complete your analysis in 5-10 minutes with Melabs' CPA-3 Pulse Polarographic Analyzer! The high resolution and the high sensitivity demonstrated by this particular analysis are possible only by pulse techniques. Simple to operate, the versatile Melabs CPA-3 Analyzer gives you the choice of four operating modes with three-electrode potential control, enabling you to work effectively with high-resistance organic solutions. Peak readout on standard recorder makes interpretation simple and accurate.

Other applications of the CPA-3 include air and water pollution studies, pesticide and pharmaceutical analyses. What's your application?

Please send for literature, bibliography and list of compounds analyzed. Write Melabs, Scientific Instruments Department, 3300 Hillview Avenue, Palo Alto, California.

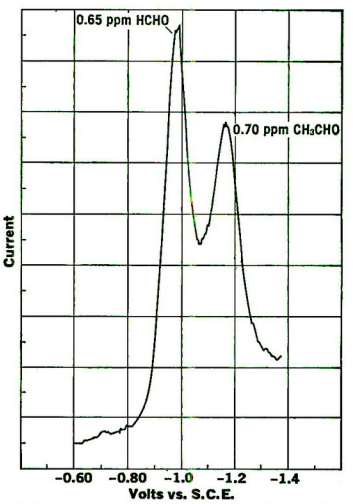

Pulse polaragram of a mixture of formaldehyde and acetaldehyde, obtained by Special Services Laboratory, Dow Chemical Company, Midland, Michigan. The aldehydes were converted to hydrazones by addition of hydrazine sulfate. This conversion greatly improves the sensitivity because the hydrazones are reduced more reversibly than the aldehydes.

Melabs®

See us at the Chemical Exposition U.S.A. Booth 901
"See Laboratory Guide for all Products/Sales Offices"
Circle No. 150 on Readers' Service Card

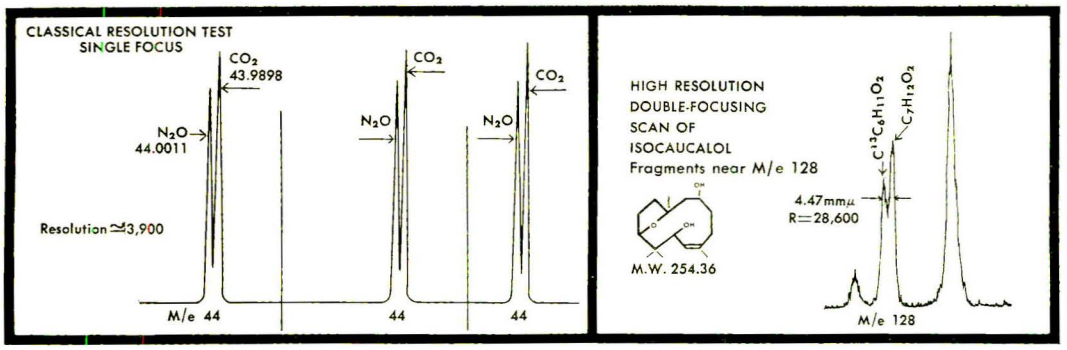

PLANNING A MASS SPECTROMETER?

The new Hitachi Perkin-Elmer RMU-6E is an instrument that gives you exceptional performance and versatility at moderate cost. It is easy to operate, compact and reliable. Its building-block design allows you to add all the analytical capability you need as your mass spectrometer program grows. For example: you can attach the electrostatic sector to allow high resolution (M/△M 10,000 routine, 30,000 attainable) and precision mass measurement (better than 1 in 200,000.) For computer-aided spectral interpretation, our new DDA-1 Digital Data Acquisition System records 12,000 twelve-bit data points per second on magnetic tape with compatible format.

• **The RMU-6E Analyzer** incorporates a 90° 8 inch-radius magnetic sector with rigid, open construction. Its high resolution results from a refined ion optical design. Aberrations are corrected to the second order, and field fringing is minimized. Its wide pole pieces give a homogeneous field across the tube. Externally adjustable slits allow translation, tilting, and width adjustments. The magnet is fully adjustable in all coordinates, and need not be re-aligned when returned to position after bakeout. The solid state electronics are designed for high resolution stability. Masses can be scanned to more than M/e 2000. Positive or negative ion scanning is standard. The all stainless steel vacuum system provides low background while allowing unattended operation without need for cold traps. Once set up, the RMU-6E analyzer requires little attention.

• **All-Glass Heated Sample Inlets** accommodate gases, liquids and solids. Sample introduction is convenient; throughput is high.

• **Dual Direct Sample Introduction into the Ion Source** produces intense spectra even at the low temperatures required with unstable samples. The amino acid spectrum below illustrates this.

• **Gas Chromatograph Connection System** heatable to 350°C with efficient all-glass helium separator allows on-the-fly identification (M/e 12-450 in 2 secs) of as little as 3 nanograms of component injected into the G.C.

• **Electron Multiplier Detector** is required for highest sensitivity and speed of analysis. It offers a gain of more than 50,000X the Faraday cup detector.

• **Precision Mass Marker** directly indicates the mass number and marks the chart for faster data interpretation.

• **Accessories** include Fox-type ion source, Knudsen cell, double collector for isotope ratio work.

The cost of a typical RMU-6E from sample inlet to electron multiplier and high speed recorder is less than $35,000. A high-resolution double-focusing instrument costs less than $60,000. Where diverse requirements exist within a single department, we have been able to install two complete high performance systems within a tight budget originally established for one mass spectrometer. For more information, or to arrange a visit to our Mass Spectrometer Demonstration Laboratory, contact Perkin-Elmer, Mass Spectrometer Department, 747 Main Ave., Norwalk, Conn. 06852.

PERKIN-ELMER

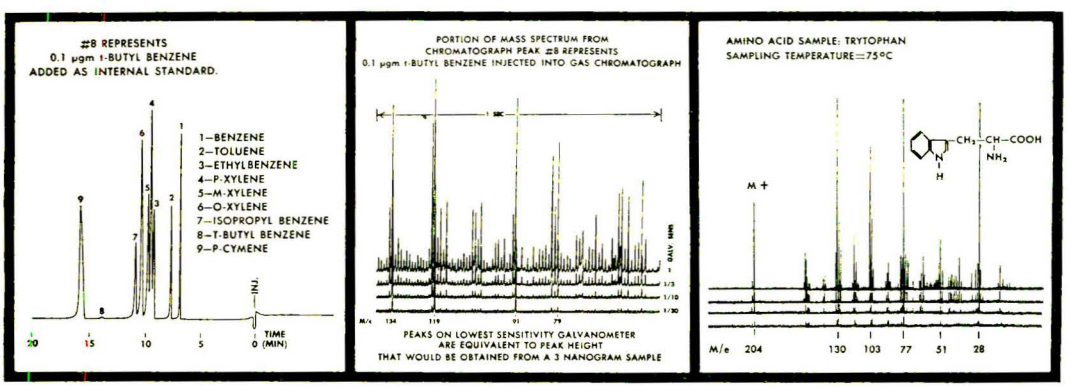

Circle No. 134 on Readers' Service Card

How to rent a mass spectrometer for three full months for $794.

(And then how to get $715 of that back.)

We are about to describe a procedure for putting a mass spectrometer in your laboratory for a full three-month period for a maximum cost to you of $794. Honest. (And the *minimum* cost can be even lower than that.) So if you have ever wished to try mass spectroscopy, this may be the time to begin.

First, the instrument in question. It's the MS-10 — a small, accurate mass spectrometer for qualitative and quantitative analysis of gases. And despite its low basic cost (only $5,290 if you'd rather buy than rent), the instrument's level of performance and accuracy doesn't have to apologize to anyone. This is a true *analytical* mass spectrometer. It is the most easily operated mass spectrometer with procedures that are quickly understood, learned and remembered. You really don't need a specialist in mass spectrometry to use this instrument. Also, the MS-10 withstands any amount of inexpert handling; it is virtually impossible to damage. (Else why would we rent them?)

The MS-10 was initially introduced in 1960 by AEI (the world leader in mass spectrometry). Since then, hundreds have gone into service throughout the world and, quite literally, there are now more MS-10's being used than any other mass spectrometer. By far. As a result, the MS-10 has been applied to more end uses than any other piece of equipment. The implication of this: the chances are good that, whatever *your* application, someone has already applied the MS-10 to it.

And comprehensive technical information on the use of the MS-10 for these many applications is available to you. Because of this, you usually don't have to start your work from scratch with an MS-10.

There are many accessories and vacuum systems available for the MS-10. Consequently, you need choose only those elements which fit the MS-10 to your specific requirements. These accessories — and every subsequent MS-10 development — are designed for easy adaptation to all existing instruments. The MS-10 will never become obsolete.

Now, we'll happily rent you an MS-10 for three months for a total cost of $794. Then, should you decide to buy it within the three-month period, 90% of your rental fee ($715) is credited to the low purchase price of $5,290.

We might as well admit that people inevitably buy the MS-10 after they've tried it. So we love to rent them. We've obviously learned that it makes sense to put the MS-10 on the road to sell itself. (To short-circuit this sequence, why not skip the rental and consider buying the MS-10 immediately?)

For more on the instrument, write for bulletin M1AC8. For more on renting the instrument, write for bulletin RM1AC8. For more on both, write for both.

PICKER AEI

PICKER NUCLEAR: 1275 Mamaroneck Avenue, White Plains, N.Y. 10605

"See Laboratory Guide for all Products/Sales Offices" Circle No. 58 on Readers' Service Card

Analytical Chemistry Is Important to the Growth of Purex

Entrance and Library at Purex Technical Center

PUREX CORPORATION has become a diversified international corporation with five operating groups. Its more than one thousand products include bleaches, toilet soaps, household and industrial detergents, and specialty cleaning compounds, floor waxes and finishes, drug and cosmetic products, paints and paint vehicles, paint strippers, various types of protective coatings, etchants and protective coatings for chemical milling, polymer emulsions and specialty resins, dye penetrant flaw-detection systems, plastic forming operations, ultrasonic cleaning devices, etc. These many and varied products call for numerous analyses and frequently the analyst must use great ingenuity to develop suitable analytical processes for some of these complex mixtures.

Corporate management, recognizing and appreciating the substantial contribution which analytical chemistry has made to the growth of Purex, has provided superior research facilities to service all operating groups by building a Technical Center at Wilmington, Calif. Analytical chemistry was one of the principal factors which influenced the decision to centralize the corporation's chemical research and development at this new facility. The cost of maintaining six small research laboratories at as many locations was becoming inordinately high, largely because of the need for library facilities and costly analytical chemical instrumentation at each of these laboratories. Management, therefore, decided to relocate all chemical research at a single place with one library and one analytical laboratory servicing all groups. This makes it possible to provide better library and analytical services for the money spent.

The Technical Center was built at Wilmington, since this was the site of the Corporation's most up-to-date and largest facility, the former Turco Products Laboratory. Also, adequate land, already owned by Purex, was available at this location. Two modern research buildings with a total floor space of 30,000 square feet were in operation at Wilmington. These buildings were tied together by a new three-level structure of 53,000 square feet floor space, giving a combined area of 83,000 square feet in the Technical Center.

The new building is rectangular in shape with a central utility core running the length of the building. Laboratories are laid out on a 10′ × 30′ modular basis on both sides of this utility corridor. All hood vents, gas, water, air, electricity, nitrogen, steam, etc., are brought in through the utility corridor, providing low cost maintenance and ready modification of facilities to meet changing needs of the various laboratories. Offices are located around the perimeter of the building with halls between the offices and laboratories.

Hoods are located at the end of each laboratory adjacent to the utility corridor to minimize duct-work connecting with that in the utility corridor. The hoods have a unique design developed by Purex. Although the hoods are relatively low in cost, their new design makes possible certain performance and operating advantages. The saving in cost in air-conditioning and heating capacity more than paid for the total cost of the hoods! The new Purex hood draws 60–80% of its air from the utility corridor, which is not air-conditioned. (In the Southern California climate no heating or cooling of this air is required. In a more severe climate, a minimum heating would be required during the very cold months.) The remaining 40–20% of the air is drawn from the laboratory, and is, therefore, air-conditioned air.

The analytical work is about equally divided between organic and inorganic determinations. Many of the mixtures analyzed contain from six to twenty components, partly organic and partly inorganic. These mixtures must be

separated by suitable techniques and the various components determined quantitatively. Extensive use is made of ion exchange, gas chromatography, infrared, visible, and ultraviolet spectrometry, as well as volumetric and gravimetric methods in these analyses.

There also are specialized analytical techniques which must be used in connection with certain processes or products. The Lawrence hydrogen detection gage is used to evaluate the possibility of hydrogen embrittlement from all cleaning, paint stripping, protective coating, or other products which are used on aircraft structural parts. Bleaching and soil removal studies have been made using radioactive isotopes as tracers and conventional counting equipment for quantitatively measuring soil removal. Our surface coating and polymer laboratories use light scattering techniques for molecular weight determinations and particle size distribution measurements. The dye penetrant and flaw detection system laboratories use optical methods in both the visible and ultraviolet regions for analyzing the results of their operations. The Chem-Mill section has special methods for evaluating maskants and etchants.

While none of the apparatus or techniques are particularly unique, they are representative of modern analytical methods requiring skill and knowledge on the part of the analyst. The significant factor to the analytical chemist is that the Purex Technical Center has provided greatly improved library and research facilities.

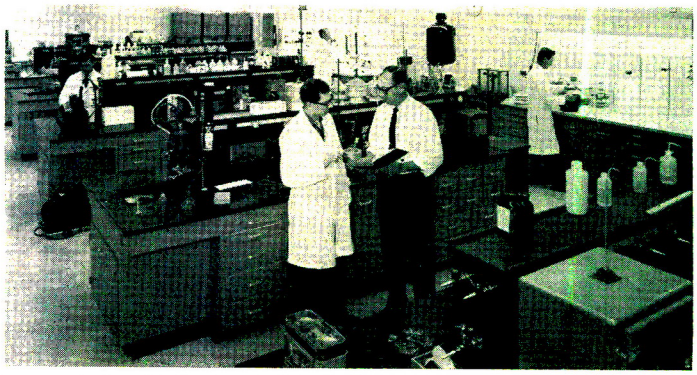

General Analytical Laboratory showing special titration benches in background

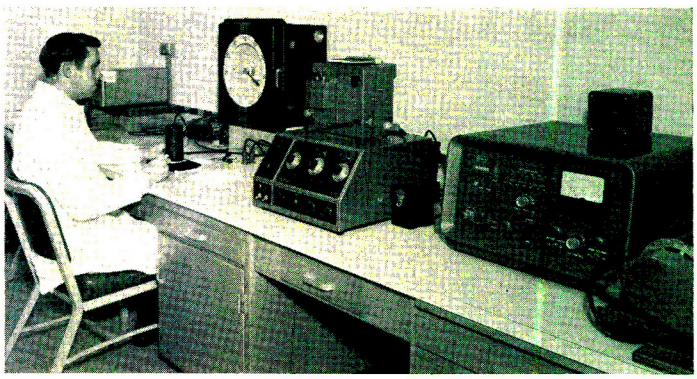

Purex evaluates the performance of its household detergents, abrasive cleansers, hypochlorite and peroxide bleaches, janitorial maintenance products, etc., by studying the quantity of a standard "soil" removed from cloth swatches, painted panels, floor tiles, vitreous enameled surfaces, etc., by reflectance measurements, fluorescent emission studies, and radioactive tracers using the illustrated equipment

LABORATORY OF THE MONTH

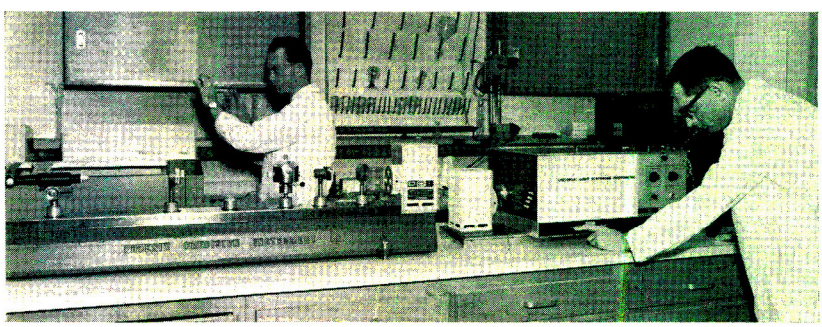

The performance of various polymeric lattices of polystyrene, polyethylene, polyacrylics depends among other things upon the molecular weight of the polymer and its distribution in addition to the particle size of these polymer particles in the emulsion. The light scattering photometer and differential refractometer are used in these analyses of particle size distribution and molecular weight distribution

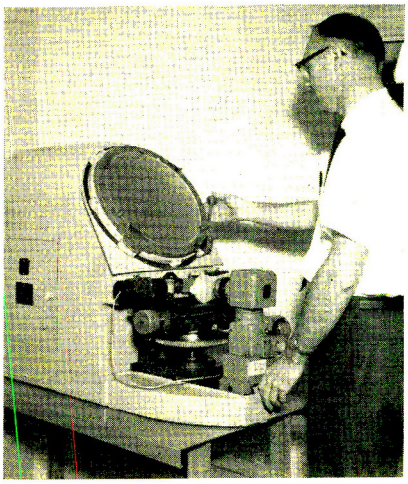

Purex blows their own plastic bottles and vacuum forms some of their other plastic containers. Thread form on the neck of bottles and wall thickness at various points are critical for the good performance of such containers. These characteristics are analyzed at frequent intervals by use of an optical comparator

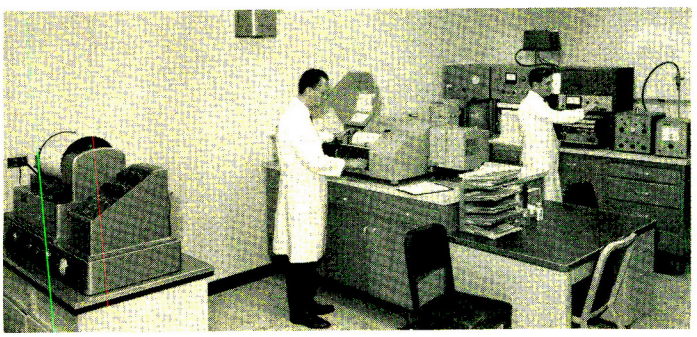

The infrared and near-infrared spectrophotometers and gas-liquid chromatographs are the work horses of the Analytical Laboratory. These are used to separate, identify, and quantitatively determine many of the organic components of surfactant, polymer, perfume, floor wax, dye penetrant, protective coating, and other complex organic mixtures normally a part of Purex business

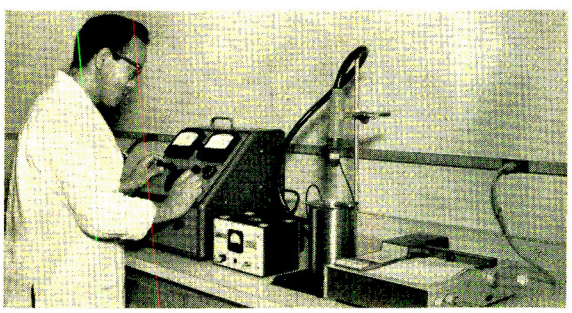

Purex uses the Lawrence hydrogen detection gage to detect possible hydrogen embrittlement resulting from the use of alkaline or acid paint strippers, alkaline detergents and other industrial cleaning compounds used in cleaning and refinishing the exterior surfaces of aircraft or other equipment where this could be a possible problem. This analysis requires the determination of hydrogen in the parts per million range in the metal under consideration

NEW DOUBLE DUTY INSTRUMENT

AGITHERM

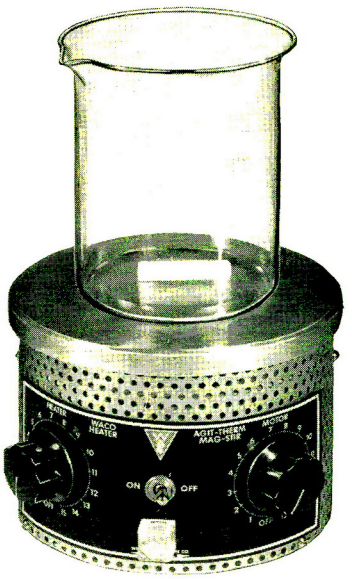

ONLY $67.50

Hot Plate—
—Magnetic Stirrer

New low cost plus advanced design features

Now you can heat and stir simultaneously with WACO AGITHERM. Heavy-duty individual controls allow use of either stirrer or hot plate independently when desired.

The 500 watt hotplate can be set thermostatically at any temperature up to 600° F. Pilot light indicates when heat is on. The perforated stainless steel case assures cool operation of motor. Compact design, 6½" diameter by 5" high.

No. F-84500 Agitherm Stirrer Hot Plate, complete with one each glass and Teflon covered stirring bars ⅜" by 1¼", for 115 volt, 60 cycle, A. C. ..... $67.50.

ORDER NOW

LABORATORY SUPPLIES AND EQUIPMENT
WILKENS-ANDERSON CO.
4525 W. DIVISION ST. CHICAGO 51, ILL.

Circle No. 77 on Readers' Service Card

When Purity is Essential

Why not go first class?

If your work requires high purity gases, why not use the best? Matheson Research Grade gases are the purest available. They are now supplied in our new ICC-approved high pressure cylinder that is far safer and more convenient than the so-called throw-away kind. Equipped with Standard CGA Connections. No deposit, no demurrage.

Ordinary Regulators Contaminate. Our No. 18 and 19 regulators were specially designed for high purity and Research Grade gas service. They have diffusion resistant metal diaphragms to prevent the contamination that often occurs with ordinary "welding type" regulators. They are equipped for direct attachment to cylinders with provisions for options on outlet connections.

Use A Good Valve. It's surprising how many researchers are using common needle valves. Our chromed brass 939 BT packless control valve attaches directly to the cylinder, provides positive seating, eliminates leakage. No "O" rings or packing to create diffusion problems.

For further information on our Research Grade gases and handling equipment, write for Matheson Catalog 25. We invite you to consult our Engineering Department concerning the design of high purity gas systems or other compressed gas problems.

P.O. Box 85, East Rutherford, New Jersey
Plants in East Rutherford, N. J.; Joliet, Ill.; La Porte, Texas, Morrow, Ga.; Newark, Calif. / Matheson of Canada, Whitby, Ont.

MATHESON

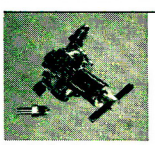

No. 18 Regulator

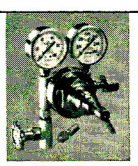

No. 19 Regulator

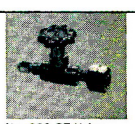

No. 939 BT Valve

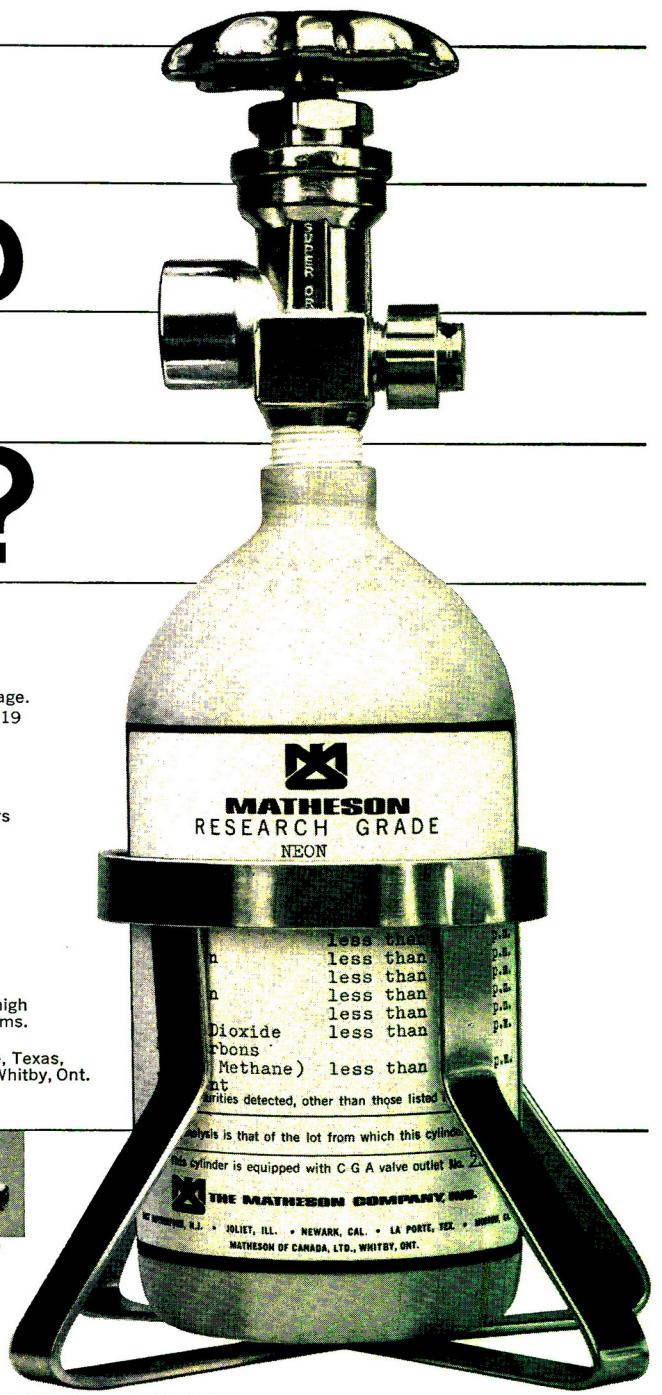

Circle No. 120 on Readers' Service Card

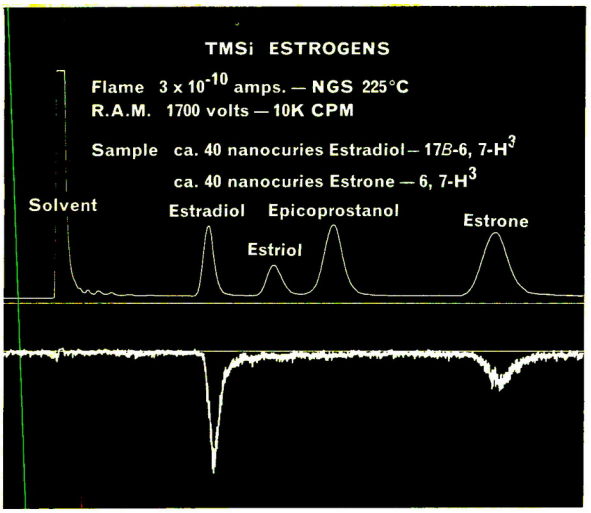

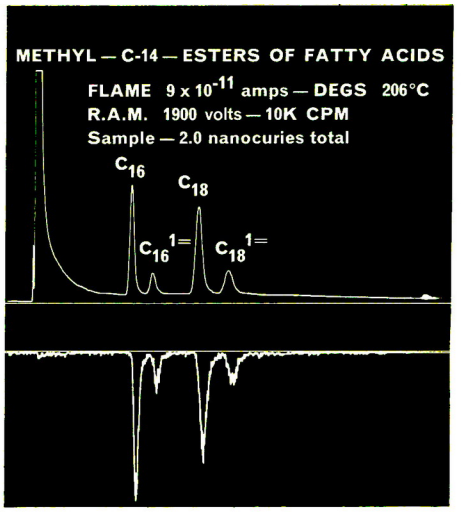

For the analysis of C–14 or H–3 labeled materials

investigate the BARBER-COLMAN radioactivity monitoring gas chromatography system

Barber-Colman Model 5190 Radioactivity Monitoring System and Series 5000 Selecta-System provide the ultimate in continuous radioactivity monitoring for either C—14 or H—3 labeled materials. Model 5190 includes a combustion furnace, proportional counter and ratemeter.

In operation, the G/C column effluent is split with part of the sample going to the mass detector and the rest to the R.A.M. System. The sample is immediately burned to CO_2 and H_2O. The H_2O is then reduced to H_2. The radioactive CO_2 and H_2 are counted at ambient temperature.

Series 5000 Selecta-System with all-glass columns and direct on-column injection is the basic G/C unit used with the R.A.M. System. Series 5000 instruments are the product of Barber-Colman's many years of experience in the biomedical field and were designed specifically for biomedical applications.

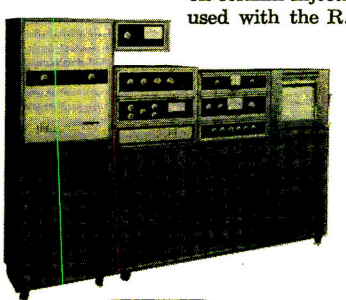

Features of Radioactivity Monitoring System

- Counter Efficiency:
  Better than 90% for C—14
  Better than 60% for H—3
- Detects as little as 0.05 nanocuries of C—14 and 0.1 nanocuries of H—3.
- Low Background — 40 CPM — assured by ambient operation of counter.
- Reliable combustion-reduction system.
- Separation — Detection — Recording — All in one simple operation — No Fraction Collection Required.

Features of Selecta-System®

- Flame Ionization Detectors
- Coiled or "U" Shaped Column Bath
- On Column Injection — All-Glass System
- Temperature Programming Capability
- Modular Construction

For more information, contact a local Barber-Colman representative or Rockford.

BARBER COLMAN

BARBER-COLMAN COMPANY

Dept. H, 15104 Rock Street, Rockford, Illinois, U.S.A.
BARBER-COLMAN of CANADA, Ltd., Dept. H, Toronto & Montreal • Overseas Sales Mgrs.: Ad. Auriema, Inc., N.Y.

"See Laboratory Guide for all Products/Sales Offices"
Circle No. 13 on Readers' Service Card

For better instrumentation for materials analysis...

Choose the supplier who assigns a service representative to your x-ray unit.

BECAUSE X-RAY instrumentation is his only business, your G-E Service Representative's primary interest is to help you get optimum performance from your G-E x-ray unit.

He's been specially trained to help you improve efficiency with your analytical work. Besides acting as a consultant for operation and application tips, he'll help you select additional supplies and accessories. Right at his office is a stock of G-E renewal parts.

The Service Representative assigned to your instrument is trained in service and maintenance. A man with electronics and x-ray experience and aptitude, he knows the ins and outs of G-E x-ray units.

On call to support him are factory application engineers. They're only a phone call away on G.E.'s own long distance system. When you buy General Electric, factory service is part of your instrument.

Find out how General Electric service can help your materials analysis. For descriptive data on General Electric instrumentation, write to General Electric, Section 4612, 4855 Electric Avenue, Milwaukee, Wisconsin.

GENERAL ELECTRIC

INSTRUMENTATION

Automatic Optical Pyrometers Measure High Temperatures

BY RALPH H. MÜLLER

THE PROBLEM of measuring very high temperatures is of continuing interest in present day science and technology. For many years, the optical pyrometer of the disappearing filament type has been the standard for the measurement of high temperatures. It was natural that attempts would be made to substitute photoelectric methods for the more precise comparison of brightness of the target and the center portion of the filament of the standard lamp. Recently, we raised the question of what had happened to commercial developments of this sort. One answer has been supplied to us by H. L. Daneman of Leeds and Northrup, who has furnished us with a description of an elegant automatic optical pyrometer. The L & N automatic optical pyrometer, Models 8640 and 8641 are manufactured by the Leeds and Northrup Co. of 4907 Stenton Ave., Philadelphia 44, Pa. A general view of the instruments is given in Figure 1, with Model 8640 on the left. The operating principle of both instruments is illustrated in the schematic diagram of Figure 2. The optical system consists of two similar optical paths, one for the target, the other for the standard lamp, that converge to a point on the photocathode of the multiplier phototube. The two paths are alternately interrupted 90 times a second by a motor-driven disk having three 60-degree slots displaced 120 degrees from each other. At any given instant, one slot permits the phototube to "see" light from one beam while the disk blocks light from the other beam. A reasonably good square wave form is produced by this method of light modulation and switch-over time from one beam to the other is relatively short.

The phototube output consists of two d.c. signal components, one proportional to the brightness of the target, the other proportional to the brightness of the standard lamp. The a.c. component of these two signals is an error signal which is amplified and then demodulated. The demodulated signal, which is proportional to the a.c. error signal, causes the integrator to change the lamp current in the direction that will reduce the error signal. When the target and lamp brightnesses are the same, the error signal is zero and the integrator holds the lamp current at a constant value that is related to the target temperature.

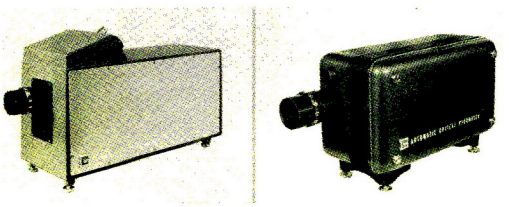

Figure 1. L & N automatic optical pyrometers, Models 8640 (left) and 8641

The synchronous demodulator is triggered by two phototransistors which are energized by separate lamps whose light is interrupted 90 times a second by the modulator disk. The output of one phototransistor is also used to generate two square wave voltages required for operation of the integrator.

Inasmuch as the radiant energy of the target increases very rapidly as the temperature increases, the system gain must be decreased for higher temperatures. This is accomplished by the automatic gain control circuit which samples the standard lamp current and automatically reduces the system gain as the lamp current increases.

The temperature can be determined by measuring the standard lamp current with a current recorder, or alternatively by connecting an external precision resistor in series with the standard lamp and measuring the voltage drop across it with a millivolt recorder, or, for the highest precision, with a type K-3 potentiometer. The instrument utilizes the same standard lamp that has been performance proven in the manually balanced L & N optical pyrometer for almost thirty years. The lamp employs a thin ribbon filament positioned between two flat windows mounted so the filament is perpendicular to the optic axis. A temperature *vs.* lamp current calibration curve is supplied with the equipment.

The 8641 Mark 1 precision automatic is the lower priced version of these pyrometers and, although less sensitive to small changes in temperature than the 8640 high precision automatic, it provides a level of precision and sensitivity which exceeds that of most commercially available instruments. A turret viewer (8640 only) permits viewing the target image on a ground glass screen or through a Ramsden eyepiece. The 8641 utilizes the latter only.

Some of the characteristics of the two instruments, stated with respect to the 8640 and 8641 are: range: 775° to 5800° C., in four ranges; and 775° to 2800° C. in three ranges. Resolution: 0.2° C. for one-second balance at the gold point (1063.0° C.) and 0.5° C., respectively. The response time for both models is approximately one second for 99% of reading

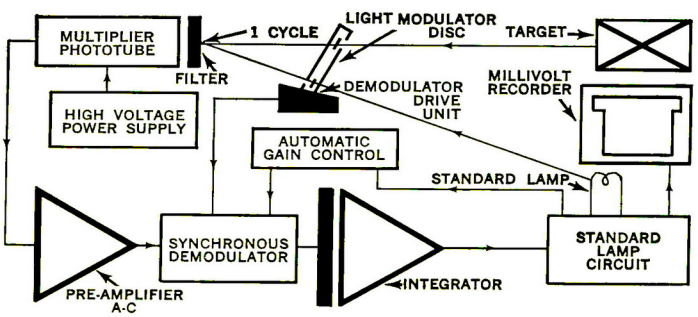

Figure 2. Schematic of the automatic optical pyrometer

← Circle No. 35 on Readers' Service Card

WANTED

NEW, CHALLENGING APPLICATIONS FOR GOW-MAC DETECTORS

to serve YOU at . . .

TEMPERATURES: —200° to 500°C

PRESSURES: 0.1 to 10 atmospheres

FLOW RATES: 1 to 1000 ml/min.

SERVICE: intermittent or continuous
corrosive or contaminated gases

with SEPARATION by Chromatographic Columns { Packed or Capillary
Laboratory or prep scale

COME AND SEE US AT THE CHEMICAL EXHIBITION OF THE A.C.S. SEPT. 13-15 BOOTH 111 NEW YORK HILTON

Flotwire

WRITE TODAY FOR GOW-MAC's NEW ISSUE

Gas Analysis since 1935

GOW-MAC INSTRUMENT CO.

100 KINGS ROAD, MADISON, NEW JERSEY 07940
TELEPHONE: (201) 377-3450

Circle No. 153 on Readers' Service Card

or automatic operation. The effective wavelengths are approximately the same, 6500 and 6450 angstroms and the radiation band passes are approximately 200 and 350 angstroms. Standard optics permit viewing distances from 12 inches to infinity and 20 inches to infinity. In the high precision, automatic, objective lens assemblies are available for special target requirements. For example, a target diameter as small as 0.01 inch can be viewed at a target distance of approximately 3 inches.

Some useful applications in the research laboratories are listed by the manufacturer, such as: studying the melting points of oxides or metals; measuring high speed transient temperatures; using as a backup for thermocouples to correct for drift; using as a comparison device for calibration of secondary standards and radiation sensors for measuring plasma temperatures; measuring fast temperature changes in induction furnaces; measuring material temperature during changes of state in an arc imaging furnace; calibrating lamps used as star simulators, etc.

This and similar instruments will be a boon to many investigators. We know of one superbly equipped metallurgical laboratory where all measurements in optical pyrometry were conducted by one technician who had no particular technical background but the ability to match target and filament brightness better than anyone on the research staff. Carefully conducted objective tests and intercomparisons with thermocouples showed that his setting errors were two or three times smaller than other observers. But despite his calmness and patience, his visual acuity would wane in time. We know a professional color matcher in New York who enlisted our interest in developing a precise photoelectric photometer to perform his tasks. We were proud of our achievement, but humiliated by the fact that he infallibly could spot differences in hue which neither our eyes nor instrument could detect. Our offering was accepted with gratitude because it would supply acceptable data twenty-four hours per day whereas his daily stint was confined to three widely spaced one-hour intervals of visual matching, a performance accepted by his employers without question.

In a different category, the late A. H. Pfund of Johns Hopkins developed a hardness tester for paint and varnish films. As he remarked ruefully, "It was not much better than the thumbnail test of an inspecter but was widely adopted because we have not yet learned to breed a race possessing sensitive and calibrated thumbnails."

Using these for data recording?

You have better things to do.

Isn't it ironic that we've automated many of the tedious manual tasks of the industrial worker while many of our finest scientific minds must still hand tabulate analytical instrument data. The price for this waste of time and talent is high; payments are made in lost opportunity for scientific progress.

Is it necessary for a scientist to perform the functions of a clerk? No. You can close the gap between laboratory instrumentation and a digital computer simply and inexpensively. How? By using a Datex Automatic Digital Data System to control laboratory instrument operation and record results in computer-compatible form (you extend instrument operating time and reduce opportunity for error in the bargain). For instance:

DIFFRACTOMETRY: The Datex Diffractometer Control and Recording System is pre-programmed to position the crystal to discrete angles, record scaler data, verify crystal position and convert this data into computer language. Like this:

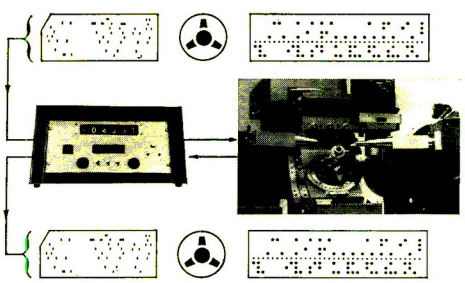

Position properly oriented crystal on diffractometer, start the computer generated tape or cards in the reader and push the button. That's it. Now you're free for those better things. Investigations go faster, too. And the Datex System can operate continuously and reliably around the clock.

SPECTROPHOTOMETRY: The Datex Spectrophotometer Data Recording System converts analog output data of spectrophotometers to digital computer language. It can be added to your present equipment or made part of a new system. Like this:

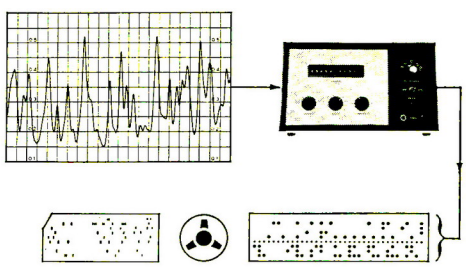

Let the computer perform least squares calculations to improve signal-to-noise ratio, or simply match patterns; unknown to known. No more hand-digitizing of analog charts; Datex output is machine ready. And all systems are available in modular form. As your requirements increase, so does the system capability.

This is only a start. Datex Systems are readily applicable to any laboratory instrument for investigation. Interested? Tell us about your problem. We'll answer promptly with a detailed technical description and price of a system tailored to fit your needs precisely.

DATEX
DIVISION OF GIANNINI CONTROLS CORPORATION
1307 South Myrtle Avenue, Monrovia, California 91016

Circle No. 97 on Readers' Service Card

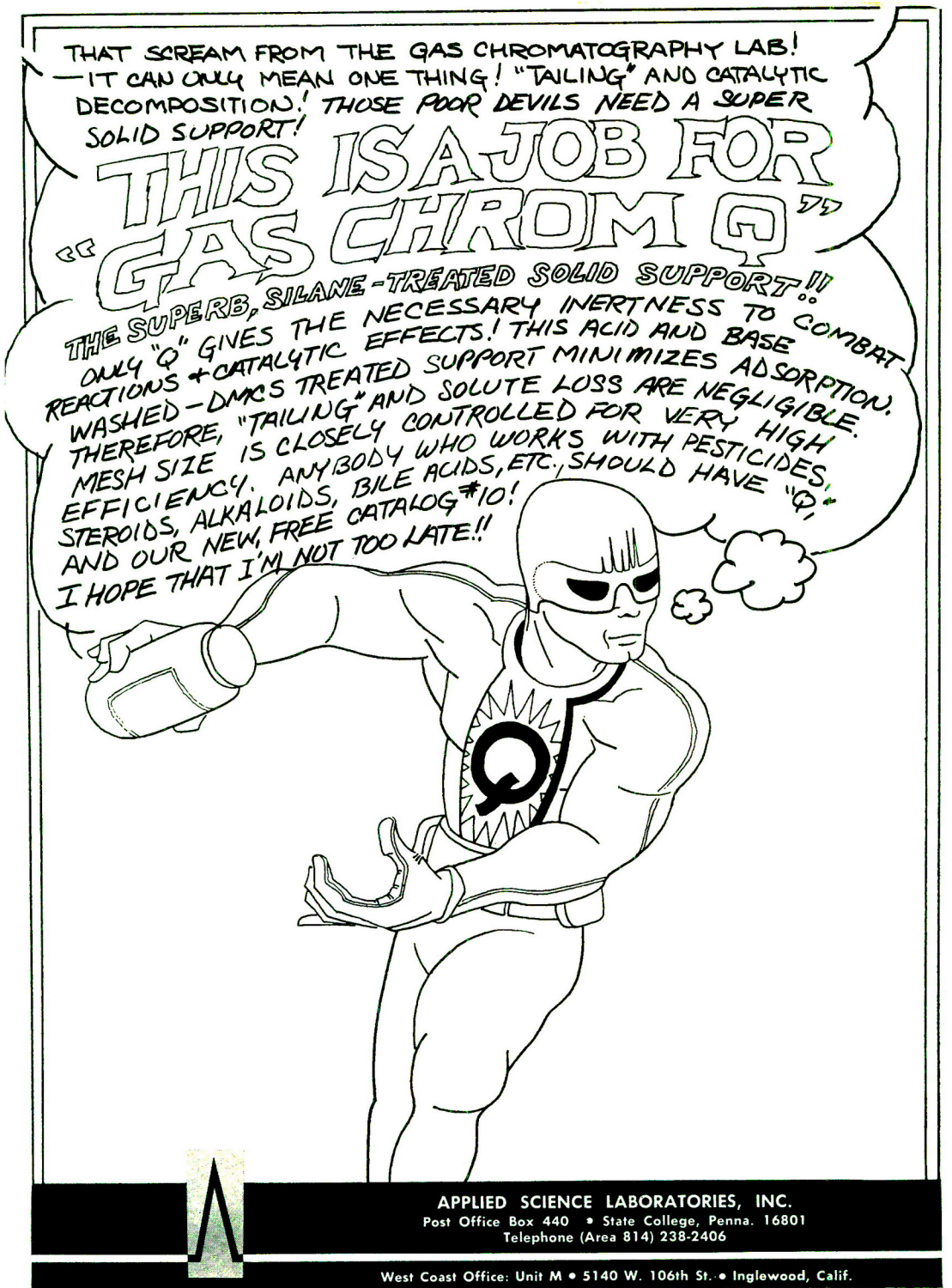

APPLIED SCIENCE LABORATORIES, INC.
Post Office Box 440 • State College, Penna. 16801
Telephone (Area 814) 238-2406

West Coast Office: Unit M • 5140 W. 106th St. • Inglewood, Calif.

Circle No. 12 on Readers' Service Card

WEIGH THE SIX FACTS LISTED BELOW

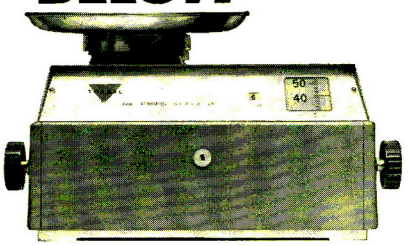

You'll find more advantages with TORBAL balances

1. From 14 kg. balances to 0.1 mg. analyticals, Torbal is the only complete balance line with friction-free pivots and bearings.

2. Only Torsion balances retain accuracy so long. With no knife-edges or friction points to be affected by dusty or abrasive atmospheres, adjustment and high sensitivity of Torsion balances last for 20 years and more!

3. Only Torsion balances are so rugged yet sensitive. The Torsion construction with no knife-edges gives greater protection against damage from objects accidentally dropped on the pans.

4. Only Torsion balances do not get sluggish with time. With no bearings to accumulate dust or foreign material, Torbals do not lose their original speed even after long, tough use.

5. The Torbal EA-1 analytical balance is the only analytical offering the advantages of a null-type read-out. This construction eliminates any effect from variations in sensitivity. Sample weighing is much easier.

6. When you use Torsion balances you don't need a service contract. Torbals are so rugged and dependable that adjustment or repairs are rarely needed.

Write today for a complete catalog of Torsion balances.

TORBAL®

THE TORSION BALANCE COMPANY

Main Office and Factory: Clifton, New Jersey, Sales Offices: Chicago, Ill., Richardson, Texas, San Mateo, Cal., Santa Ana, Cal., Pittsburgh, Pa., Lynnfield, Mass. • Plants and Offices in Montreal, Quebec and London, England

CLIP, ATTACH TO YOUR LETTERHEAD AND WE'LL SEND INFO ON ANY YOU CHECK

☐ **Fast, accurate direct read out to ±0.01 grams.** Capacity 800 grams. Also available in 1000g. capacity (PL-1) with direct read out to 0.1 gram, and 2000 gram capacity (PL-2) with direct read out to 1.0g. (0.1g. by estimation).

Model PL-800

☐ **200 gram capacity.** Weight control dial and fine weighing dial with vernier makes possible direct readings from 100 grams to 0.01 grams. 500 gram capacity model also available (DWL-5).

Model DWL-3V

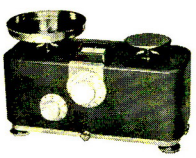

☐ **2000 gram capacity** and with 10g. x 0.1g. and notched beam 100g. x 10g. increments. Available with tare beam instead of notched beam. (DH-2(b)). 4500 gram capacity models (DH-4(a) and DH-4(b)) also available.

Model DH-2 (a)

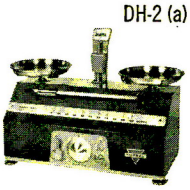

☐ **120 gram capacity.** Dials permit direct readings from 10 grams to 0.01 grams (can also be read to 0.003 grams by estimation).

Model DWL-2

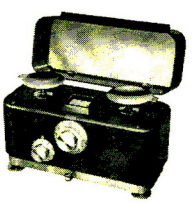

☐ **Analytical balance, direct digital readout to tenth mg., 160g. capacity.** Has exclusive solid-state electronic null indicator. Unaffected by variations in sensitivity. Ease of reading, accuracy and reproducibility greatly enhanced. Null indicator simplifies sample weighing.

Model EA-1

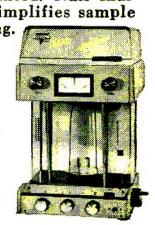

TB-217

Visit our display—Booth No. 117—at the Chemical Exposition USA 1966, N. Y. Hilton Hotel 9/13—9/15.

Circle No. 122 on Readers' Service Card

CHN Analyzer proves its performance 100 times every day

Every day, more than 100 microchemists use the F & M Model 185 Carbon Hydrogen Nitrogen Analyzer to perform elemental analyses whose accuracy is well within the accepted allowable error of ±0.3%. Some have reported a distinct improvement in the reliability of their CHN analyses since they have turned to the 185. Others have already paid the 185 the ultimate compliment by sending us a repeat order.

An important reason why the 185 is beginning to make a deep impression among microchemists is its performance under difficult circumstances in the past year.

At the recent International Symposium on Microchemical Techniques, for instance, F & M gave a live demonstration of the 185 and promptly calculated results as follows: 0.01% error for Carbon, 0.3% error for Hydrogen, 0.04% error for Nitrogen.

At the 1965 Pittsburgh Conference, in a room filled with as many as 15 visitors, F & M performed on-the-spot analyses of 18 samples submitted by the visitors . . . with results within the microchemist's 0.3% allowable error for all three elements.

In a series of 52 samples of all types, submitted "blind" by interested microchemists across the country, the overall standard deviation (σ) of duplicate analyses performed on the 185 was 0.15% for Carbon, 0.12% for Hydrogen and 0.19% for Nitrogen.

Some of the credit for the remarkable performance capability of the second-generation F & M Model 185 CHN Analyzer is due to recent design improvements: a two-stage furnace for optimum sample combustion *and* reduction temperatures, an improved single-column gas chromatographic system and an automatically timed combustion cycle . . . all of which result in even more reliable analytical data than with its predecessor . . . at the same speed advantage of 4 to 8 times over classical methods.

Not the least amazing part of the 185 story is its price: $4,995.00 including balance and recorder (f.o.b. Avondale, Pa., U.S.A.) For full information, call the Chemical Instrumentation Sales Representative at one of the 41 Hewlett-Packard sales offices in the U. S.

Hewlett-Packard, F & M Scientific Division, Route 41, Avondale, Pennsylvania, 19311. In Europe: F & M Scientific Europa N.V., Basisweg (Sloterdijk), Amsterdam, The Netherlands.

HEWLETT PACKARD hp *F & M SCIENTIFIC DIVISION*

Circle No. 38 on Readers' Service Card

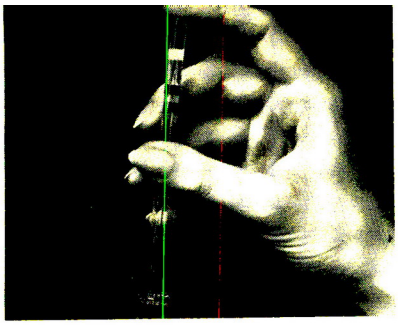

It's really a lot faster this way.

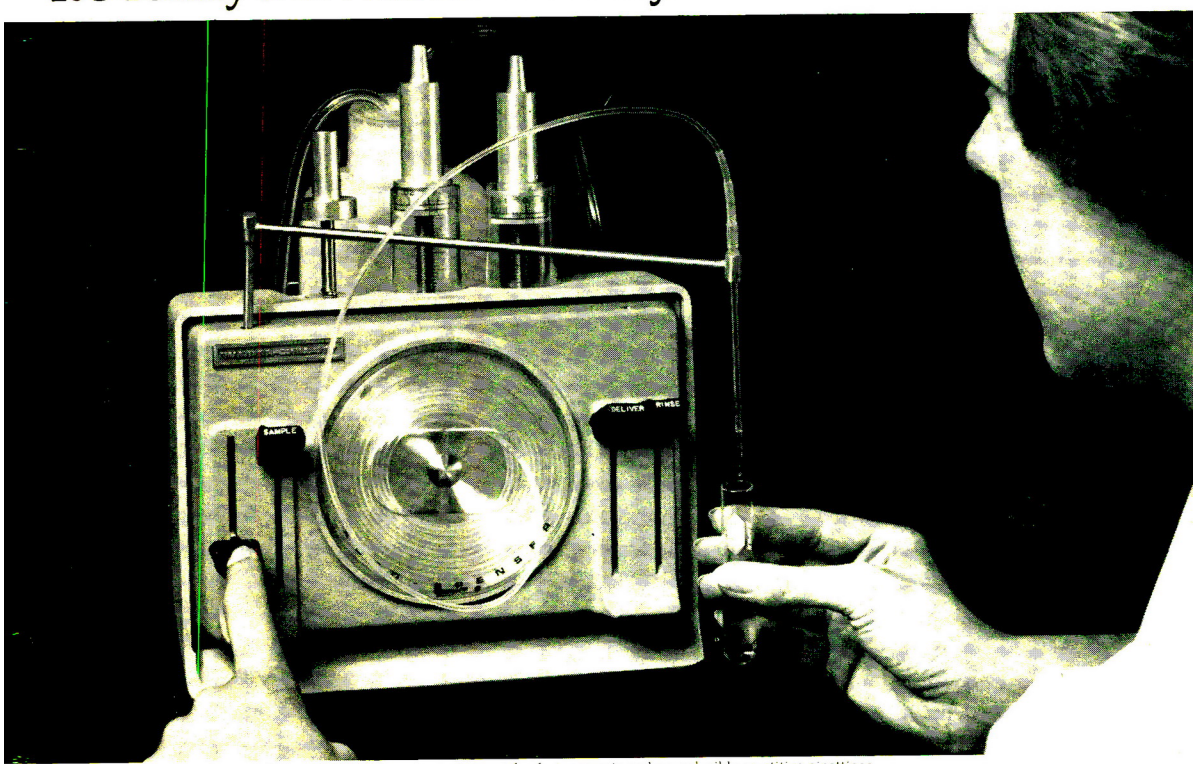

Warner-Chilcott's Auto-Spenser™—a precision laboratory instrument for fast, accurate and reproducible repetitive pipettings.

It takes only 15 seconds—or less—to pipette, add a reagent or diluent, and dispense, with Warner-Chilcott's Auto-Spenser.™ It's not only faster and safer than manual methods, but far simpler—you simply depress a lever. No pipettes to wash. You just depress a lever for that, too, and your Auto-Spenser rinses itself. Add to this the high accuracy and reproducibility of the instrument, and you'll see why we feel the Auto-Spenser belongs in every laboratory that performs repetitive pipettings. Time saved will quickly pay for its modest $195 cost!

Versatile, Trouble-Free

You can use your Auto-Spenser for pipetting, diluting, or dispensing. The self-wash feature lets you change reagents in seconds. Two micrometer-controlled pumps handle a wide range of sample and reagent volumes. It's easy to set and read sample volumes to one-half microliter—with no visual checking of liquid levels. The compact, rugged Auto-Spenser is completely mechanical. There's no electrical power needed, virtually nothing to break or replace, and no way for sample or reagent to enter the mechanism. It's practically foolproof!

"See Laboratory Guide for all Products/Sales Offices"
Circle No. 149 on Readers' Service Card

Brief Specifications

Practical Volume Ranges: Sample, 20-250 μl; Reagent, 0.5-5.0 ml. Sampling Reproducibility: ± 0.5 μl or $\pm 1\%$, whichever greater. Reagent Delivery Reproducibility: ± 0.005 ml or $\pm 0.5\%$, whichever greater.

Please write for details on Model 26500 Auto-Spenser. Address Warner-Chilcott Laboratories Instruments Division, 200 South Garrard Blvd., Richmond, California 94804.

WARNER-CHILCOTT LABORATORIES
INSTRUMENTS DIVISION
Richmond, California

PARTICLE MONITORING REPORTS 07817

HOW INDUSTRY USES ROYCO INSTRUMENTS TO COUNT AND MEASURE PARTICLES IN LIQUIDS AND GASES...

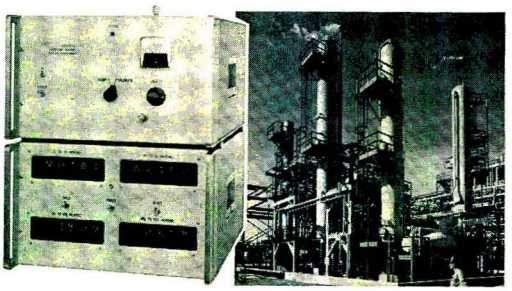

VERIFIES PURITY OF CHLORINATED SOLVENTS

Ultra high purity solvents for electronic and aerospace applications require positive control of particulate contaminants. Manufacturers supplying this rapidly growing market control product purity during processing and packaging in drums by monitoring particle content with the Royco Liquidborne Counter. Model 320 counts particles in 4 selected size ranges from 5 microns to 500 microns simultaneously and displays the individual totals.

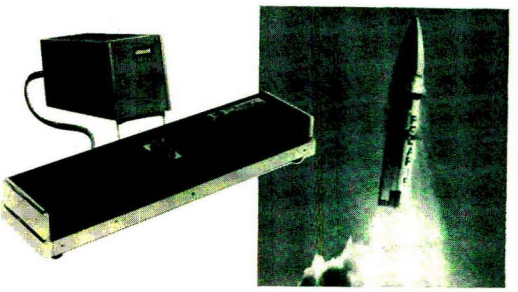

HYDRAULIC OIL PARTICLE COUNTING ON POLARIS SUBS

A new test procedure adopted for Polaris submarine operations involves systematic monitoring of hydraulic oils with the new Royco miniaturized portable particle counter, Model 340. Liquidborne particulates as small as 5.0 microns are measured and counted automatically to provide immediate data on levels of contamination. The monitoring system is composed of the 12 lb. sensor, 4" high by 6" wide by 18" long, the control module and read-out unit displaying particle counts in 5 size ranges simultaneously. Working pressure is 3500 psi at 100° F.

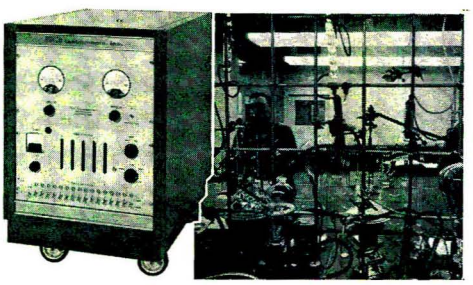

BASIC RESEARCH IN DRY AEROSOLS

Particle size as related to other physical properties of dry aerosols is an important laboratory study being conducted by a major chemical company toward improved product quality. A basic research instrument, Royco Airborne Particle Counter, Model 202, with a built-in dilution system for highly concentrated aerosols, provides the particle size concentration in 23 size ranges from 0.3 microns to 100 microns. By monitoring dry aerosol particulates in the natural environment, Royco instrumentation assures reliable, repeatable data that is continuously recorded by a Royco Digital Recorder, Model 122.

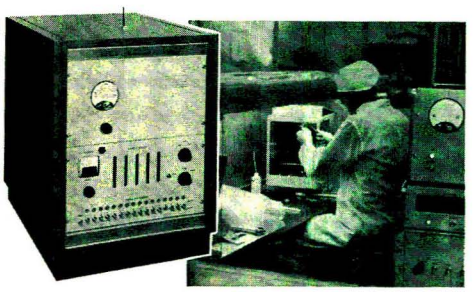

CLEAN ROOM MONITORING

Controlled environments for film manufacture and developing, miniature component assembly and other clean processing can be continuously monitored for particulate matter by Royco Airborne Particle Counter. Model 200 provides readings programmed over any desired combination of particle sizes in 15 ranges from 0.3 microns to 10.0 microns and larger. Royco Digital Recorder, Model 122, provides a continuous printed record.

ROYCO INSTRUMENTS INC., MENLO PARK, CALIFORNIA

Particle Monitoring by ROYCO

Circle No. 136 on Readers' Service Card

Alberene Stone can take it!

Now try this on the substitutes

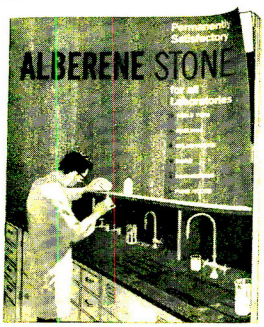

Alberene Stone for 75 years the only permanently satisfactory material for chemical laboratory table tops, shelving, sinks, splash backs, drain boards and fume hoods. Prompt delivery. Produced and fabricated by the Alberene Stone Division of the Georgia Marble Company. For our 12-page booklet or technical assistance, send the coupon or phone:

The Albermar Company
Dept. C, 386 Park Ave. South, New York, N.Y. 10016
Please send your 12-page Alberene Stone catalog

Name _____ Title _____

Company _____

Street _____

City _____ State _____ Zip _____

Offices or Agents in Principal Citi

New . . .

Thomas Magne-Vap™ FLASH EVAPORATOR

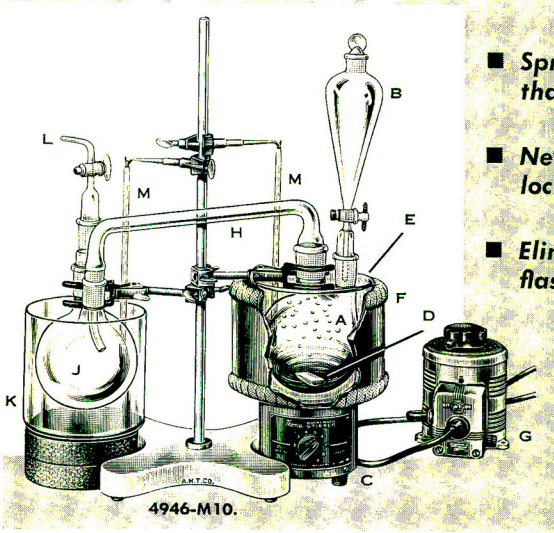

4946-M10.

- ***Spray action—efficiency double that of rotating flask type***
- ***New twin-bar stirring magnet locks in at high speed***
- ***Eliminates rotating seals—flasks secured to stationary stand***

For rapid concentration of heat-sensitive materials at reduced pressure. Evaporation rate is approximately twice that of conventional rotating flask devices. Vigorous magnetic stirring action disperses solution throughout 1000 ml evaporating flask, which is heated by a water bath in transformer-regulated mantle. Need for rotating joints is eliminated, permitting use of simple glass system with ⅎ joints.

The greatly accelerated evaporation rate results from the large surface of solution, which is dispersed as a constant spray of small droplets, continuously wetting entire flask wall. The required high speed stirring is made possible by an efficient, double-magnet bar, driven by a powerful magnetic stirrer. Lock-in effect of double magnet keeps bar in synchronization with magnetic drive at high speeds. Addition funnel allows maintenance of optimum volume for best dispersion. Condenser flask collects up to 500 ml of solvent.

System is entirely of borosilicate glass, connected by ⅎ joints. Solution to be concentrated is placed in evaporator flask *A* or in funnel *B* with Teflon stopcock for controlled addition. Agitation is provided by magnetic stirrer *C* and stirring bar *D*. Evaporator water bath *E* is heated by mantle *F*, controlled by variable transformer *G*. Vapor transfer tube *H* conducts solvent vapors to condenser flask *J* in cooling bath *K*. Vacuum connection is made at stopcock of connecting tube *L*. Thermometers *M* are provided for evaporator and condenser baths.

Vacuum Requirements. A simple type filter pump requiring minimum water pressure of 15 to 20 lbs. per square inch is usually adequate. For solvents of low volatility, a mechanical vacuum pump with suitable vapor trap should be employed.

4946-M10. EVAPORATOR, Thomas Magne-Vap, complete as shown in illustration, without filter pump. For 115 volts, 50 or 60 cycles, a.c.; 370 watts. . . . **205.00**

Thomas **ARTHUR H. THOMAS COMPANY**

Scientific Apparatus and Reagents

VINE STREET AT 3RD • P. O. BOX 779 • PHILADELPHIA 5, PA., U. S. A.

Circle No. 71 on Readers' Service Card

ANALYTICAL CHEMISTRY

August 1966, Vol. 38, No. 9

Editor: HERBERT A. LAITINEN

EDITORIAL HEADQUARTERS

Washington, D. C. 20036
1155 Sixteenth St., N.W.
Phone: 202-737-3337 Teletype WA 23

Associate Editor: John K. Crum

Assistant Editors: Josephine Pechan, Virginia E. Stewart

Editorial Assistants: Mary Ann Wingard, Martha B. Wood

Contributing Editor: R. H. Müller

Production Staff—Washington:

Art Director: Joseph Jacobs

Art and Layout: Perry Donovan, Herbert Kuttner

Production Staff—Easton, Pa.:

Associate Editor: Charlotte C. Sayre

Assistant Editor: Elizabeth R. Rufe

Advisory Board: O. U. Anders, F. C. Anson, C. V. Banks, R. G. Bates, W. J. Blaedel, S. Bruckenstein, H. W. Habgood, G. A. Harlow, D. M. Hercules, F. W. McLafferty, M. W. Mallett, G. H. Morrison, R. E. Thiers, J. C. White, D. H. Wilkins

AMERICAN CHEMICAL SOCIETY PUBLICATIONS

Director of Publications, Richard L. Kenyon

Assistant Director of Publications and Director of Research Journals, Richard H. Belknap

Director of Business Operations, Joseph H. Kuney

Executive Assistant to the Director of Publications, Rodney N. Hader

Assistant to the Director of Publications, William Q. Hull

REGIONAL EDITORIAL BUREAUS

NEW YORK, N. Y. 10017
733 Third Ave.

PHILADELPHIA, Pa. 19107
Philadelphia National Bank Building
Broad & Chestnut Streets

PITTSBURGH, Pa. 15230
530 William Penn Place

CHICAGO, Ill. 60603
36 South Wabash Ave.

CLEVELAND, Ohio 44114
1367 East Sixth St.

SAN FRANCISCO, Calif. 94104
57 Post St.

LOS ANGELES, Calif. 90005
422 South Western Ave.

HOUSTON, Texas 77002
1121 Walker St.

FRANKFURT/MAIN, West Germany
32 Grosse Bockenheimerstrasse

LONDON, W. C. 2, England
27 John Adam St.

TOKYO, Japan
Apt. 306, 47 Dai-machi, Akasaka, Minato-ku

WASHINGTON, D. C. 20036
1155 Sixteenth St., N. W.

Advertising Management

REINHOLD PUBLISHING CORP.
(for Branch Offices, see page 133 A)

For submission of manuscripts, see page 2A.

Citizenship in Science

IT MAY BE USEFUL to draw some parallels between citizenship in its social and political meanings, and citizenship in the scientific community.

One aspect of citizenship is loyalty. A good citizen shows loyalty to his family, his neighborhood, his town, his county, his state, and his country in an ever widening set of spheres depending upon the breadth of the issue under discussion. While he may take a strong position of support for one locality against another in discussing a municipal issue, these differences are properly forgotten when discussing interstate or international issues. In a parallel manner, a scientist properly shows loyalty to his own specialty in discussions within his own branch of science. But the dimensions of his loyalty expand as the boundaries of the discussion become broader. Analytical chemists, for example, might engage in a lively dispute about the relative merits of polarography or gas chromatography in the solution of a particular problem; but their differences rapidly disappear when the discussion involves the validity of the analytical approach, as compared to some other approach to the problem. What is more important, however, analytical chemists as well as other specialists should demonstrate their loyalty for chemistry as a whole, and not just to one branch of it, when discussing problems of interest to the whole chemical science; for example, undergraduate curricula in chemistry, or government support for chemistry in relation to biology or physics.

Another aspect of citizenship is voluntary service. Just as a good citizen on the political scene not only exercises his privilege of the ballot, but also contributes his time and efforts to causes he believes in, so does a scientist have obligations of voluntary service. Particularly in the postwar era, the scientific community in the United States has evolved a remarkably successful method of administering the greatly enlarged level of government support of science. The success of this procedure is vitally dependent upon voluntary services such as reviewing research proposals and serving on advisory panels. But even long before the present era of substantial federal support, the traditional scientific activities such as local section and national meetings of professional societies and the review and publication of research papers required many types of voluntary services from individual scientists. It is particularly important that younger scientists be encouraged to grow gradually into a fuller participation at the various levels of voluntary service. Not only are more services needed than ever before, but the new ideas and new influences of the younger scientists are needed to shape the directions of science in the years to come.

Symposium on Electroanalytical Instrumentation

ACS Winter Meeting
Analytical Division
Phoenix, Ariz.
January 1966

Effect of Uncompensated Resistance on Electrode Kinetic and Adsorption Studies by Chronocoulometry

GEORGE LAUER and ROBERT A. OSTERYOUNG
North American Aviation Science Center, Thousand Oaks, Calif.

▷ The presence of "uncompensated resistance" in a potentiostatic experiment results in loss of potential control, which in turn affects the results of electrode kinetic and adsorption studies. A positive feedback potentiostatic circuit permits compensation of the potential drop across this uncompensated resistance. The circuit was tested by applying potential steps to an electrical analog of an electrode-solution interface and determining heterogeneous rate constants of Cd(II) and Tl(I) reduction by chronocoulometry at a hanging mercury drop electrode. The rate constants are essentially independent of the concentration of the electroactive ions; prior work without compensation had indicated an inverse relationship. The deliberate addition of uncompensated resistance results in a variation of the apparent rate constant, which is removed if the added resistance is compensated by the electronic circuit. Problems in chronocoulometric studies of adsorption are ascribed to the presence of uncompensated resistance and an electrical analog of an interface where an adsorbed species reacts is proposed.

THE METHODS of potential step chronocoulometry and double potential step chronocoulometry have recently been shown to be useful techniques in the study of adsorption of electroactive species and of electrode reaction kinetics (*1, 2, 5, 10*). The initial studies of Christie, Lauer, and Osteryoung (*5*) reported the determination of the heterogeneous rate constants for Cd(II) reduction using the chronocoulometric technique. Some variation of the rate constant obtained with concentration of Cd(II) was indicated, but at that time it was not clear that the trend was not within experimental error. A more detailed examination of the procedure (*8*) established the dependence of the rate constant on concentration as a real effect outside the expected experimental error.

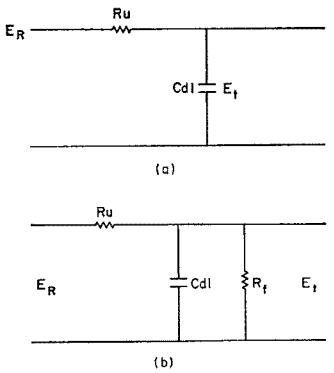

Figure 1. Assumed electrical analog

a. Ideally polarizable electrode
b. Polarized electrode with faradaic resistance R_f

In carrying out chronocoulometric studies on Tl(I) adsorption, it was recognized that the existence of uncompensated resistance, resulting in the loss of strict potential control, had a marked effect on the experimentally obtained charge curves (*14*). Some of the consequences of this situation have recently been discussed (*12, 13*), particularly as related to potential step experiments in which the current-time transient is analyzed.

Nemec (*11*) has shown that the potential "seen" by a reference probe from a spherical microelectrode is given by

$$E_R = E_t + \frac{i}{4\pi\kappa r}\left(1 - \frac{r}{r+x}\right) = E_t + iR_u \quad (1)$$

where r is the radius of the electrode, i is the net current, x is the distance of the reference probe from the surface of the electrode, κ is the specific conductance of the solution, E_R is the potential measured, E_t is the true potential across the double layer, and R_u is an "uncompensated" resistance "seen" by the reference electrode, which manifests itself in a potentiostatic circuit even though essentially no current flows through the electrode itself. The total "uncompensated" resistance is then the summation of the resistance due to the geometry of the electrode and that due to the capillary, the leads, etc.

If we consider the standard analog of an ideally polarized electrode (Figure 1, *a*), when a potential step is applied at E_R, the potential E_t is given by

$$E_t = E_R(1 - e^{-t/RC}) \quad (2)$$

Thus the true potential, E_t—that is, the potential across the double layer capacitor—is not equal to E_R for a time determined by the RC time constant.

If a faradaic current flows, the analog chosen is (Figure 1, *b*) and E_R never reaches E_t, even asymptotically. Thus, there are two interconnected effects: the slow rise of the potential, and the difference in the final E_t and the potential measured, E_R. This problem is discussed quantitatively by Oldham (*12*). The problem of ohmic drop can be overcome to a certain extent by positioning the reference capillary as close to the indicator electrode as possible. However, as Barnartt (*3*) has shown, the capillary will significantly alter the field if it is positioned too close to the surface.

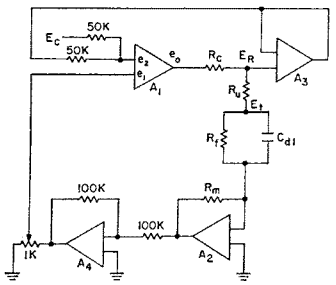

Figure 2. Schematic of potentiostatic circuit with compensation for ohmic losses

Analog shown in place of cell. R_c is resistance normally compensated by potentiostat

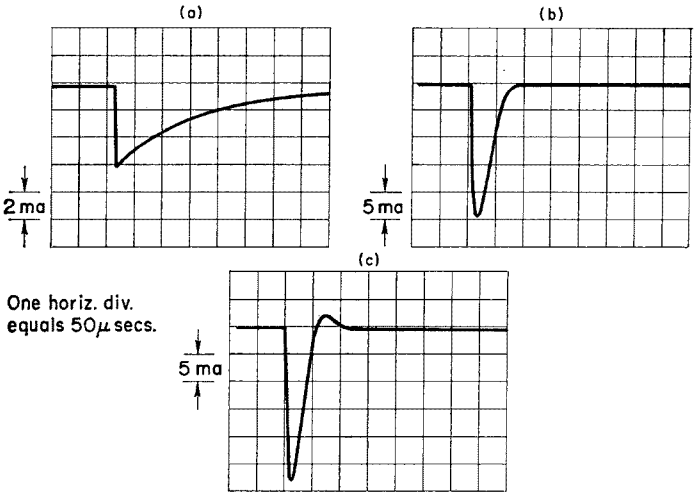

Figure 3. Current time traces following a potential step across an analog polarized electrode

a. No compensation
b. Optimum compensation
c. Overcompensation

The problem becomes severe when spherical microelectrodes such as hanging mercury drops are used, since the radius is on the order of 0.5 mm. If the reference electrode is very far from the indicator electrode, then from Equation 1

$$R_{u(\infty)} = \frac{1}{4\pi\kappa r} \tag{3}$$

The percentage reduction of $R_{u(\infty)}$ is then

$$\frac{R_u}{R_{u(\infty)}} = \left(1 - \frac{r}{r+x}\right) \times 100\% \tag{4}$$

Thus, it is necessary to position the reference electrode at exactly one radius distance from the surface to obtain a 50% reduction in R_u and at 0.111 r for a 90% reduction. We have found it impractical to position a Luggin capillary tip reproducibly at such close distances.

POSITIVE FEEDBACK SYSTEM

Instead of attempting to use a Luggin capillary, we have devised a positive feedback circuit which in essence compensates for the potential drop across R_u, the "uncompensated" resistance. [A recent paper by Pouli, Huff, and Pearson presents a compensation scheme which they indicate is operative under very limited conditions (*16*). Their analysis of the circuit appears to be in error, particularly in their concept of positive feedback and comments regarding reference electrode potentials.] The circuit is shown in Figure 2.

A_1 is a Weking fast-rise potentiostat where the Sonde terminal corresponds to e_2 and the Solspannung terminal corresponds to e_1. The other amplifiers are manufactured by G. Philbrick Researches, Boston, Mass. A_3 is a Model P75AU and A_2 and A_4 are Model SP656. The cell is represented by a resistor and a capacitor analog. Amplifier 3 is wired as a unity gain follower, amplifier 2 as an inverting current follower, and amplifier 4 as a unity gain inverter.

Considering only amplifier 1, the control amplifier,

$$e_0 = G(e_1 - e_2) \tag{5}$$

where G is the open loop gain of the amplifier and e_0, e_1, and e_2 are voltages as indicated in Figure 2. If the input and feedback resistors are equal, we can write

$$E_c - e_2 = e_2 - E_R \tag{6}$$

where E_c is the negative of the potential desired, and E_R is the potential "seen" by the reference electrode. All potentials are given with respect to ground.

We define β as the fraction of the output of amplifier 4 fed back to the positive input of amplifier 1. Since the output of amplifier 4 is precisely iR_m

$$e_1 = \beta i R_m \tag{7}$$

Solving Equation 6 for e_2 and substituting together with Equation 7 into 5, we obtain

$$e_0 = G\left[\beta i R_m - \left(\frac{E_c + E_R}{2}\right)\right] \tag{8}$$

However, $e_0 - iR_u - iR_c = E_t$ and $E_t = E_R - iR_u$, so that

$$2E_t + 2iR_u + 2iR_c = G[2\beta i R_m - (E_c + E_t + iR_u)] \tag{9}$$

$$E_t\left(\frac{2}{G} + 1\right) + iR_u\left(\frac{2}{G} + 1\right) + iR_c\left(\frac{2}{G}\right) = -E_c + 2\beta i R_m \tag{10}$$

Since $G \gg 1$, Equation 10 reduces to

$$E_t + i(R_u - 2\beta R_m) = -E_c \tag{11}$$

If the potentiometer is set so that $\beta = R_u/2R_m$, then $-E_c = E_t$, and the potentiostat controls the true potential across the double layer. If $\beta > R_u/2R_m$, the system will be out of control.

Response to a potential step is a "worst case" test for an operational amplifier network. Ideally, the potential across the double layer should be identical to the input at all times. In practice this is impossible. The initial response to a potential step requires an infinite current in a system with no uncompensated resistance. More realistically, for a 1-μf. capacitor to be charged in 1 microsecond, 1-ampere average current is required. Operational amplifiers do not have infinite gain; the 6 db. per octave gain rolloff effectively limits the response. Thus, perfect compensation cannot be obtained using the step techniques if only because response of the amplifier system to the high frequency components of the step is degraded. It was therefore of interest to evaluate the actual system performance.

POSITIVE FEEDBACK SYSTEM PERFORMANCE

The effective rise time of a potentiostatic system may be considered as that time required to charge the double layer. In the case of an ideally polarized electrode, it is the time required for the current to go essentially to zero. As a suitable analog for an ideally polarizable electrode we used the circuit shown in Figure 2, where C_{dl} is 1μf., R_u = 150 ohms, R_c is 100 ohms, and $R_f = \infty$.

In Figure 3 are shown the current-time traces obtained for the above cir-

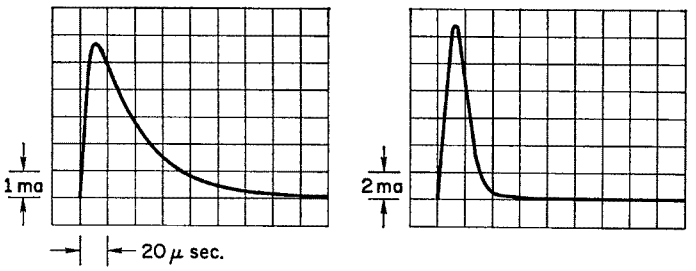

Figure 4. Current-time traces following a potential step using a hanging mercury drop (0.0291 sq. cm.) in 1*F* $NaNO_3$–0.01*M* HNO_3

a. No compensation
b. Optimum compensation

cuit with various values of $2\beta R_m$. In Figure 3, *a*, $2\beta R_m = 0$ and the rise time is greater than 500 microseconds. In Figure 3, *b*, $2\beta R_m = 98$ ohms and the rise time is approximately 80 microseconds. In Figure 3, *c*, $2\beta R_m = 110$ ohms and "ringing" is observed even though $2\beta R_m$ is less than 150 ohms. The ringing observed in Figure 3, *c*, is due to the deviations from ideality of the amplifier system. While the potential was kept constant $2\beta R_m$ was increased; the system went into violent oscillation when $2\beta R_m = 150$ ohms. At this point the system is in complete positive feedback—i.e., unstable—even though no d.c. current is passing. This "break point" may be used to determine the uncompensated resistance, as discussed below.

The system was then evaluated using a hanging mercury drop (0.0291 sq. cm.) in 1*F* $NaNO_3$ –0.01*M* HNO_3. The *i-t* traces shown in Figure 4 were obtained with a Tektronix type 564 oscilloscope using a 3A72 dual trace amplifier and a 3B3 time base. Figure 4, *a*, is for $2\beta R_m = 0$. The theoretical current time behavior is given by

$$i(t) = \frac{\Delta E}{R} e^{-t/RC} \qquad (12a)$$

or

$$\log i = \log \frac{\Delta E}{R} - \frac{1}{2.3} \frac{t}{RC} \qquad (12b)$$

Thus, with a known potential step, $\Delta E = 0.30$ volt, a plot of log *i vs. t* will have an intercept at $t = 0$ of $\Delta E/R$. Figure 4, *b*, shows the trace obtained when $2\beta R_m$ was set so that the current barely showed no ringing ($2\beta R_m = 20$ ohms). This value of β—i.e., just short of "ringing"—for a particular system is the maximum practical value of compensation used; the value of β at this point will be designated by β^*.

The "break point" of the system occurred when $2\beta R_m = 32$ ohms. Figure 5 shows the log *i-t* plot for the trace shown in Figure 4, *a*. The intercept log $(\Delta E/R)$ gives a value of *R* of 32 ohms, which is in agreement with the "break point" determination. The compensation procedure drastically decreased the effective rise time of the system.

ELECTRODE KINETIC STUDIES

The variation of the heterogeneous rate constant was believed to result from the presence of uncompensated resistance. To investigate this hypothesis in some detail, the following experiments were carried out.

The heterogeneous rate constant, $k_{s,h}$, for 5m*M* Tl(I) in 1*F* $NaNO_3$–0.01*F* HNO_3 at a hanging Hg drop was determined by chronocoulometry. In this method the potential is stepped from a potential where no current flows to a potential along the polarographic wave. The charge, *Q*, passed following such a potential is recorded as a function of time, *t*. Only the species Ox is in solution, and the potential is stepped to a point where the reaction $Ox + ne \rightarrow Red$ takes place. The charge-time behavior is analyzed by obtaining the asymptotic slope and intercept from a plot of *Q vs.* $t^{1/2}$, since it has been shown (*5*) that

$$Q_{asm} \approx \frac{2Kt^{1/2}}{\lambda\sqrt{\pi}} - \frac{K}{\lambda^2} \qquad (13)$$

where

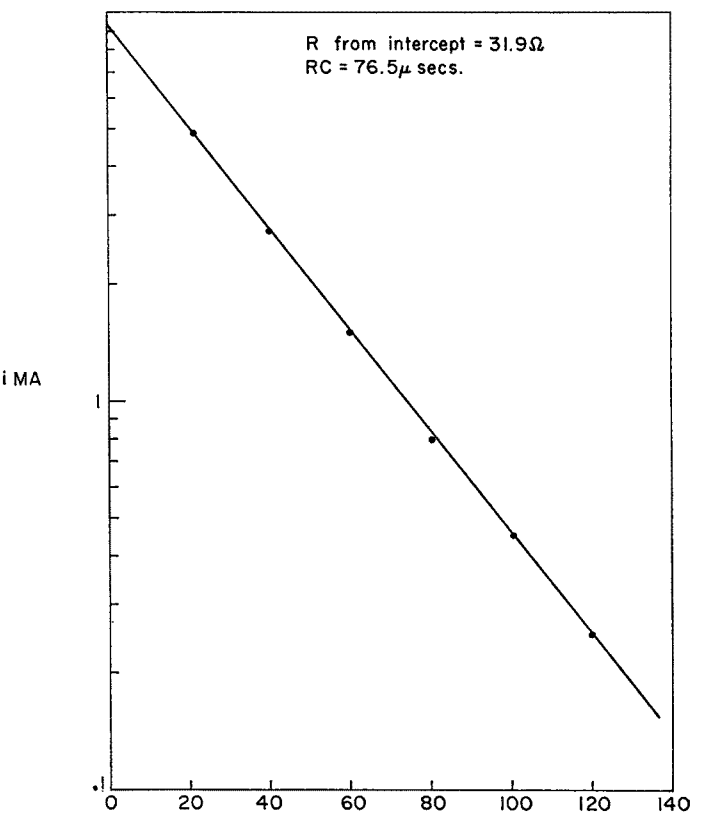

Figure 5. Log *i vs. t* plot for current decay shown in Figure 4, *a*

$$K = nFAk_{s,h}C_{ox}^{*} \exp \frac{-\alpha nF(E - E^{\circ})}{RT} \quad (14)$$

$$\lambda = k_{s,h} \left\{ \frac{\exp\left[\frac{-\alpha nF(E - E^{\circ})}{RT}\right]}{D_{ox}^{1/2}} + \frac{\exp(1 - \alpha)\frac{nF(E - E^{\circ})}{RT}}{D_{red}^{1/2}} \right\} \quad (15)$$

$k_{s,h}$ is the apparent heterogeneous rate constant (cm. per second), n, F, A, and D have their usual meaning, and C_{ox}^{*} is the bulk concentration of species Ox (moles per cc.). A correction for the coulombs required to charge the double layer is made by measuring a ΔQ corresponding to a given step ΔE in the absence of electroactive species; ΔQ is then subtracted from the experimentally obtained Q-t curve. Resistance was deliberately added in series with the indicator electrode in order to evaluate the system. The relevant data obtained are shown in Table I. All the data were collected using a high-speed digital data conversion and acquisition system (*9*, *15*).

The apparent rate constant at the operational maximum compensation, β^{*}, is remarkably constant. The value of $k_{s,h}$ decreases with resistance when $2\beta R_m = 0$. The values of $k_{s,h}$ at intermediate values of $2\beta R_m$ show less variation with added resistance as compensation is increased. If the ratio of $2\beta^{*}R_m/R_u$ is a function of the electronic system

Table I. Standard Rate Constant for 5mM Tl(I) in 1F $NaNO_3$–0.01F HNO_3

(Maximum value of β is β^{*})

Added resistance								
0 ohm			50 ohms			100 ohms		
$k_{s,h}$	α	β	$k_{s,h}$	α	β	$k_{s,h}$	α	β
0.55	0.62	0.125	0.54	0.55	0.290	0.50	0.59	0.460
0.40	0.62	0.090	0.19	0.60	0.145	0.13	0.53	0.230
0.31	0.53	0.062	0.14	0.55	0.072	0.084	0.52	0.115
0.23	0.58	0	0.11	0.53	0	0.065	0.49	0

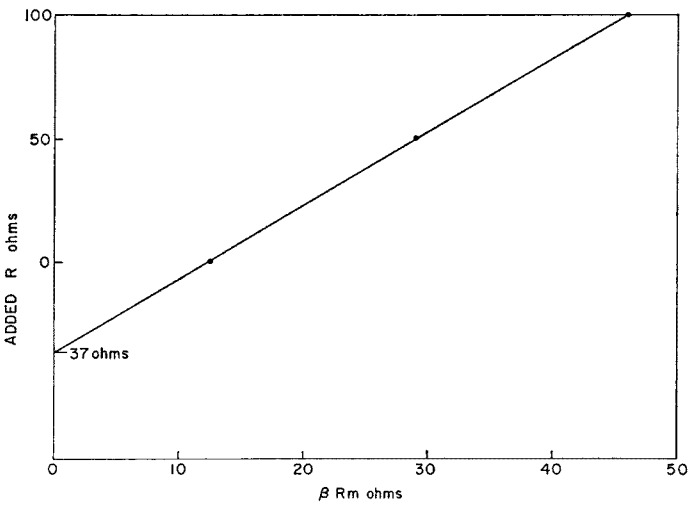

Figure 6. Plot of βR_m vs. added resistance at β^{*}

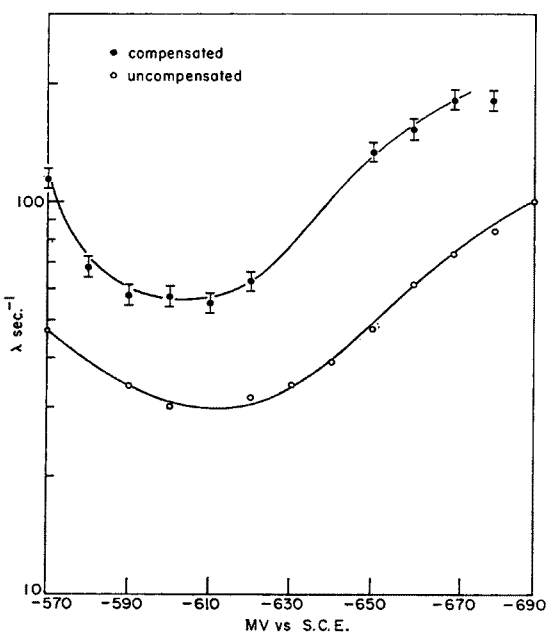

Figure 7. Log λ vs. E plot for 10mM Cd(II) in 1F Na_2SO_4

Upper line corresponds to values obtained for $\beta = \beta^{*}$, lower for $\beta = 0$

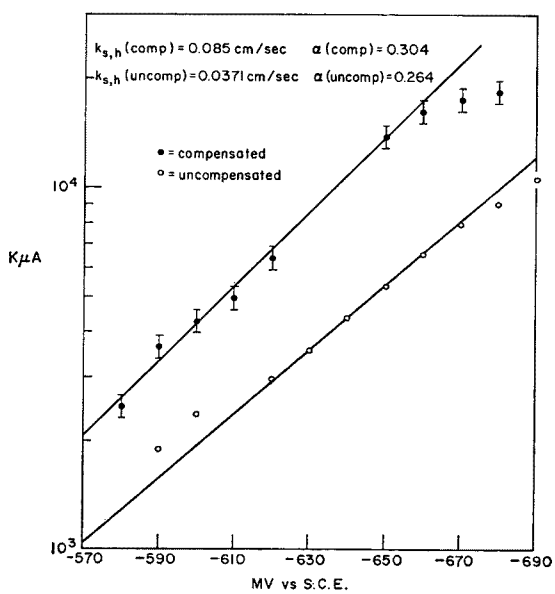

Figure 8. Log K vs. E plot for 10mM Cd(II) in 1F Na_2SO_4

Value of K at $E_{1/2}$ is $nFAC\,k_{s,h}$

Upper line corresponds to values obtained for $\beta = \beta^{*}$, lower for $\beta = 0$

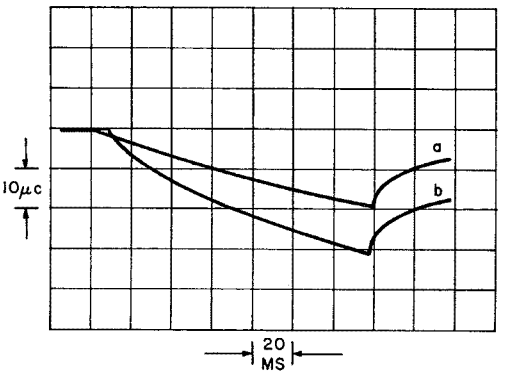

Figure 9. Q-t curves for potential step in 10mM Cd(II) in 1F Na_2SO_4

Potential step to $E_{1/2}$
a. $\beta = 0$
b. $\beta = \beta^*$

only, a constant percentage of R_u should be compensated. Therefore, a plot of $2\beta^* R_m$ *vs.* added resistance should be linear and the intercept should be the value of the uncompensated resistance of the cell alone. Figure 6 shows such a plot for the data presented in Table I. The value of R_u from the intercept is 37 ohms, in reasonable agreement with the value (32 ohms) obtained for the same solution without electroactive species.

The apparent heterogeneous rate constants for 5 and 10m*M* Cd(II) in 1*F* Na_2SO_4 at a hanging mercury drop were then determined and found to be 0.74 and 0.83 cm. per second, respectively. These numbers can be compared to those reported previously (*5*) and those reported by Lingane and Christie (*8*) using a similar method. In both previous cases an inverse relation was observed between $k_{s,h}$ and concentration. Plots of log λ *vs.* E and log K *vs.* E, with and without compensation, are shown in Figures 7 and 8 for 10m*M* Cd(II).

If one applies a sufficiently large step to the electrode, so that for $t > 0$, the surface concentration of the species undergoing reaction will be equal to 0, then the *Q-t* behavior will follow the chronoamperometric current integral

$$Q = \frac{2nFACD_{ox}^{1/2}t^{1/2}}{\pi^{1/2}} \qquad (16)$$

If, however, the surface concentration does not go to zero instantly, because of slow-rise equipment or uncompensated resistance, the Q at t will be less than the value calculated from Equation 16. One may thus consider these coulombs "lost." The error can be estimated in terms of a linear potential sweep followed by a steady potential as suggested by Booman and Holbrook (*4*). The charge passed at any time following the application of a potential step can approach that given by Equation 16 only if the potential across the double layer is constant. If, as is the case, the actual potential rises slowly, the electron transfer rate will be determined by the actual potential during the rise, and thus less than the theoretical charge will have passed at any time, t; this will alter the concentration profile at the electrode surface. Although this effect will be present in any potentiostatic method, chronocoulometry is most sensitive to this disturbance, since the integral of the current contains the history of the reaction from the time of initiation. The effect is accentuated by a high concentration of electroactive species and for potential steps to potentials around the polarographic half wave where the current is most sensitive to the true potential. Figure 9 shows *Q-t* traces obtained for 10m*M* Cd(II) compensated and uncompensated; the "loss" of coulombs in the uncompensated case is striking.

ARTIFACTS IN ADSORPTION STUDIES

In the study of adsorption of electroactive species by chronocoulometric techniques the potential is stepped from E_1 where no faradaic current flows to a potential, E_2, where the electron transfer rate is essentially so fast that the reaction is diffusion-controlled at all times. In such a case it is assumed that the species adsorbed at E_1 will reduce at E_2 instantaneously. The problem of uncompensated resistance can be very serious in such cases, as pointed out by Anson, Christie, and Osteryoung, and can result in plateaus in the *i-t* traces (*2*).

A reasonable analog for an electrode at which an electroactive substance adsorbs at E_1 and then reduces, is shown in Figure 10, where C_{dl} is the analog for the double layer capacity, D_1 is a zener diode whose breakover potential is fairly low, and R_f is the faradaic resistance.

We consider the potential across the

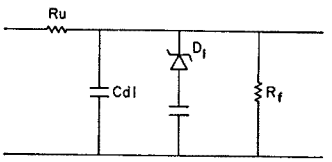

Figure 10. Operational analog for electrode showing adsorption

This analog is valid only for a potential step procedure. Potential true and corresponding current

double layer capacity for the circuit shown in Figure 10, following a potential step $\Delta E = E_2 - E_1$ applied at R_u; the potential will rise rapidly at a rate determined by $R_u C_{dl}$ until the breakover potential of the zener diode is reached. At that point the potential rise will be significantly decreased because of charging of the capacitor in series with D_1, which may be considered analogous to discharge of the adsorbed species. [This is not the analog considered by Laitinen and Randles in their studies of adsorption by means of faradaic impedance (*7*). The chronocoulometric technique can determine only the amount of material absorbed at E_1, the potential from which the step is applied, and at which no net faradaic current flows. The faradaic impedance procedure considers the adsorption as a parallel reaction path to explain "anomalous" results. Thus, in general, the faradaic impedance considers the reaction in the vicinity of the polarographic half-wave potential. Recent considerations of the merits of the two techniques as applied to detecting adsorption by Laitinen and Chambers (*6*) and Anson (*1*) appear to have overlooked this point.] Figure 11, *a*, shows the potential rise across C_{dl} for a step from 1.0 to 3.5 volts for an analog system made up of $R_u = 100$ ohms, $R_f = \infty$, $C_{dl} = 1$ μf., D_1 = 1N702 (2.6 volts), $C = 10$ μf. The corresponding current is shown in Figure 11, *b*. Figure 11, *b*, shows that there is a distinct "plateau" in the current immediately following the initial current spike. However, if 60% of the resistance is compensated, one obtains the potential rise and corresponding current shown in Figure 12, *a* and *b*. The plateau has essentially disappeared and the potential rise across C_{dl} has been sharpened.

In a recent paper, Anson, Christie, and Osteryoung (*2*) showed *i-t* traces for Cd(II) in SCN^- solutions where distinct plateaus were observed. The plateaus were assumed to occur because of reduction of the adsorbed species. Such interpretation is correct, however, only because of the presence of uncompensated resistance. A 2m*M* Cd(II) solution in 0.5*M* NaSCN–0.5*M* $NaNO_3$ solution was run. Figure 13, *a*, shows the *i-t* trace where no compensation is applied;

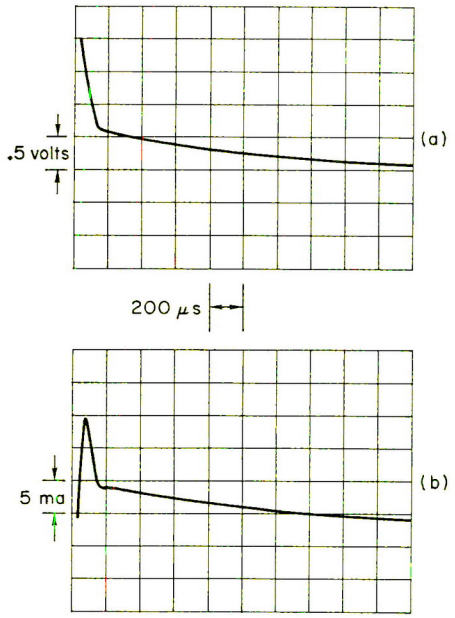

Figure 11. Potential rise and corresponding current

a. True potential across C_{dl} following application of potential step at E_i using analog shown in Figure 10 with $\beta = 0$
b. Corresponding *i-t* trace

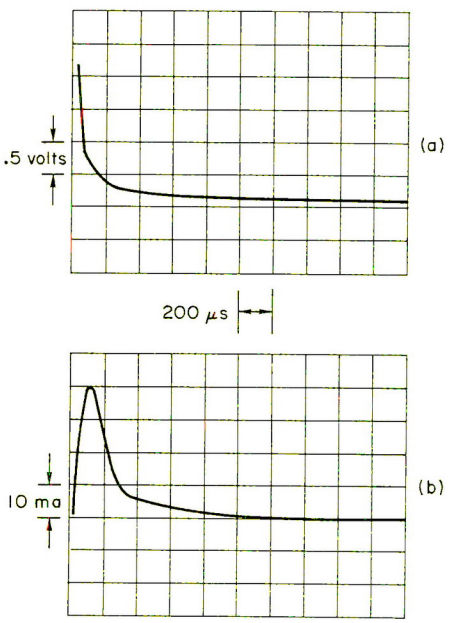

Figure 12. Conditions identical to those in Figure 11, with $\beta = \beta^*$

a. True potential across C_{dl}
b. Corresponding *i-t* trace

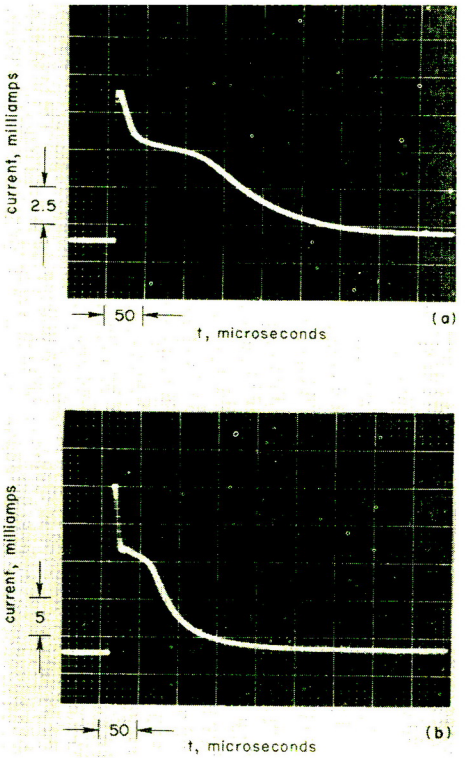

Figure 13. Current-time trace following a potential step in 2mM Cd(II) in 0.5M NaSCN–0.5M $NaNO_3$

a. $\beta = 0$
b. $\beta = \beta^*$

Figure 13, *b*, shows the corresponding trace when compensation is applied. However, such plateaus where no compensation is applied are not conclusive evidence of adsorption. If the concentration of electroactive species is made sufficiently great, a plateau will be observed even in the absence of adsorption, the plateau current being due to a massive iR drop.

CONCLUSIONS

The ohmic resistance can be compensated electronically to a degree dependent on the quality of the electronic circuitry. In the case of potential step methods the scheme is effective and necessary. The compensation can be increased to higher values for voltage sweep methods than for the step method, as phase shift problems will be less severe. Similar considerations hold for a.c. polarographic methods (*17*). The method is effective for all potential control methods except polarography. This special problem will be treated in a separate communication.

ACKNOWLEDGMENT

The authors thank F. C. Anson and J. H. Christie for helpful discussions.

LITERATURE CITED

(1) Anson, F. C., ANAL. CHEM. **36**, 932 (1964).
(2) Anson, F. C., Christie, J., Osteryoung, R., *J. Electroanal. Chem.*, in press.
(3) Barnartt, S., *J. Electrochem. Soc.* **108**, 102 (1961).
(4) Booman, G., Holbrook, W., ANAL. CHEM. **37**, 795 (1965).
(5) Christie, J., Lauer, G., Osteryoung, R., *J. Electroanal. Chem.* **7**, 60 (1964).
(6) Laitinen, H., Chambers, L., ANAL. CHEM. **36**, 7881 (1964).
(7) Laitinen, H. A., Randles, J., *Trans. Faraday Soc.* **51**, 54 (1955).
(8) Lingane, P., Christie, J., *J. Electroanal. Chem.* **10**, 284 (1965).
(9) Lauer, G., Osteryoung, R., ANAL. CHEM. **38**, 1137 (1966).
(10) Murray, R. W., Gross, P. J., *Ibid.*, **38**, 392 (1966).
(11) Nemec, L., *J. Electroanal. Chem.* **8**, 166 (1964).
(12) Oldham, K. B., *Ibid.*, **11**, 171 (1966).
(13) Oldham, K. B., Osteryoung, R. A., *Ibid.*, **11**, 397 (1966).
(14) Osteryoung, R., unpublished results.
(15) Osteryoung, R., Lauer, G., Electroanalytical Symposium, Winter Meeting, ACS, Phoenix, January 1966.
(16) Pouli, D., Huff, J., Pearson, J. C., ANAL. CHEM. **38**, 382 (1966).
(17) Smith, D., Electroanalytical Symposium, Winter Meeting, ACS, Phoenix, January 1966.

RECEIVED for review April 19, 1966. Accepted June 10, 1966. Electroanalytical Instrumentation Symposium, Winter Meeting, ACS, Phoenix, Ariz., January 1966.

Kinetic Current Measurements with Controlled Potential

Application to the Uranium(V) Disproportionation Reaction

DALLAS T. PENCE[1] and GLENN L. BOOMAN[1]

Phillips Petroleum Co., Atomic Energy Division, Idaho Falls, Idaho

▶ **The correct interpretation of kinetic current measurements that are obtained by the use of controlled potential polarography at short times requires a thorough understanding of the electrical characteristics of the cell and of the potentiostat. This paper demonstrates the practical application of transfer function measurements to test the design and to determine the response time of a controlled potential polarograph. Errors involved in the measurement of kinetic currents at short times and methods proposed for their correction are discussed. The uranium(V) disproportionation reaction was studied over the time region of 1 msec. to 10 sec. using the controlled-potential method. The determined value of the rate constant is 192 liter^2 mole^{-2} sec.$^{-1}$ for 1M perchloric acid medium.**

THE LARGE AMPLITUDE, potential-step method of controlled potential polarography has developed slowly compared to other electrochemical techniques. The controlled-potential method has been compared with other methods by Gerischer and Staubach (*9*) and more recently by Reinmuth (*22*). The use of any of the large amplitude methods to obtain kinetic current data at short times is limited by a lack of knowledge of the effect of the double-layer capacitance. To a degree, the controlled-potential method depends less on a precise understanding of the double-layer capacitance at short times than do other methods. A second advantage is that data interpretation is simplified because in cases involving parallel reactions, the directly measured current is the linear summation of the individual reaction currents. A third advantage is that nearly all the information about a reaction can be obtained for a set of selected conditions with a single voltage pulse. Finally, absorption of interfering ions at the electrode surface is a lesser problem with the controlled-potential method because kinetic current effects are more easily discriminated from adsorption current effects.

The greatest single factor that has limited the popularity of the large amplitude, potential-step method of controlled potential polarography for short time measurements has been the complexity of the required instrumentation. The stringent bandwidth, current, and gain requirements for the operational amplifiers also have been limiting factors. Lastly, data collection has been a tedious task. The continued improvement of commercial operational amplifiers and automatic data acquisition equipment, and recent advances in the theory of controlled potential polarography undoubtedly will lead to its increased use.

The purpose of this paper is to illustrate the important aspects in the collection and interpretation of kinetic current data taken at short times by use of controlled potential polarography. As a practical demonstration, data are presented and discussed for the uranium(V) disproportionation reaction in 1*M* perchlorate media. Also the use of transfer function measurements is demonstrated as a means of determining system response time.

EXPERIMENTAL

Instrumentation. The block diagram showing the functional breakdown of the various components used to time, control, measure, and print out the collected data has been presented in Figure 1 of Reference *1*. Because details of the fast data acquisition system are given in the same reference, only a brief description is presented here. The start signal, initiated by depressing the start switch in the digital timing and control section, gates the pulse from the digital-to-analog waveform generator to the potential control circuit and the cell. This also initiates the timing routine which controls the read signals to the analog-to-digital converter. The timing routine is preprogrammed on a patchboard in the digital timing and control section. The analog-to-digital converter measures and converts the analog voltages from the current-measuring circuit. The digital information is stored in the core memory unit. At the completion of the measurements, the stored information may be recalled and printed out by operating a manual switch in the digital timing and control section.

The potentiostat, shown in Figure 1, is a simplified version of the one described by Booman and Holbrook (*3*) and contains the same operational amplifiers, plug-in units, and modifications. Because the various components of the potentiostat and their relationships to each other are discussed below at some length, the modified circuit diagram of the potentiostat is presented here. The control amplifier is represented by *A*-1 with R_1, R_2, and C_1 comprising the stabilization network. The voltage follower for the reference electrode is *A*-2. The current-measuring circuit consists of the current follower, *A*-3, and the load resistor R_6. The bias and pulse voltages are applied to the control amplifier through the summing resistors R_3 and R_4, respectively. Resistor R_5 is a series cell resistance and resistor R_7 is additional uncompensated cell resistance.

[1] Present address, Idaho Nuclear Corp., CPP, National Reactor Testing Station, P.O. Box 1845, Idaho Falls, Idaho 83401

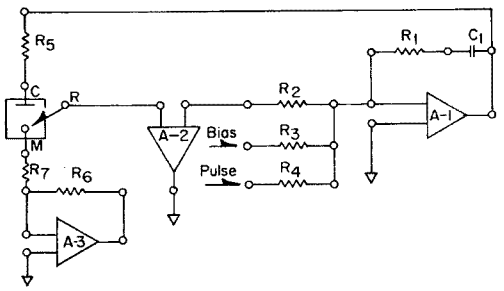

Figure 1. Electrochemical cell and potentiostat

Electrochemical Cell and Reagents. The electrochemical cell was a conventional three-electrode type. The counter electrode, a helically-wound platinum wire, surrounded the reference electrode probe and the measuring electrode.

The reference electrode was an H-cell with three compartments, each separated by an ultrafine, fritted glass disk. The reference cell was a silver-silver chloride electrode, with 0.1*M* hydrochloric acid electrolyte, enclosed in a porous-Vycor-tipped, 7-mm. glass tube. The reference cell was fitted in one arm of the H-cell. Contamination from the reference cell was prevented by the continuous passage of supporting electrolyte, 1*M* perchloric acid, through the center compartment and the compartment containing the reference cell. The supporting electrolyte overflowed into a large glass reservoir through an outlet located in the compartment containing the reference cell. Contamination of the reference cell by the supporting electrolyte was prevented by maintaining a positive head of pressure on the hydrochloric acid solution in the reference cell. The reference electrode probe, also a porous-Vycor-tipped glass tube filled with supporting electrolyte, was connected to the other arm of the H-cell with Tygon tubing.

The measuring electrode, a two-drop, hanging drop mercury electrode (HDME) was similar to that described by Shain (*23*). A commercial 6- to 12-second dropping mercury electrode (DME) delivered the drops to a glass scoop for transfer to the HDME. The potential of the DME was maintained at a constant value, equal to that of the reference electrode, during the collection of the mercury drops. This was accomplished by connecting the output of the voltage follower to the DME mercury reservoir and grounding the measuring and counter electrodes. An accurately timed, automatic drop knocker, installed on the DME, improved the reproducibility of the drop size.

The cell container was a 100-ml. weighing bottle surrounded by a glass seal for circulating water thermostated to 25° ± 0.1° C. The lid, made of Teflon, provided a tight seal on the weighing bottle. Holes were drilled in the lid for the various electrodes, degassing dispersion tube, and scoop. The cell, DME mercury reservoir, DME drop knocker assembly, and reference electrode were attached to a framework which was shock-mounted with several layers of firm sponge rubber sandwiched between sheet lead.

The uranium perchlorate stock solution was prepared by dissolving U_3O_8, NBS standard sample 950a, in 71% perchloric acid. The solution was diluted to be 0.1*M* in uranium perchlorate and 1*M* in perchloric acid. The test solutions were prepared from the diluted stock solution as needed.

Measurements. The uranium perchlorate test solutions were purged for 20 to 30 minutes with argon before each set of measurements. The amplitude of the potential step was 0.6 volt, and the bias potential was set at 0.2 volt anodic to the half-wave potential of the uranium(VI) reduction wave. To obtain the desired signal-to-noise ratio and to retain the fastest possible system response time, the kinetic current measurements, taken over four decades of time, were split into two parts. The load resistor, R_6 in Figure 1, was a six-decade, 0.05% unit. The data for the first 1.5 decades of time (1 to about 15 msec.) were obtained with a low resistance value which was increased for the final 2.5 decades. The maximum values of the load resistor for the first 1.5 decades of time and the last 2.5 decades were 4000 and 8000 ohms, respectively. A 0.05-μfd. capacitor was placed in parallel with the load resistor during the final 2.5-decade measurements. The effect of this shunt capacitance was determined to be negligible.

The current-time transient responses of the uranium perchlorate–perchloric acid system were calculated from the recorded voltage-time responses of the current follower amplifier, *A*-3 in Figure 1. Twelve sets of 41 voltage measurements were obtained for each of three concentrations of uranium perchlorate, 0.002*M*, 0.005*M*, and 0.010*M*, in 1*M* perchloric acid. Two sets of voltage measurements were required for each test solution to give a complete set of measurements for the desired 4 decades of time because of the necessary load resistance change after about 1.5 decades. Six complete sets of measurements, all obtained the same day, are defined as a run. A fresh mercury drop electrode was used for each transient response measurement. The voltage measurements were taken on a logarithmic time scale at a rate of 10 measurements per decade of time.

One-molar perchloric acid blanks were measured using the same load resistance values as were used on the test solutions. After the voltage measurements for a test solution were averaged for each of the 41 times and the averaged background voltages were subtracted, the current values for each time of the run were determined by dividing the voltages by the appropriate load resistance values. Voltage values for a typical run are shown in Table I along with the current values of all the runs. The three runs of each of the uranium perchlorate solutions were taken at approximately one week intervals.

The average radii and surface areas of the hanging mercury drops were calculated from the weight of 50 DME drops, which were collected in the test solution after each run. The current values for each run were normalized to a standard drop surface area (0.0519 $cm.^2$) for overall evaluation and for precision calculations.

The per cent relative standard deviations were calculated to obtain a measure of the within-run reproducibility of the mercury electrode drop size and of the electronic measurement equipment. The precisions of the six sets of voltage measurements were determined for each time of the various runs. As expected, the precisions were lower for both short times and for long times as compared to the intermediate time region, particularly at long times where the signal-to-noise ratios were small. At both ends of the time scale (about 1 to 10 msec. and 1 to 10 seconds), the precisions were as low as several per cent. Within the range of 1 msec. to 1 second, however, the precision values were all less than 1%, with an average value of slightly less than 0.5%. Within-run precisions for one of the runs is shown in Table I.

RESULTS AND DISCUSSION

Determination of System Response Time. To evaluate the measurement of kinetic currents at short times, the response time of the system must be determined. The term system includes the potentiostat, the electrochemical cell, and the current-measuring circuit. The best method of determining the response time is to measure the transfer function of the system. The use of transfer function measurements for the selection of components and for the general design of operational amplifier circuits for controlled-potential instrumentation has been discussed by Booman and Holbrook (*2*, *3*). A table of feedback network values is available (*3*) for a variety of cell characteristics which

Table I. Kinetic Current Values and Precision for Various Concentrations of Uranium Perchlorate in 1M Perchloric Acid

Time	Typical voltage measurements and precision for six transients (Run IA) Voltage measurements,[a] mv.						Current,[b] ma.	σ_a	Current values for average of six transients, normalized to standard drop size, and precision between runs: $0.002M$ $UO_2(ClO_4)_2$ Run number[c] IA	IIA	IIIA	σ_b	$0.005M$ $UO_2(ClO_4)_2$ Run number[c] IB	IIB	IIIB	σ_b	$0.010M$ $UO_2(ClO_4)_2$ Run number[c] IC	IIC	IIIC	σ_b
1 msec.	2041	2028	2046	2036	2029	2032	0.5008	0.35	0.4989	0.5071	0.5105	1.18	1.2857	1.2795	1.2918	0.48	2.6985	2.6664	2.7030	0.74
1.3	1741	1744	1754	1740	1737	1743	0.4293	0.34	0.4277	0.4340	0.4375	1.15	1.1024	1.0921	1.1008	0.50	2.2830	2.2565	2.2800	0.64
1.6	1549	1548	1562	1552	1545	1549	0.3818	0.38	0.3804	0.3870	0.3890	1.17	0.9727	0.9696	0.9758	0.32	2.0090	1.9847	2.0030	0.63
2.1	1336	1335	1343	1335	1329	1339	0.3313	0.35	0.3301	0.3327	0.3343	0.64	0.8314	0.8337	0.8373	0.36	1.7116	1.6930	1.7040	0.55
2.6	1191	1188	1202	1192	1191	1191	0.2930	0.41	0.2919	0.2968	0.2985	1.16	0.7452	0.7430	0.7453	0.17	1.5203	1.5030	1.5100	0.57
3.2	1069	1068	1076	1071	1070	1072	0.2633	0.26	0.2623	0.2659	0.2675	1.00	0.6683	0.6658	0.6683	0.22	1.3579	1.3429	1.3490	0.56
4.1	942	943	949	947	942	946	0.2320	0.31	0.2357	0.2367	0.2353	0.31	0.5871	0.5858	0.5875	0.15	1.1986	1.1799	1.1830	0.84
5.1	844	841	851	843	841	849	0.2075	0.50	0.2108	0.2093	0.2105	0.38	0.5260	0.5241	0.5258	0.20	1.0665	1.0547	1.0570	0.59
6.2	764	764	768	767	764	766	0.1878	0.23	0.1909	0.1907	0.1920	0.37	0.4762	0.4723	0.4773	0.55	0.9659	0.9550	0.9560	0.63
8.3	661	662	667	665	658	663	0.1625	0.47	0.1644	0.1637	0.1650	0.40	0.4113	0.4101	0.4113	0.17	0.8344	0.8248	0.8240	0.70
10	603	605	607	604	600	603	0.1480	0.38	0.1501	0.1493	0.1500	0.29	0.3746	0.3734	0.3743	0.17	0.7610	0.7515	0.7520	0.71
13	531	528	535	530	528	530	0.1298	0.48	0.1317	0.1309	0.1315	0.32	0.3289	0.3282	0.3285	0.13	0.6690	0.6612	0.6610	0.60
16	478	481	482	475	477	477	0.1168	0.55	0.1188	0.1179	0.1188	0.44	0.2969	0.2959	0.2970	0.21	0.6045	0.5974	0.5960	0.76
21	415	416	417	422	418	422	0.1020	0.72	0.1037	0.1017	0.1038	1.15	0.2595	0.2589	0.2590	0.12	0.5293	0.5236	0.5230	0.66
26	1896	1904	1896	1896	1906	1907	0.0934	0.28	0.0931	0.0923	0.0935	0.65	0.2335	0.2338	0.2335	0.07	0.4767	0.4722	0.4705	0.68
32	1712	1724	1716	1717	1725	1725	0.0844	0.42	0.0843	0.0833	0.0845	0.76	0.2116	0.2118	0.2115	0.08	0.4327	0.4287	0.4275	0.63
41	1519	1526	1519	1521	1529	1529	0.0747	0.31	0.0745	0.0739	0.0748	0.62	0.1874	0.1874	0.1873	0.04	0.3849	0.3813	0.3795	0.72
51	1369	1373	1368	1371	1376	1376	0.0672	0.25	0.0670	0.0664	0.0672	0.63	0.1690	0.1692	0.1690	0.07	0.3487	0.3454	0.3435	0.76
62	1243	1249	1247	1246	1253	1249	0.0610	0.27	0.0608	0.0602	0.0614	0.99	0.1539	0.1539	0.1538	0.05	0.3186	0.3155	0.3140	0.74
83	1079	1086	1085	1084	1088	1089	0.0531	0.33	0.0529	0.0523	0.0532	1.21	0.1345	0.1346	0.1342	0.16	0.2803	0.2773	0.2755	0.87
100 msec.	992	994	992	996	999	998	0.0485	0.30	0.0483	0.0478	0.0488	0.93	0.1234	0.1235	0.1230	0.21	0.2583	0.2551	0.2540	0.87
130	874	878	877	879	881	882	0.0428	0.33	0.0426	0.0422	0.0429	0.82	0.1095	0.1095	0.1090	0.26	0.2306	0.2284	0.2270	0.80
160	795	800	796	799	799	800	0.0389	0.27	0.0388	0.0383	0.0390	0.93	0.0997	0.0999	0.0995	0.20	0.2117	0.2092	0.2080	0.90
210	703	706	705	707	708	709	0.0344	0.30	0.0343	0.0337	0.0345	1.23	0.0888	0.0888	0.0883	0.33	0.1898	0.1875	0.1870	0.88
260	638	644	641	641	644	643	0.0313	0.36	0.0312	0.0305	0.0312	1.32	0.0812	0.0813	0.0808	0.32	0.1746	0.1725	0.1715	0.91
320	583	588	585	585	587	587	0.0285	0.31	0.0284	0.0278	0.0285	1.35	0.0743	0.0744	0.0743	0.09	0.1612	0.1594	0.1585	0.60
410	525	527	525	527	531	527	0.0255	0.42	0.0254	0.0250	0.0255	1.03	0.0675	0.0674	0.0670	0.39	0.1473	0.1456	0.1445	0.97
510	479	480	480	481	480	483	0.0233	0.28	0.0232	0.0228	0.0232	1.00	0.0619	0.0619	0.0623	0.37	0.1358	0.1344	0.1340	0.71
620	439	445	442	443	446	444	0.0214	0.56	0.0213	0.0208	0.0215	1.70	0.0574	0.0574	0.0573	0.12	0.1265	0.1252	0.1250	0.65
830	396	396	398	396	400	398	0.0191	0.41	0.0190	0.0185	0.0191	1.69	0.0518	0.0518	0.0521	0.33	0.1141	0.1132	0.1125	0.71
1 sec.	368	369	367	368	369	369	0.0177	0.21	0.0176	0.0172	0.0178	1.77	0.0483	0.0481	0.0480	0.33	0.1066	0.1057	0.1055	0.44
1.3	333	335	335	338	336	336	0.0162	0.48	0.0161	0.0156	0.0161	1.82	0.0442	0.0441	0.0438	0.48	0.0974	0.0965	0.0965	0.54
1.6	309	311	311	312	315	312	0.0150	0.63	0.0149	0.0144	0.0150	2.16	0.0412	0.0410	0.0410	0.29	0.0905	0.0896	0.0895	0.61
2.1	282	285	285	286	287	285	0.0137	0.59	0.0136	0.0132	0.0136	1.70	0.0375	0.0373	0.0375	0.32	0.0820	0.0808	0.0810	0.79
2.6	262	265	265	266	268	267	0.0127	0.77	0.0127	0.0122	0.0126	2.08	0.0350	0.0348	0.0348	0.34	0.0757	0.0751	0.0755	0.41
3.2	249	249	249	248	249	248	0.0119	0.06	0.0119	0.0113	0.0118	2.74	0.0325	0.0324	0.0325	0.22	0.0700	0.0691	0.0700	0.75
4.1	231	235	229	229	231	231	0.0110	0.97	0.0110	0.0110	0.0110	0.00	0.0299	0.0296	0.0300	0.70	0.0641	0.0636	0.0635	0.50
5.1	216	218	216	215	217	217	0.0103	0.46	0.0103	0.0098	0.0104	3.13	0.0278	0.0275	0.0280	0.90	0.0591	0.0583	0.0590	0.75
6.2	204	204	206	201	206	203	0.0097	0.93	0.0097	0.0092	0.0099	3.75	0.0259	0.0256	0.0263	1.35	0.0551	0.0544	0.0550	0.69
8.3	188	191	185	183	192	189	0.0089	1.84	0.0089	0.0083	0.0092	5.22	0.0235	0.0233	0.0243	2.24	0.0496	0.0494	0.0500	0.62
10.0	176	182	180	174	185	180	0.0085	2.35	0.0085	0.0078	0.0089	6.67	0.0222	0.0219	0.0230	2.56	0.0463	0.0462	0.0462	0.28
									σ_c = 1.91				σ_c = 0.57				σ_c = 0.70			
									σ_d = 1.48 (51 msec. to 4.1 sec.)				σ_d = 0.27 (32 msec. to 2.6 sec.)				σ_d = 0.76 (10 to 830 msec.)			

[a] Load resistor changed at 26 msec. for this particular run. A fresh mercury drop electrode was used for each transient and at the load resistor change point.

[b] Calculated from the average of the voltage measurements after background subtraction.

[c] Each result is the average of six replicate determinations on the same solution. All data listed under the same run number were obtained on the same day, and each run was made at least a week apart.

σ_a = Within-run precision (per cent relative standard deviation) calculated from the six individual transient measurements.

σ_b = Between-run precision (per cent relative standard deviation) calculated from the three normalized average currents (two degrees of freedom).

$\sigma_c = \left(\frac{\Sigma\sigma_b^2}{n}\right)^{1/2}$, root-mean-square precision for four decade time region (n = 41).

σ_d = Same as σ_c except only the two-decade time region selected for the rate constant determination is included (n = 20).

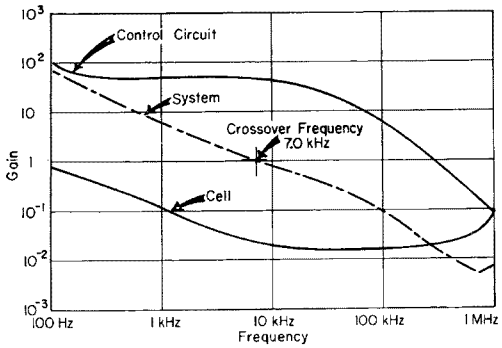

Figure 2. Measured cell, control circuit, and system transfer functions

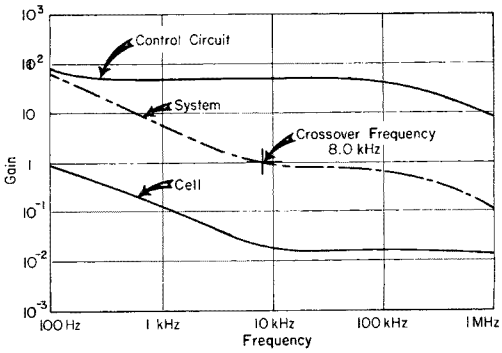

Figure 3. Calculated cell, control circuit, and system transfer functions

provides for optimum stability and frequency response for a system of the type presented in the present paper. Because frequency response and stability are sensitive to many factors, at least minor adjustments to the feedback network usually are necessary for optimum performance.

Transfer function measurements provide a fundamental test of any electronic system, and from these measurements the stability of the control system can be analyzed, the design and proper operation of the various components can be verified, and the system response can be determined. Because of the interaction between the various components of an electroanalytical system, particularly between the control circuit and the cell, the determination of the system transfer function is the most practical method to obtain the stability characteristics and the frequency response of the system. The application of transfer function measurements to verify instrument performance and to determine system response is illustrated below.

Because the transfer function of the overall system usually cannot be determined by one set of measurements, it is convenient to measure the cell and current-measuring circuit transfer function separately from the potential control circuit transfer function. Inasmuch as the two sections of the overall system chosen for transfer function measurement are not electrically independent, the individual transfer functions must be measured with the system in operation. The product of the two individual transfer functions approximately represents the overall system transfer function. For convenience, the term "cell transfer function" is defined to include the effects of the double-layer capacitance, uncompensated cell resistance, series cell resistance, reference electrode impedances, and the current-measuring circuit. Similarly, the "control circuit" is defined to include the remaining portion of the circuit comprising the voltage follower, summing network, and control amplifier with its feedback network.

It is recognized that the system transfer function as just described is not the true system transfer function. The exact definition of the transfer function of a system is the Laplace transform of the system output divided by the Laplace transform of the system input at zero initial conditions. This definition, applied to the above system, is the Laplace transform of the voltage across the double-layer capacitance divided by the Laplace transform of the voltage supplied to the summing resistor (R_4 in Figure 1) of the control amplifier input network. Even though it is not possible to directly measure the voltage across the double-layer capacitance of an actual system, the procedure outlined below gives a value that closely approximates the true system transfer function.

The double-layer capacitance was measured at various potentials with an a.c. bridge for a $1M$ perchloric acid electrolyte. Based on the geometry of the cell, the uncompensated cell resistance (the resistance between the measuring electrode and the reference electrode) was calculated to be about 0.85 of the resistance between the measuring electrode and the counter electrode. This last resistance was measured and the uncompensated cell resistance was determined. The value of the double-layer capacitance, at a potential corresponding to a point at the foot of the first cathodic uranium(VI) wave and at a frequency of 20 kHz., was determined to be 1.2 μf. for a mercury drop of radius 0.052 cm.; and the uncompensated cell resistance was estimated to be 4 ohms. From a consideration of stability, frequency response, and current-measuring sensitivity (*3*), a 1000-ohm series cell resistance, R_5, was added in the circuit (Figure 1). For the same reasons, resistance, R_7, was added in series with the uncompensated cell resistance at the measuring electrode to increase the total uncompensated cell resistance to 15 ohms. The stabilization network, first selected from Table II of Reference *3*, then was modified to provide for minimum voltage rise time across the capacitor representing the double-layer capacitance in a dummy cell.

The cell transfer function, with $1M$ perchloric acid as the electrolyte, and the control circuit transfer function, are shown in Figure 2 as a Bode diagram, a logarithmic plot of the transfer function *vs.* frequency (*2*, *3*). Also shown is the system transfer function which is the product of the cell and control circuit transfer functions. The cell transfer function was obtained by applying an a.c. signal to a resistor in the summing network, then measuring the input voltage (10 mv. or less) at the output terminal of the control amplifier and the output voltage at the input terminal of the voltage follower. The control circuit transfer function was obtained by applying the a.c. signal to a resistor at the input terminal of the voltage follower and measuring the voltage gain between the input of the voltage follower and the output of the control amplifier for a series of frequencies. Care was taken to ensure that the input resistor, through which the a.c. signal was applied, was of sufficient value not to change the loop gain of the potentiostat.

The calculated transfer functions of the cell, control circuit, and the system are shown in Figure 3. The following approximations were used for these calculations: ideal performance (defined as all summing points maintained at zero potential) for all the amplifiers; electrical independence of the cell and control circuit from each other; representation of the electrochemical cell as a series capacitance and resistance (*3*); and representation of the control circuit transfer function by the combined transfer functions of the voltage follower and control amplifier. The

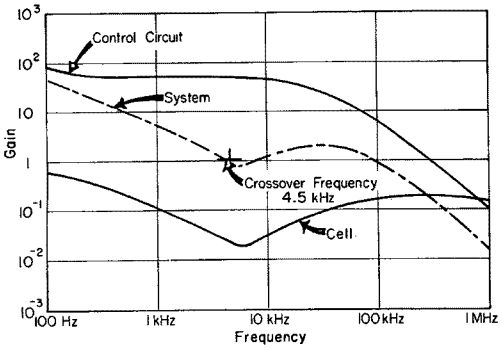

Figure 4. Measured cell, control circuit, and system transfer functions showing effects of nonideal current follower behavior

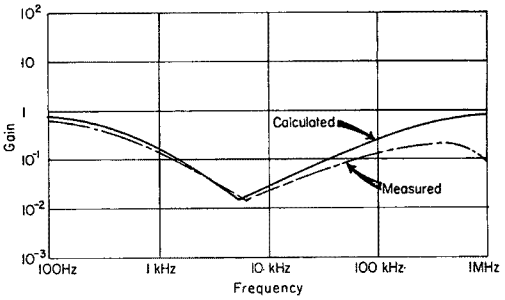

Figure 5. Calculated and measured cell transfer function with nonideal current follower effects included

details of the transfer function calculations are given elsewhere (*2, 3, 24*).

A comparison of Figures 2 and 3 shows that the measured and calculated transfer functions closely agree up to about 10 kHz. and that the unity-gain crossover frequencies agree within about 1 kHz. Several important conclusions can be drawn from these results. First, the approximations that were made in the calculated transfer functions are valid to at least 10 kHz. Second, the agreement between the measured and calculated transfer functions of the cell excellently justifies the use of the electrical equivalent model to represent the electrochemical cell even well above 10 kHz. Finally, the system functioned as designed with the best possible frequency response for the amplifiers that were used.

The deviation of the measured transfer functions from the calculated values, starting about 10 kHz., indicates that one or more of the approximations are beginning to fail. From a knowledge of the amplifier characteristics, the approximation first likely to become invalid is the one that assumes ideal amplifiers. This is supported by Figure 4 which shows the result of placing a large load resistor in the current-measuring circuit. As stated earlier, the cell transfer function calculations and measurements include the current follower. By placing a 4000-ohm load resistor in the current-measuring circuit, the unity-gain crossover frequency is reduced almost by a factor of two (Figure 4). The system response time, which is directly related to the unity-gain crossover frequency, is therefore also decreased. When the nonideal characteristics of the current follower amplifier are included in the calculations of the cell transfer function, the agreement between the measured and calculated values is quite satisfactory (Figure 5). If large load resistances are necessary to obtain the desired current sensitivities, the frequency response restrictions must be accepted or the current follower amplifier must be replaced by one with better gain characteristics. The major cause of the deviation of the control circuit transfer function above about 10 kHz. is believed to be inadequate gain characteristics of the control amplifier. To verify this by calculations would be a time-consuming task that was not deemed to be warranted.

For all experimental short time measurements, the largest load resistance in the current-measuring circuit, 4000 ohms, resulted in a unity-gain crossover frequency of about 4.5 kHz. (Figure 4). This gave a control circuit time constant of about 35 μsec. The system response time, defined as the 90% voltage rise time across the double-layer capacitance, was calculated to be about 106 μsec., using the control circuit time constant, the cell time constant (19 μsec.), and Table I of Reference *3*.

Uranium(V) Disproportionation Rate Constant. The ratio of limiting current to diffusion current is plotted *vs.* the logarithm of time in Figure 6 for the disproportionation reaction of $0.002M$ uranium perchlorate in $1M$ perchloric acid. The solid curve represents the experimental data drawn from 10 data points per decade of time. The broken line is the theoretical curve obtained by a generalized numerical solution of the second-order rate equations that describe the reaction (*4*). The experimental curve was calculated with the aid of a computer, programmed to include a shielding factor. This factor corrects for the loss in current due to the reduction in the surface area of the drop caused by its physical attachment to the HDME, but does not take into account the depletion effect caused by the shielding from the HDME. Figures 7 and 8 show the same type of plot for $0.005M$ and $0.010M$ uranium perchlorate in $1M$ perchloric acid, respectively.

To determine the experimental formal rate constants from the theoretical working curves (*4*), data for about two decades of time were used. These data include the region of the curve between the ratios of the limiting to diffusion current of about 1.02 to 1.4. The deviations of the experimental curves from the theoretical ones, noted at the longer times for the $0.005M$ and $0.010M$ uranium perchlorate solutions, are probably attributable to the depletion of the bulk concentration near the HDME caused by shielding. The observed errors from this effect agree with those obtained from approximate calculations which include the shielding effect and increase with uranium concentration. Other concentration dependent errors also may be involved but were not studied.

The formal rate constants for the uranium(V) disproportionation reaction for various concentrations of uranium perchlorate in $1M$ perchloric acid are given in Table II. A value of 0.71×10^{-5} cm.^{2} sec.$^{-1}$ for the diffusion coefficient was used for the calculations. This value was obtained by fitting the experimental curves to the unity base line of the theoretical working curves (*4*). Precisions for the kinetic current values are given in Table I. The precision of the voltage measurements is considerably better than that obtained by the conventional, oscilloscope photographic method.

Table II. Formal Rate Constants for Various Concentrations of Uranium Perchlorate in 1M Perchloric Acid

Concn. (M)	k(l^2 · mole^{-2} sec.$^{-1}$)[a]
0.002	192
0.005	192
0.010	212

[a] Formal rate constant normalized to unity hydrogen ion concentration.

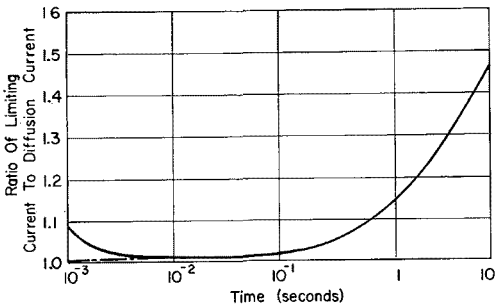

Figure 6. Ratio of limiting current to diffusion current *vs.* time for 0.002*M* uranium perchlorate in 1*M* perchloric acid

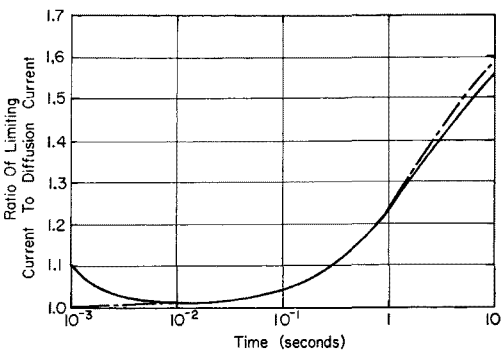

Figure 7. Ratio of limiting current to diffusion current *vs.* time for 0.005*M* uranium perchlorate in 1*M* perchloric acid

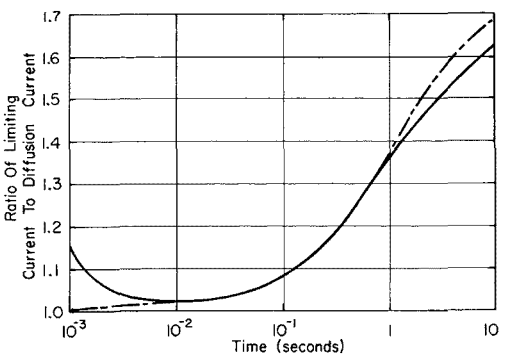

Figure 8. Ratio of limiting current to diffusion current *vs.* time for 0.010*M* uranium perchlorate in 1*M* perchloric acid

The accuracy of the formal rate constants for the 0.002*M* and 0.005*M* uranium perchlorate solutions (Table II) is estimated to be better than 10%. The accuracy of the theoretical working curves is estimated to be better than 5% and because the experimental curves were visually fit to the theoretical working curves to determine the rate constants, the 10% value is a conservative estimate. This accuracy could be improved by a least-squares fit of the experimental curves to the theoretical working curves by a computer technique. The accuracy of the rate constant obtained for the 0.010*M* uranium perchlorate solution is estimated to be 20%. The increased error is believed to result from the more pronounced shielding effect of the HDME at the higher uranium concentration.

The formal rate constant for the uranium(V) disproportionation reaction in 3*M* perchloric acid was determined earlier with a slower instrument. Three concentrations of uranium perchlorate, 0.001*M*, 0.005*M*, and 0.010*M*, were used. The kinetic currents were measured with an oscilloscope and were recorded with a Polaroid Camera. The experimental data were analyzed in the same manner as described above. The average value, normalized to unity hydrogen ion concentration was 665 ± 100 liter^2 mole^{-2} sec.$^{-1}$

The formal rate constants for the uranium(V) disproportionation reaction reported in this paper cannot be compared directly with previously reported values because of differences in ionic strength and supporting electrolyte. A rough comparison was made by plotting the logarithm of the disproportionation rate constant, normalized to unity hydrogen ion concentration, *vs.* the square root of ionic strength, as used by Masters and Schwartz (*15*). Included in the comparison were the data of Masters and Schwartz, other older data (*8*), and more recent data (*7*, *16*). The experimental data presented in this paper agree with the comparison data.

Newton and Baker (*16*) studied the uranium(V) disproportionation reaction by spectrophotometric means. They detected a stable uranium(VI)–uranium (V) complex which tends to inhibit the uranium(V) disproportionation. Because some of this complex is undoubtedly present during the electrochemical reduction of uranium(VI) to uranium(V) and its subsequent disproportionation, Newton and Baker suggested that the disproportionation rates obtained from polarographic techniques are low. They extrapolated the rate constant to zero uranium(VI) concentration for several perchloric acid solutions of low concentration.

The only polarographic data available which may be used to compare the formal rate constants extrapolated to zero uranium(VI) concentration are those of Fischer and Dracka (*8*) and those of the present paper. If the rate constant obtained by extrapolating the data of Newton and Baker (*16*) to 0.5*M* perchloric acid concentration is compared with the rate constant of 195 liter^2 mole^{-2} sec.$^{-1}$ reported by Fischer and Dracka for the same conditions, the latter rate constant value is lower, by an amount slightly exceeding the estimated experimental error. However if the rate constant obtained by extrapolating the data of Newton and Baker to 1*M* perchloric acid concentration is compared with the rate constant reported in the present paper, agreement is obtained within the limits of experimental error. The fact that the data of Fischer and Dracka did not agree with the extrapolation data but the data presented in this paper did, may be explained on the basis of the respective polarographic techniques used. The chronopotentiometric method used by Fischer and Dracka is probably more susceptible to interference caused by the formation of the uranium(V)–uranium(VI) complex than is the controlled-potential, stationary electrode method. However, the extrapolation of the data presented by Newton and Baker to 1*M* perchloric acid concentration is open to question. The disproportionation formal rate constant of 417 liter^2 mole^{-2} sec.$^{-1}$ in 2*M* perchloric acid reported by

Fischer and Dracka (*8*) and the 3*M* perchloric acid data reported in the present paper definitely indicate that the extrapolation is not valid for concentrations of perchloric acid much higher than 1*M*.

Because Newton and Baker limited their investigation of the disproportionation rate constant as a function of uranium(VI) concentration, to perchloric acid solutions of low ionic strength, a direct comparison to data obtained by polarographic techniques is not available. Newton and Baker did attempt to duplicate the condition in the DME polarographic investigations of Imai (*11*) and Koryta and Koutecky (*12*) for comparison purposes. However, the range of 2 to 4 for U(VI)/U(V) may not be realistic in terms of the DME experiments. Further work is needed to evaluate the errors involved in the polarographic determination of the uranium(V) disproportionation reaction due to the uranium(V)–uranium (VI) complex. From the limited data available, the errors do not appear to be too great. The data collected with use of the controlled-potential method are probably less affected than other polarographic methods because the uranium (VI) is completely depleted near the electrode surface.

Errors Involved in Interpretation of Kinetic Currents Measured at Short Times. To categorize the errors involved in the interpretation of kinetic current measurements is difficult, especially those taken at short times, because most are interrelated and are dependent on the instrument and cell characteristics. However, it is interesting to note that a nearly identical classification to that given below, though discussed in a different manner, recently was proposed by Oldham (*20*). The errors involved result from the finite rise time of the potentiostat, the voltage drop caused by the flow of Faradaic and double-layer charging currents, through the uncompensated cell resistance, and the difficulty in separating the Faradaic current component from the double-layer capacitance charging current component in total cell current measurements. The deviation of the experimental curves from the theoretical curves at short times in Figures 6, 7, and 8 result from these errors.

The finite rise time of the potentiostat is directly related to the system response time which has been defined to include the control-circuit time constant and the cell time constant. The effect of the finite rise time of the potentiostat on the Faradaic current can be considered as a special case of linear scan, controlled potential polarography (*3*). From basic theoretical relationships (*18*), it is evident that the net effect of the linear scan on the Faradaic current is a displacement of the current toward longer times. These relationships also show that the Faradaic current can be accurately calculated for all times despite the displacement. One would expect that the time displacement effect can be minimized by use of fast scan rates. A calculation similar to that of Booman and Holbrook (*3*), on the data of Nicholson and Shain (*18*), shows that the time displacement or time delay, t', can be approximated by

$$t' = 0.5T$$

where T is the system time response. This calculation assumes a potential step of 0.3 volt starting about 0.15 volt before the half-wave potential. It was also shown (*3*) that the time required for the time displacement error to reduce to 5% is $10t'$ and is $50t'$ for a 1% error. With a system having a response time of about 100 μsec. (such as the one described in the present paper) the times required for the time displacement error to be reduced to 5% and 1% are about 500 μsec. and 2.5 msec. Thus, short-time current measurements require a fast system-response time or the use of corrections.

The voltage drop caused by the flow of the Faradaic and double-layer capacitance charging currents through the uncompensated cell resistance results in a difference in the potential across the double-layer capacitance and that maintained by the potentiostat. The magnitude of this error is directly proportional to the uncompensated cell resistance, which, in turn, is a function of cell design and of the solution conductance. The placement of the reference electrode and the magnitude of the double-layer capacitance are considered to be included in the cell design. Nicholson (*17*) and De Vries and Van Dalen (*6*) independently derived and numerically solved the equations describing the electrode response in the presence of a voltage drop due to the flow of Faradaic current through the uncompensated resistance for the case of linear scan, stationary electrode polarography at controlled potential. De Vries and Van Dalen suggest that the voltage drop due to the double-layer charging current is probably negligible with the linear scan technique at scan rates up to about 100 volts per second. However, when using the large potential-step method where the effective scan rates during the initiation of the potential step may be from several thousand to over ten thousand volts per second, the charging current effects cannot be ignored. Hence, a satisfactory treatment of this type for the potential-step method must include the double-layer charging current as well as the Faradaic current. Unfortunately, the problem is complicated by the fact that the double-layer capacitance is a function of the applied potential. In most cases, this variation is probably significant. For example, in the 1*M* perchloric acid solution the double-layer capacitance changed about 25% over the range of the potential step.

If the potentiostat rise time and the voltage drop caused by the presence of uncompensated resistance were negligible, the current component due to the charging of the double-layer capacitance could be calculated rather easily. However, at short times the competition for the available current between the Faradaic current and double-layer charging current is complicated by the finite rise time of the potentiostat. The accurate determination of the current component due to the charging of the double-layer capacitance requires a knowledge of the voltage function across the double-layer capacitance and of the voltage dependence of the double-layer capacitance.

Most of the methods proposed (*14, 19, 20*) for the interpretation of large pulse, controlled potential polarographic data at short times are variations of the graphical extrapolation method first proposed by Gerischer and Vielstich (*10*). The recent approach by Oldham (*20*) is the most comprehensive and is the first to clearly recognize the limitations of the extrapolation technique.

The use of positive feedback to correct for the error in potential across the double-layer capacitance due to the uncompensated cell resistance has been investigated by a number of workers (*5, 9, 13, 21*). This method has considerable appeal, but it requires a system with an excellent response time to effectively correct short time data. In some systems, such as the one used in this investigation, it is necessary to add resistance in series with the uncompensated cell resistance to improve the frequency response (*3*). The use of positive feedback in a system such as this is equivalent to lowering the total uncompensated resistance. The net effect is to decrease the overall system response time. The use of amplifiers of sufficient bandwidth, current, and gain capabilities would allow the reduction of the uncompensated cell resistance to the lowest possible value limited only by cell geometry. Complete compensation would require amplifiers having infinite gain-bandwidth characteristics.

A method which appears to be the most useful for the correction of data taken at short times is an extension to the approach used by Nicholson (*17*) and De Vries and Van Dalen (*6*). If the nonconstant double-layer capacitance can be expressed in a relatively simple general form, this development, including the voltage drop due to the double-layer charging current and the correction for the charging current itself, does not appear to be too difficult. This method could be used in conjunc-

tion with positive feedback and double-pulse instrumentation. Of course, the use of better amplifiers will improve the effectiveness of all the methods for interpretation of the data taken at short times. Even with advanced instrumentation, full advantage of the potentiostatic technique will be realized only by application of correction methods.

LITERATURE CITED

(1) Booman, G. L., ANAL. CHEM. **38**, 1141 (1966).
(2) Booman, G. L., Holbrook, W. B., *Ibid.*, **35**, 1793 (1963).
(3) *Ibid.*, **37**, 795 (1965).
(4) Booman, G. L., Pence, D. T., *Ibid.*, **37**, 1366 (1965).
(5) Brown, E. R., McCord, T. G., Smith, D. E., DeFord, D. D., *Ibid.*, **38**, 1119 (1966).
(6) De Vries, W. T., Van Dalen, E., *J. Electroanal. Chem.* **10**, 183 (1965).
(7) Feldberg, S. W., Auerbach, C., ANAL. CHEM. **36**, 505 (1964).
(8) Fischer, O., Dracka, O., *Collection Czech. Chem. Commun.* **24**, 3046 (1959).
(9) Gerischer, H., Staubach, K. E., *Z. Electrochem.* **61**, 789 (1957).
(10) Gerischer, H., Vielstich, W., *Z. Physik. Chem. (Frankfurt)* **3**, 16 (1955); **4**, 10 (1955).
(11) Imai, H., *Bull. Chem. Soc. Japan* **30**, 873 (1957).
(12) Koryta, J., Koutecky, J., *Collection Czech. Chem. Commun.* **20**, 423 (1955).
(13) Lauer, G., Osteryoung, R. A., ANAL. CHEM. **38**, 1106 (1966).
(14) Lingane, P. J., Christie, J. H., *J. Electroanal. Chem.* **10**, 284 (1965).
(15) Masters, B. J., Schwartz, L. L., *J. Am. Chem. Soc.* **83**, 2620 (1961).
(16) Newton, T. W., Baker, F. B., *Inorg. Chem.* **4**, 1166 (1965).
(17) Nicholson, R. S., ANAL. CHEM. **37**, 667 (1965).
(18) Nicholson, R. S., Shain, I., *Ibid.*, **36**, 706 (1964).
(19) Okinaka, Y., Toshima, S., Okaniwa, H., *Talanta* **11**, 203 (1964).
(20) Oldham, K. B., *J. Electroanal. Chem.* **11**, 171 (1966).
(21) Pouli, D., Huff, J. R., Pearson, J. C., ANAL. CHEM. **38**, 382 (1966).
(22) Reinmuth, W. H., *Ibid.*, **36**, 211R (1964).
(23) Shain, I., "Treatise on Analytical Chemistry," I. M. Koltoff and P. J. Elving, Eds., Part I, Vol. 4, p. 2560, Interscience, New York, 1963.
(24) Shain, I., Harrar, J. E., Booman, G. L., *Ibid.*, **37**, 1768 (1965).

RECEIVED for review April 18, 1966. Accepted June 9, 1966. In part, Division of Analytical Chemistry, Winter Meeting, ACS, Phoenix, Ariz., January 1966. Work supported by the U. S. Atomic Energy Commission under Contract No. AT(10-1)-205 through the Idaho Operations Office.

Some Investigations on Instrumental Compensation of Nonfaradaic Effects in Voltammetric Techniques

ERIC R. BROWN, THOMAS G. McCORD, DONALD E. SMITH, and DONALD D. DeFORD

Department of Chemistry, Northwestern University, Evanston, Ill.

▷ The feasibility of achieving accurate, direct readout of the faradaic component in voltammetric techniques under conditions where nonfaradaic effects are substantial has been reinvestigated. Compensation of ohmic potential loss was effected with the aid of the addition of a positive feedback loop to a conventional operational amplifier potentiostat. Double-layer charging current compensation was carried out by direct subtraction of the current obtained with a solution of supporting electrolyte from the current obtained with a solution of supporting electrolyte and electroactive component. Application was made to cyclic voltammetry, fundamental harmonic a.c. polarography, and higher harmonic a.c. polarography. Readout of the faradaic component was possible with an apparent high degree of accuracy for at least moderately demanding conditions. All measurements were performed with the dropping mercury electrode. Successful application of the dropping mercury electrode was facilitated by a timing circuit which performed a number of functions including controlling and synchronizing mercury drop growth and fall in the two cells; controlling a sample-and-hold readout operation in a.c. polarographic measurements; controlling application of a triangular wave impulse in cyclic voltammetric measurements.

THE WIDELY recognized problems associated with the contributions of ohmic potential loss (iR drop) and double-layer charging current in voltammetric techniques remain a source of much concern in experimental electrochemistry (*1–11, 16–20, 25–28, 31–34, 39–42, 46, 51, 52, 56, 57, 62, 64–67, 69–71*).

In one way or another these nonfaradaic influences limit the scope of voltammetric methods in kinetic and mechanistic studies of electrode reactions as well as in analytical applications. Particularly profound are their effects in modern electrochemical relaxation methods such as cyclic voltammetry (*16, 20, 25, 42*), a.c. polarography (*55, 57, 64, 70, 71*), and high-speed potentiostatic measurements (*10, 11, 37, 55*). The contributions of iR drop and double-layer charging current in these latter techniques can be made minimal in measurements involving time scales (the period of the alternating potential in a.c. polarography and cyclic voltammetry, the measurement time in chrono-amperometry, etc.) which are large.

However, with a small time scale their contributions to instrument readout frequently are sufficiently large that even the most simple-minded mechanistic conclusions are impossible until correction for these effects has been accomplished. The complexity associated with the corrections varies, depending on the nonfaradaic effect and experimental technique in question, but the tedium associated with these operations is seldom insignificant.

Numerical correction for the double-layer charging current often is accomplished by performing two experiments: one on a solution containing supporting electrolyte and electroactive component (the sample solution) and one on a solution containing only supporting electrolyte (the reference solution) (*17*). The current observed with the reference solution is subtracted from that observed with the sample solution. The subtraction operation may involve simple scalar subtraction, as in cyclic voltammetry, or the mathematically more cumbersome vectorial subtraction, as in a.c. polarography. Due recognition must be given to the effects of iR drop before this subtraction can be effected accurately. In cases where the electroactive species significantly alter the double-layer capacity, a more sophisticated correction scheme must be employed (*21, 60*).

To correct for the effects of iR drop, one must perform the additional experiment of measuring the effective ohmic resistance (*10, 11, 17*). Once this is accomplished, the data may be corrected for iR drop in some cases by simply considering its effect on the magnitude of the applied potential, as in d.c. and a.c. polarography (*17, 52, 57*). In other techniques, the iR drop may

manifest itself in a more insidious manner by altering another important kinetic parameter. An example of the latter effect arises in linear scan or cyclic voltammetry where the ohmic resistance influences the scan rate, and thereby alters the mass transfer rate (*16, 20, 25, 42*). In such cases, rigorous correction for *iR* drop normally requires explicit incorporation of its contribution into the theory for the current-potential curve, a nontrivial operation as recent literature on cyclic voltammetry attests (*25, 42*).

These inconveniences and limitations imposed by nonfaradaic effects have led to much expenditure of effort in attempts to reduce the magnitude of their contributions to instrument readout. Reduction of the effects of charging current has been accomplished by a variety of compensation techniques essentially involving electronic simulation of the charging current signal and subtraction of the simulated signal from the cell current (*30, 33–35*) (the simulation methods). Compensation also has been tried by subtraction of current signals obtained simultaneously from sample and reference solutions (*14, 32, 52, 59, 72*) (the direct method).

Neither of these approaches has been widely employed, especially in applications of the electrochemical relaxation methods. The simulation methods are not particularly compatible with the demands of versatility and accuracy associated with quantitative kinetic applications of the relaxation techniques. For example, precision electronic simulation of the charging current–d.c. potential profile observed in cyclic voltammetry, a.c. polarography, etc. in the vicinity of the "water hump" (*47*) could be achieved only at a cost significantly greater than that of the additional polarizing unit required in the direct method.

Electronic simulation methods are also at a disadvantage in techniques involving a.c. signals. Among possible objections to the direct method of compensation are the requirement of an additional polarizing circuit and the fact that the method is invalidated whenever the electroactive compounds significantly influence the double-layer capacity. However, these disadvantages are not of sufficient consequence to dictate against widespread application of the approach. The cost of an additional polarizing unit would soon be offset by the convenience and savings in time associated with accurate compensation for charging current. Error caused by influence of electroactive species on the double-layer capacity will be negligible with a significant fraction of the systems one may encounter.

The most serious problem associated with the direct method, which may be primarily responsible for its infrequent application, is the fact that accurate compensation for charging current cannot be realized unless contributions of *iR* drop are negligible (*52*). Significant ohmic resistances normally lead to differences in ohmic potential losses in the sample and reference cells, at least where the cell currents differ, as in the vicinity of the faradaic wave. A corresponding difference in the effective potential applied to the two cells is the result.

In such situations, a significant dependence of charging current on applied potential will cause the charging current magnitude obtained from the reference cell to differ from that in the sample cell leading to error in the subtraction operation. In a.c. polarography, *iR* drop–induced differences in the phase relations associated with charging currents in the sample and reference cells will lead to an additional source of error. Error in the direct compensation method arising from *iR* drop will become most noticeable in measurements involving small time scales—precisely the situation when accurate compensation for charging current would prove most helpful.

Numerous schemes to reduce the sources of ohmic potential loss have been reported. Among the most recent and successful has been the application of the three-electrode potentiostat, a device which is frequently constructed from operational amplifiers (*10, 11, 28, 34, 56, 62, 64, 70, 71*). The three-electrode potentiostat removes many of the sources of *iR* drop operative in normal voltammetric procedures. However, it has been made abundantly clear in the literature that not all sources of *iR* drop are removed in the conventional three-electrode potentiostat (*10, 11, 28, 41, 51, 56, 64*). These devices do not compensate for *iR* drop in the working electrode and in the solution between the tip of the reference electrode probe and the working electrode. The electrode resistance is significant when a conventional dropping mercury electrode (DME) or a semiconductor electrode is employed. The solution resistance will be significant in low-conductance solvents and in high speed work in high conductance solvents.

Hayes and Reilley (*28*) presented an ingenious method which should successfully compensate in most cases for these last remnants of ohmic potential loss in phase-selective a.c. polarography. Using an electronic multiplier as the phase-sensitive detector, they incorporated the correction for *iR* drop in the electronic multiplication operation. Unfortunately, their approach appears somewhat limited in scope, not being rigorously applicable to techniques such as linear scan and cyclic voltammetry.

A method of potentially more general applicability has been suggested by Booman and Holbrook (*10*). This approach involves a minor modification of the three-electrode potentiostat in which an additional feedback (positive) loop is employed to add a signal equal to the *iR* drop to the input voltage. Hayes and Reilley (*28*) reported an attempt to implement this method in which they were unable to prevent oscillation of the control loop. Recently, Lauer and Osteryoung (*37*) and Pouli and coworkers (*51*) have reported successful applications of this technique.

Neither the numerical method nor the instrumental procedures mentioned above can completely eliminate all manifestations of *iR* drop when a large ohmic resistance (in the electrode or solution) is combined with large differences in current density across the electrode surface. In such situations a spacial distribution of *iR* loss across the electrode-solution interface exists, rather than a fixed value of *iR* drop (*1, 19, 22*), resulting in an uneven potential distribution on the solution side for large solution resistances and an uneven distribution on the electrode side for large electrode resistances. This effect has been proposed as a possible source of polarographic maxima (*22, 45*). The methods described above can, at best, effect correction for an average *iR* drop in such systems. Fortunately, a significant spacial dependence of the *iR* drop is likely to occur only in extreme cases (very large ohmic resistances and/or large variations in current density across the electrode surface) which arise infrequently in electrochemical investigations. This is particularly true in the electrochemical relaxation techniques where measurements are confined to short times and the geometry effects giving rise to uneven current distributions normally have insufficient time to become significant (*1*).

The possibility of achieving negligible influence of ohmic potential loss in electrochemical relaxation techniques performed under conditions where the ohmic resistance is significant is appealing in itself. This appeal is enhanced by the fact that such elimination of ohmic influences makes more realistic the possibilities of highly accurate implementation of the direct method of charging current compensation. These considerations led us to undertake a study of the feasibility of achieving direct readout of the faradaic current component in electrochemical relaxation techniques using the three-electrode potentiostat with the modification of Booman and Holbrook in combination with the direct method of charging current compensation. The results reported here illustrate the degree of success we have realized to date.

Fundamental harmonic a.c. polarography, higher harmonic a.c. polarography, and cyclic voltammetry, a group of relaxation techniques which are notably sensitive to nonfaradaic influences, were employed in this study.

EXPERIMENTAL

The electrochemical instrument employed in this work was constructed entirely from solid-state operational amplifiers. A variety of amplifier models was employed, none of which required noise-producing 60-Hz. power to drive electromechanical or photoconductive choppers. Whenever appropriate, specific amplifier models utilized in construction of various units will be indicated below. The notably improved instrument performance obtained with solid-state operational amplifiers relative to that observed with their vacuum tube counterparts more than justifies the additional expense. In comparison with a vacuum tube instrument described previously (*62*), the solid-state instrument employed in this work is definitely superior in characteristics such as noise level, long-term stability, and overall reliability. For example, in either normal or phase-selective a.c. polarographic measurements, drift in instrument response observed with a dummy cell seldom exceeded ±0.1% in a period of 2 to 3 hours (after a short warm-up).

Potentiostats and Compensation for *iR* Drop. Figure 1 illustrates a slightly modified version of a potentiostat in the voltage follower mode (ignore dashed line) originally given by Booman and Holbrook (*10*), which was employed in most of the work reported here. The positive feedback path provided by connecting the center-tap of the potentiometer R_c to one of the potential inputs permits, through proper adjustment of R_c, complete compensation of the ohmic losses in the cell and resistor R_L (*10*). Obviously, the same approach is applicable to many other potentiostat configurations such as the commonly used current-follower (*11*, *15*, *58*).

The current-follower version is obtained from Figure 1 as indicated in the caption. In this case, R_c is adjusted to compensate only for the cell resistance. The voltage follower configuration exhibited a noticeably wider stability margin under most operating conditions, which is the reason its application was favored. Stable operation was achieved through the use of feedback capacitors across the control and current amplifiers (*11*, *13*, *68*). The capacitors employed were of sufficient magnitude to ensure stability, but not so large that they influenced the performance of the control loop at the frequency of interest. More sophisticated stabilization networks (*11*) which might have negated the observed difference in stability obtainable with the current and voltage follower configurations were not employed in the present work. The stability problem is discussed further below.

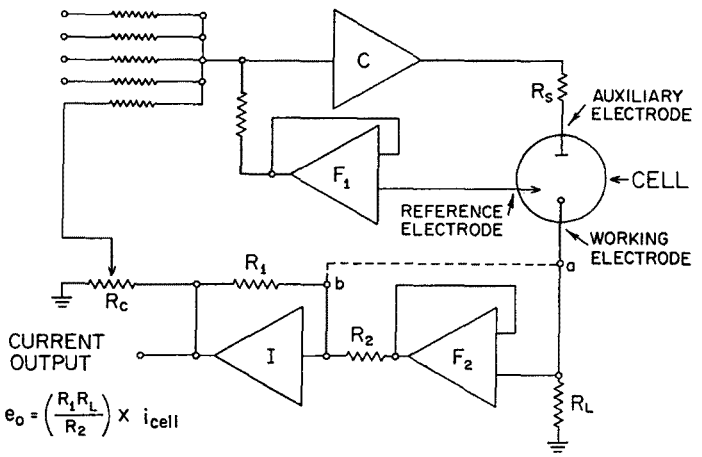

Figure 1. Potentiostat

Amplifier C—Philbrick P-2 operational amplifier with P-5 booster
Amplifiers F_1 and F_2—Philbrick P-2 operational amplifiers
Amplifier *I*—Burr-Brown 1506 operational amplifier
Input resistors of Amplifier C—100K, ±0.1%
Resistor R_1—0 to 1.2 megohm ESI Model DS1464 Dekastat Decade Resistor
Resistor R_c—1 Kohm Bourns Model 3700S-1-102, 10-turn potentiometer
Resistor R_s—1 Kohm, ±0.1% in most cases
Resistor R_L—500 Kohm, ±0.1% in most cases
Resistor R_2—1 Kohm, ±0.1% in most cases
Voltage-Follower Mode: delete dashed line
Current-Follower Mode: connect points *a* and *b* (dashed line) and delete R_1, R_L and amplifier F_2

The positive feedback approach in principle provides for complete compensation of a constant ohmic resistance. There is no provision for handling a varying ohmic resistance which one encounters with the dropping mercury electrode (*8*, *36*). This problem was solved in this work by confinement of measurements to a short period in the life of a mercury drop during which the ohmic resistance is essentially invariant. The methods employed to effect this mode of measurement are described below.

Charging Current Compensation. Compensation for charging current was achieved with the aid of two potentiostats of the type shown in Figure 1; one controls a sample cell and one controls a reference cell. The potentiostats were driven by common signal sources. The output signals from the two potentiostats were subtracted with an electronic subtractor. For these operations to have any meaning, a number of conditions must be met: (a) the concentrations of supporting electrolyte must be identical in the sample and reference cells; (b) the electroactive materials must not significantly influence the double-layer capacity; (c) the surface characteristics of both working electrodes must be identical; (d) the charging current signals generated in the sample and reference cells must correspond to the same electrode area. Item a is almost trivial and items b and c represented no problem in the present work. All of the work described here employed the dropping mercury electrode (DME) and the condition represented by item d was met as follows. Synchronization of mercury drop growth and fall in the two cells was achieved with the aid of mechanical drop-dislodgers which were activated by a timing circuit described below. Mercury flow rates were adjusted carefully to ensure that mercury drop areas were identical at the time of measurement. The final stage in this adjustment was usually performed by observing the output of the subtractor at d.c. potentials where only charging current was flowing in each cell and adjusting mercury column height until a negligible signal was observed.

Mode of Measurement. Signal conditioning in addition to the subtracting operation was unnecessary in cyclic voltammetry. Cyclic voltammograms were obtained in the normal manner by applying the output of the subtractor to the Y-axis of an oscilloscope while driving the X-axis with the triangular wave voltage source. All cyclic voltammetric investigations involved single-cycle experiments run at a slowly growing DME. Moderately fast scan rates were employed (2 volts per second to 200 volts per second) so that drop growth was negligible during the period of the triangular wave impulse. The triangular wave impulse was applied automatically to both cells late in the life of the DME's with the aid of the same timing circuit used to synchronize drop fall.

In a.c. polarographic measurements, the output of the electronic subtractor was subjected to tuned amplification (*62*) followed by conventional full-wave rectification or phase-sensitive rectification. All a.c. components of the rectified signal were eliminated with the aid of a low-pass filter of the Butterworth type (*49*). The resulting d.c. signal was applied to a sample-and-hold circuit (sampling circuit), permitting precise measurement of the a.c. polarographic signal at a point late in the life of the mercury drop (essentially at the end of drop life). Each measurement was held by the sampling circuit until the corresponding point in the life of the succeeding drop when a new sample was taken, etc. The output of the sampling circuit was recorded. This readout technique was originally employed by Barker and coworkers in square-wave, radio-frequency, and pulse polarography (*3*, *4*, *6*). It was utilized in this work to avoid the problem of the varying ohmic resistance associated with the DME (*8*, *36*). All a.c. polarographic phase angles were calculated from the information provided by total and phase-selective current measurements.

Signal Conditioning Devices. The electronic subtractor was constructed from a Philbrick P-2 operational amplifier utilizing the standard subtractor circuit (*13*, *50*) and precision (±0.1%) wire-wound 10 kohm resistors.

A previously described circuit (*62*) employing a twin-T network in the feed-back of an operational amplifier served as tuned amplifiers. A Philbrick P-5 booster amplifier in combination with a Philbrick P-2 operational amplifier comprised the amplifier section. The twin-T network was constructed from ±1% Mylar capacitors and a three-gang Model A Beckman helipot (ten-turn) as the source of resistors in the twin-T network.

The full-wave rectifier used to obtain a.c. polarograms of the total current was based on a well known precision absolute-value circuit which has been described in various sources (*13*, *29*). Philbrick P-35 operational amplifiers were employed together with ±0.1% wire-wound resistors. The performance of this circuit was outstanding. Linearity in response was within approximately ±0.1% for signal levels ranging from a few millivolts to the voltage limit of the amplifiers (~11 volts). Such performance was observed for frequencies up to 10 kHz.

The phase-sensitive rectifier utilized in this work was constructed from operational amplifiers employing a circuit (*12*) which apparently has not been published. Its performance with regard to linearity and frequency response was similar to that of the absolute value circuit mentioned above. Further details of this circuit will be given elsewhere, as they contain no features essential to the present discussion.

Low-pass filters employed to filter the output of the rectifiers were characterized by a second-order Butterworth response with a cut-off frequency of about 1.5 Hz. (*49*). Philbrick P-35 amplifiers and a circuit given in the literature (*49*) served as the basis for this unit. By utilizing the Butterworth response, it was possible to reduce the a.c. ripple on the rectified signal to less than 0.1%, even at the lowest frequencies employed (10 Hz.), without attenuating significantly (>0.1%) the response of the instrument to current oscillations associated with mercury drop growth and fall. To obtain a measurement of the instantaneous alternating current magnitude at low frequencies with a normal RC low-pass response, a time constant must be employed which is insufficient to reduce the effects of ripple to a negligible level. Thus, the low frequency performance of the instrument was notably enhanced by application of the Butterworth filter.

The sample-and-hold operation was accomplished with the aid of a Philbrick P-2 amplifier in the follower configuration, a high quality 1- to 2-μf. Mylar capacitor connected between the follower input and ground, and a normally open mercury-wetted contact relay (C.P. Clare Model HGSS1002 single-side stable relay) in series with the signal source. The circuit has been described in the literature (*53*, *64*). Usually a resistor was placed between the signal source and sampling circuit to prevent short-term overloading of the signal source. The time constant thus introduced normally was of the order of 0.03 second.

Signal Sources. The d.c. voltage sources were comprised of a precision (±0.1%) initial voltage source and a voltage ramp generator, both constructed from conventional operational amplifier circuits (*15*, *34*, *58*). A Hewlett-Packard Model 241A sine wave oscillator was employed as the source of sinusoidal voltages in a.c. polarographic measurements. The frequency stability of this oscillator is more than compatible with the demands imposed by the use of tuned amplifiers (*62*). For cyclic voltammetric measurements, a triangular-wave oscillator was constructed from a published circuit (*38*) which employs an operational amplifier integrator and a trigger (voltage comparator) with hysteresis (*13*, *50*) in a loop configuration. A Philbrick P-35 operational amplifier was employed in the integrator stage. The trigger utilized a Philbrick P-45 amplifier. Single-cycle operation was effected with the aid of a C. P. Clare Model HGSM1016 bistable mercury-wetted contact relay with a double-wound coil. The relay was placed across the feedback capacitor in the integrator stage. In a closed position, the relay prevents charging of the condensor and, thus, suppresses the oscillation.

A voltage step from an external timing circuit which is capacitively coupled to one coil winding serves to open the relay and initiate a cycle. The oscillation is terminated at the end of one cycle by capacitively coupling the output of the trigger to the second coil winding. The voltage step at the trigger output, which is associated with the end of the cycle, is of the right polarity to effect relay closure suppressing further oscillation. A new cycle does not ensue until a voltage step from the timing circuit reopens the relay, etc. Because of the finite response time of the mercury-wetted relay (~2 msec.), single-cycle experiments at scan rates in excess of 200 volts second^{-1} were not possible.

Readout Devices. Cyclic voltammograms were obtained with the aid of a Tektronix Model 502A oscilloscope and a Tektronix Model C-13 oscilloscope camera. The oscilloscope was also employed to measure amplitudes of applied potentials in a.c. polarographic measurements and as a general purpose monitor of various aspects of instrument performance.

An Electro Instruments Model 480 *X-YY'* recorder with Model 468 (*X*-axis) and Model 420 (*Y*-axis) plug-in modules was employed to record a.c. polarograms. The dual *Y*-axes feature of this recorder permitted simultaneous readout of conventional a.c. polarograms (total alternating current) and phase-selective a.c. polarograms (the resistive current component). The phase relations were then immediately calculable from these recordings.

A Hewlett-Packard Model 5243L electronic counter served to measure frequency of applied alternating potential. With a Hewlett-Packard Model 5265A plug-in, this counter was converted to a digital voltmeter which provided for precise, high resolution measurement of d.c. signal levels. A Hewlett-Packard Model 5262A plug-in permitted the use of this counter in time-interval measurements for assessment of the performance of the timing circuitry.

Timing Circuits. Figure 2 illustrates the multipurpose timing circuit which was employed to control mercury drop life, the sample-and-hold operation in a.c. polarography, and the application of the triangular wave impulse in cyclic voltammetry. A voltage ramp generator composed of an electronic integrator with a fixed input voltage serves as the clock for this unit. A scan rate of +1.000 volt per second is realized with the component values indicated in Figure 2.

The output of the ramp generator is applied at the input of two trigger (voltage comparator) circuits (*13*, *50*, *62*). The triggers are set to switch from a state of zero volts to −10 volts when the scan generator output reaches a predetermined value. This switching point is controlled by a second input network comprising a voltage divider and a 50 Kohm potentiometer. The switching points are adjusted so that trigger 1 is the first to change state to −10 volts. It remains in this state until the ramp generator output reaches the level where trigger 2 changes state. The voltage step at the output of trigger 2 closes relay R_1, discharging the capacitor of the ramp generator. This drives the output levels of the ramp generator and the trigger circuits

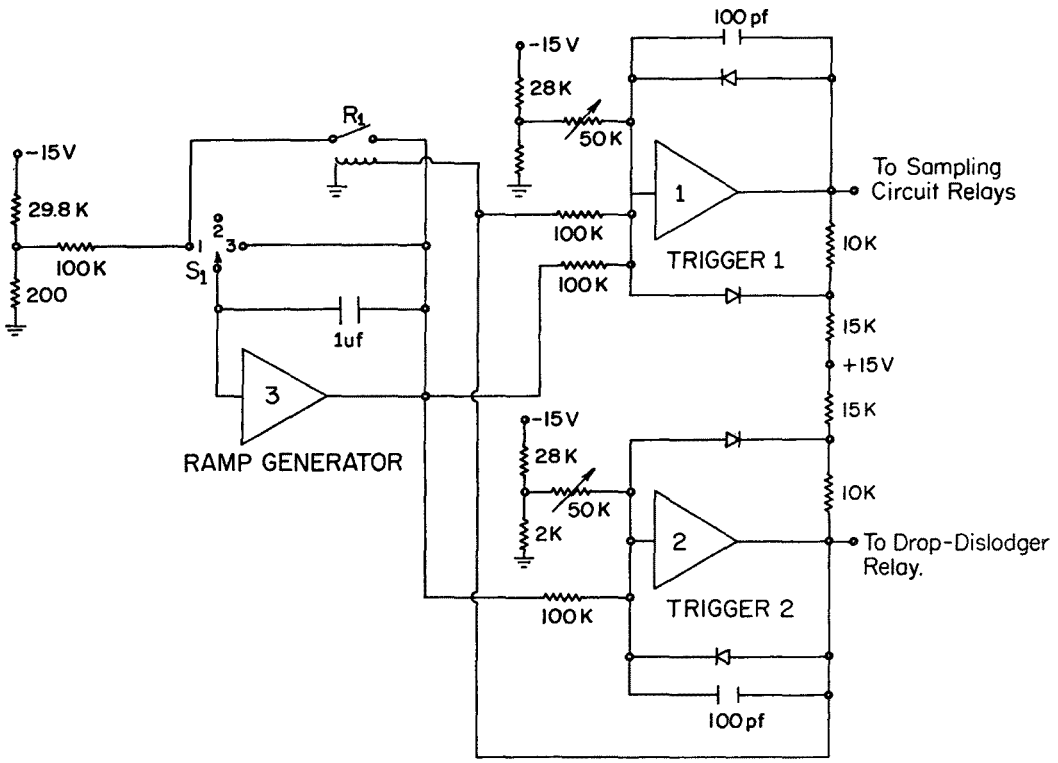

Figure 2. General purpose timing circuit

Amplifiers 1 and 2–Philbrick P-45 operational amplifiers
Amplifier 3–Philbrick P-35 operational amplifier
All fixed resistors–±0.1% wire-wound
Variable resistors (50K)–Bourns Model 3500S-2, 10-turn potentiometers
1-μF. capacitor–Southern Electronics Model MC106G1APL, ±1%
Diodes–Hughes type 1N483B
R_1–C.P. Clare Model HGSS1002 mercury-wetted contact relay
S_1–single pole 3-position switch with
position 1–operate (scan)
position 2–standby (hold)
position 3–off (reset)

back to zero volt, permitting relay R_1 to reopen, a new cycle to ensue, etc.

Thus, the timing circuit basically is a low frequency oscillator with three available waveforms. The ramp generator furnishes a sawtooth waveform. Trigger 2 furnishes a pulse train composed of narrow (~2 msec.) pulses coinciding with the end of each cycle of the ramp generator output. Trigger 1 furnishes a train of pulses whose width can be controlled from a minimum of zero (no pulse) to a maximum corresponding to the period of the sawtooth oscillation.

The outputs of triggers 1 and 2 are employed to control external circuitry as indicated in Figure 2. The output pulse of trigger 2 is employed to activate drop-dislodger circuitry making the mercury drop life equal to the period of the oscillation of the timing circuit. In cyclic voltammetry, the change in state of trigger 1 to −10 volts is used to initiate the triangular wave voltage sweep. Trigger 2 is set to change state, ending the drop life, etc., shortly after completion of the triangular wave cycle.

In experiments in which the sample-and-hold readout procedure is employed (a.c. and d.c. polarography), the change in state of trigger 1 to −10 volts serves to close relays in the sampling circuits, commencing the sampling operation. Trigger 1 is permitted to remain in the −10-volts state for a time significantly longer (0.1 to 0.2 seconds) than the above-mentioned input time constant of the sampling circuits. Under these conditions, the sampling circuits will hold a voltage corresponding to the input signal level at the end of the sampling operation (not an average of the signal over the sampling period). When trigger 1 returns to the zero volt state, the sampling circuit relays reopen, ending the sampling operation. The accompanying output pulse from trigger 2 ends the drop-life.

Obviously, it is essential that the sampling operation is terminated before the mercury drop is dislodged. To ensure this, the output of trigger 2 is connected to the input of trigger 1. When trigger 2 changes state to −10 volts it forces trigger 1 to zero volt at a time shortly before the similar effect associated with the discharge of the scan generator becomes operative. Thus, the return of trigger 1 to zero volt and the accompanying opening of the sampling circuit relays are not retarded by the time constant associated with discharge of the ramp generator. The proper sequence of events is further guaranteed by a relatively long time constant in the drop-dislodger circuitry. Timing measurements indicate that the electromechanical drop dislodgers are activated approximately 2 msec. after completion of the sampling operation.

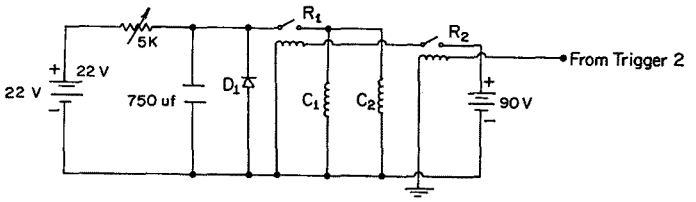

Figure 3. Drop-dislodger circuitry

R_1—Potter and Brumfield Type LM5-2500 ohm SPDT Relay
R_2—C.P. Clare Model HGSS1002, mercury-wetted contact relay
C_1 and C_2—Coils of Guardian Type 4-24 volt solenoids
D_1—GE Type 1N1695.

The electromechanical hammers serving as drop-dislodgers (Guardian Type 4-24 volt solenoids) were activated by a relay closure which discharges a 750-μf. capacitor through their coils. A separate hammer was employed for each cell. The high currents associated with this operation demanded a relatively heavy duty relay (Potter and Brumfield Type LM5-2500 ohm SPDT relay) whose closure could not be affected by direct application of the low power pulse from the P-45 operational amplifier of trigger 2. Thus, the mechanical termination of drop life was accomplished with a two-stage circuit as shown in Figure 3. Trigger 2 activates a mercury-wetted contact relay, applying a voltage to the heavy duty relay which is sufficient for closure.

The timing and drop-dislodger circuitry just described has been in use in these laboratories for over one year with excellent results. The only maintenance required in that period has been one battery replacement. Perusal of data obtained with this equipment indicates that erratic operation, such as failure to properly dislodge a drop, is a rare event. The probability of an obviously poor reading on a given mercury drop is no more than 0.001. The reproducibility of the timing operation—e.g., the reproducibility of the controlled drop life—is of the order of ± 1 msec. (average deviation).

Miscellaneous Supporting Equipment. Except where they did not contribute significantly to the response of the instrument, passive components of high quality were employed with resistors (wire-wound or metal-film) normally characterized by $\pm 0.1\%$ tolerance and capacitors (Mylar or polystyrene) of 1% tolerance. The dummy cells normally were comprised of an ESI Model DS1464 decade resistor and $\pm 1\%$ Mylar capacitors (Southern Electronics Corp.). When more precise dummy cell measurements were desired, an ESI Model DC-57 Decade capacitor originally calibrated at the factory to 0.1% was employed in place of the $\pm 1\%$ capacitors.

Sargent Model S-29390 polarographic cells thermostated by an Aminco Model 4-8600 constant temperature bath were employed. Most measurements were performed at 25° C. Sargent Model S-29417 polarographic capillary was utilized for the DME. Saturated calomel reference electrodes with Luggin probes and platinum auxiliary electrodes served as the other electrodes Reagent grade chemicals were utilized in solution preparation. Most solutions were prepared from distilled water which had been treated with activated charcoal or the solutions themselves were subjected to charcoal treatment.

Determination of Series Resistance. To employ the above-described positive feedback scheme for eliminating contributions of ohmic resistance, one must know the effective uncompensated ohmic resistance which is normally operative in the three-electrode potentiostat—i.e., the ohmic, resistance contribution observed in absence of the positive feedback loop. A number of methods have been suggested for measuring this resistance (*8, 10, 11*).

Convenience dictated our choice of method which was based on the phase-selective a.c. polarographic readout. The method involved adjusting the instrument to measure the resistive (in-phase) alternating current component and selecting a d.c. potential at which only charging current is observed. The iR compensation control (potentiometer R_c in Figure 1) was then adjusted until zero signal was observed. Under these conditions, negligible resistive component is an indication that contributions of iR drop are negligible. This procedure simultaneously achieves proper adjustment of the instrument to negate effects of ohmic potential loss and determination of the magnitude of the effective ohmic resistance which is calculable from the setting of R_c.

Care must be taken to ensure that only charging current is present when the adjustment of R_c is made. Otherwise, the method was satisfactory. Its validity was verified by dummy cell experiments. With the aqueous systems employed in this work, the predominate source of ohmic resistance was the DME capillary resistance which ranged from 60 to 90 ohms. The appropriate setting of R_c, determined in the manner just described, agreed closely with the setting required to compensate only for the capillary resistance. For this reason, compensation for ohmic resistance was effected in many of the experiments described here by simply adjusting R_c to compensate for the known capillary resistance.

Methods of Instrument Evaluation. The assessment of the success of the foregoing instrumental concepts in compensating for nonfaradaic influences was based on measurements with dummy cells and with electrochemical systems which previously had been subjected to careful experimental study. Dummy cell measurements permitted evaluation of the scope and accuracy of experimental procedures with the aid of passive components of accurately known value. Dummy sample and reference cells were constructed, simulating ohmic resistances, charging currents, and faradaic currents of values consistent with those found in electrochemical systems.

In experiments with actual electrochemical systems, the direct readout of the instrument was taken as the faradaic component and compared with theory and/or previously reported experimental data. The ferric-ferrous redox couple in 0.5M potassium oxalate (the iron system) and the cadmium ion–cadmium amalgam redox system in 0.5M hydrochloric acid (the cadmium system) were employed as systems representing diffusion-controlled or reversible systems (*8, 54, 64, 67, 70*) under the experimental conditions utilized. Results obtained with these systems were compared to theory for the reversible case (*64*).

The chromicyanide - chromocyanide system in 1.0M potassium cyanide (the chromium system) and the titanyl-titanous couple in 0.2M oxalic acid (the titanium system) were employed as representative of systems in which both heterogeneous charge transfer and diffusion play a significant kinetic role (quasireversible systems) (*64, 61*). Charge transfer rates obtained from data on these systems were compared to previously reported rate parameters.

The voltammetric waves of the iron and titanium systems occur in the region of the water hump (*47*) of the double-layer charging current-potential profile. The associated large variations of charging current with potential enhance the demands on the charging current compensation operation.

RESULTS AND DISCUSSION

Fundamental Harmonic A.C. Polarography. Figure 4 illustrates the efficiency with which compensation for charging current can be effected in a.c. polarography. Both polarograms shown in Figure 4 were recorded with compensation for the iR drop in effect. The effective ohmic resistance in this and in all other experimental data presented below was approximately 80 ohms. Conditions were such that the charging current was substantial, although not overwhelming. As Figure 4 indicates, subtraction of charging current yielded negligible back-

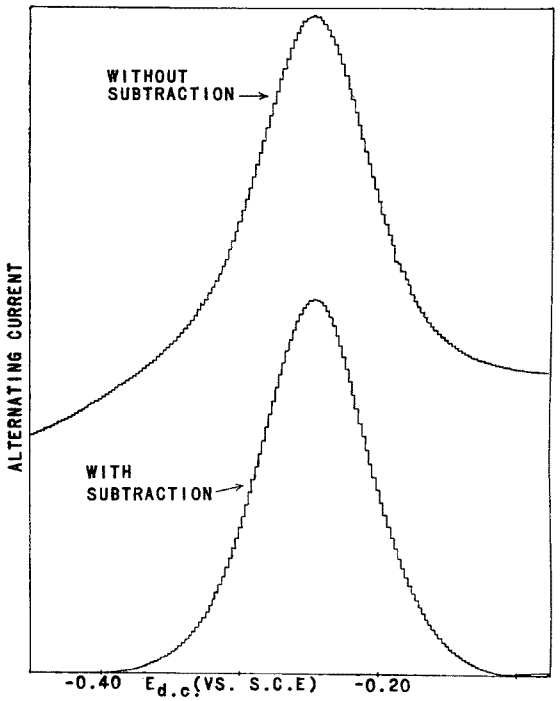

Figure 4. Fundamental harmonic a.c. polarograms of the iron system with and without subtraction of charging current

System: 0.80 × 10^{-3}M Fe(III) in 0.50M $K_2C_2O_4$
Applied: 160 Hz., 10 mv. peak-to-peak sine wave; d.c. scan rate 50 mv. per minute
Measured: 160 Hz., current component at the end of drop life with compensation for *iR* drop; ordinate uncalibrated

ground current. More significant is the fact that the polarogram obtained with alleged compensation of charging current and *iR* drop (lower polarogram in Figure 4) is of the shape predicted by theory for a reversible one-electron process which the iron system represents. For example, the half width of the wave is precisely the predicted 90 mv. These facts indicate that compensation for nonfaradaic influences was achieved quantitatively for the case in question.

The a.c. polarographic theory based on the planar diffusion model predicts that a plot of

$$\log\left[\left(\frac{Ip}{I}\right)^{1/2} - \left(\frac{Ip - I}{I}\right)^{1/2}\right]$$

(Ip is the peak alternating current and I is the current at any point along the wave) *vs.* d.c. potential should yield a straight line of $\pm(118/n)$-mv. slope at 25° C. with reversible processes (*64*). The plus sign applies to the slope on the positive side of the a.c. wave and the minus sign to the negative side. Calculations (*24*) indicate that this plot is relatively insensitive to the recently discussed effects of spherical diffusion (*23*). Figure 5 illustrates such a plot obtained from the cadmium system. The agreement between theory for the reversible wave and experiment again indicates a negligible nonfaradaic contribution. Similar agreement between theory and experiment was observed with the iron system. Although these log plots are not so sensitive to nonfaradaic effects as certain other forms of data presentation, they are nevertheless responsive to such influences. For example, failure to compensate for ohmic resistance under conditions of the experiment shown in Figure 5 yielded straight lines of 66-mv. slope, indicating a 12% contribution of *iR* drop to this characteristic. For the same conditions, a 20% decrease in peak height of the conventional a.c. polarogram resulted from failure to compensate for the ohmic resistance.

An a.c. polarographic observable which is extremely sensitive to nonfaradaic contributions is the phase angle. Results obtained with the iron and cadmium system fell close to the 45° phase angle (cot $\Phi = 1.00$; Φ = phase angle) expected for a reversible system when compensation for nonfaradaic contributions was in effect. For example, one set of a.c. polarographic data on the iron system at 40 Hz. yielded cot $\Phi = 1.01 \pm 0.04$ (± relative average deviation) over a 225-mv. portion of the a.c. wave.

The deviations of cot Φ from the expected value of unity became smaller if measurements were confined to d.c. potentials nearer the peak of the wave. Cot $\Phi = 1.01 \pm 0.02$ for d.c. potentials within 50 mv. of the peak. Equally good agreement with expectations was found with the cadmium system which was studied at frequencies between 20 and 80 Hz. As suggested above, phase angle results were particularly sensitive to effects of ohmic resistance. Failure to compensate for the 80-ohms capillary resistance with the cadmium system at 40 Hz. yielded an apparent phase angle of 29° (cot $\Phi = 1.80$) at the peak of the wave. Phase angle data also were obtained on the chromium system at frequencies of 10, 20, 40, and 80 Hz. Plots of cot Φ *vs.* $\omega^{1/2}$ yielded a straight line characteristic of a quasireversible system. The apparent k_s value (k_s = standard rate constant for heterogeneous charge transfer at $E°$) obtained from the slope of the straight line using a previously reported diffusion coefficient (*63*) was 0.21 ± 0.02 cm. second^{-1}. This result is in good agreement with previously reported values of 0.22 cm. second^{-1} (*63*) and 0.25 cm. second^{-1} (*54*).

Because this instrumentation significantly reduces the influence of charging current, the minimum concentration at which quantitative a.c. polarographic measurements can be performed is reduced correspondingly. Studies on the iron system indicated that data of nearly the quality indicated above could be obtained to concentrations at least as low as $5 \times 10^{-5}M$. At much lower concentrations, data quality was degraded significantly, particularly for measurements of total alternating current where suppression of charging current is not promoted by phase-sensitive detection. Because faradaic currents of the cadmium system exceed those of iron by more than a factor of four under similar conditions, it should be possible to obtain reasonably good quantitative data down to concentrations of about $1 \times 10^{-5}M$ in the case of cadmium. However, this has not been attempted to date.

Higher Harmonic A.C. Polarography. The measurement of higher harmonic a.c. polarographic currents contributes little to the assessment of the ability of the instrumentation to compensate for charging currents because of the small contribution of the latter (*39*, *64*, *67*). However, higher harmonic a.c. polarograms represent a sensitive index of the degree of

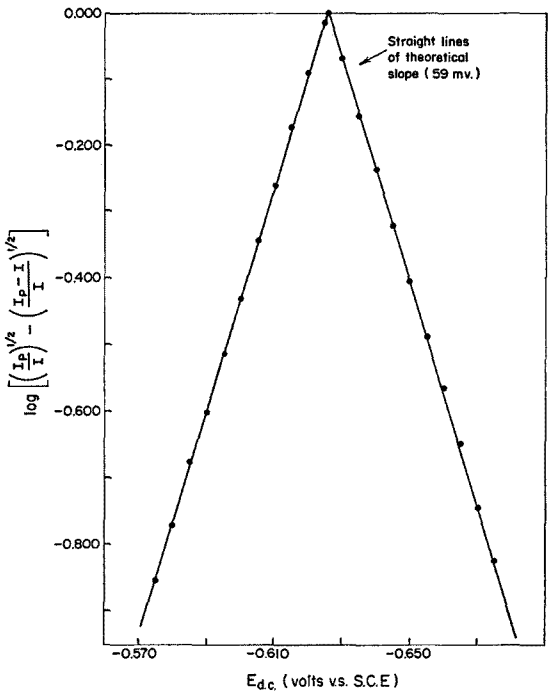

Figure 5. Plot of d.c. potential vs. $\log\left[\left(\frac{I_p}{I}\right)^{1/2}-\left(\frac{I_p-I}{I}\right)^{1/2}\right]$ from a fundamental harmonic a.c. polarogram of the cadmium system

System: 1.0×10^{-3}M Cd(II) in 0.50M KCl
Applied: 40.0 Hz., 10 mv. peak-to-peak sine wave; d.c. scan rate 25 mv. per minute
Measured: 40.0 Hz. faradaic current component at end of drop life with compensation for nonfaradaic effects

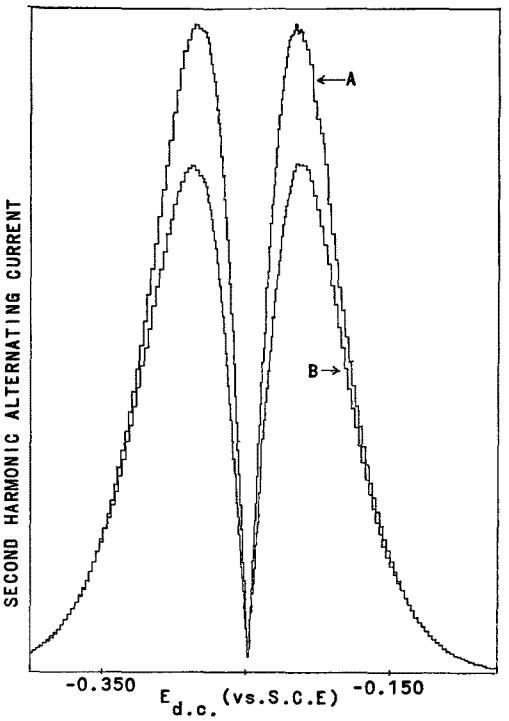

Figure 6. Second harmonic a.c. polarograms of the iron system with and without *iR* compensation

System: 2.0×10^{-3}M Fe(III) in 0.50M $K_2C_2O_4$
Applied: 42.0 Hz., 10 mv. peak-to-peak sine wave; d.c. scan rate 25 mv. per minute except between two peaks where it was reduced to 12.5 mv. per minute
Measured: 84.0 Hz. faradaic current component at end of drop life; ordinate uncalibrated
Polarogram A: With compensation for nonfaradaic effects
Polarogram B: Without *iR* compensation

success in eliminating contributions of *iR* drop because of the dependence of these polarograms on higher powers of the applied alternating potential. For small *iR* drops, the second harmonic alternating current, which depends on the square of the applied alternating potential (*64*), will be influenced by an *iR* drop roughly twice as much as the fundamental harmonic polarogram. Under similar conditions, the influence on the third harmonic currents will be roughly three times as large. The origin and nature of the effects of ohmic resistance on higher harmonic currents have been discussed at length elsewhere (*48*), where it was pointed out that, among other things, the peak separation is a good indicator of the contribution of *iR* drop.

In general, second and third harmonic a.c. polarographic results obtained with compensation for nonfaradaic effects indicated a negligible influence of *iR* drop. Figure 6 illustrates two second harmonic polarograms obtained with the iron system. The polarogram obtained with *iR* compensation is characterized by equal peak heights and a 69-mv. peak separation as expected for a reversible process (*64*). As illustrated, failure to compensate for ohmic resistance yields a smaller, second harmonic wave (peak heights are 22% smaller) with an overly large peak separation of 75 millivolts. As one would expect (*48*), the effects of *iR* drop on the second harmonic a.c. polarogram of the cadmium system are considerably larger. With *iR* drop compensation, the expected 34-mv. peak separation was observed, while a 45-mv. peak separation was obtained without compensation. Peak second harmonic currents observed with and without *iR* compensation differed by 38%. Figure 7 illustrates a third harmonic a.c. polarogram observed with the cadmium system. The peak separations are precisely as predicted by planar diffusion theory (*48*)—e.g., 29 mv. separate the central and outer peaks—indicating little influence of ohmic resistance. The predicted peak height ratio of 1:3:1 also is approximately obeyed, although the most positive peak is slightly low and the more negative peak noticeably high relative to the height of the central peak. It is difficult to attribute this disparity to an influence of *iR* drop in light of the nearly ideal peak separations and the excellent symmetry observed in the fundamental harmonic a.c. polarogram, which primarily determines the characteristics of the *iR* distortion (*48*). The disparity may manifest a slight kinetic effect of charge transfer or coupled chemical reaction. However, a contribution of spherical diffusion which has been predicted to be significant with amalgam-forming systems (*23*) appears to be the most likely source of this disparity in peak heights (*65*). The spherical correction appears to have little influence on peak separation (*65*).

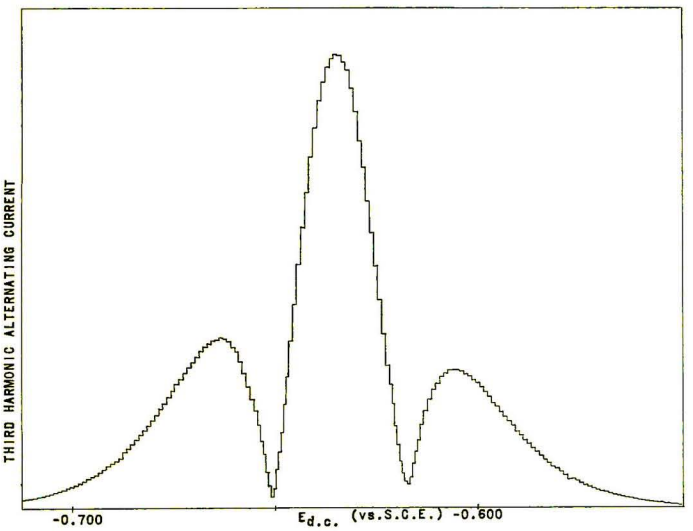

Figure 7. Third harmonic a.c. polarogram of the cadmium system

System: 1.0×10^{-3}M Cd(II) in 0.50M HCl
Applied: 26.7 Hz., 15 mv. peak-to-peak sine wave; d.c. scan rate 12.5 mv. per minute
Measured: 80.1 Hz., faradaic current component at end of drop life with compensation for nonfaradaic effects; ordinate uncalibrated

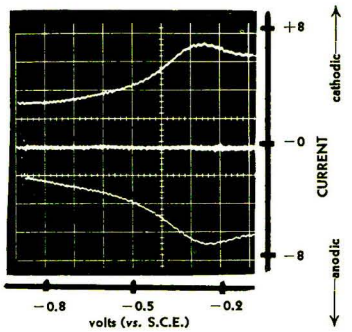

Figure 8. Cyclic voltammograms on potassium oxalate supporting electrolyte with and without charging current compensation

System: 0.50M $K_2C_2O_4$
Applied: Single-cycle triangular wave of 20 volts per second slope
Measured: Outer trace-charging current (no compensation)
Inner trace-signal with charging current compensation
Both traces obtained with iR compensation. Ordinate in units of microamperes

Triangular Wave Cyclic Voltammetry. Figure 8 illustrates the reduction of charging currents observed in cyclic voltammetric experiments with direct subtraction of charging currents as described above. The cyclic voltammogram of 0.5M potassium oxalate obtained without subtraction of charging current (outer trace) indicates that the potential range in question includes the water hump, thus maximizing the demands on the compensation circuitry. The result obtained with charging current compensation (inner trace) shows a negligible contribution of charging current. Results of single-cycle experiments on the iron system performed with scan rates in the range 2 to 50 volts second^{-1} showed the expected (*43*, *44*) 60-mv. separation between the potentials of peak anodic and cathodic currents. At the fastest scan rate, the charging current was approximately equal in magnitude to the peak faradaic current. Nevertheless, negligible charging current contributions were observed in this series of experiments when compensation was in effect. Figure 9 shows the dependence of peak current on the square-root of the scan rate. With compensation for iR drop, the expected linear relation was observed.

Failure to compensate for iR drop yielded significant deviations from linearity, as shown. At the scan rate of 50 volt second^{-1}, a separation of peak potentials of 100 mv. was recorded when iR compensation was not in effect. Measurements were performed on the titanium system with scan rates ranging from 2 to 100 volts second^{-1}. Data obtained with compensation for nonfaradaic effects corresponded to expectations for a quasireversible system with a k_s value of 5.5×10^{-2} cm. second^{-1}. This result agrees favorably with a previously reported value of 4.6×10^{-2} cm. second^{-1} obtained by a.c. polarographic measurements (*61*). Calculation of the k_s value was based on the theory of Nicholson (*43*) and observed differences in potentials associated with peak anodic and cathodic currents. A compilation of relevant data obtained with the titanium system is given in Table I. Data obtained without iR compensation are included to indicate the magnitude of the ohmic potential loss which was operative in these experiments.

Because peak separation data is somewhat insensitive to certain flaws in instrument behavior, a more complete picture of instrument performance in cyclic voltammetric measurements is given in Figure 10 which illustrates a typical single-cycle voltammogram obtained with the titanium system. The essentially ideal wave shape, lack of charging current (see initial portion of cathodic sweep), absence of ringing where the potential changes direction, and low noise level are features which indicate essentially ideal instrument response under the conditions of this experiment.

Dummy Cell Measurements. The results described above suggest that, at least under the experimental conditions in question, the instrumentation is effecting compensation for nonfaradaic influences with good accuracy. However, a definitive statement on the absolute accuracy obtainable cannot be made on the basis of results on electrochemical systems, as none of these represents a standard whose response is known and/or controllable to a high degree of accuracy

Table I. Cyclic Voltammetric Determination of k_s for Titanium System[a]

With iR compensation			Without iR compensation	
Scan rate, volt/sec.	ΔE^b, mv.	k_s, cm./sec.	ΔE, mv.	k_s, cm./sec.
5	87	5.4×10^{-2}	95	4.0×10^{-2}
10	95	5.6×10^{-2}	110	3.8×10^{-2}
20	110	5.4×10^{-2}	130	3.6×10^{-2}
50	135	5.4×10^{-2}	170	3.4×10^{-2}
100	165	5.5×10^{-2}	...	...

[a] $3.0 \times 10^{-3}M$ Ti^{+4}, 0.20M $H_2C_2O_4$.
[b] ΔE = anodic peak potential − cathodic peak potential.

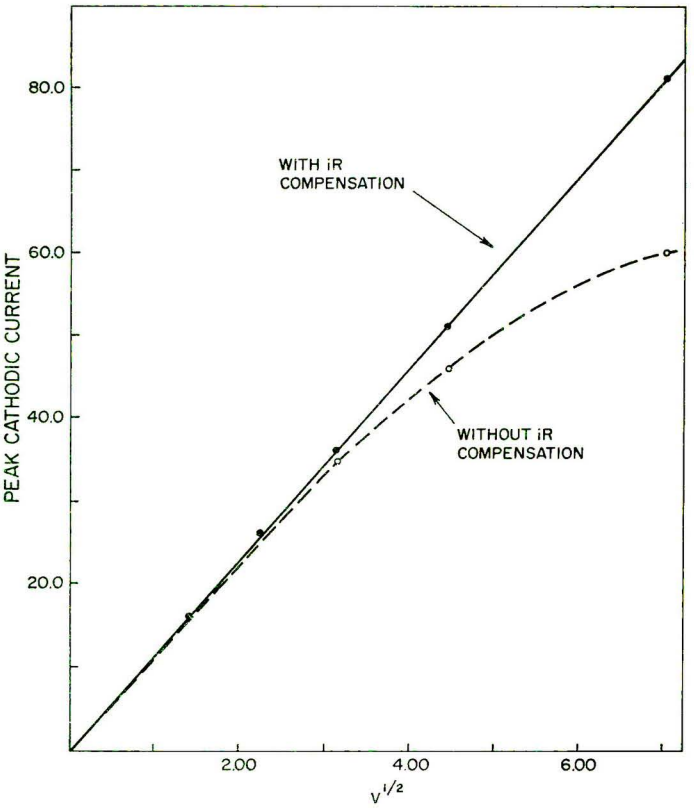

Figure 9. Plot of peak cathodic cyclic voltammetric current *vs.* square-root of scan rate for the iron system

System: 2.0×10^{-3}M Fe(III) in 0.50M $K_2C_2O_4$
Applied: Single-cycle triangular waves of slopes between 2 and 50 volts per second
Measured: Total faradaic current
● = Data obtained with compensation for nonfaradaic effects
○ = Data obtained without *iR* compensation
Ordinate in units of microamperes

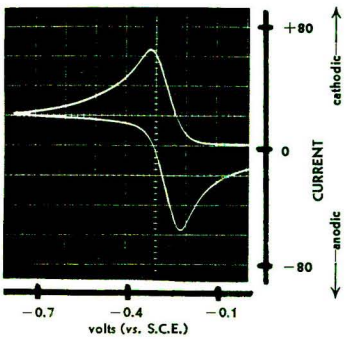

Figure 10. Cyclic voltammogram observed with titanium system

System: 3.0×10^{-3}M Ti(IV) in 0.20M $H_2C_2O_4$
Applied: Single-cycle triangular wave of 20 volts per second slope
Measured: Total faradaic current with compensation for nonfaradaic effects. Ordinate in units of microamperes

(better than 1%). Dummy cell measurements satisfied this need.

Results of a.c. polarographic dummy cell measurements indicated that for frequencies up to 200 to 300 Hz., data can be obtained with compensation for nonfaradaic effects with accuracies of ±0.5% (± relative standard deviation of data from the expected result calculated from component values). The range of deviations between instrument readout and the calculated result was normally within ±1%.

Although no actual electrochemical experiments were performed with high resistance nonaqueous solvents, successful dummy cell measurements with large simulated ohmic resistances (up to 10 *K*) suggested that the concepts tested in this work would be applicable to aprotic solvents such as acetonitrile, dimethylformamide, etc.

Band-Pass Problems. At frequencies much above the 200- to 300-Hz. limit indicated above, band pass problems became evident in results obtained with both dummy cells and electrochemical systems. Similar deterioration of performance was detected in cyclic voltammetry for scan rates in excess of 100 to 200 volts second^{-1}. It was apparent throughout this work that compensation for ohmic resistance with the aid of the positive feedback loop was achieved at the expense of the stability margin of the potential control loop. This was not unexpected in view of the work of Booman and Holbrook (*11*). Successful operation was achieved in this work at low and moderate frequencies because stabilizing capacitors (*11*, *13*, *68*) could be placed in the feedback of the control amplifiers which were of sufficient magnitude to stabilize the system, but not so large that they attenuated the response at the frequency of interest.

However, when control was attempted at frequencies over about 200 to 300 Hz., the magnitude of the stabilizing capacitor which yielded good performance at the frequency of interest decreased to the point where it was insufficient to stabilize the system when complete compensation of ohmic resistance was attempted. Stable and accurate operation was obtained above the 200- to 300-Hz. limit (up to about 1200 Hz.) by compensating for only a fraction of the effective ohmic resistance. This fraction was usually greater than one half. While accurate, the potentiostat readout reflected a small, but significant, contribution of ohmic resistance under these conditions and direct compensation of charging currents was inaccurate.

It is expected that some improvement in band-pass can be effected with the present instrument through the use of phase compensation networks (*10*, *11*) to achieve stability in place of the rather crude feedback capacitor approach employed here. The observed reduction in the stability margin with *iR* compensation may also be eliminated through properly designed phase compensation networks.

As far as band-pass is concerned, the use of Philbrick P-2 amplifiers as the active components of the potentiostat represents a rather poor choice. Our choice of the Philbrick P-2 amplifier was made at a time when the more sophisticated high frequency solid-state operational amplifiers were unavailable and, thus, was dictated by considerations other than band-pass. The P-2 amplifier is characterized by a

low unity gain crossover frequency of 120 KHz., in contrast to the 100 MHz. value characterizing some of the newer models. It appears likely that the frequency range over which effectively complete compensation of nonfaradaic effects can be realized will be extended over that observed here through the use of faster amplifiers, together with carefully designed stabilizing networks based on the phase compensation principle.

Because direct experimental evidence is not available at this time, the foregoing statements regarding application of these techniques under more extreme conditions (shorter time scales, higher ohmic resistances) amount to conjecture. However, the experimental results presented at least demonstrate the feasibility of effecting accurate, direct readout of the faradaic component in experiments involving moderately short time scales and moderate ohmic resistances where nonfaradaic effects are substantial. Such conditions are found in a considerable fraction of experimental electrochemical studies so that even if the promise of wider scope of application is not realized, the techniques employed in this work should prove to be of frequent use.

ACKNOWLEDGMENT

The authors thank Glenn Booman for helpful comments and suggestions regarding the band-pass and stability problems.

LITERATURE CITED

(1) Anson, F. C., Reinmuth, W. H., ANAL. CHEM. **33,** 1438 (1961).
(2) Arthur, P., Lewis, P. A., Lloyd, N. A., Vanderkam, R. K., *Ibid.*, p. 488.
(3) Barker, G. C., *Anal. Chim. Acta* **18,** 118 (1958).
(4) Barker, G. C., Faircloth, R. L., Gardner, A. W., *Nature* **181,** 247 (1958).
(5) Barker, G. C., Gardner, A. W., At. Energy Res. Est. C/R 2297 (August 1958); *Z. Anal. Chem.* **173,** 79 (1960).
(6) Barker, G. C., Jenkins, I. L., *Analyst* **77,** 685 (1952).
(7) Barnartt, S., *J. Electrochem. Soc.* **108,** 102 (1961).
(8) Biegler, T., Laitinen, H. A., ANAL. CHEM. **37,** 572 (1965).
(9) Booman, G. L., *Ibid.*, **29,** 213 (1957).
(10) Booman, G. L., Holbrook, W. B., *Ibid.*, **35,** 1793 (1963).
(11) *Ibid.*, **37,** 795 (1965).
(12) Brown, E. R., Weyssenhoff, H. von, Smith, D. E., DeFord, D. D., unpublished work, Northwestern University, Evanston, Ill., 1965.
(13) Burr-Brown Handbook of Operational Amplifier Applications, Burr-Brown Research Corp., Tucson, Ariz., 1963.
(14) Davis, H. M., Rooney, R. C., *J. Polarog. Soc.* **8,** 25 (1962).
(15) DeFord, D. D., Division of Analytical Chemistry, 133rd Meeting, ACS, San Francisco, April 1958.
(16) Delahay, P., "New Instrumental Methods in Electrochemistry," pp. 132–4, Interscience, New York, 1954.
(17) *Ibid.*, pp. 166–7.
(18) Delahay, P., in "Advances in Electrochemistry and Electrochemical Engineering," P. Delahay and C. W. Tobias, eds., Vol. 1, chap. 5, Interscience, New York, 1961.
(19) Delahay, P., *Anal. Chim. Acta* **18,** 13 (1958).
(20) Delahay, P., Stiehl, G. L., *J. Phys. Chem.* **55,** 570 (1951).
(21) DeLevie, R., *Electrochim. Acta* **10,** 395 (1965).
(22) DeLevie, R., *J. Electroanal. Chem.* **9,** 311 (1965).
(23) Delmastro, J. R., Smith, D. E., ANAL. CHEM. **38,** 169 (1966).
(24) Delmastro, J. R., Smith, D. E., unpublished work.
(25) DeVries, W. T., Dalen, E. van, *J. Electroanal. Chem.* **10,** 183 (1965).
(26) Ferrett, D. J., Milner, G. W. C., Shalgosky, H. I., Slee, L. J., *Analyst* **81,** 506 (1956).
(27) Hayes, J. W., Bauer, H. H., *J. Electroanal. Chem.* **3,** 336 (1962).
(28) Hayes, J. W., Reilley, C. N., ANAL. CHEM. **37,** 1322 (1965).
(29) Howe, R., *Instr. Control Systems* **34,** 1482 (1961).
(30) Ilkovic, D., Semerano, G., *Coll. Czech. Chem. Commun.* **4,** 176 (1932).
(31) Imai, H., *J. Phys. Chem.* **66,** 1744 (1962).
(32) Kanevskii, E. A., *Zh. Prikl. Khim.* **17,** 514 (1944).
(33) Kelley, M. T., Fisher, D. J., Cooke, W. D., Jones, H. C., in "Advances in Polarography," I. S. Longmuir, ed., pp. 158–82, Pergamon Press, Oxford, 1960.
(34) Kelley, M. T., Fisher, D. J., Jones, H. C., ANAL. CHEM. **31,** 1475 (1959); **32,** 1262 (1960).
(35) Kelley, M. T., Miller, H. H., *Ibid.*, **24,** 1895 (1952).
(36) Kolthoff, I. M., Marshall, J. C., Gupta, S. L., *J. Electroanal. Chem.* **3,** 209 (1962).
(37) Lauer, G., Osteryoung, R. A., Division of Analytical Chemistry, 150th Meeting, ACS, Phoenix, Ariz., January 1966; ANAL. CHEM. **38,** 1106 (1966).
(38) Morrison, C. F., Jr., "Generalized Instrumentation for Research and Teaching," p. 97, Washington State University Press, Pullman, Wash., 1964.
(39) Neeb, R., *Z. Anal. Chem.* **188,** 401 (1962).
(40) Neeb, R., *Naturwiss.* **49,** 447 (1962).
(41) Němec, L., *J. Electroanal. Chem.* **8,** 166 (1964).
(42) Nicholson, R. S., ANAL. CHEM. **37,** 667 (1965).
(43) *Ibid.*, p. 1351.
(44) Nicholson, R. S., Shain, I., *Ibid.*, **36,** 706 (1964).
(45) Okinaka, Y., Kolthoff, I. M., Murayama, T., *J. Am. Chem. Soc.* **87,** 423 (1965).
(46) Parry, E. P., Osteryoung, R. A., ANAL. CHEM. **37,** 1634 (1965).
(47) Parsons, R., in "Advances in Electrochemistry and Electrochemical Engineering," P. Delahay and C. W. Tobias, eds., Vol. 1, chap. 1, Interscience, New York, 1961.
(48) Paynter, J., Reinmuth, W. H., ANAL. CHEM. **34,** 1335 (1962); J. Paynter, doctoral thesis, Columbia University, New York, 1964.
(49) Philbrick Researches, Inc., "The Lightning Empiricist," Vol. **13,** Nos. 1 and 2, Philbrick Researches, Inc., Dedham, Mass., 1965.
(50) Philbrick Researches, Inc., "Applications Manual GAP/R, K2," Philbrick Researches, Inc., Dedham, Mass., 1956.
(51) Pouli, D., Huff, J. R., Pearson, J. C., ANAL. CHEM. **38,** 382 (1966).
(52) Powell, K. G., Reynolds, G. F., *Electrochim. Acta* **10,** 921 (1965).
(53) Propst, R. C., "A Multipurpose Instrument for Electrochemical Studies," Clearinghouse for Federal Scientific and Technical Information, National Bureau of Standards, U. S. Department of Commerce, Springfield, Va.
(54) Randles, J. E. B., Somerton, K. W., *Trans. Faraday Soc.* **48,** 937 (1952).
(55) Reinmuth, W. H., ANAL. CHEM. **36,** 211R (1964).
(56) Schaap, W. B., McKinney, P. S., ANAL. CHEM. **36,** 29 (1964).
(57) Schmidt, H., Stackelberg, M. von, *J. Electroanal. Chem.* **1,** 133 (1959).
(58) Schwarz, W. M., Shain, I., ANAL. CHEM. **35,** 1770 (1963).
(59) Semerano, G., Riccoboni, L., *Gazz. Chim. Ital.* **72,** 297 (1942).
(60) Sluyters-Rehbach, M., Sluyters, J. H., *Rec. Trav. Chim.* **82,** 525 (1963); **82,** 535 (1963); **83,** 217 (1964).
(61) Smith, D. E., ANAL. CHEM. **35,** 610 (1963).
(62) *Ibid.*, p. 1811.
(63) Smith, D. E., doctoral thesis, Columbia University, New York, 1961.
(64) Smith, D. E., in "Electroanalytical Chemistry," A. J. Bard, ed., Vol. **1,** chap. 1, M. Dekker, Inc., New York, in press.
(65) Smith, D. E., McCord, T. G., Brown, E. R., unpublished work, Northwestern University, Evanston, Ill., 1966.
(66) Smith, D. E., Reinmuth, W. H., ANAL. CHEM. **32,** 1892 (1960).
(67) *Ibid.*, **33,** 482 (1961).
(68) Strata, R., "An Operational Amplifier Application Manual," Analog Devices, Cambridge, Mass., 1965.
(69) Takahashi, T., Niki, E., *Talanta* **1,** 245 (1958).
(70) Underkofler, W. L., Shain, I., ANAL. CHEM. **37,** 218 (1965).
(71) Walker, D. E., Adams, R. N., Alden, J. R., *Ibid.*, **33,** 308 (1961).
(72) Yasumori, Y., *J. Electrochem. Soc., Japan (Japan Ed.)* **24,** 309 (1956).

RECEIVED for review April 7, 1966. Accepted June 2, 1966. Presented in part at the Division of Analytical Chemistry, 150th Meeting, American Chemical Society, Phoenix, Ariz., January 1966. This work was supported in part by a National Science Foundation cooperative fellowship (E. R. B., 1964–65), an Electrochemical Society summer fellowship (T. G. M., 1965) and by National Science Foundation grant GP-3484.

Instrumentation for Digital Data Acquisition in Voltammetric Techniques

D.C. and A.C. Polarography

ERIC R. BROWN, DONALD E. SMITH, and DONALD D. DeFORD
Department of Chemistry, Northwestern University, Evanston, Ill.

▷ **An instrument is described which was designed to effect digital readout of current and potential signals on an IBM card in voltammetric techniques involving relatively long experiment times, such as d.c. and a.c. polarography. It incorporates a combination of known electrochemical control and signal conditioning procedures with a commercial digital data acquisition system. Results of experiments designed to evaluate instrument performance in measurements involving multichannel digital readout in d.c. and a.c. polarography are presented and discussed.**

THE SUPERIOR ASPECTS of digital data acquisition over the analog approach have been well documented and proven for some time in measurement systems employed outside the realm of electrochemical experimentation (*11*). More recently, the advantages in adaptation of digital techniques to electrochemical measurements have been described (*5, 7, 13–15, 18*). In particular, a general philosophy of application of digital techniques to electrochemical measurements with a detailed description of the attending advantages has been given by Booman (*5*). Of the potential benefits associated with digital readout, those most instrumental in stimulating our efforts along these lines were the direct compatibility of digital readout with high-speed digital computers, the ease of achieving multichannel readout, and the high inherent accuracy.

Obtaining voltammetric data in a form which is directly presentable to high-speed digital computers appeared to be the most significant and far-reaching of these advantages. This is suggested by the considerable tedium associated with conventional voltammetric data processing, which includes the time-consuming operations of manually digitizing data (reading points from an analog recording), introducing scaling factors, correcting for nonfaradaic influences, plotting data in a variety of potentially informative ways and smoothing noisy data by least squares methods. Through digital readout to IBM card, punched paper tape, or magnetic tape, all of these steps may be performed by accurate, high-speed digital instrumentation, introducing a savings in time of sufficient magnitude (*7*) to make the acquisition of initially expensive digital equipment an economical approach in the long run.

The ready applicability of digital readout procedures to multichannel readout represents a significant consideration in certain voltammetric measurements. By measuring a number of current and/or potential signals of electrochemical origin in a single experimental run, a considerable improvement in efficiency over conventional data acquisition procedures can be realized. While not always applicable, this form of data acquisition is eminently suited to a number of techniques, a.c. polarographic experiments representing a notable example. A complete a.c. polarographic measurement requires readout of three signals; the applied d.c. potential and two components of the faradaic current (*3, 8, 23, 25*). A significant savings in time can be realized by obtaining these data simultaneously rather than by performing two separate experiments, as is usually done. The possibilities go well beyond this simple example. A variety of current components, all potentially informative, are available for measurement in a.c. polarography. For example, within the framework of the a.c. polarographic experiment, simultaneous measurement of the d.c. polarographic current, two components of the fundamental harmonic current—e.g., total and in-phase components—and two components of the second harmonic current would be possible in a single run, provided sufficient capacity in signal conditioning and readout devices were available. By conventional standards, this latter procedure might be looked upon as performing five techniques simultaneously; d.c. polarography, conventional a.c. polarography (*8, 25*) phase-selective a.c. polarography (*1, 8, 10, 12, 25, 28, 29*) conventional second harmonic a.c. polarography (*2, 4, 8, 19, 20, 25, 27*) and phase-selective second harmonic a.c. polarography (*26*). Third and higher harmonic components could be included in such a multichannel readout procedure. Alternative to or in combination with readout of several different current components originating from a single frequency of applied potential, one could effect simultaneous readout of the a.c. polarographic response at several frequencies. This could be achieved by simultaneously applying a number of sinusoidal potentials of varying frequency to the electrochemical cell and measuring the current components corresponding to fundamental, higher, or intermodulation harmonics of the applied frequencies with the aid of frequency selective circuits (*26, 27*). By combining the use of small amplitudes with judicious choice of applied frequencies, one can avoid complications in interpretation which can arise when higher-order current components (second harmonics, intermodulation components) originating from different applied frequencies overlap with each other or with the fundamental harmonic current components. Thus, for example, the measurement of a fundamental harmonic current of a given frequency will be unperturbed by the existence of applied potentials of other frequencies. The act of simultaneously acquiring a.c. polarographic information at a variety of frequencies and/or from a variety of types of current components (fundamental harmonics, second harmonics, etc.) might be entitled "Multiplexing in A.C. Polarography." The operational amplifier approach to electrochemical instrumentation is well suited without modification to multichannel data acquisition (*25*). Simultaneous application of several applied potential signals and/or simultaneous presentation of signals arising from various current components can be achieved readily with operational amplifier equipment described in the literature (*6, 17, 22, 24–26*). However, to effect readout of a large number of signals, recording equipment of corresponding capacity is required. Analog readout

devices capable of monitoring three signals simultaneously (X-YY' recorders) are available at a cost competitive with digital data acquisition systems. However, if more than three signals are to be recorded, the cost of additional analog recording capability is considerable, while the added cost in digital recording equipment is negligible since the capability of recording many (10–20) channels is proved by relatively low cost units. Thus, digital data acquisition appears to be the method of choice if multichannel readout is of interest.

The advantages associated with the higher inherent accuracy in digital recording are also significant. Analog recorders of 0.1% accuracy are available, but frequent maintenance is often required to hold this tolerance. The lower accuracy of high speed analog recording devices—e.g., oscilloscopes—is well known. At the same time, the least expensive digital recording equipment is capable of an accuracy of about 0.1%, and more precise units are readily available. None of these units require significant maintenance.

Reported work on adaptation of electrochemical instrumentation to digital readout procedures has appeared only recently. Herman and Bard presented instrumentation for digital readout of transition times in chronopotentiometry (*13–15*). Breiter (*7*) has described instrumentation for digital readout in low-speed cyclic voltammetric and a.c. polarographic measurements with stationary electrodes. The use of a multichannel analyzer for digitization of data in voltammetric methods, particularly potentiostatic measurements, was described by Osteryoung and coworkers (*18*). Generalized concepts and instrumentation for adaptation of digital techniques to electrochemical measurements were given by Booman (*5*).

The present paper describes instrumentation by which digital readout is effected in voltammetric experiments of relatively long duration (>1 minute, approximately) by combining known voltammetric signal conditioning procedures with a commercial digital data acquisition system of standard design. The instrumental system permits the use of digital readout procedures in measurements performed with the dropping mercury electrode, as well as with stationary electrodes. Results obtained in d.c. and a.c. polarographic measurements with a dropping mercury electrode are presented.

EXPERIMENTAL

Basic Electrochemical Instrumentation. An all solid-state operational amplifier instrument which has been described in detail in a separate communication (*9*) was employed in this work. The following main features of this instrumentation are of interest in the present discussion.

(a) Positive feedback is employed in the potential control loop to effect compensation for ohmic potential losses.

(b) Direct compensation of charging current is achieved by applying identical potential signals to two cells, one containing supporting electrolyte solution and the second containing supporting electrolyte and electroactive component, and subtracting the resulting current signals.

(c) A sample-and-hold readout mode is employed in d.c. and a.c. polarographic measurements performed with a dropping mercury electrode. The output signal represents the current component of interest at the end of each mercury drop life. The hold mode is in effect for all but about 0.1 second late in the life of the mercury drop.

(d) Synchronization of mercury drop lives and control of the sample-and-hold readout operation is achieved with the aid of a general purpose timing circuit. The output pulses of the timing circuit provide convenient command signals for synchronization of external equipment with events in the polarographic cell.

Digital Data Acquisition System. Digital readout to IBM punched card was selected for this work because it provided a readout form immediately interpretable by the operator as well as the high-speed digital computer, a feature not provided by the other choices (typewriter, printed tape, magnetic tape, punched paper tape, etc.). Readability of the data on the part of the operator was deemed important because this permits initial assessment of data quality before presentation to a computer. The choice of IBM card readout sacrificed the somewhat greater speed associated with the tape approaches, but this was not considered important for the applications of interest to us.

A Vidar Corporation Model 1025012 10-channel digital data acquisition system designed to record the voltage level at each channel on IBM punched cards with the aid of an IBM Model 526 card punch was selected for this work. A detailed description of this system is not essential to the present discussion and only the basic features will be given here. An extensive description may be obtained from the manufacturers (*16, 30*). While the Vidar system is adequate for our purposes, instruments of similar concept and design which may be equally suitable are available from a variety of other sources.

The main components of the Vidar digital data acquisition system consist of a Vidar Model 604 scanner (or "Multiplexer"), a Vidar Model 500 solid-state integrating digital voltmeter (the DVM), a Vidar Model 651-8 coupler and the IBM 526 card punch. The 10-channel scanner employs reed relays to sequentially transfer data from 1 to 10 analog signal sources to the measuring (DVM) and recording (coupler and card punch) equipment. The number and identity of the channels to be read is controlled by front panel switches. The scanner is designed to receive advance and reset commands from the coupler or by manual operation of front panel push-button controls. An advance command moves the scanner sequentially to the next input channel, transferring the associated voltage to the DVM. The reset command sets the scanner to the first selected channel, transferring this data to the DVM. From 10 mseconds to 1 second after receipt of a reset or advance command, the scanner produces a command pulse which tells the DVM to begin its measuring operation. The delay time of 10 mseconds to 1 second is adjusted by a front panel control. The digital voltmeter has five ranges from ±100 mv. to ±1000 volts full scale. An autoranging operation mode, which was employed throughout the work described here, is included. In the autoranging mode a 100% overranging capability is provided so that the DVM operates on a given range until the signal level exceeds two times the "full scale" value. Data of four significant figures are presented when the instrument is in the overranging configuration while three digits are provided for signal levels less than the full scale value. The DVM measures the voltage presented by the scanner and presents the measurement to the coupler in the form of binary coded decimal (BCD) data, a BCD location signal, and a polarity signal. The DVM effects voltage measurement through a conventional technique which involves three steps: (a) amplification of the input signal, (b) conversion of the amplified input signal to a proportional pulse train with the aid of a voltage controlled oscillator, (c) application of the pulse train to a series of decade counters for a *fixed* period of time (the integration period). A fixed integration period of 20 mseconds is controlled to better than ±0.01% by a crystal oscillator time base. The crystal oscillator output is amplified and converted into short duration pulses which serve as start and stop commands for the counter gate. A start command cannot be received until a command pulse is provided by the scanner (see above) which activates an auxiliary gate. It should be noted that the measurement time is insignificant compared to the time required for card punch operation. Upon completion of the measurement, the DVM also produces a print command which is routed through the control circuitry of the coupler to the card punch. The coupler is the key element of the system. It translates the BCD data from the DVM into a format compatible with the IBM card punch, supplies this information in a suitably amplified form to the card punch, and coordinates the operation of the other units of the system by providing reset and advance commands for the scanner, print commands for the card punch, etc. As the last character of each data point is recorded by the card punch, an advance command is

	1	2	3	4
RUN #1	002493	011844	116043	111263
RUN #2	002503	011864	115993	111143
RUN #3	002493	011814	116033	111183
RUN #4	002503	011584	115983	111123

Figure 1. Form of digital data readout presented at top of IBM card

System: 2.0×10^{-3}M Fe(III) in 0.50M $K_2C_2O_4$

Applied: 42.0 Hz, 10 mv. peak-to-peak sine wave; d.c. scan rate of 50 mv. per minute

Measured: Shows data obtained at −0.250 volt during four successive runs
Column 1: d.c. potential signal
Column 2: d.c. faradaic current signal
Column 3: total 42.0 Hz faradaic current signal
Column 4: resistive (in-phase) component of 42.0 Hz faradaic current signal
All signals measured at end of drop life with compensation for nonfaradaic effects

given to the scanner by the coupler, causing the scanner to sample the next channel. The reset command originates in the card punch each time the card punch prints the last character of information for the last channel. The command is routed through the coupler where it is delayed for 250 mseconds to permit a new card to move into place and then routed to the scanner as the reset command. Provision for control of the readout cycle by external timing circuitry is obtained by routing the reset command through a normally-open relay. A C. P. Clare Model HGSS1002 single-side-stable, mercury-wetted contact relay was used for this purpose. In this way, a reading cycle cannot ensue until an external pulse effects relay closure, transmitting the reset command to the scanner. Once the reset command is provided, readout of from 1 to 10 channels of information is achieved on a single IBM card at a rate of 100 channels per minute (0.6 second per channel) after which a new card is moved into place and the system ceases operation until an externally induced relay closure again provides a start command.

The form of the data provided is illustrated in Figure 1. Results of four measurements (four IBM cards) performed under essentially identical conditions are shown. Each measurement involved readout of four channels of information. For the present discussion it is essential to note only the form of the data. Further details regarding the significance of the data are discussed below. As shown in Figure 1, data are given in the form of six characters per word. The first character (left hand character) indicates polarity. The next four characters represent the data with the most significant to least significant digits ordered from left to right. The last character (right side) indicates the range. In the polarity character, a zero indicates positive polarity input, a one indicates negative polarity, a two indicates positive overload, and a three indicates negative overload. Range identification is effected through indication of the appropriate negative exponent of ten in the last character. Thus, the word 017653 represents +1.765 volts, and word 143204 indicates −0.4320 volt, etc.

Coupling Basic Electrochemical Instrumentation with Digital Data Acquisition System. It should be apparent from the foregoing discussion that the electrochemical instrumentation and the digital data acquisition system (the DDAS) are ideally compatible for a.c. and d.c. polarographic studies without further modification of either unit. The key elements in achieving this compatibility are the sample-and-hold readout capability of the electrochemical system and the provision for external control of the reading cycle of the DDAS. Coupling of the electrochemical instrument and the DDAS simply required the following steps. First, each channel of analog information from the electrochemical instrument was applied to the scanner inputs of the DDAS *via* sampling circuits (*9*). Second, the source of a voltage pulse from the timing circuit of the electrochemical instrument which signals the end of each mercury drop life [the output of Trigger 2 of Figure 3, Ref. (*9*)] was routed to the coil of the relay whose closure initiates a reading cycle of the DDAS. An example of one type of system resulting from such a combination of DDAS and electrochemical instrument is illustrated in a schematic form in Figure 2. Figure 2 depicts an instrument which is designed to compensate for nonfaradaic effects (*9*) and simultaneously to read out the d.c. polarographic current and two components of both the fundamental and second harmonic currents (total a.c. signal and a vectorial component). The rationale for the various analog signal paths has been discussed elsewhere (*25–27*). With a system such as illustrated in Figure 2, electrochemical data obtained with a dropping mercury electrode can be read out digitally to an IBM card, with each IBM card containing data points corresponding to instantaneous signal levels at the end of drop life (*9*) for all channels of information. The sequence of operations performed by this instrumentation in the course of effecting digital readout is as follows.

(a) Late in the life of a mercury drop, a pulse from the timing circuit simultaneously initiates sampling of all analog output signals of interest.

(b) About 0.1 second later, a pulse from the timing circuit terminates the sampling operation, sending the sampling circuits into the hold mode. The same pulse activates the drop-dislodger circuitry, ending the mercury drop life, and signals the DDAS to begin a reading cycle.

(c) During the first few seconds of the life of the new mercury drop, the DDAS goes through the operation of printing on a single IBM card the voltage outputs of the sampling circuits from each channel of information.

(d) The IBM card on which the data has been punched is moved to the storage rack, a new card is moved into place and the DDAS ceases operation until stages (a) and (b) recur a few seconds later.

The total time required to perform the preceding sequence of operations depends upon the number of channels to be monitored and places an obvious limit on the minimum drop time that can be used. This has been no problem in our applications to date, although one can envision situations where this restriction would be a disadvantage.

The operation of the instrument has been discussed only within the context of experiments employing the dropping mercury electrode because the foregoing approach to digital data acquisition is best suited to such applications where the experiment time (time required to run one polarogram) can be made relatively long without influencing the nature of the data. However, straightforward applications in experiments with stationary electrodes also exist, provided the time of the experiment is sufficient. With this restriction, adaptation of the instrument just described to measurements with stationary electrodes would require simply the removal of the drop-dislodger circuitry and possibly the sampling circuits, although the latter step is not recommended. The sample-and-hold operation makes possible the recording of data points corresponding to the same instant in time for all information channels. This is desirable regardless of the nature of the electrode because of the associated ease of comparing data from various channels.

It should be recognized that the combination of more-or-less standard electroanalytical instrumentation with the digital data acquisition system described here amounts to a special case of the generalized system configuration outlined by Booman (*5*).

Supporting Equipment. An Electro Instruments Model 480 X-YY′ re-

corder with Model 468 (X-axis) and Model 420 (Y-axes) plug-in modules was employed to record polarograms in the usual analog fashion. Analog recordings were obtained simultaneously with the digital readout to assess the consistency between the two forms of data acquisition, to determine whether the DDAS was influencing data quality, etc.

A Hewlett-Packard Model 5243L electronic counter with a Model 5265A plug-in served as a second digital voltmeter which permitted on-line checking of the data produced by the Vidar DDAS.

A California Computer Products, Inc., Model 565 digital incremental plotter made available at the Northwestern University Computing Center was employed to obtain analog plots of raw digital data produced by the DDAS. The plotter was operated in the mode in which straight lines are drawn between adjacent data points. By comparing on-line analog recordings with those produced from the digital data with the aid of the digital incremental plotter, an assessment of the noise and other sources of error introduced in analog-digital-analog conversion was possible. This was considered important because analog forms are expected to remain a most informative and efficient approach to data presentation. Thus, while data acquisition and processing may be performed by digital techniques, data presentation in *both* analog and digital forms is likely to be preferred.

The remaining supporting electronic equipment, thermostats, electrodes, cells, etc., were described in a separate paper (*9*) as were their applications. The ferric–ferrous oxalate system in 0.5*M* potassium oxalate (*21*, *27*, *29*) was employed as a model in the instrument evaluation experiments. Solution preparation was performed in the usual manner (*9*).

RESULTS AND DISCUSSION

An assessment of the performance of the electrochemical instrumentation and the DDAS as a unit was the primary objective of the experimental work presented here. Excellent individual performance of these two basic components has been established (*9*, *30*). However, successful implementation of the combined unit to produce accurate digital data demands reliable, precise, coordinated performance of a number of critical units (potentiostats, signal amplifiers, timing circuitry, sampling circuits, drop-dislodger circuitry, scanner, digital voltmeter, coupler, and card punch). A secondary objective was to assess the feasibility of the multichannel readout procedures discussed above.

A variety of experiments showed that the accuracy and reproducibility of digital data obtained with this system was comparable with the results obtained in analog readout with the same basic electrochemical instrument (*9*). For example, Figure 1 illustrates the

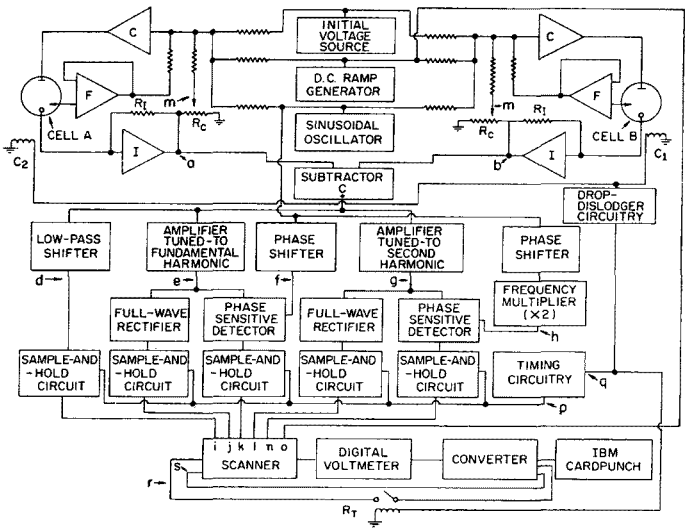

Figure 2. Schematic of instrumentation for simultaneous digital readout of d.c. polarogram, conventional fundamental harmonic a.c. polarogram, phase-selective fundamental harmonic a.c. polarogram, conventional second harmonic a.c. polarogram, and phase-selective second harmonic a.c. polarogram with compensation for nonfaradaic effects

Amplifiers *I* and C—operational amplifiers in inverting configuration
Amplifier *F*—operational amplifier in voltage follower configuration
R_f—current signal level control
R_c—*iR* compensation control
C_1, C_2—coils of drop-dislodger solenoids
R_T—readout cycle control relay
Cell A—cell with sample solution
Cell B—cell with reference solution
a—faradaic and double-layer charging current signals
b—double-layer charging current signal
c—faradaic current signal
d—d.c. faradaic current signal
e—fundamental harmonic faradaic current signal
f—fundamental harmonic reference signal
g—second harmonic faradaic current signal
h—second harmonic reference signal
i—d.c. faradaic current signal at end of mercury drop life
j—total fundamental harmonic faradaic current signal at end of mercury drop life
k—resistive component of fundamental harmonic faradaic current signal at end of mercury drop life
l—total second harmonic faradaic current signal at end of mercury drop life
m—signal equal to *iR* drop
n—in-phase component of second harmonic faradaic current signal at end of mercury drop life
o—d.c. potential signal (this signal either should be the first measured in the readout cycle or subjected to the sample-and-hold operation so that d.c. potential signal corresponding to the end of drop life is recorded)
p—timing impulse [from Trigger 1 of Figure 3, Ref. (9)]
q—timing impulse [from Trigger 2 of Figure 3, Ref. (9)]
r—reset command
s—advance command

reproducibility obtained in an experiment in which the d.c. potential, the d.c. polarographic current and two components of the fundamental harmonic a.c. polarographic current were recorded simultaneously. Each set of four data points was obtained in the course of a normal polarographic run at a particular d.c. potential (−0.250 volt) along the polarographic wave. The time elapsed between readout of the first and the last set of data was approximately 1 hour, indicating that drift in the various instrument components is negligible. Table I gives a more extensive example of typical precision observed in digital data readout in experiments of the type illustrated in Figure 1. The degradation of precision in the d.c. polarographic signal at the foot of the wave (data at more positive potentials in Table I) is partly due to a drift in d.c. offset in some of the amplifiers, a factor which is of no consequence in the a.c. measurements. This problem is readily soluble by incorporating into the instrument amplifiers characterized by less d.c. drift. It should be mentioned that d.c. polarograms obtained under these circumstances are es-

Table I. Reproducibility in Simultaneous Digital Readout of D.C. Polarographic Current, Total Fundamental Harmonic A.C. Polarographic Current and In-Phase (Resistive) Component of Fundamental Harmonic A.C. Polarographic Current[a]

D.C. potential	D.C. polarographic current				Total fundamental harmonic				In-phase fundamental harmonic			
	Run 1	Run 2	Run 3	R.A.D.[b]	Run 1	Run 2	Run 3	R.A.D.[b]	Run 1	Run 2	Run 3	R.A.D.[b]
0.230	0.0790	0.0800	0.0766	1.6	1.517	1.510	1.503	0.3	1.069	1.057	1.056	0.5
0.235	0.0885	0.0892	0.0862	1.3	1.575	1.569	1.565	0.2	1.118	1.099	1.098	0.8
0.239	0.0983	0.0988	0.0959	1.2	1.611	1.605	1.602	0.2	1.135	1.123	1.123	0.5
0.245	0.1084	0.1087	0.1059	1.1	1.621	1.617	1.612	0.2	1.140	1.113	1.126	0.8
0.250	0.1184	0.1186	0.1158	1.0	1.604	1.599	1.598	0.1	1.126	1.114	1.112	0.5
0.255	0.1282	0.1285	0.1258	0.9	1.563	1.558	1.556	0.2	1.093	1.089	1.080	0.5
0.259	0.1376	0.1379	0.1358	0.6	1.497	1.493	1.493	0.1	1.045	1.038	1.032	0.4
0.264	0.1466	0.1470	0.1450	0.5	1.416	1.410	1.410	0.2	0.982	0.974	0.971	0.4
0.269	0.1549	0.1555	0.1535	0.5	1.318	1.311	1.313	0.2	0.916	0.903	0.899	0.7
0.274	0.1627	0.1633	0.1614	0.4	1.209	1.199	1.205	0.3	0.836	0.823	0.824	0.7
0.279	0.1699	0.1705	0.1687	0.4	1.095	1.087	1.092	0.3	0.749	0.742	0.742	0.4
0.284	0.1765	0.1771	0.1751	0.4	0.980	0.973	0.977	0.2	0.667	0.654	0.663	0.8
0.288	0.1823	0.1830	0.1809	0.4	0.868	0.859	0.866	0.4	0.590	0.576	0.585	0.9
0.293	0.1874	0.1881	0.1859	0.4	0.762	0.754	0.757	0.4	0.514	0.503	0.506	0.9
0.300	0.1937	0.1946	0.1925	0.4	0.616	0.609	0.613	0.4	0.413	0.406	0.407	0.7
0.305	0.1974	0.1983	0.1960	0.4	0.530	0.524	0.527	0.4	0.355	0.348	0.353	0.8

[a] Signal levels given are those actually applied to digital data acquisition system in units of volts; data obtained with the iron system in oxalate media; applied alternating potential of 10 mv. peak-to-peak and 40 Hz.
[b] R.A.D. = relative average deviation from the mean in percentage units.

sentially identical with d.c. polarograms recorded in absence of the a.c. signal. That is, the d.c. faradaic rectification component is negligible under the experimental conditions associated with the data in Figure 1 and Table I. This was verified by both experiment and theoretical calculation which showed that the faradaic rectification component did not exceed 1–2% of the normal d.c. polarographic current and was usually much less. This contribution could be made even smaller by use of smaller amplitudes of applied alternating potential (*8, 25*).

Illustrated in Table II is the reproducibility of data obtained in experiments in which several sinusoidal potentials of differing frequency were applied to the polarographic cell and the fundamental harmonic current components at each frequency were recorded simultaneously. As shown, the reproducibility was found to be quite satisfactory. Tests also showed that the application of several simultaneous alternating potentials of different frequencies caused insignificant (<0.1%) perturbation of the current measurements at one particular frequency. Other experiments in which both fundamental and second harmonic a.c. components were recorded simultaneously also supported the feasibility of multichannel digital data acquisition.

Figure 3 shows analog polarograms of the total and resistive components of the fundamental harmonic a.c. polarographic current which were produced by the Model 565 digital incremental plotter from digital data provided by the instrumentation. In general, the quality of these analog polarograms is comparable with those obtained by on-line analog data acquisition. However, noise levels are somewhat larger than normal on the side of the polarogram corresponding to more negative potentials. This is attributable to the previously-mentioned fact that the Vidar Model 500 digital voltmeter provides only three significant digits of data for signals having values between 200 and

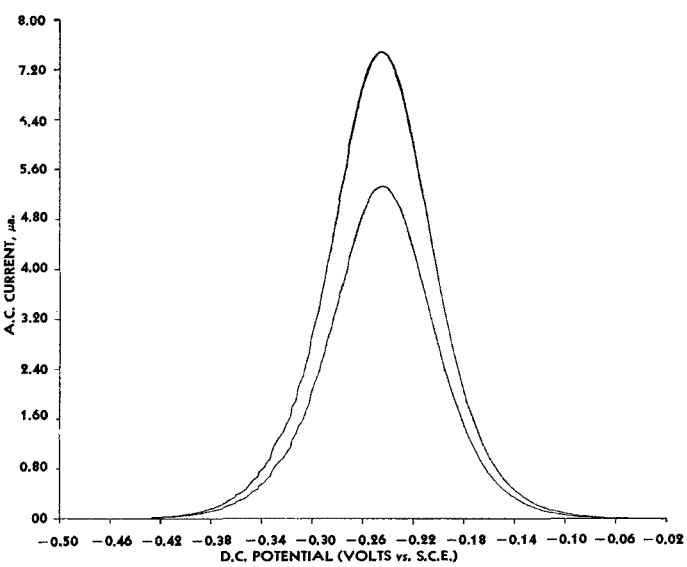

Figure 3. Analog plots of digital data obtained with the aid of the digital incremental plotter

System: 2.0 × 10^{-3}M Fe(III) in 0.50M $K_2C_2O_4$

Applied: 40.0 Hz, 10 mv. peak-to-peak sine wave; d.c. scan rate of 50 mv. per minute

Measured: Total 40.0 Hz faradaic current signal (upper polarogram), and resistive component of 40.0 Hz faradaic current signal (lower polarogram); same ordinate scale applicable to each polarogram

999 on any given range. Thus, at the positive portion of the wave, the DVM is operating on the 100-mv. full scale range and the least significant digit represents tenths of millivolts. This is the situation until the d.c. potential exceeds 0.200 volt, where the DVM switches to the 1-volt full-scale range and the least significant digit is moved to the millivolt level. The resulting uncertainty of ±1 mv. appears to be responsible for the increase in noise level at more negative potentials. Obviously, this problem could be eliminated by employing a DVM of at least four digit readout capability for all signal levels. It should be noted that this ±1-mv. uncertainty originating in the DVM will usually represent the worst case with the DVM employed in this work because the value of the d.c. potential signal (output of the ramp generator) will seldom reach the 2-volt level where the system switches to the 10-volt range, particularly when non-zero initial voltages are employed.

It was found that the IBM card punch was a rather notorious electrical noise generator, a result which was anticipated. Despite precautions such as placing the card punch in a location well removed from the main electrochemical instrument, using careful grounding practices, etc., noise spikes of significant magnitude were observed at the output of the potentiostat amplifiers whenever the card punch was in operation. Observed at the output of the follower amplifier, the noise spikes averaged 10–30 mv. in amplitude with a half-width of approximately 100 μseconds. This source of noise, presumably associated with the energizing and de-energizing of the punch solenoids, did not significantly influence less sensitive components such as tuned

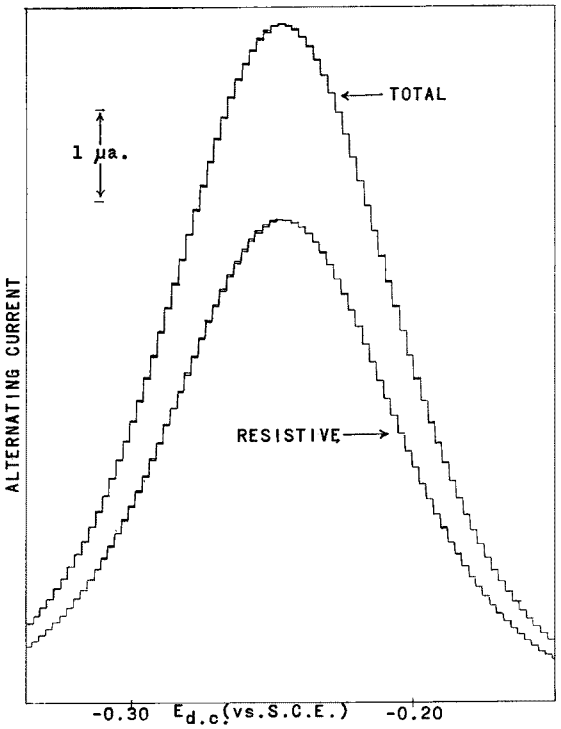

Figure 4. Analog plots of instrument readout obtained with X-YY' plotter while digital data acquisition system was in operation

System: 2.0×10^{-3}M Fe(III) in 0.50M $K_2C_2O_4$

Applied: 40.0 Hz, 10 mv. peak-to-peak sine wave; d.c. scan rate of 50 mv. per minute

Measured: Two duplicate polarograms each of the total 40.0 Hz faradaic current signal and the resistive component of 40.0 Hz faradaic current signal; same ordinate scale applicable to each polarogram

Table II. Reproducibility in Simultaneous Readout of Total Fundamental Harmonic A.C. Polarographic Current at Three Frequencies[a]

D.C. potential	Total fundamental harmonic at 40 Hz			Total fundamental harmonic at 100 Hz			Total fundamental harmonic at 150 Hz		
	Run 1	Run 2	R.A.D.[b]	Run 1	Run 2	R.A.D.[b]	Run 1	Run 2	R.A.D.[b]
0.220	0.604	0.607	0.2	0.933	0.938	0.3	1.196	1.201	0.2
0.224	0.644	0.640	0.3	0.992	0.986	0.3	1.273	1.263	0.4
0.230	0.676	0.677	0.1	1.045	1.042	0.1	1.341	1.335	0.2
0.235	0.698	0.697	0.1	1.075	1.072	0.1	1.375	1.373	0.1
0.239	0.713	0.713	0.0	1.093	1.092	0.0	1.400	1.402	0.1
0.244	0.715	0.716	0.1	1.097	1.097	0.0	1.405	1.402	0.1
0.249	0.708	0.710	0.1	1.084	1.087	0.1	1.388	1.389	0.0
0.254	0.690	0.691	0.1	1.055	1.056	0.0	1.349	1.354	0.1
0.259	0.664	0.666	0.2	1.012	1.015	0.1	1.294	1.298	0.2
0.264	0.630	0.633	0.2	0.959	0.963	0.2	1.225	1.230	0.2
0.269	0.592	0.593	0.1	0.898	0.902	0.2	1.146	1.153	0.3

[a] Signal levels given are those actually applied to digital data acquisition system in units of volts; data obtained with the iron system in oxalate media; applied alternating potentials of 10 mv. peak-to-peak.
[b] R.A.D. = relative average deviation from the mean in per cent units.

amplifiers, recorders, sampling circuits, etc. However, it was apparent that these voltage spikes were being applied to the polarographic cells and that a perturbation of the electrode process could result. Fortunately, the sample-and-hold readout mode employed in these measurements apparently negated any possibility of such a perturbation influencing the recorded data. As stated above, sampling of the current and voltage signals occurred a few seconds (at least 2 seconds) after the card punch had ceased recording data from the previous sample. In the time between termination of the card punch operation and the sampling step, any perturbation of the faradaic process due to the noise spikes apparently had decayed to a negligible level. This was suggested by the fact that analog recordings of polarograms obtained with and without the DDAS in simultaneous operation were essentially identical. Figure 4 shows two replicate analog recordings in which both total and resistive components of the a.c. polarographic currents were recorded while the DDAS was in operation. The excellent reproducibility of both signal components measured in the two runs and the general lack of noisy performance—e.g., bad readings on individual drops—attests to the fact that the noise generated by the card punch did not influence data quality in this work. However, situations may arise when readout must be carried out during or very shortly after the measurement step. The noise spikes would be intolerable in such situations, but they could be greatly reduced by employing suitable line filters and/or shielding the card punch. Connecting diodes across the punch solenoids may also be effective.

While the foregoing discussion of experimental results is directly relevant to reproducibility of data obtained in digital readout, more careful inspection of the data suggested that accuracy was of corresponding order. Quantitative aspects of the digital data obtained with the iron system were consistent with expectations for a reversible system and with previous experimental results (*9*, *21*, *27*, *29*). Dummy cell measurements also indicated a degree of accuracy similar to that observed in analog readout with the same electrochemical instrument (*9*).

These experimental data indicate that the instrument described can perform with the accuracy and precision demanded in voltammetric measurements, while providing at the same time the convenience and efficiency associated with multichannel digital data acquisition and digital data processing. It is satisfying to note that this was achieved by combining a group of techniques which are well known in electrochemical methodology (operational amplifier potential control and signal conditioning circuitry, sample-and-hold readout, electromechanical control of mercury drop life, etc.) with a commercial digital data acquisition system of conventional design. While the instrument described here is suited only to experiments involving relatively long times, digital readout in experiments of short duration (approximately 1 msecond or longer) requires one additional piece of equipment, a high-speed digital memory of modest capacity (500–1000 words) with an accompanying analog-to-digital convertor to acquire and store data in a digital form for subsequent low-speed presentation to slower readout devices such as the card punch. Combinations of analog-to-digital converters and digital memory units are commercially available in the form of the widely used signal averaging computers. The latter application is presently under investigation in these laboratories.

ACKNOWLEDGMENT

The authors are indebted to T. G. McCord for the preparation of computer programs necessary for use of the digital incremental plotter.

LITERATURE CITED

(1) Balchin, L. A., Williams, D. I., *Analyst* **85**, 503 (1960).
(2) Bauer, H. H., *J. Electroanal. Chem.* **1**, 256 (1960).
(3) Bauer, H. H., Elving, P. J., *Australian J. Chem.* **12**, 335 (1959).
(4) Bauer, H. H., Elving, P. J., ANAL. CHEM. **30**, 341 (1958).
(5) Booman, G. L., *Ibid.*, **38**, 1141 (1966).
(6) Booman, G. L., Holbrook, W. B., *Ibid.*, **35**, 1793 (1963).
(7) Breiter, M. W., *J. Electrochem. Soc.* **112**, 845 (1965).
(8) Breyer, B., Bauer, H. H., in "Chemical Analysis," P. J. Elving and I. M. Kolthoff, eds., Vol. **13**, Interscience, New York, 1963.
(9) Brown, E. R., McCord, T. G., Smith, D. E., DeFord, D. D., ANAL. CHEM. **38**, 1119 (1966).
(10) Ferrett, D. J., Milner, G. W. C., Shalgosky, H. I., Slee, L. J., *Analyst* **81**, 506 (1956).
(11) Flynn, G. J., *Electronics* **37**, 58 (May 18, 1964).
(12) Hayes, J. W., Bauer, H. H., *J. Electroanal. Chem.* **3**, 336 (1962).
(13) Herman, H. B., Division of Analytical Chemistry, 150th Meeting, ACS, Phoenix, January 1966.
(14) Herman, H. B., Bard, A. J., ANAL. CHEM. **35**, 1121 (1963).
(15) *Ibid.*, **37**, 590 (1965).
(16) International Business Machines Corp., "526 Printing Summary Punch," IBM Corp., Poughkeepsie, New York, 1959.
(17) Kelley, M. T., Fisher, D. J., Jones, H. C., ANAL. CHEM. **31**, 1475 (1959); **32**, 1262 (1960).
(18) Lauer, G., Osteryoung, R. A., *Ibid.*, **38**, 1137 (1966).
(19) Neeb, R., *Z. Anal. Chem.* **188**, 401 (1962).
(20) Paynter, J., Ph.D. Thesis, Columbia Univ., New York, 1964.
(21) Randles, J. E. B., Somerton, K. W., *Trans. Faraday Soc.* **48**, 937 (1952).
(22) Reilley, C. N., *J. Chem. Educ.* **39**, A853 and A933 (1962).
(23) Schmidt, H., Stackelberg, M. von, *J. Electroanal. Chem.* **1**, 133 (1959).
(24) Schwarz, W. M., Shain, I., ANAL. CHEM. **35**, 1770 (1963).
(25) Smith, D. E., in "Electroanalytical Chemistry," A. J. Bard, ed., Vol. **1**, Chap. 1, M. Dekker, Inc., New York, in press.
(26) Smith, D. E., ANAL. CHEM. **35**, 1811 (1963).
(27) Smith, D. E., Reinmuth, W. H., *Ibid.*, **33**, 482 (1961).
(28) Takahashi, T., Niki, E., *Talanta* **1**, 245 (1958).
(29) Underkofler, W. L., Shain, I., ANAL. CHEM. **37**, 218 (1965).
(30) Vidar Corporation, "Vidar 1025012 10-Channel Digital Data Acquisition System," Vidar Corp., Mountain View, Calif., 1966.

RECEIVED for review April 7, 1966. Accepted June 20, 1966. Presented in part at the Division of Analytical Chemistry, 150th Meeting, ACS, Phoenix, Ariz., January 1966. Work supported in part by a National Science Foundation Cooperative Fellowship (E.R.B., 1964–65) and by National Science Foundation Grant GP-3484.

Use of a Multichannel Analyzer as a Data Acquisition System in Electrochemistry

GEORGE LAUER and R. A. OSTERYOUNG

North American Aviation Science Center, Thousand Oaks, Calif. 91360

▷ **The use of a multichannel analyzer as a data acquisition system in electrochemical studies is described with particular reference to chronocoulometric studies. Interface equipment used to co-ordinate chronocoulometric potential pulses with the analyzer's timed sequential operations is described. Use of a voltage-to-frequency converter and the internal analyzer analog-to-digital converter is described. With a fixed voltage input into the voltage-to-frequency converter, the number of counts recorded decreases as the sampling rate increases. With the internal converter, the number of counts recorded with a constant voltage input is independent of the sampling rate up to a limit depending on the conversion time. Use of this system increases both the rapidity and accuracy with which data may be acquired compared to photographing an oscilloscope face.**

In many electrochemical experimental measurements, a variable (voltage, current, charge) is examined as a function of time. If the rate of change of the variable with time is rapid, an oscilloscope is generally employed to observe the variable, with the Y-axis conventionally being used for the variable, and the X-axis being a time axis as supplied by the oscilloscope time base. A photograph of the transient is obtained and the data are taken from the picture (either Polaroid or an enlargement of 35 mm. film). Lack of precision and tedium are obvious disadvantages to this method. The use of equipment possessing digital readout capability offers numerous advantages in accuracy and ease of data handling. We will discuss here the use of a multichannel analyzer as a data-acquisition system with particular reference to its use in chronocoulometric studies. It will not be the purpose of this paper to go into the detail of multichannel analyzer operation, but sufficient material will be given to facilitate appreciation and application to other than the specific analyzer used here. Consideration is given only to operation of the instrument in a time mode (rather than pulse height analyzer mode), in which case it is serving essentially as a memory oscilloscope with digital readout capability.

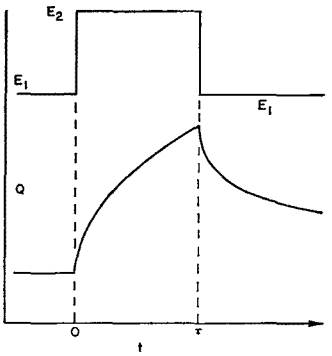

Figure 1. *E–t* and *Q–t* wave forms in double potential step chronocoulometry

To initiate the discussion, consider how a chronopotentiometric curve could be recorded on an analyzer.

A switch is closed, which results in application of a constant current to an electrochemical cell, and generation of a triggering pulse which is applied to a time-base generator. The output of this time-base generator is a series of pulses at regularly timed intervals, say 0.01 second. The chronopotentiometric potential change is measured with a high input impedance amplifier and applied to the input of a voltage-to-frequency converter (*V-F-C*). This instrument has a sinusoidal output of fixed amplitude whose frequency is directly proportional to the input potential. The output of the *V-F-C* is input to the analyzer, which may be regarded initially as a group of data scalers counting the sine wave input pulses from the *V-F-C*. Thus, for a fixed time interval, determined by the time-base generator, the analyzer counts a sine-wave whose frequency is determined by the reference-indicator electrode potential variation. An output pulse from the time-base generator, however, causes the analyzer to switch from one scaler or channel to another after the predetermined time period, in this case 0.01 second. The input from the *V-F-C* is thus averaged over the channel time period. However, before switching to another channel, the information contained in the initial channel (consisting of the number of sine-wave pulses received from the *V-F-C* in 0.01 second) is stored in the memory of the analyzer. In the case of a 400-channel analyzer and the 0.01-second time interval referred to above, 400 data points covering a 4-second time interval can be obtained. When the last channel has data written into it, the experiment is terminated and the data contained in the memory may be read out as digital information on suitable readout devices such as a typewriter or punched tape. With most analyzers, provision exists to observe the data stored in the memory as an oscilloscope trace, which is synthesized by rapid and repetitive interrogation of the analyzer memory.

APPLICATION TO DOUBLE POTENTIAL-STEP CHRONOCOULOMETRY

The main portion of this paper is devoted to a discussion of the use of a Radiation Instrument Development Laboratory (Melrose Park, Ill.) Model 34-12B multichannel analyzer as a recording device in chronocoulometric studies (*1, 2, 5, 6*). Detail of peripheral equipment which takes advantage of the capabilities inherent in the analyzer will be given.

In chronocoulometry, a potential step is applied to the electrode and the coulomb-time behavior is followed (*3, 5, 6*). Starting at a potential E_1 in a solution containing only Ox, a potential step is applied to the electrode, where the reaction at E_2

$$\mathrm{Ox} + \mathrm{ne} \rightleftarrows \mathrm{Red\ (Hg)}$$

$$E = E_2,\ t < \tau \quad (1)$$

takes place, then at a time τ stepped back to E_1 where the oxidation of Red from the amalgam takes place. Figure 1 shows the *E-t* and *Q-t* behavior expected (*1, 2, 4, 6*).

Figure 2 is a block diagram of the apparatus used. Referring to the block diagram of Figure 2, the experiment is initiated by a push button on the control box. The push button starts a sequence which:

a) provides a pulse to initiate the oscillator of the time base generator,

b) unshorts the capacitor on the operational amplifier used as an integrator,

c) receives and blocks the time-base generator pulses until after the integrator is unshorted, then

d) simultaneously supplies a voltage step into the potentiostat and permits

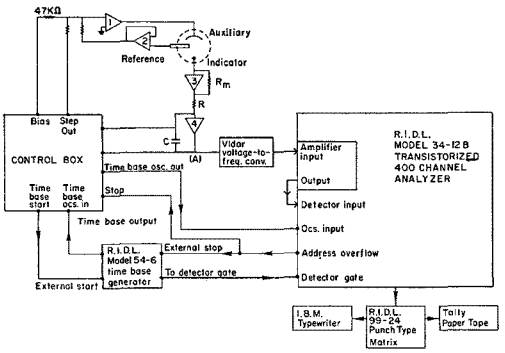

Figure 2. Block diagram of apparatus used in double potential step chronocoulometric studies

Amplifier 1 is a Wenking fast-rise potentiostat, amplifier 2 is a Philbrick P75, and amplifiers 3 and 4 are Philbrick SP656's. The R.I.D.L. 99-24 Punch type Matrix and Model 54-6 Time Base Generator are contained in a Model 29-1B instrument case and power supply. An inverting amplifier may be placed at point (A) if the voltage-to-frequency converter is unipolar and input would have wrong polarity. The Control Box detail is given in Figure 7 and is discussed in detail in the Appendix

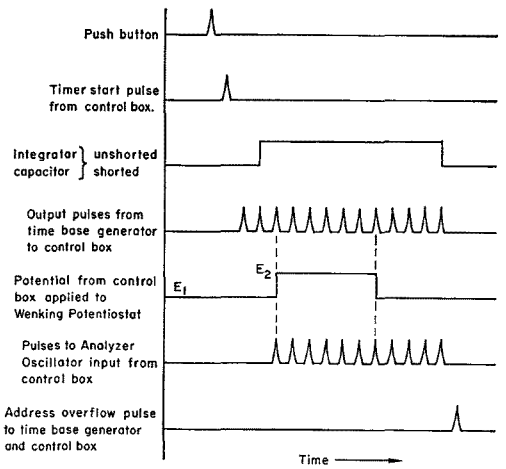

Figure 3. Sequence of control pulses and potentials as initiated by push button in control box

In this example, pulse counting circuit on control box set to remove potential step after 7 pulses (see text)

the channel advance pulses from the time base generator to pass into the Oscillator Input of the analyzer.

There is no channel advance until the first pulse from the time base generator has passed through the control box and then to the Oscillator Input of the analyzer. Channel zero will contain a number of counts corresponding to random noise generated by the system. The control box then counts the pulses from the time base generator and, after a given number of pulses, removes the potential step, bringing the applied potential from E_2 to E_1. The sequence of events is indicated in Figure 3. The output of the *V-F-C* is counted in the interval between the time base pulses. The *V-F-C* output is fed into the internal amplifier of the analyzer, and the output of this amplifier is then fed into the Detector Input of the analyzer. The pulses from the *V-F-C* at the Detector Input will pass into the analyzer and be counted unless a blocking pulse is applied at the Detector Gate Input.

When a pulse is delivered to the Oscillator Input of the analyzer, providing for channel advance, the signal at the Detector Input is blocked. The following sequence of events then occurs in the analyzer:

1) a signal is generated which causes the contents of the data scaler to be written into the part of the core-memory which corresponds to a given address or channel, say channel N,

2) the data scaler is then reset to clear it of the accumulated data,

3) an internally generated address advance pulse causes the address scaler to select that portion of the core-memory corresponding to channel $N + 1$,

4) the contents of the memory in channel $N + 1$ are then read into the data scaler,

5) the blocking pulse is removed from the Detector Gate, permitting the accumulation of data into the data scaler at channel $N + 1$.

(In the present case, the core was reset to zero in all channels in which data were to be recorded prior to running an experiment.) The time during which the analyzer is unable to accept input is its dead time and is generally a fixed interval of 12.5 μsec. controlled by the time-base generator disabling pulse at the Detector Gate Input. (The dead time has no effect on the accuracy of the experiment with either analog-to-digital converter used, since with the *V-F-C* the time interval during which data is being input is known precisely and with the internal analog-to-digital converter (see below) the time when the input is sampled, as well as the interval between samplings, is precisely known.) Figure 4 indicates, in block diagram form, the circuits involved, while the events taking place are indicated in Figures 5A, B, and C.

In the R.I.D.L. unit employed, storage may be carried out in 100, 200, or all 400 channels. At the end of the selected storage interval, after data have been input into the last channel, a completion or address overflow pulse is generated by the analyzer. This pulse cuts off the time-base generator and is applied to the control box, where it causes the integrator to be shorted, resets the circuit which counts the time-base generator pulses, and deactivates the box.

A detailed schematic of the box is given in Figure 7, and operation is discussed in the appendix.

The use of the analyzer in this manner has certain advantages and disadvantages. On the plus side is the fact that no modification of the analyzer is required. While impossible to generalize to other units, it is likely that most analyzers can be used in this manner. However, different designs (logic and interfacing) may present problems of vastly differing magnitude. Although the R.I.D.L. unit with typewriter and tape readout employed here costs about $15,000, other less sophisticated units are available at a cost not too much greater than a good oscilloscope. Converting the unit from a data acquisition mode of operation back to its pulse height analyzer mode is rapidly and easily accomplished.

One of the major advantages of using a voltage-to-frequency converter, rather than the internal analog-to-digital conversion procedure discussed below, is the great increase in precision obtainable when the signal is a slowly varying potential. Any random noise is averaged out over the time period sampled; a minor drawback previously mentioned is that in effect one averages over the time period between time-base generator pulses. However, a more serious problem involves the sensitivity of the *V-F-C*.

Typically, a current measuring resistor, R_m, of 100 ohms was used, and the integrator had an RC constant of, say, 10^{-4} sec. The *V-F-C* used had 1 megacycle output at 10 volts input. Thus, a current, I, of one microampere flowing across the 100-ohm resistor for one second, a microcoulomb, resulted in a final voltage output from the integrator of

$$E_{out} = \frac{I \times R_m \times t}{RC} = \frac{1 \times 10^{-6} \times 10^{2} \times 1}{10^{-4}} = 1.0 \text{ volt}$$

This resulted in a frequency output of $\frac{1.0}{10.0} \times 10^6 = 10^5$ cycles/sec. from the *V-F-C*. If the time-base generator was set at 400 microseconds—i.e., it gen-

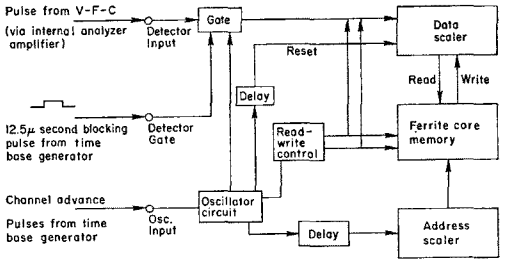

Figure 4. Block diagram of analyzer circuitry in Time-Mode of operation

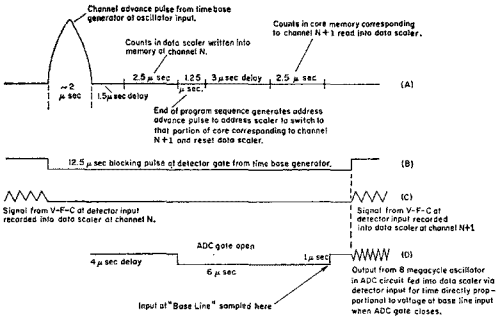

Figure 5. Sequence of events triggered by channel advance pulse from time-base generator at Oscillator Input of analyzer.

erated a channel advance pulse every 400 microseconds—then a microcoulomb corresponded to

$$400 \times 10^{-6} \times 10^{6} =$$

40 counts/microcoulomb

since each cycle input is recorded as one count by the analyzer. If the time-base generator was operating at 800 microseconds per channel advance pulse, then 80 counts equalled one microcoulomb.

In a chronocoulometric experiment with an electrode area of about 0.03 cm.^{2}, with the time-base generator set at 400 microseconds and a τ of about 25 milliseconds, 1–2 microcoulombs of charge from diffusing material will have passed at τ for a solution 1 millimolar in electroactive species. This means that, with the values for R_m, R, and C given above, one would obtain 40–80 counts at $t = \tau$. At 25 milliseconds after the potential step is applied, the faradaic current is of the order 25–50 microamperes, which means a change of only 1–2 counts every 2–3 channels. Clearly, sufficient counts must be obtained in the interval $0 < t \leq \tau$ to permit analyzing the data. If the time-base generator were operating at 200 microseconds and τ were maintained at about 25 milliseconds, only 20–40 counts would be obtained at $t = \tau$.

Although some increase in sensitivity could be obtained by varying the measuring resistor, R_m, and the RC time constant of the integrator, it was not possible to obtain sufficient counts with the time-base generator operating faster than 200 microseconds. In the step experiments, R_m is limited because the initial current which flows, largely double layer charging current, may be of the order 20–60 milliamperes and the maximum voltage output of the current-measuring amplifier is ±10–12 volts.

USE OF INTERNAL ANALOG-TO-DIGITAL CONVERTER

An alternate method of analog-to-digital conversion was also used. The analyzer contains an internal Analog-to-Digital Converter (*A-D-C*) which may be used to convert an analog voltage input into pulses which can be counted by the data scaler. In the R.I.D.L. unit, conversion is accomplished by feeding the voltage into a control or Linear Gate of the *A-D-C*. This gate permits generation of an 8-megacycle pulse train for a *time directly proportional* to the *level of the input voltage*.

This 8-megacycle signal is generated and divided down from a 16-megacycle crystal oscillator and is extremely stable. In operation, the output from the integrator (or any other voltage source) is applied to what is called the Base Line input. This input point is directly in front of the Linear Gate which controls the *time* during which the 8-megacycle signal is output from the *A-D-C*. The pulses from the time-base generator are fed through the control box into the analyzer Oscillator Input, as before, providing channel advance pulses, and are also fed into the Short Time Constant input of the analog-to-digital converter. The pulse at this input provides an enabling or strobe pulse, causing the linear gate to examine the voltage at the Base Line input and subsequently controls the 8-megacycle signal at the Detector Input which is fed into the data scaler for a time proportional to the voltage at the Base Line input; this is the conversion cycle. The sequence of events is indicated in Figure 5A, B, and D. Linearity of input voltage to output counts is shown in Figure 6. With our instrument, for example, voltage into the Base Line input resulted in a straight line of the form

$$\text{Counts} = 73 + 474 \times \text{voltage input}$$

That is, 0 volts resulted in 73 counts. Correction for this could easily be made. This sensitivity corresponds to about ±2 millivolt resolution. Provided the conversion time,

$$\frac{\text{voltage input} \times (474 + 73)}{8 \times 10^{6}}$$

is *less* than the time-base generator period, the counts/volt is *independent* of the time-base generator setting. This was not the case when the voltage-to-frequency converter input was used. In short, the internal *A-D-C* provides an order of magnitude, or better, increase in sensitivity as compared to using the *V-F-C*.

DISCUSSION

As shown in Figure 2 suitable readout equipment such as punched tape or typewriter may be employed. The advantages of obtaining digital readout in chronocoulometric adsorption or kinetic studies cannot be overstressed. Accuracy is greater than can be attained by photographic methods; ease of obtaining data is increased to such an extent that experiments are possible which were heretofore prevented largely by the length of time spent in obtaining photographs and taking data from them. The data acquisition system described here has been used in chronocoulometric studies of adsorption and kinetics (*2*, *6–8*); it is doubtful if the detail of these studies would have been possible without this equipment.

This paper is intended as an introduction to the use of multichannel analyzers to data acquisition in electrochemical studies. Applications to other work where a signal may be converted to a voltage are obvious.

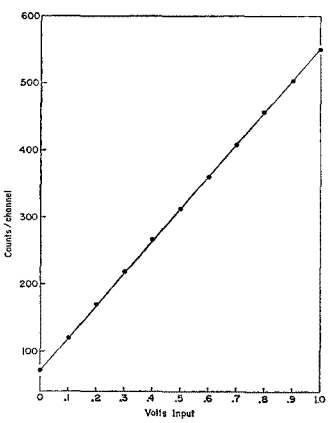

Figure 6. Counts per channel vs. input voltage—internal analog-to-digital converter with 8-megacycle pulse train

Other more or less sophisticated acquisition systems may be devised, depending only on the finances and ingenuity of the experimentalist. The use of computer-type systems, which include not only acquisitional but computational capability, may be predicted. Nevertheless, the analyzer system used in this work possesses a larger degree of versatility than one might guess at first glance. While a certain amount of "interfacing," as exemplified by the control-box, is required, it is the authors' contention that a multichannel analyzer offers a large return in capability and flexibility per dollar of investment.

ACKNOWLEDGMENT

The aid of Helmar Schlein in designing portions of the control box circuitry is appreciated. The helpfulness of John Brandt and Don Frank of R.I.D.L. is appreciated. Helpful and occasionally argumentative discussions with F. C. Anson also contributed to this work.

APPENDIX

Control Box Operation. The control box is constructed largely from Engineered Electronics Co. (Santa Ana, Calif.) units. The push-button at the extreme left of Figure 7 initiates the experiment, supplying a pulse to start the time-base generator and operating the relay which unshorts the capacitor across the integrator, and removes a −15-volt blocking input at plug-in 21, an "and" gate. The output from the time-base oscillator is applied at the second input of the "and" gate. This procedure prevents passage of these pulses until the integrator is unshorted. The time-base generator pulses are then delivered a) via pin 7 of plug-in 5 to the analyzer Oscillator Input, where it supplies channel advance pulses, b) via pin 8 of plug-in 5, to pin 5 of plug-in 8, and c) pin 4 of the binary counting circuit, comprised of plug-ins 11–19. (Note that this circuit is pre-set by depressing the push-button which starts the experiment.) The output from pin 7 of plug-in 8 supplies the pulse to trigger the potential step, via plug-ins 9 and 10 and the diode network at their right. The diode network permits obtaining positive or negative going potential pulses and further clamps the base line of the pulses to about 0 volt. This is necessary because the potential pulse is applied about the pre-set bias voltage obtained from the potentiometer at top right. The pulse at pin 5 of plug-in 9 results in a level shift from 0 to 8 volts across the 100K potentiometer at

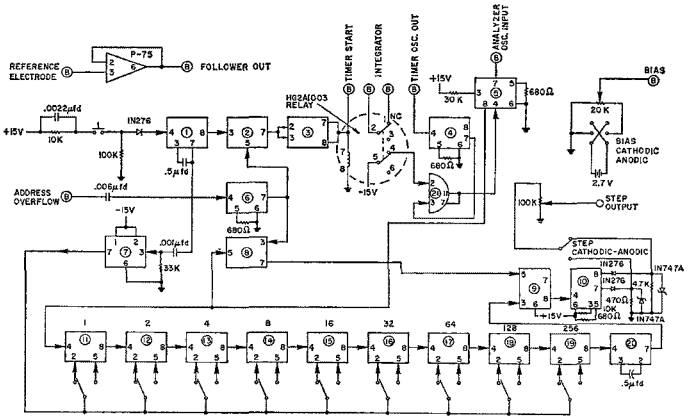

Figure 7. Control unit for application of double potential step and channel control of R.I.D.L. Analyzer

Plug-In No.

1, 20	T-166, One shot (single pulse generator)
2, 8, 9	T-103, Set-Reset Flip Flop
3	T-1102, Relay Driver
4, 5, 6, 10	T-1103, Shaper
7	T-109, Reset Generator
11–19	Modified T-101B, triggered reset Flip Flop (pin 5 shorted to junction of C6 and R10 internal of units).
2	T-641, DC logic—"and" gate

Above units are plug-ins manufactured by Engineering Electronics Co., Santa Ana, Calif. Relay is Clare HG 2A1003. Philbrick P75 amplifier serves as follower and is located on control box. Harrison Lab Power Supplies used to supply regulated ±15 volts. (B) Indicates B.N.C. connectors

the output of the diode network; the level of the pulse may be adjusted by the potentiometer control. An input pulse at pin 3 of plug-in 9 will return the output of the diode network to 0 volt. This output will be supplied via the binary counting circuit and its output, plug-ins 11–20. The counting circuit counts the time-base generator pulses, which are fed to it from pin 8 of plug-in 5. The number of counts which will result in an output from the logic circuit, removing the potential step, may be set by positioning the toggle switches shown. In the chronocoulometric work discussed elsewhere (*2*, *6*), reversal was held at channel 64, regardless of the time-base generator setting. The address overflow pulse from the analyzer, which signals that all the channels have had data input, terminated the experiment. Via plug-in 6, the overflow pulse serves to inactivate the relay, short the integrator, and the input at pin 3 of plug-in 8 resets it.

The result of all this is that

a) the integrator is opened before the potential step is applied,

b) no channel advance pulse is supplied to the analyzer until the integrator is opened,

c) the potential step rise is *exactly* synchronized to the first channel advance pulse reaching the analyzer and its removal is synchronized to any given channel advance pulse from the time-base generator as set in the logic circuit.

LITERATURE CITED

(1) Anson, F. C., ANAL. CHEM. **38**, 54 (1965).
(2) Anson, F. C., Christie, J. H., Osteryoung, R. A., *J. Electroanal. Chem.*, in press (1966).
(3) Anson, F. C., Payne, D. A., *J. Electroanal. Chem.*, in press (1966).
(4) Christie, J. H., *J. Electroanal. Chem.*, in press (1966).
(5) Christie, J. H., Lauer, G., Osteryoung, R. A., *J. Electroanal. Chem.* **7**, 60 (1964).
(6) Christie, J. H., Osteryoung, R. A., Anson, F. C., *J. Electroanal. Chem.*, in press (1966).
(7) Lauer, G., Osteryoung, R. A., paper presented at the Winter Meeting of the American Chemical Society, Phoenix, Arizona, January 1966.
(8) Lauer, G., Osteryoung, R. A., ANAL. CHEM., **39**, 1106 (1966).

RECEIVED for review March 7, 1966. Accepted April 26, 1966. Division of Analytical Chemistry, Winter Meeting, ACS, Phoenix, Ariz., January 1966.

A Digital Data Collection, Waveform Generation, and Timing Instrument for Electrochemical Measurements

GLENN L. BOOMAN[1]

Phillips Petroleum Company, Atomic Energy Division, Idaho Falls, Idaho

▶ **A digital instrument has been constructed to perform efficiently the interrelated operations of accurate timing, precise waveform generation, and automated data collection in one integrated unit. Functions such as pulse, square-wave, linear scan, linear-scan-and-hold, stair-step, and bidirectional linear-scan waveforms are obtained easily by changing prewired patchboards. With the flexibility given by patchboard control of the digital logic governing both the waveform generation and the measurement timing, the particular advantages of numerous electrochemical techniques are provided and the instrument is readily adapted to new techniques. The full information capabilities of electrochemical measurements are closely approached with the measurement time constant of 1 μsec., resolution of 0.01%, and crystal-controlled, logarithmic, multidecade, timing. Relationships between high speed data processing and rapid data collection are discussed in terms of overall objectives.**

THE INSTRUMENT COMMONLY USED for obtaining measurements at times below about one second, is the cathode ray oscilloscope. Although very useful for many types of qualitative studies and single-valued measurements, oscilloscopes are not readily adapted to precision measurements of single transients. In recent years, digital data systems have come into widespread use in applications requiring the measurement of transient phenomena. The widespread acceptance of multichannel analyzer systems in radiochemical studies is a notable example of how digital electronic systems can change an area of study.

Obtaining measurements from oscilloscope traces to evaluate current-time responses of electrochemical cells could be considered as a parallel to a radiochemist doing inadequate data collection and analysis with an oscilloscope or even a single channel analyzer, when the greater information capabilities of multichannel analysis are so firmly established. With digital instrumentation, the need to photographically record the oscilloscope trace and then tediously read, and correct for timing and amplitude non-linearities before data analysis has been overcome. In addition, the ability to collect data over five or more decades of time with a single transient, ensures consistency of the data, without the uncertainties of varying electrode surface area or changes in surface conditions. With multiple scans, measurements at shorter times and at increased sensitivity can be obtained through use of data averaging and smoothing procedures. These are easily realized with digital techniques but are either prohibitively time consuming or are not feasible by manual methods.

Requirements for an electrochemical digital data system would include versatility of timing sequences to allow use with diverse measurement techniques, rapid response to obtain data over at least five decades of time, and high resolution to provide sufficient dynamic range without complex gain switching for measuring diffusion controlled signals which normally decrease according to the $t^{-1/2}$ function. High precision measurements are especially important in kinetic rate studies, as a 1% uncertainty in current or time measurements can mean as much as 10% uncertainty in rate constant. A number of these requirements are met in unique fashion by special purpose, electrochemical, digital data collection instruments (*2*, *3*, *8*) and by commercially available digital data systems. However, a unified consideration of the overall electrochemical measurement problem, in terms of the capabilities of digital instrumentation, has not been presented.

With the wide range of digital devices available, it was possible to design an instrument meeting these system requirements without undue compromise. Almost no circuit wiring at the device level is needed as digital modules such as analog-to-digital converters and magnetic core memories are available as subsystem components.

Waveform generation of the type and flexibility required by electrochemical studies has been a continuing problem as indicated by the numerous publications (*4*, *11*, *12*). Instrumentation has recently become available (Representative examples: Hewlett-Packard Co., Palo Alto, Calif., Function Generator Model 3300A; Exact Electronics, Inc., Hillsboro, Oregon, Series 300 Function Generators; Wavetek, San Diego, Calif., Series 100 Function Generators), which is suitable for a number of applications. To overcome the limitations of waveform stability in devices using on-off switching of active devices and of restricted waveshape programming abilities, the digital approach was extended to waveform generation by including a highly accurate digital-to-analog converter module with the controlling signals obtained from the circuits already required for measurement programming.

Because functional planning of an instrumentation system is of primary importance, the design fundamentals and necessary interrelationships of the digital subsystems are stressed. Detailed implementation of the circuitry has been omitted, as the particular modular devices used for the system described have no outstanding qualification over similar devices of other manufacture, the implementation of digital logic hardware is presently a rapidly changing field, and choice of components will be influenced by the particular interests of the investigator along with the economic considerations which argue against universality.

Data interpretation, being inseparable from data collection, requires decisions to be made on the extent of the immediate experimental instrumentation, especially with regard to including further arithmetic capabilities in the digital system, to using directly or indirectly the abilities of a general purpose digital computer facility, and in making the data collection procedure harmonious with the data interpretation procedure. Computer techniques must then be considered as an integral facet of the complete experimental approach which a priori includes the instrumentation.

It is the purpose of this paper to show

[1] Present address, Idaho Nuclear Corp., National Reactor Testing Station, P.O. Box 1845, Idaho Falls, Idaho 83401

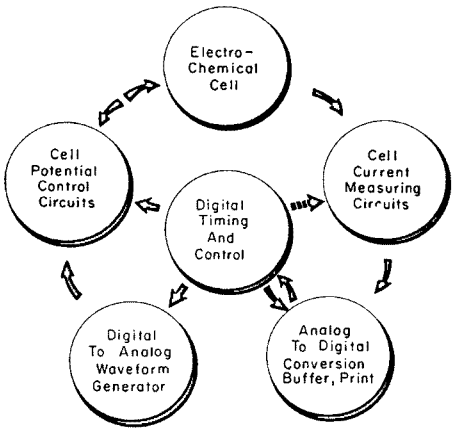

Figure 1. System configuration

the design of the digital data system in broad outline, to indicate the versatility obtained, and to attempt a definition of the overall relationship between experiment and results as influenced by high speed data systems and digital computer techniques. Definitions of digital logic terms are given in the Appendix.

INSTRUMENT DESIGN

All electrochemical measurements require knowledge of three variables, namely voltage, current, and time. Experimentally, only one of these variables is measured, as the other two are known from the externally imposed conditions. Stated in terms of instrumentation, the experimental requirements are met by the waveform generator for the input signal (driving function), a timing system, and a device for measuring the output response.

Design considerations for economical implementation of experimental measurements would indicate use of common circuitry to control the timing of both the input waveform generation and the output response measurement. Flexibility, to allow use of the equipment with the majority of the new instrumental methods and to be adaptable for future methods, is a further design requirement.

System Configuration. A complete experimental system, including the electrochemical cell, driving function control elements, timing, and output response measuring devices is outlined in Figure 1. The close interrelationships among the various components is directly evident with the principal signal paths shown. Design of the system with digital devices gives basic advantages over all-analog systems with respect to accuracy, speed, and timing. The timing is based on a crystal controlled master clock, and all control signals are obtained with the high accuracy inherent in digital count down circuits.

Data Collection. Obtaining high-speed digital presentation of the electrochemical cell voltage or current output signals overcomes previous limitations imposed by oscillographic methods and generates new capabilities in measurements of electrode responses. Figure 2 outlines typical timing sequences for data collection during the recording of a transient from a cell driven by a potential-step function.

In the sample mode, the programmed digital timing and control section puts out the signals necessary to start and to modify the driving waveform function, to sample the electrochemical output function with conversion to digital form of the analog signal held in the sample-and-hold circuit at the time of the sample command, and to store the digital numbers in the magnetic core, buffer memory unit when the conversion-complete signal is received from the analog-to-digital converter (ADC). In the readout mode, the start signal initiates transfer of the data from the core memory to the electric typewriter in the format of one measurement reading per line of printed output.

The core memory requirement is dictated by the relatively slow speed of suitable output devices such as electric typewriters, paper tape punches, and line printers. Magnetic tape, drum, or disk, and quartz delay line devices are not suitable input-output buffers because of cost and the difficulties associated with the non-predictable variations of sampling which must be left as the prerogative of the investigator.

Typewriter output gives immediate access to the experimental results, but at a relatively slow readout rate of 12 characters per second. Punched paper tape output has been included to permit computer processing of the experi-

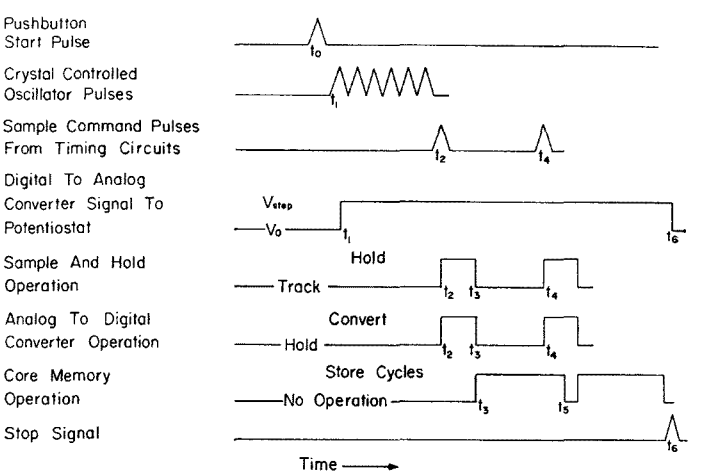

Figure 2. Timing diagram for generation of potential step, conversion of current-follower output voltage to digital form, and operation of ferrite core memory during the data collection period

A pulse from the manually operated pushbutton occurs at time t_0, the first synchronized crystal-controlled clock pulse at time t_1, the first sampling command pulse from the timing circuits at time t_2, the end of the first analog-to-digital conversion at time t_3, the second sampling command pulse at time t_4, the end of the first store-in-core-memory cycle sequence at time t_5, and the end of signal or stop pulse at time t_6. With the equipment described, t_3-t_2 is 40 μsec., t_4-t_3 is greater or equal to 10 μsec., and t_5-t_3 is 50 μsec. The sampling command pulse time sequences, t_2, t_4, etc., are set-up on the patchboard as desired and each pulse time selected is synchronous with the 1-MHz crystal-controlled oscillator

mental data without the delays and susceptibility to errors associated with manual transcription, card punching procedures. The 120 character per second speed of the paper tape punch allows data to be punched as fast as collected at measurement times greater than about 50 milliseconds after initiation of a transient. Hence many more data points can be collected, increased reliability is obtained through smoothing of random variations in the data, and multiple transients can be recorded over long time periods when the short punching time is compatible with the experimental cycle times. Again, versatility and economy result from the common timing control.

Recording of data points with less than the 50 μsec. minimum separation indicated on Figure 2 can be accomplished with sampling points interlaced on repeat transients. It is not economically practical at the present time to reduce the time between samples much below 10 μsec. even with the full scale resolution requirement reduced to 0.1 to 0.2%. Obtaining relatively few data points on each transient does not significantly lengthen the data collection time for most experiments because the permissable repetition rate increases as the length of the transient decreases. Repetitive waveform sampling is the accepted method of measurement in the nanosecond region.

Waveform Generation. Digital-to-analog conversion for generation of the driving functions is done easily because of the ready access to the digital timing circuits. A completely general function generator of high accuracy is thus available without wasteful duplication of timing control circuits in the subsystem components and at a cost which is less than most commercial waveform generators. The amplitude precision of 0.01% of full scale given within 2 μsec. by the digital-to-analog converter (DAC) module is a distinct advantage in low-level and fast-response studies. For example, the noise produced at a frequency of 1 KHz. by a 0.1% noise component on a 0.5-volt pulse amounts to an equivalent cell current of 3 μa. when applied to an electrode having a nominal double layer capacity of 1 μf. The more usual random fluctuations in the output levels of conventional waveform generators produce a random noise interference of similar nature. Use of only carefully matched diodes and precision resistors ensures the accuracy and stability of the current switches. The digital-to-analog converter technique is directly applicable to all types of step, multi-pulse, square-wave, and stair-step functions with both amplitude and sequencing available in nearly unlimited combinations. Waveforms such as ramps, ramp-and-hold, pulse with back scan, and triangular wave functions can be approximated closely through use of numerous small steps to synthesize the ramp components. Step output from the DAC can be used as input to an analog integrator for applications requiring continuous, high accuracy, ramp functions, and for the generation of functions approximating logarithmic or $t^{-1/2}$ responses. The DAC output is a current whose magnitude and direction represent the magnitude and sign, respectively, of the coded digital input. Use with operational amplifiers is convenient, as the virtual ground provided by a summing point connection provides the correct termination. The high precision reference voltages required by the DAC module are available from the analog-to-digital converter (ADC) power supply regulator. The DAC module used in the waveform generator is identical to the module used in the ADC for the two most significant decades, thus keeping the number of different modules at a minimum and permitting interchange of modules for performance checking, besides giving the economy of common use of high accuracy power supplies. Although sine-wave functions were not a primary consideration, precise timing and phase relationships can be derived by nonlinear shaping of digitally generated triangular waves as has been shown by the incorporation of this method in a recent function generator design (*6*). Application of the signal to the electrochemical cell in the form of controlled voltage, current, or charge functions is accomplished with the commonly used operational amplifier circuitry performing the necessary current-voltage transformations and enforcing the desired conditions at the measuring electrode.

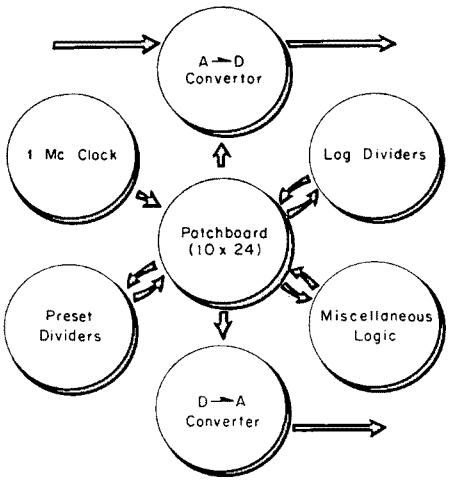

Figure 3. Patchboard functions

For stair-step function generation, the basic digital control element is a 2-decade reversible counter. A flip-flop register gate placed between the reversible counter and the digital-to-analog converter permits considerable freedom in output signal waveform selection, with only the desired counter states gated to the DAC control lines. This allows generation of non-uniform waveshapes and scaling of signals by digital logic control. The DAC resolution of 100 steps positive and 100 steps negative is more than adequate giving 5 millivolts per step with a 1-volt scan, and of course higher resolution within lesser scan regions.

Patchboard Control. Versatility is inherent in a digital system, with relatively few basic types of digital logic elements required to synthesize complex system functions. Patchboard programming of the digital timing and logic used throughout the instrument provided this versatility. The patchboard functions are shown in Figure 3. A measurement is initiated by a front-panel, push button control which gates the 1-MHz clock to the patchboard. The start time, t_1 in Figure 2, is synchronized with the 60-Hz. power line frequency to allow coherent subtraction of this component if necessary. From the patchboard, the gated clock signal can be routed through any combination of six decade dividers and six preset dividers which allow separate front panel control of any input signal division between 1 and 99 with continuous recycling by the same ratio. A logarithmic pulse divider circuit is provided which has 25 discrete time signals brought to the patchboard for the timing program. This same series of time signals is repeated for each decade recorded, hence giving uniform

data density per decade and the simplicity of standard time intervals. Although a resolution of 10 points per decade is usually sufficient, sampling can also be done on a linear basis to as high a resolution as desired when the 25 points per decade maximum resolution of the logarithmic circuit is exceeded.

Also provided on the patchboard is a selection of digital logic circuits including flip-flops, one-shots, inverters, logical "and," logical "or," two 10-position selector switches, master reset, and control lines for both the DAC function generator and the ADC measurement system (see Appendix for definition of digital logic terms). The patchboard is equipped to perform the central control functions necessary to allow immediate conversion of the instrument from one technique to another by replacing prewired patchboards. Changes of time scale and variations of control logic can be made through the front panel selector switches which are wired to the patchboard terminals.

INSTRUMENT CONSTRUCTION

Construction procedure followed standard practice with care taken to avoid ground-loops, keeping high frequency wiring to minimum length, and separating high-level digital signal leads from low-level analog wiring. Taper pin, direct point to point wiring was used on the digital module connectors and on the patchboard rear connectors, giving high reliability and ease of changing circuit configurations. The mounting frame holding the digital modules is hinged to the relay rack, allowing immediate access to all circuit points.

Particular component suppliers are listed to allow a specific description of the instrument. However, equivalent components, available from other sources, may well furnish advantages in economy or function over those mentioned.

Analog - to - Digital Converter. A standard unit made by Adage, Inc. (1079 Commonwealth Avenue, Boston, Mass. 02215) performed this function. The Adage type VS16-AD/SA3 converter incorporating a sample-and-hold module type SA3-O-D was selected to meet the particular design objectives. Three manually selected ranges of 1, 10, and 100 volts full scale are available giving a scale range of 0.1 mv to 100 volts. The resolution is ±0.01% of full scale, with the 4-decimal-digits-plus-sign output expressed in binary-coded-decimal format. The conversion time, i.e., the time required to form the digital equivalent of the analog input signal by a programed technique of succesive approximation, is less than 40 μsec. with an additional 10 μsec. maximum required for the sample-and-hold circuit to acquire the next sample voltage under the worst conditions of a full scale input change to the full 0.01% accuracy. Sample-and-hold operations are specified by an acquisition time constant of less than 1.1 μsec., a holding time of greater than 100 μsec. with less than 0.01% decay, and an aperture time of less than 0.1 μsec. Aperture is defined as the uncertainty of timing in the switching operation required to hold the value of an analog input signal. The accuracy of the ADC unit is within ±2.5 parts in 10,000 including zero drift, the internal precision reference, the sample-and-hold amplifier noise, quantizing error, and all other sources of variation.

Buffer Memory. A random access, magnetic core memory with a capacity of 256 4-bit words and a complete read-write cycle time of 10 μsec. was obtained from Rese Engineering, Inc. (A and Courtland Streets, Philadelphia, Pa. 19120) as their Ministore III, Model 3884. The 17-bit parallel output of the ADC is entered in the memory in 4-bit character format, allowing up to 51 5-character data words (data points) to be stored. The sign bit is stored in the fifth character position. Memory timing control, address register, and parallel-to-serial shift register circuits were constructed from Raytheon Computer (2700 South Fairview St., Santa Ana, Calif. 92704) 200-KHz. germanium logic modules. With use of the shift register, the 5 complete memory cycle core storage operations are completed during the 50 μsec. time period required for the sample-and-hold circuit to track the analog voltage and the ADC to obtain the digital value of the succeeding data point (see Figure 2). Also, the data can be read out of the memory serially, one character per memory cycle, as required for typewriter and paper tape punch operation.

Memory timing control is all asynchronous, a load memory cycle starting upon receiving a conversion-complete signal from the ADC followed by generation of the timing pulse sequences required to control the serial entry of 5, 4-bit data characters into the memory. In the output mode, suitable timing pulse sequences are generated to control the typewriter or paper tape punch solenoids, and to sequentially read out the memory contents. The number of core locations used is controlled by front panel switches connecting the 8 binary output lines from the memory address register to a pulse generator circuit which furnishes the signal to stop the data collection and read out cycles when the preset memory address is reached.

Typewriter - Punch. For typewritten output, an IBM Corporation Model B Output Writer was used. For punched paper tape output, a Tally Corporation (1310 Mercer Street, Seattle, Washington 98109) Model P-120 punch was used. Maximum typing speed is 12 characters per second plus carriage return time. In the output timing sequence, a 45-msec. pulse is generated to drive the typewriter digit solenoids. At the completion of this pulse a second 45-msec. pulse is generated to provide the proper delay between characters. The first pulse also advances a 5-bit digit counter. After each 5-character data word is typed, a 35-msec. pulse is generated to activate the carriage return solenoid, followed by a 400 msec. pulse to allow completion of the carriage return operation and stopping of the typewriter platen, in preparation for typing of the next line. The columnar format simplifies comparison between repeat transients. Direct drive of the typewriter solenoids is effected through a transistor power amplifier stage (Raytheon GPA1) which receives the drive signal from the core memory 4-bit output register after decoding by a binary-coded-decimal to decimal, diode network, which in turn is gated by the 45-msec. type drive signal.

The Tally P-120 paper tape perforator punches 8 channel tape asynchronously at speeds up to 120 characters per second, giving a readout speed of 2.1 seconds for the 51 data points stored in the buffer memory. Calendar date, the run serial number, and a three decimal digit, sample identification number are automatically punched at the start of each output record, allowing direct computer entry of the data without further identification and preventing errors due to improper filing. The calendar date is entered manually in a Model 321-F-6 Digiswitch (Digitran Company, 885 South Arroyo Parkway, Pasedena, Calif. 91105) a 6-decimal character switch having 4-line, binary-coded-decimal output, and the identification number is entered manually in a similar Model 321-F-3 switch. Serial numbers are advanced with each read out operation through use of a 3-decade counter comprised of decimal-counter modules having solenoid mechanisms driving rotary switches (Hecon Type FR-967 modules, Hengstler Numerics, Inc., 318 Bergen Blvd., Palisades Park, New Jersey 07650). Tape formatting was made identical to the standardized format of the multichannel pulse height analyzer, punched tape systems used for radiochemical data collection at this laboratory. Besides the compatibility thus obtained for computer input, some data processing can be accomplished during time periods the multichannel analyzer equipment is available. Signal averaging, background subtraction, oscilloscope display, and data plotting are typical operations which can be performed on this special purpose equipment once the punched tape is prepared.

Waveform Generator. A current switch, Adage Model CSD10-1-D, comprising nine diode switches, supplies or draws 0 to 0.99 ma. in increments of 10 μa. with a virtual ground connected to the output terminal. Each of the nine switches is opened and closed on command from control lines connected to each switch. Switching is accomplished to an accuracy of $\pm 0.01\%$ within 2 μsec. The polarity of the output current is determined by one of these control lines. A resolution of ± 100 steps results from the binary coded decimal operation. The reversible counter for stepwise operation of the DAC module was of conventional design (*7, 10*) with each decade operating in a 1-2-4-2 code. Control lines for the up and down clock pulse inputs, for setting the counter to zero or full scale, and for recognizing a zero or full scale condition in the counter, are on the patchboard. A gated flip-flop register, controlling all the DAC inputs, can be set to full scale, zero, or to the reversible counter value, from the patchboard. Separate patchboard control lines are provided for the sign flip-flop register. The register resets and controls are independent of the reversible counter controls. A level converter circuit was placed between the register and the DAC module to change the 0, -10 volt logic signals of the Raytheon Computer Modules to the ± 2.5 volt logic signals of the Adage DAC module. This level conversion was accomplished with a 2N708 silicon NPN transistor stage in each control line, having a 180-ohm collector resistance to a $+2.5$ volt supply, two 2700-ohm resistors between input and ground to give suitable base drive at the mid connection, and the emitter connected to a -3.3 volt supply.

Timing Circuits. The measurement timing circuits are all constructed from Raytheon Computer germanium circuit modules with 1MHz frequency capability. Timing for all purposes is derived from one clock module, type GCG2-1, operating within 2 p.p.m. of 1MHz at 25° C. and having an overall frequency stability of $\pm 0.02\%$. Decade divider modules, type GCD1-1, formed the basis for clock frequency division. Six single-decade dividers are on patchboard terminals. The 1 MHz. clock signal is gated to the patchboard in the measurement mode when three flip-flops change state. A manual push button switch operates the first flip-flop through a circuit which ensures only one pulse per switch operation. Output of this flip-flop in combination with a signal representing the measurement position of the mode switch enables the gate to the second flip-flop which is set by the rising portion of a Schmitt trigger output synchronized with the 60-Hz. line frequency. The output of the second flip-flop enables the next occurring positive swing of the master clock oscillator to set the third flip-flop, which opens a "nand" gate steering the clock pulses to the patchboard terminals.

Six dual-decade, preset dividers are provided with patchboard connections to their inputs, outputs, and inverted outputs. Continuous division by numbers from 1 to 99 is effected by resetting two type GDC1-1 decade counter modules each time the preset count is reached. The reset pulse is generated by operation of a type GOS3-1 one-shot when the output state of the two counter decades is identical to that selected by a 2-decimal-digit Digitran Model 321-F-2 binary-coded-decimal switch, having provision for the diodes used in the built in "nand" logic. Output of the one-shot is inverted, combined in a logical "nand" circuit with the signal from the master clear line, inverted again, and then routed to the reset terminals on the decade counters. Operation of the one-shot at 0.5-μsec. pulse width allows reset to occur before the next clock pulse is received.

Logarithmic time division of the clock pulses is accomplished to a resolution of 1% using standard "nand" logic circuits to decode 25 discrete states of a 2-decade counter and by gating input pulses to this counter at a rate decreased by a factor of 10 at the completion of each 100 input pulses. The extra pulse required to make timing identical in each decade covered, is generated after the 98th pulse is counted and is added to the pulse train going to the more significant decade. The indicated count sequence then becomes—96, 97, 98-08, 09, 10, 11,—, at the end of each decade. This extra pulse also advances the decade control counter. Table I shows the time steps chosen for decoding, with the steps used for 10 and 12 closely logarithmic steps indicated. The 25 time signals, in complement form, are available on the patchboard next to 25 patchboard positions leading to a logical "nand" circuit which combines the selected signals and generates a measurement command to the ADC. Accurate timing and rejection of noise pulses is assured by controlling the measurement command gate with a 0.5-μsec. pulse derived from the decade counter input pulses.

Patchboard. A panel mounted patchboard programming system with a 10×24 hole arrangement was used. Taper pin wiring connects to the gold plated contacts of the contact spring assembly. The matching, removable, front patchboards are pre-programmed with manual-type patchcords that mate in any desired pattern with the contact springs of the rear board. Previously established circuit combinations can be stored for repeated use. The AMP No. 595069-2 rear frame and AMP No. 395056 patchboards were obtained from AMP, Inc. (Eisenhower Blvd. Harrisburg, Pa. 17105). Uncommitted logic circuits which are brought to the patchboard, in addition to the timing and measurement circuits described above, include 3 gated flip-flops, 5 one-shots, 5 logical "and," 2 logical "or," and 8 inverters. Also available on the patchboard are all the contact positions for the two, 2-pole, 10-position selector switches used for rapidly changing the timing region from the front panel controls and for other rapid changes in circuit configuration.

Table I. Logarithmic Timing Sequences[a]

$1.0^{a,b}$	$2.1^{a,b}$	4.4
1.1	2.3	4.7^{b}
1.2^{b}	$2.6^{a,b}$	5.1^{a}
1.3^{a}	2.9	5.6^{b}
1.5^{b}	$3.2^{a,b}$	6.2^{a}
1.6^{a}	3.5	6.8^{b}
1.8^{b}	3.8^{b}	7.5
1.9	4.1^{a}	$8.3^{a,b}$
		9.1

[a] Steps usually used for recording 10 steps per decade are indicated by superscript *a;* for 12 steps per decade by superscript *b*.

Faradaic Dummy Cell. To evaluate the performance of the digital system combined with the potentiostat system in terms of timing as well as amplitude errors, and without the added uncertainty of electrode reproducibility, an 11-section, lumped-constant, RC transmission line was constructed to simulate a Faradaic component in step-functional experiments. The resistors in this transmission line used to simulate the $t^{-1/2}$ function had values of 3, 6.8, 18, 49, 93, 186, 500, 1800, 4700, 12,000, and 49,000 ohms resistance. These were connected in series, and non-electrolytic capacitors having values of 0.068, 0.068, 0.2, 0.5, 1.0, 2, 6, 20, 50, 150, and 500 microfarads were placed between the respective junction points of the resistor chain and the common terminal of the transmission line.

INSTRUMENT PERFORMANCE

In operation for over a year, measurements to within the instrument specifications have been obtained with no malfunction or component replacement. Extensive measurements have been made of potentiostatic transients for the uranium(V) disproportionation reaction in the time range of 1 msec. to 10 sec. which show a relative standard deviation value as low as 0.2% for a single determination (*9*). Typical data obtained with this digital system are tabulated in the cited reference (*9*), with the digital system set-up as shown in Figure 4. Measurements with the Faradaic dummy cell simulating a $t^{-1/2}$

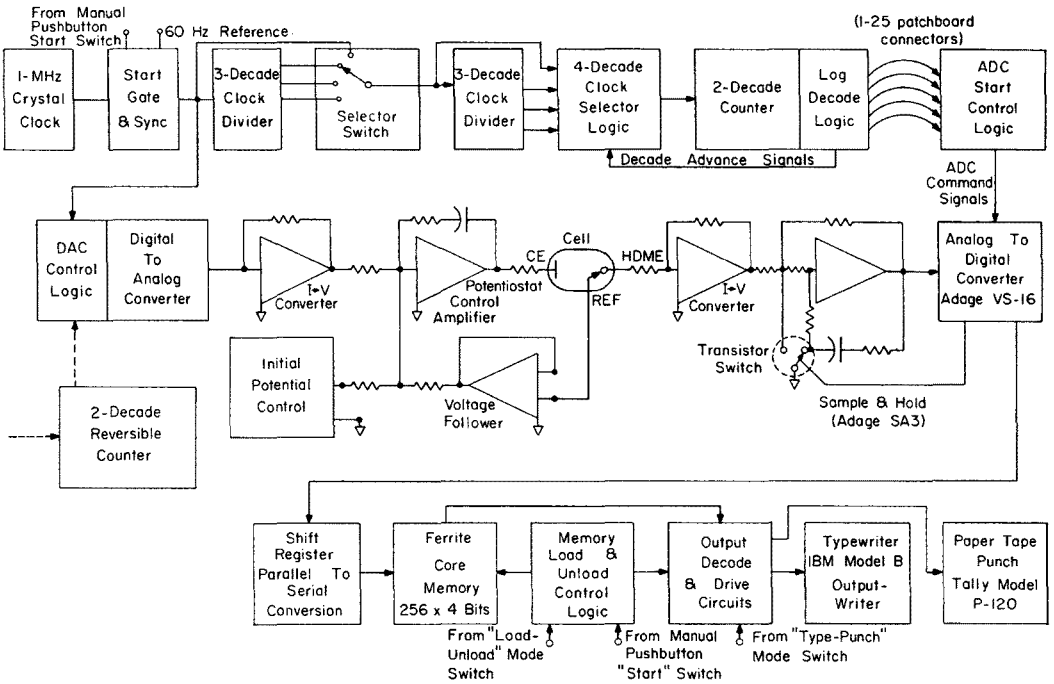

Figure 4. Operation of digital system with potential step method

Timing circuit input-outputs, analog-to-digital control lines, and digital-to-analog control lines are all set-up by patchboard wiring. The reversible counter is not used in the single potential step method. The sample-and-hold circuit is shown in the "track" mode. Operational amplifiers are Hewlett-Packard Dymec Model 2460A, except for the Adage sample-and-hold unit, Model SA3

Faradaic component, show a relative standard deviation value of less than 0.1%. Data obtained in a typical test of the complete system using a dummy cell with a simulated Faradaic component are shown in Table II. Tests of the waveform generator, using a Burr-Brown type 1644 operational amplifier (Burr-Brown Research Corp., Tucson) as a current-to-voltage converter, gave a single time constant response of 2.5 μsec. and a wave-top stability of better than the 0.01% limit of the measurement system.

Noise introduced by the measurement system was kept to within the ADC specifications. Broadband noise is the limiting measurement factor, with the 60-Hz. power line noise reduced to a negligible level through shielding and grounding precautions.

For measurements at times less than 1 msec., special care is necessary in timing synchronization or correction to compensate for delay times in the logic circuitry of the order of 1 μsec., depending on the particular configuration used.

Table II. Performance of Digital System with Faradaic Dummy Cell[a]

Transient Record Number	Time								
	msec.						sec.		
	1.0	3.2	10	32	100	320	1.0	3.2	8.3
1	7.582	4.160	2.096	1.261	0.695	0.394	0.222	0.127	0.078
2	7.582	4.161	2.097	1.259	0.699	0.397	0.220	0.128	0.081
3	7.582	4.158	2.097	1.261	0.700	0.396	0.222	0.128	0.078
4	7.582	4.164	2.096	1.259	0.695	0.395	0.222	0.128	0.080
5	7.584	4.162	2.098	1.256	0.703	0.395	0.220	0.129	0.081
6	7.582	4.164	2.098	1.260	0.700	0.393	0.222	0.126	0.081
Standard Deviation, Volts (5 degrees of freedom)[b]	0.0007	0.0026	0.0009	0.0019	0.0031	0.0014	0.0009	0.0010	0081 0.0015

[a] Table entries in volts across a 12,000-ohm load resistor on current follower. Faradaic component simulated by 11 section, lumped-constant, resistance-capacitance transmission line. Points obtained on single transient without changing the range of the ADC. Nine points are tabulated from the 40 recorded points. Voltage step applied to measuring electrode was 0.6 volts.
[b] Overall root mean square standard deviation. Volts (45 degrees of freedom, single determination) = 0.0017

DISCUSSION

With the high degree of flexibility given by the independent programming of input waveforms and output signal sampling schedules, electrochemical measurement techniques of a nearly unlimited spectrum can be quickly implemented. Application to various controlled-potential, current, or charge techniques can be directly effected. AC techniques may require some additional circuitry for ease of measurement and interpretation, but these can be added without complication within the instrument design framework. The approach used by Brown, Smith, and DeFord (*3*) for multichannel recording of AC signals is of special note. RF techniques would require little modification, as shown by Barker (*1*) in the adaptation of a square-wave polarograph for RF measurements. DC polarography, single drop current-time studies, long term adsorption studies and similar experimental measurements can be programmed easily. Unlimited output data can be obtained in these latter examples and in other measurements where the time between observations is greater than the 42 msec. required to record one data point by means of the paper tape punch. Signal averaging and various data smoothing techniques can then be effectively used with measurements in this time region to improve the signal to noise ratio, producing information that might not otherwise be obtained and making the interpretation of the results less difficult.

The digital system functions could be expanded, allowing repeat transients to be summed with data stored in the core memory, thus permitting noise reduction by the coherent addition technique. However, these and other arithmetic operations, such as testing for outliers, smoothing of random variations, normalizing data, calculating standard deviation, and more complex data reduction operations can best be done by a general purpose digital computer.

Digital computations, obtained through direct connection to a time-shared, real-time computer facility, can open new methods of investigation and greatly facilitate the interpretation of experimental results. For example, the on-line computational system could immediately furnish graphical information on a cathode ray tube screen or on a ink recorder, showing such functions as the ratio of the experimentally measured cell current to that expected for an electrode process controlled by diffusion alone at an electrode of the same geometry, thus separating out the kinetic effects from the combined kinetic-diffusion data and could easily make the plotted time axis follow a logarithmic, square root, or any other desired function. Automatic curve plotting obtained with off-line computers (*3*) has already shown the advantages of computer produced graphic presentation of electrochemical data. Limitations imposed by instrument response, uncompensated cell resistance, and other nonideal cell characteristics could be visually shown, with corrections calculated from known experimental parameters. Changes in these and other experimental parameters could be made immediately using the constant feedback from the computer data reduction programs to ensure the best possible deduction of mechanisms and to give increased reliability to the determination of reaction rates. Control of many of the experimental parameters can be done under programmed direction of the time-shared digital computer more efficiently than is possible by wired logic. For example, the switching of load resistor values in the current measuring circuit or other digital methods of changing gain could be optimized in this way, with the analog system bandwidth modified concurrently to give continuously high signal to noise ratios in the measurement of signals having large amplitude variations. In integral methods, the length of the integral segments could be program controlled in a manner, consistent with the time scale of the transient, to enhance the signal measurement with respect to non-signal contributions. Control signals of this kind are indicated by the dashed arrow in Figure 1. Auto and crosscorrelation computation can be readily implemented with digital techniques to study and measure signals masked by random noise.

Digital computer techniques are currently of great importance to the interpretation of electrochemical phenomena and will undoubtedly command a position of even greater importance. Compared with the use of high-speed computer techniques in X-ray structural studies, similar use in electrochemical studies are in their infancy. As in X-ray studies, structural information is being sought, but the intrinsic response of electrochemical measurements to interface, thin-layer, and kinetic effects makes the interpretation of these data difficult. At the same time, electrochemical measurements are of primary importance, giving in essence, dynamic structural data in rapidly changing systems from kinetic studies of interfacial and homogeneous reactions. The amount of electrochemical information obtained is directly proportional to the number of decades of time over which the measurements are taken (*5*). In order to tap this information source economically, digital systems will be required having high-speed, large volume, data collection and processing abilities.

All electroanalytical methods requiring measurements of transients could be improved by means of digital timing and logic circuits. With instruments composed of several operational amplifiers, digital circuitry can be introduced for precise timing control at a relatively small increase in cost, and these digital circuits can be expanded to control the generation of complex input waveforms and of the corresponding output measurement timing sequences to a degree of exactness not possible when restricted to a completely analog system. The use of analog-to-digital conversion devices and automatic digital recording of experimentally measured quantities is being recognized as the best approach for the great majority of measurement problems. The absence of digital equipment would only be justified in those cases where relatively simple measurements are performed on a very non-routine basis.

APPENDIX

In binary logic circuits, two states exist, a ONE state and a ZERO state, corresponding to the ON and OFF positions of a switch. The AND gate is a logic element which has a ONE output when all inputs are at the ONE level. If any of the inputs are at ZERO, the output will be at ZERO. The INVERTER logic element has a ONE output when the single input is at the ZERO level, and a ZERO output when the input is at the ONE level. Thus, the output of the INVERTER is the COMPLEMENT of the input signal. The NAND gate is equivalent to an AND logic element in series with a logical INVERTER element. The OR gate is a logic element which has a ONE output when any input is at the ONE level. It has a ZERO output only when all inputs are at the ZERO level. Logical OR operations can be implemented with series connected NAND elements. A ONE-SHOT logical element is a monostable circuit which generates a constant width output signal following an input trigger pulse. A delay is obtained by initiating succeeding operations with a signal obtained from the one-shot output upon its return to the stable configuration. A FLIP-FLOP logical element is a bistable circuit which can be triggered from one state to the other, thus being useful as a memory element to record if a signal has occurred on a given circuit line and also as a pulse train divider, giving division by two at each stage with suitable input gating.

ACKNOWLEDGMENT

The assistance of D. T. Pence in obtaining the precision data on cell measurements is gratefully acknowledged. Thanks are also due to R. I. Little, K. D.

Smith, and J. P. Morgan for helpful suggestions and circuit designs incorporated in the digital instrumentation.

LITERATURE CITED

(1) Barker, G. C., *Anal. Chim. Acta* **18**, 118 (1958).
(2) Breiter, M. W., *J. Electrochem. Soc.* **112**, 845 (1965).
(3) Brown, E. R., Smith, D. E., DeFord, D. D., ANAL. CHEM. **38**, 1130 (1966).
(4) Buck, R. P., Eldridge, R. W., ANAL. CHEM. **35**, 1829 (1963).
(5) Caldin, E. F., "Fast Reactions in Solution," p. 4, Wiley, New York (1964).
(6) Dudley, R. L., *Hewlett-Packard Journal* **17** (No. 3), 1 (Nov. 1965).
(7) Fulks, R. G., *General Radio Experimenter* **39** (No. 4), 6 (April 1965).
(8) Lauer, G., Osteryoung, R. A., ANAL. CHEM. **38**, 1137 (1966).
(9) Pence, D. T., Booman, G. L., ANAL. CHEM. **38**, 1112 (1966).
(10) Raytheon Computer Co., Santa Ana, Calif., "Digital Module Application Manual," Bull. **SP-175** (1964).
(11) Underkofler, W. L., Shain, I., ANAL. CHEM. **35**, 1778 (1963).
(12) Will, F. G., *J. Electrochem. Soc.* **112**, 1157 (1965).

RECEIVED for review March 31, 1966. Accepted June 10, 1966. Division of Analytical Chemistry, Winter Meeting, ACS, Phoenix, Ariz., January 1966. This work was supported by the U. S. Atomic Energy Commission Under Contract No. AT(10-1)-205 through the Idaho Operations Office.

END OF SYMPOSIUM

Electrode Potential Gradients and Cell Design in Controlled Potential Electrolysis Experiments

J. E. HARRAR

Chemistry Department, Lawrence Radiation Laboratory, University of California, Livermore, Calif.

IRVING SHAIN

Chemistry Department, University of Wisconsin, Madison, Wis.

▷ **The effect of potential distribution in electrolysis cells used for large-scale, controlled-potential electroanalytical experiments has been investigated, and the conditions and geometric arrangements where the working electrode potential exceeds the control potential have been evaluated. The potential distributions were characterized from existing knowledge in the field of current distribution theory, and these concepts were applied in a consideration of the design of typical cells utilizing platinum gauze and mercury pool electrodes. To illustrate the effects, the electrode potential and current distribution were investigated as a function of cell geometry with a controlled-potential cell incorporating a subdivided working electrode. In addition, controlled-potential coulometric experiments were carried out to demonstrate the effect of electrolysis cell configuration on analytical results.**

IN THE DESIGN of a three-electrode cell for controlled-potential electrolysis, the potential and current distribution in the cell are of fundamental importance. This distribution is affected by cell geometry, electrode placement, and solution characteristics, and may influence analytical and kinetic measurements. In the case of dropping mercury electrode polarography, some of these problems have received detailed study (*8*, *39*). In contrast, the effects of potential and current distribution have not been examined adequately in the case of electroanalytical techniques involving the use of large working electrodes.

The most important factor to be considered in the design of cells for large-scale electrolysis is that there may arise a local variation of electrode potential at the working electrode, as a result of the dimensions and relative positioning of the cell components. Such gradients in potential of the order of several hundred millivolts have been measured at a large mercury pool working electrode by Booman and Holbrook (*6*), by Scott, Stouffer, and Richardson (*41*), and by Fisher and coworkers (*33*, *42*). In these experiments involving reduction processes at the working electrodes, it was shown that certain electrode configurations apparently cause portions of the working electrode to become more cathodic than the control potential. This loss of potential control could be an important source of error, for example, in using controlled-potential electrolysis for separating species in which the formal E° for the systems are relatively close.

Using a mercury pool cell of exaggerated geometry, Fisher and coworkers (*33*, *42*) carried out a series of experiments designed to detect the coreduction of two species whose reduction potentials differed by less than the observed electrode potential distribution. No coreduction was detected in these experiments, and on this basis, the validity of the potential distribution measurements was questioned. Thus, this work was undertaken to clarify the theoretical basis for a gradient in working electrode potential (resulting from solution resistance effects) in three-electrode controlled-potential methods, and to illustrate the effects by a further series of experiments.

In general terms, the problem of three-electrode, controlled-potential electrolysis cell design is twofold. First, the components of the cell, particularly the counter and working electrodes, should be arranged so that a satisfactory distribution of potential at the working electrode will be obtained. The basis for understanding most of the features of potential distribution is provided by the theory of current distribution that has been developed in recent years for application in electroplating technology. However, in the literature on current distribution theory, the emphasis is on achieving uniformity of current, which tends to obscure the potential distribution aspects of the matter. Thus, an essential part of the work reported here is a review of the pertinent current distribution material from the point of view of a primary interest in potential distribution. Once the nature of the potential distribution in an electrolytic

cell is calculated or determined, the second of the two problems of cell design, placement of the reference electrode, is virtually solved, and the influence of various factors such as uncompensated iR drop upon the potential control is readily evaluated.

Two types of experiments were conducted to test some of the concepts of the theory of potential and current distribution. The first series was carried out in a cell with a subdivided working electrode which permitted a correlation to be made between the currents flowing at these electrodes and their potentials. In addition, the effect of cell geometry on the potential distribution could be ascertained by interchanging the controlling and measuring reference electrodes and positioning of the counter electrode. The second series of experiments was performed to illustrate the detrimental effects of improper electrode arrangement on an actual analytical determination; these experiments involved the determination of iridium in the presence of palladium in electrolysis cells with two different electrode configurations.

POTENTIAL CONTROL AND CURRENT DISTRIBUTION REQUIREMENTS

In general, controlled-potential experiments require not only the maintenance of a constant or controlled average electrode potential, but also a reasonable uniformity of potential over the surface of the electrode. The requirement for uniformity of potential is about the same as that for the allowable variation of the average potential, and varies considerably among the different techniques and among specific applications of a particular technique.

Probably the most stringent requirements for potential control would be in the application of controlled-potential coulometry to the precise determination of kinetic parameters (*3*, *4*, *11*, *12*). Considerably more tolerance in potential control is usually allowed in controlled-potential coulometry for analytical purposes, with the exact specification depending upon the particular application. During the electrolysis, a variation of the actual electrode potential to a value less cathodic in the case of a reduction process or less anodic in the case of an oxidation is, with certain exceptions (*15*), not detrimental to the analytical result, provided that the final electrode potential corresponds to the potential of complete electrolysis (*30*). Thus, a common technique is the deliberate limiting of the average initial potential and initial current in the electrolysis by inserting resistance in the working electrode lead or by arranging the reference electrode to include uncompensated iR drop in its measurement.

Of principal concern in analytical controlled-potential coulometry and separations are the temporary and localized excursions of the electrode potential which exceed the control potential—i.e., the electrode potential becomes more cathodic than the control potential during a reduction, or more anodic during an oxidation. An error in potential control in this direction may result in the electrolysis of a second substance and this secondary process may cause a bias in the determination. Such bias would be observed only under certain, rather restricted conditions. If the interfering substance undergoes an electrolysis reaction which is exactly reversed when the potential returns to the control value, no bias would be observed. On the other hand, an error would result if the interfering electrode process were irreversible, such as in the coulometric determinations of substances whose electrolysis potentials are close to the decomposition potentials of the solvent or supporting electrolyte. Similarly, the simultaneous electrodeposition of an interfering substance would cause a bias even though the secondary reaction by itself is reversible. Chemical interaction between the redox species of the primary and interfering electrode reactions may modify or remove the bias to an extent dependent upon the formal potentials, reaction rates, and quantities involved. Obviously, many modes of interference of varying complexity are possible.

The potential control requirements of controlled-potential electrogravimetric methods are the same as those of coulometry and separations; in addition, electrogravimetry shares with technical electroplating the need for uniformity of current density over the surface of the electrode so that the electrodeposit will have good physical properties. Electrolysis procedures involving solid electrodeposits are the only controlled-potential methods that require a uniform current density per se.

To the extent that uniform current density also indicates a uniform potential distribution, all controlled potential methods may in effect require it. However, because the relationship between current and potential distribution over the electrode surface depends on the current-potential characteristics of individual portions of the surface, considerable variation in current density without a variation in electrode potential is possible, and vice versa. For example, an electrode operating with a virtually uniform potential distribution may exhibit quite nonuniform current distribution, either because of differences in mass transfer at different parts of the electrode, or because all parts of the electrode are operating at points on the steeply rising portion of the current-potential characteristic. Neither of these two situations of nonuniform current distribution would necessarily be detrimental in a controlled-potential method. On the other hand, the most extreme cases of potential nonuniformity arise when the working electrode is completely concentration polarized. Under these conditions, the current would be determined only by the rates of mass transfer, which could be uniform, but the electrode potential would be distributed according to the ohmic losses in the cell. Thus, the effects of both potential distribution and current density distribution must be evaluated.

THEORY OF POTENTIAL AND CURRENT DISTRIBUTION

The basis for the theoretical evaluation of current distributions in an electrolysis cell involves the application of a branch of mathematical analysis known as potential theory. The mathematical problem usually is expressed as a steady state Laplace or Poisson equation in two dimensions with appropriate boundary conditions (*21*). The flow of current is assumed to be described by a straightforward application of Ohm's law, and the potential and current distribute in such a manner as to minimize the total iR loss, and to conform to the boundary conditions at the electrodes. Probably the best introduction to the method can be found in the work of Kasper (*20–22*). In addition, Kronsbein (*25*) has reviewed the field prior to about 1947 and has discussed (*26*) the basic principles of current distribution. Other material is contained in the monograph by Rousselot (*38*) and Fleck, Hanson, and Tobias (*10*) have compiled a catalog of analytical solutions for various electrolytic cell configurations, together with an extensive literature survey.

In the applications of potential theory to the electrolytic problems, it is usually assumed that the medium is electrically homogenous and isotropic. That is, the concentration gradients which arise as a result of the electrolysis are assumed to be small or restricted in extent compared with the electrolysis cell –electrode dimensions so that departures from uniform solution conductivity can be neglected. This condition is closely approached at low current densities with well-stirred solutions in which the electroactive material is present in high concentrations. It is equally valid for polarographic type solutions in which an excess of inert electrolyte is present. In addition, for simple current distribution theory to apply to electroanalytical experiments, it is necessary that the convective hydrodynamic field at the electrodes be uniform. A discussion and review of these factors affecting the applicability of potential theory to electrolysis experiments have been given by Guillou (*13*) and Newman (*34*). In addition,

Newman (*34*) has recently treated the more complicated calculation of a current distribution when both the concentration distribution in the diffusion layer and the potential distribution in the bulk solution must be considered simultaneously.

The typical current distribution problem considers that the metal of the electrodes is an equipotential and that the boundary for mathematical purposes is the adjacent layer of solution. The potential, or function of potential, that is specified for the boundary is equivalent to the usual electrochemical potential difference between the metal and this adjacent layer of solution measured with respect to some reference half-cell. The terms "electrode potential" and "potential of the surface of the electrode" refer to this potential difference at specific points on the surface of the electrode. Correspondence between theory and experiment depends on whether the electrode potentials experimentally measured at specific points on the surface of the electrode truly represent the parameter governing the flow of electrolysis current in that region. Variations in local electrode potential and current over the microscopic irregularities of the surface are not of direct concern here, although these factors also have been treated in detail (*19*).

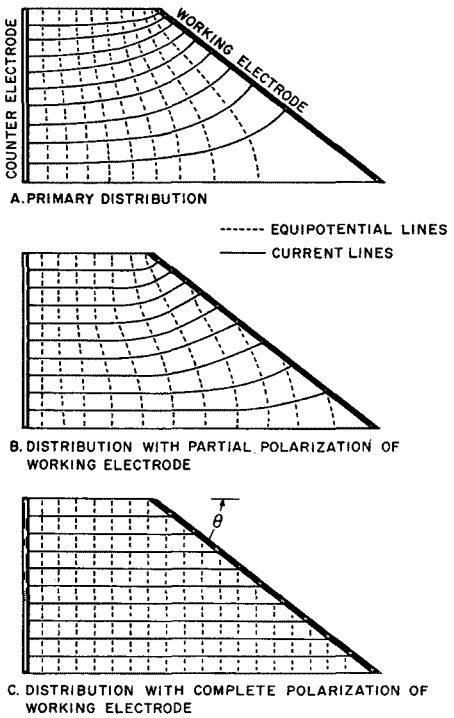

Figure 1. Potential and current distribution in the Hull cell

Primary Distribution. The distribution of current and potential in an electrolytic cell depends on the nature of the potential–current function at both conducting electrodes. If the electrodes are assumed to be completely unpolarized—i.e., the electrode potential is independent of the local current—the conducting boundary is taken to be at constant potential. Under these conditions, the current distribution is referred to as the primary current distribution (*14*) which depends only on the relative geometrical arrangement of the electrodes and cell and is independent of their absolute size. Mathematical solutions to a large number of problems of this type have been obtained (*10*). A few geometrical arrangements are known which yield a uniform current density at a working electrode, and the cell characteristics which give rise to nonuniform current distribution have been enumerated (*20, 22, 26*). Nonuniform current distribution stems from two types of geometrical factors. It may result from the relative location of the working electrode within the cell, or, independent of location, nonuniform current distribution may arise from such effects as convergent current flux which causes unshielded electrode edges or external corners to exhibit a higher current density.

The form of a primary current and potential distribution is shown in Figure 1*A*, (*37*) which is a cross section of a geometrical arrangement known as the Hull cell (*17*). The electrodes constitute the ends of the enclosure and the third dimension, perpendicular to the paper, is bounded by the bottom of the cell and the solution–air interface. The problem of defining the current and potential distribution in such a cell was first described by Moulton (*32*), and the cell has been used experimentally in the determination of solution electroplating characteristics. As in all current distribution systems, the current and potential lines are orthogonal, and because there is no polarization at either electrode, the current lines also intersect the electrodes at right angles. The current distribution at the electrodes is indicated by the convention of spacing the lines to include equal quantities of electricity. The contour of the potential and current map for the primary distribution is independent of the size of the system, the resistivity of the electrolyte, and the magnitude of the electrolysis current.

In addition to describing d.c. electrolysis experiments involving negligible polarization, primary current distribution theory corresponds very closely to experimental methods employing a.c. signals in which the faradaic impedances are low. Thus, it is interesting to note the comment of Rousselot (*38*) that most of the conductivity cells in use (*27*) have very nonuniform current distribution.

Distribution with Electrode Polarization. When polarization occurs at one or both of the electrodes, for example because of electrode kinetics or mass transfer effects, different contours of potential and current distribution are formed, as shown in Figures 1*B* and 1*C*. Considerable complexity is introduced into the mathematics of current distribution problems by the boundary condition of polarization, particularly if the relation between the current and potential at the boundary cannot be linearized. Problems involving polarization have been solved and the influence of various parameters on the distribution has been elucidated by a number of workers, including Kasper (*21*), Agar and Hoar (*1*), Wagner (*43, 44*) and Drossbach (*9*). Because of the mathematical difficulties associated with polarization, Tobias and coworkers (*10, 23*) have used numerical methods for the solution of these problems on a digital computer. Rousselot (*37, 38*) has advocated the use of analog measurement methods for obtaining current and potential distributions.

The salient feature of the theory of current distribution with polarization is that there is a gradient in potential in

the solution adjacent to the electrode, and that associated with this is a tangential as well as a normal component of the current at the electrode surface (*1*, *21*). Thus, in potential and current distribution diagrams such as Figures 1*B* and 1*C*, the equipotential lines intersect the working electrode and the current lines enter the electrodes at angles other than 90°. Of principal interest to electroplating technology is the fact that polarization tends to produce a more uniform current density at the electrode surface, and, hence, a more even electroplate.

Although not explicitly discussed in most treatments of current distribution theory, the potential distribution resulting from complete concentration polarization is of interest, especially in electroanalytical applications. Such a distribution is shown for the Hull cell in Figure 1*C*. This situation exhibits a maximum electrode potential gradient for the given geometry. In this simple arrangement, the potential gradient along the working electrode per unit of length would be $iR\cos\theta$ where i is the current density and R is the specific resistivity of the solution. As with the primary distribution, the shape of the potential-current contour is independent of the absolute size of the system, the solution resistivity, or the magnitude of the current. Cases of complete concentration polarization and a limiting, uniform current at one of the electrodes have been treated theoretically by Drossbach (*9*), Macaire, Guillou, and Buvet (*13*, *31*), Scott, Stouffer, and Richardson (*41*), and Newman (*34*).

As in cases of current distributions at unpolarized electrodes, working electrode potential distributions with polarization will depend upon both the orientation of the electrodes within the cell and whether there are electrode edges or corners which can cause unequal ohmic losses in conduction to the electrodes. Thus, the examples of uniform primary current distribution (*20*, *22*, *26*) are also the only configurations which can yield perfectly uniform working electrode potentials when the electrodes are polarized. Although edge effects can be significant in creating nonuniform electrode potentials as has been shown by Newman (*34*) for the rotating disk electrode, in most large-scale electroanalytical experiments this factor is of relatively less importance than the orientation of the counter electrode. For example, in the typical mercury-pool type cell the working electrode edge is shielded by the cell and only the counter electrode orientation needs to be considered. The edge effect will be present and should be minimized in the case of cylindrical-gauze type cells but will be important only in proportion to the ratio of edge length to electrode area.

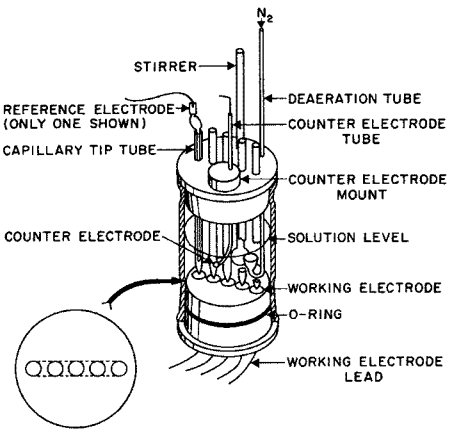

Figure 2. Potential and current distribution cell

EXPERIMENTAL

Reagents. The solution used in the potential and current distribution experiments was prepared from reagent-grade $FeSO_4 \cdot 7H_2O$ and H_2SO_4, and Commercial Solvents Co. U.S.P. 95% ethanol. The cell solution was 0.10*N* in H_2SO_4, 0.005*N* in Fe(II), and 70% ethanol by volume. Deionized water was used to prepare solutions.

The iridium solutions were prepared from Alfa Inorganics, Inc. $H_2IrCl_6 \cdot 6H_2O$ and the palladium solutions from Engelhard Industries, Inc. Na_2PdCl_4. Stock solutions of these salts were prepared to be approximately 20 mg./ml. in Ir(IV) and 3.6 mg./ml. in Pd(II), respectively; and 0.50*N* in HCl. The Na_2PdCl_4 salt was used as a primary standard based on the manufacturer's assay of Pd. Aliquots of these stock solutions were taken for the coulometric analysis experiments.

Potential and Current Distribution Cell and Electrodes. The cell (Figure 2) consisted of a glass cylinder with ⅄ 71/60 joints at each end, into which were fitted caps of Teflon which formed the top and bottom of the cell. The glass stirrer was driven at 1800 r.p.m. with a synchronous motor. The deaeration tube was terminated in a coarse porosity frit. The capillary-tip tubes containing the reference electrodes were 6 mm. o.d. drawn to a tip diameter of 0.5 mm. These tubes were firmly held in the cap of Teflon but were movable for positioning above the working electrodes. The reference electrodes were the Ag–AgCl reference electrode part of the Leeds and Northrup type 124138 miniature electrode assembly. All reference electrodes used in this work were checked periodically against a laboratory-prepared S.C.E. The potentials of these five reference electrodes remained stable and within a range of 3 mv. during the course of this work. In operation with the cell, the capillary-tip tubes were allowed to fill with the cell solution, and then the reference electrodes were inserted.

The counter electrode was a 2.5-mm.-diameter platinum sphere formed by melting the end of a 1-mm.-diameter wire. The wire was sealed into a glass tube so that only the sphere was exposed to the solution. The glass tube was curved at the electrode end, and mounted off-center in a holder made of Teflon, which was free to rotate in the cell cap. This mounting arrangement facilitated positioning of the counter electrode within the cell.

The working electrodes were fabricated from 0.032-inch-thick platinum sheet, and electrical connection was made via a wire soldered to the underside of each electrode. The electrodes were mounted in the block made of Teflon comprising the bottom of the cell, with care being taken to seat them flush with the surface of the Teflon. The cell bottom was drilled through for the electrical leads and slightly undersized, recessed seats were cut for the electrodes. After treating the seats with Teflon etchant, the electrodes were pressed in and sealed underneath with an epoxy adhesive, Resinbond No. 907 (Resin Formulators Co., Culver City, Calif.). Two cell bottoms were constructed, one with five separate working electrodes, each an 11.1-mm. diameter disk, spaced 1.0 mm. apart; and one with a single working electrode of outline shown by the dotted line in Figure 2.

The cell was operated with a solution volume of about 120 ml. at a depth of 3.0 cm. High-purity nitrogen was used to deaerate the solution and was passed first through a gas washing bottle containing another portion of the cell solution.

Potential and Current Distribution Instrumentation. To monitor the five individual electrode currents, the lead from each working electrode was connected to the input of an operational amplifier (Philbrick Researches Inc., type UPA-2) connected with an appropriate feedback resistor as a current follower (*40*). Each of the outputs from the current followers was connected through a low-pass RC filter to one channel of a 12-point Brown recorder having a 1-second, 10-mv.

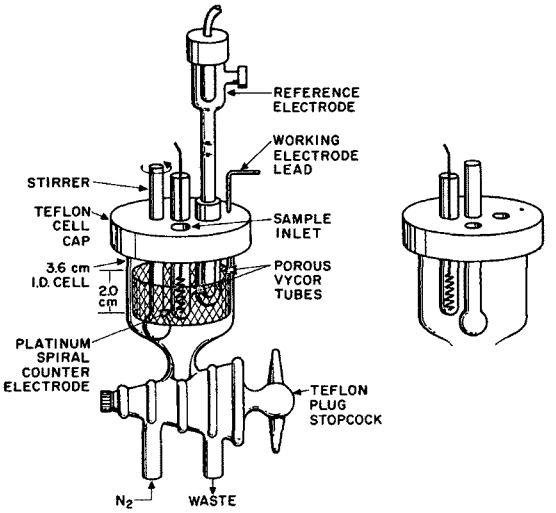

Figure 3. Controlled potential coulometry cell

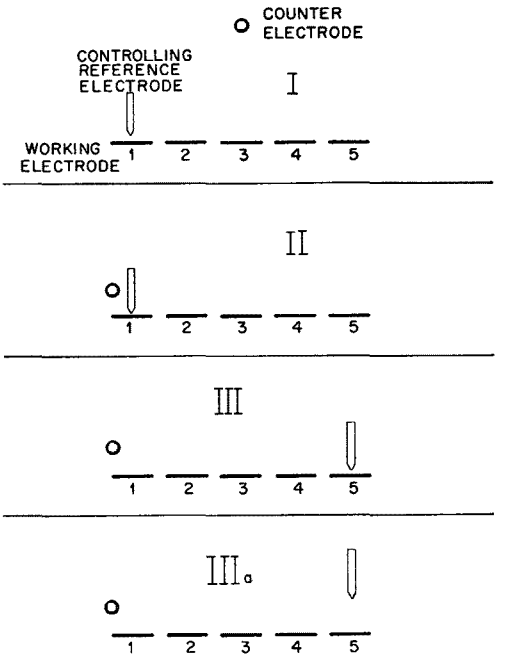

Figure 4. Configurations of the electrodes in the potential and current distribution cell

full-scale response. The recorder was modified so that it sampled and recorded one channel per second.

To record the potential distribution in the cell, each of the five reference electrodes (including the one used as the controlling reference electrode and connected to the potentiostat) was connected through a Philbrick type P65 amplifier functioning as a voltage follower to five additional channels of the recorder. Another recorder channel was directly connected to the counter electrode to measure the total cell voltage.

The potentiostat consisted of a Philbrick type P2 amplifier with a transistorized power booster in a conventional circuit configuration [Figure 4*h* in Ref. (*40*)]. The potential-scan circuit consisted of a second P2 amplifier connected as an integrator-type ramp generator. The control potential, E_c, was scanned at a rate of 96 mv. per minute. In measuring the currents, five individual voltammetric curves were thus recorded simultaneously. At the same time, the counter electrode voltage, the control potential, and the potentials at the four other reference electrodes were recorded, each with respect to circuit ground. Since the metal of the working electrodes was maintained at virtual ground by the current followers, measurements thus were obtained of the total cell voltage and the electrode potentials of the five working electrodes.

The specific resistivity of the cell solution was measured with an Industrial Instruments Inc., type RC conductivity bridge operated at 1000 c.p.s.

Coulometric Cells and Electrodes. The experiments with the controlled potential determination of iridium involved the use of a single set of components arranged in two different cell configurations as shown in Figure 3. The only difference between these two configurations was that the stirrer and the counter electrode were interchanged to alter the symmetry of the cell. The working electrode was a double thickness of 45-mesh platinum gauze, 50 sq. cm. in unfolded planar area. The salt bridge tubes were obtained from the Corning Glass Works and consisted of Vycor tubes, the lower, bulbous end of which was Glass No. 7930 porous Vycor. The porous section was 7 mm. in diameter on the tube containing the counter electrode and 10 mm. in diameter on the reference electrode tube. The porous section was 1.5 cm. long on both tubes and the tubes were positioned so that this section was located within the volume of solution enclosed by the working electrode. The cell was operated with 1.0*N* H_2SO_4 in the counter electrode tube and with the analytical supporting electrolyte, 0.20*N* HCl, in the reference electrode tube. The reference electrode was a Beckman No. 39178 asbestos-fiber probe electrode. The cell solution volume was 20 ml.

Coulometric Instrumentation. The controlled-potential electrolyses were carried out with the same potentiostat used in the potential distribution study. Careful attention was paid to the behavior of the electrode potential control as the cell-potentiostat system was switched on to ensure that no transient overshoot occurred. The electrolyses were initiated by closure of the working electrode lead with a mercury-wetted-contact relay. The initial transient potential and current signals were observed at the operating electrodes and at an independent reference electrode immersed directly in the solution by means of a Tektronix type 564 storage oscilloscope. With the potentiostat phase compensation networks adjusted properly for each cell configuration, the potentiostat was output voltage limited at 24 volts for about 120 msec., and then recovered to maintain the average control potential without overshoot. During this initial double-layer-charging period, the average electrode potential was less cathodic than the control potential.

The integrator used in the coulometric experiments was based on a UPA-2 operational amplifier and its readout voltages were measured with a Non-Linear Systems Model 484A digital voltmeter.

The voltammetric curves of iridium and palladium were obtained with the potentiostat and potential-scan circuit together with an Electro-Instruments, Inc. Model 400 X-Y recorder. Separate solutions of iridium and palladium were electrolyzed in the coulometric cell in configuration A at a scan rate of 1.08 volts per minute. The determination of palladium was carried out with a Cary Model 14 spectrophotometer using the analytical method of Jacobs (*18*).

RESULTS AND DISCUSSION

Potential and Current Distribution Experiments. To illustrate the variation of potential and current distribution as a function of electrode position and to correlate the currents obtained with the measured potentials, a series of experiments was carried out in the cell shown in Figure 2. The experimental approach of measuring the current distribution in an electrolysis cell at a series of individual working electrodes functioning as one—i.e., with a subdivided working electrode—although justifiably criticized by Kronsbein (*25*) because of edge effects, has been used successfully by Orr and Wirth (*35*) in a test of current-distribution theory. The relative importance of edge effects will depend on the exact geometry, but the largest contribution to nonuniform current distribution occurs when the electrodes are only slightly concentration polarized. At the limiting-current potentials, the effect would be minimized. Potential distribution errors, on the other hand, would be more pronounced at the limiting current. To provide some indication of this effect, data were obtained in this study with two kinds of working electrodes: the subdivided electrode with five individual disk electrodes closely spaced on a line and a single electrode corresponding to the five individual electrodes with the spaces between them filled in. The differences in measured potential distribution between cells incorporating these two kinds of electrodes were minor at all values of current. Thus, edge effects did not cause major distortions in the potential field. All data reported except the cell potential map were obtained with the subdivided electrode cell.

In the measurements of the potential distribution near the electrodes, the tips of the reference electrode tubes were positioned no closer than 1.0 mm. to avoid excessive distortion of the hydrodynamic and potential fields at the electrodes (*2*, *5*). Thus, some iR drop was included in the measurements; however, the magnitude of this iR drop cannot be calculated *a priori* in the manner of Barnartt (*5*) because the potential field in these experiments was not parallel to the electrodes. Moreover, in some cases when the equipotential lines were nearly perpendicular to the electrode, there would appear to be virtually no iR drop correction. In any case, the data were self-consistent, and on this basis it was concluded that no major error was introduced by not making corrections for the uncompensated iR drop.

The solution composition selection was based on the desire to operate under polarographic conditions—i.e., with an excess of supporting electrolyte—while still having sufficient solution resistivity to cause reasonably large iR drops at the current level that could be generated. The solution of 0.005N Fe (II) and 0.10N H_2SO_4 in 70% ethanol, which had a specific resistivity of 290 ohm-cm., proved to be satisfactory. Analytical controlled-potential electrolyses in aqueous, acidic media usually involve solution resistivities lower than this value, but correspondingly higher current densities are generated so that iR drops of approximately the same magnitudes are encountered. The hydrogen ion also functioned to depolarize the counter electrode, which was immersed directly in the solution.

Complete voltammetric curves were determined with the subdivided electrode cell in four different electrode arrangements (Figure 4). In configuration I, the counter electrode was symmetrically located above the center working electrode and near the surface of the solution. In each of the other three configurations, the counter electrode was placed at the edge of working electrode 1, and 0.5 cm. above it. The potentiostat controlled the cell potential via reference electrode 1 in configuration II and through reference electrode 5 in configuration III. Configuration III*a* was the same as III, except that the top of the controlling reference electrode tube was positioned 2.0 cm. above the surface of working electrode 5.

Current–voltage curves obtained for configuration I are shown in Figure 5. The current of each working electrode is plotted as a function of the control potential, E_c, which in this configuration is also the potential of working electrode 1, E_1. These current-potential characteristics exhibit a limiting current for the oxidation of Fe(II) from about +0.60 to +0.80 volt *vs.* S.C.E. The limiting current region also reveals a distribution of current among the five working electrodes in a manner to be expected from the hydrodynamics of the stirring. The stirrer was near the center of the cell and the highest limiting current occurs at the center working electrode, No. 3, with a decrease in limiting current toward the periphery of the cell. The five curves show no significant difference in half-wave potentials, and these results indicate that for this configuration, the potentials of the working electrodes do not vary significantly.

The potential distribution across the cell is also shown in Figure 6, where the difference between the individually measured working electrode potentials and the control potential ($E_n - E_c$) is shown for the four cell configurations. For configuration I, where the counter electrode is symmetrically located and far away from the working electrodes, the five individual working electrodes are at a relatively uniform potential. On the other hand, large variations in the individual working electrode potentials are observed for the other three cell configurations.

For configurations II and III, the variations in potential across the cell are similar in form and magnitude (about 200–250 mv., total) but differ in the direction of the deviation from E_c. Configuration III represents the case in which the control potential is exceeded at points on the working electrode closest to the counter electrode, and thus would be subject to errors resulting from a secondary reaction. Configuration III*a* was designed to illustrate the effect of positioning the controlling reference electrode to include iR drop in its measurement, so

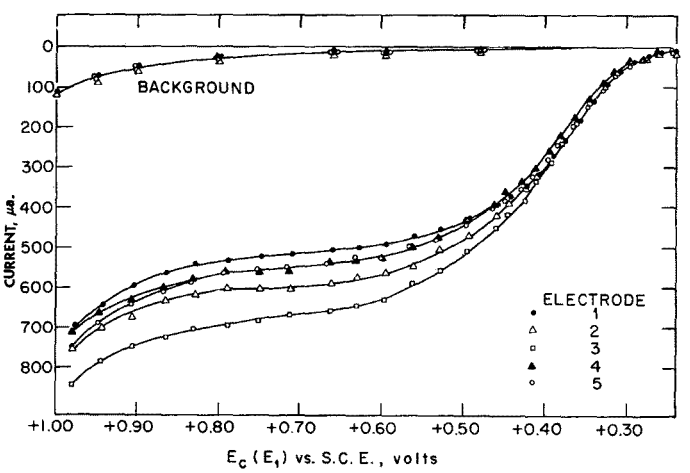

Figure 5. Currents as a function of control potential, E_c, for the five working electrodes, cell configuration I

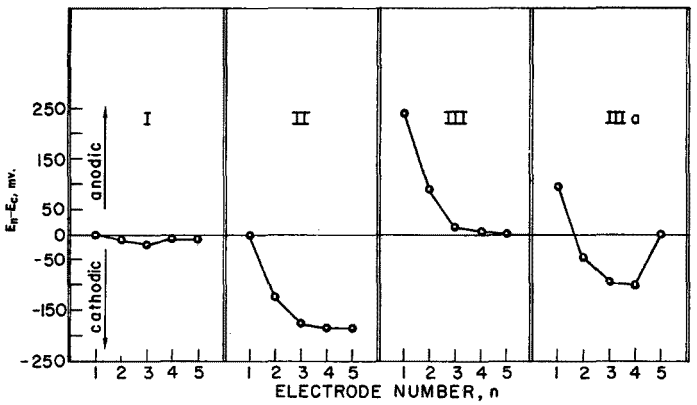

Figure 6. Distribution of working electrode potentials in the four cell configurations. Control potential, E_c, about +0.70 volt vs. S.C.E.

as to decrease the error arising from the unsymmetrical placement of the counter electrode. The distribution shown in Figure 6, III*a*, indicates that the error is indeed decreased, but that working electrode 1 was still 100 mv. more anodic than the control potential.

The behavior of the potential and current in the cell operating in configuration III is shown in more detail in Figure 7. The upper curves show the deviation of electrode potentials and the lower curves, the currents, as a function of the control potential, which in this configuration is also the potential of working electrode 5. Only data for electrodes 1, 2, and 5 are shown for improved clarity. In general, these data are consistent with the results shown in Figure 6, which indicated that in configuration III, the working electrodes were progressively more anodic in the vicinity of the counter electrode. Thus, for example, at working electrode 1, the current which is caused by decomposition of the solvent, begins at an apparent control potential of +0.60 volt (measured at working electrode 5) whereas this secondary reaction does not actually start at working electrode 5 until a potential about 200 mv. more anodic is reached. In addition, the current–voltage curve rises more steeply for working electrodes 1 and 2, compared with 5.

The upper curves of Figure 7 reveal that the individually measured electrode potentials diverge until the currents reach their limiting values and then the differences remain constant, at least to +0.95 volt *vs.* S.C.E. It is significant that the difference in potential between working electrodes 1 and 5 does not change when the former begins to exhibit the second electrolysis process, beginning at about an E_c of +0.60 volt *vs.* S.C.E. This results from the fact that while this additional current for the solvent decomposition flows only to working electrode 1, it does not affect the potential gradient across the other working electrodes. It is only when the electrolysis current must flow transverse to the working electrodes, as is the case with the electrolysis current for the oxidation of the Fe(II), that the transverse potential distribution appears. With this geometry, the working electrodes progressively nearer to the counter electrode experience potential scan rates progressively greater than the rate of scan of E_c. This magnification effect causes the current–potential curves to appear steeper and also results in increased high frequency noise in the current and potential signals at these working electrodes. Another experimental difficulty illustrated is that the background current corrections at the remote electrodes cannot be based only on the control potential scale, E_c, because when the currents are low, the large potential gradients shown in Figure 7 are absent.

If the current–voltage curves are recalculated with respect to the individually measured electrode potentials the apparent distortions due to nonuniform potential distribution largely disappear. This is illustrated in Figure 8 by an example with working electrode 1 in configuration III. Here, the curve for the current of electrode 1 *vs.* E_c of Figure 7 is reproduced together with the same data from configuration I. The points resulting from replotting the current data of electrode 1 in configuration III *vs.* its measured potential, E_1, are shown, and this curve is seen to coincide closely with that of configura-

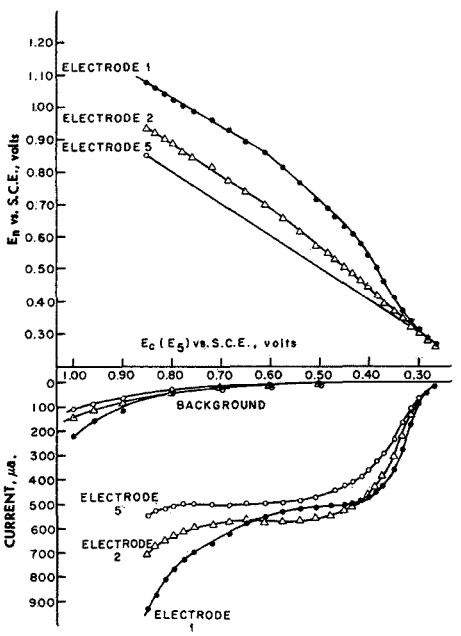

Figure 7. Working electrode potentials and currents as a function of control potential, E_c, cell configuration III

Upper curves: electrode potentials
Lower curves: electrode currents

tion I. Similar correspondence can be achieved with data from each of the electrodes and configurations, indicating that the method of electrode potential measurement is valid.

The potential distribution effects in this particular cell were also correlated with the form of the potential field in the electrolysis solution as a whole. Using the cell with the one-piece working electrode, the reference electrode tubes were raised above the working electrode to obtain a series of measurements of the potential in the body of the solution and these values were used to construct an equipotential map. The results shown in Figure 9 were obtained with cell configuration III and the polarity of the potential values is that of the reference electrode with respect to the working electrode at virtual ground. The control potential was +0.628 volt *vs.* S.C.E. and the distribution at the electrode surface is similar to that observed with the subdivided electrode. In this cell potential distribution, the equipotentials are nearly perpendicular to the working electrode in the vicinity of the counter electrode, but nearly parallel to the working electrode on the opposite side of the cell. The equipotential map reveals more clearly the reason that raising the controlling reference electrode to a position 2.0 cm. above working electrode 5 did not compensate entirely for the potential error in configuration III*a*. At this position, the reference electrode merely controlled on an equipotential which extended to a point between working electrodes 1 and 2.

Controlled Potential Coulometric Experiments. The coulometric method of Page (*36*), in which Ir(IV) is determined by reduction of $IrCl_6^{-2}$ to $IrCl_6^{-3}$ in 0.20*N* HCl, was selected to demonstrate the effect of electrolysis cell configuration upon analytical selectivity. Voltammetric curves obtained with solutions of iridium and palladium (Figure 10) indicated a possible difficulty in separating these two elements if significant errors in potential control were present in a coulometric analysis. Accordingly, determinations of Ir(IV) in an iridium solution containing $PdCl_4^{-2}$ were carried out at a series of control potentials in the vicinity of the recommended value of +0.40 volt *vs.* S.C.E. Two different cell configurations were used, shown in Figure 3, of which one (configuration *A*) would be considered to be a much better geometrical arrangement in the light of potential distribution theory, because the counter electrode is placed symmetrically with respect to the working electrode.

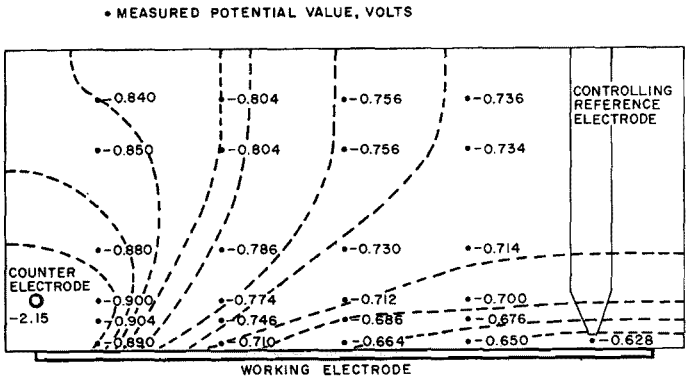

Figure 9. Equipotential map of the single working electrode cell in the plane of the reference electrodes

The voltammetric data were recorded with solutions in the coulometric cell in configuration *A* by scanning in the cathodic direction. The peak-shaped Ir(IV) wave resulted from depletion of this species in the bulk of the solution during the scan. The presence of Ir(III) in the solution caused the small oxidation current beginning at +0.80 volt *vs.* S.C.E., but this was of no importance in these experiments. In the region of potentials where Pd(II) was rapidly reduced, a very dark deposit of Pd metal formed on the electrode. On reverse scans, this Pd was reoxidized starting at about +0.40 volt *vs.* S.C.E.

The coulometric experiments were carried out with aliquots of iridium solution which, in the absence of palladium, were found to contain 10.12 mg. of Ir(IV) with a relative standard deviation of 0.1% for five determinations in each cell configuration. This value was also independent of control potential between +0.475 and +0.30 volt *vs.* S.C.E. In this potential range, the initial current was between 100 and 120 ma. and the time of the electrolysis was 6 to 7 minutes for both cell configurations. Thus, the cell efficiency was not changed significantly by rearrangement of its components. At potentials more anodic than +0.475 volt *vs.* S.C.E., the electrolysis of Ir(IV) was incomplete. The electrolysis was terminated and the readout measured when the current reached 100 μa. Background corrections were applied using the values of readout obtained when the 0.20*N* HCl alone was electrolyzed; these corrections were not larger than 0.05 mg. of Ir(IV) and were reproducible to ±0.005 mg.

The results of the analyses of Ir(IV) in presence of Pd(II) were found to be complicated by a reaction between Ir(IV) and the electroplated Pd metal. Determinations of Ir(IV) alone gave low results when the working electrode had previously been plated with Pd. It

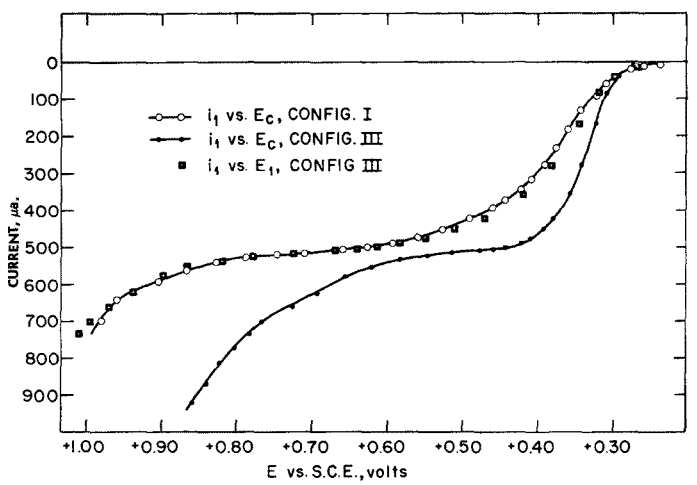

Figure 8. Working electrode 1 current as a function of potential in cell configurations I and III

could be seen that the dark deposit was stripped off the electrode by the Ir(IV) during the solution deaeration period. Thus, an electrode pretreatment procedure was adopted to ensure that no Pd was present on the electrode at the beginning of each electrolysis. This consisted of a 1-minute polarization of the electrode at +1.10 volts *vs.* S.C.E. in 0.50*N* HCl, which effectively stripped all the Pd from the electrode, followed by polarization in 0.20*N* HCl at the potential to be subsequently used, until the current decreased to 10 μa.

The results of the determination of 10.12 mg. of Ir(IV) in the presence of 10.9 mg. of Pd(II) are shown in Figure 11. The qualitative behavior of the electrolysis was the same and the precision of the results was the same as with the pure Ir(IV) solutions, with no difference between the two cell configurations except at the most cathodic control potential. At +0.325 volt *vs.* S.C.E. in cell configuration *B*, there appeared a dark deposit about 1 cm. in diameter on the portion of the working electrode adjacent to the counter electrode tube. This was identified by x-ray fluorescence as Pd and attests that the electrode potential was most cathodic in this area. The data of Figure 11 indicate clearly a difference between the two cells in the tolerance to Pd interference in the analysis. Further confirmation that this difference was due to Pd having been electroplated was sought by stripping the electrode at +1.10 volts *vs.* S.C.E. into a fresh HCl solution after each analysis. These solutions were analyzed spectrophotometrically by the procedure of Jacobs (*18*) and a good correlation was found between the observed bias and the amount of Pd found in the strip solution as a function of potential and cell configuration.

Because Ir(IV) reacts with the freshly plated Pd, the results of coulometric analyses performed without the stripping pretreatment, as would normally be done, would be dependent on the level of Pd in the previous sample and the amount of Pd already on the electrode. This is an example of a case in which expected interference is decreased by a chemical reaction between the primary reactant and the product of the interfering electrode reaction in a cyclic process. A reaction of this type could account for the lack of bias in the experiments reported by Fisher and coworkers (*33, 42*).

Both cell configurations have some imperfection in potential control because of the use of the reference electrode inside the porous glass tube. This effectively changes the area of solution sensed by the reference electrode in a manner such that increased *iR* drop is included in the measurement compared with the case in which the tip is placed directly in the solution close to the working electrode. However, this is a much less important error than that due to the placement of the counter electrode.

A general implication of these coulometric experiments which should be considered in designing an analytical procedure is that the level of tolerance to many interferences in controlled potential electrolysis methods may depend upon the type of electrolysis cell that is used.

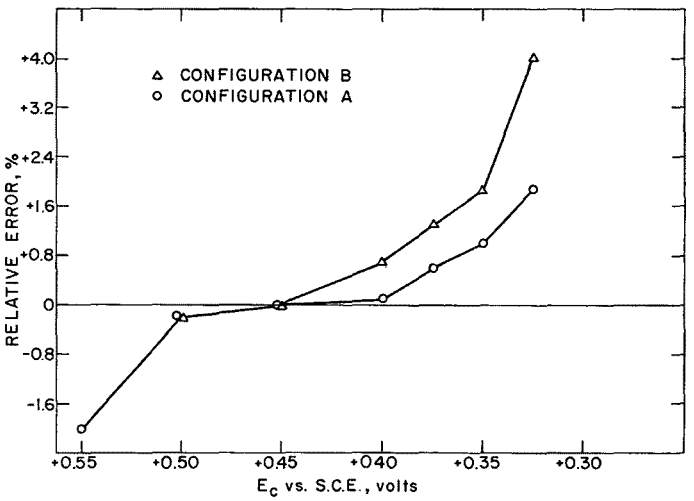

Figure 11. Accuracy of determination of Ir(IV) in the presence of Pd(II) by controlled-potential coulometry in two different cell configurations

THREE-ELECTRODE CELL DESIGN

Most of the controlled potential electroanalytical experiments which involve the use of large working electrodes employ either a cylindrical gauze or a mercury pool electrode in a cylindrical electrolysis vessel. Based on the knowledge of current and potential distribution in two-electrode cells and with the experiments and general theory outlined above as a background, some specific details of the design of three-electrode cells can be discussed. One very important design requirement is obtaining an arrangement as compact as possible to maximize the ratio of working electrode area to solution volume. Thus, the use of a remote counter electrode to produce uniform working electrode potential is not possible, and compromises in design goals usually must be made.

Cells with Cylindrical Gauze Working Electrodes. Use of a cylindrical gauze working electrode, provided the counter electrode is located coaxially within it, offers the best means for achieving uniform electrode potential distribution. A good example of this is the classical arrangement for electrogravimetry (*23*). Detailed mathematical treatments of distri-

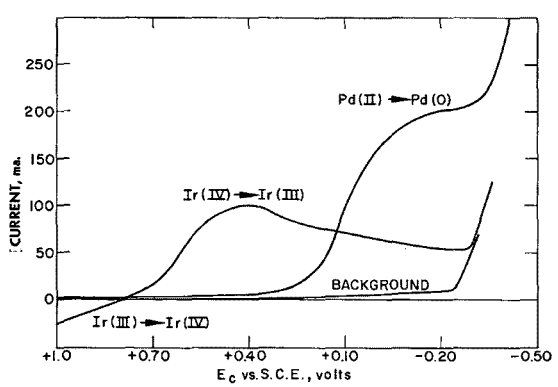

Figure 10. Voltammetric curves for Ir(III), Ir(IV), and Pd(II) in 0.20*N* HCl

butions in cells with cylindrical electrodes, including cases in which the counter electrode is external to the working electrode, can be found in the papers by Kasper (*20*, *22*) and Kronsbein (*24*, *26*). Breiter and Guggenberger (*7*) have studied the effect of reference electrode positioning in a cell with cylindrical symmetry and a centered, wire, working electrode.

Because the counter electrode frequently is isolated from the analytical solution by means of a salt bridge, the effective source of current is usually a fritted disk. This complicates the theoretical assessment of the arrangement, but the work of Kasper (*20*) indicates that to a good approximation the fritted disk may be considered an equipotential, uniform-current source if the counter electrode is located at least one disk diameter away inside the tube. Although no theoretical work is available for a disk source together with a cylinder, some estimates can be made of the desirability of certain configurations. Centering of a salt-bridge tube and fritted disk within the working electrode would probably be satisfactory, but a better arrangement would be the use of a cylindrical, conforming source such as the porous Vycor tube used in the coulometric experiments. Electrolysis vessels based on H-cells in which the counter electrode is located in one arm of the cell are likely to exhibit marked nonuniformity of potential at the working electrode.

Except when the working electrode is completely polarized, the current density will be greater at the top and bottom edges of the electrode even though the electrode potential is uniform. At the limiting current, a gradient in electrode potential will exist as a result of the electrode edges. However, these effects are decreased if the level of the solution is aligned with the top of the electrode and if the electrode is near the bottom of the cell.

Proper placement of the reference electrode in the cylindrical gauze cell is dictated by the potential distribution rather than the current distribution. Because of the wire mesh nature of the working electrode, each individual wire would have an equipotential encircling it. However, because of the open structure of the wire mesh, the entire electrode can be envisioned as having a series of concentric equipotentials inside the electrode which are repeated on the outside, provided the counter electrode is concentrically positioned. The spacing of the equipotentials in the solution on the outside would be greater because of decreasing current density at increasing distance. However, uniformity of electrodeposition obtained in this type of cell attests to the uniformity of current density *at the electrode*, and on both sides. The close agreement of inside

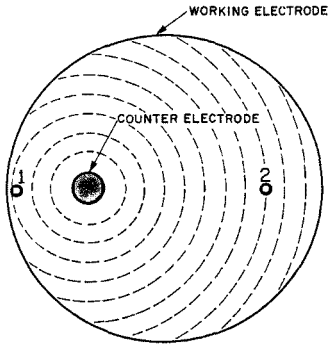

Figure 12. Distribution of potential inside a cylindrical gauze working electrode with an eccentric, cylindrical counter electrode

and outside potentials measured near a gauze electrode has been verified by experiment (*16*). Thus, the controlling reference electrode tip can be placed on either side of the gauze, but, in the interest of cell compactness, the logical position for the reference electrode tip is inside the cylindrical working electrode. At a given distance from the gauze, more uncompensated iR drop would be introduced into the control by placement of the reference electrode inside the working electrode (*29*, *30*), but there is no other inherent potential control difficulty in this arrangement and the possibly larger iR drop error is not detrimental in most analytical methods.

When the cell configuration and electrolysis conditions are such that the only appreciable electrode potential gradients are due to the edges of the electrode, the reference electrode tip should be placed at the edge. This region is where the electrode potential will be the most anodic in the case of an oxidation or most cathodic during a reduction.

If the two current-carrying electrodes in the cell are not concentrically positioned, the optimum placement of the reference electrode is further restricted. This can be seen in Figure 12 which shows a cross section of an idealized potential distribution on the inside of an eccentric cylindrical configuration under concentration polarization conditions. If the reference electrode is placed at location 2, the electrode potential would exceed the control potential in the region of location 1. To avoid exceeding the control potential, the reference electrode tip must be positioned on an equipotential which does not intersect the working electrode, and to minimize uncompensated iR drop errors, on the equipotential which approaches the working electrode most closely. The reference electrode tip thus can be located at a point on the line of minimum separation between the counter and working electrodes to achieve satisfactory potential control for analytical purposes. Thus formulated, these rules apply to all types of geometrical arrangements.

Cells with Mercury Pool Working Electrodes. Satisfactorily uniform potential distribution at the working electrode in cells of the mercury-pool type can be obtained only if the counter electrode or source approaches the diameter of the vessel in size, or is positioned a considerable distance from the pool. These conditions conflict with the size limitations of the other cell components and the requirement of minimum electrolysis solution volume. Nevertheless, if it is not necessary to isolate the counter electrode from the analytical solution, a basically good design which has been used frequently is that which incorporates a wire counter electrode which is wound in a large-diameter spiral in a plane parallel to the pool surface.

The cell design is more difficult when a counter electrode separator must be used. In analogy to the unshielded spiral counter electrode configuration above, Booman and Holbrook (*6*) described a ring-shaped separator which they reported gave negligibly low electrode potential gradients. If a conventional fritted-disk type separator is employed, the effects of such factors as the size of disk and its location must be evaluated. This boundary value problem was considered by Stouffer and Richardson (*41*), who obtained an equation relating the potential difference ΔE between the center of the working electrode and its periphery with the other experimental parameters:

$$\Delta E = \frac{2iR}{s} \sum_{j=1}^{\infty} \frac{J_1(\lambda_j s)\ [1 - J_0(\lambda_j r)]}{\lambda_j^2 J_0^2(\lambda_j r) \sinh\ (\lambda_j a)}$$

Here, i is the current density at the working electrode; R is the specific resistivity of the solution; r is the radius of the cylindrical cell; and s is the radius of the disk source, concentrically located at the same height, a, as the level of the solution. The J_n terms are Bessel functions of the first kind, and the parameter λ_j is evaluated from the zeros of $J_1(\lambda_j r)$. The disk was assumed to be a uniform-potential, uniform current-density source, and the problem was solved with the boundary condition of a uniform current at the working electrode. A somewhat similar problem was solved by Drossbach (*9*). The expression is relatively easy to evaluate because the series converges rapidly and the J_0 terms are constants at a given j. Because it is restricted to the specific configuration in which the disk is centered in the cell, the equation defines a best case as far as one cell characteristic is concerned; unsymmetrical cells would show larger total potential gradients. Although this equation cannot be used quantitatively in evaluating potential distributions

except in cells with this specific geometry, it provides a very useful general correlation between the experimental parameters. Thus, the influence of a and s on the potential distribution is defined, and as with all experiments in which the working electrode is completely polarized, the potential gradient is directly proportional to the current density and solution resistance.

On the basis of these considerations, the proper location for the reference electrode is obvious, provided the exact potential distribution is known. In the general case when the potential distribution is known only approximately, the best approach is to use the same procedure as described with wire mesh electrodes—i.e., the reference electrode should be placed on the line of minimum separation between the counter and working electrodes.

ACKNOWLEDGMENT

The authors express their appreciation to Ervin Behrin for the design of portions of the instrumentation, to Ralph G. Gutmacher and Donald McCoy for the x-ray fluorescence analysis, and to Roman Bystroff for assistance in the spectrophotometric determinations. The helpful comments on this work by Dale J. Fisher of the Oak Ridge National Laboratory are gratefully acknowledged.

LITERATURE CITED

(1) Agar, J. N., Hoar, T. P., *Discussions Faraday Soc.* 1, 158, 162 (1947).
(2) Aletti, R., *et al.*, *Proc. Intern. Comm. Electrochem. Thermodyn. Kinet.*, 3rd Meeting, Manfredi, Milan, p. 30 (1952).
(3) Bard, A. J., Mayell, J. S., *J. Phys. Chem.* 66, 2173 (1962).
(4) Bard, A. J., Solon, E., *Ibid.*, 67, 2326 (1963).
(5) Barnartt, S., *J. Electrochem. Soc.* 108, 102 (1961).
(6) Booman, G. L., Holbrook, W. B., ANAL. CHEM. 35, 1793 (1963).
(7) Breiter, M., Guggenberger, T., *Z. Elektrochem.* 60, 594 (1956).
(8) deLevie, R., *J. Electroanal. Chem.* 9, 311 (1965).
(9) Drossbach, P., *Z. Elektrochem.* 56, 599 (1952).
(10) Fleck, R. N., Hanson, D. N., Tobias, C. W., U. S. Atomic Energy Comm. *Rept.* UCRL-11612 (1964).
(11) Gelb, R. I., Meites, L., *J. Phys. Chem.* 68, 630 (1964).
(12) Geske, D. H., Bard, A. J., *Ibid.*, 63, 1057 (1959).
(13) Guillou, M., *Bull. Soc. France Electriciens* 5, 439 (1964); *C.A.* 61, 15662a (1964).
(14) Haring, H. E., Blum, W., *Trans. Electrochem. Soc.* 44, 313 (1923).
(15) Harrar, J. E., ANAL. CHEM. 35, 893 (1963).
(16) Harrar, J. E., Lawerence Radiation Laboratory, Livermore, Calif., unpublished research, 1963.
(17) Hull, R. O., *Monthly Rev. Am. Electroplaters Soc.* 26, 753 (1939).
(18) Jacobs, W. D., ANAL. CHEM. 33, 1279 (1961).
(19) Kardos, O., Foulke, D. G., in "Advances in Electrochemistry and Electrochemical Engineering," Vol. 2, 145–233, C. W. Tobias, ed., Interscience, New York, 1962.
(20) Kasper, C., *Trans. Electrochem. Soc.* 77, 353, 365 (1940); 82, 153 (1942).
(21) *Ibid.*, 78, 131 (1940).
(22) *Ibid.*, p. 147.
(23) Klingert, J. A., Lynn, S., Tobias, C. W., *Electrochim. Acta* 9, 297 (1964).
(24) Kronsbein, J., *J. Electrodepositors Tech. Soc.* 17, 83 (1942).
(25) Kronsbein, J., *Plating* 37, 851 (1950).
(26) *Ibid.*, 39, 165 (1952).
(27) Lingane, J. J., "Electroanalytical Chemistry," 2nd ed., p. 174, Interscience, New York, 1958.
(28) *Ibid.*, pp. 351–3.
(29) *Ibid.*, p. 357.
(30) *Ibid.*, pp. 365–6.
(31) Macaire, M., Guillou, M., Buvet, R., *J. Chim. Phys.* 60, 775 (1963).
(32) Moulton, H. F., *Proc. London Math. Soc.* (Ser. 2) 3, 104 (1905).
(33) Mueller, T. R., U. S. Atomic Energy Comm. *Rept.* ORNL-3750, 5 (1965).
(34) Newman, J., *Ibid.*, UCRL-16665, UCRL-16747 (1966).
(35) Orr, C. H., Wirth, H. E., *J. Phys. Chem.* 63, 1150 (1959).
(36) Page, J. A., *Talanta* 9, 365 (1962).
(37) Rousselot, R. H., *Metal Finishing* p. 56, October 1959.
(38) Rousselot, R. H., "Repartition du Potentiel et du Courant dans les Electrolytes," pp. 22–3, Dunod, Paris, 1959.
(39) Schaap, W. B., McKinney, P. S., ANAL. CHEM. 36, 29, 1251 (1964).
(40) Schwarz, W. M., Shain, I., *Ibid.*, 35, 1770 (1963).
(41) Scott, F. A., Stouffer, J. C., Richardson, R. L., *Doc. No.* HW 80365, Hanford Atomic Products Operation, Richland, Wash., 1964.
(42) Stelzner, R. W., Kelley, M. T., Fisher, D. J., U. S. Atomic Energy Comm. *Rept.* ORNL-3537, pp. 9–12 (1964).
(43) Wagner, C., in "Advances in Electrochemistry and Electrochemical Engineering," Vol. 2, 8–14, C. W. Tobias, ed., Interscience, New York, 1962.
(44) Wagner, C., *J. Electrochem. Soc.* 98, 116 (1951).

RECEIVED for review April 28, 1966. Accepted June 17, 1966. Work supported by U. S. Atomic Energy Commission Contract Nos. AT(11-1)-1083 and W-7405-eng-48.

Evaluation of Stationary Electrode Polarography and Cyclic Voltammetry for the Study of Rapid Electrode Processes

S. P. PERONE

Department of Chemistry, Purdue University, Lafayette, Ind.

▷ **The application of stationary electrode polarography and cyclic voltammetry to the study of very rapid electrode processes has been evaluated using a solid-state operational amplifier potentiostat. Several different redox systems, representing reversible, irreversible, and quasi-reversible behavior, were investigated. Potential scan rates varying from 1.0 to 50,000 volts/second were employed. In addition, to test further the time-response characteristics of the potentiostat and electrolysis cell, potentiostatic current–time experiments were performed under diffusion-limited conditions with measurements made in the 5- to 200-μsec. region. It is concluded that scan rates as fast as 2000 volts/second may be employed with confidence in fast sweep experiments where the response characteristics of the potentiostat and electrolysis cell have been optimized. Scan rates as fast as 20,000 volts/second or greater appear possible under these conditions, but the interpretation of data in some cases may be difficult due to sweep distortion by potentiostat response or uncompensated ohmic losses. The results of these experiments indicate that chemical rate processes coupled to the charge transfer step may be studied with time resolution of the order of 1–100 μsec., using linear sweep techniques.**

THE ELECTROCHEMICAL techniques of stationary electrode polarography and cyclic voltammetry offer a distinct advantage for the investigation of complicated electrode processes. Variation of the scan rate parameter results in peak current and/or peak potential changes characteristic of the mechanism of the particular electrode process. In addition, kinetic data for coupled homogeneous chemical reactions may be evaluated quantitatively from rigorously derived expressions relating the rate parameters to the characteristics of current–voltage curves obtained (*9*). Furthermore, in theory, the time scale of an experiment in stationary electrode polarography or

cyclic voltammetry may be adjusted to match the kinetics of the process being studied by increasing or decreasing the scan rate to the appropriate range.

Although successful applications of these stationary electrode techniques for studies of slow to moderately fast processes (using scan rates up to about 200 volts/second) have been reported (*8*, *15*), their extension to the study of very rapid processes (scan rates greater than 200 volts/second) have not been reported. Two primary reasons for the lack of application to rapid electrode processes can be pointed out: First, charging currents become large compared to faradaic signals, even for millimolar solutions, when scan rates greater than 100 volts/second are employed. Moreover, because charging current depends on the first power of scan rate and faradaic current depends on the square-root power, further increases in scan rate result eventually in the complete obliteration of the faradaic signal.

The second and most important problem involved in the study of rapid electrode processes is that concerning instrumental and cell response. The essential characteristics of this problem have been discussed extensively recently (*2*, *3*, *14*); although these treatments have been oriented toward response to a step-function input signal, the conclusions can be applied in principle to the linear sweep case considered here. The important experimental factors involved are the rise-time, stability, and current capacity of the potentiostat; the total cell resistance; the uncompensated resistance; and the double-layer capacity. The primary objective of the work reported here was to optimize these experimental factors such that the investigation of electrode processes with microsecond time resolution might be possible utilizing linear sweep techniques.

EXPERIMENTAL

Instrumentation. The potentiostat used in this work was constructed from a P35A solid-state differential operational amplifier and a P66A solid-state current booster amplifier obtained from G. A. Philbrick Researches, Inc., Dedham, Mass. The P66A was wired with external ballast resistors, allowing currents of ±100 ma. to be drawn (*11*). The power supply was a Philbrick PR-300, ±15 volts, ±300-ma. supply.

The circuit for the controlled potential experiments performed here is shown in Figure 4*b* of Schwarz and Shain (*13*). The working electrode was grounded directly; the reference electrode potential was sampled directly at the inverting input of the P35A. The noninverting input of the P35A was driven by the ground-referenced potential function to be imposed across the working and reference electrodes; the output of the P35A was followed by the P66A booster and was applied to the counter electrode. A floating load resistor was placed in the feedback loop, and currents were measured by sampling the *iR* drop with the differential input of a Type D plug-in unit in a Model 536 Tektronix oscilloscope. For cyclic scan experiments, the horizontal deflection of the scope was driven by the reference electrode potential, using a Type G plug-in. For single cathodic sweep experiments, the Type T time-base plug-in was used to generate a horizontal sweep. Oscilloscope traces were recorded with a DuMont No. 2620 Polaroid camera.

Square-wave and triangular-wave signals were generated by a Hewlett-Packard Model No. 3300A function generator with a No. 3302A plug-in trigger unit. Single or continuous scans could be generated from frequencies of 0.008 to 100,000 c.p.s. Sawtooth signals were generated by taking the sawtooth output of a Tetronix Type T plug-in unit and dividing it down to an appropriate level. For all cyclic experiments, the triangular-wave amplitude was 0.50 volt; for all single cathodic sweep experiments, the amplitude was 1.00 volt.

The characteristics of the operational amplifiers used in the potentiostat circuit have been published (*11*, *12*). The selection of the P35A as the control amplifier was a compromise choice based on its bandpass (4 Mc.) and input impedance (1.5 megohms). A higher bandpass differential amplifier would be preferable, but none was available with sufficiently high input impedance. The choice of the P66A as booster amplifier was arbitrary. Other booster amplifiers are available (particularly vacuum tube type) which can deliver significantly more power. One of these should be used for maximum performance with potential-step type experiments or with large area electrodes (*2*). However, for linear sweep experiments with microelectrodes at scan rates less than 100,000 volts/second, the current capacity of the P66A was considered adequate. No significant improvement in frequency response, and considerable loss of stability, resulted when a Krohn-Hite DCA-10 10-watt booster amplifier replaced the P66A.

For slow scan experiments, to minimize high-frequency noise, a variable capacitance was connected from the output of the P35A to its inverting input. Very small capacitance values were required (0.0001 to 0.01 mf.), and no alteration of response characteristics for slow scans was observed. For scan rates greater than about 200 volts/second, no feedback capacitance was required. No attempts to add stabilizing circuits, such as those discussed by Booman and Holbrook (*3*), were made, because the potentiostat remained stable and responsive under the most extreme conditions imposed in this work.

Evaluation of Optimum Response and Uncompensated Resistance. The most critical experimental maneuver in this work was the adjustment of the reference electrode probe–working electrode separation for optimum response. A Luggin capillary probe was used and placement of the mercury drop electrode was as close as possible to the probe without loss of stability in the potentiostat. As pointed out by Booman and Holbrook (*3*), potentiostat stability and control are lost when the uncompensated resistance is reduced to zero. On the other hand, it was observed in this work that the electrode separation could be reduced in most cases to less than 0.1 mm. without loss of stability or control. Thus, for each system investigated, the cell response was optimized, at the fastest scan rate to be used with that system, by gradually bringing the working electrode closer to the reference probe until loss of control was indicated by large oscillations in the voltammetric curves. The working electrode was backed off from this point until the circuit had just re-achieved stability, and just tolerable oscillations were obtained. This position was considered optimum and was readily reproducible. For relatively low conductivity solutions, this situation was achieved just at the point of light contact between the Luggin capillary and the mercury drop. In very high conductivity solutions, the optimum separation of Luggin capillary probe and working electrode was the order of 0.1 mm.

The uncompensated resistance, R_u, could be estimated in one of two ways. The electrolyte conductivity and reference probe placement could be combined to calculate R_u as described by Booman and Holbrook (*2*). This approach requires an accurate measure of the working electrode–reference probe separation for best results. Another approach applied in this work was to use a system which behaved reversibly up to very fast scan rates where relatively large currents would flow. At a scan rate where the first definite measurable shift in E_p occurred, an estimate was made of the uncompensated resistance which would completely account for the shift. This set an upper limit to R_u under the conditions obtained in the electrolysis cell. This value of R_u could be used for correcting peak shifts in the investigation of systems with similar conductivity and reference probe placement. In any event, the lowest estimated upper limit of R_u was used. For example, an estimated value of R_u of 1.0 ohm was obtained in the investigation of Cd(II) in 1.0*M* KNO_3 from the initial shift of E_p at 2000 volts/second. [The procedure of Booman and Holbrook (*2*) predicts an upper limit of 3 to 4 ohms for R_u.] This lower value of R_u was used in correcting data obtained in 1.0*M* Na_2SO_4 solution, because very similar conductivity was obtained, and placement of the Luggin capillary was identical.

For the high conductivity solutions, such as 3.7*M* H_2SO_4 used in this work, R_u was estimated to be 0.6 ohm by the procedure of Booman and Holbrook (*2*).

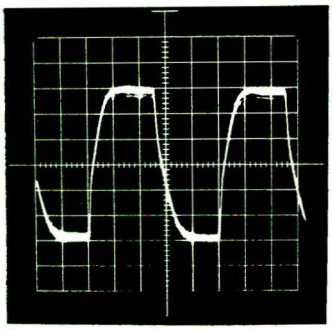

Figure 1. Response to square-wave input

Plot of working *vs.* reference electrode potential. Vertical scale, 0.050 volt/div.; horizontal scale, 2 μsec./div. Sample solution $1 \times 10^{-3}M$ Cd(II), 1.0*M* KNO_3; hanging mercury drop electrode; load resistor, 5 ohms

Cells and Electrodes. The cell and electrode assembly has been described previously (*10*). The only changes for this work were that the counter electrode was a 6-cm., 22-gauge platinum wire coiled in a 2-cm. diameter circle around the working electrode and that a Luggin capillary salt bridge (*4*) was used to isolate the reference electrode from the sample solution. The large saturated calomel reference electrode was separated from the Luggin salt bridge, which contained the same inert electrolyte as the sample solution, by a fine porosity sintered glass disk. The end of the Luggin probe was bent into a U-shape with the tip pointed up and positioned directly below the working electrode. This arrangement allowed easy and reproducible manual adjustment of the reference–working electrode separation.

The radii of the hanging drop electrodes used in this work were the order of 0.05 cm.

All experiments were performed at ambient temperatures between 23° and 25° C.

Reagents. All chemicals used in this work were reagent grade. The water used in preparing all solutions was purified either by triple-distillation or by passage of single-distilled water over a mixed-bed cation–anion exchange resin. No significant difference in electrochemical behavior was observed for the different sources of purified water.

High purity nitrogen was used for deaeration.

RESULTS AND DISCUSSION

The most important question in this work is that of evaluating the response characteristics of the instrumentation and electrolysis cell. One approach to this problem is to evaluate the transfer functions of the potentiostat electrolysis cell and predict the response limitations imposed by various combinations of cell resistance, uncompensated resistance, and double-layer capacitance (*2, 3, 14*). This approach is strictly applicable only for the case where faradaic currents are negligible (*3*), although the general principles involved are useful guidelines. [The combined effects of faradaic and capacitive currents in the potential-step approach have been discussed by Booman and Holbrook (*3*)].

An alternate approach to evaluating response characteristics would be to monitor the potential difference between the working and reference electrodes in the actual electrolysis cell and compare this with the input signal. This method would give an estimate of the fastest rise-time obtainable; that is, the response would reflect the characteristics of the potentiostat upon driving a capacitive load through the experimentally attainable uncompensated resistance. However, the actual time-dependence of the working electrode potential might be distorted due to uncompensated ohmic losses (*6, 7*).

Perhaps the best way to evaluate combined instrumental and cell response is to investigate an electrode process whose behavior could be predicted accurately for very rapid scan rates.

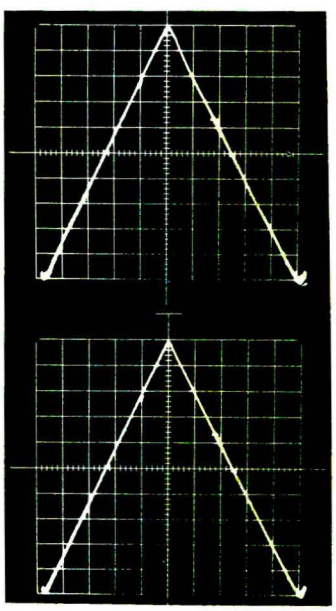

Figure 2. Response to triangular-wave input

10,000 volts/second; vertical scale, 0.050 volt/div.; horizontal scale, 10 μsec./div. Lower trace: output of function generator Upper trace: plot of working *vs.* reference electrode potential with triangular wave input at 10,000 volts/second. Load resistor, 5 ohms; sample solution same as for Figure 1; hanging mercury drop electrode

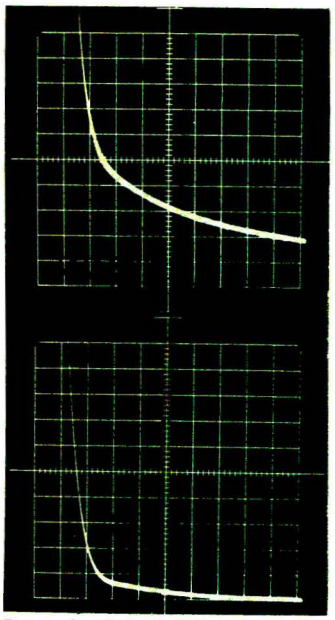

Figure 3. Potentiostatic current–time curves

$1 \times 10^{-3}M$ Cd(II), 1.0*M* KNO_3; hanging drop electrode; vertical scale, 2 ma./div.; horizontal scale, 5 μsec./div.
Upper trace: potentiostatic reduction of Cd(II)
Lower trace: blank, in 1.0*M* KNO_3

For example, a process which exhibited reversible cyclic-voltammetric behavior from slow scans through megacycle frequencies would be ideal. However, no such system has been reported. Thus, one is limited at best to investigating quasi-reversible processes. On the other hand, the voltammetric behavior of these processes may be predicted theoretically as a function of scan rate (*8*), and the study of these processes proved useful in this work.

Potentiostat Response Characteristics. The combined response of the solid-state potentiostat and the electrolysis cell to both square-wave and triangular-wave input signals is illustrated in Figures 1 and 2. For a step function, the rise-time appears to be the order of 2 to 3 μsec. Furthermore, for the triangular-wave signal no significant distortion appears at scan rates below about 50,000 volts/second.

To further characterize the rise-time of the potentiostat a potential-step experiment was performed with $1.0 \times 10^{-3}M$ Cd(II) in 1.0*M* KNO_3. The potential was stepped from −0.47 to −0.77 volt *vs.* S.C.E., where $E_{1/2}$ is −0.60 volt. Thus, diffusion-controlled currents were expected, and a linear plot of i *vs.* $t^{-1/2}$ should have been obtained (*5*). Figure 3 shows the shapes of the electrolysis current–time curve

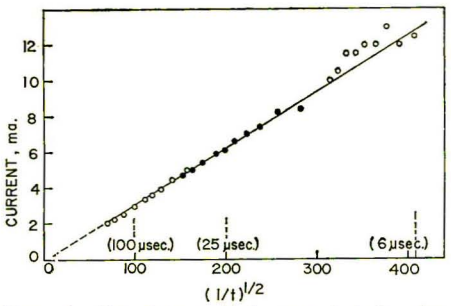

Figure 4. Plot of i vs. $t^{-1/2}$ for potentiostatic reduction of Cd(II) at the hanging drop electrode

and the blank obtained in the first 50 μsec. Figure 4 shows a plot of data obtained from 3 different current–time curves covering the range from a few μsec. to 200 μsec. The currents are corrected for blanks, and a linear plot of i vs. $t^{-1/2}$ is indeed obtained with measurements at times as short as 6 μsec. Scatter in the data at short times is due to random errors in subtracting comparable numbers. Blank-corrected currents at shorter times were consistently low, perhaps indicating that the uncompensated ohmic loss at short times was so large that the working electrode could not attain a sufficiently cathodic potential for diffusion control.

A 6-μsec. potentiostatic rise-time does not necessarily define the limiting response for linear sweep experiments. With linear sweep techniques charging current flows continuously at a relatively constant level, whereas in controlled potential-step experiments extremely large current surges are required to charge the double layer in a few microseconds (*2*). The response-limiting step for linear sweep experiments is the attainment of a charging current level sufficient to maintain the imposed scan rate. Although this accomplishment may not be instantaneous, if the potentiostat catches up with the input signal before the foot of the voltammetric wave, no scan rate error occurs. (Of course, some sweep distortion may occur during the faradaic peak due to uncompensated ohmic losses.) Observations of the shapes of charging current curves, with the reference electrode probe located for minimum uncompensated resistance, indicated that the initial induction period required before the imposed voltage coincided with the input signal varied with the value of uncompensated resistance obtained. Thus, in 1.0M KNO_3 the induction period was the order of 10 to 15 μsec.; in 3.7M H_2SO_4 the induction period lasted only 2 to 4 μsec. No data were reported in this work for cases where this induction period appeared to extend beyond the foot of the voltammetric wave.

Rapid Linear Sweep Experiments with Various Electrode Processes. Reversible and Irreversible Systems. Three systems were selected for study as typical reversible and irreversible processes. These were Fe(III) in 0.3M oxalate–0.1M oxalic acid solution, Cd(II) in 1.0M KNO_3, and Ni(II) in 0.2M KNO_3. The first two are ordinarily considered to be among the fastest electrode processes, whereas the last system is completely irreversible. None of the three systems studied with single-sweep experiments was found completely satisfactory for characterizing the overall instrumental response. Ni(II) behaved as predicted (*9*); the reduction peak shifted cathodic with increasing scan rate, but became obscured by solvent reduction for scan rates greater than 100 volts/second. Both Fe(III) and Cd(II) remained reversible up to scan rates of about 1000 volts/second, (as indicated by constant values of E_p and $i_p/v^{1/2}$). However, for faster scan rates, deviation from reversibility was observed, which could not be accounted for by uncompensated ohmic losses alone. On the other hand, no deviation occurred at scan rates lower than 1000 volts/second. Thus, confidence in the overall instrumental response for scan rates up to this range was established. Figure 5 compares linear sweep current–voltage curves for Fe(III) at a slow scan rate and at 1000 volts/second.

Quasi-Reversible Systems. The investigation of typical quasi-reversible systems proved satisfactory for the evaluation of instrumental response, because deviations from reversibility occurred at slower scan rates, where heterogeneous kinetic parameters could be measured with confidence. Correlation with values obtained at faster scan rates then provided a reliable check on instrumental limitations.

Nicholson (*8*) has described the theoretical cyclic voltammetric behavior expected with quasi-reversible systems. The behavior depends on the fundamental parameters, k_s and α, and on a

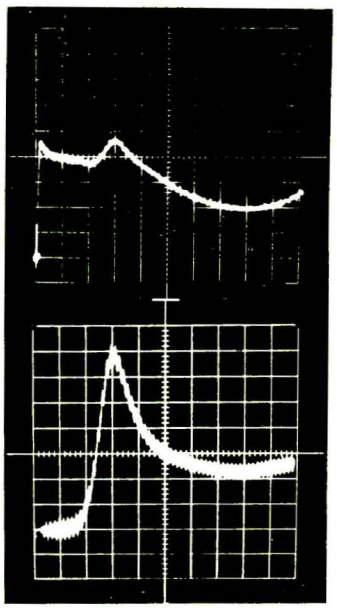

Figure 5. Linear-sweep current–voltage curves for Fe(III) at the hanging drop electrode

1×10^{-3}M Fe(III), 0.3M oxalate, 0.1M oxalic acid. Single-sweep experiments
Upper trace: 1000 volts/second; vertical scale, 200 μa./div.; horizontal scale, 0.100 volt/div.
Lower trace: 1.0 volt/second; vertical scale, 1.4 μa./div.; horizontal scale, 0.100 volt/div.

defined variable, ψ. k_s is the standard heterogeneous rate constant; α is the transfer coefficient; and ψ is defined as $\gamma^{\alpha}k_s/(\pi a D_0)^{1/2}$, where a is nFv/RT, v is the scan rate, γ is $(D_0/D_R)^{1/2}$, and the other symbols have their usual significance. The separation of cathodic and anodic peaks is dependent on ψ. Experimentally, the peak separation with a particular scan rate is compared to a working curve of $(n\Delta E_p)$ vs. ψ. With ψ evaluated, a value of k_s may be obtained as long as the constant terms are known. As Nicholson points out (*8*), the value of α has relatively little effect on the working curve, and theoretical curves with $\alpha = 0.5$ may be used with reasonable accuracy for $\psi > 0.1$.

In the work reported here, values of ψ less than 0.1 were encountered. Thus, an accurate evaluation of α had to be made for each system to compare experimental to theoretical data. The technique used to evaluate α involved a determination of the symmetry of the cyclic voltammetric curve under conditions where large peak shifts had occurred. The observed symmetry was then compared with the predicted symmetry for various values of α. Theoretical computations were made using the IBM 7094 computer and

Table I. Effhct of α on Symmetry

α	$n(E_{pc} - E_{1/2})$, mv.	$n(E_{pa} - E_{1/2})$, mv.
0.25	−182	82
0.40	−133	94
0.50	−114	103
0.60	−101	116

For all data in Table, $\psi = 0.10$.

Nicholson's numerical solution (*8*). A switching potential of $350/n$ mv. past $E_{1/2}$ was used arbitrarily for all calculations. The cathodic peak shifts, anodic peak shifts, and total peak separations were computed for α-values of 0.25, 0.4, 0.5, and 0.6 with ψ- values from 0.030 to 0.75. At the uppermost ψ-value insignificant differences between computations for each α-value were obtained.

To illustrate the relationship between symmetry and α, Table I gives cathodic and anodic peak shifts at $\psi = 0.10$ for the various values of α. For an accurate evaluation of α, it was necessary to obtain data for ψ less than 0.20.

The two quasi-reversible systems selected for study here were Cd(II) in 1.0*M* Na_2SO_4 and in 3.7*M* H_2SO_4. The first system was selected for comparison to kinetic data obtained by Nicholson (*8*) who used scan rates varying from 48 to 120 volts/second and obtained a k_s-value of 0.24 cm./second. The second system was selected because the high acid electrolyte provided nearly the highest conducting medium available. Thus, uncompensated resistance problems were minimized in the sulfuric acid solution, and the most rapid measurements were made in that medium.

Cyclic voltammetric curves were obtained from both single- and multi-sweep experiments. Although slight differences in the peak heights were observed, differences in peak separations were negligible. These observations were consistent with those of Nicholson (*8*). Thus, multi-sweep data were used for all correlations reported here, because oscilloscopic observations could be made more conveniently under steady-state conditions.

Tables II and III summarize the cyclic voltammetric data obtained with each system at the hanging mercury drop electrode. Figure 6 shows typical curves obtained near the upper limit of scan rates employed. The values of k_s given in Table II for 1.0*M* Na_2SO_4 are in good agreement with Nicholson's results. Confidence in the values of k_s evaluated in both Na_2SO_4 and H_2SO_4 is justified by the consistency observed with scan rates varied from 50 to 5000 or 10,000 volts/second. The value of α obtained in 1.0*M* Na_2SO_4 (0.53) does not agree well with that obtained by Nicholson (*8*). However, for his work an accurate value of α was not required, and his reported value of 0.25 was admittedly a rough estimate. Moreover, a value of 0.37 has been obtained by Bauer and Elving (*1*) with a.c. polarographic measurements in 1.0*M* Na_2SO_4.

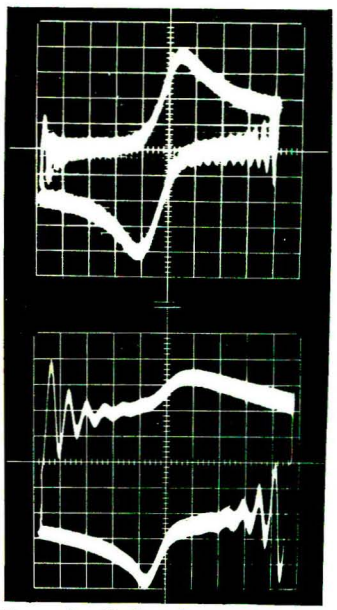

Figure 6. Cyclic voltammetric curves for Cd(II) at the hanging drop electrode

Upper trace: 1.0 × 10^{-3}M Cd(II), 1.0M Na_2SO_4; 1000 volts/second; vertical scale, 0.5 ma./div.; horizontal scale, 0.052 volt/div. Lower trace: 1 × 10^{-3}M Cd(II), 3.7M H_2SO_4; 5000 volts/second; vertical scale, 1.25 ma./div.; horizontal scale, 0.052 volt/div.

Table II. Cyclic Voltammetric Data for Cd(II) in 1.0M Na_2SO_4 at the Hanging Drop Electrode

Scan Rate, v, volts/second	$n\Delta E_p$, mv.	ψ	k_s, cm./second
50	86	0.91	0.33 ± 0.06
100	98	0.61	0.31 ± 0.04
200	117	0.38	0.28 ± 0.04
500	140	0.26	0.31 ± 0.05
1000	160	0.20	0.33 ± 0.06
2000	188	0.14	0.32 ± 0.05
5000	244	0.074	0.27 ± 0.05

ψ-values based on $\alpha = 0.53$. Uncertainties in k_s reflect uncertainty in measuring peak separations.

Table III. Cyclic Voltammetric Data for Cd(II) in 3.7M H_2SO_4 at the Hanging Drop Electrode

Scan rate, v, volts/second	$n\Delta E_p$, mv.	ψ	k_s, cm./sec.
200	89	0.80	0.59 ± 0.11
500	104	0.54	0.63 ± 0.08
1,000	122	0.38	0.61 ± 0.08
2,000	141	0.26	0.61 ± 0.10
5,000	160	0.19	0.69 ± 0.09
10,000	200	0.12	0.63 ± 0.07

ψ-values based on $\alpha = 0.58$. Uncertainties in k_s reflect uncertainty in measuring peak separations.

The peak shifts reported in Tables II and III were corrected for uncompensated ohmic contribution in the conventional manner (*7*). The uncompensated resistance in each case was estimated as described in the Experimental section. In the worst case for 3.7*M* H_2SO_4 (10,000 volts/second), the correction amounted to 12 mv. out of a total 112-mv. peak separation. The worst case for 1.0*M* Na_2SO_4 (5000 volts/second) involved 8 mv. out of a total 130-mv. peak separation. This type of correction, of course, does not account for any distortion of the sweep rate around the peak. For large ohmic losses this could cause considerable error because the peak location is theoretically scan rate dependent. For this reason, reported data for scan rates beyond about 2000 volts/second with these systems at the hanging drop electrode may be in error.

Cyclic Voltammetric Data with a Smaller Working Electrode. To make measurements where uncompensated ohmic losses were negligible at the

fastest scan rates investigated, cyclic voltammetric data were obtained using as a working electrode only the mercury-plated platinum wire tip (*16*) from which mercury drops were ordinarily hung. The area of the working electrode formed this way, and hence the corresponding voltammetric currents, were about an order of magnitude smaller than for the hanging mercury drop electrode. The surface was replenished for each run by hanging two drops in sequence and knocking them off. The area reproducibility was poor and depended upon how much mercury adhered when a drop was knocked off. However, if only a measure of the peak separation was required, the approach was satisfactory.

Table IV summarizes the cyclic voltammetric data obtained with this small area working electrode for $1 \times 10^{-3}M$ Cd(II) in $3.7M$ H_2SO_4. Figure 7 shows typical current–voltage curves obtained. With the small area electrode uncompensated ohmic losses appeared negligible up to a scan rate of 20,000 volts/second. However, because of the increased proportion of charging current at the higher scan rates it is very difficult to locate peak potentials with good accuracy for scan rates greater than 10,000 volts/second. One approach used satisfactorily in this work was to increase sensitivity and look at only one branch of the cyclic curve at a time.

Table IV. Cyclic Voltammetric Data for Cd(II) in $3.7M$ H_2SO_4 at a Mercury Electrode of Reduced Size

Scan rate, v, volts/second	$n\Delta E_p$, mv.	ψ	k_s, cm./second
200	90	0.80	0.58 ± 0.11
500	114	0.40	0.60 ± 0.08
1,000	126	0.35	0.57 ± 0.08
2,000	148	0.24	0.55 ± 0.10
5,000	176	0.16	0.59 ± 0.09
10,000	204	0.11	0.58 ± 0.07
20,000	240	0.077	0.58 ± 0.07
50,000	290	0.048	0.55 ± 0.08

ψ-values based on $\alpha = 0.58$. Uncertainties in k_s reflect uncertainty in measuring peak separations.

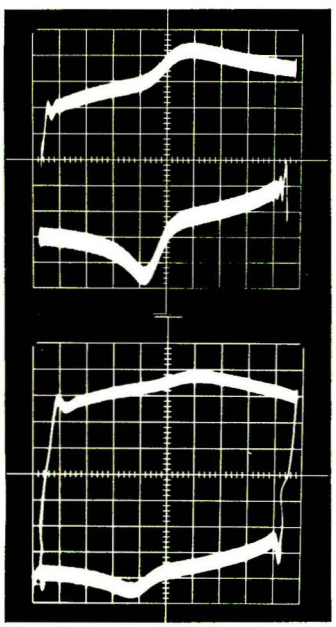

Figure 7. Cyclic voltammetric curves for Cd(II) at a reduced-size mercury electrode

1×10^{-3}M Cd(II), 3.7M H_2SO_4
Upper trace: 5000 volts/second; vertical scale, 65 μa./div.; horizontal scale, 0.052 volt/div.
Lower trace: 20,000 volts/second; vertical scale, 250 μa./div.; horizontal scale, 0.052 volt/div.

Good agreement exists between data obtained with the hanging mercury drop electrode, with correction for ohmic losses, and the data with the smaller electrode where no significant uncompensated ohmic loss was involved. This correlation indicates that the method of evaluation of and correction for uncompensated resistance used in experiments with the hanging drop were reasonably accurate. On the other hand, attempts to use the smaller electrode with less highly conducting solutions were only moderately successful, because placement of the working electrode for minimum uncompensated resistance was more critical. The small size of the working electrode and the design of the Luggin capillary made it quite difficult to find and reproduce optimum placement. Further work in the design of an electrolysis cell utilizing the smaller working electrode is in progress.

From the data in Table IV one might conclude that scan rates as fast as 50,000 volts/second may be employed in the study of rapid electrode processes. However, one must recognize that the experimental conditions obtained for data reported in Table IV may not always be realizable. Working with typical nonacid electrolyte media of 0.1 to $1.0M$, the fastest scan rate attainable with confidence is probably about 1000 to 5000 volts/second. However, considering the major portion of a typical stationary electrode polarogram to encompass about 100 mv., a scan rate of 1000 volts/second enables one to observe a complete polarographic experiment in the order of 100 microseconds. Moreover, a scan rate of 50,000 volts/second corresponds to a complete polarographic experiment in about 2 μsec. Thus, the study of chemical rate processes coupled to charge transfer with first-order rate constants as large as 10^4 to 10^6 second^{-1} ought to be possible.

ACKNOWLEDGMENT

The author acknowledges the stimulating conversations of Irving Shain and Richard Nicholson regarding this work. The author also acknowledges the assistance of C. V. Evins who carried out the numerical calculations.

LITERATURE CITED

(1) Bauer, H. H., Elving, P. J., ANAL. CHEM. **30**, 341 (1958).
(2) Booman, G. L., Holbrook, W. B., *Ibid.*, **35**, 1793 (1963).
(3) Booman, G. L., Holbrook, W. B., *Ibid.*, **37**, 795 (1965).
(4) Delahay, Paul, "New Instrumental Methods in Electrochemistry," 2nd ed., p. 393, Interscience, New York, 1954.
(5) *Ibid.*, p. 51.
(6) *Ibid.*, p. 132.
(7) Nicholson, R. S., ANAL. CHEM. **37**, 667 (1965).
(8) *Ibid.*, p. 1351.
(9) Nicholson, R. S., Shain, I., *Ibid.*, **36**, 706 (1964).
(10) Perone, S. P., Mueller, T. R., *Ibid.*, **37**, 2 (1965).
(11) Philbrick Researches, Inc., *Bull.* **P66A/1B1**, Rev. June 1, 1965.
(12) Philbrick Researches, Inc., *Bull.* **P35A/1B1**, Rev. April 1, 1965.
(13) Schwarz, W. M., Shain, I., ANAL. CHEM. **35**, 1770 (1963).
(14) Shain, I., Harrar, J. E., Booman, G. L., *Ibid.*, **37**, 1768 (1965).
(15) Shuman, M. S., Shain, I., Great Lakes Regional ACS Meeting, Chicago, Ill., June 1966.
(16) Underkofler, W. L., Shain, I., ANAL. CHEM. **33**, 1966 (1961).

RECEIVED for review April 6, 1966. Accepted May 31, 1966. Great Lakes Regional Meeting, ACS, Chicago, Ill., June 1966. Work supported by Public Health Service Research Grant No. CA-07773-02 from the National Cancer Institute.

Automatic Determination of Weak Organic Acids by Partition Column Chromatography and Indicator Titration

LEO KESNER and EDWARD MUNTWYLER

Department of Biochemistry, State University of New York Downstate Medical Center, Brooklyn, N. Y. 11203

▶ Quantitative determination of organic acids in the range 0.05 to 3 μeq. per acid may be performed rapidly and automatically by partition chromatography on a silica gel column, followed by indicator titration. Developing fluid is pumped to the column at a constant rate and the effluent from the column is mixed with an excess of indicator salt delivered at a constant rate by a second pump. As acid appears, the indicator salt is converted to its hydrogen form, the absorbance of which is continuously monitored by a recording photometer. Complex mixtures from physiological sources may be analyzed with no preliminary extraction in about 5 hours. Less complex mixtures may be analyzed within an hour. Thirteen organic acids of biological interest can be completely resolved. Acids of a yet undetermined structure have been found in urine and tissue fluids. Ultraviolet and radioactive detection may be included when desired.

In the past, organic acid analysis has been performed by a variety of techniques. Individual acids have been selectively estimated by procedures which rely upon chemical or enzymatic transformations (*14*). Groups of related acids have been determined by fractional distillation, paper electrophoresis, partition chromatography, and ion exchange chromatography. More recently gas chromatography has been used for limited separation of volatile acids or acid derivatives (*1, 4*). In general, most of these methods have suffered from limitations of sensitivity, reproducibility, applicability to large groups of acids, or ease of detection.

Column partition chromatography for estimation of carboxylic acids is a fairly well established procedure (*8, 14*). In general, this method relies upon an acidified inert support material such as silica gel, and a gradient elution system of nonpolar plus polar solvents. Because the carboxylic acid functional group cannot be easily derivatized in a quantitative manner for photometric estimation, it is customary to titrate with dilute alkali to an indicator end point fractions collected from such a separation. This is both tedious and time consuming. In addition, the lowest practical limits of detection in the manual titration methods range from 10 to 20 μeq. of each acid per determination.

The purpose of this investigation was to establish a technique for continuously and automatically monitoring the amounts of each carboxylic acid in the column effluent in a manner analogous to the ninhydrin method for automatic amino acid analysis (*13*). This was accomplished by mixing the effluent containing the weak acids with a miscible solvent system having an excess of indicator in the salt form. By applying some of the recently developed techniques for automatic partition chromatography (*8, 9*) it was possible to use longer columns at rapid flow rates in a highly reproducible manner. The result is a method of analysis having a considerable increase in speed and resolution, and a 20- to 40-fold increase in sensitivity; the data are automatically recorded.

EXPERIMENTAL

Reagents. Silica gel [Mallinckrodt, Acid Silicic A.R., 100 mesh (powd.). Suitable for chromatographic analysis by the method of Ramsay and Patterson] was dried to constant weight at 110° C. and stored in a desiccator in a plastic-lined screw-cap jar.

Chloroform, reagent grade was redistilled.

tert-Amyl alcohol, [(practical grade *tert*-pentyl alcohol), 100° to 103° C., Distillation Products Industries, Division of Eastman Kodak Co., Rochester 3, N. Y.] was redistilled in an all-glass apparatus. The distillate was collected over a 1° C. temperature range.

Ethanol, 95%, was redistilled over sodium hydroxide.

Indicator Solution. One gram of *o*-nitrophenol sodium salt (Distillation Products Industries, practical) was dissolved in 500 ml. of freshly boiled ethanol with heat and stirring. To this was added 500 ml. of *tert*-amyl alcohol and 1 liter of chloroform. The solution was stored in a brown glass bottle protected from carbon dioxide by a soda-lime tube.

Apparatus. The basic instrument for automatic organic acid analysis, consists of a gradient producing device, a Varigrad made of glass and Teflon (Buchler Instruments, Fort Lee, N. J., Model 4001); a pump (Milton Roy pump, CHMM1-B57, Milton Roy Co., 1300 East Mermaid Lane, Philadelphia 18, Pa.) for propelling the solvents at constant flow rate through a hydrated silica gel column; a pump, CHMM-1-B29, for infusing indicator salt at a constant rate into the effluent stream; a small magnetic stirring device for rapid mixing of components; and a recording photometer. A third pump is necessary if stream splitting for radioactive analysis is desired. The indicator solution is delivered at a rate of 50 ml. per hour, and the solvent pump for column operation is run at 200 ml. per hour under the standard working conditions described. It is preferable to have pumps whose delivery rate can be varied to allow for changes in experimental conditions and for application to different photometric instruments.

Fluid Connections. All connections between tubings of Teflon and glass or metal are made with Swagelok fittings (Crawford Fitting Co., 884 E. 140 St., Cleveland 10, Ohio). Pump outlet to $^1/_{16}$-inch i.d. flexible tubing of Teflon (Pennsylvania Fluorocarbon Co., Clifton Heights, Pa.) requires a 200-1-2-316 fitting. Pump inlet to tubing of Teflon uses a 200-2-2-316 fitting. Tubing of Teflon to glass connections are at both ends of the magnetic stirrer mixing vessel, at the socket connection below the column and at the ball connector on the top of the column. These are made with 400-6-2-316 reducing unions utilizing a ferrule of Teflon on the $^1/_4$-inch side. A pressure gauge ($2^1/_2$ inch P500; range 0 to 200 lb., $^1/_4$-inch bottom, $^1/_4$-inch flushing connection, $^1/_4$-inch process connection, 316 stainless housing complete with M and G type seal; Industrial Gauge and Instrument Co., 1407 E. 180 Street, New York 60, N. Y.) is inserted between the pump and column utilizing two Swagelok 200-2-4-316 fittings. The tee connection joining the column effluent and the indicator stream is a 200-3-316 fitting. When an ultraviolet photometer and radioactive strip counter is employed, another tee for effluent

splitting and additional Swagelok fittings for the third pump are necessary.

MIXING CHAMBER. The mixing chamber is made from a 6-cm. length of 6-mm. o.d. tubing. A flattened bulb is blown into the center of the tube with a diameter sufficient to allow free rotation of a $^3/_8$- × $^1/_8$-inch magnetic stirring bar coated with Teflon (No. 9235-U8, Arthur Thomas Co., Philadelphia, Pa.) The total volume of the chamber is about 1 ml.

COLUMNS. A 0.9- × 50-cm. glass column with JS 28 × 12 socket at the top and JS 12 × 1 ball at the bottom is used (similar to JC 2800 with jacket; Scientific Glass, Bloomfield, N. J.). The column is equipped with a medium-porosity fritted disk.

RECORDING PHOTOMETERS. Any stable recording photometer system may be used which is capable of reading at 350 mμ. The Beckman DB spectrophotometer, Technicon Phototube colorimeter, and Waters recording colorimeter are suitable. For ultraviolet recordings at 280 mμ, the Beckman DB and Waters photometer can be used.

RECORDER. A multipoint recorder is convenient for the estimation of area measurements, but any 0- to 10-mv. single pen recorder whose input is compatible with the photometer output may be employed. For the Beckman DB and Waters instruments, a Bristol Model 4P12H11X571, four-point 0- to 10-mv. recorder was used.

TIMER. A 15-hour timer (Dimco-Gray, 207 E. 6 St., Dayton, Ohio; with 3 blade parallel plug and receptacle) served to turn off equipment on runs which extended after working hours. Several multioutlet boxes were connected through the clock to accommodate all the equipment.

ULTRAVIOLET RECORDINGS. It is often important to determine whether the acidic substances being measured absorb in the ultraviolet, because many phenolic and heterocyclic acids absorb strongly in the 260- to 280-mμ region. Ultraviolet absorbing peaks are revealed by passing the effluent from the column through a suitable detector prior to mixing with the indicator (Figure 1). The output from the ultraviolet detector along with the output from the 350-mμ photometer may be displayed on the same chart by means of a two-pen or multipoint recorder.

CONTINUOUS COUNTING OF RADIOACTIVE MATERIALS FROM COLUMN EFFLUENT. The presence of organic solvents precludes the use of commercially available flow-counting scintillation systems. Organic solvents have quenching effects and may dissolve the cell housing and scintillating materials. To avoid these difficulties a fraction of the effluent stream is withdrawn by a pump, usually at a maximum rate of 30 ml. per hour (Figure 1) and applied to a moving strip of $1^1/_2$-inch Whatman No. 4 filter paper which is transported past the point of application at a rate of 12 inches per hour. The drive mechanism is part of the Actigraph II, Model 1026, 4π strip

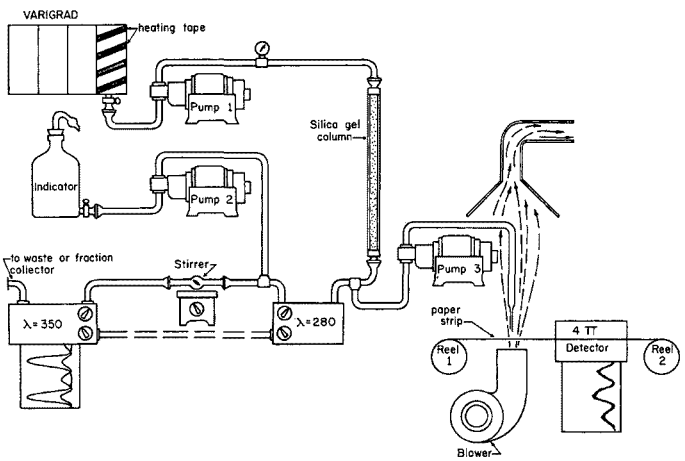

Figure 1. An organic acid analyzer with modules for determining ultraviolet absorption and continuous radioactive scanning

counter (Nuclear Chicago, Des Plaines, Ill.). The solvent is rapidly evaporated from the paper by a heater-blower located directly below the point of application of solvent. The paper strip is correctly positioned by passing it through a brass guide fastened to the top of the blower. The heater-blower is constructed from a hair dryer adapted with special wiring for a 75-volt heating element whose temperature is controlled by a variable transformer.

In summary, Figure 1 illustrates the basic system for simultaneously recording the acidic function, the ultraviolet absorption, and the radioactivity.

Procedure. SOLVENT SYSTEM. Although a variety of solvents and gradient devices have been used with some measure of success, the Varigrad has been the most convenient. It is also important to deaerate the solvents to prevent column disruption and to obtain exact metering by the pumps. This can be accomplished by heating the solvent in chamber 1 to a few degrees below the boiling point of the solvent mixture. A silicone-rubber insulated heating tape (Glas-Col, $^1/_2$ inch × 6 feet, 70 volt) is wrapped around the bottom third of chamber 1 and is held in place by adhesive tape coated with Teflon (Temp-R-Tape t-18, $^1/_4$ inch; Connecticut Hard Rubber Co., New Haven 9, Conn.). The temperature is controlled by a variable transformer.

For complex mixtures of acids such as those found in physiological fluids, a five-chamber concave gradient is generated. Chamber 1 is filled with 200 ml. of chloroform. Chambers 2 and 3 contain 7% (v./v.) *tert*-amyl alcohol/chloroform, chamber 4 contains 30% (v./v.) *tert*-amyl alcohol/chloroform, and chamber 5 contains 50% (v./v.) *tert*-amyl alcohol/chloroform. The volume of solvents used in chambers 2 through 5 is determined by the density of their solvent mixtures. A volume equal in weight to the 200 ml. of chloroform in chamber 1 is placed in these latter chambers.

This gradient was suitable for a 42-cm. column of hydrated silica gel (5.0:9.2 v./w.) with an input volume of 200 ml. per hour. Less complex mixtures may be separated at faster rates using simpler gradients and shorter columns. For example, propionic, acetic, and formic acids can be determined in less than 40 minutes with a 25-cm. column, a two-chamber gradient composed of 200 ml. of chloroform and 7% (v./v.) *tert*-amyl alcohol/chloroform, and a pump speed of 400 ml. per hour.

COLUMN PREPARATION. The hydration of the silica gel is a critical factor in the separation of certain organic acids. Although organic acid separations using chloroform and *tert*-amyl alcohol are not as sensitive to changes in hydration as are DNP-amino acids (*9*), variations in hydration can influence relative elution of acids. Thus, when the hydration of the silica gel was decreased from 62.5 to 37.5% aqueous phase without change of gradient or column height, the positions of the hydroxyl-bearing carboxylic acids—β-hydroxybutyric, lactic, malic, and citric acid—were shifted to a greater extent than the other acids.

To 92 grams of oven-dried silica gel in a screw-cap jar is added 50 ml. of 0.1*N* sulfuric acid. The mixture is stirred with a heavy glass rod until it is lump free and the powder no longer adheres to the walls. Several small glass rods are added to aid in dispersing the powder and the cap is tightly fitted in place. The jar is then rotated for 15 minutes on a ball mill.

For a 0.9- × 40-cm. column, approximately 25 grams of the hydrated gel is used. The gel is mixed with approximately 40 ml. of chloroform and the slurry is poured into a clean, dry column up to the socket. An 18- ×

Table I. Reproducibility of Standard Organic Acids

	No. detn.	Area/mole	Std. dev.	Rel. std. dev., %
Fumaric	4	2.13	0.046	2.2
Glutaric	7	1.92	0.047	2.5
β-Hydroxybutyric	4	0.98	0.034	3.5
Lactic	5	0.88	0.056	6.4
Succinic	7	2.08	0.068	3.3
α-Ketoglutaric	5	1.86	0.061	3.2
Malic	5	1.84	0.070	3.8
Citric	6	2.59	0.128	4.9

21-mm. washer (cut with cork borers from a sheet of $^1/_{64}$-inch silicone rubber MD-50; R-Way Synthetic Products, Division Ronthor Reiss Corp., Little Falls, N. J.) is placed in the dry socket and the ball is secured with a clamp (Size 28, Catalog No. C5155; Scientific Glass Apparatus Co., Bloomfield, N. J.). The socket is connected to the bottom of the column in a similar manner and chloroform is pumped through until the level of the silica gel remains constant. The upper ball is then removed, the excess chloroform above the silica gel is aspirated, and the remainder of the slurry is poured in. The procedure is repeated until a packed height of 42 cm. is obtained.

Preparation of a column requires about 15 minutes and must be performed for each run. Silica gel from the previous run is removed by inverting the column over a sink and slowly passing a narrow plastic tube with running water up through the gel. The column is rinsed with distilled water followed by acetone and then air dried. The flow cell and indicator mixing chamber are periodically rinsed with water and acetone to remove material which sometimes deposits on their surfaces.

Sample Addition to Column. To prevent spreading of peaks, the volume of aqueous solution containing the acids should not be greater than 1 ml. The sample is first made acid to Congo Red by the addition of 1 or 2 drops of 6*N* sulfuric acid. Enough oven-dried silica gel is then added to make a free-flowing powder; each 0.5 ml. of solution requires approximately 0.8 gram of silica gel. The free-flowing powder is then quantitatively added through a 3-cm. layer of chloroform which covers the top of the silica gel column. The sample is stirred with a glass rod to release air bubbles and chloroform is added up to the socket. The washer and ball are placed in position and the pump is activated. Pump performance may be evaluated by timing the collection of solution in a graduated cylinder as it leaves the colorimeter. The collection rate is recorded.

Calibration. Calibration is undertaken once optimum conditions for separation have been established for the substances being investigated. Stock solutions of acids are prepared in a 50% (v./v.) acetone–water mixture in concentrations of approximately 0.01*N*. From the stock solutions a mixture of acids is prepared by combining 1- to 10-ml. aliquots of each acid and diluting to a known volume, usually 100 ml. To standardize each acid in the mixture, a sample equal to the amount transferred using the same pipet is titrated. This minimizes pipetting errors caused from poor draining which is characteristic of nonaqueous solutions. The stock acids are titrated to a phenolphthalein end point with 0.01*N* sodium hydroxide using a stream of nitrogen for stirring. It has been our experience that calibration on a weight basis is less reliable than standardization by titration. If an acid is not obtainable in a pure free form, its sodium salt may be used. The salt can be titrated potentiometrically with a platinum silver–silver chloride electrode pair. One milliliter of a 0.1*N* aqueous solution of the salt is diluted to 25 ml. with glacial acetic acid and the mixture is titrated with 1.0*N* perchloric acid in glacial acetic acid. Potassium hydrogen phthalate serves as the reference standard for both acid and salt titrations.

Known mixtures of carboxylic acids are analyzed in the concentration range 0.05 to 5 μeq. per acid. The area under the peaks is obtained by multiplying the net height of a peak in absorbance units by the width at half the peak height (*13*). A calibration constant for each acid is thus obtained. To determine the area of a curve over a sloping base line, a line is drawn which follows the base-line slope under the peak. A vertical line from the highest point of the peak to the drawn base-line represents the net height. The line at one half the net height is made parallel to the chart abscissa, not parallel to the drawn base line.

Table I presents a typical set of results for a series of calibrations from a single preparation of standards. In a static system containing uniform concentration of chloroform, alcohol, and indicator it is possible to equate changes in absorbance per microequivalent of acid regardless of whether the carboxylic group is contributed by a mono-, di- or tricarboxylic acid. However, in a flowing system where there is a continuous change in the composition of the solvent, a uniform calibration constant in terms of absorbance units per microequivalent of acid is not possible. This is a result, in part, of a change in the spectral characteristics of the indicator with changes in solvent composition. Consequently, calibration constants are not uniform for all acids and are dependent upon the position of the curve at which they are eluted. A second effect arising from this phenomenon is a downward sloping base line early in the run and an upward sloping base line near the end of the run. The latter is also due in part to the leaching of small amounts of sulfuric acid from the column near the end of the run. However, the sloping base lines do not introduce serious errors in the calculations and are relatively constant as long as the procedure is held constant.

Following the elution of weak organic acids, the absorbance rises markedly as sulfuric acid in large concentrations now is eluted from the column. During the course of a run the top of the column becomes translucent as the hydration of the silica gel is changed. The sulfuric acid comes off as the translucent area reaches the bottom of the column.

Variations in gradient, silica gel preparation, flow rates, or column height may influence the calibration factor. Hence it is important to carry out the calibration after these variables have been standardized and thereafter adhere strictly to the same procedure. The standard organic acids prepared in acetone and water deteriorate on standing. For example, a standard mixture stored at 4° C. for 5 months exhibited a loss of 25% of *cis*-aconitic and malic acids; a loss of 15 to 20% of citric, β-hydroxybutyric, and pyruvic acids; and a loss of 5% or less of fumaric, glutaric, lactic, succinic, and α-ketoglutaric acids.

Analysis of Biological Fluids and Tissues. No preliminary extraction or concentration of urine or plasma is required prior to analysis; 0.2 to 0.5 ml. of urine is usually required for a complete analysis. Because of the small amount of urine needed for a determination, it is possible to follow the pattern of acid excretion in individual rats by analyzing each sample of urine voided (*7*).

Protein containing fluids such as plasma are analyzed in a similar manner. A 0.5 or 1.0 ml. sample is acidified with 6*N* sulfuric acid. Dry silica gel is added and the mixture is stirred until free flowing. The entire mixture is added to the top of the column. No prior protein precipitation is required.

Whole tissue such as liver, muscle, and kidney are treated in an analogous manner except that acidification and mixing is done in a ceramic mortar to ensure disruption of cells and uniform distribution of the intracellular material. The tissue should be instantly frozen, weighed, and then ground to ensure against metabolic alteration of acid constituents.

Sulfuric acid is used in preference to other acids such as trichloroacetic or perchloric acid where it is necessary to terminate a biochemical reaction. Most of the commonly used protein-precipitating reagents appear as peaks on the chromatogram and will swamp a particular area of analysis. The pH of the sample is adjusted to below 2 to keep the acids in an unionized form. Because of the increased sensitivity of the method, the requirement for preliminary extraction and concentration

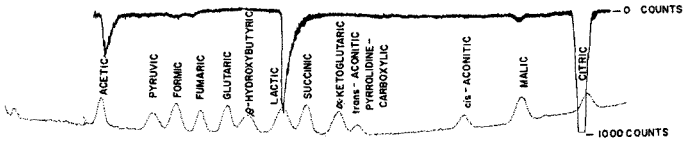

Figure 2. Analysis of an artificial mixture of acids of physiological importance with continuous radioactive scanning

is unnecessary in most instances. Hence better yield, fewer artifacts, and smaller losses from volatilization or polymerization of certain substances are obtained.

RESULTS AND DISCUSSION

Principle of Indicator Titration. Isherwood (*6*) described a procedure in which an indicator salt was used to locate the appearance of acids in the effluent of a chromatographic column. This was done so that the acid could be collected and titrated. The procedure described here utilizes an indicator salt not only in the capacity of an indicator but also as the titrant. To continuously and automatically monitor the amount of carboxylic acid in the column effluent, an excess of the indicator salt in an appropriate, nonaqueous, miscible solvent is continuously mixed with the effluent stream from the column. The indicator salt is partially converted to its hydrogen form as the carboxylic acid is neutralized. By directly measuring the increase in absorbance of the unionized indicator formed, the amount of carboxylic acid can be evaluated.

In applying this principle of "indicator titration" to the effluent of partition columns, several factors must be taken into account. First, the relative pK of the indicator in the nonaqueous solvent should be such that complete reaction can occur. On the other hand, the indicator salt must not be so basic as to react with the weakly acidic alcohol used as an eluting agent. Second, the indicator salt should be soluble in a solvent which is readily miscible with the entire gradient which passes through the column. Third, the maximal wavelengths of the salt and acid forms of the indicator should not overlap in the concentrations used.

Apparently very few indicators satisfy the above requirements, with the solvents employed. Of the various indicators tested, sodium *o*-nitrophenol was most suitable with respect to sensitivity, solubility, ease of preparation, and range of applicability.

Elution Pattern of Organic Acids. The analysis of an artificial mixture of organic acids of physiological importance is shown in the lower tracing in Figure 2. The superimposed tracing represents a radioactive scan of the same sample. Each organic acid in the mixture was present in a concentration of approximately 0.5 μeq. and, in addition, 0.1, 0.2, and 0.5 μc. of acetic, lactic, and citric acid, respectively, were added. To prevent the loss of volatile acids, such as acetic acid, during the evaporation of solvents from the moving strip of filter paper for radioactive scanning, it was necessary to precoat the paper with pH 7, 0.1*M* phosphate buffer. This precaution was, of course, unnecessary for nonvolatile acids.

The tracing in Figure 2 calls attention to certain problems. The erratic shape of the pyruvic acid peak is characteristic of the pattern obtained with temporary pump failure—e.g., when a check valve does not seat properly. *Trans*-aconitic acid is always found in samples of *cis*-aconitic acid. The radioactive pattern contains minor peaks, which are probably minor contaminants in the commercial radioactive materials.

Oxaloacetic acid is not sufficiently stable to be chromatographed on columns containing 0.1*N* H_2SO_4 as the stationary phase. In the presence of 6*N* H_2SO_4, oxaloacetic acid is relatively stable and is eluted, but under these conditions there is a high blank and indicator titration can not be used for the complete run. Oxaloacetic acid shows absorption in the ultraviolet region permitting ready detection when eluted from the column.

Fractionation of Organic Acids in Biological Materials. Figure 3 demonstrates organic acid fractionation upon analysis of 1 ml. of rat plasma and 350 mg. of rat liver. Utilizing paper chromatography, Nordmann and Nordmann (*11*) demonstrated the presence in human blood plasma of citric, malic, succinic, hippuric, lactic, and pyrrolidonecarboxylic acids. The absence of pyrrolidonecarboxylic in the plasma chromatogram shown in Figure 3 is noteworthy. Apparently, the mild treatment involved in the present procedure reduces the possibility of artifact formation. The extensive pretreatment of plasma that is required to obtain an ultrafiltrate and subsequent concentration causes loss of volatile acids and cyclization of glutamine to form pyrrolidonecarboxylic acid.

When unknown mixtures are chromatographed there is a possibility that peak effluent volumes may overlap with one of the known acids. Irregularities in the symmetry of the peak may be sufficient to designate this. However, when this situation is suspected, the eluate corresponding to the peak can be collected and its purity confirmed by paper chromatography (*10*) in a variety of developing solvents. In addition, improved resolution may be obtained by varying the hydration of the silica gel or by changing the length of the column, the temperature, and the gradient. Chemical characterization may involve the use of oxidizing agents such as permanganate or ceric sulfate. Since only specific structures are attacked by these reagents, analysis of the products of such a reaction may provide information useful in identifying the structure of the original compound. Figure 4 shows the separation of an organic acid mixture before and after treatment with acidic ceric sulfate (*2*). Losses are observed for citric, malic, α-ketoglutaric, and pyruvic acids, with oxidation products appearing in the areas of acetic, formic, β-hydroxybutyric, and succinic acids.

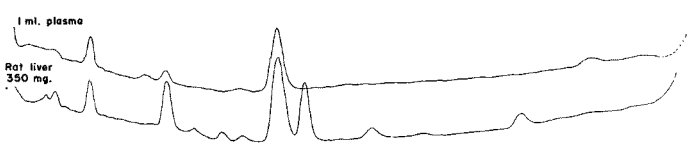

Figure 3. Organic acid analyses employing 1 ml. of rat plasma and 350 mg. of rat liver

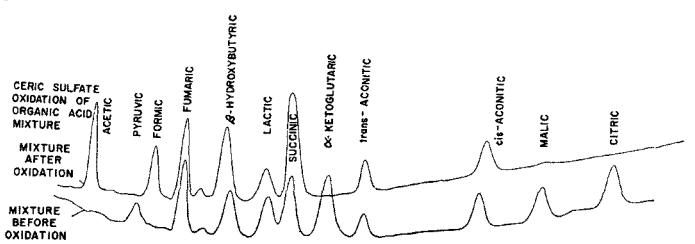

Figure 4. Separation of organic acids in an artificial mixture before and after treatment with acidic ceric sulfate

Sources of Error. Limitations in reproducibility are the result of a number of factors, of which the calculation of the peak area may be of considerable magnitude. The height-width method (*13*) for determining area is the most convenient procedure when utilizing a nonlinear absorbance photometer. Errors may also arise from lack of photometric stability or potentiometer reproducibility and deviations in the pump rates of the two or three pumps used.

Other Methods for Continuous Analysis. Previous attempts to automatically monitor the acids in column effluents have relied upon recording titrimeters (*3, 5*) or recording refractometers (*12*). Resolution of acids on an ion exchange column without the use of a buffered gradient, as is required for both refractometric monitoring (*12*) and potentiometric titrations (*5*), is rather limited in scope. With recording titrimeters in a partition system the extraction of acids into water prior to titration (*3*) is required. Although gas chromatography may become the most rapid and sensitive method for analysis of organic acids, its application to these substances is still beset by difficulties at present. Alcock has reported (*1*) the separation of nine acids as their methyl esters in 28 minutes. However, this procedure required 16 hours of preliminary extraction and esterification and was not applied to complex physiological solutions. In addition, double peaks appeared for some acids with the possible production of isomers of other acids during sample preparation.

ACKNOWLEDGMENT

The authors express their appreciation for the technical assistance of Margaret Mulladey and Grace Franusiak. We also thank Grace Griffin who was instrumental in the design and testing of the radioactive counting module.

LITERATURE CITED

(1) Alcock, N. W., *Anal. Biochem.* **11**, 335 (1965).
(2) Aronoff, S., "Techniques of Radiobiochemistry," Iowa State College Press, Iowa, 1956.
(3) Forsander, O., Neuenschwander, P., *J. Chromatog.* **5**, 515 (1961).
(4) Gee, M., ANAL. CHEM. **37**, 926 (1965).
(5) Harlow, G. A., Morman, D. H., *Ibid.*, **36**, 2438 (1964).
(6) Isherwood, F. A., *Biochem. J.* **40**, 688 (1946).
(7) Kesner, L., *J. Biol. Chem.* **240**, 1722 (1965).
(8) Kesner, L., Muntwyler, E., *J. Lab. Clin. Med.* **61**, 604, (1963).
(9) Kesner, L., Muntwyler, E., Griffin, G. E., Abrams, J., ANAL. CHEM. **35**, 83 (1963).
(10) Ladd, J. N., Nossal, P. M., *Australian J. Exptl. Biol. Med. Sci.* **32**, 523 (1954).
(11) Nordmann, J., Nordmann, R., *Advan. Clin. Chem.* **4**, 53 (1961).
(12) Shimomura, K., Walton, H. F., ANAL. CHEM. **37**, 1012 (1965).
(13) Spackman, D. H., Stein, W. H., Moore, S., *Ibid.*, **36**, 1190 (1958).
(14) Swim, H. E., Utter, M. F., *Methods in Enzymology* **4**, 584 (1957).

RECEIVED for review April 11, 1966. Accepted June 16, 1966. Presented at the Winter Meeting, January, 1966, Division of Analytical Chemistry, Phoenix Ariz.

Nonaqueous Microtitration of Dibenzoylmethane and Other Weak Acids

D. A. LEE

Chemistry Division, Oak Ridge National Laboratory, Oak Ridge, Tenn.

▷ **A potentiometric method was developed for the microtitration of dibenzoylmethane and other weak acids in pyridine or ethylenediamine. Various polarized electrodes were investigated; anodized platinum and cathodized antimony microelectrodes responded best. Sharp end points were obtained for most acids with a titrant consisting of tetrabutylammonium methylate dissolved in a 90% benzene–10% methanol solution. Several very weakly acidic compounds, such as cyanoacetamide, acetylurea, 2,3-butanedione, s-diphenylurea, malonamide, dimethylglyoxime, and 2-nitropropane were titrated successfully.**

DIBENZOYKMETHANE (DBM) and other β-diketones may be quantitatively determined in nonaqueous solutions by titrimetric procedures. Thus, Fritz (*1*) titrated DBM in dimethyl formamide with 0.1*N* sodium methoxide solution, using thymol blue as a visual indicator of the end point. Fritz and Yamamura (*2*) determined DBM in acetone potentiometrically with a triethyl-*n*-butylammonium hydroxide titrant, using glass and calomel electrodes. Modifications of these procedures have also been used.

This paper describes an improved potentiometric technique for determining DBM and other weak acids in anhydrous ethylenediamine or pyridine. Polarized bimetallic electrodes replace the glass electrodes, and a stable, easily-prepared solution of tetrabutyl-ammonium methylate is used as the titrant. The electrodes respond rapidly to changes of pH, and this combination of electrodes and titrant gives large, sharp potential changes at the end point, and is readily adapted to microscale analyses.

EXPERIMENTAL

Apparatus. Simple, microscale apparatus was used. The plastic screw cap of a 20-ml. vial was adapted to receive a 1-ml. microburet with an overhead reservoir, a 4.3-ml. automatic pipet with a reservoir to dispense the solvent, a dry argon flushing tube, and the bimetallic electrodes. The electrodes were attached to a model H-2 Beckman pH meter and the change in potential was read on the millivolt scale. The solvent and titrant reservoirs were protected from the atmosphere with Ascarite–Drierite tube s A magnetic stirrer was used during the titration. A smaller apparatus was also made, including a 1-dram vial, a 0.2-ml. buret and a 0.5-ml. pipet for dispensing the solvent. The electrodes were made coaxially in a single 3-mm. probe. A Hamilton microhypodermic syringe was used to introduce the sample.

Electrodes. All of the microelectrode systems were polarized bimetallic electrode pairs. These indicating electrode–reference electrode pairs included platinum–platinum, platinized platinum–platinum, gold–platinum, platinized gold–platinum, gold–gold, antimony–antimony, and platinum–antimony. The electrodes were anodized or cathodized by electrolyzing 5% H_2SO_4 for 2–3 minutes at 3 volts. This type of electrode pretreatment has been discussed by Willard and Fenwick (*8*) and by Harlow, *et al.* (*3*). The reference electrode was electrolytically charged with a layer of hydrogen and the indicating electrode with a layer of oxygen. The behavior of the end point change for polarized electrodes in aqueous solutions has been studied by Van Name and Fenwick (*7*). We have extended these polarization studies for aqueous and alcoholic solutions of various acids and bases;

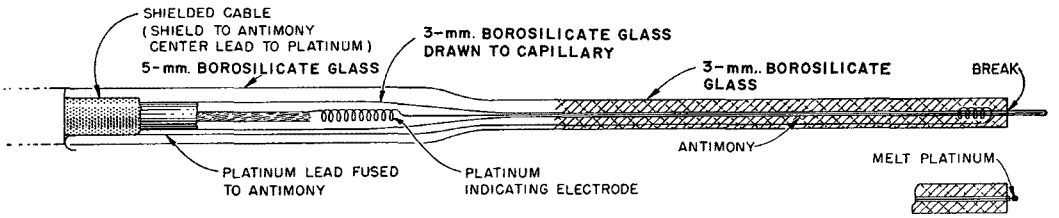

Figure 1. Concentric microelectrodes

the best results were obtained with 5% aqueous H_2SO_4. After the electrolysis, the electrodes were washed thoroughly with acetone to remove the adhering acid. The electrode pretreatment was performed twice a day. The platinum electrode was made from 0.005-in. platinum wire sealed in 4-mm. glass tubing. The exposed tip of platinum was fused into a ball about 0.025-inch in diameter. The antimony electrode was made by drawing molten antimony into a constricted glass tube. After the antimony had cooled, the tube was cut at the constriction leaving an exposed antimony surface about 0.025-inch in diameter.

For the very small-scale apparatus, a single 3-mm. probe containing both the platinum and antimony electrodes was constructed, as shown in Figure 1. The inner 0.005-inch platinum wire electrode was fitted inside a fine capillary drawn down from 3-mm. glass tubing. The capillary tip was sealed. The glass-encased platinum electrode was fitted inside a 3-mm. glass tube which had a 5-mm. shoulder. Molten antimony was drawn into the annular space between the capillary tube and the outer tube. Also in this space was a platinum electrical lead which was fused to the antimony. The inside capillary tube protruded about $^1/_4$-inch. After the antimony had cooled, the glass around the platinum protrusion was carefully broken and the platinum melted into a ball with a small hot flame.

Solvents and Titrants. The following reagents were used: pyridine, reagent grade (Baker and Adamson), ethylenediamine, 98% (Eastman), refluxed over CaH_2 and fractionally distilled, acetone, reagent grade (Baker and Adamson), tetrabutylammonium methylate in benzene–methanol (9:1), tetrabutylammonium ethylate in benzene–ethanol (9:1), tetrabutylammonium isopropylate in benzene–isopropanol (9:1).

An improved procedure for preparing the titrants was devised. Potassium metal was dissolved very cautiously in the alcohol at −80° C. to make a 0.6*M* solution. The amount of tetrabutylammonium chloride, bromide, or iodide necessary to make a 0.03*M* final solution was dissolved in an equivalent volume of 0.6*M* potassium alcoholate solution. The total volume of benzene to be used was added, causing the potassium halide to precipitate. The precipitate was filtered and the remaining alcohol was added to make the final solution 0.03*M* tetrabutylammonium alcoholate in 90% benzene–10% alcohol. The alcohols used were methanol, ethanol, and isopropanol. Potassium was used instead of sodium because potassium halide salts were less soluble than sodium salts in these solutions. The titrants were standardized against benzoic acid.

Procedure. The Pt anode and Sb cathode were preconditioned by electrolyzing 5% sulfuric acid for 2–3 minutes at 3 volts. The electrodes were then washed with acetone and air-dried. A clean, over-dried, titration vessel with a magnetic stirring bar was fitted to the apparatus. While dry argon was flushing the apparatus, an automatic pipet full of solvent was introduced into the titration vessel. The sample was added and titrated to the potentiometric end point.

RESULTS AND DISCUSSION

Several factors have contributed to the improved method which has been developed for determining dibenzoylmethane and other weak acids by nonaqueous titration. These improvements resulted from a study of various electrode systems, titrants, and solvents. Samples of dibenzoylmethane dissolved in dioxane, benzene, or methanol titrated very well, as shown in Figure 2.

Even 2*N* NH_3 in methanol did not interfere with the titration. The reproducibility of the method was illustrated by the analyses of two β-diketones. Successive determinations of a reagent-grade sample of dibenzoylmethane yielded the following results: 96.4, 95.8, and 95.4% DBM. Similar determinations of commercial grade dipivaloylmethane gave 76.6, 77.0, and 76.0% DPM. A typical standardization of the titrant Bu_4NOCH_3 against benzoic acid yielded the following data: 0.262, 0.262, and 0.260*M* Bu_4NOCH_3.

Titrations were performed using various bimetallic electrode pairs. The end points for weak acids titrated in pyridine, using an anodized platinum indicating electrode and a cathodized platinum reference electrode, were sharp. An indicating electrode of platinized platinum together with a bright platinum reference electrode often gave very good results; however, the titration curves were not always reproducible and the change in potential was sometimes erratic. Gold and platinized gold indicating electrodes were inferior to platinum indicating electrodes. A platinized gold indicating electrode with a platinum reference electrode caused a drifting potential with a small potential drop at the end point, and a gold indi-

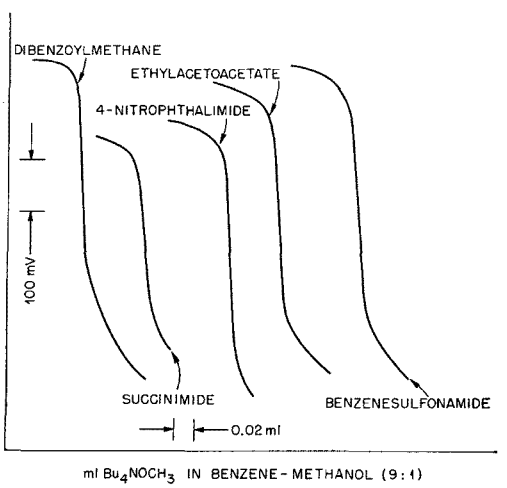

Figure 2. Titration curves for weak acids with platinum–antimony electrodes, ethylenediamine solvent

cating electrode with a platinum reference electrode produced nonreproducible curves which were very erratic. Titration curves obtained by using polarized gold–gold electrodes were nonreproducible, and the end point break was not sharp. Anodized and cathodized antimony electrodes gave good results; however, the best electrode system we studied consisted of an indicating electrode of anodized platinum and a reference electrode of cathodized antimony. The electrodes produced very stable, sensitive titration curves with sharp end points (Figure 2).

The principal solvents studied were pyridine, and the more basic solvent, ethylenediamine (EDA). Pyridine was preferred because it did not absorb carbon dioxide as easily as ethylenediamine. Extremely weak acids titrated better in ethylenediamine than in pyridine. Van der Heijde (*6*) has shown that pyridine and ethylenediamine have suitable acidity potential ranges for these titrations. For the titration of dibenzoylmethane with platinum–platinum electrodes, the end point was sharper in pyridine than in ethylenediamine; however, when platinum–antimony electrodes were used, the end point was equally sharp in ethylenediamine. One experiment was done in acetone, but the potential drop was not as large, and the end point was not as sharp, as in the basic solvents.

The titrants were tetrabutylammonium alcoholates. The order of stability of these titrants was methylate > ethylate ≫ isopropylate. A solution of tetrabutylammonium methylate in 90% benzene–10% methanol remained useful for several months; therefore, it was the preferred titrant. Heumann (*4*) has discussed alkoxides of quaternary ammonium bases as strongly basic titrants.

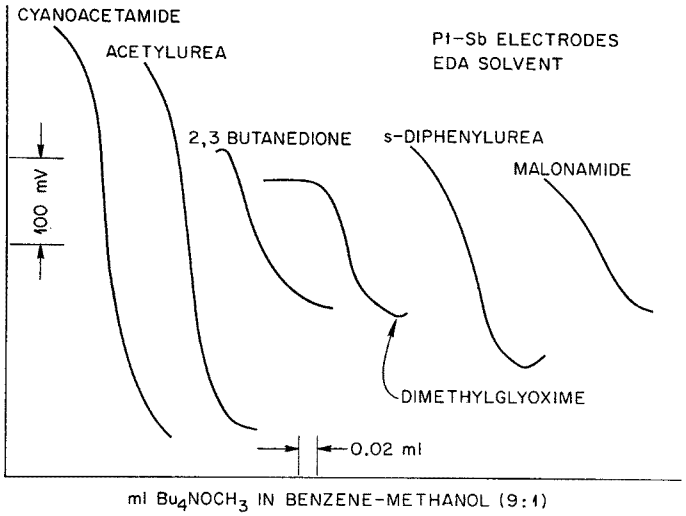

Figure 4. Titration curves for very weak acids

To determine the scope of this method for the titration of weak acids, several compounds were titrated. Dibenzoylmethane, succinimide, 4-nitrophthalimide, ethylacetoacetate, and benzenesulfonamide were titrated successfully in pyridine, using platinum–platinum electrodes and $Bu_4NOC_2H_5$ titrant. These same compounds were titrated in both ethylenediamine and pyridine with platinum–antimony electrodes and Bu_4NOCH_3 titrant. The results in ethylenediamine are shown in Figure 2. The results in pyridine were equally good.

Some very weak acids titrated well in ethylenediamine, but not in pyridine. In Figure 3, the titration curves for 2-nitropropane in the two solvents are illustrated. From the literature (*5*) several weak acids were selected which were reported as being difficult to titrate. These were titrated in ethylenediamine with 0.03*M* Bu_4NOCH_3, using platinum–antimony electrodes. The titration curves are shown in Figure 4. Although the end points were not as sharp nor the curves as stable as those for the stronger acids, still they can be used to determine these compounds quantitatively. Obviously, stronger acids, such as carboxylic acids, can be titrated in these systems with no difficulty.

A diketone which could not be titrated in either ethylenediamine or pyridine was 2,5-hexanedione. As Fritz (*1*) has stated, this may be due to the fact that the electron-withdrawing carbonyl groups are separated too far to have any noticeable effect on the hydrogens.

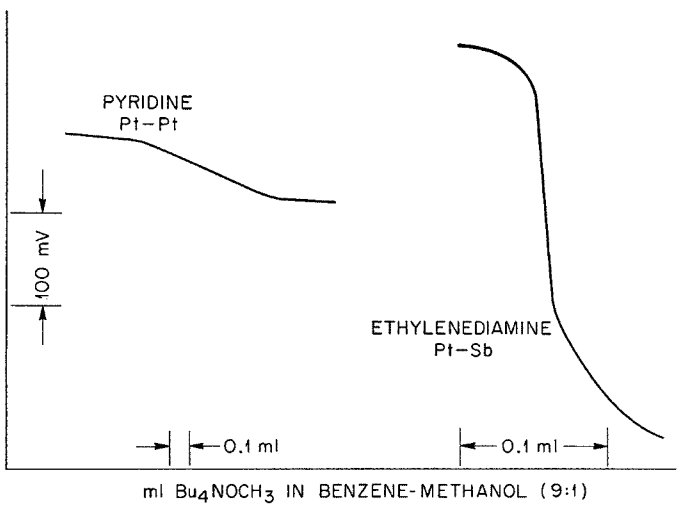

Figure 3. Titration of 2-nitropropane

LITERATURE CITED

(1) Fritz, J. S., ANAL. CHEM. **24**, 674 (1952).
(2) Fritz, J. S., Yamamura, S. S., *Ibid.*, **29**, 1079 (1957).
(3) Harlow, G. A., Noble, C. M., Wyld, G. E. A., *Ibid.*, **28**, 784 (1956).
(4) Heumann, W. R., "Titrimetric Methods, Proceedings of the Symposium on Titrimetric Methods," D. S. Jackson, ed., Plenum Press, New York, 1961.
(5) Kucharsky, J., Safarik, L., "Titrations in Non-Aqueous Solvents," Elsevier, New York, 1965.
(6) Van der Heijde, H. B., *Anal. Chim. Acta* **17**, 512 (1957).
(7) Van Name, R. G., Fenwick, F., *J. Am. Chem. Soc.* **47**, 19 (1925).
(8) Willard, H. H., Fenwick, F., *Ibid.*, **44**, 2516 (1922).

RECEIVED for review March 21, 1966. Accepted June 13, 1966. Research sponsored by the U. S. Atomic Energy Commission under contract with the Union Carbide Corporation.

A Rapid and Sensitive Method for the Determination of Iodine-131 in Milk by Ion Exchange on Silver Chloride

WILLIAM D. FAIRMAN and JACOB SEDLET

Argonne National Laboratory, 9700 South Cass Ave., Argonne, Ill. 60439

▷ Iodine-131, as iodide ion, is separated from other milk constituents by ion exchange on a silver chloride column. After elution as iodic acid from the column by acidified chlorine water, the eluate can be directly analyzed by gamma counting. The time required to analyze a 1-liter sample by this method is approximately 30 minutes (exclusive of counting time). If beta counting or increased sensitivity is required, the iodine is subjected to two oxidation-reduction solvent-extraction cycles and finally precipitated as silver iodide prior to counting. Chemical and radiochemical yields for both added and metabolized iodide are identical, and are 90 to 95% for homogenized milk and 85 to 95% for raw milk. Total time for the complete procedure (exclusive of counting time) is approximately 2 hours for a single sample. Less than 2 picocuries of total iodine-131 can be detected in 1 liter of milk, using the complete procedure. The application of the procedure to other materials is discussed.

IODINE-131 is an important radiological public health hazard when it is present in the environment since it accumulates in milk. Sensitive procedures for its determination are thus required, so that its presence and accumulation may be continually monitored.

At sufficiently high concentrations—greater than about 25 picocuries per liter—iodine-131 can be measured directly in milk without prior chemical separation if no interfering gamma-emitting nuclides are present. On the other hand, at lower concentrations, or if interfering gamma-ray emitters are present, or if a gamma-ray spectrometer is not available, chemical separation is required. This paper describes a procedure which is both rapid and specific for iodine occurring as inorganic iodide.

Since the bulk of the iodine in milk is present as inorganic iodide—the organic iodine normally comprises a maximum of 10% of the total iodine (*5*)—it was decided to develop a procedure for the determination of inorganic iodide only. The total iodine-131 present can be estimated with adequate accuracy for most purposes by assuming that the organic iodine is 10% of the total.

Separations of radioiodine that have been made specifically from milk include ion exchange on synthetic resins (*3, 5, 6, 9, 11*), solvent extraction (*2, 12*), and electrodialysis (*10*). Inorganic iodide separations that have been applied to both biological and nonbiological samples include ion exchange on synthetic resins; coprecipitation with, or ion exchange on, silver chloride; isotopic exchange on silver iodide; and solvent extraction. References to these separations are given in an earlier report (*4*).

The rapidity and potential selectivity of the anion exchange of iodide on silver chloride, and of the isotopic exchange on silver iodide, made these two techniques appear most promising for investigation. The greater ease with which the exchanged radioiodide could be eluted from the silver chloride determined the initial decision to use silver chloride for the exchange medium.

EXPERIMENTAL

Apparatus. SILVER CHLORIDE COLUMN. Glass columns approximately 2.5 cm. in diameter and with a silver chloride (20 to 40 mesh) height of approximately 7 cm. were used. The silver chloride was supported by a glass wool plug inside the column which had an addition funnel and a stopcock-controlled drip-tip, with outlet positioned such that the columnar liquid level never fell below the upper level of the silver chloride. The column was covered with black tape to make it light-tight and prevent photodecomposition of the silver chloride. A glass wool plug was placed over the silver chloride to give mechanical stability to the upper layers of silver chloride.

ULTRASONIC GENERATOR. An Ultrasonics, Inc., 80-watt, 80-kilocycles-per-second, System GC-40C was used.

Reagents. SILVER CHLORIDE. Fisher Certified Reagent silver chloride was ground in a mortar and sieved to retain the 20- to 40-mesh portion.

Procedure. Pipet 2.0 ml. of standardized potassium iodide carrier solution (approximately 10 mg. of I^- per milliliter) into the milk sample. For homogenized milk, stir with a magnetic stirrer for 15 minutes. For raw milk, place the sample in a narrow-mouthed glass bottle and cavitate for 15 minutes in an ultrasonic unit to homogenize the milk and thus prevent clogging of the column by the fat globules. (Simple stirring or shaking is inadequate for this purpose.) In addition, the 15-minute mixing periods allow time for equilibration between the various forms of iodide in the sample.

After mixing, transfer the sample with distilled water to the silver chloride column. Use a flow rate of 40 to 50 ml. per minute both in this and in subsequent columnar flows. Discard the effluent. Wash the column with 300 ml. of distilled water and discard the effluent. Add 100 ml. of 0.1*N* sulfuric acid saturated with chlorine gas to the column. After approximately 20 ml. (one column volume) of effluent (discard) has emerged from the column, stop the flow and allow the chlorine solution to remain on the column for 5 minutes; then renew the flow, collecting the effluent in a 400-ml. beaker. Add 300 ml. of distilled water to the column and collect the first 100 ml. of effluent in the same beaker. Discard the remainder of the effluent. The column is now ready for the next sample. As will be seen later, the solution in the beaker may be counted directly for gamma activity if desired.

Neutralize the contents of the beaker with 6*M* sodium hydroxide, using Hydrion paper as indicator. Add 5 ml. of excess. Bring contents to a boil and then cool to room temperature. Acidify with concentrated nitric acid and transfer the contents to a 250-ml. separatory funnel (Teflon stopcock), using a minimum amount of distilled water as transfer agent.

Add 30 ml. of benzene and 5 ml. of 1*M* hydroxylamine hydrochloride to the funnel. Shake the funnel for 30 seconds. Add 5 ml. of 1*M* hydroxylamine hydrochloride and shake again for 30 seconds. Add 3 ml. of 1*M* sodium nitrite and shake for 30 seconds. After the layers separate, drain off and discard the colorless aqueous layer. Add 30 ml. of carbon tetrachloride to the violet organic layer and then 15 ml. of distilled water containing 1 ml. of 1*M* sodium bisulfite solution. Shake until the organic layer is colorless.

After layer separation, drain off and discard the organic layer. Add 30 ml. of benzene and then 1 ml. of 6*N* nitric acid and 1 ml. of 1*M* sodium nitrite. Shake for 30 seconds. Add 1 ml. of 1*M* sodium nitrite and shake for 30 seconds. Discard the aqueous layer. Wash for 15 seconds with 15 ml. of distilled water and discard the wash. Add 15 ml. of distilled water containing 1 ml. of 1*M* sodium bisulfite. Shake until the upper layer becomes colorless and collect the lower aqueous layer in a 100-ml. beaker.

Add 1 ml. of 6*N* nitric acid to the beaker and heat, with stirring, to the boiling point and boil for 3 minutes to remove sulfur dioxide. Stop heating and add, dropwise and with stirring, 2.0 ml. of 0.1*N* silver nitrate to the hot solution. Heat the solution to a gentle boil to coagulate the silver iodide precipitate and cool to room temperature.

After cooling, filter the silver iodide onto a prepared, weighed Whatman No. 540 (2.1-cm. diameter) filter paper mounted in a two-piece fritted glass filter funnel. (The filter paper is prepared in the same manner as the precipitate is treated—i.e., washed, dried, and weighed.) Wash the precipitate with three 5-ml. portions each of distilled water and absolute ethyl alcohol. After the precipitate is almost dry, remove the top part of the filter funnel and carefully distribute the damp precipitate uniformly over the precipitate area of the filter paper with the flat tip of a stainless steel spatula. (Upon drying, the silver iodide normally possesses a "flaky" appearance and does not uniformly cover the filter paper, resulting in many open areas on the filter paper. It is, therefore, necessary to use the above precipitate distribution step to obtain reproducible counting efficiencies.) Dry the precipitate in an oven for 10 minutes at 110° C. Cool to room temperature in a desiccator and weigh. Mount the weighed precipitate and filter paper on a 2-inch stainless steel planchet, using double-coated pressure-sensitive tape for adhesion and 1/4-mil Mylar film for cover. Beta and/or gamma count.

RESULTS AND DISCUSSION

Because of the rapidity of the iodide–chloride exchange, relatively large-size (20- to 40-mesh) granules of silver chloride were used, permitting the use of high flow rates without the necessity of applying vacuum or pressure. The silver chloride in the column retained approximately 20 ml. of liquid and with the flow rates used (40 to 50 ml. per minute), the average residence time of the flowing liquid on the column was less than 1/2 minute, an indication of the fast rate of exchange obtained. The column size was more than adequate for the amount of iodide carrier (20 mg.) and sample volumes (1 liter or less) used, because the exchanged iodide was confined to the uppermost portion of the column. No additional leakage or washout of the initially exchanged carrier or tracer iodine-131 (as the iodide in alkaline sulfite solution) occurred even when the quantity of carrier and sample volume was increased by a factor of five.

Flow rates up to 100 ml. per minute have been used during the columnar wash cycles without loss of exchanged iodide. The chlorine solution acted as both eluting agent for the iodine (by oxidizing it to soluble iodic acid) and also as regenerator for the column, since the eluted iodide was replaced by chloride. The silver chloride column could thus be used repeatedly.

In the initial extraction step, hydroxylamine hydrochloride was used to reduce the iodate to elemental iodine. Because this reaction is not quantitative and a small fraction of the iodine is reduced to iodide, nitrous acid is added to oxidize this iodide to elemental iodine. While nitrous acid alone can be used to reduce iodate, under the conditions existing in the procedure prior to extraction, a much higher acid concentration is required than with hydroxylamine and considerable gas evolution occurs. The latter condition requires the use of a larger separatory funnel (500 ml.), which is awkward to handle. The initial extraction step as used in the procedure is rapid and complete, and has proven more convenient than the use of nitrous acid alone. The simultaneous use of two organic solvents in the first extraction facilitated making all extraction steps in a single vessel. The second oxidation-reduction, solvent extraction cycle was used as an additional decontamination step, the whole extraction process also serving as a volume-reduction step.

Total time for the complete procedure (exclusive of counting time) was approximately 2 hours for a single sample—proportionately less per sample for multiple sample processing.

Recovery and Sensitivity. The recovery was between 85 and 95% for both added tracer and metabolized iodine-131 in raw milk. This recovery was slightly lower and more variable than for homogenized milk, possibly because of variation in the degree of homogenization obtained in the cavitation step. When homogenized milk was processed through the complete procedure, recoveries of 90 to 95% of added iodide carrier and tracer were obtained. The losses occurred entirely in the column step and are dependent on the flow rates used. If the flow rate is decreased until residence time on the column is 2 minutes, then greater than 98% of added tracer was recovered. This increase in recovery did not seem to us to justify the necessity for a fourfold increase in sample time on the column. If the complete procedure is used, both the chemical and radiochemical recovery of iodide can be determined from the weight of the silver iodide precipitate, since the radiochemical recovery has been determined to be identical with the chemical recovery. "Recovery" will, subsequently, mean both chemical and radiochemical recovery.

As will be seen below, the iodide exchange onto the silver chloride is quite selective; therefore, after passage of the sample through the column, the silver chloride can be counted directly, if desired. Since the elution step is rapid and makes the procedure even more specific for iodine, a better approach would be to count the eluate rather than the silver chloride. If the procedure is concluded after the column step, then recovery can be assumed to be a minimum of 90% for homogenized milk or 85% for raw milk, since the remainder of the procedure has been found to be quantitative.

If larger capacities and flow rates are desirable, a larger column can be fabricated. In some of our experiments, a 7-cm. diameter by 50-cm. long column was used with a silver chloride column height of only 1.5 cm., since the exchange reaction appeared to be confined to the topmost-part of the silver chloride column. Using this column at a maximum gravity flow rate of 150 ml. per minute, recoveries equal to those of the smaller column—i.e., greater than 90%—were obtained.

Another rapid procedure involved the use of batch exchange of the iodide onto the silver chloride. In this procedure, silver chloride was added directly to the milk after addition of carrier, and the mixture was mixed by stirring or shaking. After the rapid settling of the silver halides, or after centrifugation, the supernatant was decanted or filtered off and the solid phase counted directly. To facilitate the separation of the solid halides from the milk a small amount of carbon tetrachloride was added to the milk. Upon settling or centrifugation, the silver halides accumulated in the heavier carbon tetrachloride layer, completely separated from the milk phase. After 5 minutes of mixing, recoveries have varied from 50 to 85%, using this technique with 250-ml. samples. With additional study, batch exchange could be a useful rapid technique.

Occasionally, a blank sample processed immediately after a high activity sample ($>10^4$ disintegrations per minute) will contain activity from the column of the order of less than 1% (usually less than 0.5%) of the total activity of the preceding sample. It is thus advisable to use an extra chlorine wash on the column after processing highly active samples. After the use of this second chlorine wash, activity measurements of subsequent effluents from blank samples were below detection limits.

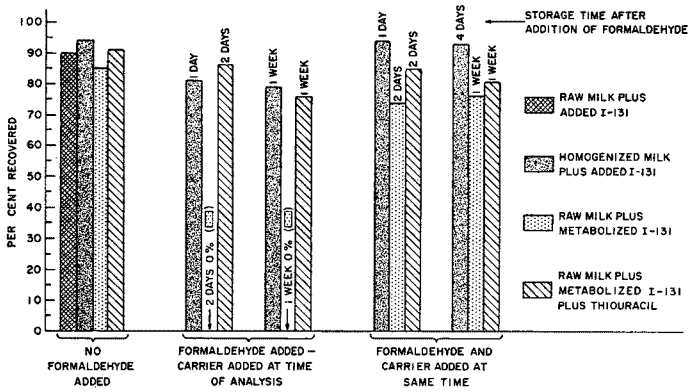

Figure 1. Effect of formaldehyde preservation on recovery of iodine-131 from milk

Because blank samples beta-counted at essentially instrumental background count level (0.3 to 0.5 c.p.m. in an anticoincidence shielded low background detector) and because the iodine-131 beta detection efficiency is approximately 30% (depending on the weight of the silver iodide precipitate), the limit of detection for the complete procedure is less than 2 picocuries of total iodine-131 in 1 liter of milk. This is based on the following assumptions: a 1-liter sample is processed; less than 10% of the iodine occurs in an organic or nonionic-iodide form; a sample count rate of 1 c.p.m. (twice the maximum background count rate) is considered positive; and a recovery of 90% is obtained.

Decontamination. Decontamination experiments were made for the radionuclides listed in Table I. The results listed pertain to the silver chloride column step only. None of the nuclides listed follow through the remaining steps of the procedure. The determination of the per cent contamination of the iodine fraction by each of the nuclides listed was limited by the experimental concentrations used, and may be smaller than that given. The listed nuclides will not interfere if gamma spectrometric measurements are made on the eluted iodine fraction.

In earlier experiments with urine (*4*), decontamination experiments were conducted at pH 1 and the following additional nuclides were also found not to interfere in the column step: cadmium(II)-109, cerium(III)-144, antimony(III)-125, ruthenium(III)-103, and a radiotellurium(IV) mixture. The halides, chlorine-36 and bromine-82, were shown to exchange at differing rates onto the silver chloride, with no elution of the chlorine-36 and partial elution of the bromine-82 (10% in 1 minute and 20% after 15 to 30 minutes). The bromine, however, was not extracted in the extraction step. Silver-110 isotopically exchanged onto the silver chloride, but was not eluted. Thus the halide radionuclides and silver would be column contaminants and after sufficient accumulation could interfere in direct gamma measurements on the column; but they would not interfere in the complete procedure nor in direct gamma measurement on the eluted iodine solution, except as noted above for bromine.

In addition, batch exchange interference studies were made on milk for tracer amounts of cesium-137 and strontium-85. These batch exchange conditions were used so that the reactions for these two most common radioactive contaminants in milk might be observed over a period of time, rather than just during column contact time. In these experiments, the tracer and iodide carrier were added to 50.0 ml. of homogenized milk. The solution was contained in a low-actinic (to minimize photolytic effects), glass-stoppered, 125-ml. Erlenmeyer flask and stirred with a magnetic stirrer. To the solution was added 7.0 grams of 20- to 40-mesh silver chloride and the mixture stirred at a speed sufficient to maintain good mixing (partial suspension) of the silver chloride in the solution. Aliquots of the supernatant solution were measured at various times. From measurements of these aliquots and of the silver chloride, it was found that less than 0.01% of cesium-137 and less than 0.1% strontium-85 were picked up by the silver chloride after 1 hour contact time.

Effect of pH. Iodine-131 tracer and carrier iodide were added to 25.0 ml. of distilled water (since milk could not be used at some of the pH's because of precipitation reactions). After adjustment to the proper pH with sulfuric acid or sodium hydroxide, the solution was stirred with the silver chloride as in the above batch experiments. At all the pH's studied (1.0, 3.0, 5.0, 7.0, and 9.0), more than 99% of the iodide had been exchanged by the end of a 1-minute mixing period, and this initial amount exchanged was not affected by an additional 1-hour contact time. Thus, for all practical purposes, the iodide exchange rate is the same for pH 1 to 9. The slightly more rapid exchange rate obtained here, as compared to the greater than 98% recovery in 2 minutes obtained in the column procedure, is probably due to the more intimate mixing of the solid and liquid phases and the slight pulverization of the silver chloride by the spinning magnet bar used to effect mixing in the batch technique.

Effect of Formaldehyde on Recovery. Formaldehyde is a commonly used preservative for milk. Several workers (*7, 8*) have pointed out that formaldehyde interferes in the ion exchange of milk iodide onto synthetic resins because it promotes an increase in the protein-binding of the inorganic iodine. Lamanna *et al.* (*7*) suggest the use of thimerosal (sodium ethylmercurithiosalicylate) as an alternative preservative.

To study the effect of formaldehyde preservation on the silver chloride–iodide exchange reaction, several experiments were made relative to room temperature storage time and the presence or absence of iodide carrier and/or thiouracil (2-thio-4-oxypyrimidine), used to inhibit the protein-binding of inorganic iodide. These experiments

Table I. Decontamination Factors Obtained with Silver Chloride Column

Isotope	Chemical form	Activity added (d.p.m.)	Per cent found in iodine fraction
Sr^{85}	$SrCl_2$	10^5	<0.01
Cs^{137}	CsCl	10^5	<0.01
Mo^{99}	$(NH_4)_2MoO_4$	10^6	<0.001
Tc^{99m}	NH_4TcO_4	10^6	<0.001
Te^{127m}	Te(IV) in HCl	10^5	<0.01
Ba^{140}	$BaCl_2$	10^6	0.17
La^{140}	$LaCl_3$	10^6	0.12
Zr-Nb^{95}	Zr(IV) and Nb(V) as oxalates	10^5	0.10

were conducted with milk containing both added and metabolized iodine-131. The results are presented in Figure 1.

Figure 1 shows that metabolized iodine-131 behaves essentially the same as added iodine-131, except in one interesting case—namely, where no carrier or thiouracil is present in the formaldehyde-preserved milk. With added iodine-131 in homogenized milk, recovery was reduced by approximately 15% when the milk was preserved with formaldehyde. On the other hand, with metabolized iodine-131 in raw milk, recovery was reduced to zero. It would thus appear that either the added iodine-131 is less susceptible than the metabolized form to protein-binding or else the pasteurization and/or homogenization process renders the proteins less capable of binding the iodine-131. This added tracer result is contrary to Lamanna's results (*7*) on pasteurized milk, using a synthetic anion exchange column, where 95% of added tracer was not recovered after a 1-day storage time and 98.5% not recovered after a 1-week storage time.

The main conclusion from Figure 1 is that formaldehyde will not seriously affect recovery rates provided iodide carrier or thiouracil is present in the milk at the time of addition of the formaldehyde. The thiouracil chemically inhibits the binding of the inorganic iodide into the protein molecules. The iodide carrier probably minimizes the "formaldehyde effect" by isotope abundance or mass effect.

Additional Applications. The procedure is not restricted to the analysis of milk samples alone. In general, the procedure may be applied to the analysis of inorganic radioiodine in aqueous media. In those cases where the iodine may be present in several oxidation states or where it is not present as iodide, a series of oxidation-reduction steps are required after addition of carrier. These redox steps are necessary to effect rapid exchange with the added iodide carrier and to convert all the iodine to iodide prior to addition of the sample to the silver chloride column. As noted earlier, the exchange of iodide ion with silver chloride was rapid and complete from solutions of sulfuric acid or sodium hydroxide in the pH range from 1 to 9. Other conditions were not studied, but the exchange may very well be usable outside that pH range and also not be limited to sulfuric acid or sodium hydroxide systems.

In addition to milk, the procedure already has been applied to urine (*4*) and environmental water samples. With urine, after addition of iodide carrier, the sample is made 0.1*N* in sulfuric acid prior to addition to the silver chloride column. All subsequent wash and eluting solutions are also 0.1*N* in sulfuric acid. The procedure is then completed the same as for milk. With water, a liter sample is first made alkaline to pH 9 with 6*M* sodium hydroxide. Iodide carrier and 25 ml. of 5% sodium hypochlorite are added and the solution brought to a boil to oxidize the iodine to periodate. After cooling to room temperature, the solution is made 0.1*N* in sulfuric acid and excess sodium bisulfite is added to destroy the hypochlorite and reduce the iodine to iodide. The sample is then added to the silver chloride column and processed in the same manner as for milk, except using 0.1*N* sulfuric acid wash solutions.

Table II. Effect of Solution Medium and Exposure to Air of Iodide-131 Evaporated Sources

Iodide-131 solution medium	Direct plated Vol., μl.	Into	Δt days	Average per cent loss	Remarks
0.01*M* HCl	25	H_2O	22.0	35.8	Average of 4 samples. Initial counting rates are nonreproducible; very large loss of iodide on exposure to air
0.005*M* Na_2SO_3	25	H_2O	22.0	23.2	Average of 4 samples. Initial counting rates are nonreproducible; but better than 0.01*M* HCl samples
0.01*M* HCl	25	0.1 ml. $AgNO_3$ (~7 μg)	21.0	7.5	Average of 2 samples. Fair reproduction of counting rates; small loss of iodide on exposure to air
0.005*M* Na_2SO_3	25	0.1 ml. $AgNO_3$ (~7 μg)	21.0	1.9	Average of 2 samples. Reproducible counting rates; little iodide loss on exposure to air

Preparation and Storage of Iodide-131 Evaporated Sources. During the course of this work, erratic behavior of trace amounts of iodide-131 was observed, as shown in Table II. If care is not exercised in the handling of iodide-131 solutions, unexpected losses of activity are encountered. Carrier-free iodide-131 (obtained from ORNL) solutions were prepared in reducing solution and in nonoxidizing acid media—namely, 0.005*M* sodium sulfite and 0.01*M* hydrochloric acid, respectively. Direct plates (evaporation under low heat from an infrared heat lamp) from each of these solutions were made into "fixing" (containing approximately 7 μg. of silver nitrate) and "nonfixing" (water) solutions on stainless steel planchets, and counted. A second count was taken approximately 3 weeks later. All of the plates appeared thin and uniform.

It can be seen from Table II that sources with reproducible counting rates were not obtained from either solution when they were evaporated in the absence of Ag(I) ion, because of volatilization of varying amounts of iodine from the plate. The effect was greater with plates made from the hydrochloric acid solution than with those made from the sulfite solution. With these "nonfixed" plates, the iodine was also lost from the plate during storage in air, probably as a result of the formation of elemental iodine or some other volatile oxidation product of iodine. The effect was again greater with those plates made from the acid solution. A somewhat similar study has been made by Anghileri who determined the extent of radioiodine losses from radiochromatograms exposed to air (*1*).

On the other hand, with direct plates made into silver nitrate solution, reproducible counting results were obtained and storage losses were lessened considerably with the acid solution and eliminated almost completely with the sulfite solution. For the preparation of direct plates of tracer iodide solutions, therefore, it is recommended that the solutions be made up in sodium sulfite solution and the direct plates be made into a solution containing a few micrograms of silver nitrate and evaporated under low heat.

ACKNOWLEDGMENT

Appreciation is expressed to C. L. Comar and F. Lengemann (Cornell University) for furnishing the milk samples containing metabolized iodine-131.

LITERATURE CITED

(1) Anghileri, L. J., *Intern. J. Appl. Radiation Isotopes* **14**, 427 (1963).
(2) Bergh, H., in *2nd U. N. International Conference on Peaceful Uses of Atomic Energy* **18**, Paper 586 (1958).
(3) Boni, A. L., *Analyst* **88**, 64 (1963).

(4) Fairman, W. D., U. S. At. Energy Comm. *Rept.* **ANL-6887** (1964).
(5) Farabee, L. B., in U. S. At. Energy Comm. *Rept.* **ORNL-3347**, p. 149 (1962).
(6) Kahn, B., *J. Agr. Food Chem.* **13**, 21 (1965).
(7) Lamanna, A., Yancik, V., Abbott, T. P., Holmes, J., *Health Phys.* **11**, 586 (1965).
(8) Murthy, G. K., in *U. S. Public Health Serv. Publ.* **999-R-2**, p. 7 (1963).
(9) Murthy, G. K., Gilchrist, J. E., Campbell, J. E., *J. Dairy Sci.* **45**, No. 9, 1066 (1962).
(10) Parsi, E. J., Ioconelli, W. B., U. S. At. Energy Comm. *Rept.* **NP-13620** (1964).
(11) Smith, H., Whitehead, E. L., *Nature* **199**, 503 (1963).
(12) U. K. At. Energy Authority, Prod. Group *Rept.* **204(W)** (1961).

RECEIVED for review March 21, 1966. Accepted May 31, 1966. A portion of this work presented at the 1965 American Industrial Hygiene Conference, May 3–7, 1965, Houston, Texas. Work performed under the auspices of the U. S. Atomic Energy Commission.

Determination of Strontium-90 in Seawater after Concentration by Manganese Dioxide

WILLIAM H. SHIPMAN

U. S. Naval Radiological Defense Laboratory, San Francisco, Calif. 94135

▷ **The adsorption of strontium by hydrous manganese dioxide was used to concentrate strontium in seawater. The important parameters involved in the concentration process were studied. A complete radiochemical procedure for Sr^{90} in seawater using the concentration method as a first step is presented. The chemical recovery is simplified by the use of Sr^{85} which can be gamma counted after Y^{90} is milked and beta counted in a low background counter. The procedure yields a good chemical recovery, satisfactory decontamination from radium and other isotopes, and a low reagent blank. This procedure has been applied satisfactorily to a large number of analyses for Sr^{90} in seawater.**

THERE is a need to assay the oceans for strontium-90, among other radionuclides, to evaluate the extent of global fallout and to test the use of these radioisotopes for describing oceanic circulation and mixing. The low levels of strontium-90 in the ocean (particularly at great depth) lead to the requirement that large volumes of seawater be analyzed.

A radiochemical procedure was devised for the determination of strontium-90 in large volumes of seawater. The strontium is isolated from seawater by coprecipitation with manganese dioxide. Then the strontium is purified through standard radiochemical procedures.

The small ratio of strontium to sodium, calcium, and magnesium in seawater complicates the isolation of strontium from seawater. Also, the amount of strontium present is insufficient to precipitate with any of the common reagents.

Other investigators (*3*, *5*) have coprecipitated the strontium with calcium by the addition of oxalate or carbonate. These methods either present difficulties in manipulating insoluble precipitates or involve massive amounts of reagents and unwieldy volumes of precipitates, thus increasing the probability that contamination is introduced during manipulation. To obviate these shortcomings, the procedure reported here was developed. It requires smaller quantities of reagents and produces smaller volumes of precipitate.

It has been observed that hydrous manganic oxide coprecipitates strontium (*1*, *2*). When this technique was applied to seawater, it was found that by selective chelation, the magnesium interference could be eliminated. When potassium permanganate is stoichiometrically combined with manganous chloride at pH 12, the hydrous manganese dioxide that forms from the resultant oxidation–reduction reaction carries the strontium almost quantitatively.

EXPERIMENTAL

Apparatus. An International centrifuge was equipped with a 3-liter manganese bronze basket and draining chamber, which allowed the centrifuge to be used as a chemical centrifuge.

Reagents. HEDTA (Hydroxyethylethylenediaminetriacetic acid, 41.3% solution as the trisodium salt) was obtained from Chas. Pfizer and Co. Strontium-85 was obtained from Nuclear Science and Engineering Corp., Pittsburgh, Pa. All other reagents were Reagent Grade and were obtained from J. T. Baker Chemical Co., Phillipsburg, N. J.

Procedure. The procedure for the determination of strontium in seawater consists of six basic steps: strontium and calcium are selectively chelated with HEDTA and magnesium is removed as the hydroxide at pH 12; strontium is freed from the chelate by the addition of copper sulfate and strontium is coprecipitated with hydrous manganese dioxide. The bulk of the calcium is eliminated by a sulfate precipitation of the strontium. The rest of the calcium and any rare earth activity are removed by two fuming nitric precipitations of the strontium. Remaining extraneous activities are removed by a ferric hydroxide precipitation, and radium by a double barium chromate precipitation. Added yttrium carrier is precipitated as the hydroxide, then the solution is acidified and yttrium carrier is added. The solution is held for 15 days for the growth of the yttrium-90 prior to final milking and counting.

The detailed procedure is as follows: To 60 liters of seawater in equilibrium with Sr^{85} tracer, 390 ml. of HEDTA are added, the pH is adjusted to 12, and the magnesium hydroxide is isolated by centrifugation and discarded.

To the supernatant solution, 81 grams of $CuSO_4 \cdot 5H_2O$, 57 grams of NaOH, 48 grams of $KMnO_4$, and 90 grams of $MnCl_2 \cdot 4H_2O$ are added in that order. Solution should be complete before each addition. The solution is stirred for 3 hours and the precipitate allowed to settle overnight.

MnO_2 is isolated by centrifugation and dissolved in a minimum volume of concn. HCl. SO_2 gas is bubbled through the solution until solution is complete. The volume is adjusted to 2.5 liters and 4.5 grams of $SrCl_2 \cdot 6H_2O$ are added.

Fifty grams of Na_2SO_4 and 200 ml. of ethanol are added, and the solution is allowed to settle. The supernatant liquid is decanted and discarded.

The precipitate is isolated by centrifugation, metathesized to the carbonate with saturated sodium carbonate, and again isolated by centrifugation.

The precipitate is dissolved in the smallest volume of 2.1*N* HNO_3 possible. Three milliliters of fuming HNO_3 are added for each milliliter of the 2.1*N* HNO_3 added. The solution is chilled in ice and the precipitate is isolated by centrifugation. This operation is repeated.

The strontium is dissolved in 10 to 15 ml. of distilled water. Ten milligrams of Fe^{+3} are added and ferric hydroxide is precipitated by the addition of carbonate-free ammonium

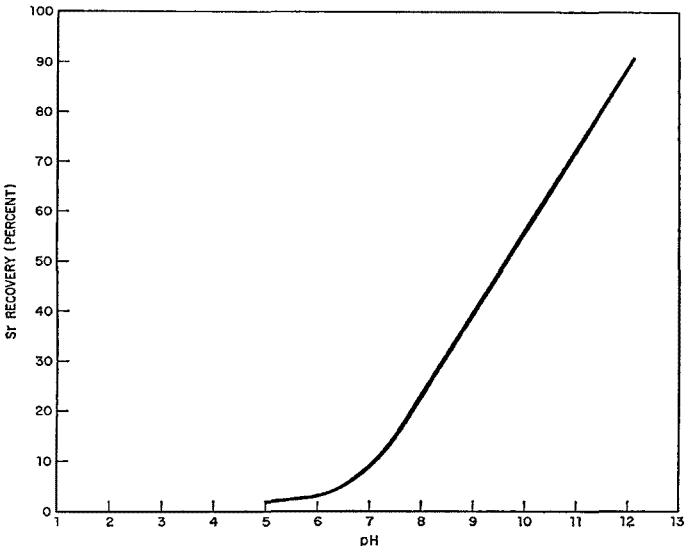

Figure 1. Effect of pH on recovery

hydroxide. The precipitate is coagulated by boiling, isolated by centrifugation, and discarded.

The solution is acidified with 6*N* HNO_3 to methyl red color change. Twenty milligrams of Ba^{+2}, 1 ml. of 6*M* CH_3COOH, and 2 ml. of 6*M* $NH_4C_2H_3O_2$ are added, and the solution is heated to boiling. One milliliter of 1.5*M* Na_2CrO_4 is added. The precipitate is isolated by centrifugation and discarded.

To the solution, 20 mg. of Ba^{+2} are added and the solution is heated to boiling. The precipitate is isolated and discarded.

Strontium is precipitated by the addition of sodium carbonate and the precipitate is isolated by centrifugation. The precipitate is dissolved in the smallest volume of 1*N* HNO_3 possible and the solution boiled to expel carbon dioxide. Twenty milligrams of Y^{+3} are added and yttrium hydroxide is precipitated by the addition of carbonate-free ammonium hydroxide. The precipitate is isolated and discarded. The date and time of this separation are needed to calculate yttrium growth.

The solution is acidified with 1*N* HNO_3, 20 mg. of Y^{+3} carrier are added, and the solution is held for yttrium-90 growth.

After not less than 15 days, the yttrium is precipitated by the addition of carbonate-free ammonium hydroxide. The precipitate is isolated and the supernatant solution saved for chemical yield determination by counting the Sr^{85}.

$Y(OH)_3$ is dissolved in 2 ml. of 1*N* HCl and 4.3 ml. of 2.1*N* HNO_3 are added. The solution is heated to boiling and 15 ml. of a saturated solution of ammonium oxalate are added. Digestion for 20 minutes, cooling, and filtering the precipitate are followed by washing with 5 ml. of water and 5 ml. of ethanol. The precipitate is dried 10 minutes at 100° C. and weighed as $Y_2(C_2O_4)_3 \cdot 9H_2O$.

The supernate saved from the first yttrium precipitation is acidified with concn. HCl and adjusted to a convenient volume. An aliquot is gamma-ray counted and compared with a standard. The chemical recovery of the strontium is calculated from these data.

RESULTS AND DISCUSSION

To establish the conditions of the procedure, four parameters affecting the recovery of strontium from seawater were studied and optimized. The ability of hydrous manganese dioxide to adsorb other radionuclides found in the ocean environment was tested under the conditions for optimum strontium recovery from seawater.

The first and perhaps the most critical of the parameters studied was the effect of the pH of the seawater on the recovery of strontium. As can be seen in Figure 1, the recovery of strontium is very sensitive to small changes of pH. To protect the solution from pH changes due to dissolved carbon dioxide, the container should be kept sealed as much as possible once the pH has been adjusted to 12.

To find the amount of manganese dioxide needed for the maximum recovery of strontium at pH 12, various amounts of manganese dioxide were

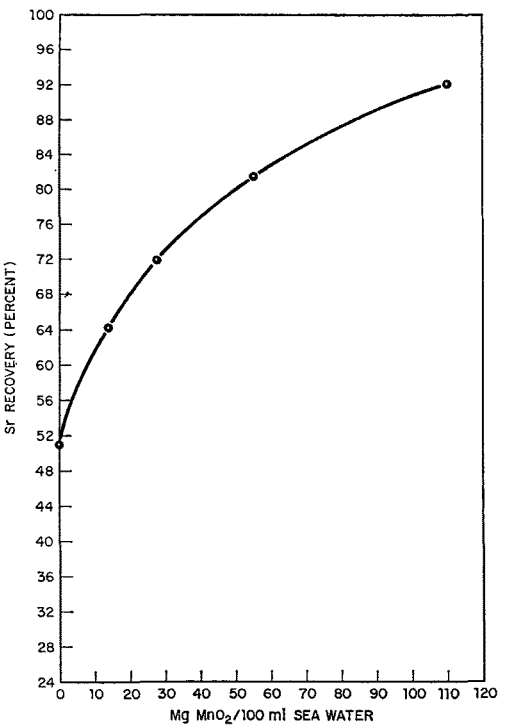

Figure 2. Effect of the amount of MnO_2 used on strontium recovery

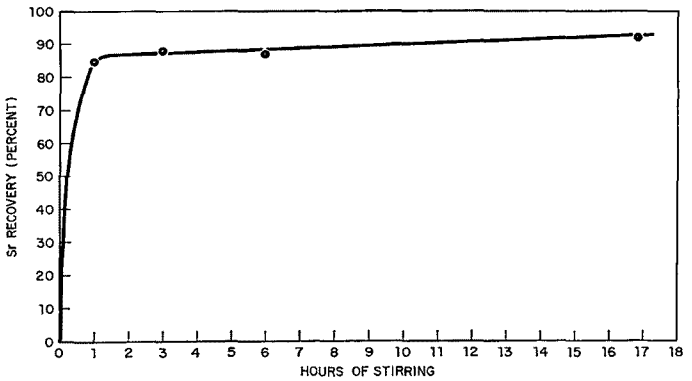

Figure 3. Effect of time of stirring on strontium recovery

introduced and the recovery of the strontium was measured (Figure 2). Based on the desire to introduce the minimum amount of reagent with maximum recovery of the strontium, a concentration of 110 mg. of MnO_2 per 100 ml. of seawater was chosen as the optimum amount. The curve relating the strontium recovery with concentration of manganese dioxide suggests that large increases in the concentration of the dioxide would give little additional increase in recovery.

The importance of the time of contact between the manganese dioxide and the seawater was studied. Figure 3 clearly shows that with 110 mg./100 ml. of manganese the bulk of the adsorption of strontium occurs in the first hour and that no significant amounts are added by prolonged stirring. In fact, a long stirring interval would introduce the problem of pH control against carbon dioxide in the atmosphere. Three hours of stirring was chosen as a compromise.

The last of the four parameters studied was the effect of excess HEDTA resulting from an insufficient addition of copper sulfate. Table I shows that small errors in the addition of copper sulfate are not important, because an error as large as 100% in the amount of HEDTA would result in only a 20% loss in the strontium recovery.

Once the procedure has been optimized, the applicability of the procedure to volumes of seawater larger than 100 ml. was tested. Table II shows that for samples of up to 2 liters, the manganese dioxide continued to be very efficient in removing the strontium from the seawater. Table III shows the recovery of strontium from larger volumes of seawater using the entire procedure. These values show that the manganese dioxide continued to efficiently adsorb the strontium at larger volumes.

The ability of manganese dioxide at pH 12 to carry other radioactivities that might be expected in a marine environment was tested. Table IV shows that under the conditions of the procedure the manganese would not scavenge other activities quantitatively. However, Yamagata (*6*) shows that at pH 8.2 manganese dioxide is quite efficient for these same radionuclides.

This procedure has been applied to the successful analysis of a large number of seawater samples from the North Pacific (*4*). Under conditions at this laboratory, a stable reagent blank of 0.31 d.p.m. of Sr^{90} per sample has been observed. This chemical recovery has been about 75% (Table III). The results shown in Table III are representative of chemical recoveries obtained on actual samples taken during a survey of the North Pacific.

Table I. Effect of HEDTA Concentration on Strontium Recovery

Stoichiometric ratio of amt. of HEDTA to amt. of strontium and calcium in seawater vol.	Strontium recovery, %
0.5	100
1.0	80.5
1.5	36.5

Table II. Effect of Volume of Seawater on Recovery of Strontium (through the initial concentration steps with MnO_2)

Vol. of seawater (liters)	Strontium recovery (%)
0.1	90
1.0	89.5
2.0	92.1
2.0	89.8

Table III. Recovery of Strontium from Large Volumes of Seawater (through the entire procedure)

Vol. of seawater (liters)	Strontium recovery (%)
57	77.2
56.6	73.1
56.9	74.7
57.1	73.8
57.0	77.6
55.2	72.0
55	76.3
56	71.9

Table IV. Isotopes Carried by Hydrous Manganese Dioxide from Seawater at pH 12

Isotope	Carried, %
Co^{60}	48.8
Cs^{137}	11.0
Ce^{144}, Pu^{144}	0.0

LITERATURE CITED

(1) Egorov, Yu. V., Pushkarev, V. V., Tkochenko, E. V., *J. Inorg. Chem. (USSR)* **6**, 256, 1961.
(2) Egorov, Yu. V., Pushkarev, V. V., Tkochenko, E. V., *Radiokhimiya (USSR)* **3**, 87 (1961).
(3) Rocco, G. G., Broecker, W. S., *J. Geophys. Res.* **68**, 4501 (1963).
(4) Shipman, W. H., U. S. Radiological Defense Laboratory, San Francisco, Calif., unpublished data.
(5) Sugihara, T. T., James, H. I., Troianello, E. J., Bowen, V. T., ANAL. CHEM. **31**, 44 (1959).
(6) Yamagata, N., Iwashima, K., *Nature* **200**, 52, (1963).

RECEIVED for review April 18, 1966. Accepted May 31, 1966.

Gas Chromatographic Determination of Pyruvic and Lactic Acids and Krebs Cycle Components

Esterification and Recovery

FRANCES L. ESTES and RICHARD C. BACHMANN

Surgical Research Laboratory, The University of Texas Medical Branch, Galveston, Texas

▷ **In addition to the components of the tricarboxylic acid (TCA) cycle, including the α- keto-, α-hydroxy-, and α,β-unsaturated acids, lactic, and pyruvic acids were esterified in good yields with diazomethane. Gas chromatographic separation on diethyleneglycol succinate gave single peaks for the esters of pyruvic, lactic, malonic, fumaric, succinic, malic, α-ketoglutaric, *cis*-aconitic and citric acids, in order of retention times. Oxalacetate gave a broad flat peak beyond citrate. The only peak observed for the methylation product of glutamic acid was identified as that of methanol. At column temperatures above 115° C. for pyruvate and above 90° C. for fumarate thermal decomposition of the esters occurred and a methanol peak appeared. Recoveries of pyruvate, lactate, malonate, fumarate, succinate, and malate were determined. The methylation of mixtures of lactic and pyruvic acids in varying proportions led to quantitative recoveries of each of the methyl esters.**

THE METHYL ESTERS of the stable (non-keto) acids of the TCA cycle, as well as the unsaturated acids, fumaric and aconitic have been identified by gas chromatography (*10, 11*). Similarly, the methyl esters of lactic and pyruvic acids have been separated from other acids (*2, 6*), and from acids of the TCA cycle including α-ketoglutarate (*2, 13*). These reports differ in the order of elution of the esters, the number of peaks given by pyruvate and α-ketoglutarate, and in the apparent isomerization of dimethyl fumarate. Rumsey *et al.* (*13*) used a column containing 15% diethyleneglycol succinate on Chromosorb W at 135° C. and observed two peaks for methyl pyruvate. Other than the emergence of methyl lactate before methyl pyruvate, the observations of Alcock (*2*) with a diethyleneglycol adipate column appeared similar to those of Gee (*6*) using a neopentylglycol succinate column. The two peaks reported by Alcock (*2*) for α-ketoglutarate were not observed by Rumsey *et al.* (*13*).

For these investigations, the methyl esters were prepared from the acids by a variety of methods including: methanol–HCl (*6, 10*), thionylchloride (*6, 10*) methanol–H_2SO_4 (*11, 13*), methanol–boron trifluoride (*2, 10*) and diazomethane (*10, 11*). The method used appeared to be dependent on the particular esters of interest and the reported applicability of the methylating agent to the acid in question.

For the long chain acids, Stoffel *et al.* (*16*) found methanol–HCl to give quantitative yields of the methyl esters, and Schlenk (*14*) observed that the quantitative esterification of long chain fatty acids by diazomethane required the addition of methanol. These observations did not appear applicable to the short chain acids. For the esterification of butyric, valeric, and caproic acids, Vorbeck (*17*) found diazomethane to give better yields than methanol–HCl, or methanol–BF_3. Luke *et al.* (*10*) also used the method of Roper and Ma (*12*) for methylation of the di- and tricarboxylic acids. McKeown and Read (*11*), however, reported that low yields were obtained when the methylation was carried out in ether solution and that the addition of methanol enhanced the yield.

Eistert (*5*) had suggested that diazomethane could add to esters of unsaturated, conjugated, dicarboxylic acids—e.g., fumaric, to form pyrazoline dicarboxylic esters, and that on heating, the pyrazoline could decompose to form cyclopropane derivatives. McKeown and Read (*11*) regarded the formation of 4,5-dicarbomethoxyl–pyrazoline as the probable explanation for the isomerization of dimethyl fumarate as reported by Luke *et al.* (*10*).

Eistert (*5*) had also indicated that with diazomethane, the α-hydroxyl group could be methylated and that methyl pyruvate could further react to give ethylenic acid. Burchfield's (*3*) comment that "the use of diazomethane should be avoided unless the mixture consists solely of saturated nonoxygenated acids such as succinic and glutaric" was consistent with these reports.

The diazomethane method of esterification, however, presented the advantage of producing nitrogen as the chief by-product which should eliminate problems of recovery of the ester that would be encountered in the other methods. In view of the previous observations, it was essential that the products formed from α-substituted, and unsaturated dicarboxylic acids on reaction with diazomethane be characterized.

Although some of the difference in the reports of the various workers may be related to column material, the work of Ackman *et al.* (*1*) suggests that thermal decomposition of the sample should be considered.

Other than the examination of the molar response of the β-ray argon detector toward straight chain α,ω-dicarboxylic fatty acids (*15*), there has been little indication of recovery or quantification of these materials.

Since our interest involved application of the method to the quantitative determination of these acids in biological systems, the chromatographic factors affecting the quantification of the esters were examined.

EXPERIMENTAL

In the initial preparation of larger quantities of the methyl ester, the method of Roper and Ma (*12*) was modified by direct addition of the free acid to an ethereal solution of diazomethane. The diazomethane was prepared from *N*-methyl-*N*-nitroso-*p*-toluene sulfonamide ("Diazald," Aldrich Chemical Co.) by the procedure of De Boer (*4*).

In all cases 35 millimoles of free acid were added directly to the ethereal solution of diazomethane. An equivalent excess of diazomethane was allowed for each carboxyl group. On completion of the reaction, the ether was removed by placing the reaction vessel in a warm water bath.

The solid esters were recrystallized from ethanol. Where possible, the liquid esters were vacuum distilled. Since the products from the diazomethylation of glutamic and α-ketoglutaric acids decomposed on heating, they were not distilled, but the lower boiling components were removed under

Table I. Properties of Methyl Esters Prepared

Ester	B.P. °C.[b] This lab	B.P. °C.[b] Ref. (7)	M.P. °C. This lab	M.P. °C. Ref. (7)	Refractive index This lab	Refractive index Ref. (7)	Density This lab	Density Ref. (7)	Yield, % This lab	Yield, % Ref. (12)
Dimethylfumarate			101	102					89.6	...
Trimethyl citrate			78	79					89	54
Methyl pyruvate	135.35	137	[a]		$1.4108^{24°}$	$1.4046^{25°}$	$1.148^{20°}$	$1.154^{0°}$	71	...
Methyl lactate	144.2	144.8			$1.4124^{26°}$	$1.4156^{15°}$	$1.051^{25.5°}$	$1.119^{0°}$	69	...
Dimethylsuccinate	106[1 mm.]	192.8			$1.4120^{26°}$	$1.4197^{18°}$	$1.119^{26°}$	$1.1202^{18°}$	86.4	33
Dimethylmalate	164[1 mm.]	242			$1.4404^{26°}$	$1.4425^{20°}$	$1.222^{22°}$	$1.226^{20°}$	73.7	...

[a] 2,4-Dinitrophenylhydrazone deriv. m.p. 144° C. Reported 142–4° C. (9)
[b] Unless otherwise indicated, boiling points were determined at 760 mm. Hg.

Table II. Effect of Temperature on Retention Time and Peak Area of Methyl Esters

Ester	Temp., 65° C.	Recovery, %	Temp., 85° C.	Temp., 100° C.	Recovery, %	Temp., 125° C.	Recovery, %
Methyl pyruvate	26.6 (388)	97.4	17.6 (371)	10.7 (368)		5.3 (274)	
Methyl lactate	32.3 (522)	100.01	20.7 (469)	12.2 (464)		5.3 (399)	
Dimethylmalonate				26.6 (350)	98.8	14.0 (322)	
Dimethylfumarate			47.4 (565)	32.8 (453)	92.6	17.4 (370)	
Dimethylsuccinate				34.0 (318)		22.3 (322)	88.5
Dimethylmalate				60.0 (219)		46.3 (280)	92.0

Retention time in minutes. Values in parenthesis are peak areas in thousands of counts. Column: 8-ft. glass column packed with 15% DEGS on Gas-Chrom-P. Flash heater: 215° C., carrier gas, argon 8 p.s.i.g. (88 ml./min. at outlet). Detector: argon Sr^{90} at 215° C. Sample: 5 μl. (10^{-2} micromoles in acetonitrile). Recovery: calculated on the basis of the free acid used for the methylation and the assumption the commercial preparations were pure.

reduced pressures at temperatures below the decomposition points of the esters.

Melting points were determined on a Fisher-Jones apparatus and refractive indices on an Abbé 3L refractometer. Boiling points were determined by distillation at the indicated pressures and densities by the weight–volume method, corrected for temperature.

For esterification of individual acids in micromole quantities, 0.02 ml. or 25 mg. of the acid were dissolved in 10 ml. of diethyl ether and the ethereal solution of diazomethane was added with shaking until a permanent yellow color appeared. A 5-ml. excess of the diazomethane solution was then added. The ether and excess diazomethane were removed from the esters on a rotary evaporator at 20° C. under vacuum. The residue of methyl esters was dissolved in 2 ml. of acetonitrile (spectro grade, Eastman Organic Chemicals) for chromatographic analysis.

For the preparation of the esters in mixtures and for studies of gas chromatography separations, the liquid acids (0.02 ml.) and the solid acids (25 mg.) were mixed and dissolved in 100 ml. of diethyl ether for esterfication. The ethereal solution of the acids was contained in the first chilled (ice bath) receiving flask so that the diazomethane distilled directly into it. For convenience, the esterified mixture was stored overnight in dry ice. To ensure complete methylation of the poly-acids additional diazomethane was added if the solutions became decolorized. For chromatography, an 8-ft. "U"-shaped column (10-mm. I.D.) packed with 15% diethyleneglycol succinate (DEGS) on 80–100 mesh Gas-Chrom-P (Applied Science Laboratories) was used in a Barber-Colman Model 15 Gas Chromatography unit with an Argon Strontium-90 Detector. Peak areas were measured by the attachment of a Model CRS-1 Chromatography Readout System (Infotronics Co.).

For esterification, the acids used were: pyruvic acid (Eastman Organic Chemicals), lactic acid (91%), succinic acid (Baker analyzed), citric acid (California Biochemical, A grade), fumaric acid and malonic acid (California Foundation for Biochemical Research, purified grade), L-malic acid (Nutritional Biochemical), *cis*-aconitic acid and oxalacetic acid (K and K Laboratories) and L-α-ketoglutaric acid (Sigma).

Commercially available esters, methyl pyruvate, methyl lactate, dimethyl malate, dimethyl fumarate, dimethyl malonate, and dimethyl succinate (K and K Laboratories) were used for comparison of retention times and recovery.

RESULTS

In the initial studies, the methyl esters were prepared in sufficient quantities for characterization. The physical properties and yields of the esters examined have been shown in Table I. Although a mole excess of diazomethane was used, there was no indication of secondary reactions for methyl pyruvate. Likewise, even after recrystallization, the yield of dimethyl ester of fumaric acid was comparable with that of succinic acid and considerably better than the yield of dimethyl malate. Glutamic acid was included because of the possibility that the methyl ester would complicate the analysis of α-ketoglutarate. As no interference was observed, the material ($\alpha_D^{26°}$ 1.3919, D $1.059^{25°}$) was not further identified. Likewise, the product of methylation of α-ketoglutaric acid has not been further identified. The 2,4-dinitrophenylhydrazone derivative (m.p. 120° C.) was formed from the product recovered ($\alpha_D^{26°}$ 1.4003, D $1.109^{25°}$).

Since our interest was in the quantification of micromole quantities of the acids, the esters were prepared in micromole quantities for subsequent studies.

The effect of temperature on the retention time and relative recovery of the individual methyl esters has been shown in Table II. As the temperature increased, the apparent peak area for methyl pyruvate, lactate, malonate, and fumarate decreased. This was most evident for fumarate between 85 and 100° C. and for pyruvate between 100 and 125° C.

Not apparent from Table II, was the observation that at temperatures above 100° C. methyl pyruvate no longer appeared as a single peak but gave three peaks; one appearing before and one

after the main pyruvate peak. It was also observed, especially for methyl pyruvate and lactate, that if the diluted samples were permitted to be at room temperature for some period of time (48 hrs.), decomposition occurred and a chromatographic peak identified as methanol appeared. The other methyl esters also exhibited this apparent decomposition to give methanol. A similar decomposition of methyl pyruvate and of methyl lactate occurred if the flash heater temperature exceeded 225° C. In all of the trials using freshly prepared methyl pyruvate at column temperatures of less than 110° C., only one peak was observed. There was no evidence of the peak generally referred to as "pyruvate-2" (*2*).

For evaluation of the methylation and possible losses in transfer, individual samples of the prepared esters were compared with known esters. The per cent recovery shown in Table II was calculated on the basis of the free acid used for the methylation and the assumption that the commercial preparations were pure. At the temperatures used for this comparison, the individual commercial esters also exhibited only a single peak. Any loss on the column would be identical for the isolated esters.

Although good recoveries of both methyl pyruvate and methyl lactate could be obtained at column temperatures below 100° C., there was no indication that such recoveries could be achieved when either of the acids were in excess. Mixtures of pyruvic acid and lactic acid in reciprocal concentrations from 0 to 25 $\times$ 10^{-2} micromole, such that the total acid concentration was constant, were prepared for methylation. Each sample of the mixed esters was taken up in 5 ml. of acetonitrile, and 5 μl. of the sample applied to the column. The results from these observations have been shown in Figure 1. Except for the sample containing 30% pyruvate and 70% lactate, all counts were within 3% of the predicted values as calculated from various concentrations of lactate and pyruvate. These observations indicate the usefulness of the method for the analysis of these specific compounds.

The data in Table II were used as a guide in programming the column temperature (65–175° C.) for the resolution of mixtures of the prepared esters. In the temperature program shown in Figure 2, several compromises were involved. For vaporization of the higher boiling components, a flash heater temperature of 225° C. was required. Likewise, in order to decrease the retention time for the longer chain compounds, the initial temperature increase was so rapid as to be at ca. 112° C. by the time fumarate was eluted. Under these conditions the decomposition of some of the ester was apparent in the consistently appearing methanol peak. Since the appearance of methanol was always associated with the higher flash heater and column temperatures, it must not be assumed that recoveries from the temperature programmed mixture would be comparable to those reported for the individual components as shown in Figure 1 or Table II. These observations indicate that the programmed situation permits identification of the components in a mixture but for quantification, the conditions for the analysis, particularly temperatures, must be related to the individual component, or group of components.

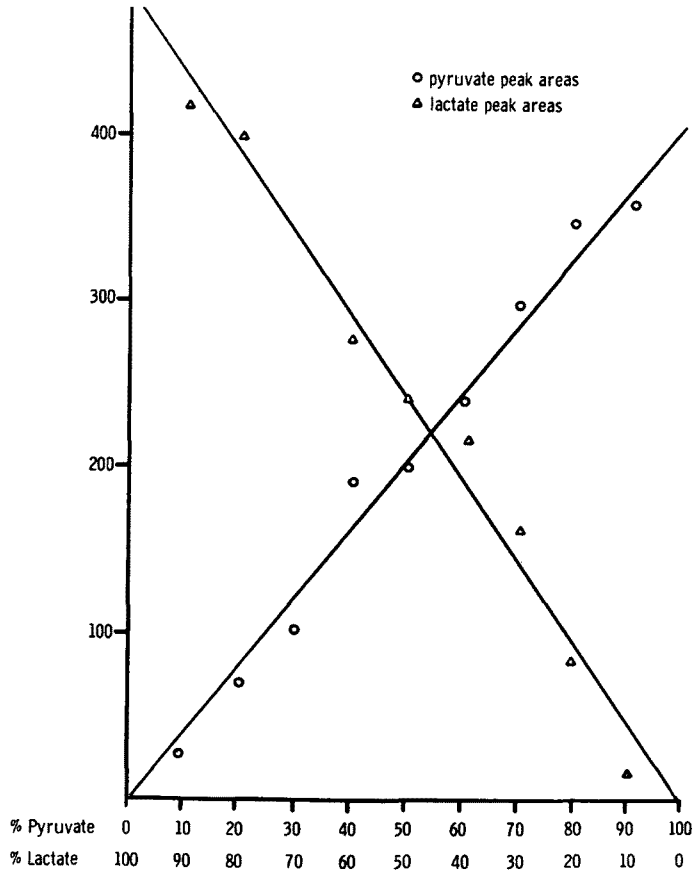

Figure 1. Recoveries of pyruvic and lactic acid as methyl esters

Relative peak areas in thousands of counts
Column temp. 85° C.
Injection port temp. 215° C.
Carrier gas (argon)
Flow rate 8 p.s.i.g. (88 ml./min.)
Sensitivity 1 $\times$ 10^{-7}
Attenuation 8

DISCUSSION

Of the esters prepared, dimethyl fumarate gave the lowest recovery. These observations are consistent with previous work (*11*) suggesting poor yields of dimethylfumarate. It is likewise in agreement with Vorbeck *et al.* (*17*) that the lower yields do not result from side reactions and there was no evidence of formation of addition products at the ethylene bond. Furthermore, even at column temperatures of 90° C., dimethyl fumarate (m. p. 102°) gave a methanol peak.

Except for Luke *et al.* (*10*), irrespective of the method of methylation, column packing material, or temperature programming, all the previously reported observations (*2, 6, 11, 13*) are in agreement with this report that dimethyl fumarate eluted as a single peak before methyl succinate. McKeown (*11*) has suggested that in the methylation Luke *et al.* (*10*) formed the 4,5-dicarbomethoxy-pyrazoline. If this ex-

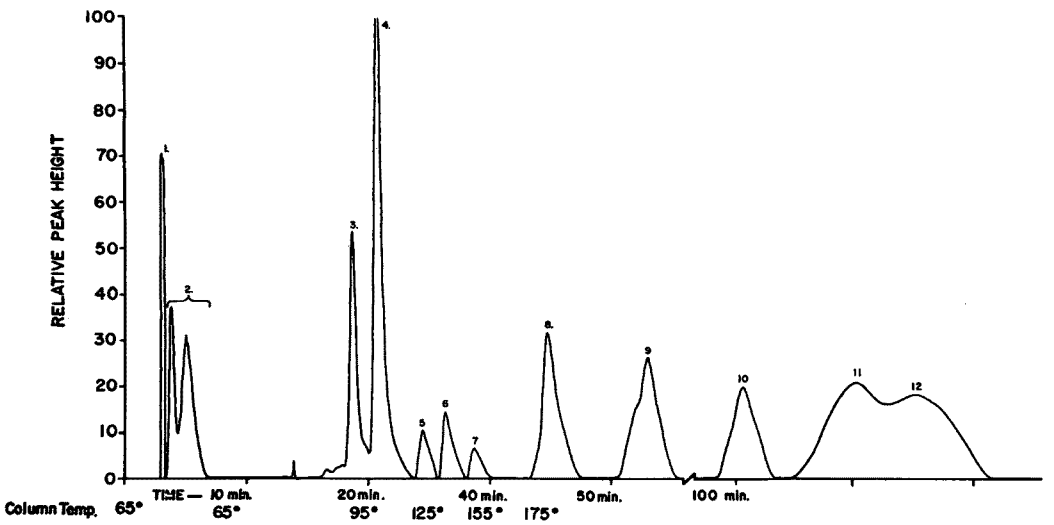

Figure 2. Programmed separation of methyl esters

Injection port 225° C., argon at 88 ml./min. Values in parenthesis are retention times relative to pyruvate, 20.7 min.

1. Methanol
2. Solvent (2 peaks)
3. Pyruvate (1.00)
4. Lactate (1.10)
5. Malonate (1.28)
6. Fumarate (1.38)
7. Succinate (1.78)
8. Malate (2.17)
9. α-Ketoglutarate (2.56)
10. *cis*-Aconitate (4.88)
11. Citrate (5.14)
12. Oxalacetate

planation is true, then it resulted from either reducing the volume in a stream of N_2, or from drying with Na_2SO_4. The results herein are not in agreement with McKeown (*11*) that reduced temperatures (−70° C.) are required to prepare dimethyl fumarate. Likewise, we were unable to confirm their (*11*) observation that better yields were obtained with methanol as a solvent for the methylation. Their use of 10% acetic acid in methanol to destroy the excess diazomethane may have contributed to the differences observed. No difficulties in methylation were encountered when the ether solution containing the diazomethane was cool, excess diazomethane was used, and the ether and unreacted diazomethane were removed in a rotary evaporator at 20° C. It was also observed that even in dry solvents, when the esters are in low concentration, prolonged standing at room temperature should be avoided.

Since both Gee (*6*) and Rumsey (*13*) used methanol to dilute their sample, any methanol resulting from the high temperature of the injection port would not have been observed. The second pyruvate peak reported by Rumsey (*13*) quite probably resulted from the column temperature used.

Although Rumsey *et al.* (*13*) found some overlapping with dimethylmalate peaks, they report the dimethyl ester of α-ketoglutarate as a single peak which is in agreement with our observations. Alcock (*2*), however, found 2 peaks for α-ketoglutarate differing in proportion from one preparation to another. In addition, while this work is in accord with Gee (*6*) that the methyl pyruvate (b.p. 137° C.) elutes before methyl lactate (b.p. 144° C.), Alcock reports the reverse order. Although the column material was diethyleneglycol adipate as compared with neopentylglycol succinate and diethyleneglycol succinate the fact that the observations involved only the keto acids suggests that the differences do not result from the packing material but possibly from the use of chloroform as a solvent.

From the data, it is apparent that methyl esters of α-hydroxyl, α-keto, and conjugated unsaturated acids can be prepared by diazomethane. The characterization and recovery of methyl lactate as determined by peak area would indicate that the α-hydroxyl group was not esterified. Likewise, the characterization and recovery of methyl pyruvate is not consistent with the formation of secondary reaction products (*3, 5*). Quite apart from the method of preparation, it is apparent that the equilibrium for methyl pyruvate is on the side of hydrolysis products, as evidenced by the appearance of the methanol peak at column temperatures above 100° C. Since heat decomposition of methyl esters of α-ketoglutaric and glutamic acid precluded distillation, it is not surprising that the methanol peak appeared with α-ketoglutarate and that methanol has been the only peak observed on gas chromatography of the dimethyl ester of glutamic acid. The latter observation indicated that application of this method to biological preparations would not be complicated by the α-aminodicarboxylic acids.

Although the observations on the resolution of the methyl ester of oxalacetic acid were not in complete agreement with those of Alcock (*2*), they are in accord with the conclusion that the resolution was not satisfactory. The problem may be one of esterification as Alcock has suggested, however, it may be inherent in the character of oxalacetic acid which is also an α-keto acid.

These observations suggest that for quantification of α-substituted dicarboxylic acids, the problem is not so much one of method of methylation as of selection of the derivative to be used. The recent report of Horii *et al.* (*8*) suggests that the trimethylsilyl derivatives might be useful for these acids.

LITERATURE CITED

(1) Ackman, R. G., Bannerman, M. A., Vandenheuvel, F. A., ANAL. CHEM. **32**, 1209 (1960).
(2) Alcock, N. W., *Anal. Biochem.* **11**, 335 (1965).
(3) Burchfield, H. P., Storrs, E. E., "Biochemical Applications of Gas Chromatography," pp. 588–92, Academic Press, New York, 1962.

(4) De Boer, T. J., *Rec. Trav. Chim.* **73**, 229 (1954).
(5) Eistert, B., "Synthesis with Diazomethane" in "Newer Methods of Preparative Organic Chemistry," p. 513, Interscience, New York, 1948.
(6) Gee, M., ANAL. CHEM. **37**, 926 (1965).
(7) Handbook of Chemistry and Physics, 44th Ed. Chemical Rubber Publ. Co., Cleveland, Ohio, 1963.
(8) Horii, Z., Makita, M., Tamura, Y., *Chem. Ind. (London)* **34**, 1494 (1965).
(9) Kuhn, R., Drury, K., *Ann.* **571**, 44 (1951).
(10) Luke, H. H., Freeman, T. E., Kier, L. B., ANAL. CHEM. **35**, 1916 (1963).
(11) McKeown, G. G., Read, S. I., *Ibid.*, **37**, 1780 (1965).
(12) Roper, R., Ma, T. S., *Microchem. J.*, **1**, 245 (1957).
(13) Rumsey, T. S., Noller, C. H., Burns, J. C., Kalb, D., Rhykerd, C. L., Hill, D. L., *J. Dairy Sci.* **47**, 1418 (1964).
(14) Schlenk, H., Gellerman, J. L., ANAL. CHEM. **32**, 1412 (1960).
(15) Sharpless, N. E., *J. Chromatog.* **12**, 401 (1963).
(16) Stoffel, W., Chu, F., Ahrens, E. W., Jr., ANAL. CHEM. **31**, 307 (1959).
(17) Vorbeck, M. L., Mattick, L. R., Pederson, C. S., *Ibid.*, **33**, 1512 (1961).

RECEIVED for review March 14, 1966. Accepted June 8, 1966. This research was supported by National Institutes of Health Research Grant NIH 5 RO1 GM 09695.

An Improved Method for the Determination of Orthophosphate Suitable for Assay of Adenosine Triphosphatase Activity

SAMUEL M. MOZERSKY, JULIO D. PETTINATI, and STANLEY D. KOLMAN

Eastern Regional Research Laboratory, U. S. Department of Agriculture, Philadelphia, Pa. 19118

▷ **In view of poor recovery and lack of reproducibility and stability frequently experienced in the assay of orthophosphate (Pi) by the method of Martin and Doty, the method has been modified in three respects: protein is precipitated with ClO_4^- at pH 1.5–1.8; the precipitate is removed prior to formation of phosphomolybdic acid; phosphomolybdic acid is measured, after extraction into isobutanol–benzene (1:1), in the unreduced (yellow) form. Optimal concentrations of H_2SO_4 and molybdate have also been determined. The method developed is superior in precision and accuracy, as well as sensitivity, to those presently available, and the product measured is stable for at least 48 hours. The procedure was applied, with satisfactory results, to the determination of the adenosine triphosphatase activity of extracts of muscle tissue and proteins isolated from such tissue.**

ORTHOPHOSPHATE (Pi) is almost always determined as phosphomolybdic acid, usually after reduction (*5*, *18*, *24*). Duval (*4*) aptly remarks on the "very numerous modifications" of the method, and of "profound contradictions on the subject of the optimal concentration of molybdic acid, of acidity, and of the temperature of reduction." He further states that if reduction is carried out at room temperature, as is commonly done, the blue color is unstable. Kondrashova *et al.* (*14*) likewise comment on the "existence of many modifications [and] the absence of a single one that is sufficiently satisfactory." Our experience fully confirms these statements.

The object of the investigation presently described was to determine conditions which are optimal for the determination of Pi and compatible with the presence of adenosine-5′-triphosphate (ATP), proteins and various salts. It was found necessary to consider the following factors: the agent used for precipitation of the protein, the necessity of removing the (precipitated) protein, the form of the phosphomolybdate during extraction and measurement, the $[H^+]$, and the concentration (aqueous) of molybdate.

EXPERIMENTAL

All spectra were obtained with a Bausch and Lomb Spectronic 505 recording spectrophotometer. Other absorbance measurements were made with a Beckman DU spectrophotometer which was calibrated for wavelength and absorbance (*12*). The level of phosphorus is expressed as final concentration in mg. of P/liter. Except where otherwise indicated, the unit of absorptivity a is $(cm)^{-1}$ (mg. P/liter)$^{-1}$. When phosphorus was extracted from an aqueous into an organic phase, the absorptivity figures refers to the concentration of phosphorus in the latter phase. In such cases the absorptivity is "apparent" in the sense that the extraction was assumed to be quantitative and the volume of the organic phase was assumed to be unaffected by equilibration with the aqueous phase.

The reduced and unreduced forms of the colored phosphomolybdate product(s) are indicated by the superscripts *B* (blue) and *Y* (yellow), respectively. Additions of inorganic phosphate were in the form of KH_2PO_4, Fisher primary standard, dried at 110° C. for 24 hours. The levels of acids and salts are expressed as final concentrations in the aqueous phase.

Adenosine Triphosphatase Assay To 1 ml. of enzyme solution containing from 10 to 400 μg. of myosin (*6*) in buffer A were added two ml. of substrate solution, containing ATP in buffer B (*24*). The samples were incubated in a water bath at 22° C. for five minutes. Some assays were carried out using the buffers suggested by Haga *et al.* (*9*).

RESULTS

I. Tests with Phosphomolybdate Blue. The procedure of Martin and Doty (*18*), as modified by Szent-Györgyi and Holtzer (*24*), was applied to a series of standard phosphate solutions. The absorbance spectrum of the blue product (Figure 1*A*) has a broad peak in the visible range, and peaks in the ultraviolet at 313 mμ and at 273 mμ. An absorptivity $a^B_{675} = 0.512$ was found, agreeing with Szent-Györgyi and Holtzer (*24*). However, fading of the extracts was observed. The fading rate increased with increasing concentration of Pi, being a first-order function of phosphate concentration up to 1.3 mg. P/liter, and a higher order function above this level. Furthermore, the rate of fading was not reproducible in different experiments. This could not be attributed to variability in reagents. Chilling the reduced extract in an ice bath improved color stability considerably, but the results were still too erratic to be acceptable. The substitution of *p*-semidine for stannous chloride, as recommended by Dryer *et al.* (*3*) was tried, but very little reduction to the blue product was obtained as measured by the color yield. The use of isoamyl acetate (iAA) as the extracting solvent, and addition of stannous chloride in the dry form, as reported by

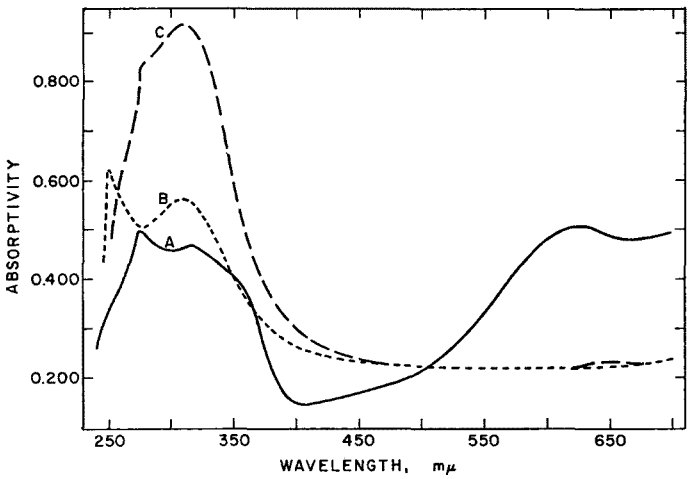

Figure 1. Absorbance spectra of phosphomolybdic acid

(A) Reduced acid in iBB, 1:1 (18)
(B) Unreduced acid in iAA
The aqueous phase contained 45.2 μg. of P (KH_2PO_4), 40 meq. H_2SO_4, and 405 μmoles $(NH_4)_6Mo_7O_{24}$ in a volume of 50 ml.
Ten ml. of the aqueous phase was extracted with 10 ml. iAA
(C) Unreduced acid in iBB
As for (B) above, except that the aqueous phase was extracted with iBB

Kirsten and Carlsson (*13*) was also attempted. Color stability at 720 mμ was improved but the fading rate was still unacceptably high. Moreover, the sensitivity found, $a^B_{720} = 0.471$, was much lower than expected (*13*).

II. Tests with Yellow Phosphomolybdic Acid: Conditions for Its Formation and Extraction.

A. Preliminary Evaluation. Figure 1 also shows the absorbance spectra of yellow phosphomolybdic acid in iAA and iBB (isobutanol–benzene, 1:1, v/v). Stability was satisfactory in both solvents, but higher sensitivity was obtained with the latter. It is also evident that greater sensitivity was obtained by measuring the heteropoly acid without reduction ($a^Y_{312} > a^B_{675}$). Furthermore, the spectrum of the yellow, unreduced acid was completely stable for at least two hours, in contrast to the poor stability of the blue reduction product. Adherence to Beer's law was demonstrated for the iBB extract.

In an attempt to prevent hydrolysis of organic phosphate (ATP) prior to extraction, the reagents used to obtain the yellow phosphomolybdate product were made up in dimethyl formamide and dimethyl sulfoxide (*20*). However, it was found that both of these solvents inhibit formation of the heteropolyacid and its extraction into iBB.

B. Optimal Molybdate Concentration. Samples containing a constant amount of KH_2PO_4 were reacted with varying amounts of molybdate [$(NH_4)_6Mo_7O_{24}$]. The products were extracted into iBB according to the procedure of Szent-Györgyi and Holtzer, and the absorbance of a portion of each organic phase was measured at 313 mμ against the corresponding reagent blank. The aqueous phase contained 2.26 μg. P, 3.84 meq. H_2SO_4, and 1–100 μmoles $(NH_4)_6Mo_7O_{24}$ in a volume of 6 ml., and was extracted with 5 ml. iBB. The data (Figure 2) indicate that optimal color development for this set of conditions occurs at a concentration of 4 to 5m*M* molybdate. A molybdate concentration of 4.17m*M* was selected for further experiments.

Since the heteropolyacid forms in, and is extracted from, an acidic medium which frequently contains salts, the effect of acidity, ionic strength, and species of ion needed careful scrutiny.

C. Optimal Acid Strength. The effect of varying acid concentration (H_2SO_4) from 0 to 3.5*N* on the yield of heteropolyacid extracted into the organic phase was measured. The aqueous phase contained 2.26 μg. phosphorous, 25 μmoles molybdate, and 0–21 meq. H_2SO_4 in a volume of 6 ml., and was extracted with 5 ml. iBB. Absorptivity was nearly independent of $[H^+]$ over the range 0.5–0.9*N* (Figure 3), where $a^Y_{313} = 0.93$. The drop in absorbance was very steep beyond an acid strength of 1*N*. For some of the experiments to be described the $[H^+]$ was set at 0.6*N*. In later work a concentration of 0.7*N* was used. The interplay of hydrogen ion concentration, ionic strength, and ionic species is discussed further in the text.

D. Interfering Substances. Preparatory to running adenosine triphosphatase (ATPase) determinations according to Szent-Györgyi and Holtzer (*24*) the buffer and salts involved were individually checked for possible interference in the measurement of phosphate as yellow phosphomolybdate. It was found that sodium chloride, imidazole, and calcium chloride, at the levels indicated, made no contribution to the absorbance at 313 mμ. Furthermore, $a^Y_{313} = 0.923$ was found for Pi when two μmoles of ATP were present in the sample. This value is in good agreement with our previously found a^Y_{313} values, where ATP was absent.

The following salts were also investigated for possible interference at levels likely to be encountered in practice: EDTA, 0.67m*M*; $MgSO_4$, 0.67m*M*; KCl, 0.4*M*. These were tested singly in the presence of calcium chloride, sodium chloride, and imidazole. There was no reduction in precision or absorptivity. In the presence of calcium chloride, sodium chloride, and imidazole, an absorptivity curve was run in the range 0–1.36 mg. P/liter of solvent phase.

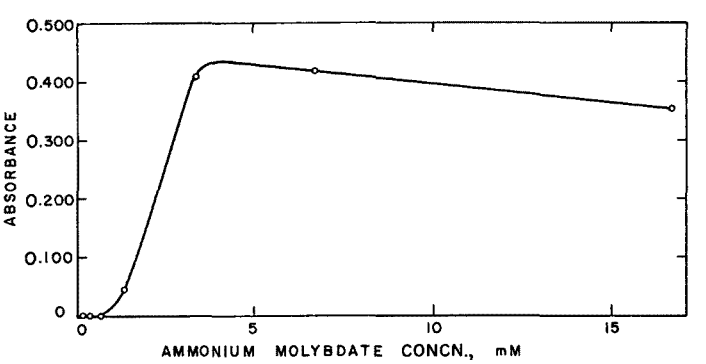

Figure 2. Absorbance of extracted unreduced phosphomolybdic acid as a function of concentration of molybdate

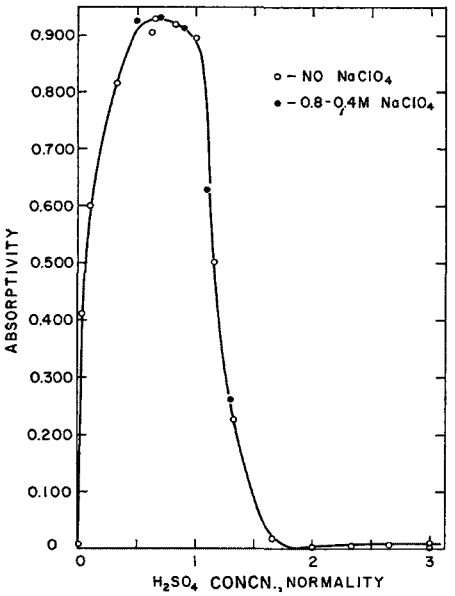

Figure 3. Absorbance of extracted unreduced phosphomolybdic acid at 313 mμ as a function of concentration of H^+

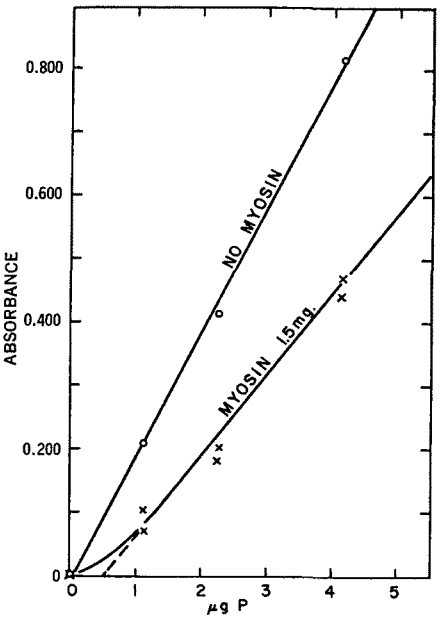

Figure 4. Absorbance at 313 mμ with and without myosin present during formation and extraction of phosphomolybdic acid

The standard deviation of absorbance was ± 0.013, corresponding to 1.4% at the 1 mg. P/liter level. Glycerol at a level of 2.28 m*M* in the aqueous phase gave no interference.

III. Investigation of Agents for Deproteinization Prior to Formation and Extraction of Unreduced Phosphomolybdic Acid. The following protein precipitants were examined:

Boiled silicotungstic acid (*18, 19*) was evaluated at three levels: 1.5, 5.0, and 8.0m*M* in the aqueous phase. The pH of the STA reagents that were used was adjusted to 1.5–1.8. It was found that the absorbances of the extracts were 0.90, 1.11, and 1.39, respectively, when read against iBB at 313 mμ; blanks having this order of absorbance would diminish photometric sensitivity. Purification of STA by recrystallization (*22*) did not improve the results.

Sulfosalicylic acid (*27*) was tried at the 0.39*M* level in the aqueous phase, but it adversely affected extraction of the yellow product by the solvent (iBB). Furthermore, it was preferentially extracted by the solvent, giving an extremely high blank (A > 2 *vs.* iBB).

Trichloracetic acid (TCA) (*17*) at the 0.20*M* level in the aqueous phase gave a reasonable blank, 0.28; a^{Y}_{313} was found to be 0.680.

Early in this investigation, perchloric acid (*26*) was used in the deproteinizing step with the intention of having it serve both as the protein precipitant and as the source of H^+ during color development. It was satisfactory insofar as sensitivity is concerned, both with samples devoid of protein and with samples containing protein (which were deproteinized). However, it was found that background color was directly correlated with the concentration of perchloric acid in the aqueous phase subjected to extraction. Furthermore, poor reproducibility and instability of the color yield were found. Also, it became apparent that perchloric acid from different sources gave very different background colors. These disadvantages led us to consider a substitute for perchloric acid.

Owing to the possibility that the high background color obtained with $HClO_4$ was produced by an impurity such as Pi, arsenate, or silicate (*25*), and in order to maintain a low $[H^+]$, the use of $NaClO_4$ (0.6*M*) at acid pH values was investigated. The recovery of protein was found to increase with decreasing pH and was complete at 1.85. This pH thus represents the minimal acid strength adequate for removal of myosin. $NaClO_4$ in an acidic medium was therefore chosen as the precipitating agent.

Figure 4 shows the results of determining phosphate in the presence and absence of protein. The aqueous phase contained the following amounts of the solutes given in a volume of 6 ml.: phosphorus, 1.13, 2.26, or 4.16 μg.; myosin (when present), 1 mg.; $NaClO_4$, 3.6 mmoles; glycine, 0.16 mmole; HCl, 0.40 mmole; H_2SO_4, 4.2 mmoles; molybdate, 25 μmoles. This was extracted with 5 ml. iBB. It is evident that the presence of protein [beef myosin (*6*)] during extraction of the heteropolyacid, as in the procedure of Martin and Doty (*18*), results in substantial loss of phosphomolybdate, in spite of the fact that the protein is in the form of a precipitate.

IV. Optimal Conditions for Formation and Extraction of Unreduced Phosphomolybdic Acid after Deproteinization.

A. Concentration of Sulfuric Acid and of $NaClO_4$.

To determine the optimal concentration of H_2SO_4 in the presence of $NaClO_4$, experiments were carried out in which the former component was varied from 0.5 to 1.3*N*; $NaClO_4$, in combination, was varied from 0.8 to 0.4*M*. This component was introduced since it was to be present in protein filtrates to be analyzed. When compared with absorbances measured in the absence of ClO_4^-, the results (Figure 3) show that absorbance was unaffected by ClO_4^-. At $[H^+]$ = 0.7*N* a^{Y}_{313} = 0.932; background absorbance was 0.20.

In a further experiment H_2SO_4 was kept constant at 0.7*N* and $NaClO_4$ was varied from 0.35 to 1.62*M* (Figure 5). It is seen that absorptivity, due to Pi,

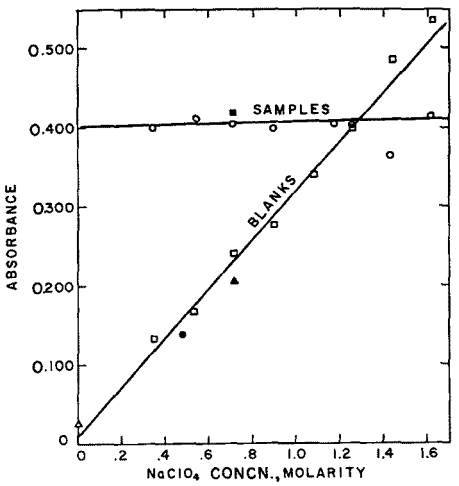

Figure 5. Absorbance of experimental samples (vs. blanks) and blanks (vs. iBB) at 313 mμ as a function of [$NaClO_4$]

The different symbols refer to experiments run at different times under the same conditions
Details as for Figure 3 except that H_2SO_4 was fixed at 4.2 meq. and $NaClO_4$ varied from 2.10 to 9.72 mmoles

is virtually independent of the sodium perchlorate concentration through the entire range, whereas background color is strongly dependent on $NaClO_4$ concentration.

Samples from which protein has been removed contain ClO_4^- at a concentration of 0.6*M*. Since a 4-ml. aliquot of this is taken into an aqueous volume of 6 ml., the perchlorate ion concentration cannot in practice be reduced below 0.4*M*. We chose to maintain the perchlorate ion concentration at 0.6*M* by adding $NaClO_4$ to the H_2SO_4 reagent; the increase in background color is small, 0.05 absorbance unit, and provision is thereby made for samples containing higher concentrations of ClO_4^-. In the latter case, the $NaClO_4$ content of the H_2SO_4 reagent would be reduced. For an inorganic phosphate test in a sample containing no protein, perchlorate can be completely eliminated.

Having selected the conditions of making the aqueous phase 0.7*N* H_2SO_4–0.6*M* $NaClO_4$, a Beer's law test was run. A straight line relationship of absorbance to Pi concentration was found, the slope yielding $a^{Y}_{313} = 0.906 \pm 0.003$ (standard deviation); background color was 0.18. The data are part of Figure 6, which will be discussed below. One of the solvent extracts was monitored at room temperature (water-cooled lamp housing) in a Gilford absorbance recording system for a 40-hour period; perfect color stability was found. Similar stability was found for deproteinized samples discussed below.

B. Effect of Protein. Solutions containing varying amounts of KH_2PO_4 and a constant amount of myosin were deproteinized and analyzed as set forth in the procedure recommended below. The data, plotted as part of Figure 6, yield a slope $a^{Y}_{313} = 0.905 \pm 0.021$; background color was 0.208. For the samples not containing protein, the aqueous phase contained the following components in a volume of 6 ml.: phosphorus, 1.13 to 4.52 μg; $NaClO_4$, 3.6 mmoles; H_2SO_4, 4.2 meq.: molybdate, 25 μmoles. This was extracted with 5 ml. iBB. For the samples containing protein, a 3-ml sample containing 1.13 to 4.52 μg. Phosphorus, 1.16 mg. myosin, 100 μmoles imidazole buffer, pH 7, 80 μmoles NaCl, and 15 μmoles $CaCl_2$ was deproteinized with 3 ml. of a solution containing 3.6 mmoles $NaClO_4$, 0.24 mmole glycine, and 0.60 mmole HCl. After removal of the precipitate by centrifugation, a 4-ml. aliquot was taken and to it was added 1.2 mmole $NaClO_4$, 4.2 meq. H_2SO_4, and 25 μmoles molybdate; the final aqueous volume was 6 ml. This was extracted with 5 ml. iBB. A statistical analysis of the data showed that, at a confidence level of 95%, the absorptivity after removal of myosin was identical to that in samples originally devoid of protein. Thus, there was no loss of Pi from samples containing the protein. An absorptivity of 0.906 therefore applies to both cases. The standard deviation is higher for the samples containing protein (2.3%) than for those that do not (0.3%).

V. Application of the Phosphate Determination to the Assay of Adenosine Triphosphatase Activity. Portions of a myosin preparation (*6*) were diluted with buffer to yield a range of protein concentrations and incubated with substrate. For most samples a 4-ml. aliquot of the incubation mixture

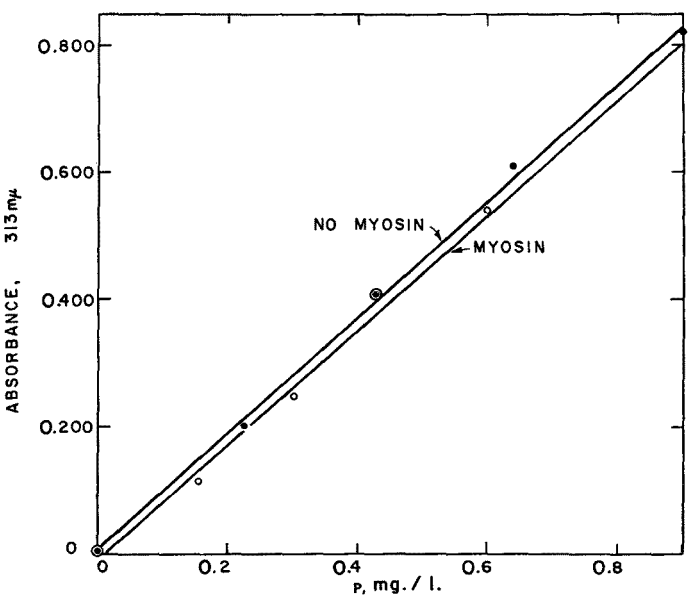

Figure 6. Effect of deproteinization with ClO_4^- on the recovery of Pi

was taken for analysis. In a number of cases, where large amounts of Pi were produced, a 1-ml. aliquot was taken and diluted to a volume of 4 ml.; $NaClO_4$ was incorporated into the diluent to maintain its concentration constant (0.6*M*) in all samples. In several tests the solvent extract was diluted with the organic phase from blank samples to reduce absorbance to a more accurate measuring range. Satisfactory results were obtained with both methods of dilution, but the first is preferred.

The yield of Pi for the five minute hydrolysis of this experiment is shown in Figure 7 as A/V, absorbance per unit volume of deproteinized aliquot, plotted against enzyme concentration. The yield of Pi is linear for the myosin range 0.04 to 0.4 mg. of protein/3 ml. of incubation mixture. The straight line portion of this curve is drawn on the basis of a least-squares fit, discarding data obtained with concentrations of myosin below the 0.04 level. Also plotted are data from a separate experiment where both extremes of the range were investigated. After hydrolysis of 50 per cent (1 μmole) of the ATP, the rate of hydrolysis decreases appreciably (the data are not shown in Figure 7). A lower rate of hydrolysis is also evident at very low concentrations of myosin. The latter effect may be attributed to denaturation, and could possibly be overcome by a stabilizer such as hydrolyzed gelatin. From the linear section of the curve the ATPase activity of the myosin preparation was 0.58 μmole of Pi per mg. protein per minute.

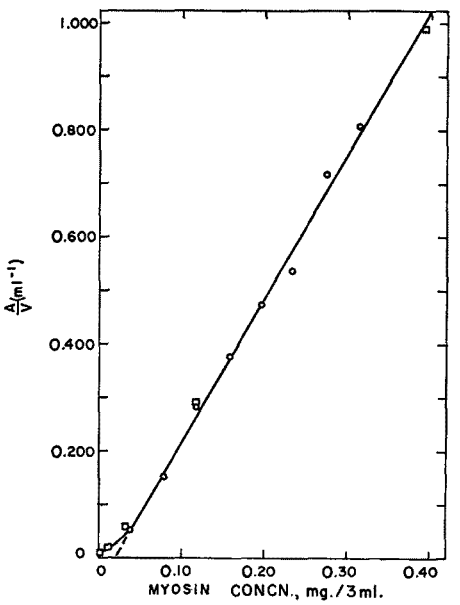

Figure 7. Application of the determination of Pi to the measurement of ATPase activity

ATP was incubated with myosin as described (Experimental) Deproteinization and subsequent steps were as for Figure 6, except that in some cases the aliquot taken for extraction was 1 ml. (see text)

IMPROVED METHOD

Reagents are as follows: protein precipitant: $NaClO_4$, 1.2*M*; glycine, 0.080*M*; HCl, 0.2*M*; diluent: $NaClO_4$, 0.6*M*; acid–perchlorate reagent: H_2SO_4, 4.2*N*; $NaClO_4$, 1.2*M*; isobutanol–benzene (iBB): isobutanol, 1 volume; benzene, 1 volume; molybdate: $(NH_4)_6Mo_7O_{24}$, 25m*M*.

Procedure. Pipet a sample containing 0.7 to 30 μg. phosphorus as Pi into a 10–12 ml. screw-cap test tube, dilute with water to 3 ml., and add 3 ml. of protein precipitant. It is preferable to add this and all other reagents with automatic syringes of all-glass construction. Cover the tube tightly with a screw-cap lined with Teflon and mix. After ten minutes, centrifuge at 6200 × g. for twenty minutes. (We centrifuge at 10° C., but this operation can usually be done at room temperature.) An aliquot of the supernatant containing 0.5 to 5 μg. phosphorus is taken and diluted, if necessary, to 4 ml. with 0.6*M* $NaClO_4$. Add 1 ml. of acid–perchlorate reagent and mix. Add 5 ml. of iBB and 1 ml. of molybdate. Mix the phases completely by inverting 15–20 times during a period of 15–20 seconds. Centrifuge for 10–15 minutes at 3300 × g. to provide complete separation of the phases. Place a portion of the organic phase in a cuvet with a ground glass joint, stopper, and read the absorbance at 313 mμ against a suitable blank treated identically.

Comments. The inorganic phosphate should be extracted and isolated from the aqueous phase without undue delay, since residual nucleotide phosphate does slowly hydrolyze in the acidified medium. Under the conditions described for "Adenosine Triphosphatase Assay" (Experimental section), this hydrolysis occurs at the rate of 0.1 micromole ATP (5% of the amount of ATP initially present) per hour. When isolated, the absorbance of the organic phase is constant for at least 48 hours.

It should be noted that once the incubated samples have been deproteinized, the remaining steps of the procedure should be run at room temperature. In an experiment where 0 to 3° C. was maintained from the protein precipitation step until measurement of absorbance, the absorbance was low and nonreproducible.

To maintain an adequate excess of molybdate (*14*), the aliquot taken for reaction with this reagent should contain not more than the recommended limit of 5μg. of phosphorus.

DISCUSSION

This investigation was initiated by our requirement for a reliable means of measuring the ATPase activity of muscle extracts and proteins isolated therefrom. Existing methods gave surprisingly erratic results, in agreement with the findings of other investigators (*4*, *14*). It was established that the difficulty was not associated with the enzymatic incubation but rather with the determination of Pi itself.

Isolation of Pi. We chose the solvent extraction of Berenblum and Chain (*1*), as modified by Martin and Doty (*18*), since it appeared that it would be applicable to large numbers of samples with relative ease. To avoid the troublesome reduction step, we investigated the possibility of measuring the yellow phosphomolybdate directly. The results were highly rewarding in that it was shown to be possible to eliminate the reduction without the concomitant loss of sensitivity, which has generally been assumed unavoidable (*8*); a gain in sensitivity was in fact obtained. In addition, the results indicate that ATP is not measurably hydrolyzed during the formation and extraction of the heteropolyacid. Whether ATP is itself extracted into the organic phase as a molybdate complex (*17*) is open to question. In any case, no Pi is formed in the organic phase subsequent to the extraction.

Having chosen the method for isolating Pi in a stable and measureable form—i.e., as yellow (unreduced) phosphomolybdic acid in iBB, the effect of protein in the original samples on the yield of the product measured was investigated. The results indicated

Table I. Key Features of Various Methods of Orthophosphate Determination

Organic solvent[a]	λ (mμ)	Absorptivity	Ref.
iB	White light	ca. 0.5	(1)
None	825	0.75	(4)
None	660–720	0.12	(5)
iAA	720	0.731	(13)
B	310	0.64	(17)
BC	310	0.800	(25)
iBB	625–725	0.546	(18)
iBB	313	0.906	This paper

[a] iAA, isoamyl acetate; B, butanol; iB, isobutanol; iBB, isobutanol-benzene, 1:1 (v/v); BC, butanol–chloroform.

(Figure 4) that if protein (myosin) is present during extraction, the yield of phosphomolybdic acid in the organic phase is seriously reduced. Three alternatives are thus open for separating Pi from protein: extraction without prior removal of protein (*18*), with consequent loss of sensitivity and reproducibility; deproteinization, leaving Pi in solution; and precipitation of Pi, as in the method of Sugino (*23*), leaving the protein in solution. The first alternative being undesirable we chose deproteinization, since it is then unnecessary to redissolve the phosphate.

Deproteinization. Various methods of deproteinization were tried, as described in section III. Boiled STA (*18*) was found unsatisfactory. This is not surprising when one considers that silicate forms a heteropoly acid with molybdate (*2*, *25*). TCA was not extensively investigated but is considered less desirable than a perchlorate medium, since extraction of phosphomolybdic acid from the former is more difficult (*10*), and since its use can be a source of error in the presence of small amounts of silicate (*2*).

$HClO_4$ was suggested as a protein precipitant by Neuberg *et al.* (*21*) and has been used for deproteinization prior to determination of Pi by Lowry and Lopez (*16*), Hagihara and Lardy (*10*), Hashimoto *et al.* (*11*), and Fukazawa *et al.* (*7*). We found this reagent, as commercially available, unsuitable, for reasons already given (Results).

It was found that myosin precipitated completely with 0.6*M* ClO_4^- at pH 1.85, but not at higher pH's (Section III), and Pi was quantitatively recovered in the supernatant (Figure 6). The ClO_4^- concentration used was suggested by the level of $HClO_4$ effective for precipitation of serum proteins (*26*, *27*). The effect of pH on precipitation of proteins by anions such as ClO_4^- can be attributed to a requirement for protonation of carboxylate groups. In this connection it is interesting to note that Lipmann and Tuttle (*15*), working with different proteins and a different precipitant, TCA, found that "an acidity of below pH 1.8 .... was necessary to bring about a complete precipitation of protein ...."

Optimal Conditions for Formation and Extraction of Unreduced Phosphomolybdic Acid. As pointed out by Duval (*4*), color yield due to phosphomolybdic acid is a complex function of both hydrogen ion concentration and molybdate concentration; the $[H^+]$ which is optimal at one molybdate concentration is not optimal at another, and vice versa. Furthermore, the optimal $[H^+]$ varies with the anion, being different for example, for $HClO_4$ than for H_2SO_4. The thorough analysis by Duval was unfortunately limited to the blue reduction product, but our experience indicates that even the yield of the unreduced heteropoly-acid is a complex function of the above kind. Thus, multiple experiments were required to choose the conditions necessary to maximize the yield of this acid. The results of some of the experiments of this series relative to optimal concentrations of molybdate and H_2SO_4 are shown in Figures 2 and 3. In our method $NaClO_4$ is also present, at a concentration of 0.60*M*, together with a small amount of glycine and HCl, these components having been used during deproteinization.

Comparison of Methods. A comparison of the method proposed with representative methods taken from the literature is given in Table I.

Conclusion. The method of Martin and Doty (*18*) was found to be unsatisfactory. The difficulty was traced to the use of silicotungstic acid, the presence of protein during extraction of phosphomolybdic acid, and reduction of the latter to the blue form.

An improved method was developed which eliminates these sources of error. Protein (myosin) is removed after precipitation with ClO_4^- at pH 1.5–1.8, and the heteropoly acid is measured, after extraction into isobutanol benzene, in the unreduced form. The extracted product has an absorptivity at 313 mμ of 0.906 $(cm.)^{-1}$ $(mg.\ P/liter)^{-1}$.

The improved method is superior to its predecessors with respect to reproducibility, stability, sensitivity, and ease of operation. The assay is suitable for application to the measurement of adenosine triphosphatase activity.

LITERATURE CITED

(1) Berenblum, I., Chain, E., *Biochem. J.* **32**, 286, 295 (1938).
(2) DellaMonica, E. S., Bingham, E. W., Zittle, C. A., ANAL. CHEM. **30**, 1986 (1958).
(3) Dryer, R. L., Tammes, A. R., Routh, J. I., *J. Biol. Chem.* **225**, 177 (1957).
(4) Duval, L., *Chim. Anal. (Paris)*, **45**, 237, (1963).
(5) Fiske, C. H., Subbarow, Y., *J. Biol. Chem.* **66**, 375 (1925).
(6) Fryar, A. J., Gibbs, R. J., *Experientia* **19**, 493 (1963).
(7) Fukazawa, T., Hashimoto, Y., Yasui, T., *J. Food Sci.* **26**, 541 (1961).
(8) Glick, D., "Quantitative Chemical Techniques of Histo- and Cyto-chemistry," Vol. II, 79, 80, 85, Interscience, New York, 1963.
(9) Haga, T., Maruyama, K., Noda, H., *Biochim. Biophys. Acta* **94**, 226 (1965).
(10) Hagihara, B., Lardy, H. A., *J. Biol. Chem.* **235**, 889 (1960).
(11) Hashimoto, Y., Fukazawa, T., Niki, R., Yasui, T., *Food Res.* **24**, 185 (1959).
(12) Haupt, G. W., *J. Opt. Soc. Am.* **42**, 441 (1952).
(13) Kirsten, W. J., Carlsson, M. E., *Microchem. J.* **4**, 3 (1960).
(14) Kondrashova, M. N., Lesogorova, M. N., Shnol, S. E., *Biokhimiya* **30**, 491 (1965).
(15) Lipmann, F., Tuttle, L. C., *J. Biol. Chem.* **153**, 571 (1944).
(16) Lowry, O. H., Lopez, J. A., *Ibid.*, **162**, 421 (1946).
(17) Marsh, B. B., *Biochim. Biophys. Acta* **32**, 357 (1959).
(18) Martin, J. B., Doty, D. M., ANAL. CHEM. **21**, 965 (1949).
(19) Mitchell, D., Shaw, E. H., Jr., Frary, G. G., *Proc. S. Dakota Acad. Sci.* **24**, 108 (1944).
(20) Mokrash, L. C., ANAL. CHEM. **33**, 432 (1961).
(21) Neuberg, C., Strauss, E., Lipkin, L. E., *Arch. Biochem.* **4**, 101 (1944).
(22) North, E. O., in "Inorganic Syntheses," (Booth, H. S., Ed.) Vol. *I*, 129, McGraw-Hill, New York, 1939.
(23) Sugino, Y., Miyoshi, Y., *J. Biol. Chem.* **239**, 2360 (1964).
(24) Szent-Györgyi, A. G., Holtzer, H., *Biochim. Biophys. Acta* **74**, 709 (1963).
(25) Wadelin, C., Mellon, M. G., ANAL. CHEM. **25**, 1668 (1953).
(26) Weimer, H. E., Quinn, F. A., *Clin. Chim. Acta* **3**, 419 (1958).
(27) Winzler, R. J., Devor, A. W., Mehl, J. W., Smyth, I. M., *J. Clin. Invest.* **27**, 609 (1948).

RECEIVED for review February 16, 1966. Accepted June 13, 1966. It is not implied that the U. S. Department of Agriculture recommends the companies mentioned or their product to the exclusion of others in the same business.

Nucleation Rate and Crystal Growth Rate of the Complex as Factors in Microscopical Fusion Analysis of Quinone–Carcinogenic Agent Complexes

DONALD E. LASKOWSKI

Department of Pathology, Western Reserve University, Metropolitan General Hospital, Cleveland, Ohio

▷ The study of quinone–carcinogenic agent complexes by microscopical fusion methods revealed that complexes frequently nucleate and grow slowly compared to the starting components. Thus, metastable eutectics are obtained rather than the thermodynamically stable complexes unless special precautions are taken to ensure the opportunity both to nucleate and to grow. Conditions favorable for nucleation are achieved by allowing the preparation to crystallize under a variety of conditions leading to varying degrees of supercooling of the melt. Growth of the complexes is achieved by cycling between two temperatures, the precise temperatures being a function of the individual system under study. Methods are described for rapidly determining these two sets of conditions, so that fusion methods may be used to determine if a complex forms in a given binary system and the melting characteristics of that complex even though it exhibits rate effects.

EARLIER microscopical fusion studies of the interaction of quinones and hydrocarbons (*2*) have been extended to include additional hydrocarbons, substituted hydrocarbons, and heterocyclics as well as additional quinones. These studies will be reported elsewhere; however, certain technique modifications were found necessary to avoid false negatives due to slow nucleation rates or slow crystal growth rates of some complexes. These modifications should be of value to any individual employing microscopical fusion techniques to study complex formation in binary systems.

EXPERIMENTAL

Equipment and Reagents. A Koffler hot bar (W. J. Hacker, Inc.) was used to make fusion preparations with starting components melting below 220° C. An alcohol lamp was used with substances melting above this temperature. Micro melting points were determined with a Reichert hot stage (W. J. Hacker, Inc.) previously calibrated with Koffler micro melting point standards.

The quinones were purified by sublimation. Hydrocarbons were used without purification.

Procedure. The mixed fusion preparation is made as described (*3*); however, with high melting components and the highly volatile quinones it is frequently not possible to melt both components simultaneously. In this case, the higher melting component is melted with the alcohol lamp and allowed to solidify so that it occupies about half of the area under the cover glass. The quinone is then melted on the hot bar so that it flows under the cover glass into contact with the solidified first component. The preparation is then moved up the hot bar to an elevated temperature but one below the temperature at which quinone boils or evaporates rapidly.

Regardless of preparation procedure, the preparation is placed immediately on a metal block set in a plastic container filled with ice. After solidification, the mixing zone is observed microscopically for evidence of a complex. The mixing zone is observed on heating from room temperature at about 3° C. per minute. The growth during heating of a new solid phase differing in color or appearance from the original solid mixing zone indicates the probable presence of a complex. Formation of a complex during this stage is differentiated from a polymorphic transformation of the starting components by subsequent melting behavior.

The hot stage is turned off when a thin line of melt appears in the mixing zone. The temperature rises slowly several degrees and then decreases slowly past the solidification point. The mixing zone is observed for growth of a complex during both the heating and cooling period. If no complex is seen at first, the stage is turned on a few degrees below the melting temperature of the mixing zone and the process is repeated several times.

If no complex grows by the above procedure, the hot stage is allowed to heat 10° to 15° C. above the melting point of the mixing zone and the preparation is observed during heating and subsequent spontaneous cooling for formation of a complex. This process is also repeated several times.

If no complex has been seen to this point, the preparation is melted on the hot bar and then placed on the cold block to solidify the mixing zone. The chilled preparation is then placed on the hot stage at about 5° above the melting point of the mixing zone as the stage is cooling from a temperature in excess of this value. The mixing zone is observed for small crystals of complex increasing in size as the hot stage cools below the solidification temperature. If no such crystals are seen, the entire process is repeated several times before it is concluded that this particular procedure fails to yield a solid complex.

If no complex is produced by the above procedures, the preparation is observed for formation of a complex as it solidifies at elevated temperatures. The hot stage is heated to a temperature in excess of the mixing zone melting point and allowed to cool spontaneously. The preparation is melted to the extent allowed by the volatility of the quinone and observed as it resolidifies on the warmed hot stage, at 5° to 10° intervals between the melting point of the mixing zone and room temperature.

If, under any of the conditions, a solid phase differing in color or appearance from the starting components is observed in the mixing zone, the temperature of the stage is allowed to heat slowly to the point at which this solid phase melts. The stage is then turned off and the preparation is observed on cooling for formation of a complex. If no complex is observed under any of these conditions, it is assumed that the particular binary system under study does not form a stable solid complex. If a complex is observed, its melting point and the melting points of the eutectics are measured.

EXPERIMENTAL RESULTS

The system chrysene-duroquinone forms a yellow-green complex under appropriate conditions. Because of the high melting point of the hydrocarbon and the high volatility of the quinone, it is not possible to make a fusion preparation on which both components exist as liquid phases in contact.

Microscopical observation of a fusion preparation containing solidified hydrocarbon in contact with hot molten quinone reveals the following sequence of events. At first the liquid in contact with the hydrocarbon has a slight yellow-green coloration. During cool-

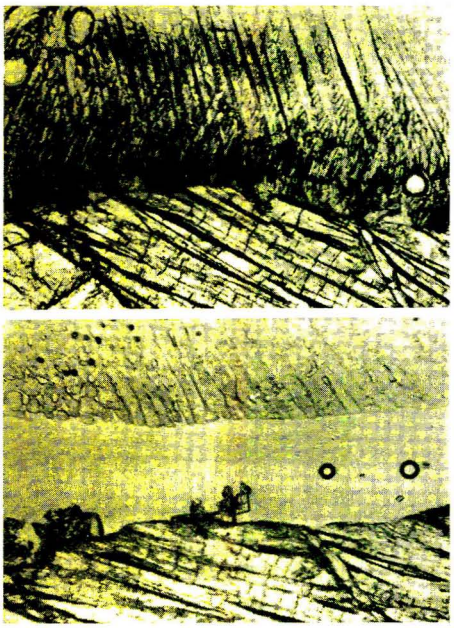

Figure 1. Chrysene and duroquinone

Upper. Metastable eutectic (center) between chrysene (bottom) and duroquinone (top)
Lower. Molten eutectic (center) with isolated crystals of complex near air bubbles on right and along chrysene crystal front (lower center and lower left)

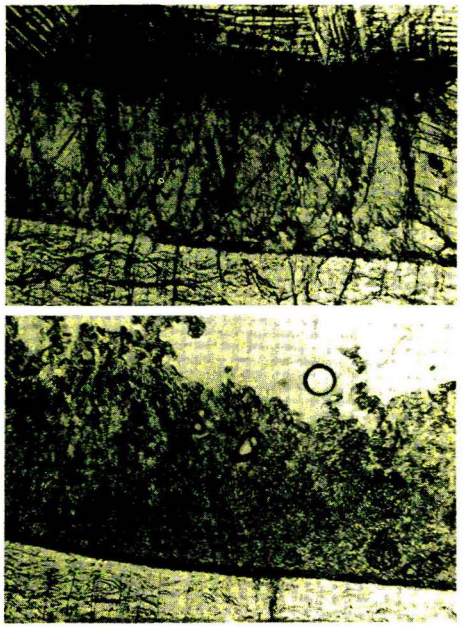

Figure 2. 1,2,5,6-Dibenzanthracene and 1,4-naphthoquinone

Upper. Metastable eutectic (center) with isolated areas of complex along quinone front. These exist in darkened areas, upper center
Lower. Complex formed throughout entire mixing zone with area of molten eutectic separating complex from quinone (top of field)

ing, the hydrocarbon grows slowly underneath the mixing zone and the color intensity decreases. At some point, the quinone grows very rapidly into contact with the hydrocarbon, the color discharges, and a eutectic mixture is seen (Figure 1, upper). No complex is visible.

On heating, no change is seen until melting occurs in the mixing zone at 100–3° C. When the mixing zone has melted, several crystals of yellow-green solid may be seen, some surrounded by melt (Figure 1, lower). If heating is continued, these crystals dissolve at some temperature below 115° C. If the stage is turned off immediately on formation of the melt, these crystals grow slowly and new nuclei form and grow, usually at the expense of the hydrocarbon that had previously grown under the mixing zone. If the stage is cycled several times between 100° and 105° C., an intact line of this yellow-green crystalline phase is seen to exist along the chrysene crystal front. Once a good line of crystalline complex is formed, it is possible to measure its eutectic temperature with the quinone and to determine that it melts incongruently at 115° C. The complex usually does not crystallize spontaneously on slow cooling of the preparation from temperatures in excess of 115° C.

Areas of nucleation of the complex can be observed in preparations allowed to solidify at temperatures below about 60° C. Numerous areas are seen if the preparation has solidified on the cold block. This system therefore is one in which nucleation of the complex is reasonably rapid under a variety of conditions but growth of the complex is slow compared to growth of the two starting components in the mixing zone. Since nuclei form and grow randomly in the mixing zone, they normally are surrounded by areas of melt rich in quinone after remelting. Unless conditions are properly adjusted for their growth after melting occurs in the mixing zone, they simply dissolve and may remain completely undetected if none happens to be in the field of vision.

The system 1,2,5,6-dibenzanthracene and 1,4-naphthoquinone is one in which the rate effects described above are reversed. The hydrocarbon melts at too high a temperature to allow simultaneous melting of both components. The sequence of events observed during the solidification process is the same as that described previously, except that the initial mixing zone has an orange coloration. With this system it is difficult to achieve nucleation of the complex by any of the crystallization procedures. If no nuclei of complex are present, the mixing zone melts at 114–15° C. If the preparation is heated above 145° and observed on slow cooling the hydrocarbon slowly grows under the mixing zone. As the hydrocarbon grows, the color discharges and when the temperature reaches about 100° C., the naphthoquinone suddenly nucleates at the hydrocarbon front and grows with extreme rapidity throughout the melt.

However, if several preparations of these components are made and allowed to solidify on the cold block, careful scanning of the solidified mixing zones will show at least one area of faint red-orange solid. Such an area is present in Figure 2 (upper). If this area is observed as the stage is heated, it is seen to grow rapidly at about 108° C. A good molten mixing zone is obtained by 115° C. and the orange complex is clearly visible (Figure 2, lower). Once the complex is formed, its incongruent melting point, 145–6° C., may be determined. If the stage is turned off immediately after the complex melts, the complex can be seen to nucleate and grow rapidly along the hydrocarbon front. Apparently even after melting, enough nuclei remain for the complex to grow. It can

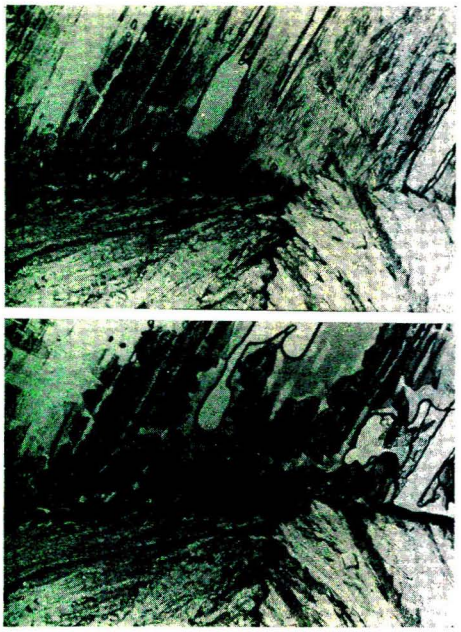

Figure 3. 6-Methylbenz(a)pyrene and 2,6-dimethyl-1,4-benzoquinone

Upper. Complex (center left) in contact with metastable eutectic (center right)
Lower. Complex growing throughout mixing zone during remelting

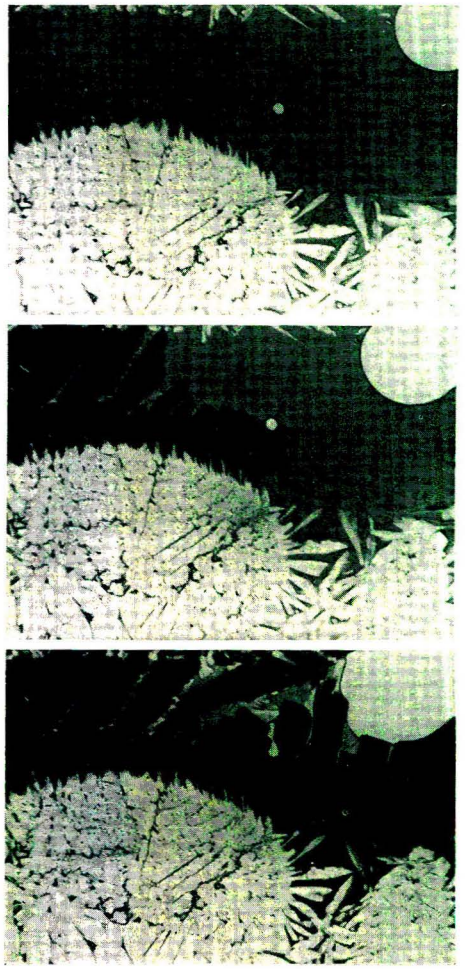

Figure 4. 2-Fluoreneamine and 2,3-dimethyl-1,4-benzoquinone

Upper. Metastable complex along amine front
Center. Stable complex growing at room temperature
Lower. Stable complex growth completed

be proved that this substance is a complex and not the product of an irreversible chemical reaction, by reheating the same preparation on the hot bar and then observing its behavior during solidification from 145° C. The complex does not reappear unless conditions are first adjusted so that nuclei form and survive as crystals.

An outstanding feature of this particular system is its variable behavior under apparently identical conditions. For instance, a preparation solidified at 35° C. yielded rapid growth of the complex after the temperature of the hot stage exceeded 108° C. A preparation solidified on a room temperature block yielded no complex, while two preparations solidified on the cold block yielded complex and one yielded no complex. This behavior is apparently characteristic of 1,2,5,6-dibenzanthracene, because similar behavior was noted with this hydrocarbon and all quinones studied. The complexes between 1,2,5,-6-dibenzanthracene and the quinones 1,4-benzoquinone, 2-methyl-1,4-benzoquinone, 2,5-dimethyl-1,4-benzoquinone, and 1,4-naphthoquinone were undetected by previous techniques (*2*).

The system 6-methylbenz(*a*)pyrene with 2,6-dimethyl-1,4-benzoquinone is one of intermediate behavior. It is possible to make a preparation in which both components exist as liquids in contact, if the hydrocarbon is melted first and then allowed to supercool before the quinone is placed outside the cover glass. Nucleation of this complex is sporadic if solidification occurs at room temperature or higher, and false negatives are common. If solidification occurs on the cold block, then multiple nuclei are formed even though a colorless metastable eutectic also appears and the areas of nucleation are obscured. If a nucleus happens to have grown to the point where a small crystal of the complex is present in the solidified mixing zone, then the complex is seen to grow slowly through the mixing zone after the temperature exceeds 55° C. As the temperature is increased and a good molten mixing zone is present, the complex grows at a more rapid rate. Figure 3(upper) shows the complex with the stage having been turned off before the complex had grown into an intact line across the hydrocarbon front. The crystals of quinone grew much more rapidly than the complex into the mixing zone. The complex is clearly visible, but the crystals of quinone have grown into contact with the hydrocarbon and a colorless metastable eutectic is seen in contact with the red-orange complex. One or two temperature cycles between 55° and 60° yield an intact line of complex suitable for melting point measurement. Figure 3(lower) shows the same area after heating was resumed.

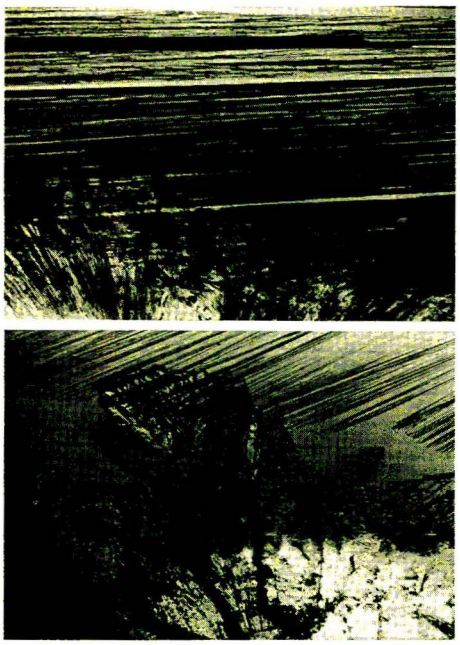

Figure 5. 9,10-Dimethyl-1,2-benzanthracene and 2,6-dimethyl-1,4-benzoquinone

Upper. Crystals of quinone (top) with areas of colored melt trapped between
Lower. Same preparation remelted and chilled on cold block. Complex growing in liquid mixing zone

The red-orange complex formed from 3,4-benzpyrene and 2-methyl-1,4-benzoquinone behaves similarly with respect to nucleation. However, nuclei of this complex have a tendency to form surrounded by areas of solid quinone. The metastable eutectic with this system melts at about 54° with a good molten mixing zone appearing by 57°. However, once the mixing zone has melted, any surviving crystals of complex do not grow on further heating but rather they dissolve. Hence, with this system it is essential that the hot stage be cycled between 50° and about 57° C. to obtain the complex in a form suitable for melting point measurement. This particular complex was undetected by previous techniques (*2*).

The system 2-fluoreneamine with 2,3-dimethyl - 1,4 - benzoquinone represents an extreme case of slow nucleation and growth of the complex. These two components may be melted easily together and the orange-brown mixing zone is liquid at room temperature. Preparations have been left at room temperature for 3 days without the appearance of a complex. If the preparation is placed on the cold block immediately, a brown metastable complex is formed. Figure 4(upper) shows the metastable complex with molten eutectic and two areas of purple-blue stable complex at room temperature. These grow slowly throughout the entire mixing zone; Figure 4(center) shows this process at an intermediate stage and Figure 4(lower) shows the process completed. It is essential that this system be subjected to low temperatures for the complex to nucleate; once nucleated, it grows throughout the mixing zone.

2,7-Diaminofluorene and 2,3-dimethyl-1,4-naphthoquinone form a purple mixing zone that supercools to a glass at room temperature. If this glass is incubated on the hot bar at a slightly elevated temperature, it gradually transforms to a colorless metastable eutectic melting at about 94°. If the identical preparation is remelted on the hot bar and then chilled on the cold block, a glassy mixing zone still results. However, as it is heated on the hot stage crystals of complex (pale blue to pink, pleochroic) grow slowly through the glassy mixing zone. This system is one that would usually be classified as negative, since the normal procedure with a glassy mixing zone is to allow crystallization to occur at an elevated temperature. On one occasion, the complex was seen to grow after solidification at room temperature, but it is usually necessary to chill on the cold block.

The complex formed from 7,10-dimethylbenz(*c*)acridine and 2,3-dimethyl-1,4-benzoquinone is recognizable as a complex if solidification occurs on the cold block. Isolated spherulitic growths of green complex are seen, surrounded by molten mixing zone. However, the complex does not grow readily into an intact line suitable for melting point determination unless the preparation is cycled several times between the cold block and the warmed hot stage (30° to 40° C.).

9,10 - Dimethyl - 1,2 - benzanthracene and 2,6-dimethyl-1,4-benzoquinone may be melted together on the microscope side. The orange mixing zone supercools but gradually solidifies to a colorless metastable eutectic melting at 48–49° C. During the solidification process, it can be seen that the quinone crystals grow into contact with the solidified hydrocarbon, trapping areas of colored melt between them (Figure 5 upper). These colored areas gradually solidify to the colorless metastable eutectic. Even though the mixing zone exists as a liquid for an appreciable period of time, the complex does not nucleate. Nucleation of the complex can be readily achieved if the preparation is first chilled on the cold block. Figure 5(lower) shows the same preparation as Figure 5 (upper) after reheating and chilling on the cold block. The orange complex is seen growing slowly in the molten mixing zone.

The green complex formed from 1,2,-7,8-dibenzanthracene and 2-methyl-1,4-naphthoquinone nucleates in recognizable form when solidification occurs at temperatures below 50°. However, these crystals invariably form in isolated areas of the mixing zone well away from the hydrocarbon crystal front. If the preparation is heated, the metastable eutectic melts at about 85° C. and small crystals of complex are then seen in the mixing zone. They grow very slowly after the stage is turned off. However, it has not been possible by any of the techniques described here, to obtain an intact line of complex suitable for melting point measurement. Invariably, the crystals of quinone grow past the complex before it grows enough to form a line; in addition, quinone nucleates at the hydrocarbon front at some stage during the cooling cycle. The complex is definitely present and recognizable. The maximum temperature to which these have been heated before solution in the quinone-rich melt was 89° C. This value, then, is the minimum melting point that the complex may possess. This type of behavior constitutes one in which fusion methods must fail for determination of the complex melting point. With this type of system fusion methods can be used only to determine

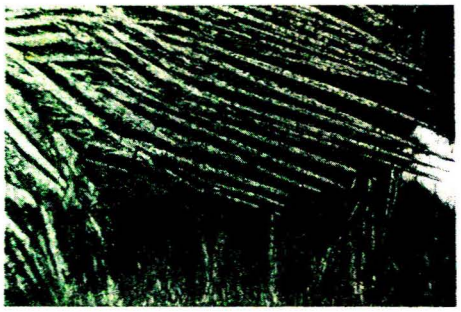

Figure 6. 1,2,7,8-Dibenzanthracene (lower) and 2-methyl-1,4-naphthoquinone (upper) complex present in isolated areas between crystals of quinone

the existence of the solid complex, its color and morphology, and the minimum temperature of its melting point. Figure 6 shows this complex formed between crystals of the quinone.

The hydrocarbon 1,2,4,5,8,9-tribenzpyrene has a very unusual behavior with either vitamin K_1 or α-tocopheryl-quinone. This may be a rate effect involving complexes but is probably a sluggish polymorphic transformation of the hydrocarbon recrystallized from either quinone. The hydrocarbon is only slightly soluble in either quinone even when the preparation is heated to 200° C. on the hot bar. A preparation so treated and then allowed to crystallize on the hot stage at 60° C. yields the crystals shown in Figure 7 (upper). These resemble a complex. If the preparation is placed on the cold block after heating and then warmed to room temperature, the multiple spherulitic growths shown in Figure 7 (center) occur. These also resemble a complex.

If the preparation containing either form is heated, a transformation to the needle structures shown in Figure 7 (lower) occurs. This generally begins near 110° and is complete by 120°. If the hot stage is turned off when the transformation is partially completed, the transformation does not reverse nor does it go to completion as the hot stage cools to room temperature. A partially transformed preparation was left for 3 days at room temperature without apparent further change. This behavior could be interpreted to conclude that the structures shown in Figure 7 (upper and center) are actually an incongruently melting complex formed from the quinone and the hydrocarbon. However, a preparation containing spherulites similar to Figure 7 (center) was placed on the hot stage maintained at 85° C. After $^1/_2$ hour, a substantial number of the needle forms were present and transformation to the needle form was complete in 2 hours. This behavior is more characteristic of a sluggish polymorphic transformation.

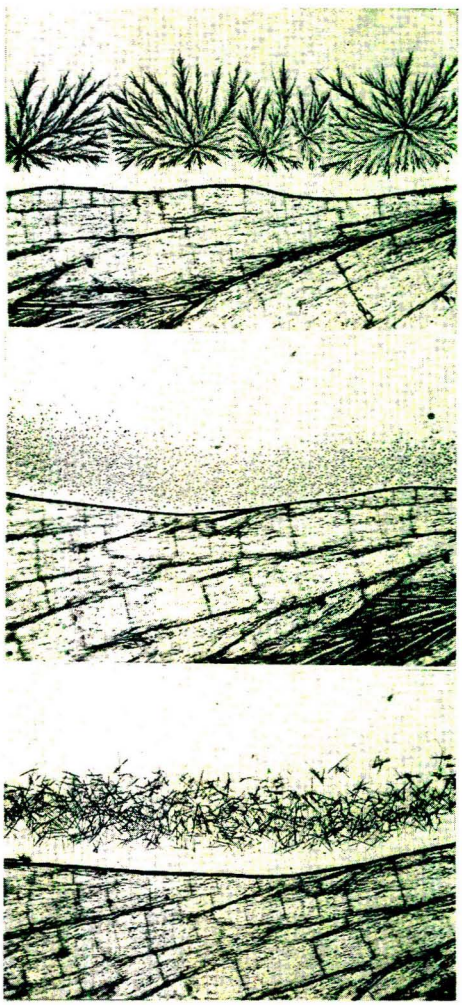

Figure 7. 1,2,4,5,8,9-Tribenzpyrene and vitamin K_1

Upper. Hydrocarbon crystallized at 60° C. from liquid quinone *Center.* Spherulites formed by heating preparation to 200° C., chilling on cold block 10 minutes, and warming to room temperature *Lower.* Needles formed from spherulites on heating to 112° to 120° C.

If this is indeed polymorphism, it must be concluded that the techniques used to circumvent rate effects can also lead to some very deceptive artifacts.

Table I summarizes the melting point data for all complexes mentioned here.

DISCUSSION

Fusion methods are rapid and economical of reagents for the detection of complex formation in binary systems. However, to apply these methods to a broad complex formation survey, it is essential that the assumptions on which they rest be valid for all systems studied.

When the fusion preparation is made from starting components A and B, there exists on the microscope slide an area of pure A and an area of pure B with zones of all intermediate compositions running parallel to the edges of A and B and changing progressively with distance from pure A to pure B.

If the equilibrium phase diagram of the system A and B is one with complex formation, during the solidification process the complex will nucleate and grow throughout the zone where the

composition is that of the complex. The eutectics will behave in similar fashion. The resultant solid complex will be an intact line across the entire preparation.

During the heating process, the line of complex will remain intact, with a line of melt rich in component A on one side and a line of melt rich in component B on the other side. This condition will continue until the melting point of the complex is reached, at which temperature it becomes liquid.

In the majority of binary systems in this study exhibiting complex formation, these assumptions are sufficiently valid to enable detection of the complex and measurement of its melting point. In a small but significant number of cases, one or more of these assumptions were not valid until special precautions were taken. In these cases false negatives were obtained at first.

The first assumption is valid, provided it is possible to melt both components on the microscope slide so that for a period of time they both exist in contact as liquids. Spontaneous diffusion leads to the required composition gradient in the mixing zone. However, if the two components differ widely in melting point and volatility, it is frequently not possible to melt both simultaneously on the microscope slide. In this event, the requisite composition gradient may exist only for a brief period during the recrystallization process. If, in systems of this type, the complex is also slow to nucleate or grow, the summation of the two effects may well lead to failure to detect the complex.

The second assumption involves the rate of nucleation and the rate of growth of the complex as compared to the rate of growth of the two starting components and ultimately of the potential metastable eutectic between them. In order for the existence of the complex to be recognized by the investigator, it must nucleate and grow to a size sufficient to be seen microscopically. The results reported here show that no one set of conditions may be used with confidence to ensure that this happens in all cases. Although a given binary system may form a complex, its nucleation rate may be so slow that the particular system usually crystallizes as a metastable eutectic. If a few nuclei form, they may well be outside the field of vision and not be seen. If they also grow slowly, they may not grow into the field of vision. Instead, the starting components grow through the mixing zone past the crystals of complex, thus altering the composition of the mixture adjacent to the complex. Remelting the preparation then leads to their dissolution in the melt at temperatures substantially below the true melting point of the complex. Unless ample opportunity is provided for nuclei to form and, once they form, for them to grow, the existence of the complex may not be recognized.

Table I. Fusion Data for Complexes

Binary system	Color of complex	Melting point, °C. Eutectic with quinone	Eutectic with carcinogen	Complex
Chrysene-duroquinone	Yellow-green	104	[a]	114–15[b]
1,2,5,6-Dibenzanthracene–benzoquinone	Yellow	110–11	[a]	147–48[b]
2-methylbenzoquinone	Yellow-orange	63–65	[a]	102–05[b]
2,5-dimethylbenzoquinone	Yellow-orange	115–17	[a]	153–55[b]
1,4-naphthoquinone	Yellow-orange	116–17	[a]	145–46[b]
6-Methylbenz(*a*)pyrene–2,6-dimethylbenzoquinone	Red-orange	59–61	86–87	94–95
3,4-Benzpyrene–2-methylbenzoquinone	Red	55–57	[a]	66–68[b]
2-Fluoreneamine–2,3-dimethylbenzoquinone	Blue + purple	43–44	58.5	58.8
2,7-Diaminofluorene–2,3-dimethylnaphthoquinone	Pale blue and pink	94–95	[a]	99–100[b]
7,10-Dimethylbenz(*c*)acridine–2,3-dimethylbenzoquinone	Green	40–42	53	60–61
9,10-Dimethyl-1,2-benzanthracene–2,6-dimethylbenzoquinone	Red-orange	51–52	[a]	59–61[b]
1,2,7,8-Dibenzanthracene–2-methylnaphthoquinone	Green	?	?	89[c]

[a] Eutectic absent because complex melts incongruently.
[b] Incongruent melting point.
[c] Minimum melting point of complex.

Four types of behavior were observed in this study:

The usual situation in which the rates of nucleation and growth of the complex are rapid compared to the metastable eutectic.

The rate of nucleation of the complex is slow but the growth rate is fast compared to the metastable eutectic.

The rate of complex nucleation is fast but the growth rate is slow compared to the metastable eutectic.

Both nucleation rate and growth rate of the complex are slow compared to the metastable eutectic.

If a particular system happens to have the fourth behavior, it is extremely difficult even to determine if a complex forms in the system.

Several miscellaneous impressions were gained. When one of the components of the mixed fusion is high melting, rate effects are likely to occur. Thus, 1,2,5,6-dibenzanthracene and chrysene are prone to exhibit these effects. If one of the components grows very rapidly from the melt, rate effects are to be expected. 2,6-Dimethyl-1,4-benzoquinone is an example of this behavior and rate effects were encountered almost uniformly with this quinone. In many of the systems exhibiting rate effects one or both of the starting components were noted to crystallize as unstable polymorphs. This may be a contributing factor. In general, complexes melting incongruently are more prone to exhibit rate effects than those melting congruently. The metastable eutectics usually appear to melt within a few degrees of the melting point of the stable eutectic between complex and one of the components. The melting point of the complex, on the other hand, may be substantially higher than that of the metastable eutectic.

It is characteristic of systems exhibiting rate effects that observed behavior is extremely variable from preparation to preparation. Thus it is possible with any of the systems described here to make a preparation and obtain an easily recognizable complex immediately on solidification. A second preparation made and treated in an apparently identical fashion may yield only a metastable eutectic. This leads to confusion on the part of the investigator unless the existence of these rate effects is recognized and procedures are adjusted to compensate for them.

It is known (*1*) that the curves relating growth rate and nucleation rate to temperature of solidification from the melt have similar shapes. Both rates are zero at the melting point of the substance, reach a maximum at some temperature below the melting point, and then gradually approach zero again at lower temperatures. The relative positions of the maxima vary from compound to compound. The investigator attempting to determine if a given binary system forms a complex does not know in advance the rate characteristic of the suspected complex. Conse-

quently the methods employed must be sufficiently general to encompass a wide variety of potential behaviors. The procedure recommended here is designed to place the fusion preparation under a variety of conditions for both nucleation and growth of the suspected complex.

The most effective single step is to raise the preparation to an elevated temperature and to allow crystallization to occur on the cold block. Most of the systems yield recognizable crystals of complex by this one step. Once recognizable crystals of complex are formed, it is usually possible to cycle the preparation between two temperatures so that a satisfactory line of complex forms. Over 1900 binary systems have been investigated in this study and over 300 complexes were found. Of these, approximately 10% were undetected until these rate effects were understood and the negatives were reinvestigated.

ACKNOWLEDGMENT

The 2,3 - dimethyl - 1,4 - naphthoquinone was generously supplied by William Roderick, Abbott Laboratories, North Chicago, Ill. Platon Burda contributed technical assistance.

LITERATURE CITED

(1) Buckley, H. E., "Crystal Growth," pp. 16–18, Wiley, New York, 1951.
(2) Laskowski, D. E., ANAL. CHEM. **32**, 1171 (1960).
(3) Laskowski, D. E., Grabar, D. G., McCrone, W. C., *Ibid.*, **25**, 1400 (1953).

RECEIVED for review April 11, 1966. Accepted May 25, 1966. Research supported by Grant E-329A, American Cancer Society, and Grant CA-07754-03, National Institutes of Health.

Fast Scan High Resolution Mass Spectrometry

Operating Parameters and Its Tandem Use with Gas Chromatography

W. J. McMURRAY, B. N. GREENE,[1] and S. R. LIPSKY

Department of Medicine, Yale University School of Medicine, New Haven, Conn.

▷ **A technique has been developed whereby high resolution mass spectra may be readily obtained from fast magnetic scans of gas chromatographic effluents. With resolving powers of between 1 in 10,000 and 1 in 12,000, mass spectra have been produced from samples containing less than 1 μg. during scans of a decade in mass in 8 seconds. Mass spectral analyses requiring resolutions higher than 1 in 12,000 with samples introduced into the ion source via a direct insertion probe may be easily acquired by employing somewhat longer scan times and larger samples. The accuracy of mass measurements obtained by using this method are, generally, better than 10 p.p.m. With these accuracies element maps can be produced from the data. With the exception of the input of the necessary control information, the entire processing of the recorded spectrum is performed by the analog to digital converter and the digital computer. With the optimization of analog to digital conversion, data processing of mass spectra will approach real time.**

BEYNON (*1*) effectively demonstrated that the mass of an ion obtained from an organic compound can be measured with sufficient accuracy to determine its elemental composition. By utilizing either the peak matching technique—i.e., the determination of the ratio in accelerating voltages necessary to bring ions of known mass and unknown mass on to the collector—or the calculation of the distances between ions of known and unknown masses on a chart record, he was able to measure the mass of a few selected ions in the spectrum. Recently with the aid of an elegant data handling system, Desiderio, Bommer, and Biemann (*5*) have extended this concept by demonstrating that the elemental composition of all ions can be used for the interpretation of a high resolution spectrum. In this instance they employed the photographic plate as a recording medium. Here, by the use of a linear comparator the line images are converted to distances and the distances are then converted to masses using a square root relationship between distance and mass (*3*).

Although the methods described by Beynon were responsible for considerable developments in the application of mass spectrometry to the structural elucidation of organic compounds, they possess certain inherent disadvantages. The peak matching technique is time consuming and requires a judgement of which peaks are to be measured while the sample is still in the instrument. A relatively large sample and additional instrument time is usually required and the data are not produced in a form readily amenable to handling by means of computer techniques. On the other hand, the photographic technique gives a permanent record, allows the data processing to be independent of the mass spectrometer, and requires no preinterpretation before the final output is received. However, it too has its inadequacies which include the variabilities of exposure times and photographic processing, the sensitivity of the emulsion to damage, and the considerable time required to measure accurately the lines on the plate [usually 30 to 120 minutes per spectrum (*3*)]. Both systems have had certain limitations when applied as a recording technique for the tandem operation of the gas chromatograph with the high resolution mass spectrometer. The peak matching technique is essentially impossible without prior trapping of the sample. With the plate, rapid handling is relatively inconvenient and the time required to measure individual spectra may become significantly large if many components are present in the chromatogram. Thus the ideal system for this application appears to be one which, among other things, should approach as nearly as possible real time data processing of the recorded scan.

In the history of spectrometry there are examples in which electrical recording systems have either replaced or compete effectively with the photographic recording techniques. Nonetheless, on the basis of low resolution data, McFadden and Day (*12*) concluded that the procurement of reliable and usable high resolution mass spectra by a fast scan of the gas chromatographic eluents was impractical. Based on limited data, subsequent refutations (*8, 13*) of this argument indicated the feasibility of the electrical scan method. While these studies touched on some of the problems, sufficient information was not available to elaborate on many specific parameters involved in this technique nor to indicate its precise use in the sphere of gas chromatography.

The purpose of this study is to describe in detail an electrical scan system whereby gas chromatographic effluents containing 1 μg. or less can be rapidly

[1] Present address, Associated Electrical Industries, Manchester, England.

monitored by recording spectra on analog magnetic tape (*11*) at a resolving power of one in 10,000 or more at scan speeds down to 8 seconds for a decade in mass. The system is devised in such a manner that the data procured are readily amenable to computer techniques. Under these circumstances the mass of all the fragments produced in a spectrum can be measured to an average accuracy of better than 10 p.p.m. Moreover, it will be noted that the same system can be readily utilized to record spectra produced from samples introduced into the ion source by means of the direct insertion probe. In these instances higher resolution (1 in ~25,000 plus) is readily attained by appropriately increasing the scan time and sample size.

EXPERIMENTAL

The mass spectrometer used in this study was a double-focusing, high-resolution instrument with Nier-Johnson geometry (Model MS9, Associated Electrical Industries, Manchester, England). Several major modifications were made to the instrument.

A special 10-Kc. per second amplifier and bandwidth filter was incorporated. It was shown by Banner (*2*) for triangular peaks that, in order to produce less than about 5% loss in resolution and peak height by the amplifier system, the amplifier time constant should be less than $t_p/20$ where t_p is the width of the peak in time. Since for an exponential scan

$$t_p = \frac{t_{10}}{2.303R}$$

where t_{10} is time for a decade in mass and R is the resolving power it follows that the bandwidth should be greater than $7.3R/t_{10}$ if the peak broadening is to be less than 5%. For example, for the 8 second per decade scans at 10,000 resolution, the bandwidth was set to 10 kc. per second. For the 72-second scans, the bandwidth was reduced to 1 or 2 kc. per second according to whether the resolution was 10,000 or 20,000.

The spectra were first recorded by an FM tape recorder (Model FR1300, Ampex Co., Redwood City, Calif.), capable of bandwidths up to 20 kc. at a tape speed of 60 inches per second. The analog tapes were then played into an IBM 1912 A/D converter with a maximum conversion rate of 1.5 kc. on a single channel and a range of 0–999. By reducing the tape speed by a factor of 32, the maximum possible for the tape recorder used, the effective digitization rate was 48,000 per second. Each mass spectral peak from the 8-second-per-decade scans was thus represented by about 20 digital samples. In the case of the 72-second scan, the tape speed was only reduced by a factor of 8 giving about 20 samples per peak at 20,000 resolution.

The dynamic range of the system was limited primarily by the digitizer and tape recorder. The digitizer did not have sufficient speed to permit multichannel digitization of the 8-second scans. In order to enable all the data to be recorded on one channel, a nonlinear attenuator with an approximately logarithmic characteristic was inserted before the tape recorder. The dynamic range was thus increased from 100 to 1 to about 1000 to 1.

The rapid recording of a spectrum was made into a single step operation. A single pushbutton initiated the tape recorder and after a proper delay, about 6 seconds at 60 inches per second, for the recorder to reach a constant speed, the magnet scan was started. At the end of the scan the tape recorder was automatically stopped and the magnet scan circuit reset in preparation for the next run.

During each scan, the output from a 2-kc. per-second clock with decade dividers down to 2 cycles per second was also recorded on a separate tape channel to facilitate the location of the start and finish of each scan during the subsequent playback and digitization operation. It was also used to establish the approximate times of three of the peaks, as required by the computer to start the processing. For this purpose, the tape recorded spectrum was played back into the ultraviolet galvanometer recorder, and a conventional chart record was obtained.

The general application of any recording technique requires that the results that are obtained are reproducible and further that the instrumental procedures used to procure these results are relatively simple. One of the most important considerations here was that the instrument could be easily adjusted to the desired resolution and that this parameter may be quickly checked when necessary. Since the resolution of the mass spectrometer is determined by the width of the source and collector slits and the aberrations of the instrument, the width of the source and collector slits are ordinarily adjusted to give the desired resolution while the instrument is operated in the static mode—i.e., at constant magnetic field. At this stage also, the source controls are adjusted for maximum sensitivity and the magnet setting is adjusted for maximum final collector ion current, which corresponds to maximum resolution. The resolving power is then checked as being the desired value.

However, when the magnetic field is scanned, the position of the focus of the ion beam at the collector slit is, in general, different from that in the static mode. This change in focal plane can be readily corrected by an adjustment of the position of the magnet. Therefore, a method of checking the resolution while scanning was required, in order that the appropriate magnet position could be determined. One method is to record several scans, playback sections of each into the galvanometer recorder, and then measure the peak width in various mass ranges in each scan. From this, the position of the magnet can be optimized. However, a simpler and

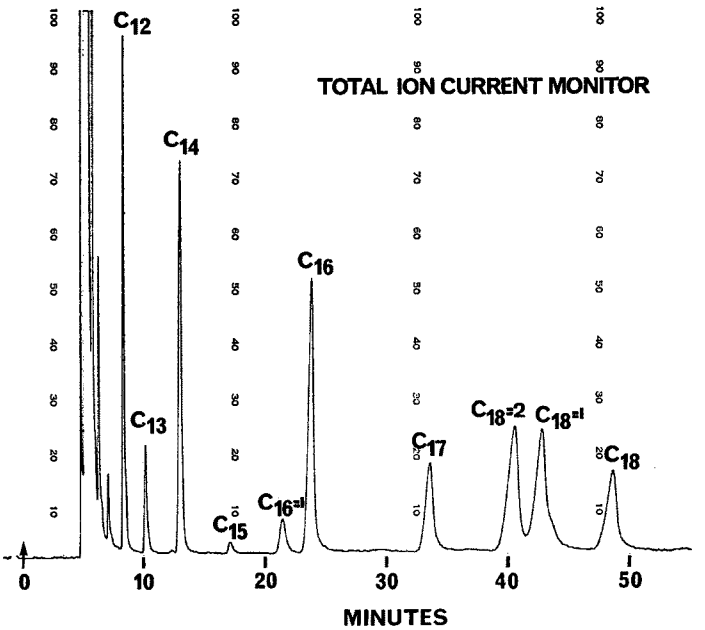

Figure 1. Gas chromatographic analysis of a mixture of fatty acids

The output was derived from the total ion beam monitor of the mass spectrometer. The 50 foot × 0.020 inch column contained a porous layer coated with Apiezon L. Column temp. 210° C. Helium flow: 10 ml./min.

equally adequate method of checking the resolving power was adopted. One of the results of the exponential scan law is that at constant resolution equal times are spent on each peak. Using a storage oscilloscope (Type RM564, Tektronix Inc., Portland, Ore.) the peaks in selected portions of the spectrum of a calibration compound, perfluorokerosene, were displayed by allowing each peak to trigger the oscilloscope time base. In as much as the record of each scan could be conveniently stored, the results of any adjustments to the magnet were compared with previous runs until the optimum conditions were obtained. By this technique changes in resolution of about 10% were distinguishable. Once the system had been set up, and the position of the magnet determined for the scanning speeds used, it was then only necessary to carry out a minimum number of checks before each series of scans. Because only a few minutes were required for the checks, this proved to be a very rapid method of optimizing the system.

For the tandem use of gas chromatography and high resolution mass spectrometry, modifications were also made to the inlet system of the mass spectrometer. A three-port ion source and source housing was provided which allowed direct connection to the source of the hot inlet system, the direct insertion probe, and the gas chromatographic inlet system. In addition, an automatic slit adjuster was incorporated into the mass spectrometer. By automatically and precisely resetting the slits within a few seconds one could, if necessary, quickly change from high (10,000) to low (1500) resolution operation during the monitoring of gas chromatographic effluents for those instances in which maximum sensitivity was required due to the unusually small sample (0.05 to 0.3 μg.) contained in a component band. The change required only a maximum of 6 seconds, and the alteration in ion intensity as measured on the beam monitor on returning to high resolution never exceeded 10%.

Table I. Theoretical Considerations of Certain Parameters for Achieving Accuracies of 10 p.p.m. or Better

Sample Size,[a] μg.	Resolution	Minimum scan time, seconds
1[b]	1:10,000	10
4	1:20,000	40
100	1:30,000	1000

[a] Based on the assumption that 0.1 μg. of sample per second enters into the ion source.

[b] In practice excellent spectra have been produced by scanning gas chromatographic effluents containing 0.5 μg. (in the ion source) in 8 seconds at 1 in 10 to 12,000.

A modified version of the pressure reduction system described by Watson and Biemann (*15*) was used to interface the gas chromatograph with the mass spectrometer. The efficiency of such devices is extremely relevant to the problem of obtaining spectra from small amounts of sample injected into the chromatograph. The efficiency—that is the fraction of injected component which actually enters the ion source—was determined as follows.

A 1-μg. sample of methyl stearate dissolved in 1 μl. of chloroform was placed in the glass capillary tip of the direct insertion probe. The solvent was carefully evaporated off by placing the probe over a hot plate. With the mass spectrometer connected to the chromatographic column via the pressure reduction system, and with helium flowing at the normal rate, the probe was inserted into its port and the sample of methyl stearate was volatilized into the ion source. With the molecular ion of methyl stearate at mass 298 focused on the collector, the ion current was measured as a function of time. The area under the curve was calculated and this value, representing the total ion charge at that mass, was defined as 100%. The same quantity of methyl stearate was then injected directly onto the gas chromatographic

Table II. A Summary of the Extrapolation of the Calibration Masses of an 8-Second-per-Decade Scan of a Gas Chromatographic Effluent Containing Methyl Palmitate

C-16 D810

THE ''TIME'' IS 0 HOURS 5.15132 MINUTES.

EXTRAPOLATION SUMMARY

	STANDARD MASSES		STANDARD TIMES		DIFF	TIME CONSTANT
	354.97930	342.97930	4.1298350	4.2459030	0.0	3.3751122
	342.97930	330.97930	4.2459030	4.3659160	0.0	3.3698026
*	330.97930	318.97930	4.3659160	4.4901654	-0.0	3.3644928
*	318.97930	304.98250	4.4901654	4.6411716	-0.0	3.3652793
	304.98250	292.98250	4.6411716	4.7759563	-273.6	3.3577375
	292.98250	280.98250	4.7759563	4.9162915	334.3	3.3556537
	280.98250	268.98250	4.9162915	5.0625741	-228.3	3.3515669
	268.98250	254.98560	5.0625741	5.2414728	87.4	3.3477015
	254.98560	242.98560	5.2414728	5.4027175	-11.9	3.3449855
	242.98560	230.98560	5.4027175	5.5719698	-55.4	3.3418182
	230.98560	218.98560	5.5719698	5.7500553	22.8	3.3380954
	218.98560	204.98880	5.7500553	5.9704692	29.6	3.3370461
	204.98880	192.98880	5.9704692	6.1714914	-176.6	3.3324174
	192.98880	180.98880	6.1714914	6.3853750	215.9	3.3316763
	180.98880	168.98880	6.3853750	6.6139061	-249.6	3.3312264
	168.98880	161.99040	6.6139061	6.7547456	-20.0	3.3299018
	161.99040	149.99040	6.7547456	7.0108421	37.0	3.3274084
	149.99040	142.99200	7.0108421	7.1697989	89.9	3.3266675
	142.99200	130.99200	7.1697989	7.4612619	-83.7	3.3252126
	130.99200	118.99200	7.4612619	7.7808557	62.6	3.3263298
*	118.99200	111.99360	7.7808557	7.9825473	-247.2	3.3274461
*	111.99360	99.99360	7.9825473	8.3597845	-0.0	3.3284984
	99.99360	92.99520	8.3597845	8.6014018	7.2	3.3299757
	92.99520	81.07050	8.6014018	9.0582690	-30.9	3.3292389
	81.07050	69.99860	9.0582690	9.5468493	303.7	3.3272080
	69.99860	61.99680	9.5468493	0.0000000	190.0	-0.0000000

STD MASS 61.99680 EXPECTED AT 0.0000000 NOT FOUND

THE ''TIME'' IS 0 HOURS 5.17168 MINUTES.

Table III. A Summary of the Extrapolation of the Calibration Masses of a 72-Second-Scan-per-Decade of Tazettine Introduced into the Ion Source by Means of a Direct Insertion Probe

TAZETTINE

THE ''TIME'' IS 0 HOURS 0.52722 MINUTES.

EXTRAPOLATION SUMMARY

	STANDARD MASSES		STANDARD TIMES		DIFF	TIME CONSTANT
	604.96330	592.96330	18.7080469	19.3932970	0.0	34.2020898
	592.96330	580.96330	19.3932970	20.0873339	0.0	33.9467530
	580.96330	566.96650	20.0873339	20.9099433	-0.0	33.7308927
	566.96650	554.96650	20.9099433	21.6267269	-962.7	33.5063553
	554.96650	542.96650	21.6267269	22.3550777	185.5	33.3187003
	542.96650	530.96650	22.3550777	23.0959134	-806.3	33.1489348
	530.96650	516.96970	23.0959134	23.9770155	-399.8	32.9820142
	516.96970	504.96970	23.9770155	24.7476909	-76.1	32.8144717
	504.96970	492.96970	24.7476909	25.5334742	14.5	32.6719337
	492.96970	480.96970	25.5334742	26.3355360	-601.5	32.5466113
	480.96970	466.97290	26.3355360	27.2927928	-424.4	32.4130926
	466.97290	454.97290	27.2927928	28.1334884	242.0	32.2930346
	454.97290	442.97290	28.1334884	28.9935539	-350.5	32.1768961
	442.97290	430.97290	28.9935539	29.8743947	-104.9	32.0732875
	430.97290	416.97610	29.8743947	30.9300592	-344.3	31.9740179
	416.97610	404.97610	30.9300592	31.8606451	-143.3	31.8684490
	404.97610	392.97610	31.8606451	32.8170204	183.8	31.7951910
	392.97610	380.97610	32.8170204	33.8001866	-972.3	31.7025857
	380.97610	368.97610	33.8001866	34.8120689	599.9	31.6166055
	368.97610	354.97930	34.8120689	36.0318298	-212.2	31.5408735
	354.97930	342.97930	36.0318298	37.1131058	-396.7	31.4421499
	342.97930	330.97930	37.1131058	38.2307081	790.6	31.3807614
	330.97930	318.97930	38.2307081	39.3871102	-1329.9	31.3136854
	318.97930	304.98250	39.3871102	40.7887425	209.8	31.2363687
	304.98250	292.98250	40.7887425	42.0394998	459.2	31.1586885
	292.98250	280.98250	42.0394998	43.3401899	14.3	31.1017170
	280.98250	268.98250	43.3401899	44.6948819	-866.4	31.0381434
	268.98250	254.98560	44.6948819	46.3504882	288.0	30.9810853
	254.98560	242.98560	46.3504882	47.8406391	-348.6	30.9128523
	242.98560	230.98560	47.8406391	49.4040790	538.3	30.8694804
	230.98560	218.98560	49.4040790	51.0478635	-1259.3	30.8116572
	218.98560	204.98880	51.0478635	53.0799503	770.6	30.7656126
	204.98880	192.98880	53.0799503	54.9337330	-778.2	30.7308211
	192.98880	180.98880	54.9337330	56.9025292	-679.0	30.6680393
	180.98880	168.98880	56.9025292	59.0032120	1796.7	30.6210003
	168.98880	161.99040	59.0032120	60.2969060	-1080.0	30.5871117
	161.99040	149.99040	60.2969060	62.6484876	-556.5	30.5536110
	149.99040	142.99200	62.6484876	64.1068983	-30.0	30.5217953
	142.99200	130.99200	64.1068983	66.7791491	-81.1	30.4868934
	130.99200	118.99200	66.7791491	69.7041235	269.9	30.4431129
*	118.99200	111.99360	69.7041235	71.5480804	852.6	30.4210403
*	111.99360	99.99360	71.5480804	74.9907703	-0.0	30.3760815
	99.99360	92.99520	74.9907703	77.1923151	2593.0	30.3417423
*	92.99520	80.99520	77.1923151	81.3795252	-770.6	30.3073971
*	80.99520	69.99860	81.3795252	85.7943935	-0.0	30.2565193
	69.99860	61.99680	85.7943935	0.0000000	2411.8	-0.0000000

STD MASS 61.99680 EXPECTED AT 0.0000000 NOT FOUND

THE ''TIME'' IS 0 HOURS 0.56320 MINUTES.

column. The ion current at mass 298 derived from the fraction of the sample which entered the ion source was measured as before and the total ion charge was again calculated. The values obtained under these circumstances were up to 20% of that noted with the direct insertion probe, depending on such factors as carrier gas flow rate, temperature, the diameter of the constrictions, and the conductance in the connecting tubes. The output from the total ion current collector, which intercepted about 50% of the total ion beam, was used to monitor the gas chromatographic effluents. By attaching a 0- to 10-mv. potentiometric recorder to the output of the ion beam monitor amplifier, and backing off the standing current due to the reference compound and carrier gas, it was possible to detect components continuously as they emerged from the column. This gave a chromatograph equivalent to that obtained from a conventional detector, but with the advantage that the peaks of the chromatogram coincided with the peaks of sample pressure in the ion source. In terms of overall sensitivity this mode of detection was sufficiently sensitive to give a signal equal to 100 times the noise for 1 μg. entering the source during a chromatograph peak lasting 30 seconds.

Two types of chromatographic columns were employed in this study. The conventional packed columns were of glass 3 to 6 feet long, by 1/8-inch i.d. Depending upon the length of the column, the inlet pressure and the nature and percentage of liquid phase present, the flow rates of helium through these columns were between 10 and 45 cc. per minute. The pressures in the ion source were influenced to a large extent

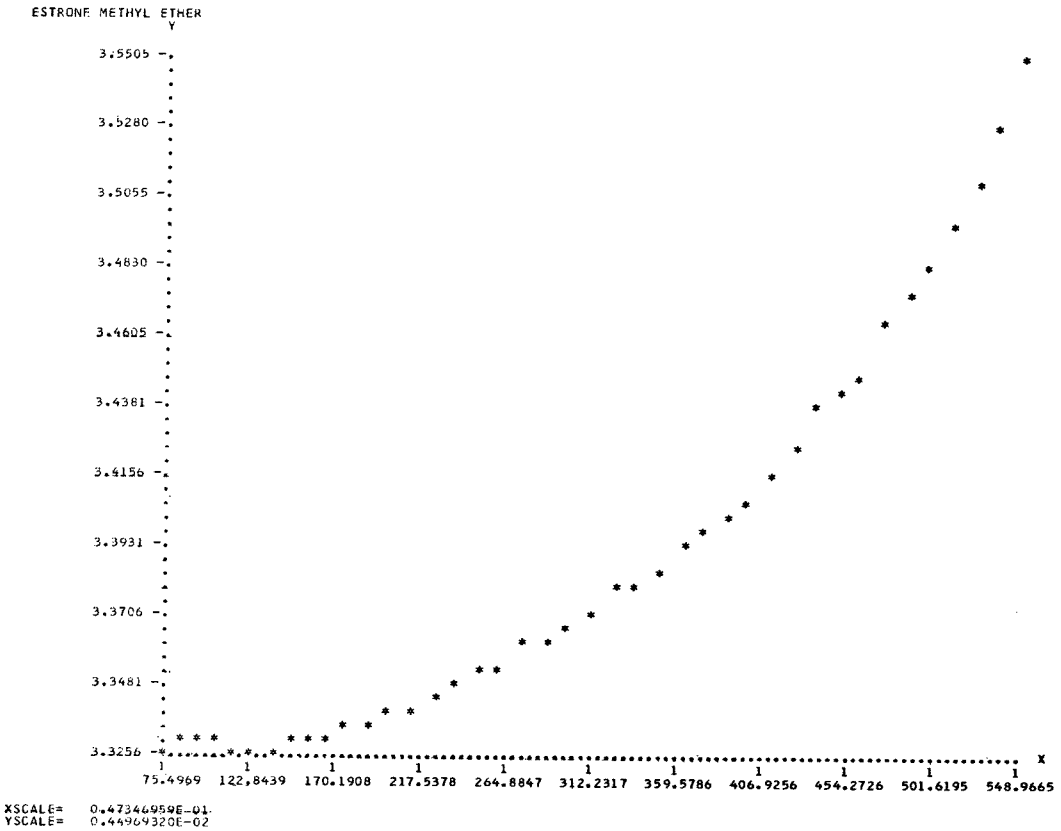

Figure 2. Plot of the time constants vs. mass for an 8-second scan per decade

Sample used was estrone methyl ether

by the "bleeding" rate of the liquid phase. Silicone rubber septums were also noted to contribute significantly to the noise level and were usually conditioned at 300° C. for 48 to 96 hours prior to use.

The other column was of the type first described by Horvath (*9, 10*). This consisted of a 50-foot by 0.020 inch i.d. metal capillary tube. A porous layer of fine particles of solid support coated with an appropriate stationary phase was made to adhere to the walls of the capillary. This type of column appears ideal for the application of the tandem use of gas chromatography–mass spectrometry to structural problems. Unlike the conventional liquid-phase, coated, open-tubular columns this column accepts a wide range of sample sizes without serious overloading. Moreover, sample splitting may be avoided or, if necessary, small sample split ratios (1 to between 4 and 8) can be used. The carrier gas flow rates are low and the concentration of solutes in the gas phase high, providing ideal conditions for the use of enrichment devices for interfacing of the two instruments. Optimal flow rates through this column for this application were in the order of 4 to 10 ml. of helium per minute. The pressure in the ion source under these conditions ranged between 0.5 and 1.5 $\times$ 10^{-4} torr. When compared to packed columns, plate numbers exceeding 500 theoretical plates per foot are easily obtained. The columns can be readily reproduced and, if necessary, can be made to contain a relatively high ratio of liquid phase volume to gas volume. They are excellent for the analysis of trace components (Figure 1).

RESULTS AND DISCUSSION

One of the true tests of any mass spectrometric system lies in the accuracy and reliability of the mass measurements. Details are now provided which indicate that this new system performs in a most satisfactory manner. An 8-second scan at 10,000 resolution gave satisfactory results and permitted operation with a chromatograph. For sample introduction from the direct insertion probe, the same scan conditions could be used, but scans at higher resolution must be obtained by scanning at a slower speed and consuming a larger quantity of sample. From a knowledge of the way in which the sensitivity of the mass spectrometer varies with resolution, to maintain the same accuracy of mass measurement at 20,000 resolution, requires that about 4 times as much sample be consumed during the scan (Table I) as at 10,000 resolution (*4*). Bearing in mind the maximum flow rate of sample into the ion source, an appropriately longer scan time must be chosen. In practice, a scan time of 72 seconds was generally used. The computer programs were written to be independent of the scan times.

To obtain the digitized tape from the IBM 1912 digitizer required approximately 6 minutes for the 8-second scan and 11 minutes for the 72-second scan.

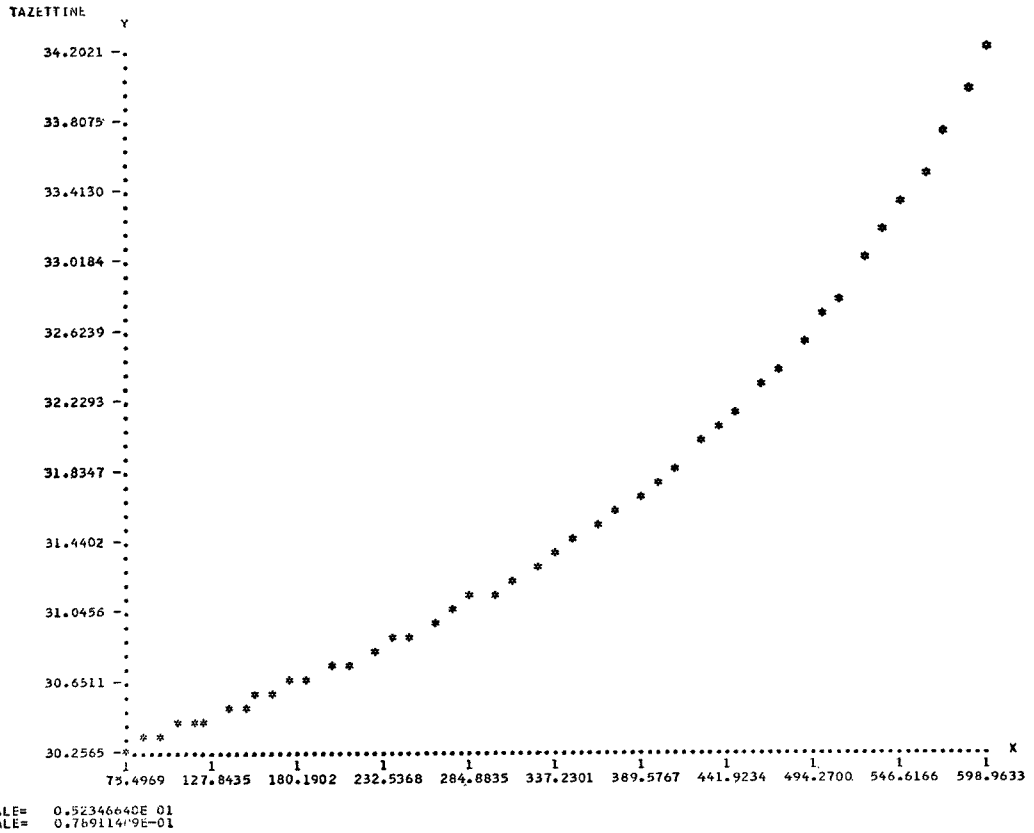

Figure 3. Plot of the time constants vs. mass for a 72-second scan per decade

Sample used was tazettine

The time here reflected the slowness of this particular digitizer. A faster analog to digital converter can essentially record all the data in real time. The digitized tape contains not only the digital values of the peak profiles but also the digital values corresponding to the base line. The first operation performed by the computer extracts the peaks from the digital spectrum. Because this in effect amounts to the reading and processing of over half a million digital values for an 8-second scan, approximately 3 minutes on a Model 7094 IBM computer are required. With a more sophisticated digitization system the threshold could be put in electronically, thus eliminating a high proportion of this computer time. Values are also amplified to correct for the nonlinear attenuation introduced in the recording. The centroid for each peak profile is then determined and used in all subsequent calculations as representing the peak time. The area under the peak is taken to represent the intensity. To convert the times to masses requires the location of the times corresponding to the fragments from the reference sample, perfluorokerosene, which has been introduced simultaneously with the sample. An extrapolation technique similar to that reported (*6*) but based on an exponential mass–time relationship is employed. As an input, the computer program requires only that the approximate time of three consecutive standard masses derived from the calibration compound, perfluorokerosene, be designated together with the time range over which the exact time corresponding to the standard mass should be found. With this information the program can then predict the time at which it expects to find the next standard mass and can then search for this time value within specified time and intensity ranges. It then substitutes the found time for the predicted time of the standard mass and repeats the sequence of predicting and searching for standard masses until it reaches a predetermined mass value at which it stops. The approximate times of the three initial standard masses are measured from a chart record, obtained by playing the analog tape record of the spectrum together with the timing signal into the galvanometer recorder. Because the scans are all made under similar conditions and the times are not required with high precision, it is usually sufficient to playback only one spectrum of a series for this purpose. Tables II and III show the result of this operation for an 8- and 72-second scan. The value in the DIFF column represents the difference in microseconds between the time predicted and the time found for the standard mass. The width of the peak in an 8-second scan at a resolution of 10,000 is about 350 μseconds, which means that the time of the next calibration mass can be predicted with an accuracy better than the time duration of a peak. The same is true for the

longer scan. The sample used for the illustration here contained less than the ideal amount of perfluorokerosene. As a result the weaker peaks either were not present or did not fit the minimum intensity criteria. The asterisks to the left of the standard masses bracket that standard mass which is absent or of low intensity. However, it should be noted that the extrapolation and therefore the subsequent conversion of time to mass could readily proceed for the entire scan. If two consecutive standard masses are not found, the extrapolation is terminated as an error has obviously occurred.

The value of this skip technique for the standard masses is illustrated in Table II. While the computer can substitute a time value for the extrapolation to continue, the masses calculated may exceed the desired error limit. Thus for example, the fragment at mass 316.97022 is in error by 12 mmu due to the absence of the standard mass at 318.9. However, the accuracy of mass calculations is usually sufficient to allow identification of the fragment ions and if necessary to substitute the mass corresponding to its composition for the standard mass if a recalculation of the masses is desired. This was done in Table II by replacing mass 80.9952 of perfluorokerosene by 81.0705 from methyl palmitate.

The values of the time constant, calculated for consecutive pairs of reference peaks assuming an exponential mass-time relationship show a small but systematic variation over the period of the scan. This is illustrated in Figures 2 and 3 which show plots of the time constant *vs.* mass for an 8- and 72-second scan. The "smoothness" of the curves is limited by the resolution of the plot output which is 100 points on the x axis and 50 points on the y axis. A simple correction to the exponential scan

Table IV. Tabular Display of a Portion of the Masses of Methyl Palmitate Emerging from the Gas Chromatographic Column and Scanned in 8 Seconds (per Decade)

C-16 D810

THE ''TIME'' IS 0 HOURS 5.20397 MINUTES.

RELI	INT	TIME	CORMASS	CALC	ERROR	C12/13	H	N	O	
12	1339	4.2459033	342.97927							CALIB. COMPD -0.03
13	1820	4.3659162	330.97929							CALIB. COMPD -0.02
9	300	4.5114036	316.97022							NO COMP CALC
11	675	4.6411716	304.98250							CALIB. COMPD 0.00
13	2428	4.7759563	292.98249							CALIB. COMPD -0.00
4	155	4.9154688	281.05140							NO COMP CALC
15	5153	4.9162915	280.98249							CALIB. COMPD -0.01
12	497	5.0343213	271.26068	271.25941	1.27	16/1	34	0	2	C-13 SPECIE
17	6351	5.0467308	270.25774	270.25606	1.68	17	34	0	2	
10	762	5.0625741	268.98251							CALIB. COMPD 0.01
13	504	5.0875368	266.98533							CALIB. COMPD -0.27
5	175	5.1379995	262.99213							CALIB. COMPD 0.13
10	954	5.2414728	254.98560							CALIB. COMPD -0.00
15	3071	5.4027175	242.98560							CALIB. COMPD -0.00
12	2635	5.4271544	241.21599	241.21691	-0.93	15	29	0	2	
8	373	5.4406979	240.24068	240.24100	-0.32	15/1	31	0	1	C-13 SPECIE
15	4825	5.4546891	239.23720	239.23765	-0.46	16	31	0	1	
6	226	5.5003877	235.98813							CALIB. COMPD 0.93
18	8683	5.5719698	230.98561							CALIB. COMPD 0.01
4	140	5.5978236	229.20437							NO COMP CALC
10	1200	5.6124309	228.20394	228.20460	-0.66	13/1	27	0	2	C-13 SPECIE
18	15494	5.6271703	227.19879	227.20125	-2.46	14	27	0	2	
5	124	5.6597042	224.99546							CALIB. COMPD 4.86
17	6203	5.7500553	218.98559							CALIB. COMPD -0.01
15	1692	5.8396646	213.18405	213.18559	-1.54	13	25	0	2	
5	184	5.8426897	212.99089							CALIB. COMPD -4.11
7	356	5.8585014	211.98409							CALIB. COMPD -3.11

Table V. Tabular Display of a Portion of the Masses of Tazettine as Determined from the 72-Second Scan per Decade

6	153	44.5650315	270.11124	270.11311	-1.87	16	16	1	3	
9	274	44.5676007	270.08886	270.08930	-0.44	16	14	0	4	
25	3035	44.6948819	268.98251							CALIB. COMPD 0.01
13	793	44.9259524	266.98550							CALIB. COMPD -0.10
9	319	45.3931012	262.99172							CALIB. COMPD -0.28
10	264	45.6197867	261.07449	261.07455	-0.07	16/1	10	1	2	C-13 SPECIE
				261.07191	2.58	13/1	12	0	5	C-13 SPECIE
9	289	45.7366052	260.09175	260.09237	-0.62	14	14	1	4	
20	1999	45.7393794	260.06845	260.07121	-2.76	17	10	1	2	
				260.06856	-0.11	14	12	0	5	
10	240	45.9761038	258.08805	258.08747	0.58	17/1	11	1	1	C-13 SPECIE
16	689	46.0969801	257.08242	257.08412	-1.70	18	11	1	1	
				257.08147	0.95	15	13	0	4	
3	84	46.2157483	256.09800	256.09745	0.55	15	14	1	3	
6	178	46.2188735	256.07215	256.07364	-1.49	15	12	0	4	
14	543	46.3380351	255.08821	255.08962	-1.41	15	13	1	3	
16	886	46.3408170	255.06528	255.06581	-0.53	15	11	0	4	
17	1113	46.3504882	254.98560							CALIB. COMPD -0.00

C-16 D810

BASE PEAK, MASS 74.03678 COMPOSITION C 3 H 6 N 0 O 2

MASS	N 0*0 0	N 0*0 1	N 0*0 2	MASS
70	5/10 --------			70
71	5/11 ----------	4/ 7 -----		71
73		4/ 9 -------		73
74			3/ 6 ----------	74
75			3/ 7 ----------	75
77	6/ 5 -----			77
78	6/ 6 -----			78
79	6/ 7 ------			79
81	6/ 9 --------			81
82	6/10 ------			82
83	6/11 ----------	5/ 7 -------		83
84	6/12 -------	5/ 8 --------		84
85	6/13 -------	5/ 9 ------		85
87		5/11 ------	4/ 7 ----------	87
88			4/ 8 --------	88
91	7/ 7 -----			91
93	7/ 9 ------			93
95	7/11 ------			95
96	7/12 ------	6/ 8 -----		96
97	7/13 --------	6/ 9 --------		97
98	7/14 -----	6/10 -------		98
99	7/15 ----			99
101			5/ 9 ----------	101
102			5/10 -----	102
107	8/11 ------			107
109	8/13 -------			109
110	8/14 ------			110
111	8/15 ------	7/11 ------		111
112		7/12 ------		112
115			6/11 --------	115
116			6/12 -------	116
121	9/13 ------			121
123	9/15 -----			123
125	9/17 ------	8/13 ------		125
129			7/13 ----------	129
130			7/14 ------	130
135	10/15 -----			135
139		9/15 ------		139
143			8/15 ----------	143
149	11/17 -----			149
157			9/17 -------	157
185			11/21 --------	185
199			12/23 --------	199
213			13/25 -------	213
227			14/27 ----------	227
239		16/31 --------		239
241			15/29 -------	241
270			17/34 --------	270
***				***
	26	14	18	

THE ''TIME'' IS 0 HOURS 1.32613 MINUTES.

Figure 4. The element map of methyl palmitate

Data derived from an 8-second scan per decade of the gas chromatographic effluent

TAZETTINE

BASE PEAK, MASS 247.08545 COMPOSITION C 13 H 13 N 1 O 4

MASS	N 0*0 0	N 0*0 1	N 0*0 2	N 0*0 3	N 0*0 4	N 0*0 5	MASS
70							70
71							71
77	6/ 5 ------						77
82							82
89	7/ 5 -----						89
91	7/ 7 -----						91
94							94
95							95
96							96
100							100
102	8/ 6 ------						102
103	8/ 7 ------						103
105		7/ 5 -----					105
112							112
114	9/ 6 -----						114
115	9/ 7 --------						115
127	10/ 7 ------						127
128	10/ 8 -------						128
129	10/ 9 ------						129
131		9/ 7 -----					131
135			8/ 7 ------				135
139	11/ 7 ------						139
140	11/ 8 -----						140
141	11/ 9 -------						141
143		10/ 7 ------					143
151	12/ 7 -----						151
152	12/ 8 ------						152
153	12/ 9 -------						153
154							154
157		11/ 9 -----					157
159		11/11 -----	10/ 7 ------				159
160			10/ 8 -----				160
168		12/ 8 ----					168
169		12/ 9 -------					169
171			11/ 7 ------				171
172			11/ 8 ------				172
173			11/ 9 -------				173
175				10/ 7 -----			175
181		13/ 9 --------					181
183		13/11 ------					183
185			12/ 9 -------				185
186			12/10 ------				186
187			12/11 -----				187
197			13/ 9 ------				197
199			13/11 ------	12/ 7 -------			199
201				*12/ 9 --------		* 9/13 -----	201
202						* 9/14 -----	202
203					*11/ 7 -----		203
209			14/ 9 -----				209
210			14/10 ------				210
211			14/11 --------				211
215				13/11 -------			215
216				13/12 ------			216
225				14/ 9 -------			225
226						*11/14 -----	226
227				*14/11 --------			227
229					13/ 9 -------		229
230					13/10 -----		230
231					13/11 -----		231
233					13/13 -----		233
238						*12/14 -----	238
239				15/11 ------			239
240						*12/16 ------	240
241				15/13 -----			241
242				15/14 ------			242
243					14/11 -----		243
247							247
249			17/13 -----				249
254						*13/18 -----	254
255					15/11 ------		255
256					15/12 -----		256
257					*15/13 ------		257
258					15/14 -----		258
260						*14/12 -------	260
261						14/13 -----	261
270					16/14 -----		270
298							298
300							300
316							316
317							317
331							331
332				*22/20 -------			332
332							332
	16	9	15	11	11	8	

Figure 5. The element map of tazettine

Data derived from a 72-second scan per decade of material introduced into the ion source by means of the direct insertion probe

law was thus necessary to ensure the completion of the extrapolation described above. About 2 seconds of computer time was required to carry out the extrapolation from mass 600 to mass 70.

The next stage in the processing is the mass calculation of all the remaining peaks in the spectrum. A correction, which was only about 6 mmu for an unknown mass spaced equidistant between two reference peaks at mass 500 decreasing to about 3 mmu at mass 300, was applied to the exponential scan law. Similar investigations in the region above mass 500 are now under way.

Illustrations of the accuracy of the mass calculations are shown in Table IV and V. Table IV represents a portion of the total tabular display of the high resolution mass spectrum of methyl palmitate as recorded in eight seconds from the effluent of a gas chromatograph. The columns reading from left to right represent: column one–the number of digital points in the peak, column two–the area under the peak and therefore a measure of the intensity of the peak, column three–the time in seconds at which the peak appeared, column four–the mass corresponding to this time, column five–the exact mass corresponding to the elemental compositions shown in columns seven through ten, column six–the error in millimass units between the two masses, and column eleven indicates those masses which are derived from the calibration compound and the error in millimass units between its exact mass and the mass calculated from the scan. The mass spectrum has been well explained (*14*) and needs no elaboration here. The elemental compositions are indicated for those which fit within an error of three millimass units or ten p.p.m. which ever is larger. The masses classified by the NO COMP CALC statement are derived from three sources, (a) from weak fragments of perfluorokerosene, (b) from failure to include the necessary elements for the calculation of the compositions, and (c) from other fragments of low abundance. For example, the composition $C_7H_{21}Si_4O_4$ (281.0517) could not be determined because silicon was not included in the calculations. The low abundance of the fragment at mass 229.2044 is responsible for the error of 3.5 mmu from the mass 229.2079 corresponding to the composition C_{12} $^{13}C_2$ H_{27} O_2. The element map output for this compound is shown in Figure 4. The format is the same as described (*5*) with the exception of the intensity scale which is based on a modified log scale.

A similar tabular display is shown for the alkaloid tazettine (Table V). The fragmentation pattern for this compound has been reported (*7*) and needs no amplification here other than to note

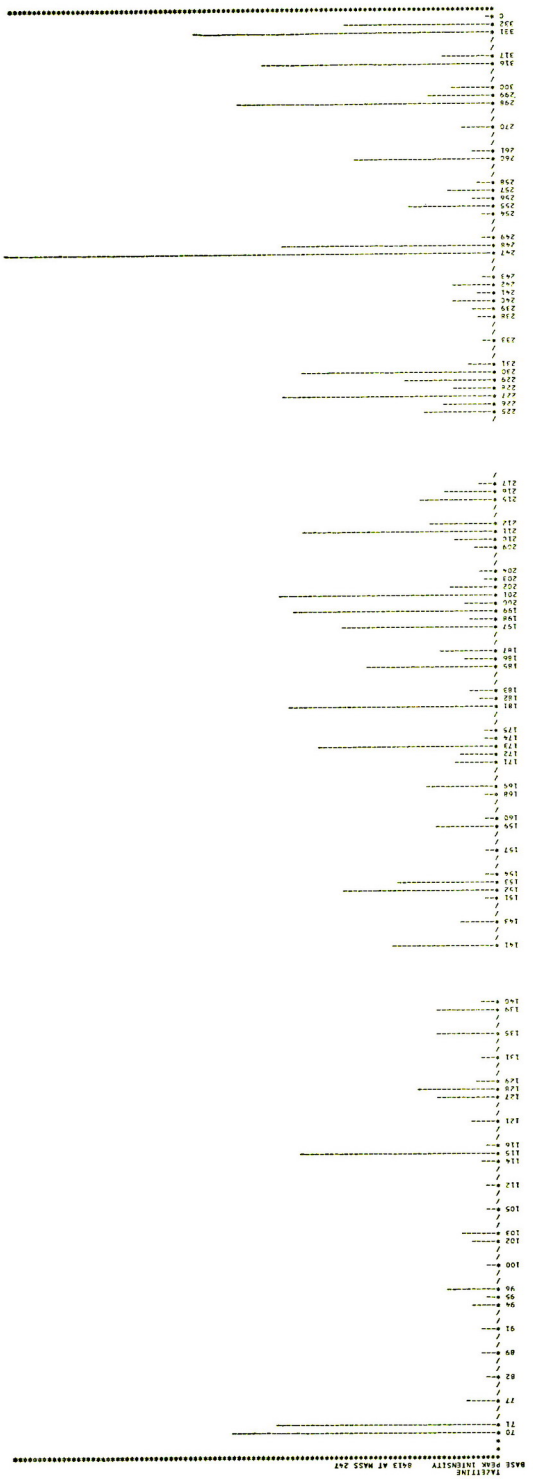

Figure 6. Computer presentation of the low resolution mass spectrum of tazettine
Data was derived from a 72-second high resolution scan

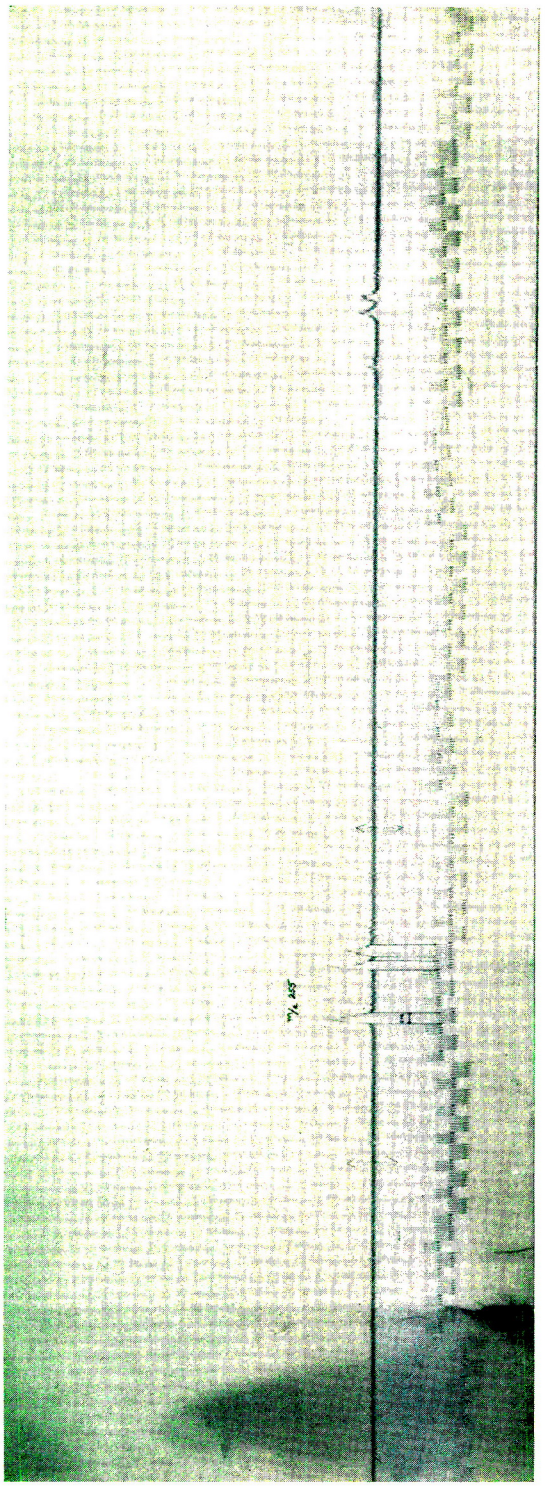

Figure 7. Oscillographic recording of the peaks derived from the *m/e* 255 region of tazettine

The peak width of the perfluorokerosene peak *m/e* 255 is 2 milliseconds. The distance between the doublets derived from tazettine represents one mass unit. Magnetic tape playback speed reduced by a factor of 8

that the elemental compositions assigned to various fragments are corroborated by the elemental compositions calculated from the complete high resolution mass spectrum. A portion of the map of tazettine showing those species containing only oxygen is shown in Figure 5. A second page showing the nitrogen-containing moieties is omitted for reasons of space. The asterisks beside the elemental compositions indicate that more than one elemental composition has been calculated for the same exact mass—e.g., those entries in the N_0O_5 column have duplicate entry in another column, in this case N_1O_2 column reflecting the doublet H_2O_3–C_3N which differs by 2.65 mmu. A low resolution presentation of the mass spectrum of tazettine as derived by the computer is shown in Figure 6. The peaks derived from the *m/e* 255 region of tazettine are depicted in order to indicate some measure of the resolution at which the scan was determined (Figure 7).

LITERATURE CITED

(1) Beynon, J. H., "Advances in Mass Spectrometry," Waldron, J. D., ed., Vol. I., Pergamon Press, New York, 1959.
(2) Banner, A. E., *J. Sci. Instr.* **43**, 138 (1966).
(3) Bommer, P., McMurray, W., Biemann, K., 12th Annual Symp. on Mass Spectrometry, Montreal, June 1964.
(4) Campbell, A. J., Halliday, J. S., 13th Annual Symp. on Mass Spectrometry, St. Louis, 1965.
(5) Desiderio, D., Bommer, P., Biemann, K., *Tetrahedron Letters*, **1964**, 1725.
(6) Desiderio, D., Biemann, K., 12th Annual Symp. on Mass Spectrometry, Montreal, June 1964.
(7) Duffield, A. M., Aplin, R. T., Budzekiewicz, H., Djerassi, Carl, Murphy, C. F., Wildman, W. C., *J. Am. Chem. Soc.* **87**, 4902 (1965).
(8) Green, B. N., Merren, T. O., Murray, J. G., 13th Annual Symp. on Mass Spectrometry, St. Louis, May 1965.
(9) Halasz, I., Horvath, C., ANAL. CHEM. **35**, 499 (1963).
(10) Horvath, C., Dissertation, Trennsaulen Mit Dunnen Porosen Schichten Fur Die Gas Chromatographic, University of Frankfort, Frankfurt, Germany, 1963.
(11) Issenberg, P., Bazinet, M. L., Merritt, C., Jr., ANAL. CHEM. **37**, 1074 (1965).
(12) McFadden, W. H., Day, E. A., *Ibid.*, **36**, 2362 (1964).
(13) Merritt, C., Jr., Issenberg, P., Bazinet, M. L., Green, B. N., Merren, T. O., Murray, J. G., *Ibid.*, **37**, 1037 (1965).
(14) Ryhage, R., Stenhagen, E., "Mass Spectrometry of Organic Ions," F. W., McLafferty, ed., Chap. 9, Academic Press, New York, 1963.
(15) Watson, J. T., Biemann, K., ANAL. CHEM. **36**, 1135 (1964).

RECEIVED for review March 31, 1966. Accepted May 24, 1966. Study supported by grants from the National Aeronautics and Space Administration (NsG-192/07-004-008) and the National Heart Institute of the National Institutes of Health (USPHS HE-03558-09).

Determination of Nonfiller Magnesium in Polyesters

JOHN E. NEWELL

Chemical Division, United States Rubber Co., Naugatuck, Conn.

▷ **A method is described for determining nonfiller magnesium in the presence of the magnesium in mineral fillers when they are together in cured or uncured polyesters. Low temperature pyrolysis of the cured sample followed by leaching of the residue with a buffered solution separates the nonfiller magnesium from that in the filler. The nature of the filler dictates the pH of the leaching solution and a method for identifying the filler by infrared spectrometry is included. For uncured samples, the acetone solubility of the organically-bound magnesium permits its separation from the filler. The magnesium is determined titrimetrically with EDTA.**

CONVENTIONAL METHODS of making polyester products containing glass fibers involve the mixing of polyester, styrene, filler, and catalyst with glass fibers. The lower the viscosity of the polyester resin mixture, the more easily it mixes with the glass fibers. However, when the impregnated fibers are molded, the higher the viscosity of the mixture, the better are the flow characteristics in the mold. A good compromise is difficult to make.

When magnesium oxide is added to the polyester resin mixture, it remains fluid for a sufficient time to be easily incorporated into glass fibers. The magnesium oxide reacts and the mixture becomes much more viscous. The impregnated glass fibers acquire much improved handling, storage, and molding properties (*2, 3, 9*). The requirements of low viscosity for easy incorporation and the high viscosity for satisfactory molding have been achieved. The thickening that occurs is due to reaction of the magnesium oxide with the polyester resin, which is unsaturated and carboxyl-terminated. The acid number of the resin is from 20 to 50.

The dispersion of the glass fiber, the characteristics of the surface, and the resistance to solvents of the cured polyester are affected by the magnesium oxide content. When the history of the sample is uncertain, the magnesium oxide content must be determined by chemical analysis.

Published methods for magnesium are mainly for its determination in the presence of other elements. The method proposed in this paper discriminates between the magnesium reacted with the resin from the magnesium present in common mineral fillers.

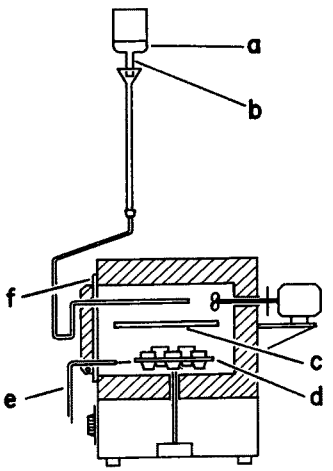

Figure 1. Diagram of furnace modified for pyrolysis

a. Hydrogen peroxide reservoir
b. Capillary tube
c. Baffle
d. Turntable
e. Thermocouple
f. Asbestos gasket

When the polymer is not cured, the organically-bound magnesium is separable from the filler and any excess magnesium oxide by its solubility in acetone. However, when the polymer is cured, it is insoluble in neutral organic solvents even at high temperatures where solution might be effected by a reaction such as ester interchange. Acid or alkaline solvents which attack the polymer also attack the fillers. Ashing the sample by conventional combustion methods leaves a dehydrated filler. Magnesium in some fillers is much more soluble in aqueous solutions after ashing.

In the method described, the organic matter in the sample is released by a controlled pyrolysis. Under the conditions chosen, the dehydration of the filler is much reduced.

The nonfiller magnesium in the residue is separated from the filler by leaching with buffered water. Contribution of magnesium to the solution by the filler or adsorption of magnesium from the solution is minimized by the choice of pH of the leaching solution. The pH of choice depends upon the filler which is identified by infrared spectrophotometry.

EXPERIMENTAL

Apparatus. The pyrolyses were done in a modified Thermolyne Type 1300 muffle furnace (Figure 1). The thermocouple supplied with the furnace was removed and a small fan was installed with its shaft going through the thermocouple opening. The speed of the fan was controlled by an autotransformer. A baffle prevented any breeze from the fan disturbing the contents of the crucibles. A slowly rotating turntable below the baffle held five crucibles. The door of the furnace was made more airtight with asbestos sheet. A thermocouple was inserted through a hole drilled in the door and a second hole permitted the introduction of hydrogen peroxide by means of $^1/_8$-inch o. d. stainless steel tubing. The rate of rise and ultimate temperature were controlled by an F and M Model 240 power-proportioning temperature programmer connected to the furnace.

The infrared spectra were obtained with a Model 421 Perkin-Elmer spectrophotometer.

Reagents. ACID WASHED CELITE. Celite Filter Aid was soaked overnight in 1:1 hydrochloric acid, filtered, water-washed, and dried at 110° C.

A BUFFERED LEACHING SOLUTION, pH 9.5, was made containing 3.6 grams of boric acid, 1.7 grams of sodium hydroxide, 1.5 grams of sodium bicarbonate, 5.0 grams of sodium oxalate monohydrate, and 1.5 grams of sodium sulfide nonahydrate in 2 liters of water. The pH was adjusted to 9.5 ± 0.1 by the dropwise addition of sodium hydroxide solution or hydrochloric acid.

A BUFFERED LEACHING SOLUTION, pH 8.2, was made containing 30 grams of ammonium acetate, 2.5 ml. of ammonium hydroxide (29% NH_3), 2.5 grams of sodium oxalate monohydrate, and 1.0 gram of sodium sulfide nonahydrate in 2 liters of water. The pH was adjusted to 8.2 ± 0.1 by the addition of drops of ammonium hydroxide or acetic acid.

A BUFFERED LEACHING SOLUTION, pH 4.7, was made containing 4.0 grams of sodium hydroxide, 12 ml. of acetic acid, 2.5 grams of sodium oxalate monohydrate, and 1.0 gram of sodium sulfide nonahydrate in 2 liters of water. The pH was adjusted to 4.7 ± 0.1 with sodium hydroxide solution or acetic acid.

BROMINATED NITRIC ACID. An excess of bromine was added to 70% nitric

acid. The stoppered bottle stood overnight to become saturated.

AMMONIUM HYDROXIDE–CHLORIDE BUFFER was made by dissolving 110 grams of ammonium chloride and 450 ml. of ammonium hydroxide (29% NH_3) in sufficient water to make 1 liter.

EDTA TITRANT, 0.0500*M*, was made by dissolving 18.61 grams of disodium ethylene diamine-tetraacetate dihydrate in distilled water and diluting to 1 liter. It was stored in a plastic bottle.

The titrant was standardized as follows: magnesium turnings were washed with benzene and dried. An accurately weighed sample of 0.010 to 0.012 gram was dissolved in 50 ml. of water to which had been added about 4 drops of hydrochloric acid. The solution was taken to dryness on a steam bath. The walls of the beaker were washed down with about 50 ml. of water and 10 ml. of 10% sodium cyanide solution, and 10 ml. of ammonium hydroxide–ammonium chloride buffer were added. With a few drops of Eriochrome Black T solution as the indicator, the solution was titrated with the EDTA titrant.

$$\text{Molarity} = \frac{1000\ (\text{wt. of turnings})}{24.32\ (\text{titer} - \text{blank})} \quad (1)$$

ERIOCHROME BLACK T INDICATOR was made by dissolving 0.25 gram of Eriochrome Black T in 50 ml. of triethanolamine. The indicator solution was kept stoppered as much as possible.

Procedure. ANALYSIS OF CURED SAMPLES. The sample was broken into small chips and a 2- to 3-gram portion was weighed into a porcelain crucible. The sample was pyrolyzed in the furnace by raising the temperature at 0.5° C. per minute from 110° C. to 340° C. and holding the temperature at 340° C. During the heat treatment the gases in the furnace were being circulated with the fan, the turntable was rotating, and 30% hydrogen peroxide was being introduced at approximately 5 ml. per hour. The total heat treatment was 16.5 ± 0.5 hours.

The crucible was cooled and reweighed. The contents of the crucible were transferred to a 250-ml. beaker. Using spatulas, the fragile residue was teased apart until the glass fiber was fluffy and the filler was a lump-free powder in the bottom of the beaker.

The contents of the beaker were poured into a second 250-ml. beaker, with tapping. A trace of filler remained in the first beaker as dust on the glass, and this dust was used to identify the filler. A small amount of finely-ground potassium bromide was added to the beaker and swirled to remove the traces of filler from the walls. The potassium bromide was transferred to a mortar, ground, and from it an infrared pellet or disk was made. From the infrared spectrum, spectra of known fillers (Figure 2), and the data in Table I, identification of the filler was made.

The glass fiber and powder in the second beaker were treated with 200 ml. of buffered leaching solution. For all fillers except alumina and clay the buffer with a pH of 9.5 was used. For alumina filler, the leaching solution with a pH of 8.2 was used and for clay it was pH 4.7. Mixed fillers were leached with the buffer of pH 9.5.

After stirring for two hours, the mixture was vacuum-filtered through a thin bed of Celite on a fine-porosity glass filter. The beaker and filter were rinsed with small volumes of buffered leaching solution.

When desired, the glass fiber content was found by washing the contents of the filter funnel through a small 325-mesh sieve. The fiber was retained on the sieve and was dried and

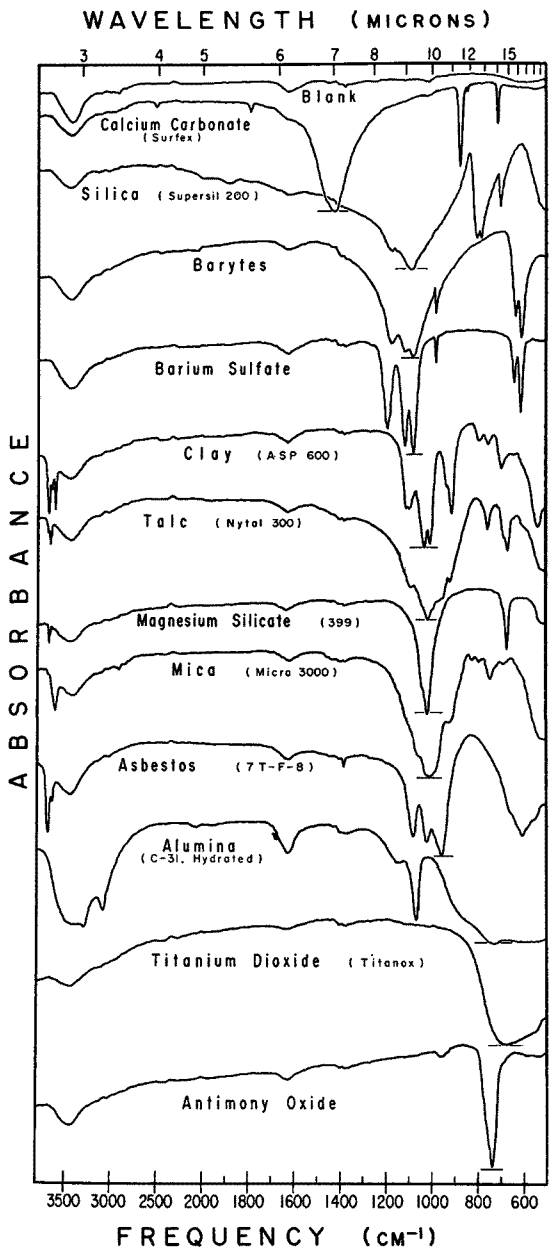

Figure 2. Infrared spectra of common fillers and additives

The spectra are displaced vertically. Minimum absorbances are approximately 0.03. Absorbances 1.0 are indicated by horizontal lines

weighed. The filler content was determined by difference.

The filtrate was evaporated to dryness in a 250-ml. beaker. To the residue were added 25 ml. of brominated nitric acid, 1.5 ml. of 70% perchloric acid, and a few carborundum boiling chips. The beaker was covered with a watch glass and boiled down to fumes of perchloric acid. The beaker was cooled and rinsed down with 100 ml. of water. The contents were reduced to about 50 ml. by boiling and were allowed to cool.

Using a pH meter, the pH was brought to 9.7 ± 0.3 by the dropwise addition of strong sodium hydroxide solution. Ten milliliters each of 10% sodium cyanide solution and ammonium hydroxide–chloride buffer solution were added. The mixture was warmed to about 40° C. and titrated to a permanent blue end point with 0.0500*M* EDTA solution. Eriochrome Black T was the indicator.

The leachable magnesium was calculated as the oxide and expressed as a per cent of the polymer (polyester resin plus styrene) in the sample by Equation 2.

$$\% \text{ Nonfiller Magnesium Oxide} = \frac{4.032M\ (\text{titer} - \text{blank})}{\text{Loss in wt. on pyrolysis}} \quad (2)$$

where M is the molarity of the EDTA solution, titer and blank are in milliliters, and the loss in weight of the sample on pyrolysis is in grams. When alumina was the filler, the "Loss in weight on pyrolysis" was corrected for the loss in weight of the filler due to its dehydration.

Analysis of Raw Samples. Approximately 20 grams of raw sample was dissolved in acetone. The filler was separated by filtration through a large paper Soxhlet extraction thimble fastened to the lip of a wide mouth Erlenmeyer flask. Residual turbidity in the filtrate was removed by filtration through a Celite bed on a porous glass filter. The solution was taken to dryness and vacuum dried at 70° C. to remove any residual solvent and styrene. One gram of the residue, accurately weighed, was ashed at 600° C. The ash was dissolved in dilute acid, and then taken to dryness. The residue was analyzed for magnesium by the method for cured polymers beginning with the addition of 200 ml. of the buffered leaching solution with a pH of 8.2.

The organically-bound magnesium was calculated from:

$$\% \text{ Organically-Bound Magnesium} = \frac{4.032M\ (\text{titer} - \text{blank})}{\text{sample wt.}} \quad (3)$$

Equation 3 expresses the organically-bound magnesium as the oxide, and as parts per hundred parts of the polyester resin in the raw sample.

RESULTS

Preparation of Known Samples. In compounding known samples, the following were varied: the polyester, the filler, and the amount of magnesium oxide. Two polyesters were used, one having an acid number of 20, the other an acid number of 42. The stocks containing the low acid number polyester had an excess of magnesium oxide, those with the high acid number had an excess of polyester. The fillers chosen were two talcs, two calcium carbonates, two clays, a mica, and a hydrated alumina. To permit more accurate compounding, glass fiber was omitted from the known stocks. The blank stocks contained no added magnesium oxide. The raw samples were stored at room temperature for a few days to allow those with magnesium oxide in them to thicken. Cured samples were made from the raw samples by the addition of benzoyl peroxide catalyst and heating overnight at 70° C.

For the results from Equation 2 to be accurate, the loss in weight by pyrolysis must be a close approximation of the actual polymer content. The data in Table II show that the loss in weight on pyrolysis is an adequate measure of the polymer content. The results of analyses of cured samples are given in Table III and for raw samples in Table IV.

Table I. Characteristic Absorption Bands for Common Fillers and Additives

(in cm.$^{-1}$, and in decreasing order of band intensity)

Calcium carbonate	1425, 875, 711, 1797
Pulverized silica	1082, 797, 780, 694
Barytes	1082, 1118, 1176, 610, 634, 984
Barium sulfate	1081, 1119, 1196, 610, 638, 984
Clay	1032, 1009, 912, 3691, 3617, 3651
Talc	1018, 669, 3674
Mica	1017, 929, 3617, 748
Asbestos	952, 1018, 1078, 601, 3685, 3635
Antimony oxide	742
Alumina	735, 1070, 1152, 3084, 3289
Titanium dioxide	675

DISCUSSION OF METHOD

The introduction of hydrogen peroxide into the furnace during pyrolysis permits the destruction of the organic matter at a lower temperature than when air or water vapor is the atmosphere. The pyrolysis of a sample with no filler was 98.2% efficient when hydrogen peroxide was introduced as

Table II. Polymer Content of Cured Samples, by Pyrolysis

Filler	% Polymer	% Loss in wt. on pyrolysis		
Alumina, C31 Hydrated	48.4	47.7[a]	46.9[a]	47.3[a]
$CaCO_3$, Atomite	49.8	49.9	49.7	49.5
$CaCO_3$, Snowflake	49.8	49.4	49.3	49.5
Clay, ASP 400	49.8	49.1	49.0	49.2
Clay, ASP 600	66.3	65.3	65.6	65.6
Mica, Micro 3000	66.3	65.5	65.8	65.8
Talc, 42R	49.8	49.3	49.2	49.6
Talc, 5490	66.3	65.4	65.3	65.0

[a] Corrected for 28% loss in weight of filler.

Table III. Analytical Data for Cured Known Samples

Filler	MgO, % Actual	MgO, % Found
None	0.85	0.84, 0.86, 0.86
Alumina		
C31 Hydrated	0.00	0.00, 0.00, 0.00
	0.86	0.75, 0.76, 0.79
Calcium carbonate		
Atomite	0.00	0.01, 0.01, 0.02
	0.85	0.85, 0.86, 0.88
Snowflake	0.00	0.00, 0.00, 0.02
	0.85	0.86, 0.87, 0.89
Clay		
ASP 400	0.00	0.00, 0.01, 0.03
	0.85	0.82, 0.84, 0.86
ASP 600	0.00	0.00, 0.00, 0.00
	0.85	0.80, 0.82, 0.84
Mica		
Micro 3000	0.00	0.00, 0.00, 0.02
	0.85	0.78, 0.80, 0.80
Talc		
42R	0.00	0.02, 0.04, 0.14
	0.85	0.96, 1.09, 1.29
5490	0.00	0.10, 0.16, 0.20
	0.85	0.96, 1.02, 1.06

Table IV. Organically-Bound Magnesium in Raw Samples

Filler	Polyester acid number	Per cent Mg, as oxide	
		Calculated	Found
Alumina C31 Hydrated	23	0.00	0.04, 0.04
	23	0.81–1.61	0.64, 0.63
$CaCO_3$ Atomite	42	0.00	0.00, 0.00
	20	0.69–1.38	0.75, 0.77
	42	1.15	1.14, 1.16
$CaCO_3$ Snowflake	42	0.00	0.00, 0.00
	20	0.69–1.38	0.80, 0.78
	42	1.15	1.14, 1.16
Clay ASP 400	42	0.00	0.00, 0.00
	20	0.69–1.38	0.82, 0.80
	42	1.15	1.04, 1.06
Clay ASP 600	42	0.00	0.01, 0.01
	20	0.69–1.38	0.78, 0.78
	42	1.15	1.09, 1.12
Mica Micro 3000	42	0.00	0.00, 0.00
	20	0.69–1.38	0.79, 0.79
	42	1.15	1.17, 1.19
Talc 42R	42	0.00	0.00, 0.00
	20	0.69–1.38	0.79, 0.80
	42	1.15	1.18, 1.19
Talc 5490	42	0.00	0.00, 0.00
	20	0.69–1.38	0.79, 0.74
	42	1.15	1.15, 1.17

described, 95.9% efficient when water was introduced and 97.1% efficient when only air was present. A minimum temperature of pyrolysis is necessary, for, if the filler loses water, it may become more soluble in the leaching solution. The temperature prescribed, 340° C., was the optimum temperature. The efficiency of pyrolysis at 329° C. under hydrogen peroxide vapors was only 90.2%.

The turntable was used to ensure uniform heat treatment. Without it the efficiency of the pyrolysis was dependent upon the position of the crucible in the furnace.

Raising the temperature slowly to 340° C. allowed the decomposition products from the plastic to evaporate as they formed and reduced the amount of char. The temperature programming rate of 0.5° C. per minute was an arbitrary choice.

The infrared spectra given in Figure 2 are typical. However, fillers of the same variety differ from each other depending on their source (*4–7*). The infrared spectrum of a particular filler also may be sensitive to the severity of the grinding with potassium bromide. The variations exhibited are usually in the width of absorption bands and the relative intensities of bands, rather than the wavelength of the absorption band. The pyrolysis treatment to 340° C. had negligible effect on the absorption spectra except for alumina. The dehydration of hydrated alumina reduced its absorption in the region of 3400 $cm.^{-1}$ Except for the reduction of absorption bands due to moisture, no changes in the infrared spectra of fillers have been observed when the potassium bromide pellets are dried by the method of Sadtler and Sadtler (*8*).

When simple mixtures of fillers have been encountered in unknown samples, the major components of the mixtures have been identifiable. When calcium carbonate was one of the components, the identification of the others was simplified by removal of the calcium carbonate by solution in dilute acid.

The leaching solutions are buffered reagents containing oxalate and sulfide ions adapted from the method of Betz and Noll (*1*). The oxalate and sulfide eliminate interference by calcium and heavy metals which otherwise could be titrated with EDTA. The use of pH 8.2 buffer for alumina fillers gives better recovery of the magnesium and avoids difficulties in the titration due to blocking of the indicator by aluminum. The pH 4.7 buffer for clay reduces the adsorption of magnesium on the clay.

The loss in weight of all the fillers tested, except alumina, upon being pyrolyzed, was negligible. When alumina was the filler in cured polyester, the polymer content found by pyrolysis was in error due to the dehydration of the alumina. The correction that was applied was based on a similar heat treatment of alumina filler alone.

DISCUSSION OF THE RESULTS

The analytical results in Table II show that the pyrolysis of the samples had an average efficiency of 98.8%. The efficiency could be improved by employing more severe conditions of pyrolysis but with an increased risk of dehydrating fillers that have hydroxyl groups in their crystalline structure.

When the filler in a cured sample is calcium carbonate, clay, or mica, the data in Table III show that the method gives satisfactory analytical results. Hydrated alumina as the filler withholds a small portion of the magnesium. The source of this loss seems to be the adsorption of magnesium on the hydrated alumina during the leaching with buffer. However, reaction between magnesium oxide and hydrated alumina during pyrolysis has not been eliminated as a possible cause. Talc gives a small amount of magnesium to the leaching solution.

The values in Table IV under the heading "Calculated" are based on the assumption that the reaction between the polyester and the magnesium oxide proceeded to the complete exhaustion of the minor component. For the stocks made from a polyester with an acid number of 20, and an excess of magnesium oxide, the organically-combined magnesium oxide can be from 0.69% to 1.38%. When the magnesium oxide joins two carboxyl-terminated molecules, the organically-bound magnesium oxide is 0.69%. However, if a basic salt should be formed, R—COOMg(OH), the combined magnesium oxide would be 1.38%. The stocks containing the polyester with an acid number of 20 had approximately a 50% excess of magnesium oxide over the amount necessary to form the basic salt. The analytical data for these samples indicate that the magnesium oxide reacts with the polyester mainly by bridging the molecules. They also demonstrate the precision of the method. The accuracy of the method and freedom from interference by fillers is shown by the data for samples made with an acid number of 42.

When hydrated alumina was the filler, the water of hydration apparently competed with the polyester for the magnesium oxide. Magnesium hydroxide is relatively inert to the polyester. The low recovery for raw samples containing hydrated alumina was not due to incomplete reaction since there was no difference in the organically-bound magnesium in samples that had thickened for three days or for nine days.

For the samples made with the polyester having an acid number of 42, the organic acidity was in excess by 30%. There is no indication of the excess acidity having reacted with magnesium in the fillers.

The method proposed in this paper requires about 40 hours. Most of this time is used for slow operations requiring no supervision, such as the pyrolysis, and evaporation of solutions to dryness. When several samples are being analyzed simultaneously, the labor per sample is about an hour and a half.

ACKNOWLEDGMENT

The author expresses his appreciation to Helen Andersen for expert assistance and to Alan Baumgartner, William Thomasino, and Charles Moruska for the preparation of samples.

LITERATURE CITED

(1) Betz, J. D., Noll, C. A., *J. Am. Water Works Assoc.* **42**, 49–56 (1950).
(2) Farbenfabriken Bayer, A.G., German Patent 1,131,881 (June 20, 1962), British Patent No. 949,869 (Feb. 19, 1964).
(3) Fisk, Charles F., (to U. S. Rubber Co.) U. S. Patent No. 2,628,209 (Feb. 10, 1953).
(4) Grim, R. E., "Clay Mineralogy," pp. 305–10, McGraw-Hill, New York, 1953.
(5) Hunt, J. M., Turner, D. S., ANAL. CHEM. **25**, 1169 (1953).
(6) Keller, W. D., Pickett, E. E., *Am. J. Sci.* **248**, 264–73 (1950).
(7) Keller, W. D., Pickett, E. E., *Am. Mineralogist* **34**, 855–68 (1949).
(8) Sadtler, T., Sadtler, P., "Improved KBr Techniques," Pittsburgh Conference on Analytical Chemistry and Applied Spectroscopy, (1965).
(9) Walton, J. P., "Pre-Thickened Polyester Resins in RFP Molding Compounds," Soc. Plas. Eng., Reg. Tech. Conf., Oct. 4–5, 1965.

RECEIVED for review March 17, 1966. Accepted May 23, 1966.

Fast and Sensitive Method for Determination of Nitrogen

Selective Nitrogen Detector for Gas Chromatography

RONALD L. MARTIN

Research and Development Department, American Oil Co., Whiting, Ind.

▷ **A fast method for determining as little as 10^{-9} gram of nitrogen is applicable to both total- nitrogen determinations and selective detection of nitrogen compounds with gas chromatography. Nitrogen compounds are converted quantitatively to ammonia in a stream of hydrogen over a nickel-on-magnesium oxide catalyst. The ammonia is titrated automatically, using a newly devised procedure, with coulometrically generated hydrogen ions. For petroleum samples, the method is quantitative and essentially free of interferences; gas oils containing as little as 0.2 p.p.m. of nitrogen can be analyzed in less than 10 minutes. The system, applied as a selective nitrogen detector with gas chromatography, has been used to determine nitrogen-compound distributions in complex petroleum materials.**

ANALYSES for organic nitrogen, while needed in most research and process laboratories, are particularly important in the petroleum industry. Because of harmful effects of nitrogen compounds, total nitrogen must be determined reliably down to about 1 p.p.m. in a variety of feeds and products. Characterization of petroleum nitrogen compounds by types and boiling point also is often desired.

This paper describes a new approach to determining nitrogen. Nitrogen compounds are converted quantitatively to ammonia over a catalyst in a stream of hydrogen, and the ammonia is titrated coulometrically. The catalyst is nickel on magnesium oxide of the type described initially by ter Meulen (*11*), improved by Holowchak, Wear, and Baldeschwieler (*3*), and applied by others (*4, 12*). Whereas earlier work with this catalyst was limited to samples in the naphtha boiling range (up to about 250° C.), improvements in operating conditions now extend the applicable range through heavy gas oil (up to about 500° C.). The ammonia is swept with hydrogen from the catalyst into a specially devised titration cell, to titrate it automatically and continuously with coulometrically generated hydrogen ions.

Liberti and Cartoni (*5, 6*), Coulson and Cavanagh (*1, 2*), and others—e.g., (*7, 9*)—have used coulometry for continuous automatic titrations. Coulson and Cavanagh designed a particularly sensitive coulometer, employing both variable current and variable voltage, and were able to titrate as little as 0.1 μg. of halide (*1*) and sulfur dioxide (*2*). None of the earlier titration systems—including the one employing hydroxyl generation or degeneration from peroxide (*2, 6*)—were adaptable, however, to the automatic titration of ammonia in a stream of hydrogen.

The catalytic and titration reactions in the new method occur so rapidly that the equipment can serve as a selective nitrogen detector for gas chromatography as well as to determine total nitrogen. The application to gas chromatography is proving very valuable in the study of the complex nitrogen distributions in petroleum.

In determining total nitrogen, the new method is two orders of magnitude more sensitive than Dumas or earlier ter Meulen methods and one order of magnitude more sensitive than Kjeldahl methods. It is at least as fast as automatic Dumas methods and an order of magnitude faster than Kjeldahl or earlier ter Meulen methods.

DISCUSSION OF METHOD

A schematic diagram of the apparatus is shown in Figure 1. Hydrogen is used as eluting gas for gas chromatography and as sweep gas. Use of the sweep gas, which bypasses the column and is humidified by bubbling through water, ensures a high velocity through the catalyst and thus preserves the narrowness of peaks eluting from the gas chromatography column. Sample-introduction ports, with silicone rubber septums for syringe injection, are provided at both ends of the column; injection at the effluent end allows determination of total nitrogen. The catalyst tube contains a 3 × 1/4 inch bed of catalyst and is housed in an oven or furnace kept at 440° ± 10° C. The exit end of the catalyst tube is connected directly to the titration cell. The coulometer (Dohrmann Instruments Co. Model C-200) supplies and controls the current used in generation of titrant within the cell. This current is recorded against time to give ordinary differential peaks, whose areas are direct measures of the amounts of titrant generated.

The exact manner of connecting the catalyst tube is diagrammed in Figure 2. For convenience in changing the catalyst, the tube is connected from the outside of the oven, using an adapter ball joint on the exit end of a permanently fixed open tube, inside which the catalyst tube fits. The sweep gas is fed through the permanent fixed tube so that the column effluent is forced directly through the catalyst tube. The entire assembly up to the adapter ball joint is kept inside the oven.

The nitrogen-analyzer apparatus, including the titration cell and other necessary equipment, is available from Dohrmann Instruments Co., which has been licensed by Standard Oil Co. (Indiana) to produce it commercially.

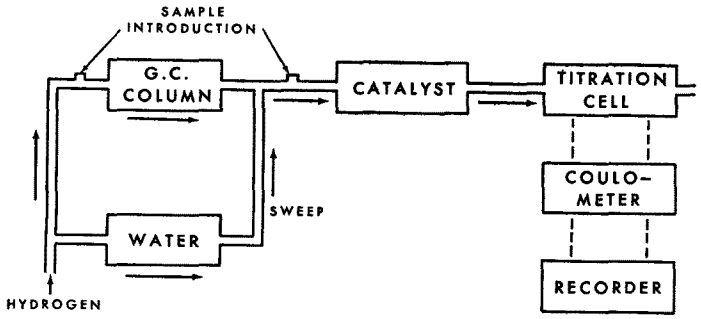

Figure 1. Apparatus

Catalytic Production of Ammonia. The combination of humidified hydrogen and a higher catalyst temperature [440° C. rather than the 300° to 360° used previously (*3, 4, 11, 12*)] permits analysis of higher boiling samples than previously. At the lower temperatures, most nitrogen compounds boiling above the kerosine range failed to yield ammonia quantitatively, largely because of "coke" formation on the catalyst. With humidified hydrogen, the rate of coke formation and, more significantly, ammonia adsorption on the coke are decreased. Without humidified hydrogen, ammonia adsorption increases as coke accumulates and the peaks soon tail too much to be measured accurately. A temperature of 440° C. is about optimum; higher temperatures give less adsorption of ammonia, but also more rapid accumulation of coke.

Even with humidified hydrogen, coke accumulation eventually precludes quantitative ammonia production, and the catalyst must be changed. The life of the catalyst in general decreases as the boiling point of the samples increases. Unusually high levels of sulfur and condensed-ring aromatics also lessen catalyst life somewhat. In a typical case, a 3 × 1/4 inch catalyst section remains totally active for 5 to 10 ml. of virgin naphtha, 2 to 4 ml. of light gas oil or heavy catalytically cracked naphtha, and 0.5 to 1.5 ml. of heavy gas oil or cycle oil. Since the usual sample size for determining total nitrogen is only 1 to 10 μl., the catalyst remains active for about 100 samples even in the worst cases. Larger catalyst sections—with correspondingly longer lives—can be used where the width of the ammonia peak is unimportant. The 3-inch section was designed to be long enough to allow many samples to be analyzed and still not so long as to make peak widths too wide for gas chromatography.

The catalyst goes through several stages of adsorptivity and reactivity. Fresh catalyst adsorbs ammonia for about 1/3 minute under normal operating conditions, but this adsorption is harmless because the ammonia peak is not given a tail nor significantly broadened. (This type of adsorption surprisingly increases with increasing catalyst temperature.) After about 100 μl. of sample have passed through the catalyst, adsorption decreases and remains relatively low until the catalyst is nearly deactivated. Then adosption increases, presumably from extensive coke formation, and badly tailing peaks are often observed. When this occurs, incomplete ammonia production can be anticipated soon. Ammonia production drops sharply, rather than gradually, when the catalyst becomes deactivated.

Attempts to reactivate the catalyst with heat and air oxidation or steaming have been unsuccessful.

Hydrogen flow rate through the catalyst tube is not particularly critical. All rates between 10 and 1000 cc. per minute have given essentially the same results. The rate chosen for usual operation—about 500 ml. per minute—is fast enough to keep peak widths relatively narrow and yet not cause significant noise in the titration cell.

Coulometric Titration of Ammonia. The ammonia titration cell (Figure 3) contains two pairs of electrodes. Hydrogen ion concentration is sensed by one pair—the platinum-blacked sensor in the center compartment and the silver–silver sulfate reference electrode in one of the two legs; any number of other reference electrodes could also have been chosen, and for future work, the lead–lead sulfate electrode would be preferred (*8*) because of the lower solubility of lead sulfate. The second electrode pair is for hydrogen ion generation and consists of the platinum-blacked anode in the central chamber and the platinum-coil cathode in one of the legs. The two electrodes in the center chamber are "blacked" with finely divided platinum (by electrolytic reduction from dilute chloroplatinic acid solution) to make them more sensitive to hydrogen ion concentration. The generator anode will also function satisfactorily when made of shiny platinum (*8*).

The ammonia cell requires a glass frit or its equivalent between the cathode leg and central chamber to restrict diffusion of hydroxyl ions generated at the cathode ($H_2O + e^- \rightarrow H_2 + OH^-$) from entering the central chamber.

The type and concentration of electrolyte in the cell are not particularly critical. A 0.003*M* solution of sodium sulfate is used, although any number of other inert salt solutions also could have been chosen. Concentrations of sodium sulfate significantly higher than 0.003*M* lead to slightly more electrical noise.

The coulometer maintains a constant concentration of titrant within the titration cell (*1, 9*). This concentration is determined by the coulometer "bias set" control, which supplies a voltage to the input of the coulometer amplifier equal and opposite to that of the reference-sensor electrode pair. When the two voltages are equal, the amplifier receives a zero signal and hydrogen ions are not generated; however, when ammonia enters, the voltage shift of the sensor electrode is sensed by the amplifier, and a flow of current is produced in the generator circuit to oxidize hydrogen gas at the anode to hydrogen ions. This generation continues until the original hydrogen ion concentration is restored and the reference-sensor voltage again equals the bias voltage.

The ammonia cell works most satisfactorily—i.e., the titrant-generation peaks are the narrowest without significant overshoot—when the original concentration of hydrogen ions is kept between about 5×10^{-6} and 5×10^{-7} *M*. This range is a compromise between high sensitivity and high stability. The cell is actually the most sensitive at a concentration of 1.0×10^{-7}—i.e., it can then detect the smallest addition of ammonia because the changes in sensor voltage are the largest; the cell, however, is unstable—i.e., the generation

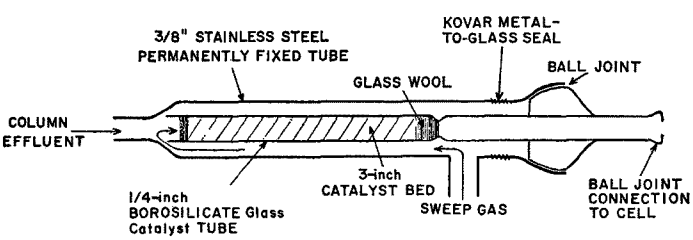

Figure 2. Catalyst tube and connections

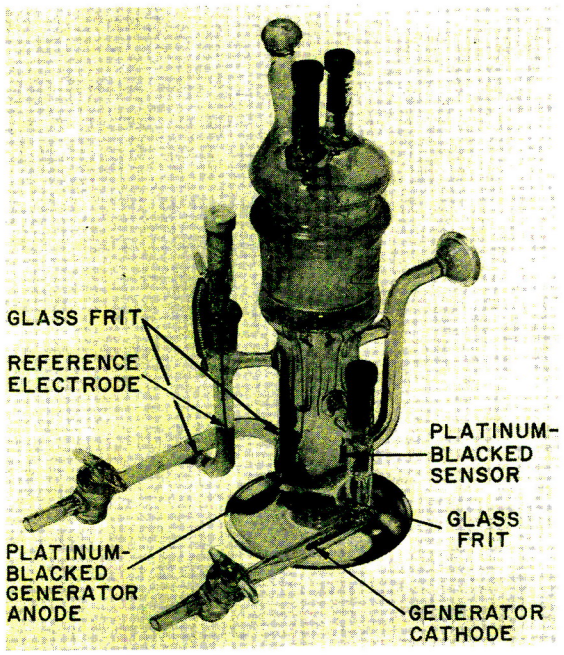

Figure 3. Titration cell

overshoots and oscillates. Higher concentrations than 10^{-7} are thus necessary to ensure stable operation; concentrations above 5×10^{-5}, however, are unsatisfactory, because the cell is then too insensitive and the peaks become broad.

Bias settings around 1.00 volt give hydrogen ion concentrations between 5×10^{-6} and $5 \times 10^{-7}M$. The bias voltage, which is equal and opposite to the sensor-reference voltage, neglecting overvoltage, can be computed approximately by:

$$E_{bias} = E^{\circ}_{(Ag\text{-}AgSO_4)} + E^{\circ}_{(H_2\text{-}H^+)} + 0.059 \log \frac{[H^+]}{[H_2]^{1/2}}$$

By this expression, when the bias is exactly -1.00 volt, the hydrogen ion concentration is $1 \times 10^{-6}M$. If generation of titrant is too fast or too slow at 1.00 volt, the bias can be adjusted a few millivolts either way until it becomes optimum. If the lead–lead sulfate reference electrode is used in place of silver–silver sulfate, the bias would be operated at about 0.10 volt.

In addition to being dependent on the bias setting, the speed of titrant generation is also somewhat dependent on the positions of the two center-compartment electrodes. For the fastest generations, the center electrodes are best placed in their least-damped position, with the sensor directly in the path of the incoming gases. Generations are slower when the center electrodes are rotated 90° counterclockwise, but noise is somewhat less.

Slow speeds of titrant generation can also be caused by particularly thick coatings of platinum black on the center-compartment electrodes. Our best results have been obtained with coatings that do not completely cover the shiny platinum.

Gas Chromatographic Separations. A gas chromatography column was sought that would give efficient separations, would not react with or strongly adsorb petroleum nitrogen compounds, and could be taken to relatively high temperatures without causing detector response or catalyst deactivation. A column satisfying these requirements was a 20-foot by $^3/_{16}$-inch i.d. stainless steel section packed with 9% by weight of polyethylene of 12,000 molecular weight (Bakelite DYLT) on Chromosorb-W precoated with 3% potassium carbonate. This column, which was unreactive and gave good separating efficiencies, was usable to 330° C., which was sufficient to elute samples as high boiling as gas oils.

The potassium carbonate and the relatively high percentage of liquid phase (9%) both are present to minimize reaction of nitrogen compounds with the solid support. Nine per cent of liquid phase was enough to minimize reaction with the support, yet not cause inefficient separations.

The molecular weight of polyethylene was chosen as a compromise to give short retention times and efficient operation. Shorter retention times, which result from the higher molecular weights, are desirable because the column can then elute higher-boiling materials. However, polyethylenes much above 12,000 in molecular weight were difficult to coat on the support and gave poorer separating efficiencies. All of the polyethylenes began to give minor amounts of decomposition products above 270° C. but were usable to about 330° C., because the products did not give significant detector response nor deactivate the catalyst.

Many conventionally used liquid phases failed in this application. Polyesters and silicone fluids both lacked sufficient temperature stability—especially in the presence of potassium carbonate—and their decomposition products gave interfering response. With silicones, the interference was at least partially due to a few parts per million impurity of nitrogen in the products. Most of the petroleum-derived oils and greases—e.g., Apiezon greases—also failed because of nitrogen impurities. Microcrystalline wax columns were usable to about 320° C., and gave excellent separations; however, after short use they caused polymerization of pyrroles and indoles.

Because the response speed of the nitrogen detection system is slower than most detectors, gas chromatographic peaks that are both sharp and incompletely separated cannot be followed perfectly. The slower response speed, which results from short time delays in both the catalyst tube and the titration cell, makes the peaks at least one-half minute wide at the base. In some cases, therefore, columns are best operated at relatively slow rates for column flow and temperature programming, so narrow peaks are avoided. This problem becomes insignificant, however, as retention time increases, because the peaks soon become sufficiently broad to be adequately followed.

DETAILS OF PROCEDURE

Preparation of Catalyst. The catalyst is prepared in a manner similar to that as described by Holowchak, Wear, and Baldeschwieler (*3*) and later by King and Faulconer (*4*).

Prepare a slurry of 125 grams of finely divided magnesium oxide in 1.25 liters of distilled water at 50° C. Prepare a solution of 400 grams of nickel nitrate hexahydrate in 4 liters of distilled water at 50° C., and add it slowly to the magnesium oxide slurry while stirring vigorously with a mechanical stirrer. Allow the precipitate to settle, decant the mother liquor, collect the precipitate on a Büchner funnel, and wash with about twenty 100-ml. portions of distilled

Table I. Analyses of Standard Samples

	Nitrogen, p.p.m. Known	Found
Pyridine	4.2	4.4
	42	42
	420	412
Pyrrole	151	153
Indole	102	104
Carbazole	92	92
Phenazine	154	158
Butylamine	140	139
Acrylonitrile	66	67
Nitrobenzene	37	38
Azobenzene	37	36
Azoxybenzene	36	35
Phenylhydrazine	110	89
O,O-Dimethyl *S*-(4-oxybenzotriazino-3-methyl)phosphorodithioate (Guthion)	119	47
3-(3,4-Dichlorophenyl)-1-methoxy-1-methylurea (Linuron)	56	55
Ethyl *N,N*-di-*n*-propylthiocarbamate (Eptam)	189	188
O-Ethyl *O*-p-nitrophenyl phenylphosphorothioate (Epn)	104	109

Table II. Analyses of Petroleum Fractions

	Nitrogen, p.p.m. Kjeldahl	Present method
Shale naphtha	1900	1920
Light catalytic cycle oil	241	233
Heavy virgin gas oil	605	600
Catalytic naphtha	0.5[a]	0.8
Percolated heavy cycle oil	2[a]	1.7

[a] Analysis made after prior concentration; estimated uncertainty about ±50% relative.

water, mixing the precipitate thoroughly with each portion before drawing off. Compact the precipitate by pushing it down firmly with a flat surface such as the end of a wide spatula. Divide the precipitate into 1/4- to 1/2-inch pieces, and dry them first in air and then in vacuum at about 100° C. Transfer the dried pieces, which should be pale green, to a 2-inch diameter borosilicate glass tube, place the tube in a furnace at about 450° C., and maintain a hydrogen flow of about 100 ml. per minute through it for 1 hour. (The nickel oxide will be reduced to nickel metal and most of any traces of nitrate still present will be reduced to ammonia and eluted.) Remove the tube from the furnace and allow it to cool before stopping the hydrogen flow. Using a sharp knife, gently break the black solid into pieces of about 4- to 8-mesh size, and screen gently through 4- and 8-mesh screens, breaking up any pieces that do not pass through the 4-mesh screen. Use the catalyst retained on the 8-mesh screen.

If desired, omit the above reduction step and conduct it instead in the catalyst tube just before use. A disadvantage of this shortcut is that the solid shrinks during reduction and gaps may form in the tube.

Preparation of Electrolyte Solution. Dissolve 4.3 grams of sodium sulfate in distilled water, add 3 ml. of 0.05*M* sulfuric acid, and dilute to 10 liters. The sulfuric acid is added to bring the hydrogen ion concentration into the range required for optimum cell operation.

Startup. Adjust furnace temperature to 440° C. Clean the titration cell by flushing it several times with acetone and fresh electrolyte. Clean the center compartment electrodes by dipping them into concentrated nitric acid and rinsing them thoroughly with distilled water. Fill the catalyst tube with a 3-inch section of catalyst. Purge the tube with hydrogen for 30 seconds, connect it into the apparatus, and adjust the flow of hydrogen to about 500 ml. per minute. Connect the titration cell to the exit end of the catalyst tube. Fill the cell with electrolyte solution to a height of 2 inches. Turn the magnetic stirrer to about 50% of its maximum rate, and purge the solution with hydrogen for 5 minutes. Lower the electrolyte level until it is about 1/4 inch above the top of the electrodes. Position the sensor electrode at the cell entrance, and set the coulometer voltage gain to about 2000. Adjust the bias to 1.00 volt and turn the coulometer function switch to "operate." The base line should level within 3 minutes, and noise should be no more than 1% of full scale on a setting of 15 ohms with a 1-mv. recorder. If noise is too high, check cell cleanliness, electrical connections, and the coulometer.

Calibrate the system with a sample of known nitrogen concentration—e.g., 2.00 µl. of a 100-p.p.m. solution of carbazole in benzene—and check the resultant peak for speed of response and quantitativity. The pen should return to base line in less than 1 minute and the overshoot should be no more than several per cent of the peak height. To increase response speed, increase the bias in increments of about 5 mv.; coulometer gain and cell cleanliness have lesser effects on response speed. Judge quantitativity by the number of coulombs used in generating the titrant. They should be at least 95% of theory; if they are less, check for leaks or install fresh catalyst.

Determination of Total Nitrogen. Add a known weight of sample by syringe through the introduction port at the column exit, measure the area of the resultant peak, compare it to that of a standard sample, and calculate the amount of nitrogen by proportioning. If the density of the sample is known, the measured volume from a calibrated syringe is satisfactory for determining sample weight; otherwise, weigh the syringe on a microbalance before and after charging. In measuring peak area, subtract any dip below the base line occurring at the front or back of the peak from the area above the base line. Run samples of known nitrogen content periodically and change the catalyst when the peak area decreases below 95% of its usual value.

RESULTS

Total Nitrogen. The accuracy of the titration was established by measuring the quantity of electricity used in titrant generation for known injections of ammonium hydroxide. The coulombs used were theoretical throughout the usable range of 10^{-5} to 10^{-9} gram of ammonia; relative deviations were within the estimated experimental error of 3%.

The response of the detection system to various types of organic nitrogen compounds is shown in Table I. These 17 samples were prepared by weighing a known amount of a single nitrogen compound into a nitrogen-free solvent; the first group comprises typical petroleum nitrogen compounds; the middle group, miscellaneous compounds; and the last group, pesticides. Agreement between the "known" and "found" values is well within experimental error for all of the petroleum nitrogen compounds and all but two of the other compounds. These two (Guthion and phenylhydrazine) were, respectively, only 39 and 81% of theory, because some of the nitrogen atoms are converted to elemental nitrogen, which cannot be converted to ammonia. With Guthion, two of the three nitrogen atoms in the triazine linkage tend to yield elemental nitrogen. Kjeldahl analyses, which also depend on ammonia production, gave similarly low results in our laboratory for Guthion and phenylhydrazine. Azobenzene and azoxybenzene, both of which contain two nitrogen atoms connected by a double bond in contrast to the single bond in phenylhydrazine, yielded ammonia quantitatively.

Total nitrogen determinations by ammonia titration on five petroleum fractions are compared with Kjeldahl analyses in Table II. All of the analyses agree well. The last two show that samples in the 1-p.p.m. range can be analyzed accurately by ammonia titration without prior concentration. The precision of replicate analyses has been about 3% or 0.2 p.p.m., whichever is larger.

Interferences to the nitrogen detection system are very slight. Acidic compounds, such as hydrogen sulfide or hydrogen chloride, do not interfere because they are adsorbed irreversibly by the magnesium oxide in the catalyst as long as the catalyst is kept below about 480° C. Basic compounds other than ammonia would interfere, but few if any such compounds would normally be present or would be formed during passage through the catalyst. No interference has been encountered from 1% concentrations of compounds con-

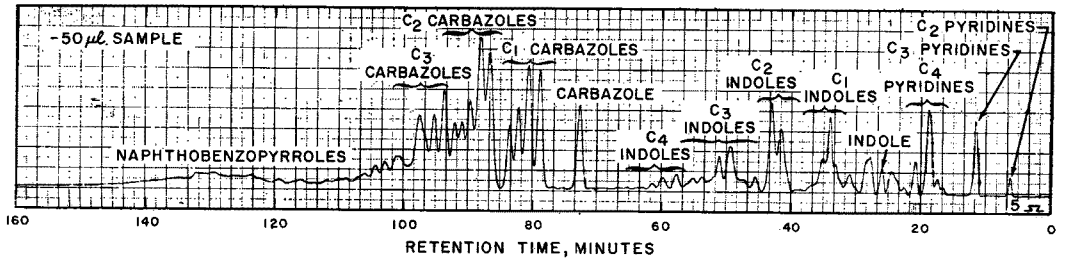

Figure 4. Nitrogen compounds in catalytic cycle oil

taining oxygen, halogens, sulfur, phosphorus, or arsenic.

The detector is essentially inert to hydrocarbons, although quantities of more than 5 to 10 μl. will cause the base line to dip slightly and then rise a corresponding amount; no problem results, however, because the dip and rise have exactly the same areas and thus cancel. The dip is caused by a momentary high concentration of hydrocarbons in the gas stream, which lowers the hydrogen activity below unity and thus changes the sensor potential slightly. As soon as the slug of hydrocarbon passes, the hydrogen activity is restored and the cell corrects for the earlier change.

Gas Chromatography. Chromatograms of a full-range catalytic cycle oil containing 260 p.p.m. of nitrogen (Figure 4) and a shale naphtha containing 1920 p.p.m. of nitrogen (Figure 5) illustrate the usefulness of combining gas chromatography with ammonia titration. Both runs were made on the polyethylene column and were programmed at 1.4° C. per minute —the cycle oil from 120° to 330° and the naphtha from 50° to 190°. The column flow rate was 200 cc. per minute for the cycle oil and 120 cc. for the naphtha. Four types of compounds dominate in the cycle oil—pyridines, indoles, carbazoles, and naphthobenzopyrroles—some overlap between the types exists, but the proportions of the types as well as their carbon numbers can be estimated from the chart areas. Nitrogen compounds in the shale naphtha are nearly exclusively pyridines; they range from pyridine itself to homologs containing alkyl substituents of six carbons.

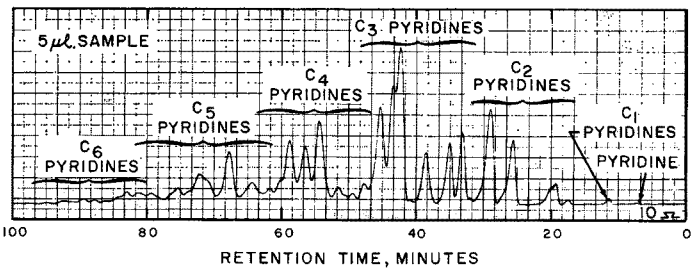

Figure 5. Nitrogen compounds in shale naphtha

CONCLUSIONS

The new detection system has shown excellent promise for both total-nitrogen determinations and gas chromatography. More work could profitably be conducted in both areas, however. Total-nitrogen determinations need to be tested in routine service, and nonvolatile samples should be tried using some type of a fragmentation procedure. Other catalytic conditions probably should also be tested. For example, McNulty (*8*) reports that a section of nickel turnings at 900° C. can, at least in some instances, be used in place of ter Meulen catalyst. If such conditions give consistent quantitative results, they could prove advantageous, because less volatile samples could be analyzed and catalyst regeneration might be possible. An alkaline absorber for gases such as hydrogen chloride and hydrogen sulfide would be needed with this type of catalyst. Catalysts with different metals (such as rhodium) or different supports (such as silica) also could be investigated.

With gas chromatography, nitrogen-compound distributions could be determined in a variety of materials that are difficult to analyze; applications to the pesticide and petroleum fields are obvious. In pesticide work, the detector could be used to distinguish pesticides containing nitrogen from those that do not. For petroleum samples, a reasonable manner of application—similar to that used previously for sulfur compounds (*10*)—would be to use gas chromatography in combination with procedures for separating nitrogen compounds by types; one or more papers describing such an approach will issue from this laboratory in the future.

The new titration cell should also be valuable in other applications. Its ability to titrate acids as well as bases should add to its usefulness. The cell should be tested, perhaps under different bias conditions, for titration of weak acids such as carbon dioxide.

ACKNOWLEDGMENT

The author gratefully acknowledges the very helpful counsel of R. L. Burwell of Northwestern University and R. J. Flannery and I. J. Oita of the American Oil Co.

LITERATURE CITED

(1) Coulson, D. M., Cavanagh, L. A., ANAL. CHEM. **32**, 1245 (1960).
(2) Coulson, D. M., Cavanagh, L. A., "Microcoulometric Detection in Gas Chromatography," Pittsburgh Conference on Analytical Chemistry and Applied Spectroscopy, March 1961.
(3) Holowchak, J., Wear, G. E. C., Baldeschwieler, E. L., ANAL. CHEM. **24**, 1754 (1952).
(4) King, R. W., Faulconer, W. B. M., *Ibid.*, **28**, 255 (1956).
(5) Liberti, A., Cartoni, G. P., *Chim. Ind. (Milan)* **39** (10), 821 (1957).
(6) Liberti, A., Cartoni, G. P., Pallotta, U., *Ann. Chim. (Rome)* **48**, 40 (1958).
(7) Klaas, P. J., ANAL. CHEM. **33**, 1851 (1961).
(8) McNulty, J. A., Dohrmann Instruments Co., San Carlos, Calif., private communication, Feb. 7, 1966.
(9) McNulty, J. A., Meyers, A. R., "Advanced Automatic Microcoulometer for Trace Sulfur and Halogen Analysis," Pittsburgh Conference on Analytical Chemistry and Applied Spectroscopy, March 3, 1964.
(10) Martin, R. L., Grant, J. A., ANAL. CHEM. **37**, 644 (1965).
(11) Meulen, H. ter, *Rec. Trav. Chim.* **43**, 1248 (1924).
(12) Schluter, E. C., ANAL. CHEM. **31**, 1576 (1959).

RECEIVED for review April 20, 1966. Accepted June 7, 1966. Pittsburgh Conference on Analytical Chemistry and Applied Spectroscopy, Pittsburgh, Pa., February 1966.

Automatic Analyzer with Direct Readout for Determining Carbon in Steel

L. L. LEWIS[1] and M. J. NARDOZZI

Applied Research Laboratory, United States Steel Corp., Monroeville, Pa.

▷ **An automatic analyzer with direct readout in per cent carbon has been developed for determining carbon in steel. The steel sample is burned in oxygen and the carbon dioxide formed is collected and measured for a total analysis time of 80 seconds. Solid state components in the programming and computing system lead to high reliability in a plant environment. Instrument stability is excellent and the need for calibration checks is infrequent. The linear operating range of the instrument is from 0.01 to 1.2% carbon, and the range can be extended down to 0.001 and up to 3.0%. Oxygen of the quality used for plant operation in a steel mill can be used for the analysis. Experiments have shown that the analyzer can be used without modification for determining oxygen in steel by the carrier gas method.**

COMBUSTION–THERMAL conductivity analyzers for determining carbon in steel have been developed by Lewis and Nardozzi (*1*), Walker and Kuo (*2*), and others in which the sample is burned in oxygen and the carbon dioxide that is formed is swept through a molecular sieve trap and collected. Advantages of this method are that high sensitivity is obtained by concentrating the carbon dioxide from the oxygen stream on the trap before measurement and that argon and nitrogen (both present as impurities in the oxygen) do not interfere because they are not retained on the trap.

Our previously reported work (*1*) showed that the relation between peak height or peak area and quantity of carbon dioxide was not linear over a broad concentration range of carbon dioxide, so calibration curves were needed for quantitative determinations. The work reported here describes how the analyzer was converted into a rapid and fully automatic instrument by providing a linear relationship between the carbon dioxide present and the peak area.

EXPERIMENTAL

The equipment consists of a combustion apparatus (*1*), an analyzer chassis, a control chassis, and a direct readout system.

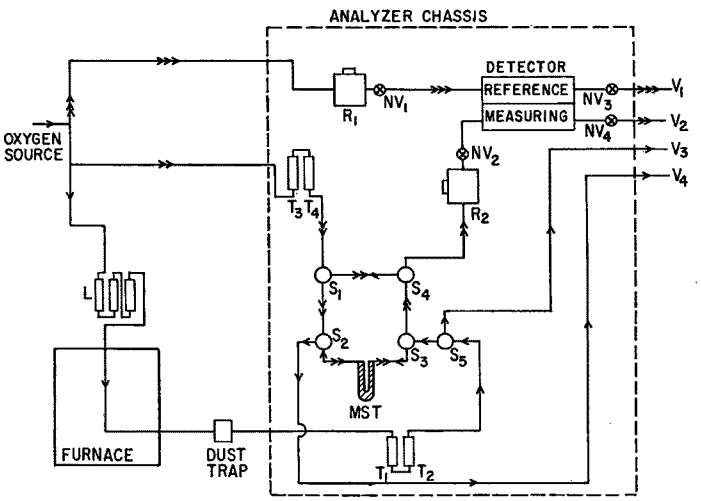

Figure 1. Gas handling system

>	Furnace flow
>>	Measuring carrier flow
>>>	Reference carrier flow
R	Flow regulator
NV	Needle valve
T	Trap
S	Solenoid
V	Vent
MST	Molecular sieve trap
L	Leco purifying train

Combustion Apparatus. A Leco (Laboratory Equipment Co.) induction furnace, Type 521, is used with a Leco Jet combustion tube, No. 550-122.

Analyzer Chassis. The analyzer chassis houses the detector, the gas handling system, purification traps, and the molecular sieve trap. The detector is a two-cell, thermistor type (No. 9677, Gow-Mac Instrument Co.) operated at a current of 6 ma. and a temperature of 40° C.

The gas handling system, Figure 1, is composed of three oxygen streams (furnace, reference, and measuring); five three-port solenoid values (S_1 to S_5, Skinner Precision Industries, type V5); four needle valves (NV_1 to NV_4, Ideal Aerosmith, No. 52-2-13); and two constant-differential-type gas flow regulators (R_1 and R_2, Moore Products Co.). Two steps are required to get the carbon dioxide into the detector for measurement. The carbon dioxide is first adsorbed from the furnace-gas stream as follows: The oxygen flow from the furnace passes through S_5, S_3, the molecular sieve adsorption trap, S_2, and then to the atmosphere through a vent, V_4; meanwhile the oxygen of the measuring carrier flow stream passes directly through S_1, S_4, and the measuring side of the detector. In the second step, the flush or desorption step, the oxygen from the measuring carrier flow stream passes, in order through S_1 and S_2, the heated molecular sieve trap, S_3, and S_4, thus carrying the desorbed carbon dioxide to the measuring side of the detector. During the desorption, the furnace stream passes through S_5 and is vented to the atmosphere through V_3.

Oxygen is supplied to the analyzer at a regulated pressure of 10 p.s.i.

[1] Present address: Chemistry Department, General Motors Corp., Warren, Mich.

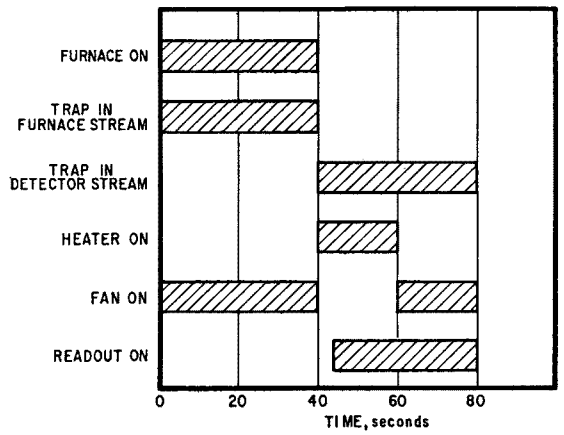

Figure 2. Programming time and sequence chart

Needle valves NV_1 and NV_2 (Figure 1) are adjusted to provide oxygen flow rates of 200 and 500 ml. per minute, respectively, through the reference and measuring sides of the detector. The oxygen flow rate through the furnace is 1200 ml. per minute. When the instrument is not being used, the detector voltage and oxygen are turned off, and needle valves NV_3 and NV_4 are then closed to protect the traps from atmospheric contamination.

For rapid determinations, a relatively high flow rate of 500 ml. per minute is required through the measuring side of the detector because of the internal volume of flow regulator R_2. This high flow rate results in dilution of carbon dioxide in the oxygen stream and some loss of sensitivity. For the best sensitivity, R_2 can be bypassed and the flow rate reduced to about 80 ml. per minute. With R_2 out of the system, linearity in integrated voltage from the detector signal will be limited to samples with less than about 0.3% carbon.

The analyzer chassis has traps T_1 and T_2 (Figure 1) to purify the furnace stream of water and sulfur oxides. Water and carbon dioxide are adsorbed from the measuring carrier stream by traps T_3 and T_4.

The trap on which the CO_2 is adsorbed is a quartz U trap (7 mm. o.d., 4 mm. i.d., and 60 cm. long) containing 7 grams of $^1/_{16}$-inch pellets of molecular sieve, Type 5A (Linde Co.). The trap is wound externally with Nichrome ribbon (Driver-Harris Co.) for resistance heating. The voltage applied to the resistance ribbon is adjusted so that the ribbon becomes red at the end of a heating cycle of 20 seconds. Longer heating periods at lower trap temperatures have been used successfully. If overheated, the molecular sieve will fuse. With proper heating, however, traps have been used for more than 10,000 cycles without sign of deterioration of the molecular sieve.

Control Chassis. The control chassis contains the electrical components and associated controls for the detector, the timing cycle (both automatic and manual), and the molecular sieve trap heater.

The timing cycle consists of: furnace purge, during which time the air trapped during sample loading may be purged from the furnace tube if desired; furnace burn, during which time the sample is burned and CO_2 is adsorbed on the molecular sieve trap; flush, during which time the molecular sieve trap is heated and the CO_2 is desorbed; and read, which activates the readout system just before the CO_2 passes through the detector. A programming time and sequence chart for the analytical cycle is given in Figure 2. Individual adjustable solid-state timers (Syracuse Electronics Corp., Type TER) control each part of the cycle and provide a versatile and completely automatic timing program. Manual on–off switches are provided for individual activation of any part of the timing cycle for maintenance purposes.

Direct Readout System. A schematic diagram of the direct readout computing system is shown in Figure 3. The input signal from the detector is amplified by a value of R_2/R_1 by operational amplifier A_1. Variable resistor R_2 is used as a linear weight compensator to automatically correct for samples of varying weight; the value of the feedback resistor R_2 was selected to give a sample weight range of 0.85 to 1.15 grams. The amplified signal coming from the detector is integrated by operational amplifier A_2. The potential across the capacitor C_1 is measured across resistor R_4 by the digital voltmeter (DVM). By adjusting R_4 in the calibration procedure, the desired voltage is read on the DVM for direct readout. Component values are chosen so that 0.1-volt output is equivalent to 0.01% carbon, 1-volt to 0.1% carbon, etc.

When the carbon dioxide from a sample is to be measured, the read part of the program is activated by the opening of relay RL_1. The short across C_1 is removed as RL_2 opens and the integration period begins. When the integration time is ended, RL_1 and RL_2 close and the capacitor is discharged. The voltage reading is stored on the DVM, however, by a reading retention circuit that is activated through P_1. Toggle switch S_1 is closed

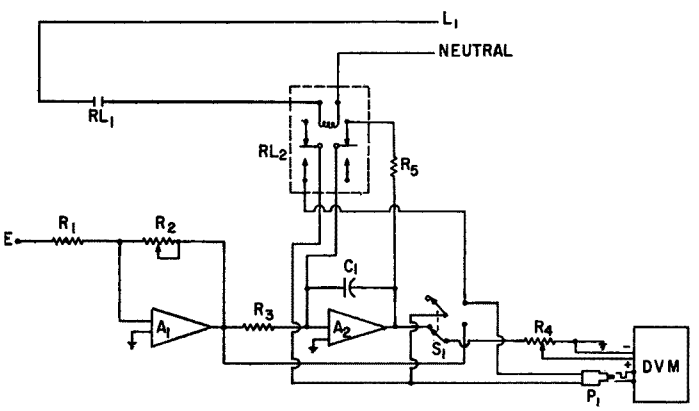

Figure 3. Direct readout wiring diagram

RL_1	Read delay timer
RL_2	Relay, DPDT, Potter & Brumfield No. KRP11AG
E	Detector signal
A	Operational amplifier
S_1	Switch, spring loaded, DPDT, Arrow-Hart & Hegeman, No. 21858-X
C_1	0.5 mf., 200-VDC, Mallory, PVC-205
P_1	Phone jack
DVM	Digital voltmeter
R_1	1.0 kohm., 1-W, Dale Products, No. RS-1B
R_2	120 kohm., 5-W, 3 turn, 0.25% linear tolerance, Clarostat, No. 59-14-JA
R_3	15 Meg, 1-W, International Resistance Co., No. DCF
R_4	200 kohm. 5-W, 10 turn, 0.25% linear tolerance, Borg, No. 2201-B
R_5	1 kohm., 1-W, Dale Products, No. RS-1B

momentarily at the beginning of a determination to check the balance of the detector bridge by means of the display on the DVM. As S_1 closes, the reading on the DVM retained from the previous determination is cancelled automatically.

The stabilized operational amplifiers used are from Philbrick Researches, Inc. Both the tube type (Model UPA-2) and the solid-state type (Model SP 656) have proved to be satisfactory for this application. The digital voltmeter is the Model Z200 made by the United Systems Corp. The quality of the readout system was studied by making measurements with known input voltages over carefully measured time periods. The reproducibility was determined to be within ±0.2%, which is satisfactory.

Operating Procedure. The instrument is calibrated with 1-gram samples of a standard sample, preferably one that contains carbon in the concentration range of interest. After the crucible that contains the standard and 1 gram of copper accelerator is placed in the furnace, switch S_1 (Figure 3) is closed and the detector bridge circuit is balanced. The automatic program is started, and when the read portion commences, RL_1 is kept open by means of a switch so that the integrated voltage will be stored in C_1. After the program is finished, R_4 is adjusted so that the carbon content of the standard appears on the DVM.

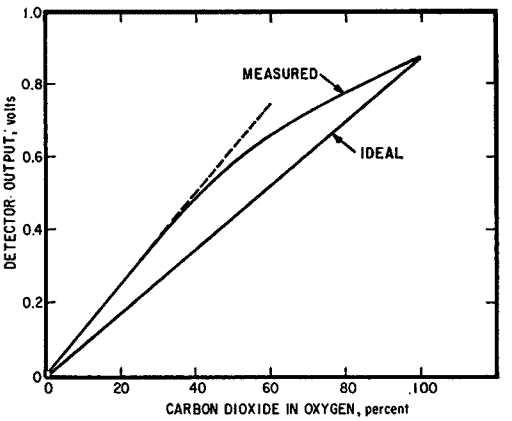

Figure 4. Detector response to carbon dioxide in oxygen

Samples are analyzed by placing the accelerator and a weighed quantity of the sample in the furnace, adjusting R_2 for the sample weight, balancing the bridge circuit, and starting the automatic program.

Experience has shown that water and carbon dioxide may be adsorbed on the molecular sieve held in the trap when the instrument is not in use and that the instrument should therefore be run through two cycles to rid the trap of these contaminants before calibration. The considerable quantity of water that must be present in a newly installed trap is best removed by heating the trap after switching it into the furnace gas stream. The resistance ribbon on the trap is heated to a red color and then the heater is turned off and the air blower is turned on; this is repeated, permitting the trap to cool each time, until the absence of a negative signal on the DVM indicates that the water has been removed.

Table I. Determination of Carbon in Standard Steel Samples

Sample	Carbon, certificate value, %	Analyzer results: Carbon av., %	Std. dev.	Rel. std. dev.
NBS 55*e*	0.011	0.0117	0.00074	6.3
NBS 166*b*	0.019	0.0212	0.0017	8.0
NBS 125*a*	0.032	0.0323	0.00076	2.3
NBS 101*e*	0.054	0.0541	0.0014	2.6
NBS 129*b*	0.094	0.0935	0.00070	0.8
NBS 20*f*	0.380	0.381	0.0018	0.5
NBS 30*e*	0.505	0.508	0.0019	0.4
NBS 50*b*	0.728	0.739	0.0087	1.2
NBS 153*a*	0.902	0.903	0.0031	0.3
NBS 51*b*	1.21	1.19	0.011	0.9

Table II. Determination of Carbon in Samples Containing More than 1.2% Carbon

Carbon, reported value, %	Carbon detd., %	Av.	Std. dev.	Rel. std. dev.
1.82	1.77	1.77	0.0036	0.20
	1.77			
	1.78			
	1.77			
	1.77			
2.16	2.05	2.03	0.025	1.23
	2.02			
	2.06			
	2.02			
	2.02			
3.18	2.72	2.71	0.018	0.66
	2.70			
	2.69			
	2.73			
	2.71			

RESULTS AND DISCUSSION

The desired range of the analyzer with a direct readout required a linear response over a concentration range of 0.001 to 3.5% carbon. Achieving this was made difficult by changes in the gas flow through the detector brought about by heating the trap and switching the trap in and out of the gas stream. When the trap was heated (from ambient temperature to about 600° C. in 15 seconds), sudden pressure increases resulted from desorbing the carbon dioxide and heating the oxygen and carbon dioxide. (The carbon from 1 gram of sample with 2.5% carbon produces 47 ml. of CO_2, STP.) Early experimental results showed linearity with up to 0.3% carbon. When the carbon content exceeded 0.3%, pressure increases caused faster gas flow through the detector and low results. Nevertheless, results were reproducible and satisfactory determinations over the whole range could be made by using a calibration curve (*1*).

Linearity was increased to 1.2% carbon (1 gram of sample) by placing a constant-differential-type flow regulator between the trap and the detector (R_2 in Figure 1). With this regulator, constant gas flow was maintained through

Table III. Data on a Low-Carbon Standard with and without Crucible Preheating

Carbon, certificate value, %	Crucible condition	Carbon detd., %
0.0044	As-received	0.0087[a]
		0.0081
		0.0096
0.0044	Preheated	0.0066[a]
		0.0058
		0.0066
		0.0067
		0.0060
		0.0061
		0.0062
		0.0063
0.0044	Preheated	0.0046[b]
		0.0046
		0.0048
		0.0044
		0.0046

[a] Instrument standardized on a sample containing 0.380% C.
[b] Instrument standardized on a sample containing 0.0040% C.

the detector regardless of increases in upstream pressure. Most steels of commercial interest contain less than 1.2% carbon, so this upper limit in linearity is not a serious problem. The 1.2% carbon limit in linearity is evidently due to nonlinearity in detector response when the gas mixture being analyzed contains more than 30 volume % carbon dioxide, Figure 4. The data for Figure 4 were collected under the conditions used for analysis, namely, a detector temperature of 40° C., a detector current of 6 ma., and a gas flow rate of 50 ml. per minute.

Results obtained on standard steel samples with a carbon content range of the greatest commercial importance (0.01 to 1.21% carbon) are shown in Table I. These data were obtained after calibrating the instrument with National Bureau of Standards (NBS) sample 20*f*, which contains 0.380% carbon. (The data for NBS sample 20*f* were obtained over a 2-hour period, during which all data were collected and during which time no instrument recalibration was necessary.) Each sample was analyzed five times. Data are given as the standard deviation from the average, and the relative standard deviation is calculated as the standard deviation from the average divided by the average. The data are of satisfactory precision and accuracy.

An attempt to increase the linearity further was made by placing a stream splitter between the furnace and analyzer to vent a reproducible fraction of the furnace gases. However, rapidly fluctuating pressures in the furnace gas stream caused by irregular usage of oxygen during combustion led to uneven splitting, as evidenced by an unsatisfactory reproducibility (within ±3%). The use of flow and pressure regulators with a stream splitter did not improve the reproducibility of the splitting significantly.

Although the linearity of the instrument was not extended beyond 1.2% carbon (1-gram sample), steels with higher percentages of carbon may be analyzed by using fractional gram samples. Of course, the instrument would not be direct-reading and the values shown on the DVM would have to be corrected. Alternatively, the customary 1-gram sample could be used with a calibration curve. The data in Table II show that in this carbon range detector response is reproducible, but not linear.

Direct readout for samples containing less than 0.01% carbon is not straightforward because blanks arising from the ceramic crucible and the copper accelerator become relatively significant. Data obtained on NBS 131*a* (0.0044% carbon) are given in Table III to illustrate the problem. When the analyzer was calibrated on NBS 20*f* (0.380% C) and the crucibles were used in the as-received condition, an average value of 0.0088% carbon was determined for NBS 131*a*. The value was reduced to 0.0063 by preheating the crucibles at 1000° C. Thus the blank can be reduced from about 0.004 to 0.002% carbon by preheating the crucibles. Direct readout in the low carbon range can be obtained by calibrating the instrument with a standard sample that contains a carbon content in the range of interest and preheating the crucibles as shown by the final data of Table III. Alternatively, the offset voltage in the operational amplifier used as the integrator may be adjusted to correct for the blank so that the instrument is direct reading over a concentration range of 0.001 to 1.2% carbon; this latter method has been preferred. Instrument sensitivity is high enough to detect carbon dioxide at the 1-μg. level. However, special efforts would be required to reduce the blank before samples with less than 0.001% carbon could be analyzed with confidence.

Water has at times interfered even though attempts are made to dry all gases completely. Both water and carbon dioxide are adsorbed on the molecular sieve at ambient temperature, and they are both desorbed in the 200° to 350° C. temperature range. However, interference from water is seldom a problem because of the small quantity present and because any water vapor present is desorbed and swept through the system to the detector more slowly than the carbon dioxide, so that the water peak occurs after the carbon dioxide peak. Water vapor passing through the detector gives a signal opposite in polarity to that of carbon dioxide and causes the integrated voltage signal to decrease. The analyzer is therefore programmed to stop the integration function as soon as the carbon dioxide has passed through the detector so that any water vapor present does not interfere.

This instrument can also be used without modification to analyze for oxygen in steel by the carrier gas fusion method. In this method, the sample is burned in a carbon crucible in a helium atmosphere, and the carbon monoxide formed by the reaction of the oxygen of the sample and carbon of the crucible is converted to carbon dioxide by passing it over iodine pentoxide. The carbon dioxide is then collected on the molecular sieve trap and measured in a helium stream. The necessary change of carrier gas from oxygen to helium requires 1 hour for temperature equilibration of the detector block. Preliminary results with carbon dioxide in a helium stream showed a linearity of response with 4 to 700 parts per million of oxygen (1-gram sample) and a reproducibility within 1%. Direct readout for such analysis would be difficult because the oxygen blank is high. Therefore, use of a calibration curve is necessary. Because an oxygen determination may require as much as a 5-minute fusion, depending on the sample size, it is necessary to check the balance of the detector bridge after the fusion and just prior to measuring the carbon dioxide.

Two carbon analyzers have been constructed. An estimated total of 60,000 carbon determinations has been made with no serious operational or maintenance difficulties on either instrument. Instrument stability is excellent, and the solid-state components in the programming and computing system have led to satisfactory reliability in a plant environment. Oxygen of the quality used for production operations in a steel mill has been used without difficulty because nitrogen and argon, common contaminants of oxygen, are not adsorbed on the molecular sieve trap and therefore do not interfere with the analysis.

ACKNOWLEDGMENT

The authors thank P. P. Eismont, J. J. Giglio, and S. W. Damian for their keen interest and thorough evaluation of the instrument.

LITERATURE CITED

(1) Lewis, L. L., Nardozzi, M. J., ANAL. CHEM. **36**, 1329 (1964).
(2) Walker, J. M., Kuo, C. W., *Ibid.*, **35**, 2017 (1963).

RECEIVED for review March 2, 1966. Accepted May 18, 1966. Pittsburgh Conference on Analytical Chemistry and Applied Spectroscopy, Pittsburgh, Pa., March 1966.

Spectrophotometric Determination of Platinum with 3,4-Diaminobenzoic Acid

LARRY D. JOHNSON[1] and GILBERT H. AYRES
The University of Texas, Austin, Tex.

▷ **Platinum in solution reacts with 3,4-diaminobenzoic acid when the mixture, at pH 9.8 to 12.2, is heated; the blue to blue-green solution has maximum absorption at 715 mμ. The absorbance is not highly sensitive to reagent concentration, pH, or normal room temperature fluctuations. Developed samples are stable for at least 4 hours. The system conforms to Beer's law over the optimum concentration range of 0.35 to 1.20 p.p.m. of platinum for measurement at 1.00-cm. optical path. The only ions which interfere enough to require separation are palladium, osmium, and ruthenium. Separation procedures are easily applied. Spectrophotometric solution studies show that 3,4-diaminobenzoic acid reacts with platinum to form a 2 to 1 complex. Ion exchange studies show that the complex is anionic in alkaline solution and cationic in acid solution. Products thought to be potassium salts of the anion and chloride salts of the cation were synthesized, but could not be obtained with consistent composition.**

THREE excellent review articles (*3, 4*) have summarized the state of platinum metals spectrophotometry up to early 1964. At that time, the tin(II) chloride (*2*) and the *p*-nitrosodimethylaniline (*13*) methods were preferred. Since February 1964, three new spectrophotometric methods for platinum have appeared (*6, 11, 16*), but have not yet been subjected to the test of time and critical evaluation. Because relatively few spectrophotometric procedures for platinum have been published, more work in this field was desirable.

Thirty-five reagents were investigated briefly for ability to form colors with platinum. During this study additional facts not mentioned in the original paper (*15*) were learned about *o*-phenylenediamine; by briefly heating an acidic sample, cooling, and then making it strongly alkaline, an intensely colored purple precipitate was formed. Very similar behavior was shown by solutions of platinum and 3,4-diaminotoluene. Several reagents containing two amino groups adjacent to one another on an aromatic ring, and also containing some feature to increase water solubility, were tested. Platinum formed water-soluble colored complexes with 3,4-diamino-5-hydroxypyrazole sulfate, 2,-3 - diaminopyridine, 4,5 - diaminopyrimidine, and 3,4-diaminobenzoic acid. A colored complex formed with *o*-aminobenzenethiol was insoluble in aqueous solutions, but soluble in many common organic solvents and thus was extractable. From the preceding group of compounds 3,4-diaminobenzoic acid (DBA) was chosen for further study as a spectrophotometric reagent for platinum.

EXPERIMENTAL

Apparatus. Absorbance measurements at varying wavelengths for the temperature effect studies were recorded with a Beckman Model DK-1 spectrophotometer equipped with a cell thermostat. All other absorbance measurements at varying wavelengths were recorded with a Cary Model 14 spectrophotometer. Absorbance measurements at a fixed wavelength were made with a Beckman Model DU quartz spectrophotometer set at high and constant sensitivity. Matched silica cells of 1.00-cm. optical path were used.

A Beckman Zeromatic pH meter equipped with a saturated calomel–glass electrode system was used for all pH measurements.

All analytical weighings were made with a Mettler Type H5 analytical balance or a Mettler Type M5 microbalance.

Reagents. 3,4-Diaminobenzoic acid was obtained from the Aldrich Chemical Co. and used as received. Solutions were prepared by dissolving the desired amount (usually 0.3 gram) in 10 ml. of dimethylformamide and diluting to 50 ml. with distilled water.

N,N-Dimethylformamide (DMF), Eastman No. 5870, was used as received.

Potassium tetrachloroplatinate(II) was obtained from the Fisher Scientific Co. It had been checked for platinum content (*1*) and found to contain the theoretical amount.

Standard platinum(IV) solution was prepared by dissolving 1.0000 gram of grade 1 platinum thermocouple wire, 99.99% pure, in hot aqua regia. The resultant solution was taken almost to dryness, a small amount of hydrochloric acid was added, and the solution was again taken to dryness. This treatment was repeated three times in order to destroy any nitroso complexes. After the final evaporation, 10 ml. of hydrochloric acid was added and the solution was made up to 1 liter with distilled water. More dilute platinum solutions were prepared as needed by volumetric dilution of this stock. This procedure has been shown by Ayres and McCrory (*1*) and Janota (*9*), as well as earlier workers in this laboratory, to yield solutions of the concentration calculated from the weight of platinum taken. To check against mechanical loss or some other error in the dissolution step, two standard platinum solutions were prepared by exactly the same procedure and found to give exactly the same spectrophotometer readings when carried through the standard analysis scheme.

All other reagents were ACS reagent grade.

Recommended Procedure. A sample containing 35 to 120 μg. of platinum in a volume of 25 ml. or less was placed in a 100-ml. borosilicate-glass volumetric flask; 2 ml. of the DBA reagent solution was added and the pH of the solution was adjusted below 3 in order to avoid hydrolysis effects during the heating step. The flask containing the solution was floated for 15 minutes in a large beaker of boiling water, then removed and cooled to room temperature. At this point the sample was light amber in color and sometimes contained a precipitate. The sample was made alkaline by adding an excess of either 0.1*M* or 1*M* sodium hydroxide, depending upon the amount of acid present. The sodium hydroxide was added from a buret until a green color appeared in the solution. An amount of sodium hydroxide equal to one third of the amount already added was then run in. At this point the sample was blue-green and the precipitate was completely dissolved. The sample was made up to 100 ml. with distilled water, and its absorbance was measured within 1 hour at 715 mμ. The reagent blank was negligible at 715 mμ, but was employed as an added precaution.

RESULTS AND DISCUSSION

Calibration, Range, and Sensitivity. Data for calibration and a check for conformity to Beer's law were obtained by measuring the absorbance at different concentrations of platinum after treatment by the recommended procedure (Table I). Each absorbance

[1] Present address, Chemstrand Research Center, Durham, N. C.

value given is the average of three closely agreeing replicates. The system follows Beer's law over the calibrated range. The optimum concentration range for measurement at 1.00-cm. optical path is 0.35 to 1.20 p.p.m. of platinum. The mean specific absorptivity for the calibrated range is 0.585 p.p.m.$^{-1}$ cm.$^{-1}$, corresponding to a molar absorptivity of 1.14×10^5 liter mole^{-1} cm.$^{-1}$

Reproducibility. Twenty-three identical samples, each with a final platinum concentration of 0.80 p.p.m., were treated according to the recommended procedure, and their absorbances were measured. The mean absorbance was 0.468, with a standard deviation of 0.002 absorbance unit. This study was an attempt to measure the inherent precision of the method and was performed under ideal and constant conditions; the precision obtained in actual analyses of samples will probably be somewhat lower.

Effect of pH. When the pH was varied by the use of appropriate buffers, no appreciable absorbance (at 715 mμ) was produced at pH below 4. Between pH 6 and 8 the absorbance increased rapidly, and leveled off at a constant high value between pH 9.8 and 12.2. The recommended procedure produced samples of pH about 11.5.

Development Time. The time required for full color development in the hot water bath varied with sample volume, sample concentration, DBA concentration, and pH. For the conditions used in the recommended procedure, full color development took about 10 minutes. Continued heating up to 30 minutes produced no further change in absorbance.

Effect of Temperature. After color development by the standard procedure, absorbance was measured at three temperatures (25°, 42°, and 75°) in a thermostatically controlled cell compartment. With increasing temperature only a slight decrease in peak absorbance was produced. Normal room temperature fluctuations were without measurable effect.

Effect of Reagent Concentration. Samples containing 100 μg. of platinum (IV) were developed by the recommended procedure, except that the concentration of DBA was varied. Maximum color development required about a 50-fold molar excess of reagent. Better precision on multiplicate samples could be attained by the use of an even larger excess of reagent. The 2 ml. of DBA solution used in the recommended procedure supplies a ratio of 128 to 1 if the sample contains 120 μg. of platinum.

Effect of DMF Concentration. When the recommended 2 ml. of DBA solution was used, up to 10 ml. of DMF had little or no effect on the absorbance. With smaller amounts of DBA, low results were sometimes produced when several milliliters of DMF were present. It was therefore thought best to keep the concentration of this solvent reasonably low, and to exclude it completely during the continuous variations studies.

Effect of Foreign Ions. The effect of foreign ions was studied by adding a solution of the ion to a sample containing 80 μg. of platinum, and developing by the standard procedure. The tolerance to a given ion was defined as the maximum concentration which could be present without causing an error of 0.010 in the absorbance reading of the sample. All tolerance values given are averages of very closely agreeing triplicate determinations. Anions were added as solutions of their sodium, potassium, or ammonium salts. Cations were added as solutions of their chlorides, nitrates, or sulfates. The platinum metals came from solutions left over from previous investigations, and were usually chloride complexes. Except for substances used as masking agents, the highest concentration levels tested were 100 p.p.m. for anions and 50 p.p.m. for cations. Anions which did not interfere at the 100-p.p.m. level were bromide, iodide, nitrate, perchlorate, sulfate, phosphate, molybdate, tungstate, tartrate, and formate. Cations which were tolerated at the 50-p.p.m. level without masking were zinc, lead, and ammonium. Nitrite, dichromate, and iron(III) oxidized the reagent. Tolerances for other ions tested are listed in Table II.

When the tolerance for a foreign ion was below 0.8 p.p.m., a search was made for a suitable masking agent. Several of the heavy metals required masking to prevent precipitate formation, even though no reaction with DBA was evident. Cobalt slowly formed an interfering color even when masked; if the absorbance was measured within 10 minutes after sample development, relatively large amounts of cobalt(II) could be tolerated.

Removal of Interfering Ions. Interference from palladium(II), ruthenium(III), and osmium(III) was sufficient to warrant their removal, which was accomplished at the 10-p.p.m. level. Palladium was easily removed by two extractions of its complex with 1-(2-pyridylazo)-2-naphthol (PAN) into chloroform, and the chloroform layer is suitable for spectrophotometric determination of palladium (*5, 14*). Osmium and ruthenium were volatilized from a dilute hydrochloric acid solution to which ammonium peroxydisulfate was added. This process produced a solution with fewer extraneous ions than other methods tried. The method was not tested for larger amounts of osmium and ruthenium, so its general applicability is unknown.

Table I. Calibration Data

Platinum, p.p.m.	Absorbance	Specific absorptivity, p.p.m.$^{-1}$ cm.$^{-1}$
0.400	0.235	0.588
0.500	0.291	0.582
0.600	0.352	0.587
0.700	0.412	0.589
0.800	0.468	0.585
0.900	0.526	0.583
1.00	0.581	0.581
1.10	0.639	0.589
1.200	0.694	0.587
	Av.	0.585

Table II. Tolerance for Foreign Ions

(Platinum concentration, 0.80 p.p.m.)

Ion	Tolerance, p.p.m. Without masking	With masking
Gold(III)	0.3	2[a]
Vanadium(IV)	2	
Iron(II)	Precip.	10[b]
Nickel(II)	Precip.	50[c]
Cobalt(II)	Precip.	10[c]
Manganese(II)	Precip.	20[c]
Copper(II)	Precip.	50[c]
Cadmium(II)	Precip.	50[c]
Chromium(III)	Precip.	50[d]
Mercury(II)	Precip.	50[a]
Iridium(IV)	4	
Palladium(II)	0.2	
Rhodium(III)	0.8	
Ruthenium(III)	0.1	
Osmium(III)	0.5	
Acetate	10	
EDTA	10	

[a] Masked with iodide, 300 p.p.m.
[b] Masked with EDTA, 10 p.p.m.
[c] Masked with tartrate, 3 g. per liter.
[d] Masked with formate, 1 g. per liter.

Stability of Developed Samples. Absorbance measurements at frequent time intervals showed the samples to be stable for at least 4 hours.

Stability of DBA Reagent Solutions. The 0.6% reagent in 20% DMF-water solution could be used for from 2 days to a week; in practice, fresh solution was prepared every other day. In 0.1% concentration, the reagent was more stable, and solutions in pure DMF were even more stable; but this amount of DMF in the final solution was undesirable. Solutions of DBA in sodium hydroxide were even less stable than the reagent solution recommended. In any case, slight instability of the reagent solution is not a serious difficulty.

STUDY OF REACTIONS AND PRODUCTS

Absorption Spectra. Figure 1 shows the absorption spectrum of a sample containing 80 μg. of platinum(IV) developed by the recommended procedure. Absorbances at both peak wavelengths were proportional to the platinum concentration. Another sample containing 80 μg. of platinum(II)

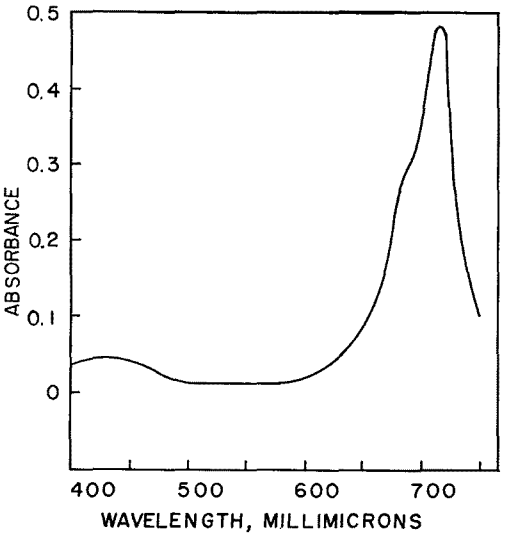

Figure 1. Absorption spectrum of platinum complex with 3,4-diaminobenzoic acid

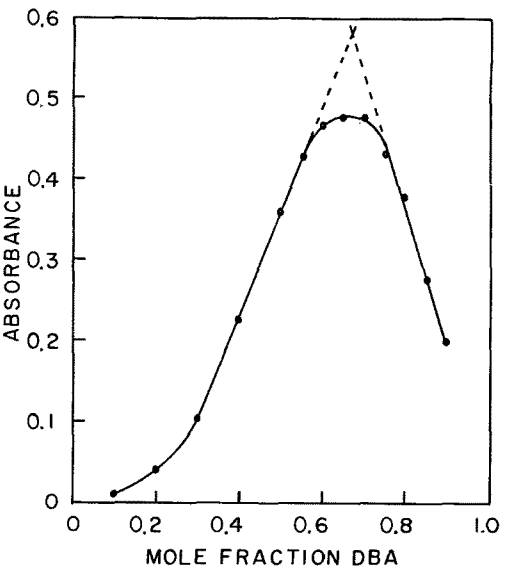

Figure 2. Continuous variations plot for platinum-DBA complex

was treated in the same manner; its spectrum was identical with that in Figure 1 except that there was no absorption in the 400-to 500-mμ region. The DBA blank absorbed very slightly in this region, but samples of DBA which had been oxidized by either air or ammonium peroxydisulfate absorbed strongly. The maximum of the blank and of the two oxidized samples of DBA coincided exactly in wavelength with the maximum in that region of Figure 1. It appears, therefore, that the absorption in the 400-to 500-mμ region is due primarily to oxidized DBA. Since this absorption increased with an increase in platinum(IV) in the starting material but remained at blank level for all concentrations of platinum(II) tested, it also appears that the DBA reduced the platinum(IV) to platinum (II) and was oxidized in the process.

Ullmann and Mauthner (*18*) state that when DBA is oxidized with iron (III) the product is 7-amino-6-hydroxyphenazine - 2 - carboxylic acid. Their claim is neither supported nor disputed in the present work. If this compound is the correct product for the reaction of DBA with iron(III), it is likely that the same oxidation product would be produced by reaction with platinum (IV). Reactions and products of a similar nature have been reported (*7, 8, 17*) for the oxidation of *o*-phenylenediamine with iron(III).

Method of Continuous Variations. The method of Job (*10*) as modified by Vosburgh and Cooper (*20*) and others (*12, 19, 21*) was applied to a study of this system, first to a series of solutions of total concentration of platinum(II) plus DBA = $2.05 \times 10^{-5}M$. The continuous variations plot (Figure 2) has a maximum at 0.67 mole fraction of DBA, indicating a 2 to 1 DBA-platinum ratio. Absorbance measurements at three different wavelengths produced no shift of the position of maximum, and the spectra of all samples above mole fraction 0.5 were identical except for concentration differences. Existence of other complexes is therefore improbable. The curvature in the neighborhood of 0.20 mole fraction might be an argument for the existence of another complex in the system. This possibility cannot be completely ruled out, but it seems very doubtful. Even a mole fraction value of 0.25 would correspond to a complex with three platinum atoms and one ligand molecule, and smaller mole fraction values would correspond to even less probable arrangements. The curvature near mole fraction 0.20 is more probably due to a fairly high dissociation of the complex or to hydrolysis of the excess platinum in the alkaline solution. A series of solutions of total concentration of platinum(II) plus DBA of $5.13 \times 10^{-5}M$ produced a continuous variations plot identical with the first except for higher absorbance values.

The method of continuous variations was applied to two series of platinum (IV) samples corresponding in total concentration to the values previously used with platinum(II). The plots obtained had inflections between mole fraction 0.30 and 0.40, and maxima at 0.73. By use of more concentrated solutions of platinum(IV) and DBA and absorbance measurements at both 715 and 445 mμ, it was found that a sharp change in slope occurred at 0.38 mole fraction, which corresponds to oxidation of DBA by reduction of platinum(IV) to platinum(II).

When successive complexes are formed with a given metal and ligand, each peak will still occur at, or near, the mole fraction value corresponding to its particular stoichiometry (*12, 19, 20*). The present case is different, in that the ligand is destroyed (for our purposes) by the redox reaction. Thus, the major break in the curve must occur at a mole fraction corresponding to a reaction ratio including the total amount of ligand in both the redox and the complexation steps.

It therefore appears that 3 moles of platinum(IV) are reduced by 2 moles of DBA (mole fraction 0.4). The 3 moles of platinum(II) formed require 6 additional moles of DBA for complexation, giving a total reaction ratio of DBA to platinum of 8 to 3 (mole fraction 0.73). The redox behavior agrees with that observed for the previously cited reactions of iron(III) with DBA and with *o*-phenylenediamine (*7, 8, 17, 18*).

Mole Ratio Method. This method was inconclusive as to the reaction ratio, on account of the very great rounding of the curve of absorbance against mole ratio of DBA to platinum.

Ion Exchange Studies. An alkaline solution of the colored complex was not retained by a cation resin, but was retained very strongly on an anion resin. An acidic solution was retained

quantitatively on a cation resin, and partially retained on an anion resin; the acidic form was easily removed from the cation exchanger by use of dilute sodium hydroxide; the material on the anion column was slowly eluted with 1 to 1 hydrochloric acid.

Isolation of Product. By use of much more concentrated solutions of reactants, at pH about 3, heating the mixture for 30 minutes just below the boiling point produced a yellow-brown precipitate. The mixture was made alkaline (pH 10.5) with potassium hydroxide; the precipitate dissolved and the solution turned an intense blue. Cooling in an ice bath and addition of isopropyl alcohol to decrease the solubility resulted in formation of a precipitate (probably the potassium salt of the anionic complex). The precipitate was filtered, washed, and dried. The product was usually very dark blue (almost black), although occasionally a bright purple solid was obtained. Elemental analysis for carbon, hydrogen, and nitrogen varied considerably from batch to batch. Portions of the salts were titrated with hydrochloric acid, with potentiometric and conductometric detection of the end point; although sharp breaks were obtained in the titration curves, results were variable from batch to batch. The yellow-brown precipitate originally formed in acidic solution likewise gave variable analyses for carbon, hydrogen, and nitrogen for different preparations.

LITERATURE CITED

(1) Ayres, G. H., McCrory, R. W., ANAL. CHEM. **36**, 133 (1964).
(2) Ayres, G. H., Meyer, A. S., Jr., *Ibid.*, **23**, 299 (1951); *J. Am. Chem. Soc.* **77**, 2671 (1955).
(3) Beamish, F. E., *Talanta* **12**, 743 (1965).
(4) Beamish, F. E., McBryde, W. A. E., *Anal. Chim. Acta* **9**, 349 (1953); **18**, 551 (1958).
(5) Busev, A. I., Kiselva, L. V., *Vestnik Moskov. Univ., Ser. Mat., Mekh., Astron., Fiz., Khim.* **13**, No. 4, 179 (1958); *Chem. Abstr.*, **53**, 11105f (1959).
(6) Chechneva, A. N., Podchainova, V. N., *Izv. Bysshikh Uchebn. Zavedenii, Khim. i Khim. Tekhnol.* **7** (5), 731 (1964); *Chem. Abstr.* **62**, 9760c (1965).
(7) Fischer, O., Hepp, E., *Ber.* **22**, 356 (1889).
(8) Greiss, P., *J. Prakt. Chem.* **3**, 143 (1871).
(9) Janota, H. F., Ph.D. dissertation, University of Texas, 1963.
(10) Job, P., *Ann. Chim.* **9** (10), 113 (1928); **6** (11), 97 (1936).
(11) Karpova, L. V., Alyanchikova, V. N., Simirnov, P. P., Gut'ho, A. D., Ryserva, G. V., Morozova, N. F., Labkovskaya, D. B., *Vopr. Analiza Blogorodn. Metal., Akad. Nauk SSSR., Sibirsh. Otd., Tr.5-go (Pyatago) Vses. Soveshch.* **1963**, 30; *Chem. Abstr.* **61**, 10038b (1964).
(12) Katzin, L. I., Gebert, E., *J. Am. Chem. Soc.* **72**, 5455 (1950).
(13) Kirkland, J. J., Yoe, J. H., ANAL. CHEM. **26**, 1340 (1954).
(14) Sawada, T., Kato, S., *Bunseki Kagaku* **11**, 544 (1962); *Chem. Abstr.* **57**, 5297h (1962).
(15) Sen Gupta, J. G., *Anal. Chim. Acta* **23**, 462 (1960).
(16) Senise, P., Pitombo, L. R. M., *Talanta* **11**, 1185 (1964).
(17) Ullmann, F., Mauthner, F., *Ber.* **35**, 4302 (1902).
(18) *Ibid.*, **36**, 4032 (1903).
(19) Underwood, A. L., Toribara, T. Y., Neuman, W. F., *J. Am. Chem. Soc.* **72**, 5597 (1950).
(20) Vosburgh, W. C., Cooper, G. R., *Ibid.*, **63**, 437 (1941).
(21) Woldbye, F., *Acta Chem. Scand.* **9**, 299 (1955).

RECEIVED for review May 16, 1966. Accepted June 3, 1966. Condensed from a dissertation submitted by Larry D. Johnson to the graduate school, The University of Texas, in partial fulfillment of the requirements for the doctor of philosophy degree, June 1966. The authors gratefully acknowledge the financial support of National Science Foundation grant G14479, and fellowships provided by Procter and Gamble, Monsanto Co., and the Dow Chemical Co.

Analysis of a High-Molecular-Weight Phenolic Inhibitor

H. S. KNIGHT and HERBERT SIEGEL

Shell Development Co., Emeryville, Calif.

▶ **Gas chromatography and phase solubility analysis were combined to achieve a more definitive analysis of a high-molecular-weight phenolic inhibitor than would have been possible by either technique alone. Phase solubility analysis showed that the material was about 99% pure, and about 1% of a related phenol was found by gas chromatography. The agreement of the two techniques showed that this was the only significant impurity present.**

THE OXIDATION-INHIBITING PROPERTIES of certain hindered phenols have given these materials widespread commercial interest. In the manufacture of films and fibers which may be subjected to high temperature during processing, it is desirable that the inhibitor be of high molecular weight and correspondingly low vapor pressure to avoid evaporation losses. High molecular weight also contributes to low extractability of the inhibitor from the polymer on contact, for example, by foods packaged in films.

A phenolic inhibitor having a molecular weight of 775 and a vapor pressure of 0.014 mm. at 180° C., suitable for use in food packaging materials, is 1,3,5-trimethyl - 2,4,6 - tri(3,5 - di - *tert*-butyl-4-hydroxybenzyl)benzene, Shell trade-named Ionox 330. The application of this inhibitor in the food and drug industry leads to the need for detailed and precise knowledge concerning its purity, which was believed to be 98% or more.

Two complementary techniques were employed to obtain a more definitive analysis than would have been possible by either technique alone or by other available procedures. Phase solubility analysis, a known but little used technique, was applied to determine nonvolatile impurities but was not suitable for light materials. Gas chromatography was employed for the volatile components but could not be used to determine polymers or other nonvolatile impurities. Final agreement of the two techniques showed that only one impurity was present in significant concentration. This was identified by gas chromatography on the basis of its retention volume compared with that of a known compound.

In the course of the gas chromatographic study, it was found possible to determine the Ionox 330 itself. This is believed to be the highest-molecular-weight phenol to be successfully eluted from a gas chromatographic column.

Analytical techniques that have been successfully used for lower-molecular-weight phenols include various forms of spectrometry, determination of weak acidity, gas chromatography, and determination of physical properties such as melting point. Spectrometry and titration were not specific for Ionox 330 which might be expected to contain phenolic impurities, although nuclear magnetic resonance could detect these impurities if they were present at a sufficiently high level. No gas chromatographic method was available in the 775 molecular weight range. The melting point of high-molecular-weight materials is strongly influenced by traces of low-molecular-weight impurities and therefore does not provide a practical measure of purity.

Phase solubility analysis consists of

measuring at constant temperature the solubility of a solid sample in a relatively poor solvent as a function of sample size. From these data, interpretations with respect to purity, concentration of impurities, and even the number of impurities can frequently be made. A detailed discussion of various systems has been adequately presented by Mader (*6*).

Much work on analysis of phenols by gas chromatography has been published, and a few selected papers will be mentioned here. The techniques employed can be divided into two categories, depending on whether the phenol is determined directly or after conversion to a less polar derivative to avoid adsorption and tailing or to reduce decomposition.

Mixtures of phenols of structural complexity up to di-*tert*-butyl were analyzed directly by Duvall and Tully (*2*) who employed a packed column containing a mixture of Carbowax 4000 and DC-550 silicone. Close-boiling isomeric phenols such as 2,4- and 2,5-xylenol were resolved fairly well by Brooks (*1*), using a packed column containing 2,4-xylenyl phosphate on acid-treated Celite. Tominaga (*8*) resolved di- and trinuclear phenols, the latter on a 40-cm. column packed with 10% Apiezon L on Celite. Porcaro (*7*) analyzed bisphenols on columns as short as 8 to 10 inches.

Grant and Vaughan (*5*) converted 66 low-molecular-weight phenols to trimethylsilyl ethers and analyzed them on a capillary column coated with a silicone. They reported low conversion for hindered phenols. Freedman and Charlier (*3*) described conditions for obtaining complete conversion, and recommended a capillary column coated with 2,4-xylenyl phosphate. Gill (*4*) was unable to repeat Tominaga's work with di- and trinuclear phenols because of tailing. He used columns as short as 3 inches to analyze these compounds after acetylation.

In techniques used in this laboratory hindered phenols have not tailed seriously and short low-loaded packed columns have given satisfactory separations of many high-boiling materials. Therefore, direct gas chromatography was explored for Ionox 330.

At first, a marker technique was employed to determine the impurities and the Ionox 330 was obtained by subtracting the impurities from 100%. Later a procedure was developed in which the Ionox 330 itself emerged from the column and was measured.

EXPERIMENTAL

Phase Solubility Analysis. Apparatus and Reagents. The apparatus included 8-dram screw-capped vials with Poly-Seal caps, and a shaker for rocking the vials horizontally. The work was performed in a constant temperature room at 22.2° ± 0.6° C. Reagents were Phillips 99%m isooctane which was flashed before use, and a stock of Ionox 330 which had been recrystallized once from isooctane.

Procedure. Six vials were numbered 1 through 6, cleaned, dried, capped, and weighed. Recrystallized Ionox 330 was weighed into vials 1 and 2. A sample size of 1 gram was used in each case. Commercial grade Ionox 330 was weighed into vials 3, 4, 5, and 6. Sample sizes of 0.2, 1.0, 2.2, and 3.4 grams were used. Ten grams of isooctane were accurately weighed into vials 1, 3, 4, 5, and 6. These vials were then capped tightly. Approximately 10 grams of isooctane were added to vial 2, which was heated to 75° to 85° C. in an oil bath for 75 minutes with frequent shaking. This step was carried out to ensure that one of the solubility measurements for the recrystallized Ionox 330 was made using a saturated solution. Vial 2 was then capped and weighed to obtain the weight of the added isooctane. The six vials were mounted horizontally on the shaker in the constant temperature room and rocked continuously for 66.3 hours.

At the end of the 66.3 hours, the vials were reweighed and showed slight losses in weight amounting to only 0.5% in the worst case. Possibly, the polyethylene cones in the Poly-Seal caps softened upon the prolonged exposure to the isooctane leading to a slight leaking around the seal. These losses in weight were assumed to be entirely isooctane; for each vial, the weight of the initial isooctane used was corrected for the measured loss.

Six additional 8-dram vials were numbered 1 through 6. These vials were cleaned, dried, capped, and weighed. The contents of each vial containing the mixture of sample and isooctane were filtered into a corresponding numbered empty vial. Each vial plus filtrate was capped and weighed. The vials were uncapped and placed in a water bath at 50° C. The filtrate in each vial was then evaporated to constant weight under a stream of nitrogen which was dried with Drierite and filtered through glass wool.

From the weights of the initial sample, initial isooctane (corrected for losses by leaking of capped vials) and from the weights of the residues obtained by evaporation of the filtrates, the following calculations were made for vials 3 through 6.

$$W = \frac{W_s}{W_o} \cdot 100$$

where

W = composition of system, grams of sample per 100 grams of isooctane
W_s = weight of sample, grams
W_o = weight of isooctane, grams

$$w = \frac{W_r}{W_f} \cdot 100$$

where

w = composition of solution (liquid phase), grams of solute per 100 grams of isooctane
W_r = weight of residue obtained by evaporating filtrate, grams
W_f = weight of isooctane in filtrate, grams

For vials 1 and 2, only w was calculated and the average of these values was taken as the solubility of pure Ionox 330 in isooctane at 22.2° ± 0.6° C. (72° ± 1° F.).

Vial	Solubility grams Ionox 330/100 grams isooctane
1	0.4142
2	0.4147
	Av. 0.415

Gas Chromatography. Apparatus. An apparatus with hydrogen flame ionization detector was employed which made use of a Beckman Thermotrac for temperature programming. The apparatus was designed for $^3/_{16}$-inch columns because this size tubing provides a good match between detector and column optimum flow requirements. The column was suspended from an insulating board in the programmer. The injector and detector were mounted on top of the board and were independently heated to 300° to 325° C.

Early marker analyses were carried out with a 1-foot by $^3/_{16}$-inch column packed with 20% DC-710 silicone (Dow Corning) on Chromosorb W (Johns-Manville). Later direct determinations of Ionox 330 were carried out with 16-gauge (heavy-walled) stainless tubing having an internal diameter less than that of $^1/_8$-inch copper tubing, about $^1/_{16}$-inch. This column was packed with 2% SE-30 (General Electric) on Chromosorb W, 80 to 100 mesh. In spite of the lower polarity of the SE-30 silicone, tailing was not objectionable. The SE-30 was a faster solvent and was more stable thermally.

Procedure. The solid samples were dissolved in acetone or carbon disulfide, and about 1 μl. of 5% solution was injected. The SE-30 column was then temperature programmed from 200° to 300° C. in 10 minutes. Somewhat milder conditions were used for the DC-710 column. The carrier flow was maintained at about 40 ml. per min. even in the small bore column, in a sacrifice of efficiency for speed of elution.

THEORY OF PHASE SOLUBILITY ANALYSIS

Mixtures of the solid sample and solvent at concentration W (grams of sample/100 grams of solvent) are brought to equilibrium by thorough mixing at constant temperature. The liquid phase of each equilibrated mixture is analyzed for the amount of solute present at concentration w (grams of solute/100 grams of solvent). In many cases the amount of solute can be conveniently obtained by evaporating the liquid phase and weighing the non-

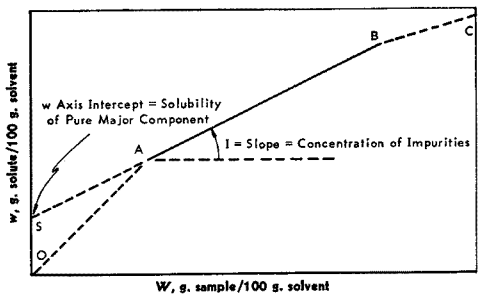

Figure 1. Plot of data obtained by phase solubility analysis

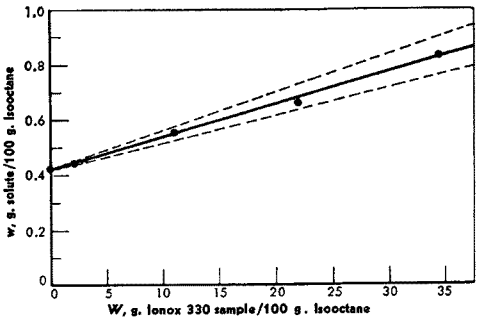

Figure 2. Phase solubility analysis of an Ionox 330 sample

volatile residue. The major component of the sample dissolves in the solvent according to its solubility S (grams of component/100 grams of solvent) at the temperature of the system. For the system under consideration, it is assumed that the impurities are completely soluble in the liquid phase of each sample-solvent mixture. Accordingly, the concentration of impurities in each liquid phase is equal to their concentration I (grams of impurities/100 grams of sample) multiplied by the sample-solvent concentration W. The concentration w of solute in the liquid phase of each sample-solvent mixture is then as follows.

$$w = I \cdot W + S$$

The plotted (W, w) data obtained for this system follow a straight line as shown by AB in Figure 1. The slope of this line is equal to the concentration of impurities I in the sample, and the intercept of the line on the w axis is equal to the solubility S of the pure major component with the particular solvent and temperature used. If one of the impurities exceeds its solubility, then a discontinuity occurs as at B. Beyond this point, the data follow a new line BC whose slope represents the concentration of the remaining impurities. It is, therefore, possible in some cases to detect and determine several impurities individually. When the concentrations of the major component in the solvent are below its solubility, the unsaturated region OA with a slope of unity is reached. Nonvolatile impurities that are completely insoluble can in principle be detected by examining the unsaturated region. These insoluble residues form a solid phase which is reflected in line OA having a slope less than unity.

RESULTS AND DISCUSSION

Phase Solubility Analysis. The phase solubility data (W, w) for an Ionox 330 sample are plotted in Figure 2. The solubility of recrystallized Ionox 330 is plotted as a point on the w axis. The (W, w) data and the solubility point on the w axis fall on an excellent straight line as shown in Figure 2. The line has the following equation:

$$w = \frac{1.2}{100} \times W + 0.415$$

The slope corresponds to a nonvolatile impurity concentration of 1.2% w so that the concentration of Ionox 330 in the sample is accordingly 98.8% w. The gas chromatographic method found 1.2% impurities.

The dashed lines drawn in Figure 2 with slopes corresponding to 1.4 and 1.0% w impurities, respectively, indicate the current estimate of the precision of the method to be $\pm 0.2\%$ w, which is three times the standard deviation. The excellent linearity of the phase solubility data depicted in Figure 2 can be appreciated by the calculations summarized in Table I. In these calculations, a slope was computed for each hypothetical straight line drawn between a (W, w) point and the solubility of Ionox 330 plotted as the intercept on the w axis.

The procedure using recrystallized Ionox 330 gave the following solubility values: 0.4142 and 0.4147 grams Ionox 330/100 grams isooctane at 22.2° ± 0.6° C.

Gas Chromatography. Ionox 330 is apparently the highest-molecular-weight phenol to be determined by gas chromatography to date. It seems desirable to present the evidence that the peak observed is actually the starting phenol.

With a flame detector, oxygen in the phenol molecule does not respond. About 7.5% of the Ionox 330 is oxygen. The area-to-weight calibration factor actually measured relative to xylene was 1.05. Higher factors were occasionally observed, indicating decomposition, and were reduced by rinsing the injector with sodium bicarbonate solution or sometimes just by injecting several samples. The factor for Ionox 330 was reasonable compared to other similar phenols, showing that a very large percentage of the injected sample is included in the peak.

By analyzing a series of phenols and waxes of known structure it was shown that the material that emerges when Ionox 330 is injected is well over C_{30}. The fairly symmetrical peak was trapped in a few inches of hypodermic tubing, dissolved, and reinjected. It emerged at the same time as before. Several peaks were then trapped together and examined by nuclear magnetic resonance, which gave a spectrum consistent with the starting material. There was not enough sample for an unequivocal identification.

The sample of the inhibitor which had been subjected to phase solubility analysis was analyzed by gas chromatography. It was found that 1.2% of the sample appeared in a single peak at about 250° C. and the remainder, identified as Ionox 330, emerged after about 5 minutes at 300° C. The early peak coincides with a phenolic compound similar to the Ionox 330, namely 1,3,5 - trimethyl - 2,4 - di(3,5 - di - *tert*-butyl-4-hydroxybenzyl)benzene. The calibration factor for this material relative to xylene was also 1.05. Small amounts of volatile impurities were found by conventional gas chromatographic techniques. The agreement

Table I. Linearity of Phase Solubility Data

(W, w) point	Slope = concentration of nonvolatile impurities, % w
1	1.19
2	1.22
3	1.12
4	1.20
	Av. 1.18 ± 0.04[a]

[a] Standard deviation based on three degrees of freedom.

between gas chromatography and phase solubility analysis was considered excellent.

ACKNOWLEDGMENT

Certain phenols suspected of being impurities were prepared by T. H. Colby. The gas chromatographic apparatus was designed by F. M. Nelsen.

LITERATURE CITED

(1) Brooks, V. T., *Chem. Ind. (London)* 1959, p. 1317.
(2) Duvall, A. H., Tully, W. F., *J. Chromatog.* 11, 38 (1963).
(3) Freedman, R. W., & Charlier, G. O., ANAL. CHEM. 36, 1880 (1964).
(4) Gill, H. H., *Ibid.*, p. 1201.
(5) Grant, D. W., Vaughan, G. A., in "Gas Chromatography," M. van Swaay, ed., p. 305. Butterworths, London, 1962.
(6) Mader, W. J., "Organic Analysis," J. Mitchell, Jr., ed., Vol. II, p. 253, Interscience, New York, 1954.
(7) Porcaro, P. J., ANAL. CHEM. 36, 1664 (1964).
(8) Tominaga, Sachiyuki, *Bunseki Kagaku* 12, 137 (1963); Lowry Abstract Card 37, 6-15-63.

RECEIVED for review March 7, 1966. Accepted June 6, 1966.

Identification of Normal Paraffins, Olefins, Ketones, and Nitriles from Colorado Shale Oil

TAKEO IIDA, EIICHI YOSHII,[1] and EITARO KITATSUJI

Faculty of Pharmaceutical Sciences, Toyama University, Toyama, Japan

▷ Straight-chain components of a Colorado shale oil distillate boiling from 280° to 305° C. were obtained through urea adduct formation, and analyzed principally by chromatographic separation methods. They were found to be a mixture of paraffins (C_{13} to C_{18}), olefins (C_{13} to C_{18}) with predominantly 1-alkenes, nitriles (C_{12} to C_{15}), and ketones (C_{13} to C_{16}) in which 2-alkanones are predominant. A useful and convenient chromatographic method for the separation of hydrocarbon components uses a silica gel–silver nitrate mixture. A mixture of ketones and nitriles is most effectively separated by sodium borohydride reduction followed by adsorption chromatography.

SHALE oil is a complex mixture of saturated, olefinic, and aromatic hydrocarbons, as well as nitrogen-, oxygen-, and sulfur-containing compounds. The nonhydrocarbon constituents that make up approximately half of the shale oil are an outstanding characteristic of shale oil as compared to petroleum. It is important to know the types of these compounds and desirable to determine the structures of individual components, not only in connection with processing techniques for fuel oil production but also the use of by-products with industrial raw materials. U. S. Bureau of Mines workers (*14*) and others (*5, 6, 9–12*) have made valuable contributions to the identification of the shale oil naphtha components consisting of tar bases, tar acids, neutral nitrogen and oxygen compounds, and hydrocarbons. However, high boiling fractions which constitute a major portion of shale oil distillate have not been so extensively investigated. The type analyses of individual concentrates separated according to physical properties have been principally carried out (*2–4*).

In 1956, one of the present authors (T. I.) began to study the components

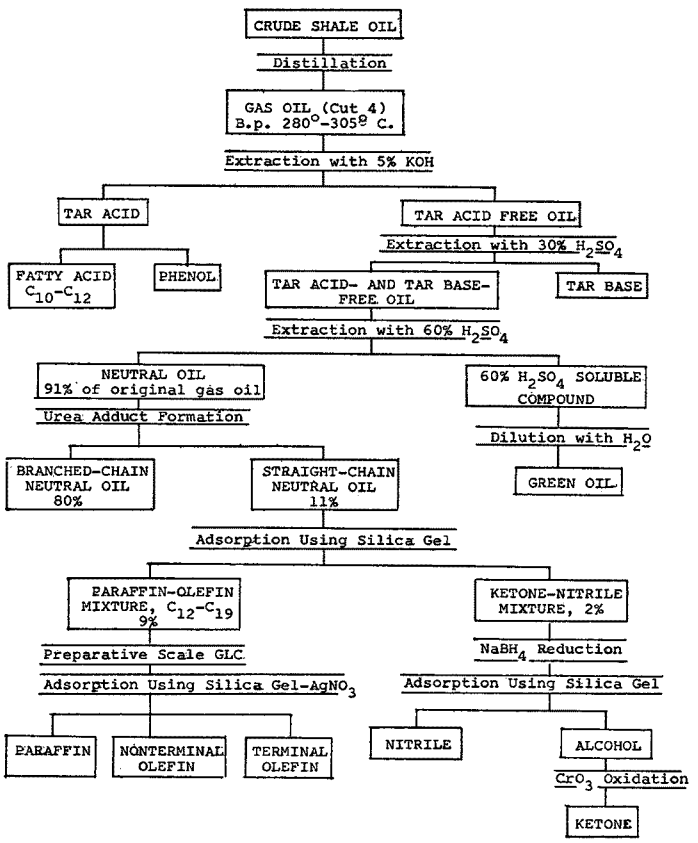

Figure 1. Separation of groups of compounds from shale oil

[1] Present address, Department of Chemistry, Columbia University, New York, N. Y.

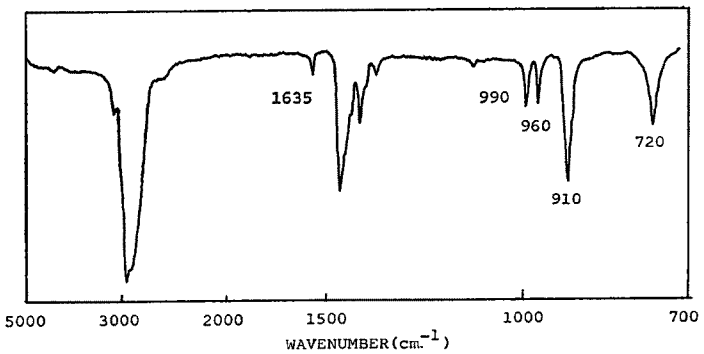

Figure 2. Infrared spectrum of straight-chain paraffin and olefin mixture from cut 4

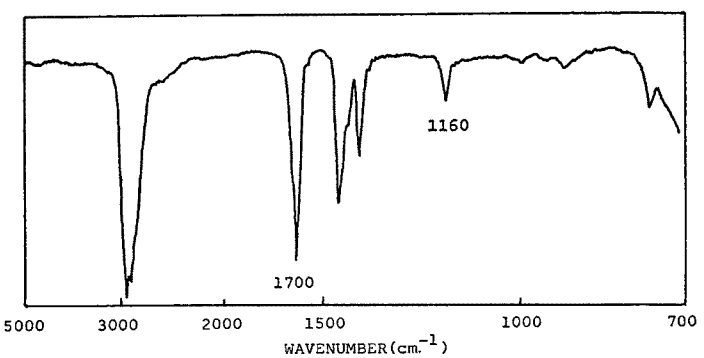

Figure 3. Infrared spectrum of straight-chain ketone and nitrile mixture from cut 4

of Colorado shale oil under a cooperative agreement between the U. S. Bureau of Mines and Toyama University. He discovered in a heavy oil fraction the presence of a class of middle layer base which consists largely of long-chain 2,4,6-trialkylpyridines (*8*). The present work is concerned with the constituents of neutral straight-chain compounds obtained from the distillate boiling from 280° to 305° C. Specific emphasis was placed on the separation and identification of an olefin mixture and a ketone-nitrile mixture. The result could be applicable to other fractions of shale oil distillate as well as related oils.

EXPERIMENTAL

Preparation of Starting Material. Crude shale oil obtained from Colorado oil shale by N-T-U retort at the Rifle plant (*7*, *13*) was separated into seven fractions by fractional distillation under reduced pressure. Boiling ranges corrected to 760 mm. of Hg as well as yields of each fraction are given in Table I.

The work discussed in the present paper was done on the cut 4 gas oil boiling in the range from 280° to 305° C. This oil was successively washed with 5% aqueous potassium hydroxide, 30% sulfuric acid, and 60% sulfuric acid to remove tar acids, tar bases, and "green oil" probably containing pyrroles (positive Ehrich test) (*9*). The neutral oil thus obtained was resolved into straight-chain and branched-chain compounds through a urea complex formation technique. Further separations of groups of compounds are schematically outlined in Figure 1.

Table I. Boiling Points and Yields of Shale Oil Fractions

Cut no.	B.p., °C.	Yield based on crude oil, %
1	... 215	5.6
2	215–50	5.3
3	250–80	5.5
4	280–305	5.6
5	305–25	5.6
6	325–50	5.7
7	350–70	5.7
Residue		61.0

Reagents. Silica gel impregnated with silver nitrate for elution column chromatography was prepared by thoroughly mixing 40 grams of silica gel (Merck, 0.2 to 0.5 mm.) and 8 grams of 50% aqueous silver nitrate, followed by drying in the dark at 120° C. for 4 hours (*15*). Thin-layer plates of silica gel–silver nitrate were prepared by spraying the usual 250-micron layer of kieselguhr G (Merck) with 20% aqueous silver nitrate, followed by reactivation at 110° C. for 10 to 15 minutes. The developing solvent system used for the separation of hydrocarbons was a *n*-hexane–benzene mixture (20 to 1). Spots were detected by spraying 60% sulfuric acid and heating at 100° to 150° C., when dark spots appeared, or by spraying a 0.2% ethanolic solution of fluorescein sodium, when yellow spots were observed on an orange-red background under visible light or yellow fluorescent spots under ultraviolet light (*1*).

Apparatus. For preparative scale gas-liquid chromatography (GLC) a Beckman Megachrom instrument with eight 6-foot columns in parallel was used. The column packing was 7% methyl silicone polymer (SE-30) coated on 40- to 60-mesh Microsorb F. The temperature range was from 193° to 203° C. For the analytical GLC, a Shimazu Model GC-1B instrument was used in conjunction with a hydrogen

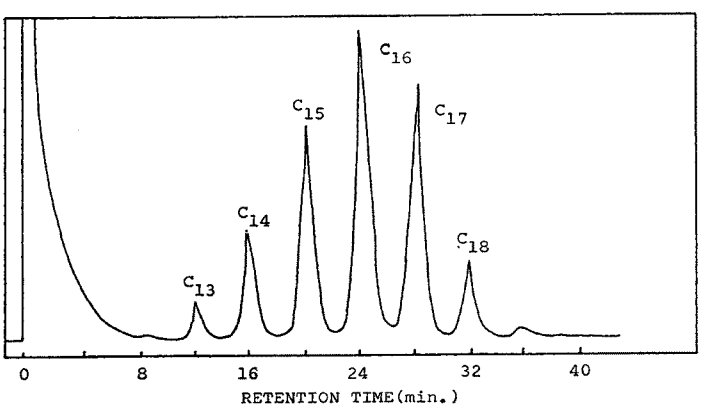

Figure 4. Gas chromatogram of straight-chain hydrocarbon from cut 4

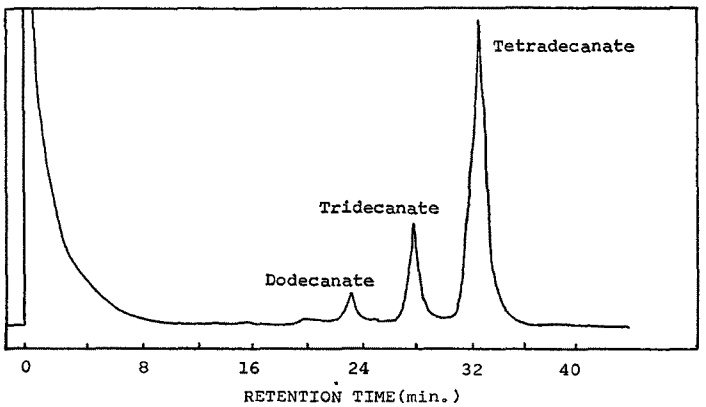

Figure 5. Gas chromatogram of carboxylic acid methyl esters obtained from straight-chain C_{16} nonterminal olefins

flame detector. Dual columns, 4 mm. in diameter and 150 cm. in length packed with 2% SE-30 on silanized Chromosorb W, were generally used with a temperature program of 2° C. per minute. Infrared spectra were taken by Hitachi-Perkin Elmer Model 125 and Nippon Bunko IR-S spectrophotometers. All data were obtained on thin film.

Procedure. The sample was first separated by elution column chromatography using silica gel into hydrocarbon and a ketone-nitrile mixture. The former concentrate was obtained by elution with *n*-hexane and the latter with a *n*-hexane–benzene mixture (4 to 1). Infrared spectra of both fractions are shown in Figures 2 and 3.

HYDROCARBON. TLC (silica gel–silver nitrate) showed three spots, assigned by infrared spectra to be, in order of R_f, paraffin, nonterminal olefin, and terminal olefin. Analytical GLC is shown in Figure 4. Each peak, which consists of hydrocarbon of the same carbon number, was fractionated by preparative scale GLC and subjected to silica gel–silver nitrate chromatography. The amount of paraffin, terminal olefin, and nonterminal olefin was obtained by direct weighing of the concentrates. The double bond distribution in nonterminal olefin was estimated by ozonolysis followed by GLC analysis of the derived carboxylic esters. A typical GLC result on C_{16} nonterminal olefins is given in Figure 5.

NITRILE AND KETONE. The hydrocarbon-free nitrile-ketone mixture was reduced with a methanolic solution of sodium borohydride, and the resulting nitrile–secondary alcohol mixture was subjected to elution chromatography over silica gel. Elution with a *n*-hexane–benzene mixture (4 to 1) gave nitriles which were characterized by infrared spectrum (Figure 6) and also by sulfuric acid hydrolysis to amides. Chain length was determined by analytical GLC (Figure 7).

Further elution of the column with benzene afforded secondary alcohols, from which original ketones were recovered by oxidation with chromic acid in acetic acid. Chain length distribution of the ketone mixture was determined by converting into the corresponding paraffins by the Huang Minlon reduction method, followed by GLC analysis. For the estimation of carbonyl group distribution in the chain, the sample was fractionated by preparative scale GLC and then Schmidt reaction was applied to each fraction.

$$\mathrm{R{-}CO{-}R' \xrightarrow[H_2SO_4]{HN_3} R{-}NH{-}CO{-}R' + R{-}CO{-}NH{-}R'}$$

$$\xrightarrow[HCl]{H_2O} \mathrm{R{-}NH_2,\ R'{-}NH_2} + \mathrm{R{-}COOH,\ R'{-}COOH}$$

An example carried out on C_{15} ketones fraction is given. Pentadecanones were treated with sodium azide in the presence of sulfuric acid, and the resulting amides were hydrolyzed by concentrated hydrochloric

Table II. Determination of Major Normal Hydrocarbon Fractions Obtained from Cut 4 Oil

Fraction	Alkane, %	1-Alkene, %	2-Alkene, %	Other alkenes, %
C_{16}	65	30	3.5	... 1.5
C_{17}	67	25	3.8	... 1.0

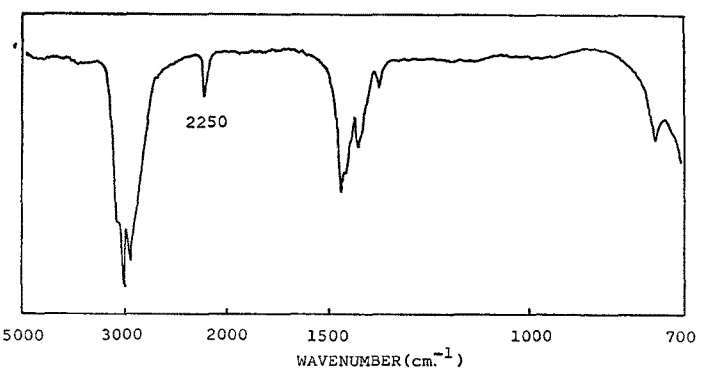

Figure 6. Infrared spectrum of straight-chain nitriles from cut 4

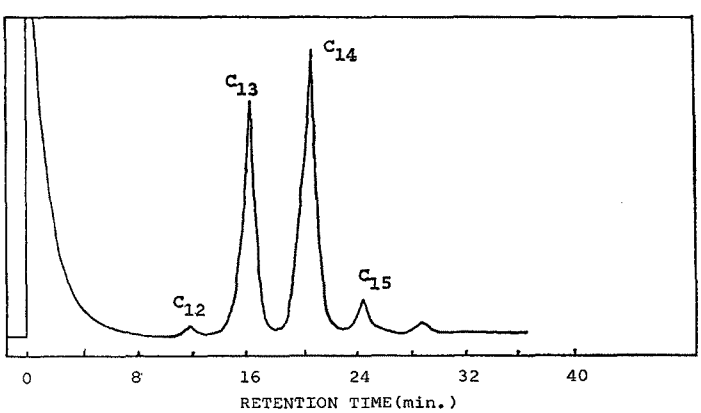

Figure 7. Gas chromatogram of straight-chain nitriles separated from cut 4

acid in a sealed tube at 200° C. for 6 hours. After the usual workup, carboxylic acids were analyzed by GLC as methyl ester and primary amine as trifluoroacetamide. Tetradecanoic acid was found to be a major constituent in the acidic product. In the basic fraction C_{13} amine was predominantly found.

RESULTS AND DISCUSSION

Hydrocarbons. In the investigation of the hydrocarbon components of shale oil distillate, elution adsorption chromatography using silica gel has been successfully applied for the separation of paraffin from olefin (*3*). Further separation of isomeric olefins by this method, however, is almost impossible. The present work has shown that silica gel impregnated with silver nitrate is a useful adsorbent for the type analysis of shale oil hydrocarbons. Paraffin, terminal olefin, and nonterminal olefins were completely separated from each other on TLC as well as by elution chromatography. Among olefins, the terminal one was most strongly adsorbed; as the double bond goes to the center of the chain, it was less strongly adsorbed. Olefin concentrates were easily characterized by infrared spectra: terminal olefins at 910 and 990 cm.$^{-1}$ (deformation bands) and 1635 cm.$^{-1}$ (stretching band); nonterminal olefins at 960 cm.$^{-1}$ (deformation band). Analytical results on C_{15} and C_{17} hydrocarbons are given in Table II. A noticeable fact about the straight-chain olefinic components is that double bond distribution is strongly favored toward the end of the chain. The same situation would be expected in fractions of both higher and lower boiling point.

Nitriles. Separation of the ketone-nitrile mixture into each functional component by elution adsorption chromatography was not practical because of their close polarities against various kinds of adsorbents. However, selective reduction of ketonic compounds with sodium borohydride to the corresponding secondary alcohols made it possible to isolate nitriles by silica gel chromatography. Whether or not the shale oil distillate contains aliphatic nitrile has been questioned (*14*). As a matter of fact, it is impossible to find in the infrared spectrum of the distillate the characteristic stretching vibration band of nitrile. As shown in Figure 8, only strong ketone (1700 cm.$^{-1}$) and double bond absorption bands (1635, 990, 960, and 910 cm.$^{-1}$) are observed. The present investigation confirmed the presence of nitriles of C_{12} through C_{15} in the distillate boiling from 280° to 305° C., although in small amount (0.2%).

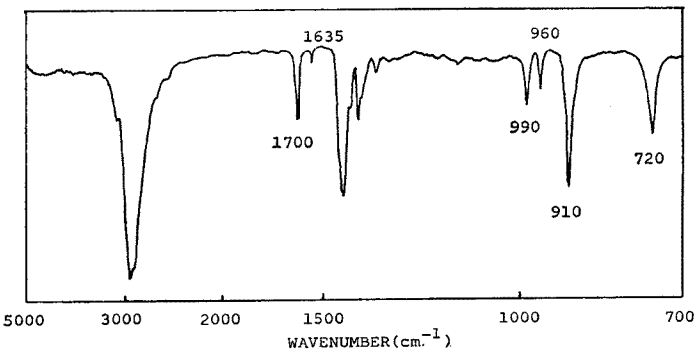

Figure 8. Infrared spectrum of straight-chain neutral oil from cut 4

Ketones. Alkanones of C_{13} through C_{16} were identified. The Schmidt reaction method which was used for the estimation of carbonyl position distribution is not necessarily the best method. There is no definit evidence about the side of the carbonyl group to which the imino group is preferably introduced in the case of the long-chain ketone. However, degradation experiments on fractions of the same carbon number showed that one carbon less carboxylic acid and two carbon less amine were predominantly formed. This suggests that 2-alkanone is the major component in the shale oil distillate of the present investigation.

ACKNOWLEDGMENT

The authors are grateful to E. Ochiai for his encouragement throughout this work, and to K. Mitsuhashi of Toyama University for his helpful suggestions. They also express their thanks to M. Ishikawa and T. Tsuchiya, Tokyo Medical and Dental University, for carrying out preparative scale gas-liquid chromatography, to C. H. Prien, Denver University, and B. Guthrie, U. S. Bureau of Mines, for their kind supply of Colorado shale oil, and to Idemitsukosan Co., Ltd., for the transportation of shale oil.

LITERATURE CITED

(1) Barrett, C. B., Dallas, M. S. J., Padley, F. B., *Chem. Ind. (London)* **1962**, 1050.
(2) Dinneen, G. U., Cook, G. L., Jensen, H. B., ANAL. CHEM. **30**, 2026 (1958).
(3) Dinneen, G. U., Smith, J. R., Van Meter, R., Allbright, C. S., Anthoney, W. R., *Ibid.*, **27**, 185 (1955).
(4) Eisen, O., Goryuch, S., *Khim. i Tekhnol.* **1961**, 213.
(5) Eisen, O., Rang, S. A., *Ibid.*, **1961**, No. 4, 200.
(6) Eisen, O., Rang, S. A., Arumeel, E. K., *Kim. i Tekhnol. Topliv i Mosel* **8**, 38 (1963).
(7) Hull, W. Q., Guthrie, B., Sipprelle, E. M., *Ind. Eng. Chem.* **43**, 2 (1951).
(8) Iida, T., *J. Pharm. Soc. Japan* **82**, 144, 151 (1962).
(9) Iida, T., *Pharm. Bull.* **1**, 209 (1953).
(10) Iida, T., Tanaka, M., *J. Pharm. Soc. Japan*, **64**, 162 (1944).
(11) Iida, T., Tanaka, M., *Pharm. Bull.* **1**, 211 (1953).
(12) Klesment, I. R., *Eesti NSV Teaduste Akad. Toimetised* **13**, 297 (1964).
(13) Ruark, J. R., Berry, K. L., Guthrie, B., *U. S. Bur. Mines Rept. Invest.* **5279** (1956).
(14) Van Meter, R., Bailey, C. W., Smith, J. R., Moore, R. T., Allbright, C. S., Jacobson, I. A., Hylton, V. M., Ball, J. S., ANAL. CHEM. **24**, 1758 (1952).
(15) Wagner, H., Goetschel, J. D., Lesch, P., *Helv. Chim. Acta* **46**, 2986 (1963).

RECEIVED for review March 10, 1966. Accepted June 10, 1966. Work supported by a grant from the Ministry of Education of Japan.

Correction

Estimation of Medium Effects for Single Ions and Their Role in the Interpretation of Nonaqueous pH

In this article by Orest Popovych (ANAL. CHEM. **38**, 558 (1966)], the e. m. f. of the cell described on page 559 below Equation 9 should be equal to $(E_j - k \log_m \gamma_H)$.

In the title of Table III on page 561, the scale should read "molal," instead of "molar."

Absorptiometric Methods in Rapid Silicate Analysis

C. O. INGAMELLS

College of Mineral Industries, The Pennsylvania State University, University Park, Pa.

▷ **The lithium metaborate–nitric acid solution technique makes possible the determination of all major elemental constituents of silicate rocks and minerals except carbon, hydrogen, and oxygen on a single sample. A complete analysis is often possible with 50 mg. of material. The whole-rock solution is examined using instrumental and chemical techniques. Rapid colorimetric methods for SiO_2, P_2O_5, Al_2O_3, Fe_2O_3, TiO_2, MnO, NiO, and Cr_2O_3 are described.**

THE preparation of a lithium metaborate–nitric acid solution of silicate rocks and its use for their spectrometric and flame photometric analysis have been described (*8*, *14*). Results compare favorably with those obtained by other rapid methods; however, until direct-reading spectrometers are everywhere available, rapid chemical procedures will be needed. Phosphorus is a common constituent of silicate rocks, and cannot as a rule be determined spectrometrically. In addition, even with unlimited instrumentation, it is desirable to have alternative methods for cross-checking results. If a spectrograph is used instead of a spectrometer, chemical procedures will be more attractive for those elements for which satisfactory absorptiometric methods exist, partly because the reading of spectrographic plates is time-consuming, and partly for the sake of higher precision. The spectrographic approach will usually be preferred for Ba, Sr, Zr, Mg, and less common minor constituents such as Be and Zn. With a direct-reading spectrometer, results for most metals are so rapid and precise that colorimetric procedures will seldom be used if such an instrument is available, except for P_2O_5, Cl, F, and perhaps SiO_2.

The procedures outlined below are applicable to all ordinary silicate rocks and minerals and have been worked out for use with the same solution prepared for emission spectrometry. An indication of the variety of samples which yield clear lithium metaborate–nitric acid solutions is given in Figures 3 and 6. In addition to the materials listed therein, solutions of tourmaline, muscovite, serandite, catapleiite, ilmenite, magnetite, illite, and other refractory minerals have been prepared and analyzed without difficulty. Variations of the original solution procedure (*14*) are described, which may be preferred when the emphasis is on colorimetric methods or when the available sample is small. The cobalt nitrate addition, which is essential to the spectrographic or spectrometric methods, is included. Although the supposition that it is without effect in the colorimetric procedures seems reasonable, all the methods have been developed with cobalt present in the solution, and the possibility of omitting it should not be accepted without trial.

Application of spectrometric (or spectrographic), flame photometric, and colorimetric techniques to the same solution makes possible the determination of all major elemental constituents of silicates except carbon, hydrogen, and oxygen on the same sample, which may be as small as 20 mg. In addition, several minor elements (Ba, Sr, Zr, etc.) may be determined spectrometrically with little added effort. If a spectrograph is used, unusual or unexpected constituents are quickly detected.

EXPERIMENTAL

Preparation of Sample Solution. REAGENTS REQUIRED. Lithium metaborate, anhydrous, $LiBO_2$, available from the G. F. Smith Chemical Co., Columbus, Ohio. The reagent should be examined spectrographically for impurities. Lithium tetraborate is not a satisfactory substitute. Methods for purifying $LiBO_2$ have been described (*14*).

Cobalt Nitrate Stock Solution. Dissolve 113 grams (1/4 pound) of $Co(NO_3)_2 \cdot 6H_2O$ in 1 liter of water. Filter, and store in a tightly sealed bottle. Preparation of this concentrated solution avoids frequent restandardization.

Dilute Cobalt Nitrate. Dilute 50.00 ml. of cobalt nitrate stock solution to exactly 1 liter with water.

Dissolving Solution (with cobalt internal standard). Dilute 50.00 ml. of dilute cobalt nitrate with 30 ml. of concentrated nitric acid to exactly 1 liter with water.

Dilute Nitric Acid (1 to 24). Dilute 40 ml. of concentrated nitric acid to 1 liter with water.

PROCEDURE. Transfer 0.2000 gram of a −200-mesh sample to a 25-ml. platinum crucible. If required, determine weight loss at 105° C. (H_2O-). If sulfides or large amounts of ferrous iron are present, roast overnight at 550° C.

Add 1.00 gram of lithium metaborate, mix thoroughly with a platinum rod, and support the crucible on a clean silica triangle. Cover, and heat with a Meker burner, making sure that the flame is strongly oxidizing. (A good test for an oxidizing flame is made by replacing the platinum with a nickel crucible of the same size: If a bright metallic surface is observed, decrease the gas flow until an oxide film forms.) Fusion in a reducing flame will result in loss of base metal to the platinum. Excess oxygen in the flame is essential to the decomposition of chromite and some other ferrous minerals.

Several times during the fusion, mix the contents of the crucible by rotating it in the flame, then heat for a further 5 minutes (longer with samples containing refractory minerals). Let the viscous melt flow over the walls, and place the crucible (while still red hot, so that the molten material is cooled rapidly to a glass) in a 100-ml. beaker containing 25 ml. of dilute nitric acid (1 to 24). When cool, add 50 ml. more of dilute nitric acid, filling and submerging the upright crucible. Put a small Teflon-covered stirring bar in the crucible, and stir gently over a magnetic stirring unit to complete solution. Addition of a drop of 3% hydrogen peroxide may be required with manganese-bearing samples.

Add 5.00 ml. of dilute cobalt nitrate, and transfer to a 100-ml. volumetric flask, washing the beaker, crucible, etc., with water. Dilute to the mark and mix. As soon as practicable, prepare a 1 to 19 dilute solution for the Si, Al, and Fe determination.

SOLUTION PREPARATION FOR SMALL SAMPLES. Transfer a sample of 20 mg. or less to a 30-ml. platinum crucible, roast overnight at 550° C., mix with 5 times its weight of lithium metaborate, and fuse over a Meker burner for 10 to 15 minutes. Cool quickly. Add 1.00 ml. of dissolving solution (with cobalt internal standard) for each 2 mg. of sample, cover, and stir, using a small Teflon-covered bar, until solution is complete. Transfer to a stoppered container without rinsing the crucible.

A solution for Si, Al, and Fe may be prepared by diluting 2.00 ml. of the sample solution to 50 ml. (or 1.00 ml. to 25). In this case, take 5.00 ml. of the dilute solution (instead of 4.00 ml.) for these determinations. One fifth the specified volumes of solutions and reagents can be used in the colori-

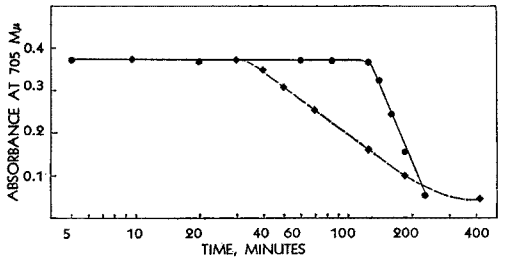

Figure 1. Persistence and fading of silicomolybdenum blue: solution prepared from a granitic rock according to the recommended procedure

◇— 1.0 ml. of stannous oxalate solution
○—10 ml. of stannous oxalate solution

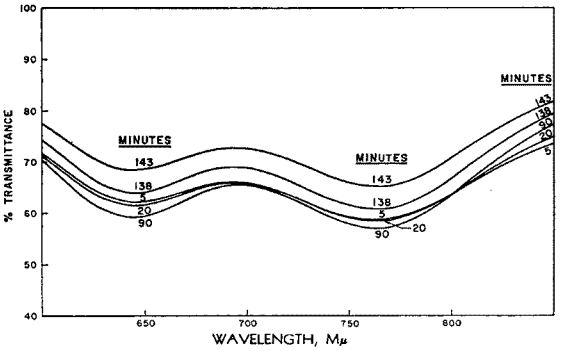

Figure 2. Absorption spectra of silicomolybdenum blues

metric procedures when necessary without much inconvenience, if suitable absorption cells are available.

A sample solution may also be prepared after fusion in a graphite crucible. This technique and its very considerable advantages have been described (*14*). Fusion in platinum in an electric furnace has proved to be unsatisfactory.

Polymerization of silicate and aluminate proceeds slowly in these solutions (though no visible precipitation occurs), and leads to low results, particularly for Si and Al, if analysis is delayed for more than a few hours.

Determination of Silicon. The most successful colorimetric procedures for Si in silicates are those in which its heteropoly molybdenum acids are reduced to silicomolybdenum blues and measured photometrically.

When silicic acid reacts with molybdate, at least two silicomolybdates are formed, the relative proportions of which are strongly dependent on pH and temperature. On reduction, these produce corresponding silicomolybdenum blues with differing absorption spectra (*2*).

Strong acid must be added before reduction of silicomolybdate; otherwise molybdic acid itself is reduced to molybdenum blue. The latter is a distinct species with an absorption spectrum unlike that of the silicomolybdenum blues (*2*).

Many reducing agents have been used. After thorough investigation (*2*, *7*), stannous oxalate in sulfuric–oxalic acid–sodium formate solution has been found most satisfactory.

While a complete understanding of molybdenum blue reactions is not claimed, the following mechanism has proved to be a useful approximation.

$$\text{Mo(VI)} + \text{Sn(II)} \rightarrow \text{(Slow)} \rightarrow \text{Mo(IV)} + \text{Sn(IV)} \quad (1)$$

$$\text{SiMo(VI)} + \text{Sn(II)} \rightarrow \text{(Fast)} \rightarrow \text{SiMo(IV)} + \text{Sn(IV)} \quad (2)$$

$$\text{Mo(VI)} + \text{Mo(IV)} \rightarrow \text{(Fast)} \rightarrow 2\text{Mo(V)} \text{ (Colorless)} \quad (3)$$

$$\text{SiMo(IV)} + \text{Mo(VI)} \rightarrow \text{(Fast)} \rightarrow \text{SiMo(V)} \text{ (Blue)} + \text{Mo(V)} \text{ (Yellow)} \quad (4)$$

$$\text{SiMo(V)} \text{ (Blue)} + \text{Mo(V)} \rightarrow \text{(Slow)} \rightarrow \text{SiMo(VI)} + \text{Mo(IV)} \quad (5)$$

The formulas in Equations 1 to 5 should not be taken literally. There are numerous molybdenum atoms per molecule in these species, and the valence changes indicated will be recognized as nominal. The over-all reaction is

$$4\,\text{Mo(VI)} + 2\,\text{Sn(II)} \rightarrow (4 - x)\,\text{Mo(V)} \text{ (Colorless)} + x\,\text{Mo(V)} \text{ (Yellow)} + 2\,\text{Sn(IV)} \quad (6)$$

Thus SiMo(V) (Blue) is a reaction intermediate, maintained in the presence of Sn(II) and excess molybdate.

That the silicate-molybdate complexes remain intact through repeated redox cycles is shown by complete restoration of color to a fading solution by adding more reductant. The existence of two distinct reduced molybdenum end products, designated Mo(V) (Colorless) and Mo(V)(Yellow), is indicated by a final yellow color which varies with the amount of reductant added and also with the silicomolybdate present. At the concentrations involved, SiMo(VI) is not perceptibly yellow.

The intensity of the blue color is essentially independent of the amount of stannous salt added, but its persistence, and also its rate of fading, increase with increased reductant addition (Figure 1). This indicates that its transient character is due to reaction with reduced molybdenum species (Equation 5). Addition of more reductant to a faded solution restores the original color, indicating stability of the reducible species.

Procedures have been devised which give a more permanent blue. While some of these work well in pure solutions, color intensity depends on factors which cannot be kept under control in the presence of the miscellany of elements found in silicates. For example, ferric iron inhibits the development of silicomolybdenum blue if an excess of strong reductant is not used, presumably because of the equilibrium

$$\text{SiMo(V)} \text{ (Blue)} + \text{Fe(III)} \rightleftarrows \text{SiMo(VI)} + \text{Fe(II)} \quad (7)$$

This is put to good use in the determination of phosphorus (see below). Gentry and Sherrington (*4*), who used ferrous iron as a reductant in silicon determination, recognized the effect of Fe(III).

The measured color intensity is slightly, but not excessively, sensitive to the effect of temperature on the several reaction rates. For concordant results, temperature should be the same in all determinations.

Silicic acid, particularly in undiluted sample solutions, polymerizes on standing. Completely acceptable results are not possible without a depolymerization step even if determination immediately follows solution preparation; if several days elapse before preparation of the diluted sample solution, relatively little silicomolybdenum blue appears. Depolymerization is accomplished by heating the freshly prepared sample solution with molybdate at optimum pH for 2 hours. On reduction, the solution shows an absorption minimum in the neighborhood of 700 mμ (Figure 2), which is not far from the isobestic point (735 mμ) between the two maxima demonstrated by Eckert (*2*). Measurements made between 700 and 735 mμ are least dependent on the relative proportions of the various species, and on other factors which may vary somewhat from sample to sample. The change in absorbance with time indicates the presence of more than one species. Different spectra are obtained in solutions which have not been heated.

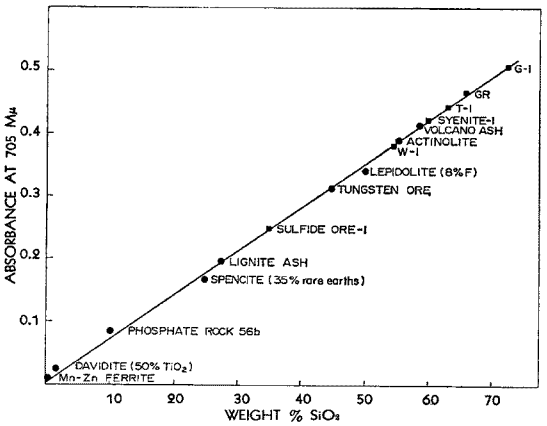

Figure 3. Determination of SiO_2

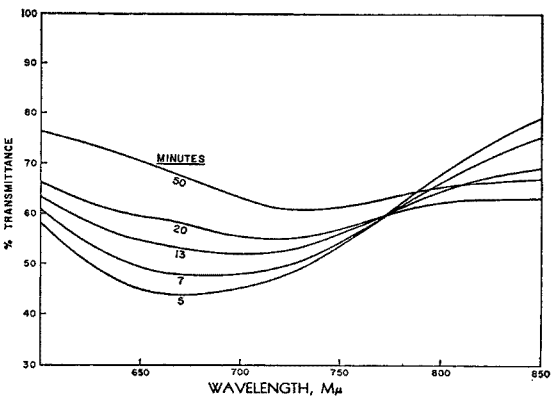

Figure 4. Absorption spectra of phosphomolybdenum blues

Absorbance changes least with time at 705 mμ, and photometric measurement is made at that wavelength. However, the best wavelength setting depends to some extent upon the band pass of the instrument used.

SOLUTIONS REQUIRED. Ammonium Molybdate. Dissolve 50 grams of large crystals of $(NH_4)_6Mo_7O_{24}\cdot 4H_2O$ in 1 liter of water. Filter into a polyethylene bottle. Some products sold as ammonium molybdate are mixtures of complex molybdates and molybdic acids. These are not satisfactory.

Stock Stannous Chloride. Weigh 350 grams of $SnCl_2\cdot 2H_2O$ into a 1000-ml. volumetric flask and add 200 ml. of concentrated hydrochloric acid. Warm gently until a perfectly clear solution is obtained. Dilute to 1000 ml. with water and mix.

Stannous Oxalate. Dissolve 25 grams of oxalic acid dihydrate in 1 liter of cold water. Add all at once 80 ml. of stock stannous chloride. Swirl once, and allow to stand for an hour. Filter through glass frit or glass fiber, and wash thoroughly with cold water to remove chloride. Dry at 50° C.

Stannous Oxalate Solution. In 1900 ml. of water dissolve in the order given 33 grams of oxalic acid dihydrate, 32 grams of sodium formate, and 21 ml. of 90% formic acid. Dilute to 2000 ml. As needed, dissolve 1.7 grams of stannous oxalate in 200 ml. of the mixture.

Dilute Sulfuric Acid (1 to 3). To 1500 ml. of water add 500 ml. of concentrated sulfuric acid. Mix and cool.

PROCEDURE. Transfer 4.00 ml. of dilute sample solution (1 to 19) to a 200-ml. volumetric flask. The flask should not have a ground-glass closure. Add 5.0 ml. of dilute nitric acid (1 to 24), 10 ml. of ammonium molybdate, and 50 ml. of water. Mix, and heat on the steam bath for 2 hours. Cool to room temperature, add 25 ml. of dilute sulfuric acid (1 to 3), mix thoroughly, and then without delay add all at once 10 ml. of stannous oxalate solution, using a 10-ml. graduate or a rapid-delivery pipet. Mix immediately, dilute to the mark with water, and again mix. Read absorbance after 20 to 30 minutes against a water reference at 705 mμ, using 13-mm. cells. Alternatively, 2-cm. cells may be used; it is then better to make the dilution to 250 ml. instead of 200 (dilutions to less than 200 ml. or more than 250 ml. are not advised). Higher precision may be attained by differential measurement against similarly prepared standards, using 5-cm. cells.

Unless the process is very carefully controlled, and measurement can be made near 705 mμ, it will be necessary to run a high and a low standard with each batch of samples.

The effect of the small amounts of silica dissolved from the glassware is small and reproducible if the flasks are in new condition.

INTERFERENCES. Fluorine causes low, and phosphorus high, results, but the effects are relatively small, and will seldom be appreciable with ordinary silicates. The general applicability of the method is illustrated in Figure 3. Large amounts of P_2O_5 (phosphate rock) cause high, and fluorine (lepidolite) low, results. Large amounts of rare earths (spencite) and of TiO_2 (davidite) have an appreciable effect. Silica from glassware and reagents results in a blank of about 0.3 to 0.5% SiO_2.

Determination of Phosphorus. Phosphorus is determined in a manner similar to silicon, by reducing phosphomolybdates to phosphomolybdenum blues. Interference by silicate is blocked by pH control and by adding a large excess of ferric iron. Two reduced phosphomolybdenum compounds are formed (Figure 4). The species with an absorption maximum at about 650 mμ forms first, and is gradually converted into a second species with an absorption maximum at about 850 mμ. Photometric measurements are made at the isobestic point (775 mμ). A dynamic equilibrium is established as in the silicon determination, during which, however, one of the two blues increases at the expense of the other before the reductant is exhausted and both disappear. The presumed mechanism is as follows:

$$Mo(VI) + Sn(II) \rightarrow (Slow) \rightarrow Mo(IV) + Sn(IV) \quad (1)$$

$$Mo(VI) + Mo(IV) \rightarrow (Fast) \rightarrow 2\,Mo(V) \quad (3)$$

$$PMo(VI) + Sn(II) \rightarrow (Fast) \rightarrow PMo(IV) + Sn(IV) \quad (8)$$

$$PMo(IV) + Mo(VI) \rightarrow (Fast) \rightarrow PMo(V)\ (Blue\ 1) + Mo(V) \quad (9)$$

$$PMo(VI) + Mo(IV) \rightarrow (Fast) \rightarrow PMo(V)\ (Blue\ 2) + Mo(V) \quad (10)$$

$$PMo(V)\ (Blue\ 1, 2) + Mo(V) \rightarrow (Slow) \rightarrow PMo(VI) + Mo(IV) \quad (11)$$

Reaction 10 is the reverse of the corresponding silicate reaction. Its rate relative to that of Reaction 9 presumably increases as reaction proceeds. Because of the resulting continuous change in the proportion of the two colored species, colorimetric measurement is made near the isobestic point (775 mμ).

There must be enough ferric iron in the solution to remove SiMo(V) (Blue) by Reaction 7 as fast as it is formed. Oxalate and fluoride in the formate buffered solution adequately control the Sn(II) and Fe(III) concentrations, and also prevent precipitation of Sn(IV) compounds. Under the recommended conditions, phosphomolybdenum blue develops rapidly, and can be measured with time to spare before depletion of Fe(III) and increasing Fe(II) result in a

slowly increasing absorbance due to silicomolybdenum blues. Eventually the Sn(II) becomes exhausted, and all blue species disappear, via Reactions 5, 11, and 3. When silicate is absent, absorbance at 775 mμ remains constant for as long as 1 to 2 hours, or until the reductant is exhausted. As expected, the period of color stability decreases as phosphorus concentration increases.

In the presence of zirconium, it is essential to heat the sample solution with acid and ferric salt to release phosphate for combination with molybdate. Syenite-1, for example, with 0.5% ZrO_2, shows very little phosphorus when this step is omitted. Release of phosphate becomes increasingly difficult as the solution ages; thus determination should be accomplished as soon as practicable after solution preparation, especially when much zirconium is present.

Phosphomolybdenum blues are more temperature-sensitive than their silicate counterparts; however, the error introduced by ignoring this is small, if all solutions are kept at a reasonably constant room temperature.

Freshly prepared stannous oxalate solution must be used, the full-strength reagent being required for sufficiently rapid reduction of phosphomolybdate in the presence of ferric iron. The wave length setting which will give the best results depends, as in the silicon determination but to a somewhat greater extent, on the band pass of the spectrophotometer.

It is necessary to pay some attention to the quality of the sodium molybdate reagent. Of three reagents investigated (all reagent grade $Na_2MoO_4 \cdot 2H_2O$), only one gave satisfactory results when used in a freshly prepared solution; all could be used successfully if the reagent solution was allowed to age for a few days. One of the three yielded a solution which remained stable and usable for several months; the other two deposited crystalline material within a few days or weeks.

SOLUTIONS REQUIRED. Ferric Nitrate. Dissolve 70 grams of $Fe(NO_3)_3 \cdot 9H_2O$ in water containing 30 ml. of concentrated nitric acid, and dilute to 1 liter with water. Filter through Whatman No. 42 paper.

Molybdate Formate. To 900 ml. of water add and dissolve in the order given 9.0 grams of $Na_2MoO_4 \cdot 2H_2O$, 15.5 grams of sodium formate, 10.5 ml. of 90% formic acid, and 46 ml. of dilute sulfuric acid (1 to 3). Allow the solution to stand in the dark for 2 to 3 days before use. This solution is light-sensitive, slowly acquiring a deep blue color if kept in daylight. Discard a strongly colored solution, or one which has deposited insoluble salts.

Sodium Fluoride. Dissolve 10 grams of NaF in 1 liter of water in a polyethylene bottle.

Table I. Comparison of Results for P_2O_5

Sample	% P_2O_5 Present	% P_2O_5 Found
Limestone, 403	0.04[a]	0.05
Limestone, 402	0.05[a]	0.07
Granite, G-1	0.09[b]	0.09
Granite, GA	0.10[c]	0.12
Diabase, W-1	0.14[b]	0.15
Tonalite, T-1	0.17[b]	0.17
Basalt, BCR-1	0.39[b]	0.40, 0.46
Andesite, AGV-1	0.50[b]	0.53
Basalt, BR	1.03[c]	1.24, 1.23
Syenite	1.06[a]	1.03
Minette	2.86[a]	2.53

[a] Separated and weighed as $Mg_2P_2O_7$.
[b] Separated and weighed as ammonium phosphomolybdate.
[c] Preliminary value reported by Petrographic and Geochemical Research Centre, Nancy, France.

PROCEDURE. To 5 ml. of the undiluted sample solution (use less with samples containing much more than 1% P_2O_5, and make up the volume difference with water) add 5 ml. of ferric nitrate, and mix. Cover, and heat on the steam bath for 15 to 20 minutes. The operation is best carried out in a wide-mouthed flask, conveniently a 250-ml. milk flask. Cool to room temperature (15 minutes on a cold stone or metal surface), add 5 ml. of molybdate formate, and allow to stand for 15 minutes. Be careful to leave no molybdate on the walls of the flask, where it will form molybdenum blue on contact with the reductant during the next addition. Add 10 ml. of stannous oxalate solution (freshly prepared), all at once from a rapid-delivery pipet. Mix immediately and thoroughly, and after 20 to 30 seconds add 25 ml. of sodium fluoride. Measure the transmittance after 5 minutes at 775 mμ against a water blank.

After about 10 minutes, absorbance (at 775 mμ) slowly increases because of reduction of Fe(III) and resulting development of some silicomolybdenum blue.

INTERFERENCES. The most seriously interfering element is zirconium, and its effect can in many cases be almost entirely overcome by observing the precautions indicated, and carrying out the determination immediately after preparation of the sample solution. Some typical comparable results are given in Table I.

Determination of Aluminum. Until recently, the misconception that lake formation is essential to the chromogenic reaction between aluminum and aluminon has prevented its most effective use. Recent work by Hsu (*6*) demonstrates convincingly that in acetate-buffered solution at pH 3.8, the reaction is essentially ionic. A series of experiments using Job's method of continuous variations showed a 1 to 2 complex, but higher complexes are also indicated. The latter adversely affect the performance of some commonly used procedures. The equilibria involved are complex and are strongly dependent on pH and temperature. Absorption spectra of the aluminon-aluminum complexes show maxima at about the same wave length as the dye itself (*6*).

By the addition of borate, the blank absorbance is diminished; more reagent can be used, and the concentration of aurintricarboxylate is controlled so as to suppress formation of higher complexes. The result is a more exactly linear relation with absorbance over a wide range of aluminum concentrations.

A difficulty in the use of aluminon is that of obtaining a high-quality reagent. In this connection reference may be made to the work of Scherrer and Smith (*11*) and Smith, Sager, and Siewers (*13*): Of five batches of aluminon obtained at random from four different manufacturers, only two were satisfactory for good quantitative work. Table II summarizes the performance of the five reagents applied to a granite carried through the recommended procedure.

Attempts to purify the reagents of Table II showed a surprising lack of uniformity in their behavior—for example, the good Fisher reagent was almost completely precipitable from aqueous solution by silver nitrate. A

Table II. Comparison of Aluminon Reagents from Various Sources
(Absorbance measured at 530 mμ, 30° C.)[a]

Supplier	Color of aq. soln.	Blank absorbance (*vs.* water)	Sample absorbance (*vs.* blank)	Color: Blank	Color: Sample	Remarks
M C & B	Almost black	1.17	0.358	Dark amber	Brown	Unusable
Eastman	Brown orange	0.533	0.381	Amber brown	Dark brown	Poor
Fisher	Red-orange	0.169	0.259	Faint pink	Pink	Insensitive
Fisher	Red-orange	0.481	0.706	Orange-amber	Pink-red	Good
BDH	Red-orange	0.312	0.456	Pink-orange	Pink	Usable

[a] Final concentration of Al_2O_3 about 60 μg. per 100 ml. of solution.

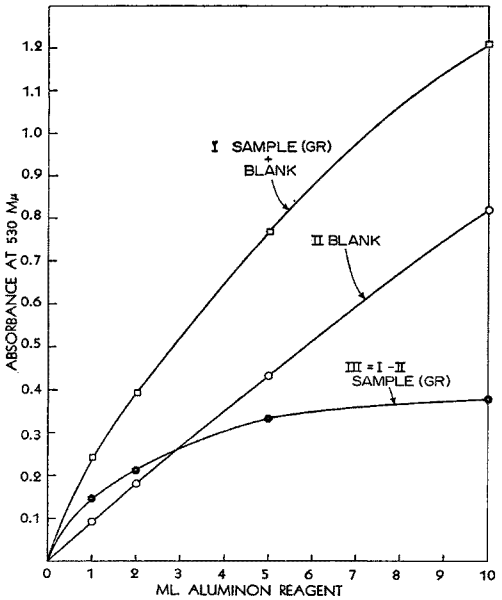

Figure 5. Effect of aluminon concentration on the determination of Al_2O_3

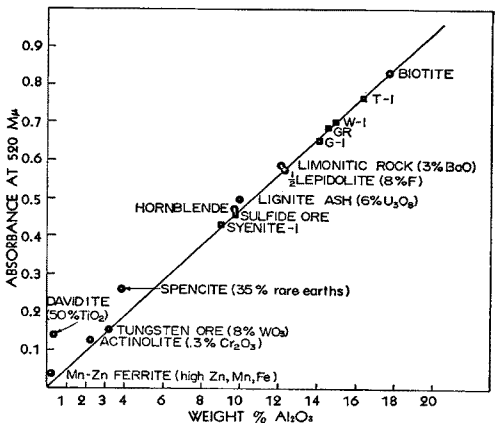

Figure 6. Determination of Al_2O_3 with aluminon

reagent prepared by treating the insoluble silver salt with ammonium chloride, and removing silver chloride by filtration, performed slightly better than the untreated aluminon. However, the Eastman reagent could not be purified in this way, since its silver salt was not precipitable.

Possibly the simplest way to determine the adequacy of a particular reagent is to carry a sample through the method, using varying amounts of 0.1% aluminon solution, but keeping all other conditions constant. Results should be similar to those illustrated in Figure 5. Enough reagent should be used to approach the horizontal of curve III without unduly increasing the blank absorbance (curve II). The recommended addition of aluminon does not give the maximum attainable absorbance—it represents a compromise, necessary to keep the absorbancy of the blank within reasonable limits. A reading on the steeply ascending portion of curve III with the recommended aluminon addition is indicative of nonchromogenic impurity, and results will be unsatisfactory because of their critical dependence on an exact reagent addition. Some reagents (Table II) are unusable because the blank absorbancy becomes untenably high when enough is used to approach the horizontal of curve III (Figure 5).

An important factor which seems to have sometimes escaped notice is that color intensity is temperature-dependent; this leads to difficulty if not recognized and taken into account. Further, equilibrium is not attained immediately, so that the solutions must be held at constant temperature for some time before measurement. Readings of both blank and samples must be made without permitting temperature change. In the absence of agents which destroy aluminon or form precipitates, the color is otherwise stable for long periods.

For complete color development, aluminum must be in the ionic state at the time of pH adjustment and reagent addition (*6*). If the initial pH is too high, polymeric species are present which will not produce a full color. The difficulty is overcome by heating the acidified solution on the steam bath before buffering to the correct final pH.

SOLUTIONS REQUIRED. Acetate-Borate Buffer. Filter 700 ml. of 2*M* sodium acetate through Whatman No. 42 paper, then add 700 ml. of water and 550 ml. of glacial acetic acid. Filter before acid addition. To 1 liter of this solution add 10 grams of sodium tetraborate pentahydrate. Filter.

Aluminon. Dissolve 1.00 gram in 1000 ml. of water. After several hours, filter through Whatman No. 42 paper. Refilter if the solution does not remain perfectly clear.

Sodium Thioglycollate. Dissolve 1.0 gram in 200 ml. of water. Some batches of thioglycollate contain impurity which strongly suppresses the aluminum color.

PROCEDURE. Transfer 4.00 ml. of the dilute sample solution (1 to 19) to a 100-ml. volumetric flask. Add 1.0 ml. of dilute nitric acid (1 to 24) and 50 ml. of water. Heat on the steam bath for 2 hours. Without cooling, add 1.00 ml. of sodium thioglycollate, mix, and after 1 to 2 minutes add 5.00 ml. of acetate-borate buffer and 5.00 ml. of aluminon. Measure all additions exactly. Dilute nearly to the mark and place in a constant temperature bath at 30° C. until temperature equilibrium is attained. Then dilute to exactly 100 ml., mix, and return to the bath for about 18 hours (overnight). Prepare a reagent blank, carrying it through all the steps of the procedure. Read absorbance at about 520 mμ in 5-cm. or 2-cm. cells. The pH of the final solution should be very close to 3.8. It is best to determine the wave length setting which gives maximum absorbance, since this depends to some extent on the band pass of the instrument and on the quality of the reagent.

The procedure is applicable to samples containing up to about 20% Al_2O_3. With greater aluminum concentrations, greater dilution and proportionately larger volumes of reagents should be used; otherwise precipitation may occur, and results will be low. With low-alumina samples (dunite, limestone, etc.) the undiluted sample solution may be used in the same procedure.

Since the absorbancy of both blank and sample is temperature-dependent, measurements should be made quickly enough to avoid appreciable warming of the solutions in the cell compartment of the spectrophotometer; routines which leave the reference solution in the instrument during the reading of several samples must be avoided.

INTERFERENCES. Under the proper conditions, aluminon is nearly specific for aluminum in silicate rocks and minerals. Beryllium, chromium, and the rare earths show the most interference, but it is seldom appreciable. Titanium in normal amounts interferes only slightly. Figure 6 illustrates the applicability of the procedure to variety of materials, and also gives the interference of TiO_2

(davidite), rare earths (spencite), U_3O_8 (lignite ash), ZnO (ferrite), and Cr_2O_3 (actinolite). Of these, only Cr_2O_3 is often present in silicates in amounts sufficient to cause serious error. Since, weight for weight, Cr_2O_3 produces almost the same color as Al_2O_3, a correction is easily made.

Determination of Iron. *o*-Phenanthroline is employed for the iron determination. The procedure is widely used and well known. A satisfactory variation applicable in the present case is as follows:

SOLUTIONS REQUIRED. *o*-Phenanthroline, 0.1% (w./v.) in water.

Hydroxylamine hydrochloride, 10% (w./v.) in water.

2*M* sodium acetate, filtered through Whatman No. 42 paper.

1*M* sodium citrate, filtered through Whatman No. 42 paper.

PROCEDURE. Transfer 4.00 ml. of the dilute sample solution (1 to 19) to a 50-ml. volumetric flask. Add 5 ml. of hydroxylamine hydrochloride. Let stand for 5 to 10 minutes (or for 1 hour if citrate buffer is to be used), and add 10 ml. of *o*-phenanteroline and 5 ml. of 2*M* sodium acetate (or 1*M* sodium citrate). Dilute to the mark, mix, and let stand overnight. Measure transmittance against a reagent blank at 508 mμ, using 5-cm. or 1-cm. cells, depending on the amount of iron present.

When much iron is present, superior results may be obtained by using bracketing standards and making differential measurements.

If very little iron is present, the undiluted sample solution, or a larger aliquot of the diluted solution, may be used. Precipitation sometimes occurs with acetate buffer, particularly when the undiluted solution is used. In such cases, citrate may be substituted; however, iron must be completely reduced before citrate addition. In most cases acetate is preferred.

Determination of Manganese. To 10.0 ml. of the undiluted sample solution in a 50-ml. volumetric flask add 3 ml. of colorless concentrated nitric acid. Add 10 ml. of 1% (w./v.) periodic acid solution, and heat on a boiling water bath overnight. Cool to room temperature, then add 1 ml. of 1 to 1 phosphoric acid, and dilute to volume. Measure transmittance against water or a reagent blank at 545 mμ in 5-cm. cells.

Determination of Titanium. To 10.00 ml. of undiluted sample solution in a 50-ml. volumetric flask, add 5 ml. of dilute sulfuric acid (1 to 3) and 5 ml. of 3% hydrogen peroxide. Dilute to the mark and mix. Prepare a similar solution, omitting the peroxide addition, for use as a reference. Measure transmittance at 410 mμ in 5-cm. cells. The reference solution is essential because Fe(III) absorbs appreciably at 410 mμ.

Vanadium and molybdenum interfere. Chromium may cause low results because of CrO_4^{-2} in the blank.

The titanium solutions may be reserved for the determinations of chromium and nickel (see below).

If it was necessary, because of the presence of manganese, to add peroxide during solution preparation, it should be removed by heating on the steam bath before attempting the TiO_2 determination. Reference and sample solutions must be at exactly the same temperature at the time of photometric measurement, because the absorbancy due to Fe(III) is strongly temperature-dependent. If traces of chromate are likely to be present, the addition of a very little ferrous salt to the blank is advisable.

Some typical results for Fe_2O_3,MnO, and TiO_2 are given in Table III.

Table III. Comparison of Results for Fe_2O_3, MnO, and TiO_2

Sample	% Fe_2O_3		% MnO		% TiO_2	
	Present	Found	Present	Found	Present	Found
Granite, GA	2.85	2.82	0.08	0.08	0.36	0.38
Granite, GH	1.36	1.38	0.04	0.04	0.11	0.09
Basalt, BR	12.88	12.77	0.21	0.21	2.64	2.61
Granite, G-2	2.72	2.72	0.03	0.03	0.47	0.45
Peridotite, PCC-1	8.16	8.31	0.12	0.11	0.00	0.00
Dunite, DTS-1	8.75	8.75			0.00	0.00
Granodiorite, GSP-1	4.27	4.20	0.04	0.04	0.64	0.64
Basalt, BCR-1	13.40	13.20	0.19	0.20	2.22	2.22

Table IV. Comparison of Results for Cr_2O_3 and NiO

Sample	% Cr_2O_3		% NiO	
	Present	Found	Present	Found
Peridotite, PCC-1	0.34	0.32	0.31	0.34
Dunite, DTS-1	0.48	0.48	0.31	0.33
Sulfide ore—1	0.04	0.05	1.92	1.90
Diabase, W-1	0.02	0.02		

Determination of Chromium. Transfer the whole of the peroxidized titanium solution from the previous procedure (or a fresh 10-ml. aliquot, plus dilute sulfuric acid and peroxide) to a 150-ml. beaker. Add 8 ml. of 10*N* sodium hydroxide and 1 drop of 4% (w./v.) potassium permanganate solution. Heat on the steam bath overnight. Evaporate to about 40 ml., and cool completely. Transfer to a 50-ml. volumetric flask, dilute to the mark, mix, and filter through a dry 541 Whatman paper. Measure transmittance at 365 mμ against a reagent blank, using 5-cm. cells.

Determination of Nickel. SOLUTIONS REQUIRED. Bromate-Bromide. Dissolve 20 grams of KBr and 5 grams of $KBrO_3$ in 1 liter of water.

Citric Acid. Dissolve 400 grams of citric acid in 1600 ml. of water. Filter, and add a drop of toluene as a preservative.

Dimethylglyoxime. Dissolve 0.2 gram in 100 ml. of 5% (w./v.) Na_2CO_3, warming gently to hasten solution.

PROCEDURE. To each of two 100-ml. volumetric flasks, add 5.0 ml. of the undiluted sample solution and 5 ml. of dilute sulfuric acid (1 to 3). (The reference solution from the titanium determination may be used.) To both add 5 ml. of bromate-bromide, allow to stand 1 to 2 minutes, add 10 ml. of citric acid and then, after a further 2 minutes, add 50 ml. of water and 15 ml. of 1 to 1 ammonia. Check with test paper to be sure the solution is alkaline. To one solution, add 5 ml. of dimethylglyoxime, and to the other 5 ml. of 5% sodium carbonate. Dilute to volume, and measure transmittance after 15 minutes at 520 mμ in 1-cm. or 5-cm. cells, depending on the amount of nickel present.

Measurement is made at 520 mμ rather than at the isobestic point at 445 mμ (*10*) because of the greater absorbancy of iron(III) at the latter wavelength.

Some results for Cr_2O_3 and NiO are given in Table IV.

DISCUSSION

Use of the same sample solution for many determinative procedures lends considerable flexibility to the proposed approach to rapid silicate analysis. Determinative techniques can be selected according to sample type, available equipment, and the accuracy required. An obvious extension of the method is the use of flame absorption techniques.

An advantage of the solution technique is the possibility of preparing standards with unusual elemental concentrations simply by salting known samples with measured amounts of metal nitrate solutions added to the dissolving acid; the method of standard additions may be applied when necessary.

Neither this nor any similar scheme will give results for major constituents comparable in accuracy to those obtainable by the more sophisticated methods on which it depends for the essential standards. This cannot be too strongly emphasized, especially since the important distinction between primary and secondary methods appears to remain generally unrecognized. While absorp-

Table V. Summary of Interferences

Element determined	Observed Interference		Probable interference from
	Serious	Slight[a]	
Si		F, P, Ti, R.E.	
Al	Cr	Zn, Ti, U, Ba, R.E.	Be
P	(Zr)	Si, Zr	As, V
Fe	No gross interferences observed		
Cr	U		
Ti	Mo, V	Cr	U
Mn	No gross interferences observed		Cl
Ni		Mn, Cu	

[a] Interferences listed as "slight" will normally cause no appreciable error in analysis of silicates if suggested precautions are taken. Samples containing unusually high concentrations of these elements will probably require special treatment. For example, the procedure for nickel is inapplicable to manganese minerals.

tiometric methods applied to pure solutions can be made accurate to better than 0.1% by differential measurement, the practical difficulty of completely eliminating all interferences in a rapid procedure without separations makes this possibility of academic interest only.

The greatest absolute errors will usually appear in the silica and alumina. A 1% error in SiO_2, while it gives rise to a high or low total, is of little consequence in many applications. Routine gravimetric Al_2O_3 determinations are often high because of failure to correct for all associated oxides: Direct colorimetric values may be more accurate, despite their lower precision, if reliable standards are available.

Interelement interferences in the recommended colorimetric procedures are in most cases small. Special efforts have been made to circumvent those which might commonly lead to error. As a single example, the effect of zirconium on the phosphorus determination (which might have gone unnoticed if the CAAS sample of syenite-1 had not been available) required revision of the original procedure. Some observed interferences are summarized in Table V.

One of the major problems in using and evaluating rapid secondary methods for the analysis of silicate rocks is the dearth of useful standards. Until recently, the only thoroughly analyzed samples of wide distribution were granite G-1 and diabase W-1. The situation has improved with the issuance of syenite-1 and sulfide ore-1 by the Nonmetallic Standards Committee of the Canadian Association for Applied Spectroscopy (*1*), granite GR by the Centre de Recherches Petrographiques et Géochimiques of Nancy, France (*5*), and tonalite T-1 by the Geological Survey of Tanganyika (*15*). Exhaustive analyses of these rocks have been published (*9*, *16*). The National Bureau of Standards issues several less complex and less completely analyzed samples which are sometimes very useful; but frequently it is desirable to make accurate analyses of a few of each large suite of samples, to provide standards for the rapid methods. An alternative, easily applied in the suggested scheme, is to make appropriate additions of critical elements to solutions of available standards.

Three new rocks, GA, GH, and BR, have recently been prepared by the Centre de Recherches Petrographiques et Géochimiques, and the U. S. Geological Survey has issued six new samples for analysis. These will eventually be useful as standards, and are now being analyzed in our laboratories. Some results on these samples are reported in the tables.

In preparing calibration graphs, we have used our own preferred analytical values of G-1, W-1, T-1, GR, syenite-1, and sulfide ore-1. These were determined for the most part by primary methods outlined elsewhere (*9*). Several unusual samples were used to investigate interferences (Figures 3 and 6).

Those who are now using other rapid chemical schemes of analysis may find it worth while to investigate the applicability of their established determinative procedures to the lithium metaborate–nitric acid solution. No claim is made that the suggested colorimetric methods are much superior to others—for example, those recommended by Shapiro and Brannock (*12*). There is not much doubt, however, concerning the advantages of the solution procedure, particularly over those using hydrofluoric acid, in which numerous rock-forming minerals may be incompletely decomposed, and in which the near-impossibility of entirely removing fluoride leads to difficulties and errors.

LITERATURE CITED

(1) Canadian Association for Applied Spectroscopy, Non-metallic Standards Committee Report, *Appl. Spectry.* **15**, 159 (1961).
(2) Eckert, G., *Z. Anal. Chem.* **161**, (6) 421 (1958).
(3) Fleischer, M., Stevens, R. E., *Geochim. Cosmochim. Acta* **26**, 525 (1962).
(4) Gentry, C. H. R., Sherrington, L. G., *J. Soc. Chem. Ind.* **65**, 90 (1946).
(5) Govinaradju, K., Extrait de la Publication du G.A.M.S. 3/1963, 4/1963.
(6) Hsu, P. H., *Soil Sci.* **96**, 230 (1963).
(7) Ingamells, C. O., *Chemist-Analyst* **45**, 10 (1956).
(8) Ingamells, C. O., *Talanta* **11**, 665 (1964).
(9) Ingamells, C. O., Suhr, N. H., *Geochim. Cosmochim. Acta* **27**, 897 (1963).
(10) Sandell, E. B., "Colorimetric Determination of Traces of Metals," 3rd ed., Interscience, New York, 1959.
(11) Scherrer, J. A., Smith, W. H., *J. Res. Natl. Bur. Stds.* **21**, 113 (1938).
(12) Shapiro, L., Brannock, W. W., U. S. Geol. Surv. Bull. **1036C** (1956), **1144A** (1962).
(13) Smith, W. H., Sager, E. E., Siewers, I. J., ANAL. CHEM. **21**, 1334 (1949).
(14) Suhr, N. H., Ingamells, C. O., ANAL. CHEM. **38**, 730 (1966).
(15) Thomas, W. K. L., *Bull. Geol. Surv. Tanganyika, Msusule Tonalite*, Supp. 1 (1963).
(16) Webber, G. R., *Geochim. Cosmochim. Acta* **29**, 229–48 (1965).

RECEIVED for review March 28, 1966. Accepted June 3, 1966. Work financed in part under National Science Foundation Grant GP 3853.

Determination of Nickel by Atomic Fluorescence Flame Spectrometry

SIR: Recently it has been demonstrated that for a limited number of metallic elements, atomic fluorescence flame spectrometry is a very sensitive analytical procedure (*5, 9*). For these metals it has been possible to obtain very intense discharge lamps with unreversed emission lines. A primary requirement for the production of atomic fluorescence emission is the availability of an appropriate high-intensity light source. Also, it is advantageous if the element of interest possesses in the ultraviolet region an atomic resonance line with a high transition probability. Below 280 mμ, where flame background emission and atomic emission from the flame are relatively weak, considerably better fluorescence signal-to-noise ratios can be obtained. Even if the radiation from the light source is modulated and the resulting modulated fluorescence signal is selectively amplified, a portion of the unmodulated emission from the turbulent flame will have frequencies that are within the bandpass of the tuned amplifier, and this emission will cause signal noise.

Nickel has a satisfactory resonance line at 232.0 mμ and a sensitive emission line at 352.5 mμ, but previous attempts to observe the fluorescence emission with conventional nickel hollow-cathodes (*1, 6*) were unsuccessful. This was undoubtedly due to the weak emission intensities from the hollow-cathodes then available. The recent development of high intensity hollow-cathodes (*7*) has now made it possible to obtain intense unreversed line sources for a much wider variety of metals.

This study was undertaken to evaluate the usefulness of the new lamp for atomic fluorescence flame spectrometry. Strong nickel fluorescence was observed when aqueous solutions containing nickel nitrate were aspirated into an air–hydrogen flame. An oxygen–hydrogen flame was also tested for comparative purposes and found to be less satisfactory for nickel fluorescence work. Included in this paper are the analytical working curves, the detection limits, and a series of other wavelengths at which nickel fluorescence was observable in the air–hydrogen flame.

EXPERIMENTAL

Apparatus. The experimental arrangement is shown in Figure 1. The source was a high-intensity nickel hollow-cathode manufactured by Atomic Spectral Lamps Pty. Ltd. It has two separate electrical discharges, and therefore two stabilized d.c. power supplies were required. The primary discharge produces atoms by cathode sputtering and some excitation while the secondary discharge causes the main excitation of the atomic vapor. The maximum recommended currents are 20 ma. for the primary discharge and 400 ma. for the secondary discharge. Besides the two power supplies, it was also necessary to have a current source capable of supplying about 5 amp. at 1.5 volts to heat the cathode filament in the secondary discharge circuit. This heater current was turned off after the discharge was sustained and so did not have to be stabilized.

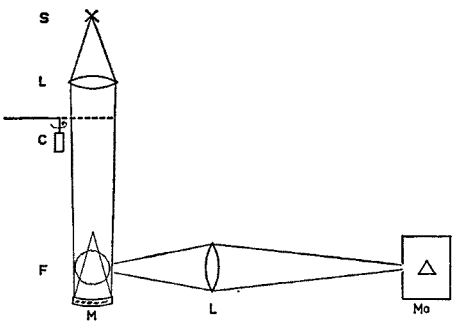

Figure 1. Optical arrangement for atomic fluorescence studies

S: source; *L:* quartz lens; *C:* chopper; *F:* flame; *M:* mirror; *Mo:* monochromator

The radiation from the source was first modulated at 50 c.p.s. with a mechanical chopper to discriminate between the fluorescence emission and the other forms of emission from the flame. After being modulated, the source radiation was passed through the flame to the front-surfaced mirror, *M*, and then directed back through the flame to a focus as shown. The addition of the concave mirror increased the resulting fluorescence intensity about three-fold, undoubtedly because it permitted the source radiation to be concentrated in the observed portion of the flame. The 50-c.p.s. fluorescence emission from the flame was focused on the entrance slit of a Hilger Watts Uvispek monochromator equipped with a quartz prism and was detected by a selected RCA 1P28 photomultiplier tube operated at 1250 volts. The resulting signal was amplified with a Model RJB lock-in amplifier manufactured by Electronic, Missiles, Communications, Inc., Mount Vernon, N. Y. The output from the narrow frequency bandwidth amplifier was then displayed on a recorder. A voltage stabilizer placed between the line voltage and the electrical components ensured the maximum instrumental stability.

The burner employed was a Beckman (No. 4020) medium-bore hydrogen burner operated with flow rates of 4.8 liters per minute for air and 13.6 liters per minute for hydrogen.

Procedure. In practice, the primary discharge current was set at 18 ma. After the cathode of the secondary discharge circuit was heated for 5 minutes with 3 amp., the secondary discharge voltage was applied and the secondary discharge current was slowly increased to 80 ma. This was the maximum output of the available power supply. Once the secondary discharge was obtained, it was unnecessary to continue heating the cathode filament, and therefore that voltage was switched off. The subsequent steps for measuring the atomic fluorescence intensity have already been presented in detail (*9*).

RESULTS AND DISCUSSION

First, the experimental variables were adjusted to give the optimum nickel fluorescence emission at 232 mμ. A study of the dependence of fluorescence intensity upon the secondary discharge lamp current showed a direct proportionality between them. The hollow-cathode lamp was therefore operated at the highest current possible. The gas flow rates and height of observation in the flame were not critical factors in regard to the fluores-

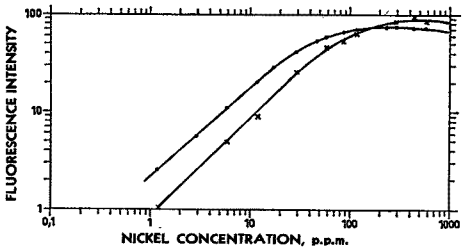

Figure 2. Analytical working curves for nickel fluorescence intensities with the air–hydrogen flame

O 232 mμ
× 352 mμ

cence intensity. However, the water droplets in the flame scattered the radiation from the hollow-cathode and caused an appreciable background signal. For that reason the lowest flow rate of air at which maximum fluorescence could be attained was used. Also, measurements were made in the highest portion of the flame where dispersion of droplets and evaporation of water were more complete. The region of the flame observed was 50 to 70 mm. above the burner tip.

An investigation of the nickel fluorescence signal and the noise level at 232 mμ as a function of the monochromator slitwidth showed that the widest slitwidth possible, which was 2.0 mm., gave the highest signal-to-noise ratio. This unexpected result can be attributed to the following three factors. Most important was the relative absence of signal noise caused by the nonfluorescence radiation from the air–hydrogen flame. Although the fluorescence signal was modulated, comparable data taken with the same burner using oxygen instead of air gave a prohibitively high noise level at slitwidths greater than 1.0 mm., even when only pure water was aspirated into the flame. Thus it was apparent that modulation did not allow complete isolation of the fluorescence signal from the unmodulated emission. A second reason for the improved results using a wide slitwidth was the contribution of fluorescence emission from nickel lines other than the 232.0-mμ line. As the slit was opened from 0.4 to 2 mm. and the bandwidth increased from 0.4 to 2.0 mμ, the intensity increased approximately to the 1.4 power of the slitwidth. Had only one line been observed, the intensity would have been proportional to the first power of the slitwidth, as was the case for slitwidths below 0.4 mm. On the other hand, if a continuum were observed, the intensity would have been proportional to the second power of the slitwidth. The 231.1-mμ resonance line and the 231.2-mμ, 231.4-mμ, and 231.7-mμ atomic nickel lines all have high transition probabilities and low lying ground state levels (*2*), and undoubtedly fluorescence emission from these transitions also contributed to the total measured signal. When the nickel fluorescence spectrum was scanned with a slitwidth less than 0.4 mm., two broad peaks, one at 232.0 mμ and the other at 231.1 mμ, could be resolved. A third reason for the observed advantage of a wide slitwidth was that as the slit was opened and the fluorescence signal increased, the noise components from the amplifier and recorder became less significant.

In Figure 2 are given the experimental working curves for the nickel fluorescence intensity *vs.* the nickel concentration at 232 mμ and 352 mμ. Aqueous nickel nitrate solutions were used to obtain these results. The slitwidth at 352 mμ was 0.5 mm. All the experimental points shown have been corrected to account for the signal from the scattered hollow-cathode radiation. Although the measured fluorescence intensity at 232 mμ was not markedly greater than at 352 mμ, the signal at the former wavelength was much more stable. The unmodulated emission at 352 mμ from the turbulent flame caused appreciable noise. The air–hydrogen flame does not have enough energy to produce appreciable nickel emission at 232 mμ, but at 352 mμ the atomic nickel emission is very intense. As the nickel concentration was raised from 1 to 50 p.p.m., the signal-to-r.m.s. noise ratio at 352 mμ increased to a maximum of 20:1. Above 50 p.p.m., the ratio became progressively less. At 232 mμ the signal-to-r.m.s. noise ratio attained a maximum of 70:1 for 100 p.p.m. nickel, and then it remained relatively constant for more concentrated nickel solutions.

The nickel detection limit at 232 mμ was calculated according to the procedure described by Herrmann and Alkemade (*4*). Twenty values of the scattered light intensity were obtained by aspirating twice-distilled water into the flame. The mean intensity $\bar{X}_B$ and the standard deviation σ_B of the values were calculated. Substitution of these two values into the equation

$$X = \bar{X}_B + 3\sqrt{2}\,\sigma_B \qquad (1)$$

gave the meter reading at the detection limit, X. From the working curve the nickel concentration at the detection limit was seen to be 0.3 p.p.m. Four separate fluorescence emission values for a 1-p.p.m. nickel solution had a relative standard deviation of 3.6%. The good analytical reproducibility near the nickel detection limit was the result of the relatively large signal for the pure water solution. Distilled water gave a signal of 1.6 units, and 1-p.p.m. nickel solution gave a signal of 3.8 units. The value 3.8 could be reproduced quite well, however a large portion of that value was due to the scattered light and not to fluorescence. Sufficient data were not taken to correctly calculate a detection limit at 352 mμ, but an estimation of 0.7 p.p.m. based on only a calculation with four values for distilled water can be given.

For the 232-mμ fluorescence line the nickel concentration necessary to give a signal-to-r.m.s. noise ratio of 0.75:1 was calculated so that a comparison between the results of this work and earlier publications (*5, 9*) could be made. When pure water was aspirated into the flame, the r.m.s. noise level of the signal was 0.3 unit. Thus a nickel concentration of 0.1 p.p.m. would have given the desired signal-to-noise ratio.

A brief investigation of the fluorescence intensity at 232 mμ from an oxygen–hydrogen flame was performed with the same burner to determine if in the hotter oxygen–hydrogen flame more nickel atoms would be formed. This would result in additional fluorescence emission. As in the case of the air–hydrogen flame, the fluorescence intensity was not critically dependent on the gas flow rates. A maximum emission was obtained with 4.3 liters per minute of oxygen and 15.5 liters per minute of hydrogen. At higher oxygen flow rates the fluorescence signal was not enhanced and the noise level was somewhat greater. Because the oxygen–hydrogen flame gave much more background radiation at 232 mμ than the air–hydrogen flame, the slit was closed 1.0 mm., and then the comparison between the two flames was carried out.

A 100-p.p.m. nickel solution aspirated into the oxygen–hydrogen flame gave slightly less fluorescence emission than that obtained from the air–hydrogen flame with a 1.0-mm. slitwidth. Moreover the signal-to-r.m.s. noise ratio with the oxygen–hydrogen flame was only 20:1, whereas it was 60:1 with the air–hydrogen flame. The noise level from the oxygen–hydrogen flame was even greater than that observed with

the air–hydrogen flame and a slitwidth of 2.0 mm. It is evident that the cooler air–hydrogen flame is as efficient for producing nickel atoms as the oxygen–hydrogen flame.

Additional spectral regions where nickel fluorescence emission could be expected were investigated with the air–hydrogen flame. The slitwidth was reduced to 0.2 mm. to better resolve the lines. A number of nickel fluorescence emission peaks were observed and are given in Table I with their relative intensities. None of the intensity measurements were corrected for the phototube response or the monochromator transmission characteristics. Since the bandwidth was about 1.0–1.5 mμ in the spectral region between 300 and 360 mμ, each peak consisted of more than one fluorescence emission line.

The use of atomic fluorescence flame spectrometry for the analytical determination of nickel appears to be very promising. A severe limitation to the fluorescence technique with the apparatus used was the short range in which the analytical working curves were linear. However, it is believed that significant improvements can be made in the nickel detection limits and the linear range of the analytical curves. The hollow-cathode radiation can be easily increased when a power supply, capable of supplying greater current to the secondary discharge of the lamp, is available. In addition, the hollow-cathode radiation could be passed through the flame an additional number of times. The elimination of the water droplets in and around the flame would also lead to improved results. The addition of a burning sheath of air and hydrogen that surrounds the flame would reduce the amount of scattered source radiation and increase the rate of nickel atom production. The sheath would more efficiently evaporate water droplets and salt particles that escape from the side of the flame without sacrificing the sample flow rate or worsening the problem of self-absorption. Also, the sheath would reduce the turbulence of the flame (*3*) and thereby stabilize the fluorescence emission. Using organic solvents would increase the solvent evaporation, but a disadvantage would be the resulting increased noise level caused by the additional flame background emission.

A detailed study of chemical interferences with the nickel fluorescence emission has not as yet been undertaken. It was noticed that nickel sulfate solutions between 10 and 50 p.p.m. nickel gave about 25% less fluorescence emission than the corresponding nickel nitrate solutions. Also, the presence of 0.02*M* lanthanum nitrate enhanced the fluorescence emission of a 50-p.p.m. nickel nitrate solution 15%. Since the atomic fluorescence intensity is dependent upon the number of nickel atoms in the ground state, the chemical interferences encountered should be similar to those reported for comparable atomic absorption techniques. Although interferences arising from changes in the quenching of the fluorescence radiation were not investigated, it is believed that significant variation in the degree of quenching will occur only if the gases added to the flame or the type of solvent is altered. Under normal analytical conditions these variables are maintained constant. The author has studied many cation and anion interferences with the nickel absorption and emission in oxygen–hydrogen and oxygen–acetylene flames (*1*). The results should be helpful for predicting chemical interferences in the air–hydrogen flame.

A spectral interference with the fluorescence emission will occur only if two conditions are fulfilled. First, there must be an appropriate emission line of the interferent element present in the radiation source spectrum, and second, the fluorescence emission line of the interferent element must lie within the spectral bandwidth of the monochro mator. This is likely to happen if a very intense, continuous radiation source is used to produce fluorescence emission, but not when line sources for individual elements are employed. Shortly after this work was submitted for publication an excellent paper appeared (*8*) in which a continuous source was successfully used to obtain fluorescence emission.

The availability of high intensity hollow-cathodes for elements other than nickel should in the near future greatly increase the number of metals that can be analyzed by atomic fluorescence flame spectrometry.

Table I. Relative Intensities of Observed Atomic Nickel Fluorescence Lines

Wavelength, mμ	Rel. intensity
352	10
342	5.2
346	4.4
349	4.0
362	4.0
300	3.0
305	2.6
339	2.4
232	2.0
337	2.0
304	1.4
357	1.2

ACKNOWLEDGMENT

The author is very grateful to R. Herrmann and W. Lang for their helpful suggestions and interest in this project.

LITERATURE CITED

(1) Armentrout, D. N., Ph.D. thesis, Cornell University, Ithaca, N. Y., 1965.
(2) Corliss, C. H., Bozman, W. R., *Nat. Bur. Std. (U.S.) Monograph* **53** (1962).
(3) Gilbert, P. T., *Intern. Conf. Spectry.*, College Park, Md., June 1962.
(4) Herrmann, R., Alkemade, C. T. J., "Chemical Analysis by Flame Photometry," 2nd. ed., p. 257, P. T. Gilbert, trans., Interscience, New York, 1963.
(5) Mansfield, J. M., Winefordner, J. D., Veillon, Claude, ANAL. CHEM. **37**, 1049 (1965).
(6) Robinson, J. W., *Anal. Chim. Acta* **24**, 254 (1961).
(7) Sullivan, J. V., Walsh, A., *Spectrochim. Acta* **21**, 721 (1965).
(8) Veillon, Claude, Mansfield, J. M., Parson, M. L., Winefordner, J. D., ANAL. CHEM. **38**, 204 (1966).
(9) Winefordner, J. D., Stabb, R. A., *Ibid.*, **36**, 165 (1964).

D. N. ARMENTROUT

Abteilung für Med. Physik
Univ.-Hautklinik
63 Giessen, Germany

RECEIVED for review February 4, 1966. Accepted April 25, 1966. Investigation supported by Public Health Service Fellowship 1-F2-GM-28, 353-01 from the National Institute of General Medical Sciences.

Application of the Rule of Six to the Separation of Diastereoisomeric Esters by Gas—Liquid Chromatography

An Exchange of Comments

SIR: A recent paper on the separation of diastereoisomeric esters by gas–liquid chromatography attributed the degree of resolution to a possible combination between bulk dissymmetry and the distance between the two optical centers (*7*). It was concluded that the data obtained were suggestive of certain steric effects, particularly in regard to an energetic preference for a favorable conformational distribution at the *alcoholic asymmetrical carbon atom* of a diastereoisomeric ester. The improved resolutions noted with the polar liquid phase [1,2,3-tris-(2-cyanoethoxy)-propane], as contrasted to the nonpolar phase (silicone oil), must be due to a strong secondary bond interaction between the lactic ester carbonyl and the cyanoethoxy moiety. The same suggestion has been invoked for the resolution of some diastereoisomeric esters on an optically active substrate, and a somewhat related gas chromatographic separation of diastereoisomeric alcohols has been explained by an analysis of various conformational influences on intra- and intermolecular hydrogen-bond formation (*3*, *4*). Likewise, the variance in R_f values on Sephadex liquid–solid chromatography for several diastereoisomeric dipeptides is attributed to the formation of a hydrogen-bond stabilized ring formation in the DL compounds, while the LL dipeptides reside selectively in the open chain conformation (*9*).

A generalized concept of the effects observed here in the gas chromatography of the diastereoisomeric esters is in the possible operation of the "Rule of Six" (*6*). Commencing the count with the carbonyl oxygen, then the number of atoms in position six is called the "six number" and varies from 6 in 2-hexyl *O*-acetyllactate (Ia) to 3 for the corresponding 2-methyl-1-pentyl (Ib) and 3-methyl-1-pentyl (Ic) esters. The essential data are summarized in Figure 1. It is assumed that the normally coiled structure of the atom chain allows the atoms in the six position to approach the oxygen more closely and indirectly block additions to the carbonyl group from certain directions. A high six number is therefore directly associated with increased steric hindrance to secondary bond formation. As the magnitude of this effect will be dependent on absolute configuration, it will be different for each diastereoisomer and so lead to a corresponding separation of isomers for Ia. Again, a low six number is connected with the formation of a stronger secondary bond with both diastereoisomers, and this condition ultimately furnishes a poorer resolution for Ib and Ic. This argument fits the results described earlier for the hexyl esters and has been applied with equal success to the actual gas chromatographic retention patterns given by eight diastereosiomeric dipeptides (*5*). It is evident that an improved resolution is seen directly as an increase in the relative retention times or α value, which is related to a more negative Δ (ΔG°) sum.

Another series of secondary esters was chromatographed in the paper under discussion, but a modified explanation is required for these compounds. Although these derivatives have the same over-all six count, there is considerable variation in the number of six hydrogens and carbons. The necessary information is summarized in Figure 2. It would appear that excessive branching of the alkyl side chain will hinder the development of the secondary bond in one diastereoisomer, but not in the related conformer. A separation would be expected for the *t*-butyl ester, which possesses three methyl groups, but not for the ethyl ester where there is no alkyl branching. This explanation confirms the resolution patterns drawn for these compounds—poor for IIa, moderate for IId, and good for IIe. The six number does not distinguish between IIa–c, as the count remains constant, and small alkyl eclipsing (skew) factors are dominant here (*2*, *8*). This latter suggestion may be associated with the slow rise in the number of six carbons, due to branching, in this particular series of compounds.

The proposal is ventured that the preparation and gas chromatography of 3,3 - dimethyl - 2 - butyl - *O* - acetyllactate (Id) will produce an excellent α value, as it contains the elements of maximum methyl interaction, yet retains the net six number for this particular group of compounds. It is recognized that 2-methyl-3-pentyl-*O*-acetyllactate (Ie) has an identical six pattern, but an inferior separation is expected here as severe alkyl eclipsing and inter-

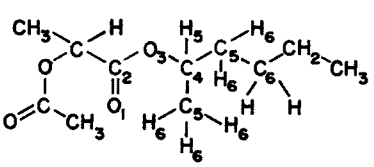

Ester	Structure	6 No.	6 C's	6 H's
Ia	$-CH(CH_3)CH_2CH_2CH_2CH_3$	6	1	5
Ib	$-CH_2CH(CH_3)CH_2CH_2CH_3$	3	2	1
Ic	$-CH_2CH_2CH(CH_3)CH_2CH_3$	3	2	1
Id	$-CH(CH_3)C(CH_3)_3$	6	3	3
Ie	$-CH(C_2H_5)CH(CH_3)_2$	6	3	3

Figure 1. Six numbering system for Hexyl esters

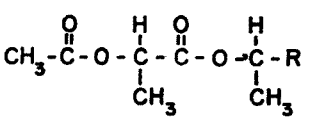

Ester	R	6 No.	6 H's	6 C's
IIa	$-C_2H_5$	6	5	1
IIb	$-C_3H_7$	6	5	1
IIc	$-C_4H_9$	6	5	1
IId	$-CH(CH_3)_2$	6	4	2
IIe	$-C(CH_3)_3$	6	3	3

Figure 2. Diastereoisomeric esters of secondary alcohols

nal strain effects begin to play increased roles at this point (*1*).

In a reply to this Communication (see following Comment), it has been said that the Rule of Six would favor a separation of 3-heptyl-*O*-acetyllactate over 2-hexyl-*O*-acetyllactate; yet, the reverse situation is actually observed on gas chromatography. As stated previously, a clear distinction cannot be made between two compounds when the six count remains constant and a six carbon summation may be the deciding factor. An inspection indicates that the 3-heptyl ester possesses more internal strain than the 2-hexyl ester because of a pronounced 1,6-methyl interaction. On this basis, the 2-hexyl-*O*-acetyllactate should give a better separation than 3-heptyl-*O*-acetyllactate.

In conclusion, one might seek further quantitative data to support and possibly extend the suggested role of steric factors, computed empirically by the Rule of Six, in the separation of diastereoisomers by gas chromatography. A measurement and discussion of diffusion coefficients for the various compounds in the liquid phases mentioned here would certainly furnish valuable supplemental data.

LITERATURE CITED

(1) Cram, D. J., "Steric Effects in Organic Chemistry," M. S. Newman, ed., p. 270, Wiley, New York, 1956.
(2) Dauben, W. G., Pitzer, K. S., *Ibid.*, p. 1.
(3) Galt, Y., Felkin, H., *Bull. Soc. Chim. France* **1965**, 742.
(4) Gil-Av, E., Feibush, B., Charles-Sigler, R., *Tetrahedron Letters* **1966**, 1009.
(5) Halpern, B., Westley, J. W., Weinstein, B., *Nature* **210**, 837 (1966).
(6) Newman, M. S., "Steric Effects in Organic Chemistry," M. S. Newman, ed., p. 206–8, Wiley, New York, 1956.
(7) Rose, H. C., Stern, R. L., Karger, B. L., ANAL. CHEM. **38**, 469 (1966).
(8) "Stereochemistry of Carbon Compounds," E. L. Eliel, p. 124, McGraw-Hill, New York, 1962.
(9) Wieland, T., Bende, E., *Chem. Ber.* **98**, 504 (1965).

BORIS WEINSTEIN
Department of Chemistry
Stanford University
Stanford, Calif. 94305

WORK supported by the National Institutes of Health under Grant No. GM-12120-01.

SIR: In the previous paper Weinstein (*4*) has invoked Newman's Rule of Six as a generalized concept of the effects observed in a publication by Rose, Stern, and Karger (*3*) (R.S.K.) on the gas chromatographic separation of diastereoisomeric esters. The Rule of Six correctly predicts several of the trends observed in the R.S.K. paper and therefore, the rule is to be recommended as a first order approximation of the causes of diastereoisomeric ester separation.

We wish, however, to place the Rule of Six in proper perspective. As Newman states in describing his rule (*2*): "It should be emphasized that the Rule of Six is empirical and is to be used only as a substitute for molecular models. The examination of models is the best way of estimating steric factors." One must examine structure, configuration, and conformation in order to elucidate the factors responsible for separation, as we have partially done in our original paper (*3*).

Weinstein, himself, agrees that the Rule of Six cannot explain the change in $\Delta(\Delta G°)$ values for compounds IIa–IIc of his paper, in which the six count remains constant. He suggests small alkyl eclipsing, a rather vague term, to explain this trend. He further predicts that 3,3-dimethyl-2-butyl-*O*-acetyllactate (Id) should produce a better separation than 2-methyl-3-pentyl-*O*-acetyllactate (Ie) due to severe alkyl eclipsing and internal strain. We have recently examined compounds Id and Ie, and the Weinstein prediction is correct as shown in Table I. However, a more reasonable way of looking at this result is in terms of a change in the time average population of preferred conformations at the alcoholic asymmetric center, compound Id being more conformationally rigid than compound Ie (*1*).

A striking example of the failure of the Rule of Six can be seen in a comparison of compounds Ia (2-hexyl-*O*-acetyllactate) and If (3-heptyl-*O*-acetyllactate) in Table II. Applying the ideas of Weinstein, compound If should produce a better separation than Ia because, while the six number is the same, the number of alkyl groups in the six position is greater in If. However, compound If is 32 cal./mole smaller in $\Delta(\Delta G°)$ than compound Ia.

A detailed interpretation of the mechanism of diastereoisomeric ester separations in terms of preferred conformation at both the acidic and alcoholic asymmetric centers will shortly be published (*1*). This interpretation not only agrees with the trends observed, but also is able to explain the fact that the LD-DL racemic ester pair always has a longer retention time than the DD-LL pair.

In conclusion, while the Rule of Six may be a useful empirical method for predicting the relative degree of separation, it is not useful if one is concerned with the details of the mechanism of separation. In order to understand the many and subtle effects responsible for separation, a detailed examination of steric and electronic effects is necessary.

LITERATURE CITED

(1) Karger, B. L., Stern, R. L., Rose, H. C., Keane, W., Sixth International Symposium on Gas Chromatography and Associated Techniques, Sept. 20–23, 1966, Rome, in press.
(2) Newman, M. S., "Steric Effects in Organic Chemistry," M. S. Newman, ed., p. 206 (footnote), Wiley, New York, 1956.
(3) Rose, H. C., Stern, R. L., Karger, B. L., ANAL. CHEM. **38**, 469 (1966).
(4) Weinstein, B., *Ibid.*, p. 1238.

BARRY L. KARGER
ROBERT L. STERN
Department of Chemistry
Northeastern University
Boston, Mass. 02115

WORK supported by the National Science Foundation under Grant No. GP-5742.

Table I. Separation Data on 20% 1,2,3-Tris(2-Cyanoethoxy) Propane AW Chromosorb P, DMCS, T = 125° C.

Compound	$\Delta(\Delta G°)$, cal./mole
(Id) 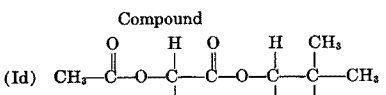	−80
(Ie) 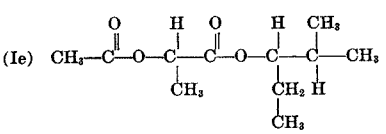	−36

Table II. Separation Data on 20% 1,2,3-Tris-(2-Cyanoethoxy)Propane AW Chromosorb P, DMCS. T = 125° C.

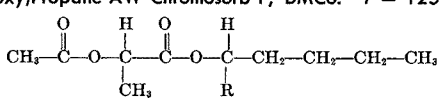

Ester	R	6No	6C's	6H's	$\Delta(\Delta G°)$ cal./mole
Ia	$-CH_3$	6	1	5	−65
If	$-CH_2CH_3$	6	2	4	−33

p-Bis-(o-Methylstyryl)Benzene, Useful Secondary Fluor for Liquid Scintillation Counting

SIR: Our laboratory routinely runs several different radioassays for enzyme activity which require the use of a liquid scintillation counter. The solvent systems required for these assays are all different, but the primary and secondary solutes employed as fluors are common to all systems. Diamine oxidase activity (*3*) is assayed using toluene, monoamine oxidase activity (*4*) is assayed using anisole, and histidine decarboxylase activity (*2*) is assayed using a mixture of dioxane, anisole, and dimethoxyethane (DAD). The radioactive substrate for the various enzyme determinations is usually assayed in a toluene–ethanol mixture. The primary fluor used is 2,5-diphenyloxazole (PPO) and the secondary fluor is *p*-bis-[2-(4-methyl-5-phenyloxazolyl)]benzene (dimethyl POPOP). A new secondary fluor, *p*-bis-(*o*-methylstyryl)benzene, (bis-MSB) has recently become available commercially. This secondary fluor was substituted directly in place of dimethyl POPOP in four of our liquid scintillation counting solvent systems and an increase in counting efficiency was observed in every case (Table I).

EXPERIMENTAL

Materials. Tritiated water, 1.368×10^6 d.p.m./ml., tritiated toluene, 2.14×10^6 d.p.m./ml., and C^{14} toluene, 3.83×10^5 d.p.m./ml. were obtained from New England Nuclear Corp. C^{14}-carboxyl-labeled DL-histidine (Merck, Sharpe, and Dohme, Canada) was made up to contain 1.91×10^5 d.p.m./10 μg. DL-histidine/0.1 ml. aqueous solution. PPO and bis-MSB were obtained from Pilot Chemical, Inc. Dimethyl POPOP was obtained from Arapahoe Chemicals, Inc. All solvents were reagent or analytical grade from Distillation Products or Fisher Scientific Co.

Apparatus. The liquid scintillation counters used were a Packard, Model 314 EX-2, and a Nuclear-Chicago, Model 725. For carbon-14 assay, one pair of discriminators (channel 1) was set so that approximately 50% of the carbon spectrum including the 156-k.e.v. beta emission was in the window. The second pair of discriminators (channel 2) was set so that approximately 75% of the carbon spectrum including the 156-k.e.v. beta emission was in the window. The ratio, channel 1/channel 2, is an accurate monitor for absolute counting efficiencies between 15 to about 55% (*1*). For tritium assays, the discriminators were set for the best figure of merit (efficiency^2/background) and the counting efficiency was determined by the addition of an internal standard.

Solvents Systems. TOLUENE. Toluene contained 0.5% PPO and 0.01% of either dimethyl POPOP or bis-MSB. To 10 ml. of this solution was added either 38,300 d.p.m. of C^{14} toluene (0.1 ml.) or 214,000 d.p.m. of tritiated toluene (0.1 ml.).

ANISOLE. Anisole contained 0.6% PPO and 0.01% of either dimethyl POPOP or bis-MSB. To 10 ml. of this solution was added either 38,300 d.p.m. of C^{14} toluene (0.1 ml.) or 214,000 d.p.m. of tritiated toluene (0.1 ml.).

TOLUENE–ETHANOL. This mixture contained 7 parts toluene to 3 parts absolute ethanol (v./v.), 0.35% PPO, and 0.01% of either dimethyl POPOP or bis-MSB. To 10 ml. of this mixture was added 0.2 ml. of water containing either 273,600 d.p.m. of tritium (as water) or 191,000 d.p.m. of C^{14} as DL-histidine (10 μg.).

DAD. This mixture contained 6 parts dioxane, 1 part anisole, 1 part DAD (v./v.), 0.7% PPO, and 0.005% of either dimethyl POPOP or bis-MSB. To 15 ml. of DAD was added 2 ml. of water containing either 191,000 d.p.m. of C^{14} as DL-histidine (10 μg.) or 273,600 d.p.m. of tritium (as water).

DISCUSSION

Similar results were obtained with the Packard and the Nuclear-Chicago liquid scintillation counters. No attempt was made in this survey to determine optimum concentrations of the fluors used. In view of the fact that a modest improvement in counting efficiency was noted in every case by the direct substitution of bis-MSB for dimethyl POPOP in the radioassay solvent mixtures used in our laboratory, this observation is reported as a possible aid to others who may be seeking means of improving counting efficiency. It should be noted, however, that there was no apparent relationship between the improvement in counting efficiencies due to the bis-MSB and the absolute counting efficiencies. It is entirely possible that a systematic study of varying concentrations of primary and secondary fluors will lead to even greater gains than these reported here.

Table I. Effect of Substituting bis-MSB as a Secondary Fluor for Dimethyl-POPOP in Various Solvent Systems Used in Liquid Scintillation Counting

	Carbon-14			Tritium		
Solvent system	bis-MSB, c.p.m.	Dimethyl POPOP, c.p.m.	Increase, %	bis-MSB, c.p.m.	Dimethyl POPOP, c.p.m.	Increase, %
Toluene	21,600	21,000	2.8	51,000	50,700	0.7
Anisole	15,200	13,400	13.4	43,500	38,600	12.7
Toluene–EtOH	41,500	39,200	5.8	16,600	15,900	4.4
DAD	60,000[a]	55,600[a]	7.9	14,600	13,200	10.6

All counts are averages of duplicate samples counted a total of 30 minutes.

[a] Counted at higher gain settings because of severe quenching.

ACKNOWLEDGMENT

The author gratefully acknowledges the technical assistance of Robert J. Seymour and Jacob Kupelian.

LITERATURE CITED

(1) Baillie, L. A., *Intern. J. Appl. Radiation Isotopes* **8**, 1 (1960).
(2) Kobayashi, Y., *Anal. Biochem.* **5**, 284 (1963).
(3) Okuyama, T., Kobayashi, Y., *Arch. Biochem. Biophys.* **95**, 242 (1961).
(4) Otsuka, S., Kobayashi, Y., *Biochem. Pharmacol.* **13**, 995 (1964).

YUTAKA KOBAYASHI

Worcester Foundation for Experimental Biology
222 Maple Ave.
Shrewsbury, Mass. 01545

Supported, in part, by Contract AT(30-1) 2085 with the U. S. Atomic Energy Commission.

Relative Efficiency of a New Liquid Scintillation Fluor, p-Bis-(o-Methylstyryl) Benzene

SIR: This report compares a recently announced secondary solute for liquid scintillation counting, *p*-bis-(*o*-methylstyryl) benzene (bis-MSB) with two previously available fluors. The conditions which must be specified when comparing fluors are discussed in a recent study (*1*) of relative efficiencies among some primary and secondary solutes in liquid scintillation counting. The usefulness of a secondary solute depends upon the optics of the counter being used (*4*) and upon the kind and degree of quenching in the sample. At low concentrations, a secondary solute functions as a wavelength-shifter by absorbing the emission of the primary fluor and reemitting at a longer wavelength. Because this process is less than 100% efficient, the resulting loss of light is compensated only if the longer wavelength results in a sufficient increase in multiplier phototube sensitivity, in reflectivity of the counting chamber, and/or transmission in the counting chamber and sample. A counter in which Lucite was interposed between the sample and the multiplier phototube was found (*1*) to be more wavelength-sensitive than those which had an air gap only. In some modern commercial counters the addition of a secondary solute to an unquenched sample of primary solute caused a small decrease in counting efficiency, and in others an increase.

At higher concentrations the secondary solute may function in some cases to increase the light output from the sample. Two additional excitation mechanisms become important at high secondary concentration: radiationless transfer of energy from the primary fluor (*2*) and direct solvent excitation. In the latter case the secondary is acting as a primary solute. (Because it is usually considerably less soluble than a good primary, it will not, in general, give as great an efficiency when used alone. A high concentration of a secondary may be between 0.2 and 4 grams/liter.)

These last two mechanisms contribute to the increase in efficiency observed when a secondary is added in sufficient quantity to samples containing certain chemical (colorless) quenching agents. Although solvent quenching by chemical quenchers predominates over direct quenching of fluors, some halogen compounds, ketones, acids, and bases quench the fluor molecules as well as the solvent. The primaries which emit at short wavelengths are in general more quenched than the secondaries. If a secondary is present in sufficient concentration, it may compete with the quencher for the excitation energy of the primary through radiationless transfer, recovering for light production some energy which would otherwise be lost. It may also act as a less-quenched primary. It was of interest to test the effectiveness of the new fluor in reducing quenching, as well as in the role of wavelength-shifter.

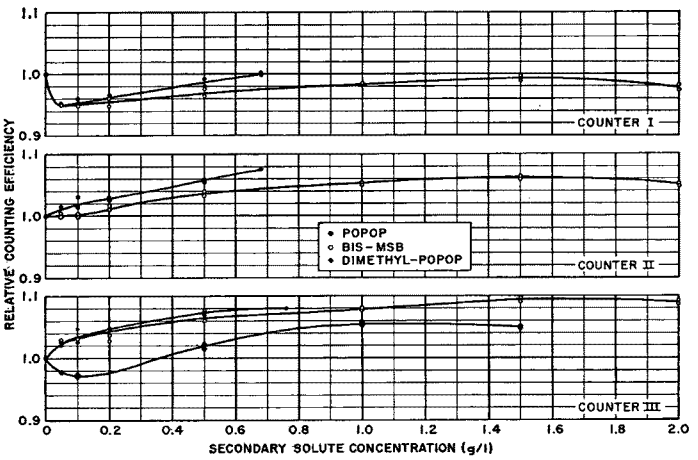

Figure 1. Tritium counting efficiencies as a function of concentration of secondary solute in unquenched samples containing 4 grams/liter PPO, in three liquid scintillation counters

EXPERIMENTAL

Bis-MSB samples and PPO (2,5-diphenyloxazole) were obtained from Pilot Chemicals, Inc. POPOP (*p*-bis-2-(5-phenyloxazolyl)-benzene) and dimethyl-POPOP were obtained from Arapahoe Chemicals, Inc. Reagent grade toluene was used as the solvent, and toluene-H^3 was used to label all samples, which were in equilibrium with air. Counting was performed in Nuclear-Chicago Corp. Model 725 spectrometers with both quartz-face and glass multiplier phototubes, and in a Packard Instrument Co. Model 3002.

RESULTS AND DISCUSSION

A range in counter response to wavelength-shifting is shown in Figure 1, where counting rates of unquenched samples containing secondary solute + 4 grams/liter PPO are given relative to that of a sample containing the PPO only. The top two sets of curves were obtained with Nuclear-Chicago counters and the lower set with a Packard counter. The latter shows the greatest change in sensitivity with wavelength, as indicated by the steeper initial rise in efficiency with secondary concentration [at a concentration of 0.05 gram/liter wavelength-shifting is virtually total, as shown by spectrofluorometric measurements by the author and by others (*3*)]. Differences between counters with identical optics are attributable to variation among individual multiplier phototubes. Counter I shows the least change in sensitivity with wavelength and illustrates the loss in efficiency which may be suffered when only a small amount of secondary solute is added.

The increase in efficiency at higher concentrations is the contribution from the secondary solute functioning as a primary. In the absence of PPO, at concentrations of 0.6 and 2 grams/liter, respectively (nearly maximal at 4° C.), POPOP and bis-MSB gave H^3 efficiencies of 17% and 28.5% in Counter I. A saturated solution of dimethyl-POPOP (<2 grams/liter) gave 26%. In any counter, if a secondary solute is to be used at all, it is best used at a high concentration. This is true for both quenched and unquenched samples.

In the presence of quenching agents which do not directly quench fluors, but are solvent quenchers only—i.e., the majority of sample components encountered in liquid scintillation counting—the relative efficiencies of samples containing these secondary solutes are expected to be the same as in unquenched samples (*1*). The detection of any direct fluor quenching effect by a quenching agent is best made by a spectrofluorometric measurement, in

which solvent quenching can be bypassed by exciting only the fluor. Such data have not been obtained for bis-MSB and dimethyl-POPOP. Previous spectrofluorometric studies, however, showed that those compounds which caused substantial quenching of other long wavelength fluors did so only at concentrations which were prohibitively high for liquid scintillation counting, because of their concurrent severe solvent quenching. Although some compound may be encountered which will severely quench one of these secondaries and alter its efficiency relative to the others, this is expected to occur only rarely.

Because in many counters the principal usefulness of a secondary solute is in compensating for direct quenching of the primary solute, the three secondaries were compared for effectiveness in samples containing one of three compounds known to quench PPO: CCl_4, 4-hydroxy-4-methyl-2-pentanone, or PPO itself at 30 grams/liter. This latter is particularly important because the optimal primary solute concentration may be quite high in the presence of other quenching agents. Each secondary was used at or near its maximal concentration at 4° C.: POPOP at 0.6 gram/liter, bis-MSB at 2 grams/liter, and dimethyl-POPOP at saturation (a precipitate formed when samples at 2 grams/liter were cooled to 4° C.). With each quencher, efficiency was improved by the secondaries in the order bis-MSB > dimethyl-POPOP > POPOP. Tritium efficiencies in samples with bis-MSB were 1.1 to 1.2 times those in POPOP samples, while dimethyl-POPOP samples were 1.03 to 1.07 times more efficient than POPOP. The relative efficiencies vary somewhat with the kind and degree of quenching, but the values observed in these experiments are indicative of the order of magnitude to be expected.

When comparisons were made at equal concentrations by weight of secondary solute, efficiencies with POPOP were 1.01–1.03 times those with bis-MSB in samples with 30 grams/liter PPO, and were 1.08–1.18 times those with dimethyl-POPOP with each of the quenching agents. The order POPOP > bis-MSB > dimethyl-POPOP is the same as for unquenched samples.

The chief advantage of the new fluor, bis-MSB, is its higher solubility. It should find its greatest usefulness at high concentrations in samples in which the primary fluor is quenched by some other sample component or through self-quenching.

LITERATURE CITED

(1) Bush, E. T., Hansen, D. L., "Radioisotope Sample Measurement Techniques in Medicine and Biology," p. 395, International Atomic Energy Agency, Vienna, 1965.
(2) Birks, J. B., "The Theory and Practice of Scintillation Counting," p. 314–15, Macmillan, New York, 1964.
(3) Hayes, F. N., *et al.*, U. S. At. Energy Comm. *Rept.* LA-1639 (1953).
(4) Ott, D. G., "Liquid Scintillation Counting," C. G. Bell, F. N. Hayes, eds., p. 101–7, Pergamon Press, Oxford, 1958.

ELIZABETH T. BUSH

Nuclear-Chicago Corp.
333 E. Howard Ave.
Des Plaines, Ill.

The Rate of Oxidation of Platinum Electrodes

SIR: Feldberg, Enke, and Bricker (*2*) have reported that the oxidation charge accumulated at constant potential in the anodic oxidation of platinum in perchloric acid is proportional to the logarithm of oxidation time over a wide range of time and applied potential. Quite similar results were obtained by Smith (*6*) in sulfuric acid solution. The first authors have given an interpretation of this behavior by writing a conventional electrochemical rate equation and making the assumption that the forward rate constant decreases with increased oxidation of the surface in an exponential manner. The origin of this Temkin-like behavior is uncertain, but the introduction of an exponential term of this kind appears to be justified by experimental data. Such a treatment implies that the slope of the oxidation charge *vs.* log time curve should be independent of potential at high oxidation potentials. At lower oxidation potentials, the curves are less linear, and the slopes depend upon potential. The work reported here attempts to extend the treatment to lower potentials.

It is well known that the nature of an anodically oxidized platinum electrode is not completely specified by a specification of the oxidation charge present upon the electrode, but rather, depends strongly upon the time and potential history leading to the formation of the oxide charge. The hysteresis in the anodic and cathodic curves for platinum oxidation and reduction may be cited (*3*).

The magnitude of charge capable of existing on smooth platinum electrodes corresponds in many cases to nine or ten electrons per surface platinum atom, if a roughness factor not much greater than one is taken. This large charge cannot be accommodated by any reasonable oxidation state of surface atoms alone. The fact that oxygen atoms readily reach positions below the surface has been demonstrated by low energy electron diffraction (*7*) and by field ion microscopy (*5*). Recently, Warner and Schuldiner have used the term "dermasorption" for such subsurface oxides (*9*).

It is proposed here that the exponential decay of the rate constant may be taken as the limiting form in a two-step process, the first of which is regarded as an electrochemical reaction at the surface. This is followed by a potential-independent transfer of oxide to the underlying platinum structure. Alternatively, film growth by metal atom transfer may be involved. The two steps are quite different from those discussed by Feldberg, Enke, and Bricker (*2*).

EXPERIMENTAL

Apparatus. The circuitry used for constant potential electrolysis and integration of charges accumulated was similar to that previously described (*1*).

Electrodes. Two types of test electrodes were used. A single crystal platinum electrode approximately 2 mm. in diameter was mounted in the end of a piece of glass tubing with black sealing wax. This electrode had an exposed geometric area of 0.091 $cm.^2$ The second electrode was polycrystalline platinum wire sealed into soft glass tubing. After annealing, this electrode was polished using kerosene-levigated alumina supported on a felt disk mounted on a dental engine. The exposed geometric area was 0.110 $cm.^2$ Electrochemical measurements made with the single crystal were found to be the same as those made with the wire electrode within experimental uncertainty, after allowing for differences in area. Most of the data reported here were obtained with the wire electrode.

Cell and Electrolyte. All electrolyses were made in $0.5M$ H_2SO_4 prepared by diluting reagent grade acid with water distilled from alkaline permanganate in a borosilicate glass still. The electrolyte was freed of oxygen by purging with nitrogen obtained from evaporation of liquid nitrogen and passed over heated copper. The working electrode of platinum gauze in $0.5M$ H_2SO_4 was in a compartment separated from the test electrolyte by a glass frit. Potentials were measured against a saturated calomel electrode connected by a capillary filled with $0.5M$ H_2SO_4. Potentials are herein referred to saturated calomel. Stirring the electrolyte had no effect upon the charges observed;

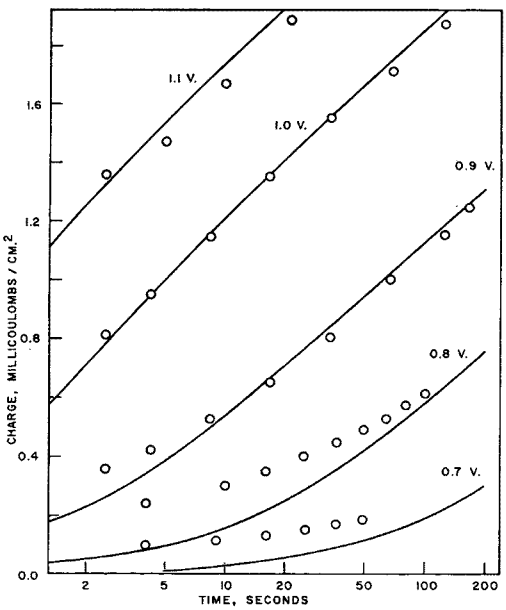

Figure 1. Oxidation charge *vs.* time

Circles, experimental; lines, computed

electrolyses were made in unstirred solution.

Electrode Pretreatment and Storage. Electrodes were stored in 0.5*M* H_2SO_4 under continuous nitrogen purging and kept at +0.2 volt *vs.* S.C.E. It was necessary to treat the electrode in this way for several hours after anodization, to obtain reproducible results. No other treatment was used.

RESULTS AND DISCUSSION

Cyclic Potential Experiments. Starting from a well-reduced electrode, a one-second anodic pulse of constant potential was applied. The potential was then switched to +0.20 volt for one second, then a second one-second anodic pulse was applied, and the sequence continued many times. The charge accumulated was continuously recorded. In separate experiments, anodic potentials of from +0.70 to +0.90 volt were used. The charge consumed at anodic potential was always greater than that released at +0.20 volt. Both charges were transferred very quickly, the current dropping to a very low value in less than the one-quarter second response time of the recorder. Thus there was a fairly rapid oxidation charge, most of which could quickly be recovered. Such charges increased with increasing number of cycles, reaching a steady value in from ten to two hundred cycles, and were greater at higher potentials. Such charges were several hundred microcoulomb cm.$^{-2}$, too large to be accounted for solely from double layer charging. In addition to the recoverable charge, the total charge increased with cycling at an ever diminishing rate but did not approach any steady value at several hundred cycles. A quantitative treatment of the above cannot be given, but the results suggest that the oxidation of platinum be considered as a two-step process, the first of which is rapid and easily reversible, and is followed by a slow, irreversible step. Several hours storage at +0.20 volt was required for complete removal of the charge stored in the slow process.

Anodic Oxidation at Constant Potential. Of the many two-step formulations which could be written, we have chosen one which we believe to be as simple as possible and yet reflect the above observations. Assuming the activity of the oxidized part of the surface is proportional to the fraction of the surface θ/θ_o, we write for the easily reversible surface reaction

$$r_f = k(\theta_o - \theta) \exp \alpha nF(E - E^\circ)/RT \quad (1)$$

$$r_b = k\theta \exp (\alpha - 1)nF(E - E^\circ)/RT \quad (2)$$

where θ is surface charge and θ_o is surface charge at complete coverage, k is the heterogeneous rate constant, and E° becomes the potential at which a half-covered surface is in equilibrium with respect to the electrochemical reaction. The second step, transfer of charge to underlying structure, may be written

$$\frac{d\phi}{dt} = a\frac{\theta}{\theta_o} \exp - c\phi \quad (3)$$

where ϕ is the charge stored in subsurface layers. Here the reverse process can be ignored. The form of Equation 3 is justified only by the observed behavior of platinum at high potentials and long times. The change of surface coverage, then, is

$$\frac{d\theta}{dt} = r_f - r_b - \frac{d\phi}{dt} \quad (4)$$

Total oxidation charge $(\theta+\phi)$ can be obtained by simultaneous integration of Equations 3 and 4, taking the initial charge as zero. These equations were integrated numerically for a variety of parameters, using an International Business Machines Type 650 computer. The equations include a large number of parameters, but certain of these can be evaluated independently, or reasonable values assumed.

At long times, θ should approach an equilibrium value given by equating Equations 1 and 2. Under these circumstances, Equation 3 may be integrated, with the result

$$\phi c = \ln(1 + ac\theta t) \quad (5)$$

Thus, c may be calculated from the slopes of the charge *vs.* ln time curves at long times. For the electrode used here, we find c = 0.0038 microcoulomb^{-1} cm.^{2}, the same as found by Smith (*6*) for a different electrode, but much smaller than that calculated from the data of Feldberg, Enke, and Bricker [(*2*), Figure 12]. We assume θ_o = 960 microcoulomb cm.$^{-2}$ for true surface area, four electrons per surface platinum atom; and a roughness factor of 1.15, essentially that of Laitinen and Enke (*3*). It can be seen that the ratio, $k\theta_o/a$, strongly determines the shapes of the calculated oxidation charge *vs.* $\log_{10}$ time curves, but the absolute values simply determine the positions of the curves on the time axis. A large number of curves were computed using various values of these parameters, with the result that curves of the approximate shapes of the experimental curves could be obtained only if this ratio were taken close to unity. The curves in Figure 1 were obtained using k = 1 sec.$^{-1}$ and a = 1000 microcoulomb sec.$^{-1}$ cm.$^{-2}$ These values imply an exchange current roughly equal to the minimum exchange current needed for polarographic reversibility for dissolved reactants at about millimolar concentration. A value of α = 0.5 has been used, since greatly different values give curves spaced too closely with respect to potential either above or below E°. The parameters,

E° and n, can be adjusted to fit the computed curves to the experimental data with respect to potential, once curves of the proper shape and scale have been obtained. For the curves in Figure 1 we have taken $E^\circ = +1.00$ volt *vs.* S.C.E., but found that n must be taken as approximately 0.5 to obtain a proper spread in charge with respect to potential. We would have preferred to take $n = 1$ to reflect a stepless removal of protons from the solvent sheath on the electrode. Vermilea (*8*) has found that, in the oxidation of tantalum, the activation energy of the primary process is not a simple linear function of potential and that the preexponential factor is a function of potential. Use of these ideas in formulating different forms for Equations 1 and 2 would permit a better fit with a more reasonable value of n. Similar effects could be obtained by allowing α to vary with coverage. Such modifications would introduce additional arbitrariness not justified by available data. No allowance for double layer charging has been made in the computed curves, but this is a small error.

It is not intended to suggest that the above parameters are the correct ones. In particular, it appears that the formulation of surface activity is quite in error. It is suggested, however, that a two-step model involving a nearly reversible surface reaction, followed by an exponential transfer to underlying layers is capable of explaining much of the kinetics of electrochemical oxidation of platinum. It provides for the storage of large amounts of charge in the subsurface form and partially shielded from the influence of applied potential, hence the hysteresis in the reduction of such surfaces; and for the observation that the total charge does not determine the nature of the surface. In this connection, the above computations show large fractions of the total charge in the subsurface form, even at low potentials and short times. It is of interest that equations of the form of Equation 3 have been used to treat the growth of very thin films by place exchange of metal and oxygen atoms (*4*). It should be noted that results similar to, but not identical with, those obtained experimentally above were obtained if charges were measured by cathodic stripping of repeatedly oxidized electrodes, rather than by direct oxidation of well-reduced electrodes.

LITERATURE CITED

(1) Booman, G. L., Morgan, E., Crittenden, A. L., *J. Am. Chem. Soc.* **78**, 5533 (1956).
(2) Feldberg, S. W., Enke, C. G., Bricker, C. E., *J. Electrochem. Soc.* **110**, 826 (1963).
(3) Laitinen, H. A., Enke, C. G., *Ibid.*, **107**, 773 (1960).
(4) Lanyon, M. A. H., Trapnell, B. M. W., *Proc. Roy. Soc.* **A227**, 387 (1955).
(5) Muller, E. W., "Structure and Properties of Thin Films," C. A. Neugebauer, J. B. Newkirk, D. A. Vermilea, eds., p. 476, Wiley, New York, 1959.
(6) Smith, J. G., Thesis, University of Washington, Seattle, 1960.
(7) Tucker, C. W., *J. Appl. Phys.* **35**, 1897 (1964).
(8) Vermilea, D. A., *J. Electrochem. Soc.* **102**, 655 (1955).
(9) Warner, T. B., Schuldiner, S., *Ibid.*, **112**, 853 (1965).

KARL H. POOL[1]
JAMES G. SMITH[2]
A. L. CRITTENDEN

Department of Chemistry
University of Washington
Seattle, Wash. 98105

[1] Present address, Department of Chemistry, Washington State University, Pullman, Wash.
[2] Present address, Pennsalt Chemicals Corporation, King of Prussia, Pa.

Quantitative Determination of Individual Tocopherols by Thin Layer Chromatographic Separation and Spectrophotometry

SIR: The natural antioxidants such as the tocopherols are important factors affecting the shelf life of vegetable oils. The fact that the various tocopherols differ considerably both in their biological activities and in their ability to protect these oils from oxidative degradation emphasizes the need for good analytical methods. The high molecular weight and chemical similarity of the various tocopherols have hindered their efficient separation.

In the past few years a number of workers have reported thin layer chromatographic systems for the separation of the tocopherols (*1*, *2*, *7–12*). Several analytical methods have been reported which utilize such separation. Seher (*10*) determined the tocopherols semiquantitatively from the area of the spot obtained on the thin layer plate. Dilley and Crane (*2*) determined the tocopherol content, after thin layer separation, from the absorbance difference obtained after a two-step procedure involving oxidation followed by reduction. Katsui, Ichimura, and Nishimoto (*7*) analyzed only standard α-tocopherol solutions using the Emmerie–Engel reagent.

The method described here was developed for the analysis of tocopherols in peanut oil and involves saponification of the oil sample and the separation of the tocopherols in the nonsaponifiable fraction by thin layer chromatography. The α-, γ-, and δ-tocopherols were removed from the thin layer plate and determined spectrophotometrically by the Tsen (*13*) modification of the Emmerie–Engel method for total tocopherols (*3*) using bathophenanthroline. This modification increases the sensitivity of the original Emmerie–Engel procedure 2.5 fold. The method was applied to peanut oil samples and the precision of the method was evaluated.

EXPERIMENTAL

Reagents. All reagents were of analytical grade. Bathophenanthroline was purchased from the G. Frederick Smith Chemical Co.; α-tocopherol was obtained from Merck and Co., Inc.; β-, γ-, and δ-tocopherol were obtained from Hoffmann-LaRoche, Inc. The bathophenanthroline reagent was $6.0 \times 10^{-3}M$ in ethanol and was stored in an amber bottle in the refrigerator. The ferric chloride solution was $1.0 \times 10^{-2}M$ in ethanol, and was prepared fresh each day and protected from light by an amber bottle. Orthophosphoric acid solution was $0.1M$ in ethanol; pyrogallol was 5% in ethanol. Potassium hydroxide solution was prepared by dissolving 160 grams in 100 ml. of distilled water. All distilled water used was boiled to remove dissolved oxygen. Potassium ferricyanide and ferric chloride were 5% in distilled water. Mallinckrodt anhydrous ether was found preferable; others gave irregular results due to peroxides.

Saponification. One gram of peanut oil, 4 ml. of 5% pyrogallol in absolute ethanol, and 20 ml. of additional ethanol in a three-neck, 100-ml., round-bottom flask were brought to reflux under a N_2 atmosphere. One milliliter of KOH (160 grams/100 ml. distilled H_2O) was quickly added, and refluxing continued for 1 hour. The reaction mixture was cooled by immersing the flask into an ice bath without removing it from the reflux condenser or N_2 atmosphere. Boiled, cooled, distilled water (20 ml.) was then added while the mixture was still under N_2. The flask was then removed from the condenser and N_2 atmosphere and quickly stoppered. After the reaction mixture had dissolved in water, it was extracted five times with fresh anhydrous ethyl ether. The ether extract was kept under N_2 until the extraction was completed. The extract was then washed with boiled, cooled, distilled water, until free of base. The ether was evaporated, and the dry nonsaponifiables were dissolved in 5 ml. (V_1) of ethanol. Four milliliters (V_2) was removed to a 20-ml. round-

bottom flask and the ethanol evaporated from both portions of nonsaponifiables. Ten milliliters (V_3) of ethanol was added to the 0.2 portion A (1 ml. V_4), which was then ready for the modified Emmerie–Engel procedure. One milliliter (V_5) of benzene was added to the 0.8 portion B and known microliter amounts were placed in a band on a large thin layer, silica gel G plate for subsequent elution and recovery of tocopherols. Benzene was used as the solvent for placing nonsaponifiables on the thin layer plates because it evaporates much faster than ethanol.

Chromatography. Four-tenths milliliter (V_6) of the benzene solution (fraction B) was spotted in a 15-cm. band across a large (8 × 8 inch × 1 mm.) silica gel plate, which had been activated in an oven at 100° C. for 1 hour and cooled. This left space for a 15-μl. test spot of the same solution and a test spot of each standard tocopherol solution. The plate was then developed with chloroform to a distance of 16 cm. After removal and drying, the test spots were sprayed with 5% $K_3Fe(CN)_6$ followed by 5% $FeCl_3$ to determine tocopherol positions. The appropriate zones were removed with a 1-cm.-wide blade by holding the plate in a vertical position over a funnel placed in a 15-ml. centrifuge tube. Silica gel adhering to the tube with 10 ml. (V_7) of ethanol for α- and γ-tocopherols and 5 ml. (V_7) of ethanol for δ-tocopherol. The contents were stirred well and then centrifuged for 3 to 5 minutes. The modified Emmerie–Engel determinations were made directly on 3 ml. of the individual supernatants.

Spectrophotometric Determination. The modified Emmerie–Engel color test used in determining the amount of tocopherol present consisted of adding 0.5 ml. of bathophenanthroline ($6.0 \times 10^{-3}M$) in ethanol and 0.5 ml. of $FeCl_3 \cdot 6\ H_2O$ ($1.0 \times 10^{-3}M$) in ethanol to 3 ml. (V_8) of solution to be tested. A reaction time of 15 seconds was allowed for α- and γ-tocopherols; 3 minutes were allowed for δ-tocopherol, total tocopherol, and blank determinations. The blank value was determined using 3 ml. of ethanol instead of the test solution. The reaction was then terminated by adding 0.5 ml. of H_3PO_4 ($0.1M$) in ethano l(4.5 ml. V_9). The absorbance values of the solutions were obtained at a wavelength of 534 mμ with absolute ethanol in the reference beam. The ethanol blank value was subtracted from the test solution value. The absorbance value obtained was inserted into a previously constructed calibration curve (Table I) for the tocopherol being measured.

Values for μg. of various tocopherols per gram of oil were then calculated using the weight of oil taken for analysis and the appropriate formula below.

$$T_{\text{Total}} = \frac{V_1V_3V_9t}{V_4V_8g} = \frac{75t}{g}$$

Table I. Calibration Standards

α-Tocopherol		γ-Tocopherol		δ-Tocopherol	
μg./ml.	Absorbance	μg/ml.	Absorbance	μg./ml.	Absorbance
1.41	0.139	1.33	0.145	0.80	0.074
2.82	0.284	2.67	0.292	1.60	0.163
4.22	0.430	4.00	0.450	2.40	0.255
5.63	0.575	5.34	0.592	3.20	0.337
7.07	0.737	6.67	0.740	4.00	0.422
8.47	0.890	8.00	0.900	4.80	0.503
9.87	1.05	9.34	1.04	5.60	0.592
11.3	1.18	10.7	1.16	6.40	0.700
12.7	1.32	12.0	1.30	7.20	0.760

Table II. R_f Values for Silica Gel G Thin Layer Chromatography

Development time, 35 minutes; distance, 16–17 cm.

Solvent	Tocopherol (R_f)			
	α	β	γ	δ
Benzene	0.26–0.32	0.17–0.22	0.17–0.22	0.10–0.15
Chloroform	0.42–0.53	0.30–0.36	0.30–0.36	0.20–0.24
Petroleum ether–ether (5:1)	0.32–0.38	0.28–0.33	0.24–0.29	0.19–0.24

$$T_{\text{individual}} = \frac{V_1V_7V_9V_8t}{V_2V_8V_6g} = \begin{matrix} T_{\alpha,\gamma} = \dfrac{46.9t}{g} \\ T_{\delta} = \dfrac{23.4t}{g} \end{matrix}$$

V_1 = (5 ml.) volume to which nonsaponifiables were diluted.
V_2 = (4 ml.) volume taken to give portion B.
V_3 = (10 ml.) volume to which portion A was diluted.
V_4 = (1 ml.) volume taken to give portion A.
V_5 = (1 ml.) volume to which portion B was diluted.
V_6 = (0.4 ml.) volume placed on chromatographic plate.
V_7 = (5 ml. or 10 ml.) volume used to elute tocopherol from silica gel.
V_8 = (3 ml.) volume of spectrophotometric test solution.
V_9 = (4.5 ml.) volume of spectrophotometric test solution and reagents.
t = weight of tocopherol obtained from calibration curve.
g = weight of oil taken for analysis.

DISCUSSION

Saponification was necessary to remove excess lipids which caused streaking and poor separation of the tocopherols in the chromatographic step. Care should be taken during saponification to rigorously protect the tocopherols from oxidation, especially when base is present. Only freshly opened peroxide-free ether should be used for the extraction.

The division of the solution into two portions, A and B, in order that portion A may be used for analysis of total tocopherols, required very little additional effort and gave an important check on the determination of the individual tocopherols. The values for total tocopherols usually ran slightly higher than the sum of the individual tocopherols, however, because of small amounts of nontocopherol reducing substances which were still present at this point. The values obtained for total tocopherols before chromatography were calculated as α-tocopherol and are therefore not completely valid since there is a small difference in the standard curves for each tocopherol.

Using chloroform as a solvent in the chromatographic procedure failed to separate β- and γ-tocopherols (Table II), but gave a good separation of α-, γ-, and δ-tocopherols. Peanut oils have been shown to be essentially devoid of β-tocopherol (*4*).

The 15-μl. test spot and test spots of standard tocopherol solutions were used as a guide in removing the tocopherol bands for analysis. After development, the plate was masked with another glass plate and the test spots were sprayed with potassium ferricyanide solution followed by ferric chloride solution which reveal reducing materials as bright blue spots. Care must be taken not to contaminate the other parts of the plate which must be removed for analysis. Quantitative removal of tocopherols from the plate was not a problem because they tend to move toward the outer surface of the thin layer during evaporation of the chloroform.

The Emmerie–Engel method is based on the quantitative reduction of ferric ions by tocopherol and the excess ferric ions are subject to photoreduction if the solutions are exposed to strong light. No difficulty is encountered if the work is done under dim artificial light. After addition of the orthophosphoric acid solution, danger of photoreduction is eliminated because the excess ferric ions complex with the phosphate.

RESULTS

Table III shows the results obtained by application of the method to a sample of New Mexico Valencia peanut oil.

Table IV shows the results obtained on the same peanut oil containing added amounts of each tocopherol. An average percentage recovery was obtained for each tocopherol from the values of Tables III and IV. Values for total tocopherol analysis, which involves saponification and application of the modified Emmerie–Engel procedure directly to the nonsaponifiable material, are also reported. The average recovery of total tocopherol from saponification was 97.9% with a standard deviation of ±5.94. Values for α-, γ-, and δ-tocopherol analysis, which involves thin layer chromatographic separation, are also reported. The average recovery values are 93.2%, 87.9%, and 75.1%, respectively, with standard deviations of ±6.85, ±4.97, and ±6.79, respectively. The order of recovery as exhibited by our analyses agrees with the relative antioxidative effectiveness of each tocopherol which increases in the following order: α-, β-, γ-, δ-tocopherol (*6*). It is therefore reasonable to obtain greater losses due to oxidation with γ- and δ-tocopherol.

Table III. Tocopherol Analyses on New Mexico Valencia Peanut Oil

	Tocopherols (μg./gram)			
	Total	α	γ	δ
	400, 394	176	199, 186, 185	11.6, 15.4
	402, 402	159	176, 181, 186	12.0, 15.4
	395, 399	164	185, 188, 191	27.5, 15.8
	422, 402	156	150, 184, 159	15.6, 11.0
	404, 387	166	186, 194, 166	12.6, 15.7
	390, 387	153	189, 188, 176	11.0, 10.8
	387,	150		12.5, 12.5
		122		
Av:	398	156	182	14.2

Table IV. Tocopherol Analyses on New Mexico Valencia Peanut Oil with Added DL-α-, DL-γ-, and DL-δ-Tocopherols

	Total tocopherols		α-Tocopherol		γ-Tocopherol		δ-Tocopherol	
Sample[a]	After saponification (μg./gram)	Recovery (%)	(μg./gram)	Recovery (%)	(μg./gram)	Recovery (%)	(μg./gram)	Recovery (%)
1	708	92.3	269	107	368	93.0	39.6	85.0
2	712	93.5	216	...[b]	326	...[b]	27.7	79.4
3	731	99.1	263	101	369	93.5	39.2	83.7
4	726	97.7	249	87.7	345	81.6	35.8	72.3
5	733	99.7	250	88.7	368	93.0	34.0	66.4
6	749	104	260	98.2	367	92.5	36.5	74.7
7	755	106	214	...[b]	331	...[b]	33.1	63.3
8	737	101	261	99.2	362	90.0	38.9	82.7
9	751	105	254	92.4	362	90.0	36.5	74.7
10	734	100	246	85.0	353	85.6	36.2	73.6
11	664	86.9	248	87.8	358	88.0	...	...
12	766	100	246	84.9	340	79.1	60.0	76.5
13	716	86.8	226	...[b]	323	...[b]	57.6	72.6
14	786	106	261	99.2	366	92.1	56.8	71.2
15	751	96.4	219	...[b]	346	82.1	46.1	...[b]
16	737	92.6	248	86.8	346	82.1	59.4	75.5
Av.		97.9		93.2		87.9		75.1

[a] 106 μg. α-tocopherol and 200 μg. γ-tocopherol were added to all of the above samples.
30 μg. δ-tocopherol was added to samples 1–10.
60 μg. δ-tocopherol was added to samples 12–16.
[b] These values were omitted from determination of the average because they were found to be low because of incomplete removal of the layer from the plate or storage of the sample before analysis.

Table V. Averaged Corrected Values of Tocopherols[a]

	Tocopherol (μg./gram)				
Sample	Total after saponification	α	γ	δ	Total after chromatography
Spanish Type					
Dixie Spanish	400 ± 10.5	130 ± 7	235 ± 9.5	22.1 ± 2.0	387 ± 18.5
Argentine	391 ± 11	99.8 ± 8.1	238 ± 17	8.4 ± 2.8	346 ± 27.9
Starr	406 ± 12.5	113 ± 9	229 ± 13.5	11.7 ± 2.0	354 ± 24.5
Spantex	350 ± 10.5	84.0 ± 7.2	204 ± 11	8.3 ± 1.7	296 ± 19.9
Virginia Type					
Virginia Bunch 46-2	377 ± 11	149 ± 10	208 ± 14	10.9 ± 2.0	368 ± 26.0
Georgia 119-20	399 ± 12.5	137 ± 9	197 ± 13	8.3 ± 1.9	342 ± 23.9
Virginia 61R	446 ± 12	178 ± 9.5	213 ± 14	13.5 ± 1.8	405 ± 25.3
Florigiant	413 ± 10.5	177 ± 9	216 ± 12.5	13.2 ± 1.8	406 ± 23.3
NC 2	472 ± 12	175 ± 9.5	223 ± 11.5	8.4 ± 1.7	406 ± 22.7
NC 5	411 ± 12.5	137 ± 9	195 ± 13.5	8.9 ± 2.0	341 ± 24.5
Florida 393	540 ± 14.5	197 ± 10	288 ± 15	12.4 ± 2.9	497 ± 27.9
Runner Type					
Southeastern Runner 56-15	542 ± 12.5	230 ± 9	306 ± 12	25.0 ± 2.0	561 ± 23.0
Early Runner	505 ± 14	196 ± 10.5	253 ± 14	18.6 ± 2.2	468 ± 26.7
Dixie Runner	453 ± 12	129 ± 8	225 ± 11.5	10.9 ± 1.8	365 ± 21.3
Georgia 186-28	488 ± 12.5	128 ± 8	282 ± 12.5	13.8 ± 2.0	424 ± 22.5
Virginia Bunch 67	409 ± 12.5	191 ± 10.5	200 ± 14	14.1 ± 2.1	405 ± 26.6
Florida 416	418 ± 11.5	122 ± 8	228 ± 11.5	6.9 ± 1.7	357 ± 21.2

[a] The oil samples were obtained from sound mature seed grown at Holland, Virginia, in 1964.

Table V shows the results obtained on 17 peanut oil samples. The values have been adjusted to 100% recovery; averages and the error allowed by one standard deviation are also shown. This was calculated in the following manner: Standard deviations were calculated for the values shown in Table III. These deviations were applied to sample values shown in Table V because the experimental procedure was identical. The limits of one standard deviation for an average value obtained on a particular sample were calculated using standard methods (*5*). The number of measurements for Table V varied from two to four.

LITERATURE CITED

(1) Dilley, R. A., *Anal. Biochem.* **7**, 240 (1964).
(2) Dilley, R. A., Crane, F. L., *Ibid.*, **5**, 531 (1963).
(3) Emmerie, A., Engel, C., *Nature* **142**, 873 (1938).
(4) Fore, S. P., *et al.*, *J. Am. Oil Chemists' Soc.* **30**, 298 (1953).
(5) Freund, J. E., "Modern Elementary Statistics," Prentice-Hall, Englewood Cliffs, N. J., 1952.
(6) Griewahn, J., Daubert, B. F., *J. Am. Oil Chemists' Soc.* **25**, 26 (1948).
(7) Katsuki, G., Ichimura, Y., Nishimoto, Y., *Arch. Pract. Pharm.* **23**(4) 299 (1963).
(8) Lambertsen, G., Myklestad, H., Braekkan, O. R., *J. Sci. Food Agr.* **13**, 617 (1962).
(9) Schmandke, H., *J. Chromatog.* **14**, 123 (1964).
(10) Seher, A., *Mikrochim. Acta* **1961**, 308.
(11) Skinner, W. A., Parkhurst, R. M., Alaupovic, P., *J. Chromatog.* **13**, 240 (1964).
(12) Stowe, H. D., *Arch. Biochem. Biophys.* **103**, 42 (1963).
(13) Tsen, C. C., ANAL. CHEM. **33**, 849 (1961).

PRISCILLA A. STURM
R. M. PARKHURST
W. A. SKINNER

Department of Pharmaceutical Chemistry
Stanford Research Institute
Menlo Park, Calif.

WORK supported by U. S. Department of Agriculture, Oilseed and Industrial Crops Research Branch, Beltsville, Md., Contract No. 12-14-100-7745(34).

Gas Chromatographic Study of the Separation of Resin Acid Methyl Esters on a QF-1 Column

SIR: In preparation for our work involving some of the resin acids isolated from natural sources, the use of gas chromatography as one criterion of homogeneity of the isolated acids seemed very attractive. The literature cites the use of various polar and nonpolar liquid phases in conjunction with a thermal detector cell to monitor the separation of the diterpene acids present in gum rosin (*1, 2, 5–9*). To date no one column has been found to resolve satisfactorily the seven commonly known resin acids.

It appeared desirable to utilize a lower operating oven temperature to reduce the extent of thermal isomerization of the resin acid methyl esters on the column. Also bypassing the thermal conductivity cell which operates generally 30° to 50° C. above the column temperature by using a flame ionization detector appeared advantageous. Furthermore, the increased sensitivity of this detector cell would aid in the detection of trace impurities in our isolated samples. The use of a 4% QF-1 column provides better separation of the resin acid esters than anything previously reported.

EXPERIMENTAL

Equipment. Gas–liquid chromatographic separation of the gum rosin was accomplished using an Aerograph A-600 B unit equipped with a flame ionization detector and a Brown Honeywell 1-mv. full-scale recorder. The column used, prepared by Wilkins Instrument and Research Corp., Walnut Creek, Calif., was a 10-foot × 1/8-inch aluminum column packed with 4% QF-1 fluorosilicone on 60/80 mesh Chromosorb W, acid-washed, and treated with dimethyldichlorosilane.

The column was conditioned before use for 24 hours at 210° C. with a slow stream of nitrogen, which was employed as the carrier gas. Hydrogen was generated by an Aerograph hydrogen generator, Model 650. The flow rate, determined by a soap bubble flow meter, was 30 cc./minute hydrogen and 31 cc./minute nitrogen.

Materials. Resin acid samples were isolated by established procedures from W/W gum rosin. The acids were analyzed as methyl esters and were prepared by diazomethane treatment of an ethereal solution of the acid, followed by removal of solvent under nitrogen. The methyl esters were injected as a carbon disulfide solution with a Hamilton 5-μl. syringe.

Determination of Relative Retention Times. The point of initial emergence of the solvent peak was taken as reference. The retention times were measured as the difference in time between the reference peak and the peak in question. Relative retention times were taken with reference to methyl neoabietate.

RESULTS AND DISCUSSION

As can be seen from Figure 1 a complete analysis of the gum rosin can be accomplished in 30 minutes. Dehydroabietic, abietic, and neoabietic acids can be cleanly separated (as methyl esters) on this column. Of the remaining two resin acids in the abietic-type series, palustric and levopimaric acids can clearly be differentiated. Previous reports have mentioned the failure in resolving these two homoconjugated dienes with Versamid 900 (*1*), butanediol succinate (*5*), and diethylene glycol succinate (*6*) substrates.

Abietic-type acids

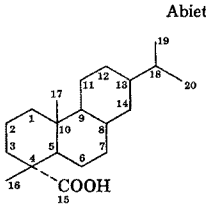

Abietic	$\Delta^{7,13(14)}$
Dehydroabietic	$\Delta^{8(14),9(11),12}$
Levopimaric	$\Delta^{8(14),12}$
Palustric	$\Delta^{8(9),13(14)}$
Neoabietic	$\Delta^{8(14),13(18)}$

Pimaric-type acids

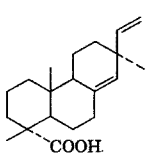

Pimaric

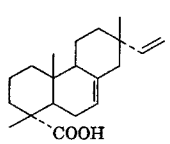

Isopimaric

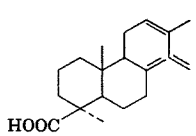

Elliotinoic

Table I. Relative Retention Data for Resin Acid Methyl Esters on QF-1 Column

	r^a	$r_N{}^b$	$r_{1/2}{}^c$
Pimarate	14.5	0.506	
Sandaracopimarate			
Elliotinoate	16.0	0.558	1.10
Palustrate	17.7	0.616	1.10
Levopimarate	19.2	0.670	1.09
Isopimarate	20.1	0.702	1.04
Dehydroabietate	22.4	0.781	1.11
Abietate	25.0	0.872	1.12
Neoabietate	28.7	1.000	1.14

[a] Retention times (minutes).
[b] Retention times relative to neoabietate.
[c] Retention relative to preceding peak.

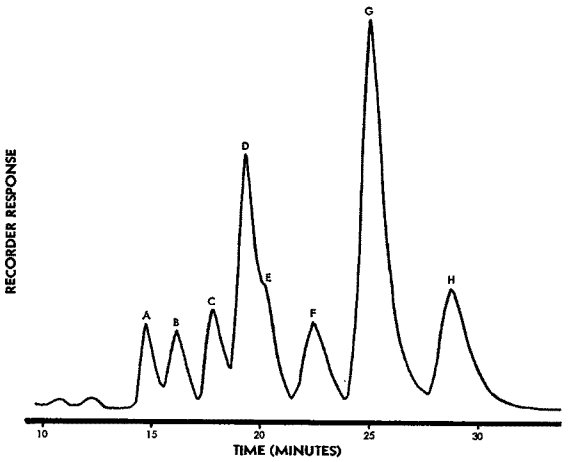

Figure 1. Gas phase chromatogram of methyl esters of gum resin

A, pimaric acid, sandaracopimaric acid; *B*, elliotinoic acid; *C*, palustric acid; *D*, levopimaric acid; *E*, isopimaric acid; *F*, dehydroabietic acid; *G*, abietic acid; *H*, neoabietic acid.
Column: 10-foot × 1/8 inch 4% QF-1 on 60/80 Chromosorb W
Column temp.: 193° C.
Input impedence: 10^9 ohms
Output sensitivity: 1 ×
Attenuation: 1
H_2 flow rate: 30 ml./minute
N_2 flow rate: 31 ml./minute

Pimaric and isopimaric acids, which represent two of the pimaric-type acids, are also separable on this column. These acids are nonconjugated dienes differing in the configuration of the groups at C-13 and in the positions of one of the double bonds at $\Delta^{8(14)}$ (pimaric) and Δ^7 (isopimaric). Sandaracopimaric acid, a minor component of gum oleorosin (ca. 1%) (*4*), has the same structure as pimaric acid except for the reversed configuration of the groups at C-13. Unfortunately, the methyl ester cannot be separated from methyl pimarate on this column. In fact, the chromatogram of a sample of methyl pimarate-sandaracopimarate (80–20 mixture) showed only a peak with slight tailing. Tahara and Hoshino (*9*), however, were able to obtain partial separation of these epimers on a 1% QF-1 column.

Of particular interest is the presence in the gum rosin of elliotinoic acid, a bicyclic diterpene acid whose C-4 carboxyl group has the beta configuration (*3*). This peak, occurring between the pimarate and palustrate peaks, represents the only nontricyclic resin acid in the fingerprint region associated with the seven common resin acids.

Table I gives the retention times and the relative retention times of the resin acids (relative to neoabietate = 1). As in previous reports, methyl neoabietate is the last resin acid to exit the column. The relative separation between adjoining peaks can be summarized by the separation factors, $r_{1/2}$, which represent the ratio between the succeeding peak and the peak in question.

The partial isomerization of methyl levopimarate into methyl abietate and methyl dehydroabietate was first reported by Hudy (*2*) who attributed the acidity of the supports used in the column as one of the factors causing isomerization. This observation was substantiated also by Brooks, *et al.* (*1*) who had found that in addition to methyl abietate and dehydroabietate, methyl neoabietate and methyl palustrate are also isomerization products. The latter finding was obscured in the earlier studies by the nonresolution of the methyl levopimarate-methyl palustrate peaks but was later confirmed by both ultraviolet spectrometry and optical rotation studies (*1*).

The use of the flame ionization detector precludes the study of the extent of isomerization of methyl levopimarate under the influences of heat and the acidity of the solid support. However, this investigation has shown that good separation of six of the seven common resin acids can be achieved with a QF-1 column and that the previously inseparable palustrate-levopimarate peak is resolvable.

ACKNOWLEDGMENT

We thank R. V. Lawrence for the gum rosin and for samples of methyl elliotinoate, isopimaric acid, and a 80:20 mixture of pimaric–sandaracopimaric acids.

LITERATURE CITED

(1) Brooks, T. W., Fisher, G. S., Joye, N. M., Jr., ANAL. CHEM. **37**, 1063 (1965).
(2) Hudy, J. A., *Ibid.*, **31**, 1754 (1959).
(3) Joye, N. M., Jr., *et al.*, *J. Org. Chem.* **30**, 429 (1965).
(4) Joye, N. M. Jr., Lawrence, R. V., Gough, L. J., *Ibid.*, **31**, 320 (1966).
(5) Lawrence, R. V., Naval Stores Laboratory, Olustee, Fla., private communication, November 20, 1964.
(6) Nestler, F. H. M., Zinkel, D. F., ANAL. CHEM. **35**, 1747 (1963).
(7) Norin, T., Westfelt, L., *Acta Chem. Scand.* **17**, 1828 (1963).
(8) Rudloff, E. von, Sato, A., *Can. J. Chem.* **41**, 2165 (1963).
(9) Tahara, A., Hoshino, O., *Sci. Papers I.P.C.R. (Japan)* **57**, 19 (1963).

CLIFFORD W. J. CHANG
S. W. PELLETIER[1]

Department of Chemistry
The University of Georgia
Athens, Ga. 30601

[1] To whom inquiries should be addressed.

WORK supported in part through funds provided by the Georgia Forestry Research Council, Macon, Ga. Cooperative project of the School of Forestry and the Department of Chemistry.

Determination of Chloride in Glass by Pyrohydrolysis

SIR: Determination of small amounts of chloride in glasses has been carried out in several ways, including gravimetric methods (*8*) and potentiometric titrations (*5*, *9*). Most of these methods are long and tedious and are not well suited for the determination of low concentrations of chloride (<0.1%). The present paper describes a simple, rapid method for the determination of small amounts of chloride in glasses. The method involves separation of the chloride by pyrohydrolysis, followed by the spectrophotometric measurement of the chloride in the distillate. The spectrophotometric determination of chloride is a modification of the procedure described by Clark (*2*) for the analysis of water. The method is based on the formation of weakly ionized mercuric chloride upon the addition of excess mercuric nitrate. The chloride is determined indirectly by measuring the concentration of excess mercury as the mercury-diphenylcarbazone complex.

Since the aspects of the quantitative separation of halides were presented by Warf, Cline, and Tevebaugh (*7*), several authors (*1*, *3*, *6*) have described procedures for the separation of fluoride from glasses. The only method appearing in the literature involving the pyrohydrolytic separation of chloride is that of Gahler and Porter (*4*) for the separation of chloride from titanium sponge.

EXPERIMENTAL

Apparatus. The pyrohydrolysis apparatus is shown in Figure 1. The combustion tube was fabricated from Vycor tubing and standard taper joints. The vertical arm from the steam generator should be wrapped with asbestos tape. An electric heating tape, controlled by a Variac, should be used around the horizontal portion of the tube between the steam inlet and the furnace to prevent condensation of steam in that area. The steam generator was heated with a Glas-Col heating mantle controlled by a Variac.

The combustion furnace was a Burrell Model H-1-9. The combustion boats used were Combax, size A (Fisher Scientific Co., Catalogue No. 7-651). The boats should be placed in the pyrohydrolysis apparatus under operating conditions for about 15 minutes to remove any chloride contamination.

All spectrophotometric measurements were made with a Beckman Model DU spectrophotometer equipped with 1-cm. Corex cells.

Reagents. Standard chloride solution was prepared by dissolving 82.4 mg. of reagent grade sodium chloride in water and diluting to 1 liter. One milliliter of this solution contains 0.050 mg. of chloride.

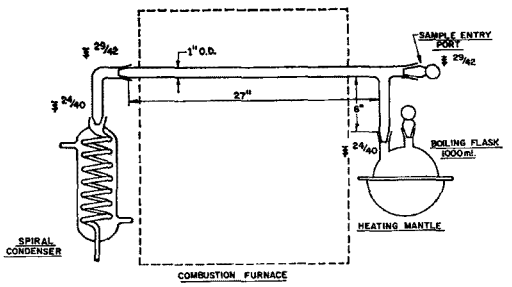

Figure 1. Pyrohydrolysis apparatus

Mercuric nitrate solution (0.001*M*) was prepared by dissolving 0.2166 gram of reagent grade mercuric oxide in 3.8 ml. of nitric acid and diluting to 1 liter.

Diphenylcarbazone solution (1%) was prepared by dissolving 1.00 gram of the reagent in 100 ml. of 95% ethanol.

Uranium oxide (U_3O_8) was prepared by igniting uranyl acetate at 1000° C. until the material was black. The U_3O_8 was ground to a fine powder.

Procedure. Grind the glass sample to pass through a 100-mesh sieve. Weigh a sample containing up to 0.3 mg. of chloride. Sample size must be limited to 1 gram because of the capacity of the boat. Thoroughly mix and grind the sample with an amount of uranium oxide equal to twice the sample weight in an agate or mullite mortar.

Transfer the mixture to a combustion boat. When the furnace is operating at about 1050° C. and when the water is boiling at a rate to produce about 4 ml. of distillate per minute, push the boat into the hottest part of the furnace using a length of stiff wire, and then close the sample entry port. Collect 100 ml. of distillate in a 250-ml. beaker.

Transfer the distillate to a 200-ml. volumetric flask. Add 3 ml. of 30% hydrogen peroxide, 5.00 ml. of the mercuric nitrate solution, and 2.00 ml. of the diphenylcarbazone solution in that order. Dilute the solution to volume and measure the absorbance immediately at 520 mμ against a water blank. Determine the amount of chloride in the sample from a calibration curve.

Preparation of Calibration Curve. Transfer aliquots (containing up to 0.3 mg. of chloride) of the standard chloride solution into 200-ml. volumetric flasks containing about 100 ml. of water. Add the reagents as given in the procedure, dilute to volume and measure the absorbance. Plot absorbance against milligrams of chloride.

RESULTS AND DISCUSSION

Temperature Requirements. Chloride is quantitatively separated from glasses, such as NBS 89 lead-barium glass, at temperatures as low as 950° C. Soda-lime glasses, which contain much higher percentages of the alkali and alkaline earth elements, require a higher temperature for complete separation. Pyrohydrolysis at 1050° C. appears to be adequate for all ordinary glasses.

Accuracy and Precision. Eleven aliquots of a standard potassium chloride solution (containing 0.100 to 0.217 mg. of chloride) were pipetted with micropipets onto 1-gram portions of uranium oxide contained in a mullite mortar. The mixture was dried under a heat lamp, mixed by grinding, and transferred to a combustion boat for pyrohydrolysis. The percentage of chloride recovery ranged from a low of 97.5 to a high of 102.1. The average recovery of the 11 determinations was

Table I. Precision of Results

	Chloride determined, %	
NBS 89 (Pb-Ba glass), certificate value 0.05%	Optical glass	Plate glass
0.052	0.42	0.018
0.049	0.40	0.018
0.051	0.40	0.019
0.050	0.41	0.021
0.048	0.42	0.020
0.048		0.018
0.050		
0.051		
Std. dev. 0.050 ± 0.001	0.41 ± 0.01	0.019 ± 0.002

99.7%. The standard deviation was ±1.5.

National Bureau of Standards 89 lead-barium glass, a plate glass, and an optical glass were used to investigate the precision of the method. These glasses represent a range of from 0.02 to 0.4% chloride. The results of these determinations, along with the standard deviations are shown in Table I.

A good estimate of the accuracy of the method is not possible because of a lack of suitable standards. The agreement between the measured value and the certificate value of the NBS 89 glass in Table I is excellent. However, analysis of NBS 93 borosilicate glass (certificate value 0.036% Cl) produced a mean value of 0.046%. The possible interference of boron was checked because some boron will be removed from the glass by pyrohydrolysis (*10*). No interference was found. This method is believed to be accurate because the chloride recovery data obtained with potassium chloride are acceptable, and the results obtained in testing various glasses are reproducible.

Interferences. When sulfur is present in the sample it is removed as SO_2 by pyrohydrolysis (*6*). The resulting sulfite ions in the distillate bleach the color of the mercury-diphenylcarbazone complex causing high results. This interference is easily avoided by the addition of hydrogen peroxide to the distillate to oxidize the sulfite ions to sulfate.

Arsenic is partially removed by pyrohydrolysis as arsenic(III). This was shown by pyrohydrolyzing arsenic-containing glasses or sodium arsenate ($Na_2HAsO_4 \cdot 7H_2O$) and titrating the distillate with iodine. The amount of arsenic normally found in glasses does not cause any interference. Antimony is not removed from the sample by pyrohydrolysis and does not interfere.

LITERATURE CITED

(1) Adams, P. B., Williams, J. P., *J. Am. Ceram. Soc.* **41**, 377 (1958).
(2) Clark, F. E., ANAL. CHEM. **22**, 553 (1950).
(3) Cluly, H. J., *Glass Technol.* **2**, 74 (1961).
(4) Gahler, A. R., Porter, G., ANAL. CHEM. **29**, 296 (1957).
(5) Glaze, F. W., *Bull. Am. Ceram. Soc.* **33**, 45 (1954).
(6) Nardozzi, M. J., Lewis, L. L., ANAL. CHEM. **33**, 1261 (1961).
(7) Warf, J. C., Cline, W. D., Tevebaugh, R. D., *Ibid.*, **26**, 342 (1954).
(8) Welcher, F. J., ed., "Standard Methods of Chemical Analysis," 6th ed., Vol. **2**, Part B, p. 2235, Van Nostrand, Princeton, 1963.
(9) *Ibid.*, p. 2239.
(10) Williams, J. P., Campbell, E. E., Magliocca, T. S., ANAL. CHEM. **31**, 1560 (1959).

V. E. CALDWELL

Pittsburgh Plate Glass Co.
Box 11472
Pittsburgh, Pa. 15238

Determination of Long-Chain Alkyl Sulfates as Chloroform-Soluble Azure A Salts

SIR: For the determination of anionic surfactants, cationic dyes have been in use for several years. Generally, the dye–surfactant complexes formed are extracted into chloroform or a similar solvent and the absorbance of the resulting solution is measured. The dye most widely used is methylene blue (*2–5, 8, 9*), introduced by Jones (*5*). Some publications propose the use of other dyes, such as pinacyanol (*6*) and basic fuchsin (*11*). A serious drawback of these procedures is the sensitivity to various interfering anions—e.g., nitrate and thiocyanate. These anions form chloroform-soluble salts with the dye, thus giving too high results in surfactant determinations.

Procedures to counter such difficulties—e.g., Degens' (*3*)—are costly, as regards the time and solvent quantities required. Therefore, experiments were undertaken to develop a simpler method. The dye azure A was found to have remarkable advantages over methylene blue [See Reference (*1*) for the properties and formulas of these dyes]. We arrived at the following azure A–chloroform procedure.

EXPERIMENTAL

Azure A was obtained as a preparation of adequate purity (certified dye content 91%) from Allied Chemical Corp., National Aniline Division. Paper chromatography (*7*) showed this dye to be virtually free from colored contaminants. The azure A reagent solution used in the following procedure contained 40 mg. of dye and 5 ml. of 0.1*M* sulfuric acid in 100 ml.

Procedure. In a 250-ml. volumetric flask, 50 ml. of the sample solution, which should be neutral or weakly acidic and which should contain 0.01–0.15 μmoles of the alkyl surfactant (C_{12}–C_{17} alkyl chains), is brought together with 5 ml. of 0.1*M* sulfuric acid and 1 ml. of the azure A reagent solution described. Then 10 ml. of chloroform is added, and the mixture is shaken for 5 minutes by a Griffin flask shaker. The mixture is transferred to a measuring cylinder (100 ml.) and the phases are allowed to separate. A large part of the lower phase is removed and brought into a centrifuge tube. Centrifugation in stoppered tubes removes water droplets (3000 r.p.m., 5 minutes). The absorbance of the dye complex in the clarified chloroform solution is measured at 630 mμ. The surfactant concentration in the initial solution is obtained from a reference graph. Beer's law was found to hold for up to 0.15 μmoles of surfactant.

DISCUSSION

By means of the basic procedure described the influence of the following experimental variables was investigated.

Shaking Time. Two minutes of shaking resulted in an almost optimal absorbance of the chloroform layer; the speed of shaking was not critical. The volume of the water layer, varied between 10 and 85 ml., did not affect the results.

Nature of Extracting Solvent. As can be seen from Table I, relatively few of the solvents examined gave a complete extraction of the dye–surfactant complex. Chloroform and 1:2-dichloroethane were both suitable in this respect.

Table I. Extraction of Heptadecyl Sulfate and Dodecyl Sulfate from Water by Various Solvents

(Procedure described in the text)

Solvent	Extd. from water phase in one extn., % C_{17}	C_{12}
Chloroform	100	100
1:2-Dichloroethane	100	100
o-Dichlorobenzene	83.6	62.5
Monochlorobenzene	70.6	28.8
1:2-Dichloropropane	77.8	43.7
Benzene	<2	<2
Carbon tetrachloride	<2	<2
2:2:4-Trimethyl pentane	<2	<2

Anion Interference. Experiments were undertaken in which the water phase contained varying concentrations of nitrate or thiocyanate to assess their transfer to the organic phase by cationic dyes. No surfactant was present. Some results obtained with nitrate solutions are summarized in Figure 1. Relatively small nitrate concentrations suffice to cause a considerable staining of the organic

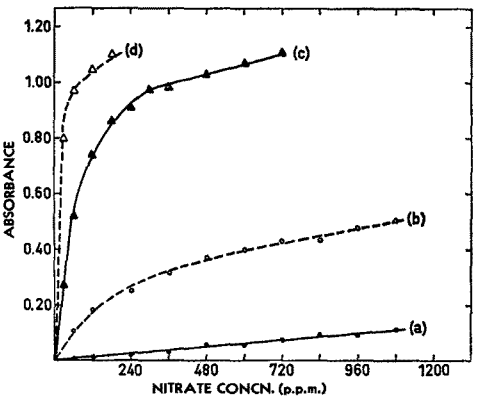

Figure 1. Extraction of dye from water phase (56 ml.) containing increasing concentrations of nitrate, measured as the absorbance of the solvent phase (10 ml.) at 630 mμ (azure A) and 655 mμ (methylene blue)

(a) O azure A–chloroform
(b) O azure A–1:2 dichloroethane
(c) ▲ methylene blue–chloroform
(d) △ methylene blue–1:2 dichloroethane

phase (chloroform or 1:2 — dichloroethane) if methylene blue is used as the cationic dye (lines *c* and *d*). With azure A, less dye transfer is effected by nitrate, especially if chloroform is used as the extractant (compare lines *a* and *b*). With a series of thiocyanate concentrations similar results were obtained. Here also the combination azure A–chloroform proved to be strongly preferable.

Up to 1000 p.p.m. nitrate and up to 200 p.p.m. thiocyanate hardly affected the results of alkyl sulfate surfactant determinations, if the azure A–chloroform procedure was adopted (Table II). Chloride (<0.1*M*), phosphate, and sulfate anions did not interfere. Up to 1 mg. of yeast ribonucleic acid in 50 ml. of water phase did not affect the results. Proteins interfered by preventing a clear separation of the liquid phases. Deproteinizing the samples, by the Nelson (*10*) procedure, abolishes this interference.

Quantitative Analysis of Mixtures. Chloroform extracts the dye–surfactant complex completely from its watery solution. With monochlorobenzene, extraction is incomplete; here the extent to which the complex is extracted depends on surfactant chain length (Table I).

The extraction of one surfactant–e.g., C_{12}–as azure A complex by monochlorobenzene is not changed by the presence of another surfactant–e.g., C_{17}–as is shown in Table III. This fact opens the possibility of an analysis of mixtures of alkyl sulfates of different chain length. Two separate applications of the azure A extraction procedure are necessary: one with chloroform and one with monochlorobenzene. With a mixture of x moles C_{12} and y moles C_{17} surfactant:

$$x + y = a \qquad (1)$$

and

$$0.288x + 0.706y = b \qquad (2)$$

where a = total quantity of surfactant extracted by chloroform, and b = total quantity of surfactant extracted by monochlorobenzene.

Table II. Extraction of Dodecyl Sulfate from Water by Chloroform, in the Presence of CNS^- and/or NO_3^-

Water phase: 85 ml.; chloroform: 10 ml. Comparison of methylene blue and azure A methods.

Dodecyl sulfate, total μmoles	CNS^-, p.p.m.	NO_3^-, p.p.m.	Dodecylsulfate found, μmoles[a]	
			Methylene blue method	Azure A method
0.0800	...	...	0.0800	0.0799
0.0800	5	...	0.1411	0.0801
0.0800	25	...	0.1962	0.0805
0.0800	100	...	0.2346	0.0830
0.0800	...	200	0.1220	0.0803
0.0800	...	800	0.1396	0.0821
0.0800	5	200	0.1840	0.0804
...	5	200	0.1020	0.0006

[a] Mean values of three detns.

Table III. Extraction of C_{12}, C_{17}, and Mixtures of C_{12} and C_{17} Alkyl Sulfates as Azure A–Complex by Chloroform and Monochlorobenzene

Water phase: 50 ml.; solvent: 10 ml.

Surfactant (μmoles)		Absorbance (630 mμ)[a]	
C_{12}	C_{17}	Chloroform	Monochlorobenzene
0.040	...	0.245	0.071
0.080	...	0.491	0.144
...	0.040	0.247	0.176
...	0.080	0.490	0.345
0.040	0.040	0.492	0.247
0.040	0.080	0.736	0.416
0.080	0.040	0.738	0.322

[a] Mean value of 3 determinations.

ACKNOWLEDGMENT

J. A. A. de Jong gave valuable technical assistance.

LITERATURE CITED

(1) Conn, H. J., "Biological Stains," 7th ed., Williams and Wilkins, Baltimore, Md., 1961.
(2) Critchfield, F. E., "Organic Functional Group Analysis," p. 171, Pergamon Press, Oxford, 1963.
(3) Degens, P. N., Jr., Evans, H. C., Kommer, J. D., Winsor, P. A., *J. Appl. Chem. (London)* **3**, 54 (1953).
(4) Freier, R. K., "Wasseranalyse," p. 113, De Gruyter, Berlin, 1964.
(5) Jones, J. H., *J. Assoc. Offic. Agr. Chemists* **28**, 398 (1945).
(6) Mukerjee, P., ANAL. CHEM. **28**, 870 (1956).
(7) Persijn, J. P., *Stain Techn.* **36**, 27 (1961).
(8) Rosen, M. J., Goldsmith, H. A., "Systematic Analysis of Surface-Active Compounds," p. 53–60, Interscience, New York, 1960.
(9) Schwartz, A. M., Perry, J. W., Berch, J., "Surface-Active Agents and Detergents," Vol. II, Interscience, New York, 1958.
(10) Nelson, N., *J. Biol. Chem.* **153**, 375 (1944).
(11) Wallin, G. R., ANAL. CHEM. **22**, 616 (1950).

JOHNNY VAN STEVENINCK
J. C. RIEMERSMA

Laboratory of Medical Chemistry
University of Leiden
Holland

Financial support for investigation received from Unilever, N.V.

On the Interpretation of Solute Vaporization Interference in Flame Photometry

SIR: Solute vaporization interferences between the analysis element and concomitants in the sprayed solution occur in flame photometry when the vaporization rate of the aerosol particles that are formed after dehydration of the spray droplets, is altered by the presence of these concomitants (*1*, *4*, *6*). For the emission or absorption signal which is determined by the content of the analyte in the vapor phase of the flame, any alteration of the vaporization rate will cause an interference effect if all of the aerosol particles are not completely vaporized at the height of observation in the flame. The most widely studied example of this kind of interference is the depression of the calcium signal by the presence of phosphoric acid in the solution. The characteristic depression curve shows initially a linear decrease of calcium signal with increasing phosphorus concentration, until at a molar P:Ca ratio of the order of unity the calcium signal remains constant upon a further increase in phosphorus concentration (so-called plateau). It should be stressed here that this is but one type of solute vaporization interference and that the interpretation of literature data may be clarified by distinguishing the following different cases.

Ia. Depression of Signal Due to Formation of a Less Volatile Compound than Analyte. The effect of phosphorus on calcium as described above is a truly chemical interference as it is based on the formation of a refractory compound molecule with a certain P:Ca molar ratio. The calcium depression results because the aerosol particles formed from the calcium + phosphorus compound are less volatile than those formed from, for example, a $CaCl_2$ solution alone. A discussion on the volatilization of different calcium salts in terms of their melting point is given in (*3*).

Ib. Enhancement of Signal Due to Formation of a More Volatile Compound than Analyte. If, however, the volatility of the compound particles is greater than that of the pure analyte particles, chemical interference may very well produce an enhancement of the analyte signal also. This case occurs, for example, when HF is added to a solution containing aluminum as analyte (*7*) or when ammonium chloride is added to a solution of a rare earth (*4*, *9*). The volatility of the AlF_3 particles formed [which have a sublimation temperature of 1200° C. (*7*)] is obviously greater than that of the aluminum particles which are formed from an aluminum solution containing no HF. The enhancing effect of oxine on the aluminum signal is said to be caused by a similar mechanism (*5*, *13*).

These are true chemical interference effects which should be distinguished from other condensed-phase effects, viz., after dehydration the analyte is found to be dispersed in a solid matrix formed by the concomitant element. Here again two cases IIa and IIb may be noted:

IIa. Depression of Signal Due to Occlusion of Analyte in a Less Volatile Matrix of Concomitant. When the matrix of the concomitant is less volatile than the aerosol particles formed from a pure analyte solution, a depression of the analysis signal may result. This depression is due to the occlusion of the analyte in a particle formed from the concomitant, that is not quickly vaporized in the flame because of its high boiling point or of its large size. This mechanism may explain the observed depression of the strontium emission (corrected for spectral interference) by addition of an excess amount of calcium (*10*). This explanation is supported by the observation that the calibration curve for the calcium band emission shows a downward curvature for high calcium concentrations. This curvature was absent when the liquid flow rate was strongly reduced (*10*). It is well known that at reduced flow rate the spray droplets become finer and consequently the size of the dry aerosol particles decreases (*6*). This decrease in size, again, promotes the vaporization rate and eliminates ultimately all solute vaporization effects.

IIb. Enhancement of Signal Due to Dispersion of Analyte in a Volatile Matrix of Concomitant. If, however, the matrix formed by the concomitant is more quickly decomposed than the solid particles formed from the analyte alone, an enhancement of the signal may follow. Quick vaporization of the matrix in which the analyte was finely dispersed, then results in a finer comminution, and because of it, a better vaporization of the analyte substance. This mechanism should explain the enhancement of the calcium signal in the presence of an excess of aliphatic salts in a turbulent O_2/H_2 flame (*14*).

The distinctions made above may help to understand better some further typical observations reported in the literature on the basis of solute vaporization interference.

When an interference effect of type Ia occurs between two elements and if both emit radiations in the flame, a close connection between the depressions of their intensities is to be expected. If self-absorption of the atomic lines at higher concentrations is corrected for, then the ratio of their mutual depressing effects should be related to the molar ratio of these elements in the chemical compound formed between them. Measurements on the depressing effect of the calcium emission by addition of H_3BO_3, as well as of the boron oxide band emission by addition of calcium, could point to such a relationship (*3*).

Mutual depression effects are not necessarily to be expected when a solute vaporization interference of type II is present. If after dehydration the aerosol particles formed by calcium alone would be much more easily decomposed than those formed by gallium alone, then occlusion of calcium in a matrix formed by gallium would naturally lead to a depression of the calcium signal upon adding gallium, but not inversely. One could rather expect a (slight) enhancement of the gallium signal upon adding calcium, because dispersion of gallium in the more volatile matrix formed by calcium could promote the vaporization of this analyte (cf. IIb). Such asymmetry between the mutual interference effects of calcium↔gallium has, indeed, been reported (*3*).

Depression effects of type Ia are still noted when the concentration of the concomitant is noticeably less than that of the analyte. The extent of compound formation and the depression caused by it is proportional to the (relatively small) amount of interfering element present. However, interference of type II due to occlusion or dispersion effects is expected to become operative only, if the concomitant concentration is at least of the same order of magnitude as the analyte concentration. This may explain why the calcium or magnesium depression by added gallium or titanium sets in only if the gallium or titanium concentration in the solution exceeds a nonvanishing minimum value (*3*, *11*).

The different behaviour of calcium depression by the addition of $AlCl_3$ and $Al(NO_3)_3$, respectively, may also be readily explained as different kinds of solute vaporization interference. The effect of aluminum chloride is quite similar to that of phosphoric acid; the depression curve of calcium emission *vs.* aluminum chloride concentration shows the familiar features of an initial

linear decrease, followed by a knee and a plateau (*6*). The plateau value increases markedly with increasing height of observation in the flame. Obviously an interference effect of type Ia is present here between calcium and aluminum. However, when $Al(NO_3)_3$ is added, the calcium emission drops smoothly to zero with increasing aluminum concentration and depends hardly on the height of observation (*6*). An interference of type IIa has to be assumed to play a part here. It is well known that the presence of $Al(NO_3)_3$ in the solution leads to the formation of highly refractory particles in the flame. Occlusion of the analyte in such particles at relatively high aluminum concentrations explains the different behavior of calcium depression by $Al(NO_3)_3$.

In practice solute vaporization interferences may appear to be much more complicated than is suggested by our simple scheme above. Interference effects of both types I and II may occur in combination for a given pair of analyte and concomitant—e.g., in the case of calcium depression by $Al(NO_3)_3$. When more than two elements are present together in the solution, competition effects between their mutual chemical reactions in the aqueous phase should also be considered (*2*). Moreover, in turbulent flames with total-consumption aspirator-burners (so-called atomizer-burners) these interference effects may appear to be smeared out and more capricious because of inhomogeneities in flame temperature and metal flame content and because of the nonuniform size distribution of the spray droplets. These complications might perhaps explain the occasional observation that a minimum in analyte emission as function of concomitant concentration is followed by a gradual increase or even a maximum of emission (*3*, *12*). The remarkable observation with a turbulent atomizer-burner flame that the calcium depression by indium is relatively smaller at the base of the flame than at larger heights (*3*), which contrasts with the usual observation in (laminar) flames (*6*), might be explained by the incomplete evaporation of spray droplets at the flame base. This incomplete evaporation is a well-known feature of this kind of flames with aqueous solutions (*6*) and as a consequence only the smaller droplets present in the spray will contribute to the formation of dry aerosol particles at the flame base. Since a small droplet will naturally lead to the formation of a small aerosol particle and hence to a quicker vaporization, the resulting solute vaporization interference could appear to be less at the flame base than at larger heights where grosser droplets contribute also.

LITERATURE CITED

(1) Dean, J. A., "Flame Photometry," McGraw-Hill, New York, 1960.
(2) Dinning, J. I., ANAL. CHEM. **32**, 1475 (1960).
(3) Doty, M. E., Schrenk, W. G., "Developments in Applied Spectroscopy, Vol. III, p. 196, J. E. Forrette and E. Lanterman, eds., Plenum Press, New York, 1964.
(4) Gilbert, P. T., "Analysis Instrumentation—1964," (Proc. 10th Natl. Anal. Instr. Symp., San Francisco, June 1964) Plenum Press, New York, 1964.
(5) Guédon, J., Voinovitch, I. A., *Chem. Anal. Warsaw* **5**, 193 (1960).
(6) Herrmann, R., Alkemade, C. Th. J., "Chemical Analysis by Flame Photometry" (transl. by P. T. Gilbert) Interscience, New York, 1963.
(7) Konopicky, K., Schmidt, W., *Z. Anal. Chem.* **174**, 262 (1960).
(8) Margoshes, M., Vallee, B. L., ANAL. CHEM. **28**, 180 (1956).
(9) Poluektov, N. S., "Techniques in Flame Photometric Analysis," (transl. by C. N. Turton and T. I. Turton) Consultants Bureau, New York, 1961.
(10) Pungor, E., Konkoly-Thege, I., *Mikrochim. Acta* **1959**, 712.
(11) Schmidt, W., Konopicky, K., Baum, M., *Tonind.-Ztg. Keram. Rundschau* **87**, 157 (1963).
(12) Strasheim, A., Wessels, G. J., *Appl. Spectry.* **17**, 65 (1963).
(13) Wallace, F. J., *Analyst* **88**, 259 (1963).
(14) West, A. C., ANAL. CHEM. **36**, 310 (1964).

C. TH. J. ALKEMADE
Physical Laboratory
State University
Utrecht, The Netherlands

Radiochemical Determination of Cesium Using Permanganate as a Precipitant

SIR: The reagents commonly used as the final precipitant in the radiochemical determination of cesium are perchloric and chloroplatinic acids (*3*, *4*). The chemical yield in these procedures is determined by weighing the precipitated cesium salt and comparing this weight with the expected weight based on the amount of cesium initially added. However, if even small amounts of ammonia are accidentally introduced into the laboratory area and dissolved in these acids, an error in the estimate of the chemical recovery results because of the low solubility of the corresponding ammonium salts. Experience has shown that under normal laboratory conditions where ammonium hydroxide is used, the probability of accidental introduction of significant amounts of ammonia into the final stage of the cesium analysis is quite high.

Other problems, in working with these reagents, are the hazards involved in using perchloric acid–ethanol mixtures and the difficulties of redissolving the chloroplatinate salts if flame photometric techniques are to be used for chemical yield determinations. Also, cesium-131 tracer with its short half-life (9.7 days) has been used to determine the cesium chemical recovery when there is a probability of ammonium contamination (*2*). This approach presents some difficulties with very low levels of cesium-137, since the x-rays of the cesium-131 daughter (Xe^{131}) contribute to the beta background.

To obviate these problems of determining the cesium recovery, other precipitants were sought.

Sodium permanganate was evaluated as a precipitant for cesium because other investigators (*1*) have found it to be a satisfactory precipitant. The direct weighing of cesium permanganate to determine the chemical recovery is precluded by the presence of manganese dioxide formed when a high concentration of permanganate ion comes in contact with extraneous oxidizable substances such as filter paper. However, the difficulties involved in determining the chemical yield are overcome by dissolving the cesium permanganate after counting and assaying the cesium by flame photometry.

In the development of this procedure, the important parameters studied were the optimum ratio of cesium ion concentration to the amount of sodium permanganate added and the effect of different acids and their concentration on the flame emission. Once values of these parameters were fixed, a self-absorption curve for the beta-ray counting of Cs^{137} was constructed.

EXPERIMENTAL

Reagents. Cesium chloride and sodium permanganate were Purified Grade from Fisher Scientific Co., Fair Lawn, N. J. Phosphoric acid, sulfuric acid, and sulfurous acid were Reagent Grade from J. T. Baker Chemical Co., Phillipsburg, N. J.

A cesium chloride standard solution was prepared by dissolving cesium chloride in distilled water. The amount of cesium in solution was determined gravimetrically with chloroplatinic acid in an ammonia free atmosphere. The

completeness of the cesium chloroplatinate precipitation was established by isotopic dilution using cesium-137 as the tracer and then counting of the supernatant liquid to determine the fraction of unprecipitated cesium.

Cesium-137 tracer was obtained from Oak Ridge National Laboratory. Its absolute disintegration rate was determined by 4π beta counting.

Instruments. A Beckman DU spectrophotometer with a flame attachment was used to assay for cesium.

Procedure. The procedure described here starts after the cesium has been removed from the sample (for instance, seawater) and purified of possible interfering nuclides.

Chloride ion, which reduces MnO_4^-, is removed from a purified cesium solution by the addition of 1 ml. of concentrated H_2SO_4 and evaporation to fumes of SO_3.

Then 10 ml. of water, 1 ml. of 85% H_3PO_4, and 0.5 gram of $NaMnO_4$ are added in that order. After complete solution of the $NaMnO_4$, the solution is chilled in an ice bath.

The resulting cesium permanganate precipitate is isolated by filtration. It is then dried, weighed (for self-absorption, self-scattering correction), mounted, and counted.

After counting, the precipitate is dissolved with 5 ml. of concentrated H_2SO_3 and approximately 5 ml. of water containing 0.5 ml. of concentrated H_2SO_4.

When the precipitate is completely in solution, the filter paper is removed, rinsed, and discarded.

The clear solution is evaporated to fumes of SO_3, cooled, and diluted to 100 ml.

Then the solution is submitted to flame analysis, using an oxygen-hydrogen flame, on the spectrophotometer. Cesium is determined at 852 mμ.

Since both the beta-ray counting self-absorption and the per cent optical transmittance curves are linear for the conditions utilized, their equations can be derived and, for simplicity, combined.

The equation for optical transmittance as measured by the flame photometer is

$$T = CW_p + D$$

The equation for self-absorption and self-scattering in the beta-ray counting of Cs^{137}, neglecting the chemical yield correction, is

$$\frac{\text{d.p.m.}}{\text{c.p.m.}} = AW_o + B$$

Because the chemical yield is W_p/W_a, the disintegration rate of Cs^{137} in the sample can be found by dividing the disintegration rate of Cs^{137} in the counting sample by the chemical yield, to give

$$\text{d.p.m.} = \text{c.p.m.}\ (AW_o + B)\left(\frac{CW_a}{T - D}\right)$$

where

- A = slope of self-absorption curve
- B = intercept of self-absorption curve
- C = slope of transmittance curve
- D = intercept of transmittance curve
- W_o = weight of $CsMnO_4$ observed by weighing
- W_a = weight of Cs added initially
- W_p = weight of Cs used in construction of transmittance curve
- T = per cent transmittance as measured by the flame photometer

Table I. Effect on Chemical Yield of Cesium of Amount of $NaMnO_4$ Used Relative to Cesium

Stoichiometric ratio of $NaMnO_4$ to Cs	Recovery of Cs, %
2	58.8
4	84.1
8	97.1

Table II. Quantities of MnO_2 in $CsMnO_4$ Precipitate

Wt. of $CsMnO_4$ and MnO_2 found, mg.	Wt. of $CsMnO_4$ from flame assay, mg.	Wt. of MnO_2, mg.
54.4	53.2	1.2
42.7	40.9	1.8
40.3	37.9	2.4
27.9	26.0	1.9
27.6	25.6	2.0

X = 1.9 ± 0.5

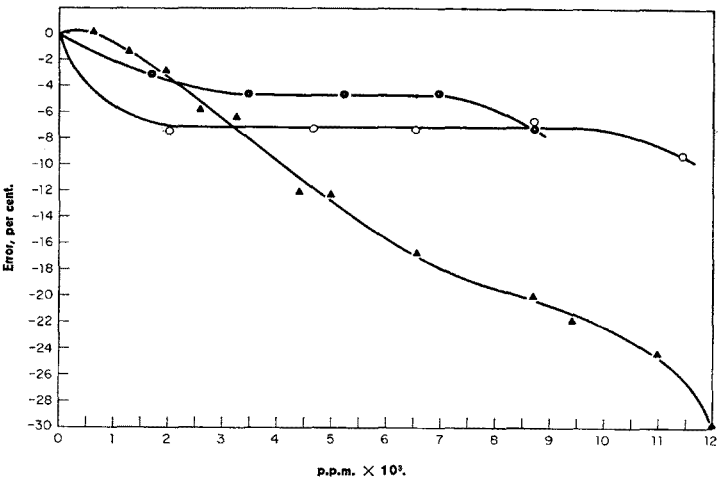

Figure 1. Effect of acids on flame analysis
● $HClO_4$, ○ H_2SO_4, ▲ HCl

RESULTS AND DISCUSSION

A study was made to adjust the important parameters to values which would give a large chemical yield, a high counting efficiency, and a high sensitivity in determining the chemical yield.

A significant factor in obtaining a large chemical yield is the ratio of permanganate to cesium concentration in the precipitating solution. Table I shows that if there is about an eightfold excess of a stoichiometric amount of $NaMnO_4$ to Cs, the recovery of cesium is nearly quantitative.

Since small amounts of MnO_2 are precipitated along with the $CsMnO_4$ precipitate, the cesium yield cannot be determined accurately by direct weighing. Table II shows that the quantities of MnO_2 precipitated are fairly constant even though the weight of $CsMnO_4$ varied by a factor of two.

Since it is necessary to have an acidic solution to dissolve the $CsMnO_4$ after counting, a study was made of the sensitivity of the flame emission to the presence of HCl, H_2SO_4, and $HClO_4$. Figure 1 shows the per cent error in the cesium assay as a function of acid concentration. The long plateau exhibited by H_2SO_4 suggested the use of H_2SO_4 in the procedure. The addition of 0.5 ml. of concentrated H_2SO_4 to the sample and the subsequent evaporation to fumes of SO_3 leave the sample with an amount of H_2SO_4 that is on the plateau (Figure 1) but free of any possible interfering chloride ions.

A calibration curve was constructed of the per cent flame transmittance as a function of cesium concentration. The results showed a linear relationship out to a concentration of 30 mg. of Cs per 100 ml. of solution. The calibrations were made at a wave length of 852 mμ, a slit width of 0.1 mm., an oxygen pressure of 10 lb./sq. inch, and a hydrogen pressure of 4 lb./sq. inch.

A curve to correct for physical geometry and the scattering of the cesium

beta-rays was constructed by precipitating known amounts of Cs^{137} with various known weights of $CsMnO_4$. The counting rate on the low-background counter used in these studies can thus be corrected for geometry, self-absorption, and self-scattering to obtain the Cs^{137} disintegration rate. This curve showed a linear relationship over the weight range of 25 to 55 mg. of precipitate.

The method presented for obtaining a cesium precipitate in a satisfactory form for counting and chemical yield determination has eliminated the problem of ammonia interference. This method is currently being used successfully in a procedure to determine activity levels of Cs^{137} as low as 1 d.p.m. (total) from 55-liter samples of seawater.

LITERATURE CITED

(1) Caley, E. R., Deebel, W. H., ANAL. CHEM. **33**, 309 (1961).
(2) Noshkin, V. E., Woods Hole Oceanographic Institution *Rept.* **NYO-2174-33, NYO-3145-5**, (1965).
(3) Rocco, G. G., Borecker, W. S., *J. Geophys. Res.* **68**, 4501 (1963).
(4) Sugihara, T. T., James, M. I., Troianello, E. J., ANAL. CHEM. **31**, 44 (1959).

WILLIAM H. SHIPMAN
DAVID MUELLER

Applied Research Branch
U. S. Naval Radiological Defense Laboratory
San Francisco, Calif. 94135

Determination of Deuterium Ion Concentration in Dilute Unbuffered Deuterium Oxide Solutions

SIR: This work concerns the determination of deuterium ion concentration in the D_2O that serves as coolant and moderator in the nuclear reactors of the Savannah River Plant. To minimize corrosion of aluminum components during reactor operation, the D_2O is maintained at a pD of 5 with nitric acid. Determination of the pD of this dilute solution is difficult because it is unbuffered. Routine in-line measurements by electrical conductivity are nonspecific and in-line measurements by pH meter with glass and calomel electrodes were not always satisfactory.

Three laboratory methods for determination of acidity were investigated: conventional potentiometric measurements with glass and calomel electrodes, conductometric titration of the acid with base, and colorimetric determination of pD with an acid-base indicator. In the colorimetric method, which comprises the bulk of this communication, conventional pH indicator colorimetry (*1*) was adapted to D_2O solutions, and indicator constants for bromophenol blue (BPB)and bromocresol green (BCG) in D_2O were determined by a method that did not require standard buffer solutions. Contrary to their customary usage, these indicators were employed as one-color indicators.

EXPERIMENTAL

Reagents. The BPB (Eastman Organic Chemicals, No. 752) was used as received; the BCG (Matheson Coleman & Bell, No. NB114) was recrystallized first from glacial acetic acid and then from benzene.

The acid forms of the indicators were dissolved in deionized H_2O or D_2O to give ~0.02% solutions. The molarity of the indicator solutions was calculated from the weight of indicator dissolved and confirmed by conductometric titration with base.

Adjusted indicator for pH or pD determinations was made by neutralizing the solution of the indicator acid until pH or pD equalled pK. In the present application, for example, where BPB was used to determine pD of reactor moderator, the BPB was neutralized to a pD of 4.62; the pH meter was calibrated with the D_2O buffer of pD 5.23 (*2*), and H_2O glass and calomel electrodes were used.

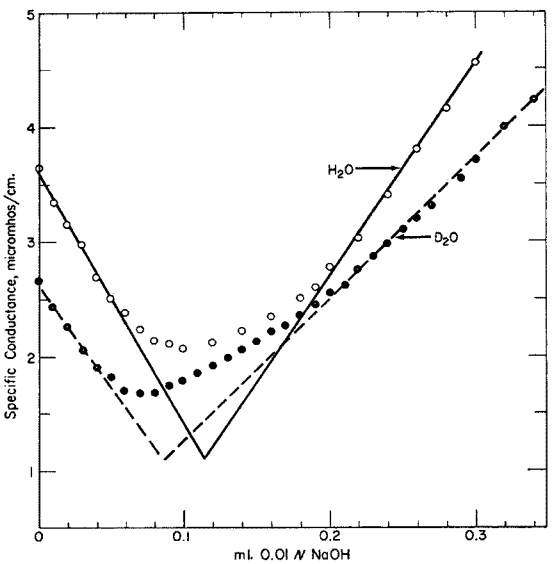

Figure 1. Examples of conductometric titration curves of $10^{-5}N$ nitric acid in H_2O and D_2O

Procedure. All measurements were made at room temperature, ~24° C.

pD MEASUREMENT. Adjusted BPB indicator (100 μl.) was diluted to 25 ml. with sample solution; another 100 μl. were diluted similarly with $0.05M$ Na_2CO_3. The absorbance of each solution was determined spectrophotometrically at 592 mμ with a 50-mm. path length.

DETERMINATION OF K. Absorbances of solutions of indicator acid at known concentrations in freshly deionized H_2O or D_2O and in $0.05M$ Na_2CO_3 were measured at wavelengths of 592 mμ for BPB and 615 mμ for BCG. The ratio of the absorbance of the sample to that of Na_2CO_3 solution was defined as α, the fraction of the indicator converted to the base form.

DISCUSSION

Potentiometric Measurements. Measurements in $10^{-6}N$ acid solutions by a pH meter with glass and calomel electrodes generally gave values that were high. Results were similar, whether the solutions were made in H_2O or D_2O, or whether electrodes with H_2O or D_2O internal solutions were used. Satisfactory results were obtained with $10^{-4}N$ solutions. The cause of the high results is unknown; perhaps some of the acid reacted with the glass. Potentiometric measurement of pH in dilute un-

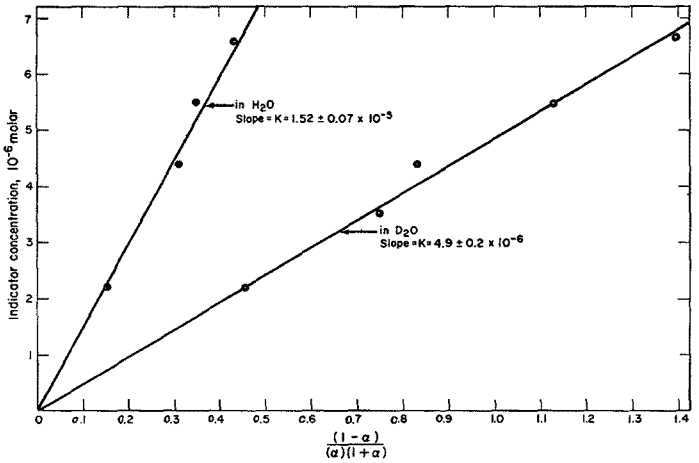

Figure 2. Determination of dissociation constants of BCG in H_2O and D_2O

buffered solutions is difficult (*1*). It was concluded that, without further refinement, potentiometric measurements were not suitable for this determination.

Conductometric Titration. The acid concentration of reactor moderator is more dilute than normal for conductometric titration. However, as shown in Figure 1 and Table I, the equivalence point was located with reasonable certainty. The absence of a sharp end point was attributed to the presence of CO_2; the reactants were not purged of CO_2, although contact with air during the titration was eliminated. Conductometric titration provided an alternative independent method to complement the indicator measurements described below.

Colorimetric Determination with Indicator. The blue base forms of BCG and BPB were used in the determinations because they had higher extinction coefficients than the yellow acid forms. BCG and BPB could be treated as one-color indicators because neither the acid nor the undissociated species interfered at the wavelength of measurement. For one-color indicators, measurement of absorbance at only one wavelength is required, but the absorbance of an identical concentration completely converted to the base form must also be measured. Beer's law was obeyed in these systems so that the absorbance values were proportional to concentration and could be used directly for calculation of α.

Determination of pK Values. The standard relationship (*1*)

$$pD = pK + \log\left(\frac{\alpha}{1-\alpha}\right) \quad (1)$$

was used as a basis for pD determination. The concentrations at which measurements were made were sufficiently dilute to allow activity coefficients to be neglected.

pK values for the indicator acid in D_2O at low ionic strengths were needed. For these sulfonephthalein indicators, it was reasoned that, in dilute solution, dissociation of the sulfonic acid group would be complete, and that the constant for the second dissociation, which produces the blue color of the base form, would be given by:

$$K = \frac{(H^+)\,(B^{-2})}{(HB^-)} \quad (2)$$

$$= \frac{[(1+\alpha)c]\,[\alpha c]}{[(1-\alpha)c]} \quad (3)$$

$$= \frac{(\alpha)\,(1+\alpha)}{(1-\alpha)}\,c \quad (4)$$

K could then be determined from measurements of α at known concentrations, c, of the indicator acid. Water that is free from acids or bases—e.g., freshly deionized water—was required to obtain the effective dissociation of the indicator only. With measurements at different indicator concentrations, Equation 4 indicates that the results should produce a straight line of slope K when c is plotted against $[(1-\alpha)/(\alpha)\,(1+\alpha)]$.

Data are plotted in Figures 2 and 3 for BCG and BPB in H_2O and D_2O. The straight lines have been fitted to the data points by the least-squares method, with the requirement that the intercept be located at the origin. Each point is the average of two or more determinations. The uncertainties in K are $\pm 2\sigma_K$ values.

In Table II, pK values for BCG and BPB are summarized. The method is

Table I. Comparison of pD Determinations

Standard DNO_3 solutions[a]	Indicator method	Conductometric titration
pD = 5.24	5.24	...
pD = 5.02	4.98	5.02
pD = 4.74	4.77	...
Reactor moderator samples	4.79	4.84
	5.03	5.01
	5.12	5.14
	5.20	5.15

[a] Diluted from 0.01*N* solutions that were standardized by potentiometric titration with standard 0.1*N* NaOH.

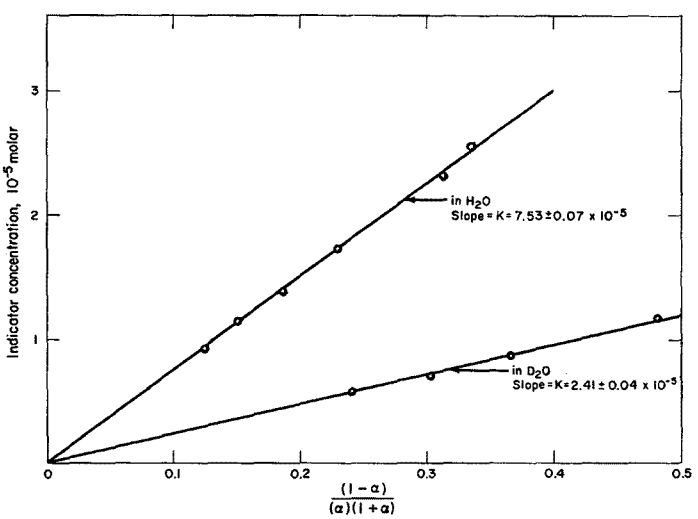

Figure 3. Determination of dissociation constants of BPB in H_2O and D_2O

verified by the satisfactory agreement of pK values in H_2O with literature values for BPB and BCG at infinite dilution. pK values in D_2O at an ionic strength of about 0.05 molar were determined colorimetrically with the pD 5.23 buffer solution.

Application of Indicator to pD Measurements. The pD of the unbuffered sample solution is necessarily decreased by addition of indicator, which is itself an acid. The perturbation was reduced to less than 0.05 pD unit by using the lowest concentration of indicator feasible for accurate absorbance measurements ($\sim 10^{-6}$ molar) and by neutralizing the indicator acid to the midpoint of its transition interval, where pD is equal to pK. pD values with unadjusted indicator were as much as 0.2 pD unit too low. The acid contribution of the indicator could have been completely eliminated by use of isohydric indicator solutions, but this elegant technique was not considered necessary for the accuracy required or desirable for routine analysis.

Table II. pK Values in H_2O and D_2O at ~24° C.

Ionic strength, molar	BCG		BPB	
	H_2O	D_2O	H_2O	D_2O
0	4.90[a]	...	4.10[a]	...
$\leq 10^{-5}$	4.82 ± 0.02	5.31 ± 0.02	4.12 ± 0.01	4.62 ± 0.01
~0.05	4.70[a]	5.27	4.00[a]	4.59

[a] Reference 3.

Because of the greater association of the indicators in D_2O, pK values are higher in D_2O than in H_2O. Thus, BCG was only marginally suitable for measurement of pD in reactor moderator, and BPB was used. As with all indicators, the range of usefulness is only within the transformation interval of pK ± 1 (1); for BPB this corresponds to a pD of 3.6 to 5.6. Reasonable agreement of the indicator method with standards and with the conductometric titration method (Table I) demonstrates that the indicator method can determine acidity satisfactorily. The inherent simplicity of the indicator method makes it suitable for automation or in-line analysis.

LITERATURE CITED

(1) Bates, R. G., "Determination of pH—Theory and Practice," pp. 131–67, 378–9, Wiley, New York, 1964.
(2) Gary, R., Bates, R. G., Robinson, R. A., *J. Phys. Chem.* 69, 2750 (1965).
(3) Kolthoff, I. M., Rosenblum, C., "Acid-Base Indicators," p. 293, Macmillan, New York, 1937.

ELIZABETH W. BAUMANN
Savannah River Laboratory
E. I. du Pont de Nemours & Co.
Aiken, S. C.

Information contained in this article was developed during work under contract AT(07-2)-1 with the U. S. Atomic Energy Commission.

Determination of Dissolved Ammonia by Gas Chromatography

SIR: Colorimetric methods of ammonia analysis are subject to interference by many common organic materials and inorganic ions which form precipitates or colors with the reagents (2). In most cases the ammonia must be separated from the interfering substances before analysis.

The separation and determination of ammonia by gas chromatography has been reviewed briefly by Jeffery and Kipping (1). The separation from amines usually requires supported liquid-phase adsorbents at elevated temperatures and therefore has the disadvantage of column bleeding. In addition, the poor sensitivity of thermal conductivity cells to ammonia may require the use of more expensive apparatus. Finally, ammonia in aqueous solution must be separated from the water prior to analysis.

These disadvantages are avoided by an extension of a gas chromatographic technique developed for determining dissolved fixed gases in aqueous solutions (4, 5). The new method is based on measurement of the N_2 liberated by the quantitative oxidation of ammonia by alkaline hypobromite.

$$2NH_3 + 3BrO^- \rightarrow N_2 + 3Br^- + 3H_2O \quad (1)$$

The technique provides several advantages in simplicity of instrumentation and operation. The liberated N_2 is stripped from solution by the carrier gas and transported directly into the chromatograph for analysis, a molecular sieve column is used at room temperature, and the thermal conductivity detector is considerably more sensitive to N_2 than to NH_3. The method is free from interference by all substances which are not converted to N_2 by BrO—e. g., amines, amides, proteins, nonnitrogenous organics, and metallic ions. Urea and hydrazine interfere. In addition to being relatively free from interference and requiring only a small sample, the method is rapid, reproducible, and independent of sample color or turbidity.

EXPERIMENTAL

The apparatus was used as previously described (4, 5), with some modifications. The plumbing of the gas chromatograph was rearranged so that only one chromatographic column and one detector thermistor were used. A 5-foot × 1/4 inch 40 to 60-mesh molecular sieve column was preceded by a drying column and an absorbent for CO_2. The instrument was operated at 29° C.

A solution of ~0.04*M* BrO^- and NaOH is prepared by dissolving 3.6 grams of NaOH in 400 cc. of water in 0.1*M* then slowly adding 100 cc. of saturated bromine water as the solution is stirred. This method avoids the hazardous transfer of liquid bromine and permits the reaction to proceed at room temperature without appreciable formation of bromate. The hypobromite solution does not require standardization and may be used for several weeks.

The solution to be analyzed is slightly acidified (pH ~3) before analysis to prevent stripping of NH_3. This is done either by adjusting the pH prior to injection of the sample or by first injecting the appropriate amount of acid into the stripping chamber. The solution is deaerated in the stripping chamber by purging with the helium carrier gas. Helium-purged BrO^- solution is then injected to convert the ammonia to nitrogen by Reaction 1. The sample and the reagent may be injected by syringe or by the six-way valve. [Figure 1 of (5)]. If the sample is injected by the valve, the reagent also should be injected in this way to ensure reaction of the small fraction of the sample which remains in and below the frit. The results reported below were obtained by syringe injection of 3-cc. samples and valve injection of 6 cc. of hypobromite solution. To ensure complete conversion, it is essential to have BrO^- in excess of all reducing agents and to have the final mixture strongly alkaline. The liberated N_2 is stripped and analyzed in the usual way (4, 5). After each analysis the chamber is rinsed with water to remove residual BrO^-.

The apparatus may be calibrated with N_2-saturated water at measured temperature and pressure (4) or, more

Table I. Calculated and Observed Ammonia Concentrations Obtained from Ammonium Sulfate Standards

NH_3 calcd., mM	NH_3 found, mM
0.080	0.076
0.160	0.162
0.200	0.198
0.300	0.300
0.500	0.504
0.784	0.788
1.00	0.998
1.50	1.46
2.00	2.03
3.00	2.99
5.00	5.08
1.00	1.02[a]
2.00	2.00[a]
3.00	3.04[a]
4.00	4.01[a]

[a] Solution contained 1mM each of methylamine, hydroxylamine, and acetamide.

conveniently, with a standard solution of ammonium sulfate.

The ammonia concentration in the sample is given by

$$C = \frac{C_0 v_0 A}{A_0 v} \qquad (2)$$

where C is ammonia or ammonium ion concentration in micromoles/liter, v is sample volume in cubic centimeters, A is peak area in square centimeters, and the subscripts denote calibration values. If $v = v_0$, the volume need not be known and the equation becomes

$$C = \frac{C_0}{A_0} A \qquad (3)$$

The calibration factor $C_0 v_0 / A_0$ averages 34.8 for the present apparatus.

DISCUSSION

Solutions containing various amounts of NH_4^+ were analyzed by this procedure and the effect of other reduced forms of nitrogen was checked by using samples containing (in addition to NH_4^+) 1mM each of methylamine, hydroxylamine, and acetamide. A least-squares analysis of the results presented in Table I showed a linear relationship with a zero blank correction and a slope statistically indistinguishable from unity. There was no interference from the other reduced nitrogen species present. Solutions containing only methylamine, hydroxylamine, or acetamide did not produce appreciable amounts of N_2. This indicates that their presence will not affect the accuracy of determination of very small amounts of ammonia.

It has been reported that BrO^- converts substantial amounts of ammonia to N_2O in the presence of cupric ions (*3*). We have obtained quantitative conversion of 0.5mM NH_3 to N_2 in the presence of 20mM $CuSO_4$. Likewise the stoichiometric amount of N_2 was obtained upon analysis of 0.5mM $Fe(NH_4)_2(SO_4)_2 \cdot 6H_2O$.

Reproducibility of the method was tested in a series of 10 replicate determinations of a $5.00 \times 10^{-4} M$ NH_4Cl solution. The average area was 42.98 cm.^{2}, with ± 0.37 cm.^{2} (0.86%) standard deviation and ± 0.12 cm.^{2} (0.28%) standard deivation of the mean.

The use of 10-cc. samples in conjunction with 10-fold amplification of electrical response will make the method sufficiently sensitive for ammonia analysis of natural waters.

LITERATURE CITED

(1) Jeffery, P. G., Kipping, P. J., "Gas Analysis by Gas Chromatography," p. 131, Macmillan, New York, 1964.
(2) Kruse, J. M., Mellon, M. G., ANAL. CHEM. **25**, 1188 (1953).
(3) Riley, R. F., *et al.*, *J. Am. Chem. Soc.* **76**, 3301 (1954).
(4) Swinnerton, J. W., Linnenbom, V. J., Cheek, C. H., ANAL. CHEM. **34**, 483 (1962).
(5) *Ibid.*, p. 1509.

R. W. JENKINS, JR.
C. H. CHEEK
V. J. LINNENBOM

U. S. Naval Research Laboratory
Ocean Sciences and Engineering Division
Washington, D. C. 20390

Derivation of Expression for Integrated Luminescence Intensity When Using Pulsing Techniques in Luminescence Spectrometry

SIR: In a recent paper on the influence of phosphoroscope design on the measured intensities in phosphorimetry, O'Haver and Winefordner (*3*) gave equations which related the measured and instantaneous phosphorescence intensities to the decay time of the phosphorescence species and to the characteristics of the mechanical shutter mechanism. The equations may be extended to apply to a measurement system using a pulsed flash tube for excitation and a pulsed multiplier phototube for observation of sample luminescence. Pulse systems of this type have been used by Hendee and Brown (*2*), Peterson and Bridenbaugh (*4*), and Bhaumik *et al.* (*1*), and the reader is referred to these references for detailed experimental descriptions of the optical and electronic construction of these systems. The expressions given here are valuable for evaluating any given pulse system for analytical applications, as well as for predicting the optimum instrumental condition of measurement.

A simplified diagram of the events taking place during one cycle of sample excitation and observation in a typical pulse system is given in Figure 1. The sample luminescence is excited by a very short, intense burst of light from the flashtube. The half-intensity width of the flash is called t_f (see Figure 1). The intensity of the sample luminescence (dotted line) increases during the flash, reaches a maximum, and then decays exponentially after the flash. If the flash intensity were maintained at its peak value for an indefinite time, the sample luminescence would eventually reach a steady-state value, called I_{P_0}, which is proportional to the peak flash intensity. At a time t_D, the delay time, after the end of the excitation flash, a high voltage negative gate is applied to the multiplier phototube dynode chain, activating it for a time t_P, the multiplier phototube gate width. The instantaneous luminescence intensity at the leading edge of the photomultiplier gate is called I_{P_1}. At some time after the trailing edge of the multiplier phototube gate, another cycle of excitation and observation occurs. The number of such cycles occurring per second is called the pulse repetition frequency, f. In a pulse system, t_D, t_P, t_f, and f are all independently adjustable, within certain limits.

The integrated luminescence intensity observed per cycle, P_P, is the area under the curve of luminescence intensity *vs.* time during the photomultiplier gate, and is shown as the shaded area in Figure 1. The value of P_p (*3*) is given by:

$$P_P = I_{P_0} \left\{ \frac{\tau \exp\left(-\frac{t_D}{\tau}\right)\left[1 - \exp\left(-\frac{t_P}{\tau}\right)\right]\left[1 - \exp\left(-\frac{t_f}{\tau}\right)\right]}{1 - \exp\left(-\frac{1}{f\tau}\right)} \right\} \qquad (1)$$

where all the terms are defined above. The reader is referred to the paper of O'Haver and Winefordner (*3*) for the derivation of an analogous expression

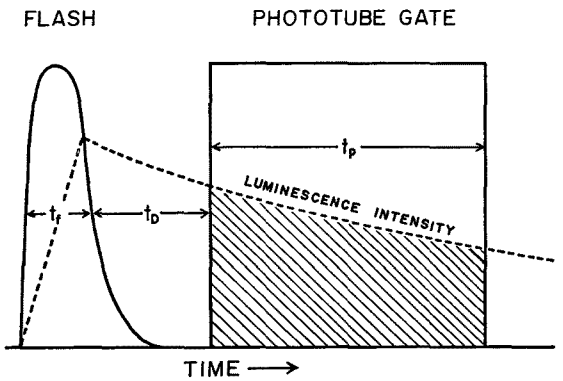

Figure 1. Simplified diagram of events taking place during one cycle of sample excitation and observation in a typical pulse system (see text of paper for definitions of t_f, t_D, and t_P)

Time and intensity axes are not to scale but only indicate the events occurring

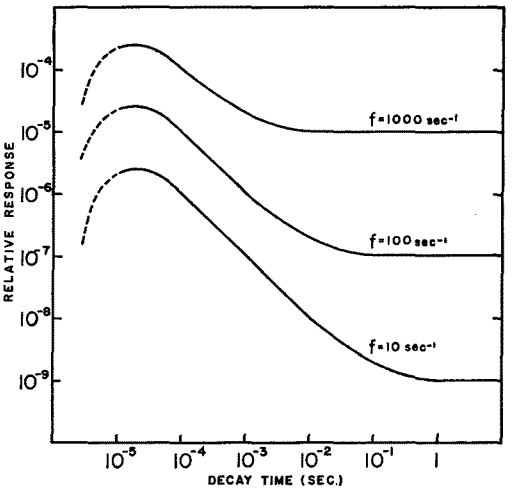

Figure 2. Plot of relative response (ratio of integrated intensity, I, to the steady state integrated intensity, I_{P_0}) vs. sample decay time, τ, for three different pulse repetition frequencies, f (solid lines were calculated using equations in text; dotted lines indicate expected trend although equations in text are not strictly valid for these regions)

The parameters used to calculate the curves are as follows: $t_f = 10^{-6}$ sec.; $t_P = 10^{-5}$ sec.; $t_D = 10^{-5}$ sec.

for P_P for a measurement system using a mechanical shutter mechanism. For the purposes of the derivations to follow, the excitation flash width t_f will be assumed to be very small—i.e., one tenth or less, compared to the decay time, τ, of the sample. This allows the flash to be treated approximately as a rectangular pulse of width t_f, during which the sample luminescence intensity increases nearly linearly at a rate directly proportional to the flash intensity and inversely proportional to the decay time, τ, of the sample. The condition that $t_f \ll \tau$ is not a serious limitation, since the flash width t_f can be made very short. Typical values of t_f are of the order of 1 μsec., allowing the treatment here to apply to species with decay times of the order of 10^{-5} sec. or greater. Practically all phosphorescent organic molecules, as well as many fluorescent rare earth ions, have decay times greater than 10^{-5} sec. Introducing the condition that $t_f \ll \tau$, Equation 1 may be rewritten as

$$P_P = I_{P_0} \times \left\{ \frac{t_f \exp\left(-\frac{t_D}{\tau}\right)\left[1 - \exp\left(-\frac{t_P}{\tau}\right)\right]}{1 - \exp\left(-\frac{1}{f\tau}\right)} \right\} \quad (2)$$

Generally, an average reading d.c. meter is used to measure the output of the multiplier phototube (I). The meter reading is then proportional to the integrated luminescence intensity observed per unit time, I, given by:

$$I = fP_P = I_{P_0} \times \left\{ \frac{ft_f \exp\left(-\frac{t_D}{\tau}\right)\left[1 - \exp\left(-\frac{t_P}{\tau}\right)\right]}{\left[1 - \exp\left(-\frac{1}{f\tau}\right)\right]} \right\} \quad (3)$$

In Figure 2, I (normalized by dividing by I_{P_0}) is plotted as a function of τ according to Equation 3 for three values of the pulse repetition frequency. Note the peak value of I which indicates that there is an optimum experimental system for any luminescent molecule. The values of the parameters t_D, t_P, and t_f are given in the figure heading. Equation 3 can be greatly simplified for four limiting cases. These are discussed below.

CASE *1*. If τ is much greater than $1/f$, t_f, t_D, and t_P then Equation 3 becomes

$$I \cong I_{P_0} f^2 t_f t_P \quad (4)$$

This corresponds to the flat portion of the curves on the right-hand side of Figure 2. Most phosphorescent organic compounds are described by this case.

CASE *2*. If τ is short compared to $1/f$ and long compared to t_f, then

$$I \cong I_{P_0} f t_f \exp\left(-\frac{t_D}{\tau}\right) \times \left[1 - \exp\left(-\frac{t_P}{\tau}\right)\right] \quad (5)$$

This corresponds to the center and left-hand portions of the curves in Figure 2, and includes Case 2*a* and 2*b* as special cases. This is generally applicable to fluorescence and phosphorescence of organic molecules with decay times less than 10^{-3} second and is especially suitable for organic molecules exhibiting fast decaying phosphorescence (decay times of 10^{-5} to 10^{-3} second) and rare-earth ion fluorescence (decay times of 10^{-5} to 10^{-3} second).

CASE *2A*. If τ is short compared to $1/f$, but long compared to t_P, t_D, and t_f, then Equation 5 reduces to

$$I \cong I_{P_0}\left\{\frac{t_f t_P f}{\tau}\right\} \quad (6)$$

This corresponds to the linear, sloping portion of the curves near the center of Figure 2.

CASE *2b*. If τ is short compared to $1/f$, and t_P, and long compared to t_f, then Equation 5 reduces to

$$I \cong \frac{I_{P_0} f t_f t_P \exp\left(-\frac{t_D}{\tau}\right)}{\tau} \quad (7)$$

This corresponds to the portion of the curves to the left of the maximum in Figure 2, and is the case for fluorescence of most organic molecules.

USE OF EQUATIONS AND POSSIBLE APPLICATIONS OF PULSING METHODS

Equation 3, or its limiting cases, may be used to calculate the relative response of a pulse-type instrument to a luminescent species as a function of τ, t_P, t_f, t_D, and f. The actual meter readings depend upon I_{P_0}, the photomultiplier sensitivity, amplifier gain, and certain details of the optical system. The value of I_{P_0} depends upon the source intensity, and the nature and

concentration of the species. These factors are treated elsewhere and, therefore, won't be discussed here.

A pulse system offers some unique advantages over a mechanical shutter system in the analysis of short-lived luminescence in the presence of a long-lived interference, such as solvent background. As can be seen from Figure 2, the relative response for long (Case 1) decay times is much less than for short (Cases 2 and 2a) decay times. Therefore, the sample-to-interferent intensity ratio is increased by a certain factor on the basis of the difference in the decay times of the two species. This factor may be determined by taking the ratio of I for the sample to I for the interferent, as calculated by Equation 3. For this purpose, it is convenient to use I *vs.* τ plots for the instrument under consideration, such as in Figure 2. If the limiting cases for Equation 3 can be used, the calculations are very simple. For instance if the sample belongs to case 2 and the interferent to case 1, then

$$\frac{I_s}{I_i} = \frac{I_{P_0)s}}{I_{P_0)i}} \cdot \frac{I}{\tau_s f} \qquad (8)$$

where s refers to the sample and i to the interferent. As a practical example, suppose $\tau_i = 1$ sec., $\tau_s = 10^{-3}$ sec., and $f = 10$ sec.$^{-1}$; then Equation 8 predicts a 100-fold increase in the sample-to-interferent intensity ratio over what would be expected if the two species had the same decay time. An even greater increase would result if τ_s were even smaller. It is of interest to compare this same case when using a pulsing technique to that obtained with a mechanical chopping system. For the Aminco-Bowman Spectrophotofluorometer with phosphoroscope attachment (American Instrument Co., Inc., Silver Spring, Md.), operating at 7000 r.p.m. (top speed of phosphoroscope), the equations of O'Haver and Winefordner (*3*) for the mechanical system predict

$$\frac{I_s}{I_i} = 0.53 \frac{I_{P_0)s}}{I_{P_0)i}}$$

In this case the sample-to-interferent intensity ratio is almost halved. If ultimate sensitivity is limited by the interferent, then the pulse system would give a much lower limit of detectability in this case. The actual value of the sample-to-interferent intensity ratio depends upon the nature of the two substances and the ratio of their concentrations, but this should be relatively independent of instrumental factors. Thus a comparison of sample-to-interferent ratio enhancement is meaningful. It should be noted that for both the pulse and mechanical systems, the response falls off for very short decay times (case 2b). This, of course, provides rejection of interference from fluorescence and scattered excitation radiation.

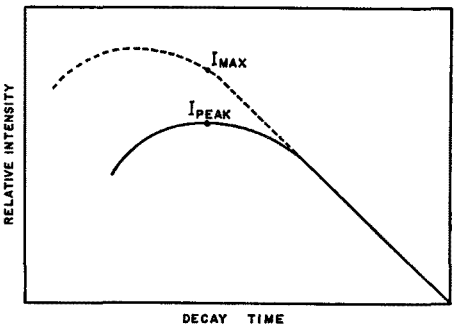

Figure 3. Curves relating I_{peak} to I_{max} (see text of paper for definitions)

Obviously, it would be desirable for the decay time of the sample to fall on the maximum in the I *vs.* τ curve (Figure 2), because maximum sample-to-interferent intensity ratio for both case 1 and case 2b interferences would then result. In addition, changes in τ of the sample (due to temperature variations, self-quenching, solvent quenching, or quenching by foreign substances) would then result in less change in I than if τ were on the sloping portion of the curve in Figure 2. This would result in higher accuracy and more nearly linear working curves. The value of τ at which the maximum I occurs, τ_{opt}, is determined by differentiating I (Equation 3) with respect to τ. Setting the result equal to zero, and solving for τ_{opt} gives

$$\tau_{opt} = \frac{t_P}{\ln\left(\frac{t_D + t_P}{t_D}\right)} \qquad (9)$$

The value of I at τ_{opt}, I_{peak}, is found by substituting Equation 9 into Equation 3. For the curves in Figure 2, Equation 9 predicts that τ_{opt} is 1.5×10^{-5} sec. and $I_{peak} = 2.5 \times 10 \times 10^{-7} f$. Since the decay time of a molecule will generally be a constant for any given experimental conditions—i.e., it is difficult to adjust τ to give τ_{opt}, and since τ_{opt} is a function of t_D and t_P, the maximum in the I *vs.* τ curve can be made to occur at τ_{opt} of any given sample (except a case 1 sample) by adjusting t_D and t_P. For instance, if t_P is fixed, then the optimum value of t_D—i.e., $t_{D)opt}$—may be found by solving Equation 9 for t_D, and so

$$t_{D)opt} = \frac{t_P}{\exp\left(\frac{t_P}{\tau}\right) - 1} \qquad (10)$$

Of course, when t_D is optimized for a given t_P and τ, then this implies that all parameters are optimized. It should be recognized that I_{peak} for a given sample is not the maximum value of I that can be obtained for given values of f and t_f. A slightly larger value of I (called I_{max} in Figure 3) would result if t_D were made smaller than $t_{D)opt}$. This would extend the linear (case 2a) portion of the I *vs.* τ curve to shorter values of τ, as shown in Figure 3. However in this condition I would be more sensitive to slight changes in τ, as mentioned before. Better overall results would generally be obtained if t_P and t_D were adjusted, according to Equation 10, to make τ_{opt} coincide with the τ of the sample.

Finally, it should be noted that, while Equation 7 indicates that a small value of f would result in a better sample-to-interferent intensity ratio, Equation 3 predicts that the actual measured signal is directly proportional to f. The smallest f that can be used will then depend on the sensitivity of the detection system.

LITERATURE CITED

(1) Bhaumik, M. L., Clark, G. L., Snell, L., Ferder, L., *Rev. Sci. Instr.* **36**, 37 (1965).
(2) Hendee, C. F., Brown, W. B., *Philips Tech. Rev.* **19**, 50 (1957).
(3) O'Haver, T. C., Winefordner, J. D., ANAL. CHEM. **38**, 602 (1966).
(4) Peterson, G. E., Bridenbaugh, P. M., *J. Opt. Soc. Am.* **53**, 1129 (1963).

T. C. O'HAVER
J. D. WINEFORDNER

Department of Chemistry
University of Florida
Gainesville, Fla. 32601

WORK carried out as part of a study on the phosphorimetric analysis of drugs in blood and urine supported by the U. S. Public Health Service (GM-11373-03).

Analysis of Cesium-134–Cesium-137 Mixtures by Gamma-Ray Spectrometric Methods

SIR: The analysis of Cs^{134}–Cs^{137} mixtures having Cs^{134}/Cs^{137} count-rate ratios as low as 0.02 or less is of practical interest (*1, 10*). These nuclides are usually found together in cesium separated from fission products that were cooled sufficiently for Cs^{136} ($T_{1/2}$ = 13 days) to be absent. Cesium-137 is a high-yield primary fission product, and Cs^{134} is a product of neutron capture by Cs^{133} formed during the fission process or present as contaminant in the fuel element.

The analysis of these two nuclides by resolution of gross decay curves is impractical because of their long half lives (2.1 years for Cs^{134} and 30 years for Cs^{137}). Various gamma-ray spectrometric methods have been described for the analysis of Cs^{134}–Cs^{137} mixtures (*2, 5, 9*). (The gamma-ray spectra of the two nuclides and a mixture are shown in Figure 1.) However, none are sensitive enough for measuring Cs^{134} when its fraction is below about 10%. Recently, high resolution lithium-drifted germanium diodes have been made applicable to gamma-ray spectrometry. At the present time, however, because of their low gamma-ray detection efficiency, these detectors are not suitable for use in routine analysis of samples with low levels of activity.

In this report two highly sensitive methods of Cs^{134} analysis are described and evaluated.

One of the methods, least-squares analysis, is probably the best for analyzing gamma-ray pulse-height spectra. It has been widely used for the reduction of gamma-ray pulse-height spectra (*8, 11*) and is applicable to the analysis of Cs^{134}–Cs^{137} mixtures. In this method, the pulse-height spectrum of a mixture is synthesized, with the aid of a computer, from normalized spectra of each of the components. Each "pure spectrum" is weighted such that the sum of the pure spectra gives a best fit to the experimental spectrum based on a least-squares criterion.

The other method, also applicable to the analysis of Cs^{134}–Cs^{137} mixtures, is gamma-gamma coincidence spectrometry. Since the two most prominent gamma rays of Cs^{134}, which have energies of 796 k.e.v. and 605 k.e.v., are emitted in coincidence and since Cs^{137} has no coincident gamma rays, Cs^{134} is amenable to analysis by this method.

In this work, these methods are evaluated with particular attention to their suitability for analyzing mixtures with low Cs^{134} content.

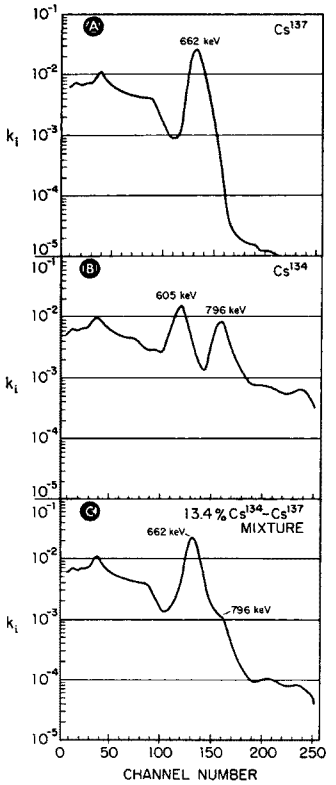

Figure 1. Normalized gamma-ray pulse height spectra of (a) Cs^{137}, (b) Cs^{134}, and (c) 13.4% Cs^{134} in Cs^{134}–Cs^{137} mixture

k_i = counts in channel i/gross count

EXPERIMENTAL

Materials. CESIUM-134. This nuclide was purchased from Oak Ridge National Laboratory and was purified by the tetraphenylboron precipitation method (*7*). Inspection of the sample by noncoincident gamma-ray and gamma-gamma coincidence spectrometry showed no apparent contaminants.

CESIUM-137. Cesium-137 was extracted from fission products. Enriched U^{235} (93.17%) was irradiated for 100 minutes in a flux of 0.81×10^{14} neutrons/sq. cm./second in the General Electric Test Reactor (GETR) at Vallecitos, Calif. The irradiation time was sufficiently short to preclude the build-up of Cs^{133}, from which Cs^{134} would be formed by neutron capture. Nine months were allowed for the decay of Cs^{136}. Cesium was separated from the fission-product mixture by precipitation with silicotungstic acid (*7*). Further decontamination was accomplished by tetraphenylboron precipitation. The noncoincident gamma-ray and the gamma-gamma coincidence spectra of the sample showed no apparent contaminants (however, see Discussion).

SAMPLE PREPARATION. Known mixtures, as well as pure sources, were prepared by evaporation of aliquots of the respective isotopic solutions in lucite planchets. The Cs^{134}/Cs^{137} count-rate ratios were varied from 0.002 to 8.

Instruments. GAMMA-GAMMA COINCIDENCE SPECTROMETER. The detector arrangement and a block diagram of the spectrometer are shown in Figure 2 and Figure 3, respectively.

Two detectors, each composed of a 4- × 4-inch cylindrical, thallium-activated, sodium iodide crystal (Harshaw Type B) coupled to a 5-inch photomultiplier tube (EMI Type 9579 B), were placed so as to face each other. A sample holder, made of 1-inch thick lead with a 2-inch diameter hole in the center, was placed between the two crystals, and a $^3/_4$-inch thick lead collar was placed about each crystal. The detectors, sample holder, and collars were mounted in an aluminum cylinder so that the geometry would remain fixed.

The detector pulses, after amplification, were fed into a Cosmic Model 801 multiple coincidence unit (Radiation Labs, Inc.). This unit contained a fast-slow coincidence circuit and two single-channel analyzers. The latter permitted selection of pulses corresponding to gamma rays of a given energy or energy range by setting appropriate windows. The resolving time of the fast coincidence circuit could be varied, but in this work was set at 90 nanoseconds. The coincidence output pulses and the outputs from the two single-channel analyzers were counted simultaneously on three scalers controlled by a common timer. Coincidence spectra were obtained by feeding the pulses from the linear amplifier of one of the detectors into a 400-channel pulse-height analyzer (Technical Measurements Corp.) and gating with the coincidence output pulses.

NONCOINCIDENT GAMMA RAY SPECTROMETER. Noncoincident gamma-ray spectra were taken on an Argonne-type, 256-channel, vacuum-tube, pulse-height analyzer (Radiation Counter Laboratories) with a fast, punched-card readout system (*6*). The detector was a 3- × 3-inch, thallium-activated, sodium iodide well crystal (Harshaw type AW). A 3-inch diameter photomultiplier tube (EMI 9578B) was used.

Counting Procedure and Data Analysis. COINCIDENCE DATA. Coincidence counting was carried out under

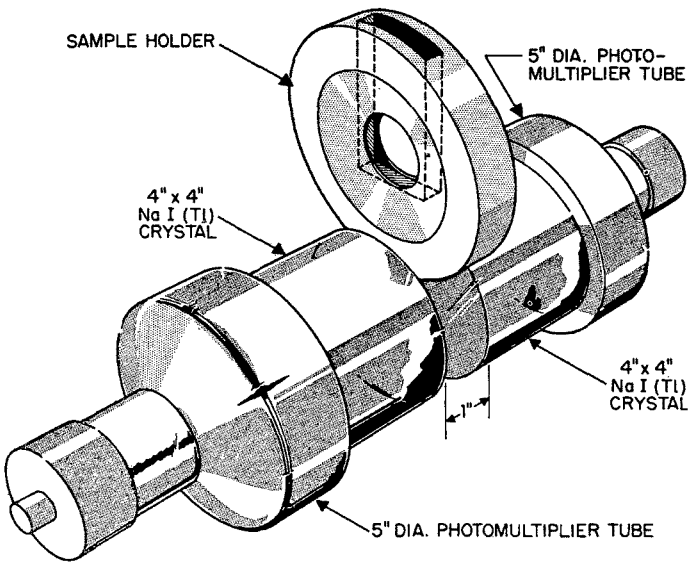

Figure 2. Gamma-gamma coincidence detector and sample holder

two sets of instrumental conditions. In one case, the single-channel analyzer window of one of the detectors was set to accept pulses corresponding to an energy range of 510 to 890 k.e.v. In other words, only those pulses corresponding to the full energy peak of the 796- and 605-k.e.v. gamma rays were selected. In practice, however, the Compton edge of the 796-k.e.v. gamma ray was also accepted by the window, because it overlaps with the 605-k.e.v. gamma-ray photopeak. All pulses whose amplitudes exceeded the base-line threshold of the instrument were accepted from the other detector. In the second case, the above energy selection was made on pulses from both detectors.

The singles and coincidence counts were measured simultaneously. The accidental coincidence rate was calculated from the singles counting rates by means of the expression

$$N_a = 2\tau N_1 N_2$$

where τ is the coincidence resolving time and N_1 and N_2 are the singles counting rates for detectors 1 and 2, respectively. The calculated accidentals and the measured background were subtracted from the observed coincidences to obtain the true coincidence counting rate. The Cs^{134} activities were estimated by comparing the true coincidence counting rates of the mixtures with that of the Cs^{134} standard.

Noncoincidence Data. As mentioned earlier, noncoincident gamma-ray spectra were taken on a 256-channel pulse-height analyzer with a fast, punched-card readout system. With this system, data is read out directly onto punched cards. All the calculations were made with an IBM 704 computer. All spectra were corrected for instrumental shifts in gain and base line by a computer correction method developed by Covell (*3*).

The relative amounts of Cs^{134} and Cs^{137} were computed by least-squares analysis of the gamma-ray spectra. The particular program used in this work was developed at this laboratory (*4*). In this method a pulse-height spectrum of a mixture is synthesized from normalized spectra of the components. Each normalized spectrum, which is called the library spectrum of the particular component, is weighted so that their sum gives a "best fit" to the experimental spectrum in a least-squares sense. In this work, a library spectrum was obtained by averaging four corrected spectra of the pure source.

RESULTS AND DISCUSSION

The coincidence spectrometric analysis results are presented in Table I. The standard deviations, which are also shown in the table, were estimated from the expression

$$\sigma = \sqrt{\frac{1}{n-1}\sum_{i=1}^{n}(x_i - \bar{x})^2}$$

where n is the number of runs, x_i the individual values, and $\bar{x}$ the average. Each sample was measured three times with a 510- to 890-k.e.v. window imposed on pulses from both detectors and three times with a window on only one detector. These results (Table I, columns 5 and 6) show that Cs^{134} can be measured accurately by the coincidence method for the entire range of mixtures studied. Mixtures with Cs^{134}/Cs^{137} ratios less than 0.01 were analyzed with an accuracy better than 5%. For example, in sample 1202, where the ratio was 0.002, the measured amount of Cs^{134} was within 4% of the actual value. The standard deviations ranged from about 3% of the measured values for low Cs^{134}/Cs^{137} ratios (less than 0.01) to about 0.5% to 1% for higher ratio mixtures.

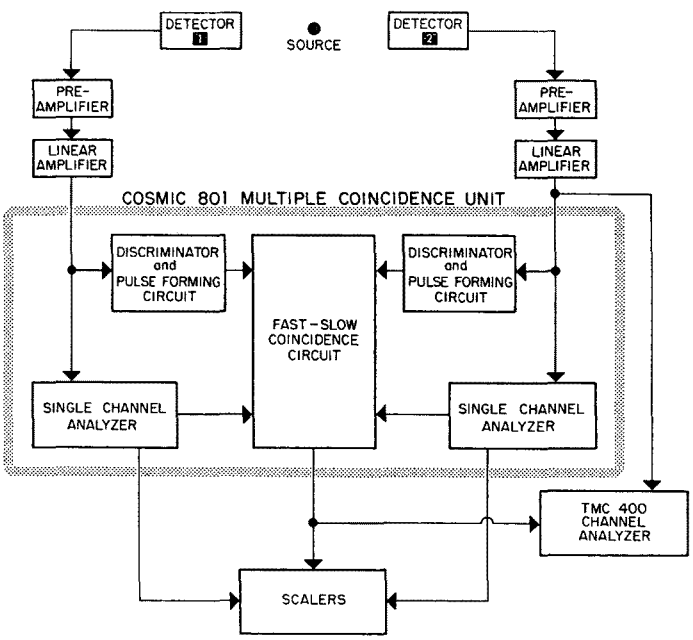

Figure 3. Block diagram of gamma-gamma coincidence spectrometer

Very little difference was observed between the two experimental conditions. Slightly better precision was noted when windows were used on both detectors. The difference probably would have been more apparent had there been some contaminant in the mixture. In such a case, selectivity could be increased further by imposing stricter pulse-height discrimination. For example, one window can be set for an energy range corresponding to the 605-k.e.v. photopeak and the other to the 796-k.e.v. photopeak.

As shown in Table I, some true coincidences were observed in the Cs^{137} sample. Since the amount was small and of the order of the experimental error, no corrections were made for this. If these coincidences are due to Cs^{134}, it must have been produced from an (n, γ) reaction on Cs^{133} impurity in the uranium sample or its container or that produced directly as fission product. As was mentioned earlier, the irradiation conditions were selected to preclude formation of Cs^{134}, which is a nuclide shielded by stable Xe^{134} from formation by beta decay of fission products of mass chain 134. During the short irradiation time of 100 minutes, the build-up of Cs^{133} will be insufficient to permit formation of detectable amounts of Cs^{134} by neutron capture in Cs^{133}.

However, assuming that the true coincidences observed in the Cs^{137} sample are due to Cs^{134}, it is interesting to speculate about its origin. If it is from cesium impurity in the enriched uranium, the observed amount corresponds to about 40 p.p.m., which seems to be inordinately high. On the other hand, if we assume the coincidences are due to Cs^{134} formed independently, its independent fission yield is found to be about $^1/_{10,000}$ the total yield of Cs^{137} On the basis of the most recent estimates (*12*), this value is much too high. This leaves two other possibilities: There is a cesium impurity in the SiO_2 container, which is a most likely possibility, or the coincidences are due to something other than Cs^{134}

The results obtained from least-squares analysis of noncoincident gamma-ray spectra are given in Table II. With this method one is able to determine Cs^{134} in mixtures where the Cs^{134}/C^{137} ratio is as low as 0.01, although precision is poor at these low levels.

This is more sensitive than any other noncoincidence method evaluated to date. However, Cs^{134} could not be determined by this method for lower ratio mixtures. The relative standard deviations for the measured per cent Cs^{134} in mixtures of 13.4% Cs^{134} and greater ranged from 0.2 to 10%, and those for the mixtures with 4.7% and 0.88% Cs^{134} were 25% and 75%, respectively (see Table III).

From these results we can conclude that gamma-gamma coincidence spectrometry is well suited for analyzing Cs^{134}–Cs^{137} mixtures, especially those with low Cs^{134} content. It is much more sensitive than the least-squares and other methods of analysis of noncoincident gamma-ray spectra. Mixtures whose Cs^{134}/Cs^{137} gross-count ratios are in the 0.002 to 0.01 region can be analyzed by the coincidence method with an accuracy and precision of better than 5% of the measured value, and for higher count ratios, 1%.

Cesium-134 can be determined by least-squares analysis of noncoincident gamma-ray spectra in mixtures in which the Cs^{134}/Cs^{137} ratio is as low as 0.01. The precision is poor at this low level, but it is 10% or better for ratios of about 0.13 and greater. The least-squares method was more sensitive than any of the other noncoincident methods evaluated to date.

Table I. Cs^{134} Activity in Cs^{134}–Cs^{137} Mixtures Determined by Gamma-Gamma Coincidence Counting

Sample No.	Cs^{134}/Cs^{137}	Counts of Cs^{137} added, c.p.m.	Counts of Cs^{134} added, c.p.m.	Measured Cs^{134} activity, c.p.m. Two windows[a]	One window[b]
1201	0	134,081	0	16	14
1202	0.0020	164,706	321	337 ± 12	297 ± 8
1203	0.0031	107,261	333	341 ± 8	336 ± 11
1204	0.0045	101,312	456	468 ± 15	465 ± 24
1205	0.0088	107,120	948	967 ± 20	970 ± 33
1206	0.049	100,203	4,949	5,027 ± 50	4,997 ± 50
1207	0.155	93,992	14,494	14,392 ± 110	14,425 ± 85
1208	0.43	71,262	30,751	30,676 ± 450	30,391 ± 390
1209	0.92	58,549	54,598	54,978 ± 320	54,763 ± 400
1210	2.06	34,780	71,680	72,129 ± 210	72,313 ± 765
1211	7.85	11,456	89,678	90,358 ± 700	90,657 ± 1130
1212	...	0	119,738	...	...

[a] Windows (510 to 890 k.e.v.) imposed on both detectors.
[b] Window imposed on one detector only.

Table II. Analysis of Cs^{134}–Cs^{137} Mixtures. Computer Analysis of Noncoincident Gamma-Ray Spectra by Method of Least Squares

Sample No.	Cs^{134}/Cs^{137}	Cs^{134}, c.p.m. Counts added	Cs^{134}, c.p.m. Measured	Cs^{137}, c.p.m. Counts added	Cs^{137}, c.p.m. Measured
1201	0	0	−484 ± 680	134,081	133,796 ± 560
1202	0.0020	321	1,022 ± 1,100	164,706	163,070 ± 1,070
1203	0.0031	333	392 ± 1,500	107,261	106,955 ± 660
1204	0.0045	456	3 ± 220	101,312	101,382 ± 440
1205	0.0088	948	1,158 ± 1,100	107,120	105,818 ± 1,900
1206	0.049	4,949	4,976 ± 1,200	100,203	99,658 ± 625
1207	0.155	14,494	16,004 ± 1,800	93,992	93,476 ± 730
1208	0.43	30,751	30,873 ± 860	71,262	70,959 ± 550
1209	0.92	54,598	55,553 ± 1,050	58,549	58,601 ± 420
1210	2.06	71,680	72,196 ± 350	34,780	34,789 ± 360
1211	7.85	89,678	90,783 ± 420	11,456	12,037 ± 390
1212	...	119,738	119,956 ± 480	0	−116 ± 240

Table III. Per Cent Cs^{134} in Cs^{134}–Cs^{137} Mixtures. Comparison of Results Obtained by Coincidence Spectrometry and Least-Squares Analysis of Noncoincident Gamma-Ray Spectra

Sample No.	Per cent Cs^{134} mixture	Coincidence Window[a] on both detectors	Counting Window on one detector	Least-squares analysis of noncoincident spectra
1201	0	0.01	0.01	−0.36 ± 0.5
1202	0.20	0.20 ± 0.01	0.18 ± 0.01	0.67 ± 0.6
1203	0.31	0.31 ± 0.01	0.31 ± 0.01	0.32 ± 1.2
1204	0.45	0.44 ± 0.01	0.46 ± 0.02	0 ± 0.2
1205	0.88	0.89 ± 0.01	0.89 ± 0.03	1.2 ± 0.9
1206	4.70	4.75 ± 0.04	4.72 ± 0.05	4.7 ± 1.1
1207	13.4	13.2 ± 0.1	13.2 ± 0.08	14.6 ± 1.5
1208	30.1	29.9 ± 0.4	30.1 ± 0.4	30.3 ± 0.5
1209	48.2	48.3 ± 0.3	48.1 ± 0.4	48.7 ± 0.6
1210	67.4	67.4 ± 0.2	67.5 ± 0.7	67.4 ± 0.4
1211	88.7	88.8 ± 0.7	89.1 ± 1.1	88.3 ± 0.4
1212	100	...	...	99.9 ± 0.2

[a] 510 to 890 k.e.v. window.

LITERATURE CITED

(1) American Society for Testing and Materials, Committee E-10 on Radioisotopes and Radiation Effects, "Tentative Methods for Radiochemical Determination of Cs^{137} in Aqueous Solutions," 1965.
(2) Aoki, F., Kurosawa, T., Yajima, S., *Bull. Chem. Soc. Japan* **30**, 583 (1957); *C.A.* **52**, 5998b (1958).
(3) Covell, D. F., *Nucl. Instr. Methods* **36**, 229 (1965).
(4) Covell, D. F., U. S. Naval Radiological Defense Laboratory *Rept.*, to be published.
(5) Ellemen, T. S., Howes, J. E., Sunderman, D. N., *Intern. J. Appl. Radiation Isotopes*, **12**, 142 (1961).
(6) Euler, B. A., Phelps, P. L., Covell, D. F., *Nucl. Instr. Methods* **34**, 266 (1965).
(7) Handley, T. H., Burros, C. L., ANAL. CHEM. **31**, 332 (1959).
(8) Heath, R. L., *Nucleonics* **20**, 67 (1962).
(9) Kinsley, M. T., Cumming, J. B., Finston, H. L., ANAL. CHEM. **32**, 1081 (1960).
(10) Liden, K., *Nature* **195**, 1040 (1962).
(11) Salmon, L., Atomic Energy Research Establishment Memorandum **AERE-M 1140** (1963).
(12) Strom, P. O., Greendale, A. E., Delucchi, A. A., Division of Nuclear Chemistry and Technology, 150th Meeting, ACS, Atlantic City, N. J., September 1965.

SACHIO YAMAMOTO

U. S. Naval Radiological Defense Laboratory
San Francisco, California 94135

Presented before the Division of Nuclear Chemistry and Technology, 150th Meeting, ACS, Atlantic City, N. J., September 1965. Work was supported by the U. S. Atomic Energy Commission.

The Effect of Water on Saponification of Organic Esters

SIR: In our recent work involving the analysis of components of woods we required a relatively simple and accurate procedure for the determination of the acetyl content. Owing to the very deep color of our test solutions, the procedure described by Mazor and Meisel (*6*), in which the sample is transesterified with sodium methoxide, was used. The volatile methyl acetate was then distilled into an alcoholic KOH solution and after saponification of the ester the excess of KOH was back-titrated with HCl. In this work we used a bulk prepared KOH solution in anhydrous methanol (0.05% H_2O) which we usually keep available in the laboratory for several other procedures.

Our initial results with the above technique showed serious variations between experiments and consistently lower values than expected. After having checked every stage of the procedure, particularly the distillation, we concluded that the only reason for the variations and low values for the ester content was the incomplete saponification with the KOH solution, and that this in turn was due to absence of water in the reagent.

Although Hine (*4*) has indicated in a general way the presence of water in alkaline and acid catalyzed hydrolysis of esters he did not stress its significance in alkaline hydrolysis nor was he able to quote any studies that would substantiate the role of water in the mechanism of hydrolysis. Consultation of several reference analytical textbooks has shown that the nature of the alcohol used in saponification reactions was either not specified at all (*6, 8, 9*) or, where the presence of water was mentioned, its significance was not indicated (*1-3, 5, 7, 10*). In the procedure recommended by the AOAC (*7*) the alcohol was purified according to a procedure recommended in 1936 using refluxing with KOH and aluminum metal. It was likely that this purification would lead to substantial dehydration of the alcohol.

In our laboratories alcoholic alkalies are usually prepared with anhydrous methanol, reagent grade, with a water content of about 0.05%. The availability of high purity reagents and anhydrous solvents is relatively recent, and their use in nonaqueous systems will generally not lead to complications, however, the saponification reaction seemed to require the presence of water. This was confirmed in a series of experiments.

Table I. Determination of Acetyl in Glucose Pentaacetate

(Transesterification to methyl acetate and hydrolysis with KOH)

100 mg. glucose pentaacetate; 30 ml. 0.1*N* KOH

Vol. of H_2O added, ml.	H_2O in KOH reagent, %	Recovery of acetyl, %
0	(0.05)	18.0
2	6.5	92.2
4	11.8	98.1
5	14.3	100.4
6	16.7	99.8
13	30.0	100.0

EXPERIMENTAL

In the first series of experiments glucose pentaacetate (100 mg.) was transesterified by boiling with anhydrous methanol in the presence of potassium methoxide (0.1*N*, 20 ml.) which acted as a catalyst (*6*) as shown below:

The liberated methyl acetate was distilled into an excess of methanolic KOH (0.1*N*, 30 ml.) and was then saponified by refluxing for 1 hour. The excess of KOH was then titrated with HCl (0.1*N*) using phenolphthalein as indicator. Controlled amounts of water were added to the saponification reagent as shown in Table I.

The above results indicated a very definite effect of water on the efficiency of hydrolysis of the ester.

In further tests (Table II) the transesterification step was omitted by using a standard solution of methyl acetate in methanol. The hydrolysis was carried out exactly as above; 39 mg. and 78 mg. acetyl was used in each series.

The above results confirmed previous findings. With larger quantities of acetyl, larger amounts of water in the alcoholic KOH reagent were necessary for complete saponification.

When methanol was substituted by ethylene glycol as the solvent for KOH, similar effects due to water were observed. However, the higher boiling point of ethylene glycol led to losses of methyl acetate during refluxing. The finally adopted procedure was as follows:

The amount of sample that would provide about 30 mg. of acetyl (CH_3COO—, mol. wt. 59) was refluxed with 20 ml. of 0.1*N* potassium methoxide in methanol (anhydrous) for 1 hour (in this step all esters were converted to methyl acetate). The reaction mixture was then distilled into 30.0 ml. of 0.1*N* KOH in methanol containing 20% H_2O, and this was refluxed for 1 hour to saponify the methyl acetate. After cooling, the excess of KOH was titrated with 0.1*N* HCl using phenolphthalein

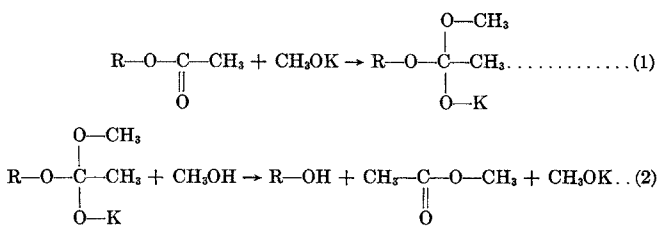

Table II. Determination of Acetyl in Methyl Acetate

(Direct hydrolysis with KOH, 40 ml. 0.1*N* KOH)

Vol. of H_2O added, ml.	H_2O in KOH reagent, %	% Recovery of acetyl with: 39 mg. acetyl	78 mg. acetyl
0	(0.05)	60.8, 47.5	25.5, 23.1
0.5	1.1	75.7, 77.2	73.2, 68.4
1.0	2.4	93.1, 93.1	90.4, 84.6
1.5	3.6	96.0, 96.0	93.8, 93.8
2.0	4.8	101.0, 100.0	95.4, 96.0
3.0	7.0	101.0, 100.0	97.2, 98.4
5.0	11.1	101.0, 100.0	99.1, 98.5

as indicator (1 ml. 0.1*N* KOH ≡ 5.9 mg. CH_3COO—).

LITERATURE CITED

(1) ASTM "1965 Book of ASTM Standards," Part 20, pp. 891–2, American Society for Testing and Materials, Philadelphia, 1965.
(2) Cheronis, N. D., Ma, T. S., "Organic Functional Group Analysis," pp. 175–6 Interscience, New York, 1964.
(3) Critchfield, F. E., "Organic Functional Group Analysis," pp. 141–3, Macmillan, New York, 1963.
(4) Hine, J., "Physical Organic Chemistry," 2nd ed., pp. 275–7, McGraw-Hill, New York, 1962.
(5) Jolly, S. C., "Official, Standardised and Recommended Methods of Analysis," pp. 79–80, W. Heffer & Sons Ltd., Cambridge, 1963.
(6) Mazor, L., Meisel, T., *Anal. Chim. Acta* **20**, 130 (1959).
(7) "Official Methods of Analysis of the Association of Official Agricultural Chemists," W. Horwith, Ed., 10th ed., pp. 185, 420, AOAC, Washington, 1965.
(8) Parr, N. L., "Laboratory Handbook," p. 7/96, George Newnes Ltd., London, 1963.
(9) Siggia, S., "Quantitative Organic Analysis Via Functional Groups," 3rd ed., p. 139, Wiley, New York and London, 1963.
(10) Snell, F. D., Biffen, F. M., "Commercial Methods of Analysis," Revised ed., pp. 343, 435–6, 725, Chemical Publishing Co., Inc., New York, 1964.

W. H. Greive
K. F. Sporek
M. K. Stinson

Owens-Illinois, Inc.
Corporate Research
Technical Center
1700 N. Westwood Ave.
Toledo, Ohio 43607

Application of Radiometric Techniques to Quantitative Paper Chromatography of Iron, Copper, Manganese, and Cobalt

Sir: Van Erkelens (*2*) mentions the possibility of performing quantitative analysis of traces of metals separated by paper chromatography. He precipitated the elements in the chromatograph with radioactive hydrogen sulfide, but gave no data whereby sensitivity or precision of the method could be estimated. In another paper (*1*), Van Erkelens described an analysis for lead using phosphate labeled with P^{32} after separation from a number of interfering elements. This method was extended by Welford (*3*) and showed high sensitivity, but again no data were presented on the precision of the method.

This method describes the quantitative determination of iron, cobalt, copper, and manganese on paper chromatograms. After the chromatographic separation, radiometric methods were used to determine these four ions. The usefulness of the radiometric method of analysis for these ions was demonstrated by an analysis of NBS Standard Reference Material No. 671, nickel oxide, which contained traces of Fe, Co, Cu, Mn, Cr, Ti, Mg, and Al.

EXPERIMENTAL

In developing a method of separation, synthetic solutions of the ions of interest were used as well as solutions of the nickel oxide sample. The first step in the procedure for the separation of the trace elements in the nickel oxide consisted of spotting several 0.01-ml. aliquots of the sample dissolved in 9*N* hydrochloric acid on Whatman No. 1 chromatographic paper which had been purified by washing with 3*N* hydrochloric acid. The separations were then accomplished by descending chromatography utilizing a solvent consisting of 8 parts concentrated hydrochloric acid and 92 parts methyl ethyl ketone. The papers were removed from the chromatographic tank, air dried, and placed in a tank saturated with ammonia vapor in order to neutralize the hydrochloric acid. They were then removed from the tank and air dried again.

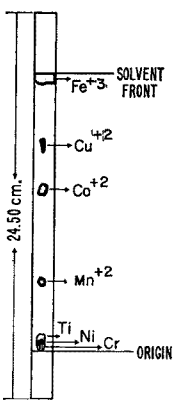

Figure 1. Separation of trace constituents in nickel oxide standard ref. material No. 671 using the solvent system: methyl ethyl ketone–conc. HCl (92:8)

In order to establish the R_f factors for the ions of interest, sufficient concentration of test solutions of the nickel oxide was used to render the spots of copper, cobalt, and iron visible when treated with alkaline sodium sulfide. The manganese was detected using sodium peroxide. The other ions, which remained near the origin, were detected with appropriate spray reagents. The R_f factors

$$\frac{\text{distance ion moved from origin}}{\text{distance solvent moved from origin}}$$

were 0.99 Fe, 0.77 Cu, 0.60 Co, 0.26 Mn, 0.08 Ti, 0.06 Cr, 0.06 Al, and 0.06 Mg, as determined by three replicate separations (see Figure 1).

After establishing the R_f factors, corresponding areas on additional chromatograms were cut out and analyzed quantitatively. The phosphates of iron, copper, and manganese were precipitated with radioactive trisodium phosphate (0.12*M* with 10^5 c.p.m. of P^{32} per ml.) in 50-ml. beakers. The papers were removed, washed with water, and air dried. The labeled precipitates were assayed with a beta proportional counter.

Manganous ion was oxidized with alkaline hydrogen peroxide (15 ml. of 30% hydrogen peroxide diluted to a liter with 1*N* sodium hydroxide), washed with water, and air dried. The paper containing the resultant manganese dioxide was equilibrated with a solution containing Co^{60} in an ammonium hydroxide–ammonium chloride buffer, pH 10.00. After washing with distilled water, the adsorbed Co^{60} was assayed using a scintillation NaI(Tl) well counter.

Table I. Analysis of a Sample of Nickel Oxide (NBS, SRM No. 671)

Cation	Amount present, %	Av. amount found, %	Rel. std.[a] dev., %	No. det.	Rel. error, %	Method of analysis
Fe^{+3}	0.39	0.37	7.1	8	−5.7	Ppt'd with phosphate labeled with P^{32}
Cu^{+2}	0.20	0.19	6.8	8	−5.0	Ppt'd with phosphate labeled with P^{32}
Mn^{+2}	0.13	0.134	39.5	6	+3.0	Ppt'd with phosphate labeled with P^{32}
Mn^{+2}	0.13	0.138	3.8	8	+5.8	Adsorption of Co^{60} on manganese dioxide
Co^{+2}	0.31	0.316	4.1	8	−1.9	Exchange of Fe^{59} with $Co_2[Fe(CN)_6]$

[a] For a single determination.

The cobalt was precipitated on the paper by reacting it with a saturated solution of potassium ferrocyanide. The papers were then washed with water, with 0.1*N* hydrochloric acid, and then with water again. The papers were equilibrated with Fe^{59} solution to allow exchange with the ferrocyanide, washed with water, dried, and counted with a NaI(Tl) scintillation well counter.

Standard curves were prepared for each element by plotting counts per minute *vs.* micrograms. The experimental points were fitted to a straight line by least squares analysis. Blanks were subtracted from all data for each element. Washing of the papers was a very important factor in minimizing the blank. The method of washing was standardized to give the highest precision. The paper was washed by gentle shaking with 5 ml. of water for 10 minutes. After the first wash the paper was removed from the beaker with forceps coated with Teflon allowing the water to drain off the paper, then the paper was placed in a second beaker containing 5 ml. of water. The procedure was repeated for a third time.

RESULTS AND DISCUSSION

Table I lists the results obtained along with data on the precision and accuracy of the method. The amounts analyzed were 3.9 μg. of iron, 2.0 μg. of copper, 3.1 μg. of cobalt, and 1.3 μg. of manganese. The limit of detection is 0.1 μg. for iron, 0.02 μg. for cobalt, and 0.01 μg. for manganese. The data show quite satisfactory precision except the labeled manganese phosphate precipitate. Efforts are under way to improve this precision.

NBS Standard Reference Material No. 671 was certified by the use of gravimetric and spectrochemical techniques. No precision or accuracy is given on the certificate, but assuming that the recommended value is close to the true amount present, an estimate of the accuracy is given in Table I.

The main advantage of the paper chromatographic method is that it permits the analysis of a number of elements in the same sample. The radiometric methods which are used to determine the separated elements have a greater sensitivity than most other methods of quantitative analysis which have been applied to chromatographic separation on paper or thin layer plates. Additional studies are in progress to extend the use of these radiometric procedures on chromatographs to other elements.

LITERATURE CITED

(1) Van Erkelens, P. C., *Anal. Chim. Acta* **25**, 570–578 (1961)
(2) Van Erkelens, P. C., *Nature* **172**, 357–8 (1953).
(3) Welford, G. A., Chiotes, E. L., Morse, R. E., ANAL. CHEM. **36**, 2350 (1964).

A. R. LANDGREBE
T. E. GILLS
J. R. DEVOE

Radiochemical Analysis Section
Analytical Chemistry Division
Institute for Materials Research
National Bureau of Standards
Gaithersburg, Md. 20760

Semiquantitative Estimation of Nitrogen in Ammonium Faujasite by Differential Thermal Analysis

SIR: The use of differential thermal analysis as a tool in the analysis of minerals and inorganic compounds (*8*) and solid catalysts (*5*) is well known, and a review of significant developments in the thermal analysis field has recently been published by Murphy (*6*). Thermal analysis techniques have also been employed in the characterization of synthetic zeolites (*2*, *9*).

In the course of studies on the properties of zeolites, we have observed an association between the presence of exotherms near 400–550°C. in the DTA pattern (run in oxygen atmosphere) of ammonium Y faujasite and the loss of zeolitic ammonium groups. Further examination revealed that the intensity of this DTA exotherm was proportional to the amount of zeolitic nitrogen (in the range of 0.2–5%). Thus, a semiquantitative method of estimating zeolitic ammonia is afforded.

EXPERIMENTAL

Apparatus. An R. L. Stone Differential Thermal Analyzer, Model DS-19 was used for DTA analyses (10° C./min., 0.2 mv. full scale, 150 mesh Vycor reference). A Consolidated Electrodynamics Corp. Model 21-103 mass spectrometer operated at 70 e.v. was used for gas analyses. A Perkin-Elmer 421 spectrophotometer was used for infrared analyses.

Reagents. The crystalline ammonium Y faujasite (NH_4Y) was prepared from a synthetic sodium Y aluminosilicate by repeated ion exchange with warm 10% aqueous NH_4Cl solution. Its unit cell composition was $(NH_4)_{48.9}\cdot(Na)_{5.1}\cdot(AlO_2)_{51}\cdot(SiO_2)_{141}\cdot(H_2O)_x$.

Procedure. Zeolite (4 grams, 5 ml. $^8/_{14}$ mesh) was placed in an electrically-heated, tubular Vycor-glass reactor fitted with axial glass thermocouple well, and a continuous flow (5 ml./min. at one atmosphere) of dry O_2 established. The reactor was then heated to the appropriate temperature and the catalyst calcined for 3 hours. The reactor was then sealed off and transferred to a dry box, where zeolite samples were placed in dry vials for Kjeldahl nitrogen determination and DTA analysis; catalyst samples for infrared analysis were prepared in the dry box by mulling with Fluorolube S (Hooker Electrochemical Co.). This procedure was repeated for NH_4Y samples calcined at temperatures of 200–500° C.

Similarly, effluent gas studies were effected by calcining zeolite samples (7.44 grams, 17.0 ml.) in dry O_2 or He (1.2 ml./min.) for 3 hours at 550° C., and collecting the total effluent gas over 10% aqueous H_2SO_4 in a conventional gas collection apparatus. After vigorous shaking to complete the adsorption of NH_3, the volume of gas was recorded, and samples were

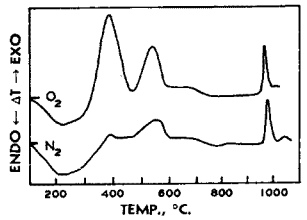

Figure 1. Comparison of DTA profiles in O_2 and N_2 atmosphere for uncalcined NH_4Y zeolite

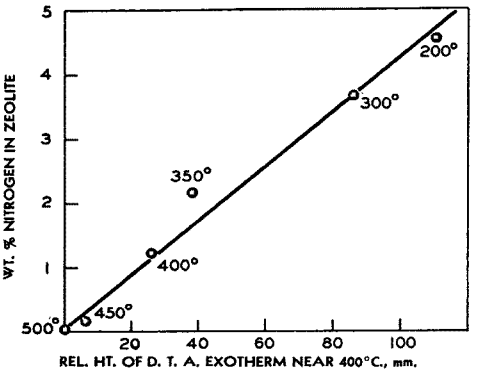

Figure 2. Correlation between wt. % nitrogen and height of DTA peak near 400° C. in NH_4Y zeolites calcined in O_2 at different temperatures

removed for mass spectrometric analyses. Precautions were taken to prevent air contamination at all stages.

RESULTS AND DISCUSSION

DTA Analysis of Uncalcined NH_4Y. Figure 1 shows a comparison of DTA profiles recorded in oxygen and nitrogen atmospheres for previously uncalcined NH_4Y. Both curves show broad endotherms near 200–300° C. corresponding to desorption of physically adsorbed water, sharp exotherms near 980° C., presumably associated with lattice reorganization and weak endotherms near 750° C. Most prominent, however, in the thermogram recorded in oxygen are two intense exotherms near 400° and 550° C. Similar exotherms, but of much weaker intensity, are present in the thermogram of the sample run in nitrogen atmosphere.

Correlations of DTA Exotherms with Loss of Zeolitic Nitrogen. As shown in Figure 2, when weight per cent zeolitic nitrogen (Kjeldahl) is plotted against the height of the exotherm near 400° C., for a series of NH_4Y samples calcined at various temperatures in oxygen, a nearly linear, empirical relationship is observed. The heights of the exotherms (DTA analyses run in oxygen atmosphere) are referred to the average base lines in the region 700–900° C.

Thus, these exotherms are absent in zeolite samples where calcination (500° C.) has removed all nitrogen. They are present however, in samples calcined at 450° C. containing 0.15% nitrogen (2.82% of calculated maximum based on sodium-free AlO_2-units), the infrared spectra of which do not show a detectable H—N—H deformation band (*7*) near 1410–1425 cm.$^{-1}$ That is, the DTA method appears to be slightly more sensitive than infrared in detecting small amounts of zeolitic ammonium groups. While the appearance of two exotherms associated with the loss of zeolitic ammonium groups may correspond to sites of different energy, it is possible that other lattice-associated processes could contribute to the overall thermochemistry of these transformations.

Analogously, an exotherm near 608° C. in the DTA profile of the ammonium feldspar buddingtonite (*4*) has been associated with ammonia loss; we have also observed an exotherm near 580° C. in the differential thermogram of uncalcined ammonium mordenite.

Role of Intracrystalline Oxidation in DTA Interpretation. Table I shows an analysis of the effluent gas collected during the calcination in oxygen of NH_4Y in a continuous-flow reactor at 550° C. From the large amounts of nitrogen gas present, it is apparent that oxidative decomposition of 44% of the zeolitic ammonium groups has occurred. Such an intracrystalline oxidation is not without precedent, since Barrer has reported a reaction conforming to the stoichiometry 4 Zeolite-$\overset{+}{O}NH_4$ + $3O_2$ → 4 Zeolite-OH + $2N_2$ + $6H_2O$ for the thermal decomposition in oxygen of the ammonium forms of mordenite and chabazite (*1*).

Thus, while recognizing the limitations inherent in comparisons of data obtained in the DTA instrument with that from a gross reactor system, we feel that the existence of an intracrystalline oxidation in the DTA sample run in oxygen atmosphere can reasonably explain the differences observed in the DTA profiles in Figure 1. Similarly, Ellis has reported an exotherm from oxidation of ammonia released during the DTA analysis of ammonia-treated bentonite (*3*).

Table I. Analysis of Effluent Gas Collected during Calcination of NH_4Y Zeolite in Oxygen at 550° C.

	O_2-Carrier	Control (He)
Total moles of gas collected	0.01199	0.01175
Mole-% N_2[a]	38.6	Trace
% Theoretical zeolite nitrogen as N_2[b]	44.2	—
% Nitrogen remaining in zeolite after calcination	0.01	0.83

[a] No oxides of nitrogen present.
[b] Based on Na-Free AlO_2-units.

ACKNOWLEDGMENT

We thank J. B. Milliken for running the differential thermal analyses and J. L. Montgomery and staff for performing the mass spectrometric analyses.

LITERATURE CITED

(1) Barrer, R. M., *Nature* **164**, 112 (1949).
(2) Barrer, R. M., Bratt, G. C., *J. Phys. Chem. Solids*, **12**, 130 (1959).
(3) Ellis, B. G., Ph.D. Thesis, Michigan State University, East Lansing, Mich., 1961.
(4) Erd, R. C., White, D. E., Fahey, J. J., Lee, D. E., *Am. Mineral.* **49**, 831 (1964).
(5) Keeley, W. M., "Application of DTA to the Evaluation and Testing of Catalysts," *Proc. 1st Toronto Symposium on Thermal Analysis*, 131–40 (1965).
(6) Murphy, C. B., ANAL. CHEM. **38**, 443R (1966).
(7) Rabo, J. A., Pickert, P. E., Stamires, D. N., Boyle, J. E., in "Proceedings of the Second International Congress on Catalysis," Vol. II, p. 2055, Editions Technip, Paris, 1961.
(8) Smothers, W. J., Chang, Y., "Differential Thermal Analysis: Theory and Practice," Chemical Publishing Co., New York, 1958.
(9) Toth, K., Flora, T., *Acta Chim. Acad. Sci. Hung.* **45**, 87 (1965).

P. B. VENUTO
E. L. WU
J. CATTANACH

Applied Research and Development Division
Mobile Oil Corp.
Paulsboro, N. J.

Fluorometric Determination of Zinc

SIR: Although the fluorescent characteristics of many zinc compounds have been investigated, only a few fluorometric methods for the determination of zinc have been reported. The fluorescence of a stabilized dispersion of zinc 8-hydroxyquinolate has been used for the determination of zinc in the concentration range of 0.4 to 12 p.p.m. (*3*). The fluorescing ether extract of a zinc–Rhodamine *s*-thiocyanate complex permits the determination of zinc at a 0.2-p.p.m. lower concentration limit (*1*). In a 70% ethanol–water mixture, the fluorescent zinc dibenzothiazolylmethane complex has been employed for the determination of zinc in the concentration range of 0.5 to 50 p.p.m. (*5*). Studies on three fluorescing zinc 2-methyl-8-hydroxyquinolate complexes have not resulted in an analytical application (*2*).

The present report describes the fluorometric determination of zinc using picolinealdehyde 2-quinolylhydrazone as a complexing agent. Characteristics of the polydentate ligand and of the zinc chelate are reported. Variables associated with metal ion complexation, with extraction of the zinc complex, and with fluorometric measurement of the zinc complex are discussed. Results on the determination of zinc in selected samples are presented. Data are included on the effects of many common ions on the fluorometric measurement.

EXPERIMENTAL

Apparatus. All fluorescence measurements were made with an Aminco-Bowman spectrophotofluorometer using 10-mm. square quartz cells. The fluorometer was equipped with a Hanovia Xenon lamp source and a 1P21 photomultiplier detector. The slits were arranged as follows: excitation beam, $^1/_8$, $^1/_{16}$, and $^1/_8$ inch; fluorescence beam, $^1/_8$, $^1/_{16}$, $^1/_8$, and $^1/_{16}$ inch. Measurements of pH were made with a Corning Model 12 pH meter.

Reagents. The chelating agent, picolinealdehyde 2-quinolylhydrazone, PAQH, was synthesized and purified in this laboratory. The starting material, 2-quinolylhydrazine, was prepared by the method described by Perkin and Robinson (*4*).

Picolinealdehyde 2-quinolylhydrazone was prepared by the addition of 3.18 grams (0.02 mole) of 2-quinolylhydrazine and 2.14 grams (0.02 mole) of 2-pyridinecarboxaldehyde to 75 ml. of absolute ethyl alcohol in a 100-ml. beaker. The solution was heated on a hot plate for 15 minutes and then allowed to cool to room temperature. The yellow product, which first started to precipitate early in the heating period, was filtered and redissolved in benzene. The desired product was obtained from benzene as a microcrystalline solid, yield 3.15 grams (64%), m.p. 204 to 204.5° C.

Anal. calcd. for $C_{15}H_{12}N_4$: C, 72.55; H, 4.88; N, 22.57. Found: C, 72.63; H, 4.67; N, 22.43.

A $8.00 \times 10^{-3}M$ solution of picolinealdehyde 2-quinolylhydrazone was prepared by dissolving 0.4968 grams of reagent in a minimum volume of 0.1*M* HCl with gentle heating. The cooled solution was diluted to 250 ml. with deionized water.

A standard zinc solution, $5.049 \times 10^{-3}M$ was prepared by dissolving 0.3301 gram of pure granular zinc in a minimum volume of dilute hydrochloric acid and diluting the resultant solution to 1 liter with deionized water.

A pH 8.0 buffer was prepared by the addition of concentrated hydrochloric acid to a solution 0.5*M* in tris(hydroxymethyl)aminomethane.

Deionized water was prepared by passing distilled water through a Barnstead Demineralizer equipped with a 0802 type cartridge.

Chloroform and all other reagents were of reagent grade quality.

Procedure. Dissolve the sample containing zinc by appropriate means. Adjust the pH of the solution to approximately 7.

To a 5-ml. aliquot containing from 1.3 to 16 μg. of zinc in a 125-ml. separatory funnel, add at least a 70-fold excess of PAQH, 10 ml. of pH 8.0 buffer, and dilute to approximately 75 ml. with distilled water.

Extract the aqueous solution with three 5-ml. portions of chloroform. Dilute the combined extracts to a volume of 50 ml. with additional chloroform. Measure the fluorescence of the chloroform solution at 535 mμ using an excitation wavelength of 485 mμ.

Determine the amount of zinc in the sample from a calibration curve prepared under identical conditions.

RESULTS AND DISCUSSION

Characteristics of the Reagent. The reagent, picolinealdehyde 2-quinolylhydrazone, is slightly soluble in organic solvents, insoluble in water, but soluble in dilute acidic solution. A stable dihydrochloride salt can be obtained as a bright yellow solid from glacial acetic acid upon treatment with gaseous hydrogen chloride. The reagent is readily extractable out of aqueous solution into chloroform over the pH range of 3.65 to 11.60. At pH 8.0, a distribution coefficient of 96 was calculated.

The reagent in chloroform exhibits weak fluorescence (Figure 1). The fluorescence is minimal relative to the strongly fluorescent zinc complex. In the analytical procedure, the fluorescence of excess reagent remains constant.

The reagent acts as a nonselective chelating agent toward many metal ions. Colored reaction products are formed with divalent cobalt, copper, iron, nickel, palladium, and zinc ions. Fluorescence is exhibited by the zinc complex. All of the reaction products are insoluble in chloride solutions and are readily extractable into common nonaqueous solvents.

Characteristics of the Zinc Complex. Zinc ion forms a water-insoluble complex with the reagent in the presence of chloride ion. The complex, with an experimentally determined empirical formula of $Zn(PAQH)Cl_2$, is soluble in benzene, carbon tetrachloride, chloroform, dimethylsulfoxide, isoamyl alcohol, and nitrobenzene. Conductance data obtained on the solid dissolved in dimethylsulfoxide indicate that the complex is essentially nonionic and undissociated in this solvent.

The zinc complex is readily extractable out of basic solution into chloroform. The resultant chloroform extract exhibits a high fluorescence intensity. Maxima in the excitation and fluorescence spectra occur at 485 mμ and 535 mμ, respectively (Figure 1). Fluorescence spectra of the solid complex dissolved in chloroform and of the complex extracted out of aqueous solution into chloroform were identical. It is assumed that the extracted fluorescent species is $Zn(PAQH)Cl_2$.

The distribution coefficient for the extraction of the zinc complex out of aqueous solution at pH 8.0 into chloroform was about 11. Three successive extractions with 5-ml. portions of chloroform are sufficient for the recovery of 99% of the complex from an aqueous volume of 75 ml.

Effects of pH and Excess Reagent. A pH study (Figure 2) showed that the zinc complex exhibits the highest fluorescence intensity at a pH of 8.9. A relatively sharp decrease in fluorescence intensity was observed at both higher and lower pH values.

At pH 8.9, maximum and reproducible fluorescence intensity was obtained over a 200- to 500-fold excess of reagent over zinc ion. At pH 8.0, maximum intensity was obtained with a 67:1 ratio of reagent to metal ion. The lower pH is to be preferred since less reagent is required.

Effect of Zinc Concentration. The zinc–picolinealdehyde-2-quinolylhydrazone complex displayed a linear relationship between concentration and fluorescence intensity over the concentration range of 0.404 to 4.847 × $10^{-6}M$ (0.026 to 0.31 p.p.m.) zinc ion. Negative deviation from linearity was

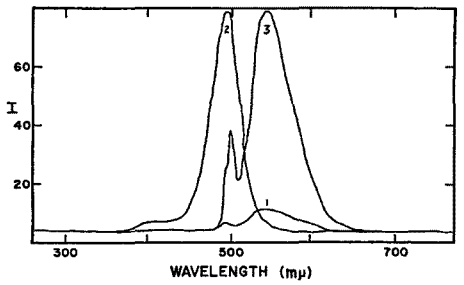

Figure 1. Fluorescence spectra of picolinealdehyde 2-quinolylhydrazone, each solution 7.775 × 10^{-4}M, pH 8.0

(1) Fluorescence of picolinealdehyde 2-quinolylhydrazone, excitation wavelength—485 mμ
(2) Excitation spectrum of zinc complex, 4.039 × 10^{-6}M, fluorescence wavelength—535 mμ
(3) Fluorescence spectrum of zinc complex, 4.039 × 10^{-6}M, excitation wavelength—485 mμ
The spectra are uncorrected

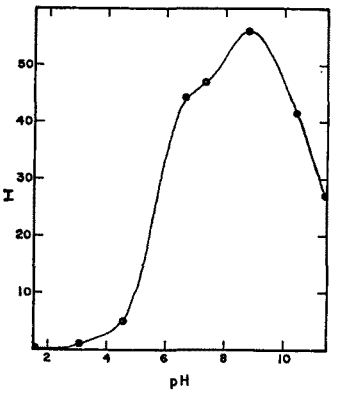

Figure 2. Effect of pH on formation and extraction of zinc–picolinealdehyde 2-quinolylhydrazone complex

1 × 10^{-4}M PAQH and 6 × 10^{-6}M zinc
Wavelength settings, 485 mμ and 535 mμ

observed at higher zinc concentrations. Concentration quenching may be the limiting factor in the applicable range of zinc concentration.

Effect of Diverse Ions. The effects of diverse ions on the formation, extraction, and measurement of the zinc complex are presented in Table I. Relative errors were calculated as indicated.

A number of metal ions interfere in the formation and measurement of the zinc complex. Cadmium, cobalt, copper, iron, mercury, and nickel ions form colored reaction products with the reagent. Reagent is consumed and although the complexes do not fluoresce, they are extracted into chloroform and absorb the excitation radiation. The addition of EDTA to eliminate metal ion interferences was detrimental to the formation of the zinc complex.

Both cyanide and thiocyanate ions enhance the fluorescence intensity of the zinc complex. However, extremely high concentrations of cyanide ion, sufficient to mask the interference of the above metal ions served to destroy the zinc complex also. Other common anions have little effect upon the system.

Analysis of Synthetic Zinc Samples. Results on synthetic samples, employing the recommended procedure, are presented in Table II. These data demonstrate that in the absence of interfering ions, the method is applicable to the determination of zinc in microgram quantities.

Table I. Effect of Diverse Ions on Fluorescence Intensity of the Zinc Complex

Zinc concentration = 0.105 p.p.m.

Ion	Concentration, p.p.m.	Source	Relative error, %[a]
Fe^{+2}	98	$Fe(ClO_4)_2$	Emulsion
Co^{+2}	104	$Co(NO_3)_2$	>−40
Ni^{+2}	100	$NiCl_2$	>−40
Cu^{+2}	100	$Cu(NO_3)_2$	>−40
Au^{+3}	184	$HAuCl_4$	Ppt. in $CHCl_3$
Pt^{+4}	48	H_2PtCl_6	−1.9
Mn^{+2}	102	$MnSO_4$	0
Ca^{+2}	99	$CaCl_2$	−1.9
Mg^{+2}	101	$MgCl_2$	−1.9
Al^{+3}	87	$AlCl_3$	−3.8
Cd^{+2}	100	$CdSO_4$	>−30
Hg^{+2}	98	$HgCl_2$	>−30
Cr^{+3}	108	$CrCl_3$	0
NH_4^+	99	NH_4Cl	+1.9
$S_2O_3^{-2}$	101	$Na_2S_2O_3$	−1.9
F^-	98	KF	−0.9
PO_4^{-3}	102	K_2HPO_4	−1.8
CN^-	99	KCN	+18
SCN^-	96	KSCN	+2.8

[a] Rel. error = $\frac{\text{I observed} - \text{I standard}}{\text{I standard}}$

Table II. Results on the Analysis of Selected Zinc Samples

Sample	Zinc present, μg.	Zinc found, μg.[a]
1	1.3	1.3
2	2.6	2.6
3	5.2	5.4
4	10.4	10.4
5	15.6	15.4

[a] Average of 3 determinations.

LITERATURE CITED

(1) Babko, A. K., Chalaya, Z. I., *Zh. Analit. Khim.* **17**, 286 (1962).
(2) Carter, D. A., Ohnesorge, W. E., ANAL. CHEM. **36**, 327 (1964).
(3) Merritt, L. L. Jr., *Ibid.*, **16**, 758 (1944).
(4) Perkin, W. H., Jr., Robinson, R., *J. Chem. Soc. Trans.* **103**, 1973 (1913).
(5) Trenholm, R., Ryan, D., *Anal. Chim. Acta* **32**, 317 (1965).

RICHARD E. JENSEN[1]
RONALD T. PFLAUM
Department of Chemistry
University of Iowa
Iowa City, Iowa

WORK supported by the National Science Foundation. First Midwest Meeting, The American Chemical Society, Kansas City, Mo., Nov. 5, 1965.

[1] Present address, Department of Chemistry, Mankato State College, Mankato, Minn.

p-Aminoazobenzene for the Spectrophotometric Determination of Sulfur Dioxide

SIR: Sulfur dioxide has many applications as a fungicide and as a preservative in pharmaceutical preparations because of its powerful toxic action upon vegetative organisms. Because of its frequent use in these preparations, a fast reliable method for its determination is needed. Early methods were based either on its acidic nature or its reducing properties. A sulfuric acid–bleached fuchsin-formaldehyde method was developed by Steigmann (*6*). Because of difficult preparation and instability of this reagent, West and Gaeke (*7*) replaced the fuchsin dyestuff with pararosaniline hydrochloride bleached with hydrochloric acid. They also utilized sodium tetrachloromercurate to stabilize the sulfite. Nauman *et al.* (*4*) studied the mechanism of the reaction of sulfur dioxide, formaldehyde, and pararosaniline in acid solution and proposed that the final reaction product is a derivative of pararosaniline containing three added methylene sulfonic acid groups. They also attributed the stabilization to the formation of a dichlorosulfitomercurate(II) complex.

Huitt and Lodge (*3*) demonstrated that the nature of the spectrally active products formed with pararosaniline is an equilibrium mixture of the mono-, di-, and trisubstituted reaction products. Pate, Lodge, and Wartburg (*5*) examined 18 samples of fuchsin and pararosaniline by spectrophotometry and in the SO_2 assay. A large variation in purity and reactivity was indicated.

In preparing a calibration curve using pararosaniline in the manner described by Barabas and Kaminski (*1*), we were unable to obtain a satisfactory curve. This could be due to a difference in dye as there is considerable variation in the commercially prepared dyes. No attempt was made to purify our dye. Instead, we used a dye chemically similar to pararosaniline but containing only one amino group which, hopefully, would result in a more sensitive procedure. This dye, *p*-aminoazobenzene (Matheson, Coleman and Bell), should give more reproducible results from laboratory to laboratory as it is readily available as a pure organic compound.

EXPERIMENTAL

Reagents. SODIUM TETRACHLOROMERCURATE SOLUTION. Dissolve 23.4 grams of sodium chloride and 54.4 grams of mercuric chloride in about 500 ml. of water and dilute to 1 liter with water.

p-AMINOAZOBENZENE SOLUTION, 0.02%. Dissolve 200 mg. of *p*-aminoazobenzene hydrochloride, previously dried for 1 hour at 80° C., in 500 ml. of ethanol; add 200 ml. of 1*N* hydrochloric acid and dilute to 1 liter with water.

FORMALDEHYDE SOLUTION, 0.2%.

STANDARD BISULFITE SOLUTION, equivalent to 200 μg. of SO_2/ml. Dissolve 325 mg. of $NaHSO_3$ in water and dilute to 1 liter with water.

Procedure. Dilute the sample with water to give a concentration equivalent to 10 μg. of SO_2 per milliliter. Place 5.0 ml. of this dilution in a 100-ml. volumetric flask containing 10 ml. of sodium tetrachloromercurate solution. Add 5.0 ml. of 0.2% formaldehyde solution, 5.0 ml. of *p*-aminoazobenzene solution, and 5.0 ml. of concentrated hydrochloric acid. Mix and dilute to volume with water. Let the solution stand for 10 minutes and read the absorbance at 505 mμ in 1-cm. cells *vs.* water in the reference cell. Subtract the absorbance of the reagent blank from that of the sample.

Prepare a standard curve by placing aliquots containing the equivalent of 20, 40, 60, and 80 μg. of SO_2 in 100-ml. volumetric flasks containing 10 ml. of sodium tetrachloromercurate solution. Treat the standards in the same manner as the sample beginning with "Add 5.0 ml. of formaldehyde. . . ." Subtract the absorbance of the reagent blank from those of the standards and prepare a graph of absorbance *vs.* micrograms of SO_2.

RESULTS

Concentration effects of acid, dye, and formaldehyde were studied to determine optimum conditions for the reaction.

ACID. During the preliminary work, we found that adding a few milliliters of concentrated hydrochloric acid to the SO_2–dye–formaldehyde solution would

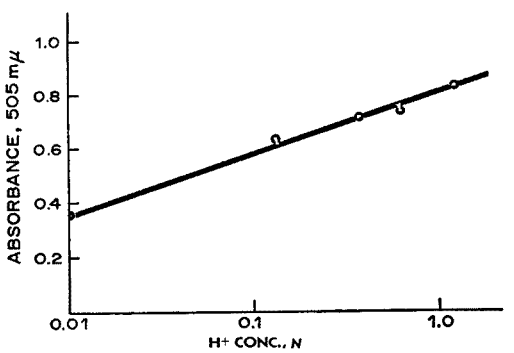

Figure 1. Effect of acid concentration on color intensity

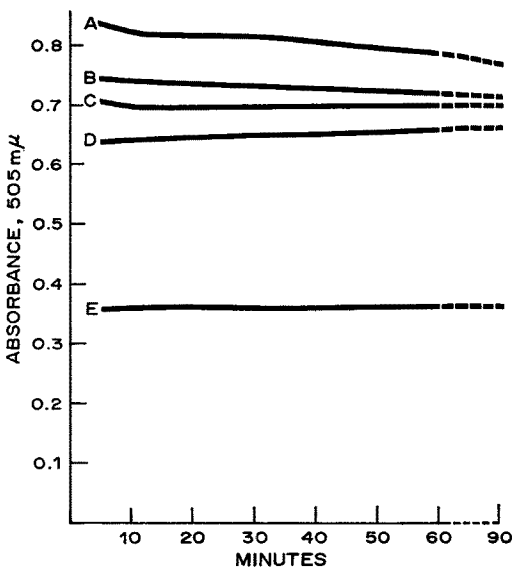

Figure 2. Stability of the complex at various acid concentrations

Curve *A*—1.21*N* HCl, Curve *B*—0.61*N* HCl, Curve *C*—0.37*N* HCl, Curve *D*—0.13*N* HCl, Curve *E*—0.01*N* HCl. All solutions contain the equivalent of 60 μg. of SO_2

intensify the color considerably. Figure 1 shows the effect of acid concentration upon the color intensity of solutions containing 60 μg. of SO_2. If the final reaction product exists as an equilibrium mixture of the protonated and nonprotonated forms similar to that described by Fieser and Fieser (*2*) for Congo Red, then the increase in color intensity with acidity would be expected.

Figure 2 shows the color stability of solutions of varying acid concentration. A final acid concentration of 0.61*N* was chosen for the reaction, as it gives a stable color of high absorbance.

DYE. The effect of dye concentration is shown in Figure 3. Curve *C* in Figure 3 shows that an increase in dye content above the 5-ml. level does not result in any appreciable increase in sensitivity.

FORMALDEHYDE. Varying the amount of formaldehyde added had only a small effect on development of the color. A variation of 1 ml. in the amount of formaldehyde reagent added resulted in a 2% change in absorbance.

DISCUSSION

Figure 1 in the publication of Barabas and Kaminski (*1*) using pararosaniline shows an absorbance difference of about 0.30 for 50 μg. of sulfur (100 μg. of SO_2). The same quantity of SO_2 by the procedure using *p*-aminoazobenzene gives an absorbance difference of 0.64 or double the sensitivity of their procedure.

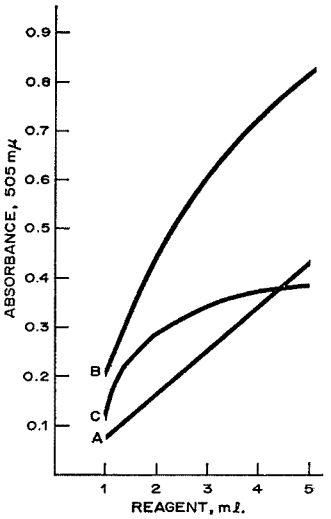

Figure 3. Effect of reagent concentration

Curve *A*—reagent blank, Curve *B*—absorbance of 60 μg. of standard, Curve *C*—difference between Curve *A* and Curve *B*

A calibration curve in the 0–10 μg. of SO_2 range can be prepared by following the procedure outlined above and measuring the absorbance in 5-cm. cells. Both the 0 to 10 μg. and the 10 to 100 μg. systems obey Beer's law.

The *p*-aminoazobenzene reagent is stable for a month.

LITERATURE CITED

(1) Barabas, S., Kaminski, J., ANAL. CHEM. **35**, 1702 (1963).
(2) Fieser, L. F., Fieser, M., "Organic Chemistry," 2nd ed., p. 934, Heath and Co., Boston, 1950.
(3) Huitt, H. A., Lodge, J. P., Jr., ANAL. CHEM. **36**, 1305 (1964).
(4) Nauman, R. V., West, P. W., Tron, F., Gaeke, G. C., Jr., *Ibid.*, **32**, 1307 (1960).
(5) Pate, J. B., Lodge, J. P., Jr., Wartburg, A. F., *Ibid.*, **34**, 1660 (1962).
(6) Steigmann, A., *J. Soc. Chem. Ind.* **61**, 18 (1942).
(7) West, P. W., Gaeke, G. C., ANAL. CHEM. **28**, 1816 (1956).

SHARON J. KNISELEY[1]
LEWIS J. THROOP[2]
Mead Johnson and Co.
Evansville, Ind. 47721

[1] Present address, Kerr-McGee Oil Industries, Inc., Kerr-McGee Building, Oklahoma City, Okla.
[2] Present address, Syntex Research, Stanford Industrial Park, Palo Alto, Calif.

Voltammetric Determination of 2,6-Di-*tert*-butyl-*p*-cresol in Hydrocarbons

SIR: There has been considerable interest lately in the determination of 2,6-di-*tert*-butyl-*p*-cresol (4M26B), since it is widely used as an antioxidant. Braithwaite and Penketh (*1*) separated the antioxidant by distillation with aqueous methanol, followed by analysis of the distillate by either colorimetry, infrared spectrometry, or gas–liquid chromatography. Phillips and Hinkel (*5*) concentrated the 4M26B on silicic acid and eluted it by successive washings with cyclohexane. The effluent was then analyzed by ultraviolet spectrophotometry.

We had need for a rapid method of analysis for 4M26B (10–2000 p.p.m.) in transformer oils which contain inherent phenols. For this reason, anodic polarography at the ceresin-wax-impregnated graphite electrode was investigated. A number of workers (*2–4, 6*) have used the impregnated graphite electrode to oxidize the phenolic group. In this method, interfering polar compounds are separated from the 4M26B by adsorption on alumina gel containing 10% water followed by the adsorption of 4M26B on dry alumina gel. The 4M26B is then eluted from the alumina gel with the polarographic solvent (isopropyl alcohol–water 0.5*M* in sodium acetate and acetic acid) and scanned from 0.0 to 0.7 volt *vs.* a S.C.E. at a rate of 1.24 mv. per second. A calibration curve is prepared from blends of the 4M26B in the polarographic solvent.

EXPERIMENTAL

Materials and Solutions. Alcoa F-20 alumina gel was dried at 180° C. for 20 hours prior to use. Alumina gel, 10% water was prepared by adding water to the dry alumina and thoroughly mixing. The polarographic solvent was prepared by dissolving 41.0 grams of sodium acetate and 30.0 grams of acetic acid in 700 ml. of isopropyl alcohol in a 1-liter volumetric flask and diluting to volume with water.

Apparatus. The adsorption columns were glass columns 7 inches long and $^3/_{16}$-inch i.d. with a 25-ml. reservoir at the top. The ceresin-wax-impregnated graphite electrode preparation is described by Morris and Schempf (*4*). The polarographic apparatus consisted of a Sargent Model XXI Polarograph equipped with a H-type electrolysis cell, a saturated calomel electrode, and a constant temperature bath.

Procedure. Depending upon the anticipated 4M26B content, mix 0.5 to 10 grams of sample with 10 ml. of pentane. This solution is percolated through a 10% water–alumina gel column at the rate of 20–40 drops per minute. The column is washed with 10 ml. of pentane, and the effluent is passed through a column packed with dry alumina gel. This column is washed with two 10-ml. portions of pentane. It is blown dry with nitrogen, and the alumina gel quantitatively transferred to an Erlenmeyer flask. By means of a pipet, 10 ml. of polarographic solvent is added. After the mixture is swirled for 15 to 20 seconds, the flask is allowed to stand at room temperature for a few minutes. The solution is decanted into the electrolysis cell, maintained at 25° ± 0.2° C., and scanned from 0.0 to 0.7 volt *vs.* a S.C.E. A fresh surface of the graphite electrode is used for each polarogram. This is accomplished by sawing approximately

Table I. Analysis of 2,6-Di-*tert*-butyl-*p*-cresol Blends

Blend	Added (p.p.m.)	Found (p.p.m.)
1	20	19.0 20.7
2	100	104 101
3	200	191 208 196 214
4	300	309 295

1/8 inch off the end of the rod with a fine-tooth saw (*6*). Ten milliliters of pentane are processed as a blank along with the sample. Since 4M26B does not give a normal diffusion plateau but a drawn-out wave with a slowly rising current, the diffusion current is taken as the difference between the current of the sample and the blank at 0.60 volt, an approximate voltage value for a normal diffusion current plateau.

RESULTS

The analysis of blends of 4M26B in transformer oil is shown in Table I.

Table I shows that the relative error of the method is 5%. It is necessary to pass the sample through the 10% water–alumina gel prior to the adsorption of 4M26B on dry alumina gel, since interfering, naturally occurring polar compounds would cause high results. By use of this technique, phenols, aromatic amines, quinones, disulfides, thiols, carbazoles, and pyrroles do not interfere if present in concentrations of less than 0.5%. The analysis time is approximately 2.5 hours for one sample and 3 hours for three samples. The method can be applied to other hydrocarbon samples, and the lower limit can be extended by using larger sample sizes. The method has not been applied to used transformer oils. Any oxidation product of 4M26B which contains the hydroxyl group would be oxidized and calculated as 4M26B, giving high results.

LITERATURE CITED

(1) Braithwaite, B., Penketh, G., ANAL. CHEM. **36**, 185 (1964).
(2) Gaylor, V. F., Conrad, A. L., Landerl, J. H., *Ibid.*, **29**, 224 (1957).
(3) Gaylor, V. F., Elving, P. J., *Ibid.*, **25**, 1078 (1953).
(4) Morris, J. B., Schempf, J. M., *Ibid.*, **31**, 286 (1959).
(5) Phillips, M. A., Hinkel, R. D., *J. Ag. Food Chem.* **5**, 379 (1957).
(6) Suatoni, J. C., Snyder, R. E., Clark, R. O., ANAL. CHEM. **33**, 1894 (1961).

JOSEPH C. SUATONI

Physical Sciences Division
Gulf Research & Development Co.
Pittsburgh, Pa.

Kinetics of Polymerization by Infrared Spectrometry

SIR: Many methods have been developed to measure rates of polymerization (*2*). Some of these are capable of determining individual rate constants, while others measure the overall rate of polymerization. Most of these methods require lengthy preparation and sensitive equipment.

The use of spectrometry is not new in kinetic studies of chemical reactions. Visible and ultraviolet spectrometry are used frequently since the absorption in one part of the spectrum will often increase or decrease in intensity as the reaction proceeds. Thus, periodic spectral analysis of the reaction mixture may indicate the course of the reaction (*6*).

Most of the previous work involving infrared measurements in polymerization kinetics entailed periodic sampling of the reaction, followed by absorption measurements of one or more reactant(s) (*1*). In the present study, a continuous sampling of the reacting solution is accomplished by incorporating a small monitoring pump in a closed cyclic system. Hence, a complete picture of the reaction is obtained while it proceeds.

EXPERIMENTAL

Reagents. Toluene, the solvent used in all the experiments, was the Baker Analyzed Reagent. The monomers were obtained from Rohm and Haas and kept in a deep freeze until required. An oxygen-free grade of nitrogen was used.

The infrared spectrometer was a Perkin-Elmer Model 337, equipped with an expanded scale read out, which was coupled to a Texas Instruments Servo Riter Recorder Type PWS. The pump was a Beckman Solution Monitoring Pump No. 74601, having Teflon (or Viton) connections and valves. A maximum output of 5 ml./minute was available. Figure 1 represents schematically the general arrangement of the apparatus. *A* is the reaction vessel, *B* a 0.1-mm. KBr cell, *C* the pump, *D* a constant temperature bath, and *E* a magnetic stirrer.

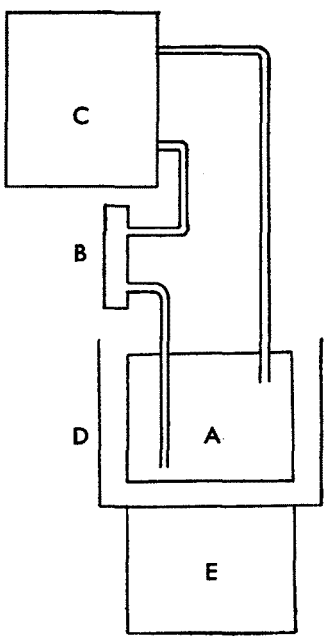

Figure 1. Schematic diagram of apparatus

The reaction vessel was an ordinary three-necked flask, with provision for a nitrogen inlet.

Method of Operation. All quantitative spectral measurements are dependent on Beer's Law (*7*). This law holds for all wavelengths and, hence, includes radiation in the infrared portion of the spectrum. There are, of course, deviations from the law, the most common of which is caused by solvent-solute interaction. The need, therefore, arises for a check on the linearity of the selected peak in relation to concentration. The criteria for the selection of a peak require that it must be distinguishable from solvent bands, decrease or increase with the speed of the reaction, and obey Beer's Law. Under these conditions, the sequence of operation is calibration of the spectrometer and polymerization.

A suitable frequency is chosen for the monomer, at which absorption decreases as the polymerization proceeds. The instrument is locked at this frequency and standard solutions are run in the spectrometer, at set slit openings, cell path lengths (0.1 mm.) and intensity of sample beam. These settings are maintained for the rest of the experiment. Thus, various absorptions are obtained (at the select frequency) which can be reproduced on the strip chart recorder coupled to the spectrometer. This recorder measures time on one axis and the degree of absorption on the other. Calibration graphs can then be drawn relating the amount of absorption to the concentration of monomer. The recorder also serves as an amplifier and, hence, increases the

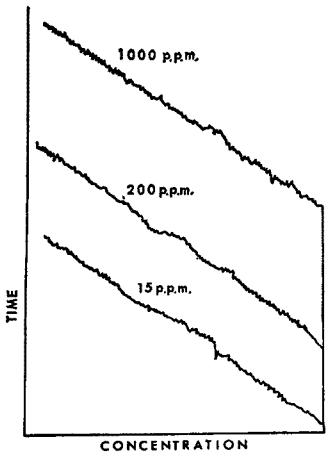

Figure 2. General form of graphs obtained from the recorder

The figures refer to the parts per million of the methyl ether of hydroquinone used as inhibitor

sensitivity of the apparatus to changes in concentration.

The reaction vessel is charged with the monomer solution, the pump started, and the initial concentration measured at equilibrium temperature; the initiator (azobisisobutyronitrile) is then added and the progress of the polymerization measured. The results are displayed on the recorder. See Figure 2.

RESULTS

We have used this apparatus to study three different types of reaction, viz., addition, decomposition (*5*), and polymerization which is discussed here. The system chosen for study was the polymerization of ethylacrylate in toluene; since the rate of polymerization is of a reasonable order at 60° C. (the thermostatic bath temperature), a peak occurs at 805 cm.$^{-1}$ in the monomer which decreases in intensity, according to Beer's Law on polymerization (this is an out-of-plane C—H deformation which is eliminated in the polymer), and the polymer, as well as monomer, is soluble in the same solvent, toluene.

Order of the Reaction. Monomer Concentration. Keeping the initiator concentration constant (1.5% based on the monomer), solutions of varying monomer concentration were polymerized (20, 12, 10, and 8%). Since,

$$\frac{d\,[M]}{d\,[T]} = K\,[I]^x\,[M]^y \qquad (1)$$

where M is the monomer concentration, I is the initiator concentration, x is the order with respect to the monomer concentration, y is the order with respect to initiator concentration,

a graph of $\log -\frac{d\,[M]}{d\,[T]}$ *vs.* $\log\ [M]$

will give a straight line with a slope equal to y. See Figure 3. Experimentally a value for y of 1.6 was found.

Initiator Concentration. Similarly, by keeping the monomer concentration constant and varying the initiator concentration, the value of x can be obtained. The rate constant K can be evaluated from the slope of the plot

$[I]^x\,[M]^y$ *vs.* $-\frac{d\,[M]}{d\,[T]}$.

Induction Period of Polymerization. The induction period of a polymerization reaction can be easily studied in this apparatus since the onset of the reaction is readily distinguished in the auxiliary recorder (Figure 2). Standard 20% solutions of ethylacrylate were polymerized with 15, 200, and 1000 p.p.m. of the methylether of hydroquinone as inhibitor. No major differences in the rate of

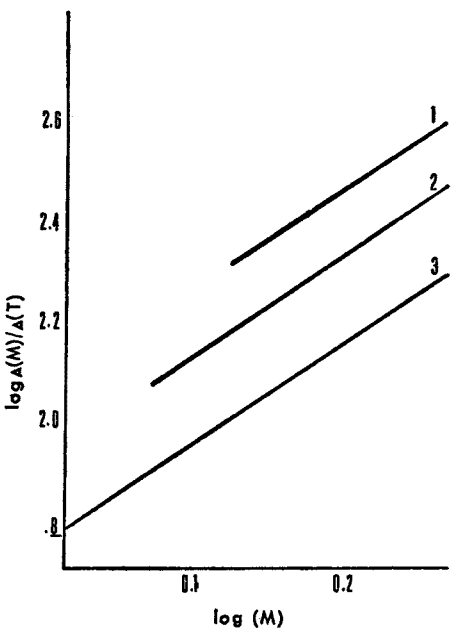

Figure 3. Order of reaction with respect to monomer concentration

M is the concentration of ethylacrylate in moles/liter. T is time in minutes
The figures refer to: 1 = 8%; 2 = 10% and 3 = 12% starting concentrations of monomer

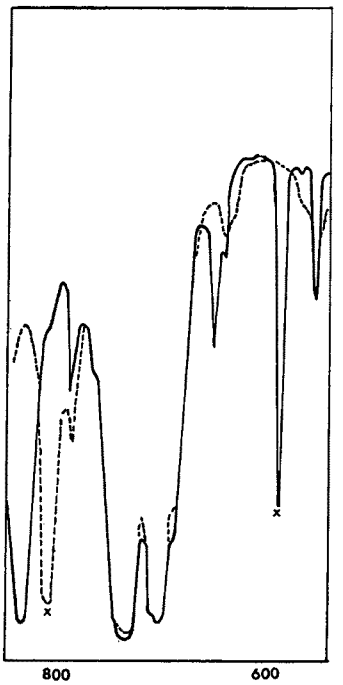

Figure 4. Infrared spectrum showing the frequencies used (marked with X) in the system ethylacrylate–maleic anhydride

— Maleic Anhydride; --- Ethylacrylate

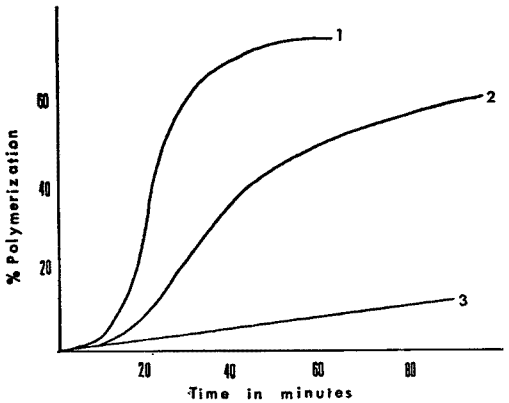

Figure 5. Graph showing copolymer relationships

1. 20% ethylacrylate. 2. A mixture of 20% ethylacrylate and 20% maleic anhydride with the ethylacrylate being recorded. 3. Same mixture as 2, but with the maleic anhydride being recorded

polymerization were observed once the inhibitor had been destroyed.

Copolymerization. The idea of following both monomers simultaneously in a copolymerization is a useful concept, giving a continuous picture of the take-up of the respective monomers into the growing polymer. Our present apparatus allows for consecutive recording only, but simultaneous recording would be possible if the spectrometer were modified to have an automatic switching of wavelengths and a two-pen recorder.

Ethylacrylate and Maleic Anhydride. The infrared spectrum allows for the measurement of both monomers (Figure 4). The peaks selected were 805 cm.$^{-1}$ for ethylacrylate and 555 cm.$^{-1}$ for maleic anhydride. For the copolymerization run, the apparatus was first calibrated for one component, the polymerization completed, and the results were plotted; then a duplicate reaction was performed, but this time the progress of the other monomer was followed. By incorporating both sets of results in one graph, the relationship between the two monomers can be seen. Figure 5 depicts such an experiment. Graph 1 represents the rate of polymerization of a 20% ethylacrylate solution. Graph 2 shows the rate at which ethylacrylate enters the copolymer formed from a solution containing 20% ethylacrylate and 20% maleic anhydride. Graph 3 repeats this last experiment observing the rate of maleic anhydride polymerization.

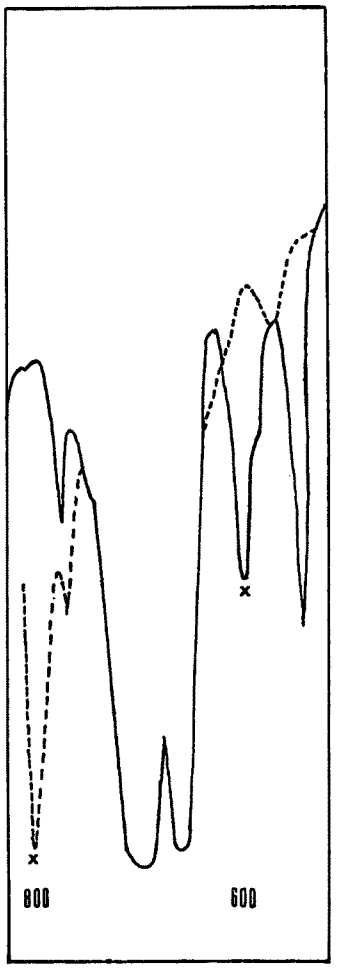

Figure 6. Infrared spectrum showing the frequencies used (X) in the system ethylacrylate–vinylacetate

— Vinyl acetate; --- Ethylacrylate

Ethylacrylate and Vinylacetate. In the copolymerization of ethylacrylate-vinylacetate, two separate frequencies can be identified which are capable of yielding quantitative results. According to Figure 6, the frequencies selected were: ethylacrylate at 805 cm.$^{-1}$ and vinylacetate at 635 cm.$^{-1}$ Figure 7 depicts the rate of polymerization of (1) a 10% ethylacrylate solution (2) a 10% ethylacrylate plus 10% vinylacetate solution, recording the ethylacrylate, and (3) recording the reaction of vinylacetate in the solution specified under (2).

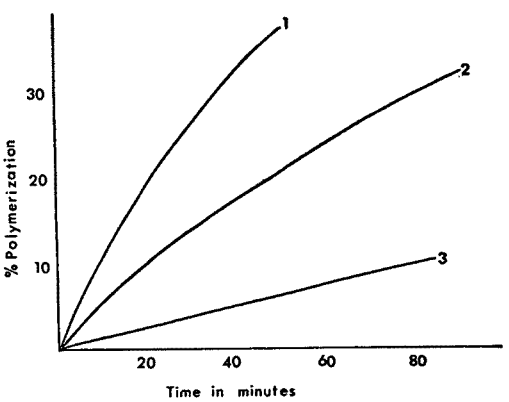

Figure 7. Graph showing copolymer relationships

1. 10% ethylacrylate. 2. A mixture of 10% ethylacrylate and 10% vinylacetate with the ethylacrylate being recorded. 3. Same mixture as 2, but with the vinylacetate being recorded

DISCUSSION

Solution polymerization of ethylacrylate was studied. Values for $x = 1.6$, $y = 0.5$, and $k = 1.6 \times 10^{-2}$ mole/liters minute^{-1} were determined. These compare with values of $x = 1.5$, $y = 0.5$, and $k = 8.9 \times 10^{-2}$ mole/liters minute^{-1} obtained by M. Devalerola, using benzoyl peroxide in benzene at 60° C. (*3*), but disagrees with previous workers at Osaka University who found first-order dependence (*4*).

The above experiments indicate that this method is satisfactory for polymerization studies. In particular it eliminates the need for intensive purification of copolymers necessary in classical chemical analysis.

However, it has its limitations: Fast reactions cannot be handled; at least 30 minutes are needed for completion of 75% of the reaction. There are spectral difficulties—i.e., the need for a unique frequency to be measured. The reactants and products must be soluble although filters could be incorporated in the apparatus. It is a macroscale apparatus—i.e., at least 150 ml. of solution is required. Due to the nature of the optics of the spectrometer, only nonaqueous systems can be studied.

LITERATURE CITED

(1) Ang, T. L., Harwood, J. H., *Polymer Preprints* **5**, (1), 306 (1964).
(2) Burret, G. M., "Mechanism of Polymer Reactions," p. 14, Interscience, New York, 1954.
(3) Devalerola, M., *Bull. Soc. Roy. Sci. Liège* **30**, 367 (1961).
(4) Hachihama, Y., Sumitomo, H., *Technology Rept. of Osaka Univ.*, **5**, No. 185, 491.
(5) Hirsch, A., Bridgland, B. E., *Appl. Spectry.* (in press).
(6) Ingold, C. K., Nyholm, R. S., Tobe, M. L., *J. Chem. Soc.* **1956**, p. 1691.
(7) Swinehart, D. F., *J. Chem. Educ.* **39**, 333 (1962).

ARTHUR HIRSCH
B. E. BRIDGLAND

Canadian Technical Tape Ltd.
Montreal, Canada

Presented in part at the 13th Canadian High Polymer Forum, Ottawa, September 1965.

The authors are indebted to the Canadian Defence Research Board for financial support of this study.

AIDS FOR ANALYTICAL CHEMISTS

Calibration Heater for Thermometric Titrations

Marvin J. Stern,[1] R. Withnell,[2] and Richard J. Raffa,[3] College of Pharmacy, Columbia University, New York, N.Y. 10023 and Chemistry Department, Brookhaven National Laboratory, Upton, L. I., N. Y. 11973

A CALIBRATION HEATER for thermometric titrations (*3*, *6*, *7*) should possess the properties of small size, low inherent heat capacity, short lag time, chemical inertness, and geometry conducive to facile cleaning between titrations. This report describes the construction and evaluation of such a calibration heater.

Figure 1 shows a cross-sectional diagram of a heater tip. The heater was constructed as follows: The insulation from a 15-ohm, 1/4-watt, carbon-element resistor was removed by careful grinding. After grinding, the resistor element had a resistance of approximately 20 ohms and measured approximately 1.8 mm. in diameter and 6.4 mm. in length. The resistor element was then coated with epoxy paint (equal parts of Nupon Converter RL12928 and Nupon Clear RL12272, Glidden Company, Reading, Pa.). One of the wire leads of the resistor was then snipped off to a stub and an insulating sleeve about 6 mm. long and 2 mm. o.d. was slipped over the second lead. The resistor element and sleeve were wrapped with a layer of silver foil which was then soldered to the stub end of the resistor. The remaining end of the silver wrapping and the long (insulated) resistor lead were soldered to insulated wire leads. The heating element was inserted into a 22-cm. length of 4-mm. o.d. glass tubing so that only the silver-foil-wrapped resistor element was exposed. This exposed tip was then coated and sealed into the glass tube with epoxy paint.

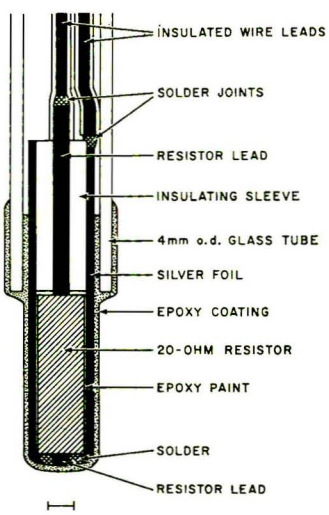

Figure 1. Cross-sectional diagram of heater tip

The heater was powered with the simple Zener diode circuit shown in Figure 2. The voltage supplied to the heating element was adjusted with the coarse and fine settings. Each successive coarse setting (1 to 6) decreases the resistance in series with the heater by 25 ohms. The fine setting (0.000 to 1.000) controls an additional variable 25-ohm series resistor. A heater setting of 4.400, which corresponds to a total series resistance of 65 ohms, implies a coarse setting of 4 and a fine setting of 0.400. A double-pole single-throw toggle switch served to activate the heater (via external control) and a precision stop clock simultaneously. For rough heating, the heater was activated with switch S2. Provision was made for measuring the current through the heater (indirectly by measuring the voltage at J1) and the d.c. voltage across the heater (at J2). The voltage stability of the power supply was evaluated by measuring the d.c. voltage across a heater while varying the a.c. input voltage. For input voltages from 100 to 135 v.a.c., the change in the

[1] Present address, Belfer Graduate School of Science, Yeshiva University, New York, N. Y. 10033.
[2] Address, Brookhaven National Laboratory, Upton, L. I., N. Y. 11973.
[3] Present address, Analytical Research Section, Quality Control Department, Chas. Pfizer and Co., Inc., Brooklyn, N. Y. 11206.

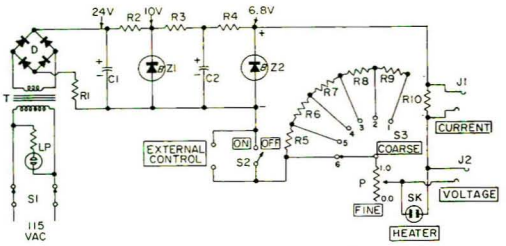

Figure 2. Power supply for heater

C1. 1000-μf., 50-w.v.d.c., electrolytic capacitor
C2. 100-μf., 25-w.v.d.c., electrolytic capacitor
D. 10DB4A bridge rectifier (International Rectifier Co.)
J1, J2. Phone jacks
LP. Neon indicator lamp
P. 25-ohm, 4-watt, 10-turn, wirewound (0.1% linearity) potentiometer
R1. 10-ohm, 10-watt, wirewound (10%) resistor
R2. 40-ohm, 10-watt, wirewound (10%) resistor
R3, R4. 5-ohm, 2-watt, carbon (10%) resistors
R5–R9. 25-ohm, 10-watt, wirewound (1%) resistors
R10. 0.1-ohm, 16 A.W.G. constantan wire (1%) resistor
S1. DPST toggle switch
S2. SPST spring return (normally open) toggle switch
S3. 6-position rotary switch
SK. Receptacle for heater leads
T. 24-volt, 1-amp. transformer
Z1. 1N1605, 10-volt, 10-watt, Zener diode
Z2. 1N1602, 6-volt, 10-watt, Zener diode

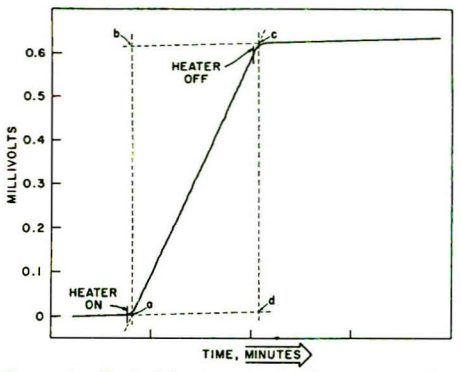

Figure 4. Typical heater curve. Heater operated for 75 seconds at heater setting 6.125

Table I. Typical Heater Calibration for Heater Setting 4.400

Date	No. of detns.	Heater output,[a] cal./sec.
2-4-65	9	0.03042 ± 0.00004
2-6-65	10	0.03046 ± 0.00004
2-16-65	10	0.03072 ± 0.00007
3-6-65	10	0.03060 ± 0.00006
4-15-65	9	0.03067 ± 0.00004
4-27-65	8	0.03068 ± 0.00009
Av.[b]		0.03066 ± 0.00003

[a] Error limits are estimated standard deviations of the means (of the grand mean for the average value).
[b] Weighted average of last four values.

voltage across the heater was less than 0.5%.

Heater output performance was evaluated with a thermometric titration apparatus to be described elsewhere (*5*). The titration cell assembly (titration cell head and special Dewar flask) was a modified version of that of Christensen, Izatt, and Hansen (*1*). Figure 3 shows a heater in the titration cell head.

Figure 4 is a typical heater curve. The short lag times between activation and response, and deactivation and termination of heat output, respectively, are apparent. The two logical indicators of the height of the heater curve are indicated as distances *ab* and *cd* in Figure 4. Since the titration cell was not perfectly adiabatic, a slight difference in these two distances was usually apparent, with the relative discrepancy increasing with increasing heating time. The reason for the difference derives from the fact that the rate of heat loss or gain to or from the surroundings changes slightly as the temperature of the liquid in the titration cell changes. If the temperature of the liquid is higher than that of the surroundings, the heat loss rate will increase when the liquid is heated; if the temperature of the liquid is lower than that of the surroundings, the heat gain rate will decrease when the liquid is heated. In either case, the slope of the final base line will be lower than that of the initial base line. The "initial height" (*ab*) should then be equal to or greater than the "final height" (*cd*).

The linearity of heater output with time of operation was studied by comparing heater curve heights for sets of three runs (120-60-30 sec. or 15-60-120 sec.) at various heater settings. Within each set, the 100 ml. of water in the titration cell was not disturbed and no adjustments of the apparatus were made except for repositioning of the recorder zero point. The deviations from direct proportionality of initial heater curve height to time of heater operation were generally within the range of deviations expected for the experimental error in the extrapolation and measurement shown in Figure 4. In these tests, as well as in additional tests of reproducibility of heater response, the use of either the final height or an average of the initial and final heights appeared to be slightly less reliable than the use of the initial height. Initial heights were, therefore, taken for calibration and subsequent use in actual thermometric titrations.

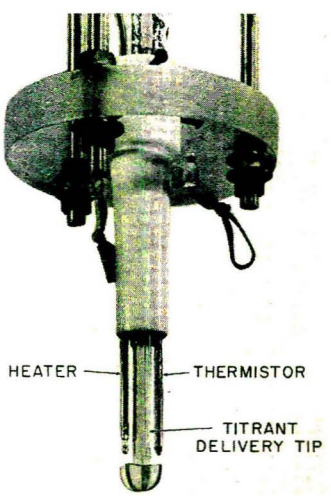

Figure 3. Thermometric titration cell head

Heaters were calibrated at individual heater settings against titrations of HCl with 1.0*N* NaOH at 25° C. A heater curve was run immediately before the initiation of titrant addition with no adjustments made on the apparatus (except for repositioning of the recorder zero point) during a heater-titration sequence. The temperature of a titration was taken to be the average of the temperatures before and after the heater-titration sequence. All calibration titrations were performed at such average temperatures of 25.0° to 25.5° C. The maximum temperature span from the beginning to the end of a heater-titration sequence was ~0.2° C. (~0.1° C. for the data presented in this report). The heater curve height was compared to the corresponding titration curve height (ΔT in Figure 8-2, Ref. *3*), in the obvious manner, in order to calculate the heater output.

Table I shows typical heater calibration data obtained from titrations of 0.005*N* HCl with 1.0*N* NaOH. The enthalpy of this neutralization reaction was taken to be −13,375 cal./mole at 25.0° C. (*2*). A sufficiently accurate first-order temperature correction of $+50(t - 25.0)$ cal./mole (*4*), where t is the temperature in °C., was added to ΔH when the titration was run at a temperature slightly higher than 25.0° C. (up to 25.5° C.). The calibration data in Table I were obtained over a period of twelve weeks. The heater was used extensively between calibration sets. A typical breaking-in period for a new heater is illustrated by the data. The error limits are probably more indicative of the experimental error in the measurements than of irreproducibility of the heater output.

ACKNOWLEDGMENT

The authors thank J. J. Christensen for a preprint of Ref. (*1*) prior to its publication.

LITERATURE CITED

(1) Christensen, J. J., Izatt, R. M., Hansen, L. D., *Rev. Sci. Instr.* **36**, 779 (1965).
(2) Hale, J. D., Izatt, R. M., Christensen, J. J., *J. Phys. Chem.* **67**, 2605 (1963).
(3) Jordan, J., Ewing, G. J., "Handbook of Analytical Chemistry," L. Meites, ed., Sect. 8, p. 3 ff., McGraw-Hill, New York, 1963.
(4) Pitzer, K. S., *J. Am. Chem. Soc.* **59**, 2365 (1937).
(5) Raffa, R. J., M.S. thesis, College of Pharmacy, Columbia University, New York, N. Y., 1966; Raffa, R. J., Stern, M. J., Malspeis, L., unpublished data.
(6) Wendlandt, W. W., "Chemical Analysis," Vol. 19, P. J. Elving and I. M. Kolthoff, eds., Chap. 8, p. 271 ff., Interscience, New York, 1964.
(7) Zenchelsky, S. T., ANAL. CHEM. **32**, 289R (1960).

Research at Columbia University supported in part by the Ciba Pharmaceutical Co., Summit, N. J. Research at Brookhaven National Laboratory carried out under the auspices of the U. S. Atomic Energy Commission.

An Electronic Coulostat

George Lauer, North American Aviation Science Center, Thousand Oaks, Calif., 91360, and California Institute of Technology, Pasadena, Calif.

IN MANY electrochemical investigations it is desired to control the quantity of charge passed, e.g. in coulostatic experiments (*2*, *7*). The published coulostatic circuits inject the charge via a capacitor charged to a very high voltage. The high voltage is required since the capacity of the injector must be much smaller than the double layer capacity of the indicator electrode. When the injector is initiated, large spikes and spurious noise are observed for 10 to 100 μseconds.

It is therefore of interest to consider the development of an electronic coulostat. This can be most easily accomplished by considering a potentiostat and feeding back the charge rather than the potential. Such a scheme can be most easily accomplished by inserting a capacitor in series with the indicator electrode and feeding back the potential drop across the capacitor.

Figure 1*a* depicts the simplest configuration. This requires a fairly stable differential input amplifier. The potential across the capacitor must be equal to E_c. If E_c is constant, the current through the cell will be zero. If a potential step, ΔE_c, is applied, the circuit acts as a coulostat in the sense of Delahay (*2*, *7*); a net charge, Q, will pass through the cell in a time determined by the rise time, current capabilities, and maximum voltage output of the amplifier. Figure 1*b* shows the equivalent circuit if a single-ended operational amplifier is used. In this case, the voltage across the capacitor is the negative of the value of E_c. Both of these methods have the disadvantage of requiring that the electrode potential be measured differentially. With available equipment it is very difficult to measure small changes in electrode potential, differentially, at the fast times required (< 100 μ*S*). This problem can be overcome by using the circuit shown in Figure 2. Amplifier A_2 is wired as a unity gain follower, A_3 as a current follower, and A_4 as an integrator. The output of A_4 is given by

$$E_o = \frac{1}{RC}\int_0^t iR_m dt \qquad (1)$$

where i is the current that flows through the cell.

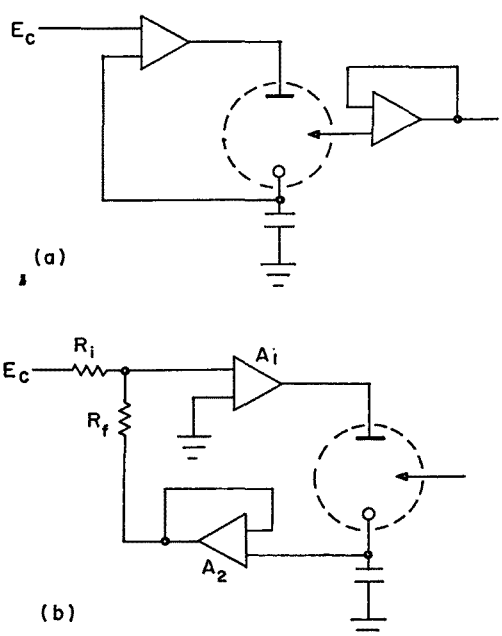

Figure 1. Basic charge control circuits

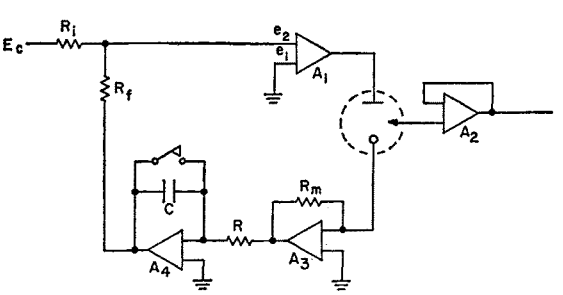

Figure 2. Charge control circuit using amplifier feedback

Considering A_1 only, the basic equation is

$$e_{out} = -Ge_2 \quad (2)$$

where G is the open loop gain of the amplifier, assumed to be very large ($> 10^7$). The bridge equation is

$$\frac{E_c - e_2}{R_i} = \frac{e_2 - \frac{1}{RC}\int_0^t iR_m dt}{R_f} \quad (3)$$

and if $R_f = R_i$, solving for e_2 and substituting into Equation 2 we obtain

$$\frac{2e_{out}}{G} = E_c + \frac{1}{RC}\int_0^t iR_m dt \quad (4)$$

If we make the usual assumption that the gain is sufficiently high so that $2e_{out}/G \approx 0$, Equation 4 reduces to

$$-E_c = \frac{1}{RC}\int_0^t iR_m dt \quad (5)$$

Thus this circuit allows the control voltage to be scaled in addition to obviating the necessity of making a differential measurement.

The control of coulombs has certain advantages over other methods. As an illustration, consider the double pulse galvanostatic technique developed by Gerischer and Krause (*3*, *4*) and by Matsuda, Oka, and Delahay (*6*). The objective in the procedure is to charge up the double layer rapidly with the initial pulse of short duration and large magnitude; this is then followed by the galvanostatic current proper. The quantity of charge injected by the first pulse is determined by the product of current and pulse duration; both variables must be precisely controlled. On the other hand, the coulostatic technique can inject the precise amount of charge required, and that is the quantity of interest. The circuit shown in Figure 3 will inject the desired charge followed by a constant current.

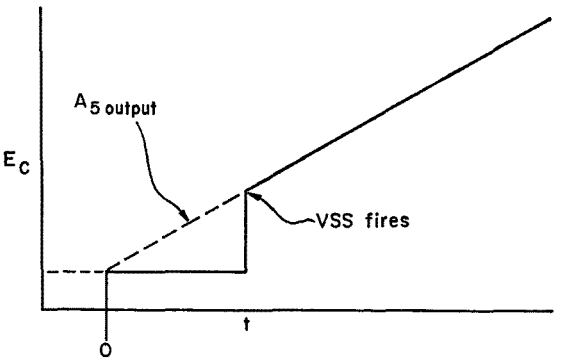

Figure 4. Voltage–time behavior at E_c in typical galvanostatic run

Amplifiers 1 through 4 are as in Figure 2. Amplifier 5 is wired as a sweep generator. The field-effect transistors act as simple electronic switches; they have a very large drain to source resistance ($R > 100$ megohms) when a negative voltage greater than 8 volts is applied and a low resistance ($R < 100$ ohms) when the emitter voltage is zero. (It may be noted that all the field effect transistors may be replaced by suitable mercury relays.) In operation, the sweep is initiated by putting T_1 into the high resistance state. When the potential of A_5 reaches the predetermined trigger value of the voltage sensitive switch (*5*) this fires and takes T_2 from the high resistance to the low resistance state. The net effect, insofar as the control voltage to A_1 is concerned, is a trapezoidal potential function as shown in Figure 4.

One can choose a ΔQ necessary to bring the potential to the desired value, and since $dQ/dt = i$, the current can be easily varied by adjusting the potentiometer until the $E - t$ plot resembles that shown by Delahay (*1*).

The charging time will be determined by the control amplifier used and the total resistance between counter and indicator electrodes. If it is desired to inject 0.1 μc. in one microsecond through a cell with 50 ohms resistance, the control amplifier will have to be capable of delivering 0.1 ampere at 5 volts with the required rise time.

The control of charge passed through the cell rather than control of potential or current can be used for a variety of other purposes by supplying suitable voltage functions at E_c.

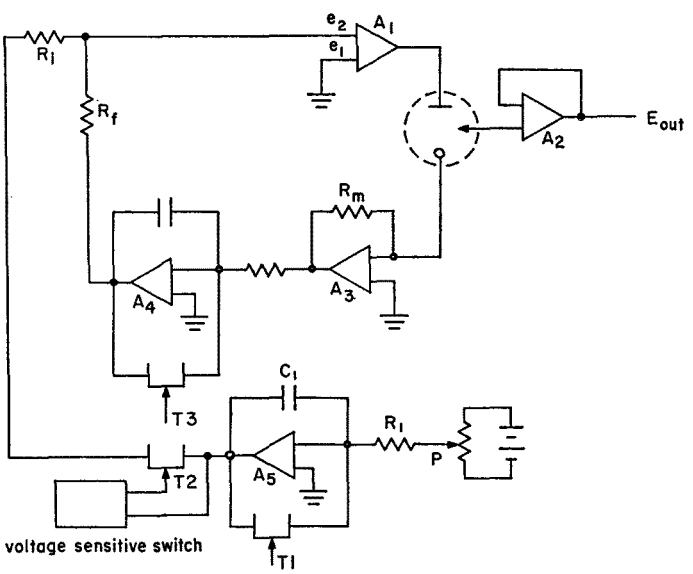

Figure 3. Improved galvanostatic circuit

ACKNOWLEDGMENT

The author thanks F. C. Anson and R. A. Osteryoung for helpful discussions.

LITERATURE CITED

(1) Delahay, P., "Advances in Electrochemistry and Electrochemical Engineering," Vol. I, p. 259, Interscience, New York, 1961.
(2) Delahay, P., ANAL. CHEM. **34**, 1267 (1962).
(3) Gerischer, H., Krause, M., *Z. Physik. Chem. (Frankfurt)* **10**, 264 (1957).
(4) *Ibid.*, **14**, 184 (1958).
(5) Lauer, G., Schlein, H., Osteryoung, R. A., ANAL. CHEM. **35**, 1790 (1963).
(6) Matsuda, H., Oka, S., Delahay, P., *J. Am. Chem. Soc.* **81**, 5077 (1959).
(7) Smith, F. R., Delahay, P., *J. Electroanal. Chem.* **10**, 435 (1965).

CONTRIBUTION No. 3345 from the Gates and Crellin Laboratories of Chemistry.

A Precision Method for Generation of Solvent Gradients

Frederick R. Blattner and John N. Abelson,[1] Department of Biophysics, Johns Hopkins University, Baltimore, Md. 21218

THE EXTENSIVE application of density gradient centrifugation in recent years has led to the development of a number of systems for generating solvent gradients (*1*, *2*). This communication describes a new type of gradient generating system based on a punched tape prepared by a digital computer. This system is capable of generating gradients of any desired shape with great precision and is generally applicable to a variety of problems requiring solvent gradients, including sucrose gradient zone sedimentation.

Operating Principle. A block diagram of the system is illustrated in Figure 1. Two reservoirs containing, for example, 1% and 25% sucrose are connected to a common mixing chamber by way of two pulse-operated solution metering pumps. These pumps deliver a small precisely determined volume to the mixing chamber each time they receive an electrical impulse. The mixing chamber, which is fitted with a magnetic stirring bar, leads via a short delivery tube in which it is desired to build the gradient.

Electric impulses which drive the pumps are generated from a punched paper tape by a photoelectric tape reader. As the tape is transported past the photoelectric cells, holes on one edge of the tape activate the 1% pump and holes on the other edge activate the 25% pump. The concentration being delivered to the mixing chamber is determined by the relative frequency of holes in the two channels. A third channel is provided to stop the tape transport.

Tape Format. At the beginning of the tape is a section which flushes the mixing chamber with 20% sucrose. Next the gradient is begun and after a volume of gradient equal to the volume of the delivery tube has been delivered, a stop appears. The operator now places the centrifuge tube into position and restarts the tape. In this way the beginning of the gradient is delivered to the bottom of the centrifuge tube. As the tape progresses, the relative frequency of holes in the two channels gradually changes, giving the desired gradient. When the end of the gradient has been delivered to the end of the delivery tube, a final stop appears and the gradient is ready for use.

Preparation of Tapes. The paper tape is punched in advance by a digital computer using a specially designed program which is detailed in Figure 2. Since the volume of the mixing chamber is not negligibly small, the tape must be punched so that the chamber output (rather than its input) conforms to the concentration gradient desired. This requires that the volume of the mixer as well as the volume of the fluid pulses be taken explicitly into account.

At any given point in the gradient the computer has three options: punch

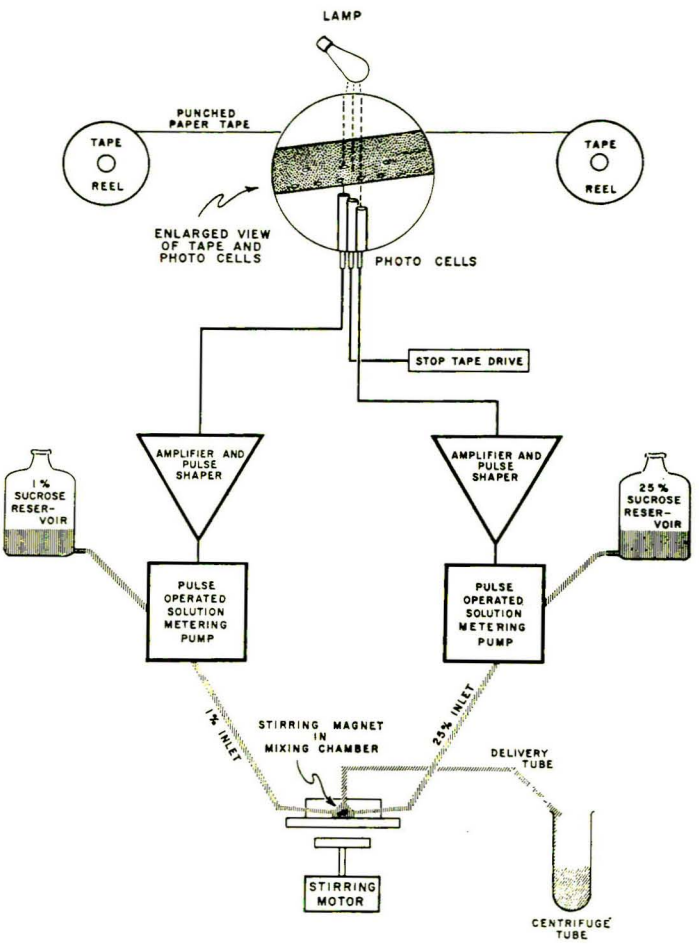

Figure 1. Block diagram of gradient generating system

[1] Present address, MRC Laboratory of Molecular Biology, Hills Road, Cambridge, England.

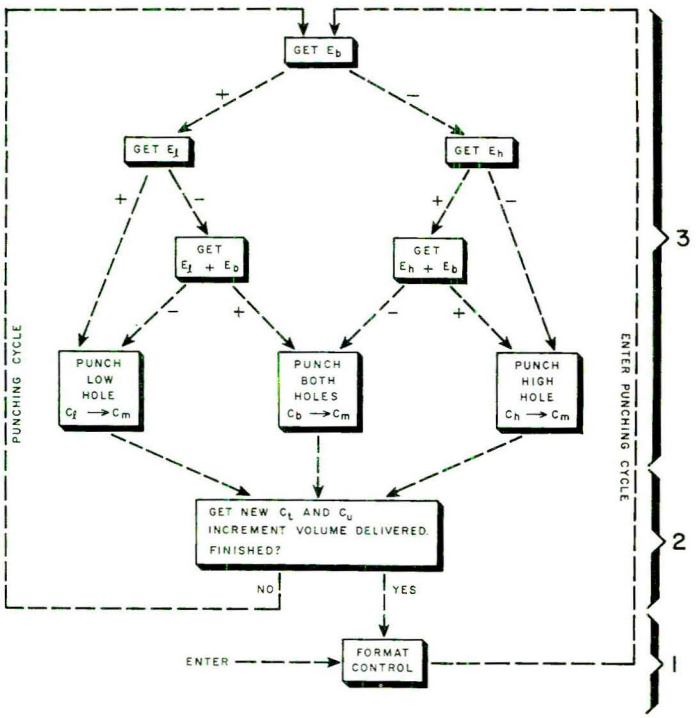

Figure 2. Flow diagram of computer program which produces tapes for gradient generator

The program has three main parts:

Section *1* determines the format of the tape and places stop punches in the proper places.

Section *2* determines the form of the gradient delivered. Each time a punching cycle has been completed the program employs a subroutine to compute the desired concentration for the next cycle. The operator can specify the form of the gradient by altering this subroutine.

Section *3* contains the logic for deciding which type of punch to place on the tape for each cycle. c_m is the concentration in the mixer. *cl*, *ch*, and *cb* are the concentrations that would result from a low, a high, or a both punch. *el*, *eh*, and *eb* are the corresponding deviations from the desired gradient. *Cl* and *Cu* are the desired concentrations one and two pulse volumes hence.

a 1% hole, punch a 25% hole, or punch both simultaneously. Given c_m, the concentration in the mixer, at that point, simple formulas can be derived giving the new values of c_m after each of the three options. By subtracting these from the desired concentration at that point an error can be determined for each option. The option giving the least error is then punched and c_m replaced by its newly calculated value. As this cycle is repeated any errors tend to cancel and the desired gradient emerges from the mixing chamber.

Apparatus. Figure 3 shows a photograph of the apparatus we have built.

The solution metering pumps (center) consist of 5-ml. multifit syringes driven by precision screws geared to solenoid-type stepping motors (Model SM-300-1, Stepper Motors Corp., Culver City, Calif.). In each of the two pumps, three syringes are driven in parallel so that three gradients can be generated simultaneously. A friction clutch is included in the gear train to prevent damage to the apparatus if the syringes reach the end of their excursion or get jammed. This also permits the screws to be rewound at the end of a run. A haircurler spring is placed around each of the syringe plungers to ensure positive feed and prevent bouncing of the plunger against the drive plate. The apparatus is mounted with the syringe outlets on top so that bubbles can be expelled easily while filling them.

The mixing chambers (right) are constructed in triplicate from lucite. A $^3/_{16} \times {}^1/_{16}$-inch stirring magnet coated with Teflon is placed in each chamber. The chamber cavities have pointed tops as detailed in Figure 1 from which the delivery tubes emerge, making it easy to expel bubbles.

The mechanical portion of the tape reader (left) was modified from a discarded microfilm reader. The electronic circuitry is conventional. Three photoconductive cells (Texas Instruments IN 2175) trigger monostable multivibrators which deliver 10 millisecond square waves. The pulses are amplified by power transistors and delivered to the stepping motors, or in the case of the stop channel, a transport motor stopping relay.

The gradient maker has mixing chamber volumes of 0.09 ml. each and the volume per pulse employed is 0.00019 ml. It takes approximately 26,000 pulses to make a gradient. Three gradients can be made in 20 minutes.

Performance Tests. Theoretical analysis of the inherent accuracy of the system using the computer reveals that for a 5% to 20% sucrose gradient the average expected absolute error throughout the gradient is ±0.008 wt. %. The average error should be 100 times smaller, since errors tend to cancel. These errors are attributable solely to the granularity of the pulse system.

Actual measurements of nine of 5–20% sucrose gradients using index of refraction revealed that the variation is less than ±0.1 wt. % at every point in the gradient for three gradients made simultaneously, and less than ±0.2 wt. % for gradients made at different times. These variations are attributed to mechanical variations and to errors

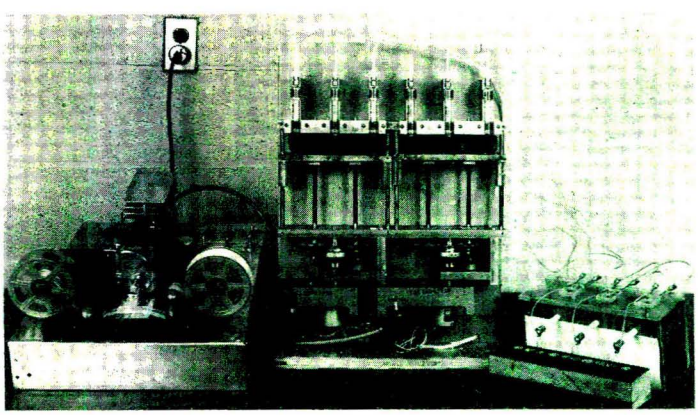

Figure 3. Photograph of gradient generating system

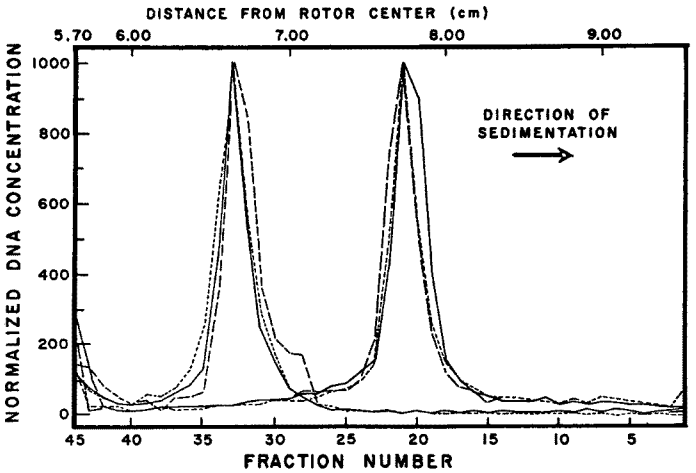

Figure 4. Test sedimentation of T7 DNA in gradients

in measuring the refractive index of the solutions.

We have tested the gradients produced by the machine in centrifugation experiments using T7 bacteriophage deoxyribonucleic acid as a standard. Figure 4 shows the profiles obtained in two runs of different durations in which identical samples were sedimented in the three buckets of the Spinco SW39 rotor. Samples of P^{32}-labeled DNA were spun for 3 hours (peak 1) and 6 hours (peak 2) at 35,000 r.p.m. The positions of the centers of gravity of the three peaks varied by no more than ±0.01 cm. in both experiments. This reproducibility makes it possible to determine the relative sedimentation coefficients of samples run in different buckets.

In other experiments we have determined the reproducibility of sedimentation distance in separate runs. When the utmost care is exercised to control temperature and speed, the reproducibility is on the order of ±0.06 cm., which corresponds to a ±2.5% variation in absolute sedimentation coefficient.

Since the machine was built, 5 or 6 workers have been using it routinely and over 1000 gradients have been satisfactorily generated. We have found it a rapid, convenient, flexible, and accurate method.

ACKNOWLEDGMENT

The authors thank C. A. Thomas, who gave this project impetus through his realization of the need for a precision gradient maker. We also thank T. C. Pinkerton and T. J. Kelly for help in performing some of the experiments reported, and W. E. Love for the use of his Royal McBee LGP-30 computer. This work was done while both of us were pre-doctoral fellows of the Public Health Service.

LITERATURE CITED

(1) Britten, R. J., Roberts, R. B., *Science* **131**, 32–3 (1960).
(2) de Duve, C., Berthet, J., Beaufay, H., "Progress in Biophysics and Biophysical Chemistry," Vol. 9, 326–69, Pergamon Press, New York, 1959.

WORK supported by Atomic Energy Commission Grant AT(30-1)-2119.

A Nomogram for Calculating the Results of an Automatic Amino Acid Analysis

W. A. Schroeder, W. R. Holmquist, and J. Roger Shelton, Division of Chemistry and Chemical Engineering, California Institute of Technology, Pasadena, Calif. 91109

SINCE the description by Spackman, Stein, and Moore (*6*) of an automatic amino acid analyzer, continued improvement has increased the number of analysis from one to several per day. On the other hand, because the time required to calculate the results of the analysis by hand from the automatic record can not be appreciably shortened per analysis, commercial integrators have become available and computer systems have been devised to do all or part of the calculation (*7*). Manual calculation is normally done by the formula $H \times W/C = \mu$moles, where H is the net absorbance of the peak, W the width at half net absorbance (in terms of the number of dots), and C a constant from the standardization (*6*). For convenience, calculation done in this way will be referred to as "the usual method." This formula is valid for Gaussian shaped curves, and, in practice, is sufficiently accurate even for curves which deviate slightly from a true Gaussian form. However, experimentally W is constant to within a few per cent over a wide range of H; theoretically, also W is independent of H for Gaussian-shaped curves if the concentration of solute is not so high as to alter the number of theoretical plates and the distribution coefficient of the system (*5*). Consequently, the quantity of an amino acid is directly proportional to H itself to the same degree that W remains constant. Because of this relationship all calculations may be made readily with a nomogram. We shall describe the construction and use of a nomogram which permits the calculation of the results of an amino acid analysis in 5 minutes. It should be emphasized that this nomogram is a graphical representation of the relationship between four variables that is expressed by

$$\mu = \frac{(P - B)}{K}$$

where μ is an amount of material whose dimensions depend on the constant K, P is the peak height, and B is the base line. It should be useful wherever such a relationship exists as it does, for example, in gas chromatograms.

USE OF THE NOMOGRAM

The five scales of this nomogram are designed to subtract the base line absorbance B from the maximum absorbance P of the peak and to convert this difference H, by appropriate intersection of a straight line with other scales, to read directly the μmoles of each amino acid. The manner in which this is accomplished is shown in Figure 1. On the left-hand scale P, the maximum absorbance of the peak is found (for example, at R) whereas, on the right-hand scale B, the absorbance of the base line is located (say at S). The net absorbance is at T where the line from R to S intersects scale H. Scale AA, which is on the left-hand side of scale

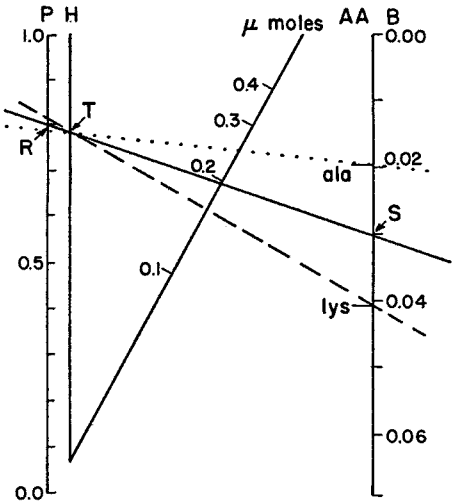

Figure 1. An illustration of the use of the nomogram for calculating the quantity of an amino acid

B, has two marks which are designated as "ala" and "lys" in Figure 1. If the quantity of lysine is to be calculated, a line is drawn between T and "lys" as shown. At the intersection of this line with the diagonal μmoles scale, the quantity of lysine in μmoles is read off. In practice, intermediate lines need not actually be drawn, because the various intersections prior to the final result can be found with a specially designed straight edge to be described later. Furthermore, the complete nomogram will have a mark on scale AA for each amino acid because scales P, B, H, and μmoles are equally applicable to all the amino acids. Thus, if a peak of alanine had the indicated absorbance and base line, its quantity would be given by the intersection of the line T to "ala" with the μmoles scale as also shown.

Figure 2 is a full-scale nomogram that is designed for use with data from the accelerated analytical system of Benson and Patterson (*2*) with high-sensitivity cuvettes (*3*). All scales have been calibrated except scale AA for which variations will occur among analyzers. The size of Figure 2 is such that it may be duplicated directly from the page and calibrated for use. Because some duplicating processes may introduce distortion, the original and the duplicates should be carefully compared. If the difference is no more than $^1/_8$ inch in length or width of the nomogram, the error introduced will be inconsequential. Calibration of scale AA may be made as follows. Suppose the standardization of the analyzer had been made with 0.2 μmole of each amino acid. For each amino acid, the value of H is found and a line is drawn from the equivalent of T (Figure 1) through 0.2 μmole on the μmoles scale and extended to scale AA where a mark is made and designated with the name of the amino acid. Although unnecessary, complete linear calibration of scale AA can be made, if desired, by using the two numerical points that are given. For other analytical systems, the nomogram may need to be modified as described in the following section.

The facility with which the nomogram can be used is hampered by the fact that the point of intersection at T must be remembered or marked so that the line from T to scale AA may be determined. The device that is shown in Figure 3 greatly speeds the use of the nomogram. For a nomogram of the size in Figure 2, a slot is milled in a plastic sheet (Figure 3*a*). After the nomogram has been taped to this sheet so the scale H is over the center of the slot, the paper over the slot is cut away.

The indicator with a fiducial line has the dimensions in Figure 3*b*. The fiducial line on the *under side* of the indicator is made by scoring the plastic with a sharp point and filling with India ink or a graduation marker for thermometers. At a point 3 inches from the end of the indicator, a short length of Lucite rod is cemented and drilled as shown in Figure 3*c*. A spring supports a pin of drill rod to which a head has been soldered, but the pin is allowed to extend about $^1/_{16}$ inch below the lower surface of the indicator. In use, the indicator is placed over the nomogram, and the pin is allowed to fall into the slot. Regardless of how the fiducial line is moved along scales P or B, the pin always follows along scale H. (A $^1/_{16}$-inch drill and a $^1/_{16}$-inch mill head will cut the plastic sufficiently oversize so that a $^1/_{16}$-inch pin will move readily in the hole and in the slot but will not fit so loosely that positioning is inaccurate.) To make the calculation, the fiducial line is adjusted to the proper absorbances on scales P and B. The pin is depressed to the bottom of the slot to form an axle about which the indicator is rotated so that the fiducial line may be moved to the appropriate mark on scale AA. The quantity of the amino acid is read at the point where the fiducial line crosses the μmoles scale.

CONSTRUCTION OF THE NOMOGRAM

Theory and methods for the construction of nomograms have been described by Allcock and Jones (*1*). The information to be given will allow the construction of a nomogram to fit the requirements of various analyzer systems now in use.

Let h and w be the height and width of the nomogram, P_M and B_M the maximum absorbance values of scales P and B, and k and K the minimum and maximum values of scale AA. In practice, the nomogram can be conveniently designed on a 7- × 10-inch grid of graph paper where the larger dimension is h. P_M and B_M use the entire height h, and scales P and B are separated by the width w.

Scale P of length h is drawn at the left of the grid with zero absorbance at the bottom and maximum absorbance P_M at the top and is graduated linearly.

At distance w from scale P, scale B of length h is drawn. Scales P and B form two sides of a rectangle. Scale B is also graduated linearly with zero absorbance at the top and B_M at the bottom.

The scale H is drawn at a distance $\left(\frac{B_M}{B_M + P_M}\right)w$ to the right of and parallel to scale P. It starts at $\left(\frac{B_M}{B_M + P_M}\right)h$ above the zero value of scale P and extends to P_M. This scale need not be graduated but, if desired, can be graduated linearly between 0 (bottom) and P_M.

Scale AA represents the net absorbance per μmole of amino acid. Therefore k and K should be chosen as somewhat less and more, respectively, than the minimum and maximum values of C/W for all amino acids. In Figure 2, the values 1.5 and 6.5 were selected for k and K, respectively. Scale AA is calibrated for each amino acid as already described but it need not be graduated numerically. If it is desired to do so, the graduation is linear with k opposite the zero value of B and K at $\left(\frac{B_M}{B_M + P_M}\right)h$ above B_M.

A mark is now made at a distance $\left[1 - \left(\frac{k}{K}\right)\left(\frac{P_M}{B_M + P_M}\right)\right]w$ to the right of scale P at the level of P_M. A line (the μmoles scale) is then drawn between this mark and the lower end of scale H.

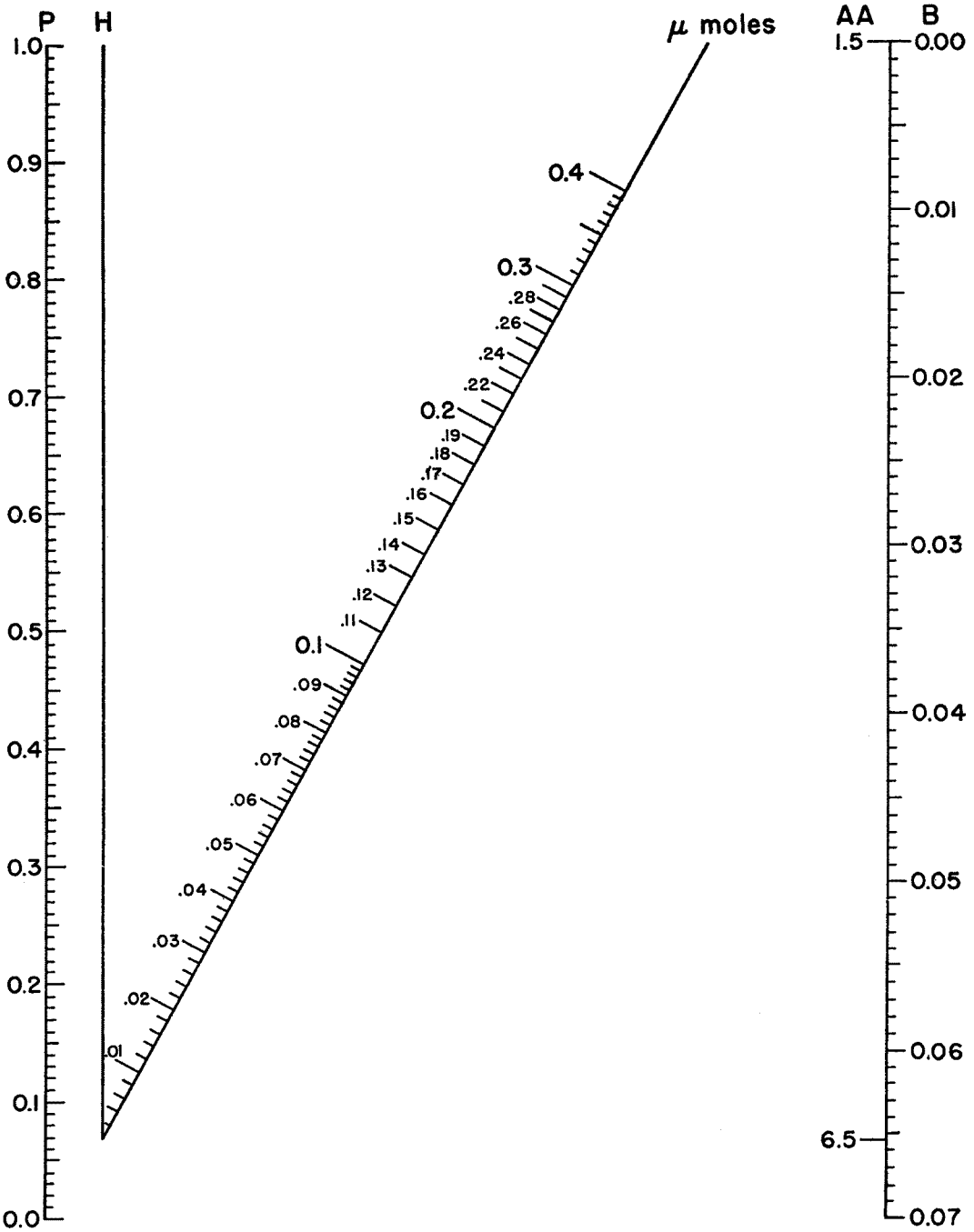

Figure 2. Full-scale nomogram without calibration of scale AA

The μmoles scale is graduated by the formula

$$d = \left[\frac{P_M}{B_M + P_M}\right] \times \left[\frac{\mu\sqrt{k^2 + (1 - k/K)^2 w^2}}{\mu(1 - k/K) + P_M/K}\right]$$

where d is the distance *along* the μmoles scale from the point of intersection with scale H and μ is the number of μmoles. This line then reads directly in μmoles of amino acid. This formula reduces to the simple form $d = \frac{a\mu}{\mu + b}$ when the constants have been entered. For making the graduation, useful values of μ such as 0.01, 0.02, . . ., 0.1, . . ., 0.2 etc. should be chosen. Also, between relatively close points such as 0.01 and 0.02, for example, linear graduation does not introduce significant error. Graduation need not be extended beyond $\mu_{max} \leqslant P_M/k$.

Scale AA is now calibrated for each amino acid as already described: the maximum absorbance and base-line values from a known number of μmoles are located on scales P and B, the pin of the indicator is depressed, the fiducial line is passed through the μmoles scale at the appropriate number, and a mark for the given amino acid is made on scale AA.

The nomogram is now ready for use. Recalibration will be necessary if the response of the analyzer should be altered by some factor such as repouring of columns, different photometer dimensions, variation in response of the ninhydrin reagent, change in flow rate, pH and salt concentration of the developer, and temperature.

DISCUSSION

Accuracy and Precision. The nomogram is, of course, inapplicable where the analytical procedure or the degree of control by the operator does not meet the requirement that the peak width at half net absorbance be independent of net peak height. The precision and accuracy of any calculation that is made with the nomogram will be lessened to the degree that this ideal is not met. Regardless of what method of calculation is used, frequent standardization of the analyzer is necessary if meaningful analyses are to be obtained. These standardizations, therefore, should be used to determine whether recalibration of the nomogram is required just as they determine whether different constants should be used in the usual method of calculation. For example, a new preparation of developer may alter chromatographic conditions slightly so that the peaks may be somewhat broadened or narrowed with resultant lowering or raising of the height. The standardization should be used to determine whether this has occurred; if it has, the values of the constants as calculated by the usual method will probably be little affected because the area will not be significantly altered but the calculation by nomogram will be affected more because the height has changed. The use of an internal amino acid standard can be helpful in maintaining proper accuracy of the nomogram.

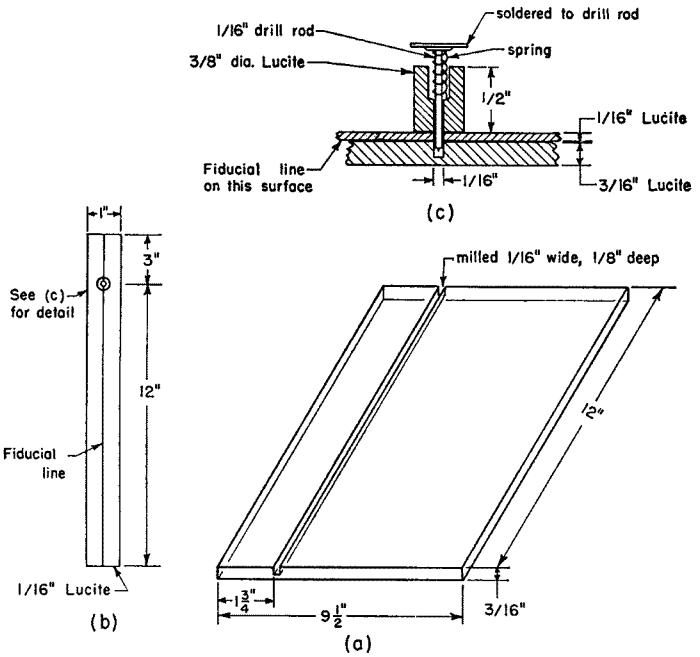

Figure 3. Indicator with fiducial line for use with the nomogram

In the accelerated procedure of Benson and Patterson (*2*), the peaks from the short column have a pronounced tendency to broaden as the column is repeatedly used. If this occurs, the nomogram must be recalibrated with a standard run or the column must be returned to its original state by regeneration and reequilibration.

In assessing the applicability of the nomogram, more than 50 analyses have been calculated both by the usual method and by the nomogram. The results from the two methods have not differed from each other by more than ±5% in the range zero to 0.3 μmole, and, actually, in about four out of five instances, the two results have agreed within ±2%. This variation is of the same order as that between two independent calculations by the usual method. This accuracy of the nomogram is all that is required for calculating the results of the analyses of peptides or of biological fluids, but the nomogram should be applied with caution for calculating the analytical data for a protein where the maximum accuracy is desired.

The necessary proportionality between net peak height and quantity that is required for accurate calculation with the nomogram appears to be met over the range of 0 to 1.0 absorbance unit for most amino acids; aspartic acid has shown the greatest variation.

The particular amino acid analyzer for which this nomogram was devised produces amino acid peaks that visibly depart from Gaussian shape. It may be that the proportionality would be more strictly maintained and the accuracy of the nomogram thereby improved with an analyzer that produced peaks essentially Gaussian in form.

Proline. The amount of proline can be calculated in the following way without resort to a special nomogram. After the values of peak absorbance at 440 mμ and base-line absorbance of a standard have been doubled mentally, the doubled values are found on scales P and B after which the mark for proline is located in the usual way on scale AA. When calculating an unknown amount, the peak and base-line absorbances must, of course, also be doubled.

Application to the Shorter Photometer Cuvette. As indicated above, the necessary proportionality for successful use of the monogram extends, in general, over the range from 0 to 1.0 absorbance unit. In most instances, the width of a peak increases at a higher absorbance than that and

the height is proportionally less. However, if the peak is very sharp as in the case of valine, isoleucine, and leucine, the proportionality is maintained up to 2.0 absorbance units. The data from the shorter photometer cuvette can then be used with the nomogram in the following way to make the calculation. Peak absorbance and base line from the shorter cuvette are located on the nomogram, and the result in μmoles is multiplied by the appropriate factor that relates the response of the two cuvettes.

Modification of the Nomogram. Certain properties of the nomogram in Figure 2 should be pointed out. If scales P, B, and H are left unchanged, then the μmoles and AA scales may be altered in inverse relation to each other. Suppose the 20-mm. cuvettes of Jones (*4*) were substituted for the 6-mm. cuvettes on which Figure 2 is based: the maximum absorbance for a given amount of amino acid would be about 3.33 times greater. The present μmoles scale can be used to graduate a scale for the longer cuvette on the opposite side. Thus, the response from the longer cuvette will be such that any quantity in micromoles μ will lie opposite 3.33 μ on the present scale. For example, 0.1 μmole will be opposite 0.333 μmole, 0.05 μmole opposite 0.167, etc. After this modification, the marks 1.5 and 6.5 on scale AA of Figure 2 would have the values of 5.0 and 21.6, respectively. Similar modification will make the nomogram applicable to the 15- and 150-cm. columns and the shorter cuvettes of the original automatic procedure (*6*).

Such modifications as these, which permit the calculation of proline and regraduation for different dimensions of cuvettes, follow from the formulas that were used to construct the nomogram initially. In addition, it should be pointed out that all scales may be extended. For example, if the nomogram in Figure 2 were calibrated on scale AA with the data from another analyzer, the geometry of this analyzer might be such that some calibration marks would be above or below the margins of the nomogram: this will not nullify the results.

Practical Considerations. Once a nomogram for specific analytical conditions has been devised, it has proved practical to duplicate some tens of copies of the nomogram without any calibration of scale AA. After attachment to the plastic sheet for use with the indicator of Figure 3, scale AA can be calibrated. If some change in analyzer constants makes it necessary to recalibrate the nomogram or if usage mars it, a new copy can be mounted on the plastic sheet and calibrated.

LITERATURE CITED

(1) Allcock, H. J., Jones, J. R., "The Nomogram," 4th Ed., Sir Isaac Pitman and Sons, Ltd., London, 1952.
(2) Benson, J. V., Jr., Patterson, J. A., ANAL. CHEM. **37**, 1108 (1965).
(3) Hubbard, R. W., Kremen, D. M., *Anal. Biochem.* **12**, 593 (1965).
(4) Jones, R. T., Weiss, G., *Ibid.*, **9**, 377 (1964).
(5) Morris, C. J., Morris, P., "Separation Methods in Biochemistry," Equation 4.48 on p. 62, Interscience, New York, 1964.
(6) Spackman, D. H., Stein, W. H., Moore, S., ANAL. CHEM. **30**, 1190 (1958).
(7) Yonda, A., Filmer, D. L., Pate, H., Alonzo, N., Hirs, C. H. W., *Anal. Biochem.* **10**, 53 (1965).

Investigation supported in part by the U. S. Public Health Service, National Institutes of Health, Grant HE-02558.

Cryoscopic Molecular Weight Determinations Using Dimethyl Sulfoxide as the Solvent

R. S. George and R. K. Rohwer, University of California, Los Alamos Scientific Laboratory, P. O. Box 1663, Los Alamos, N. M.

MANY OF THE ORGANIC nitro compounds encountered in explosives research are so insoluble in the common cryoscopic solvents that their molecular weights cannot be determined with acceptable accuracy by the freezing point method. Since dimethylsulfoxide (DMSO) appeared to be a reasonably good solvent for most organic explosives, we decided to determine whether it was otherwise suitable for cryoscopic work.

DMSO has not commonly been used for this purpose in the past, although its convenient melting point (18.5° C.) and its solvent properties (*2*) would appear to make it an obvious choice. While there are disadvantages also in its use, our conclusion from the work reported below is that DMSO is a useful and exceptionally versatile cryoscopic solvent.

EXPERIMENTAL

Chemicals. Baker Analyzed Reagent DMSO and National Bureau of Standards naphthalene were used as received. Eastman Kodak phenanthrene and xanthone were recrystallized to a constant melting point. The nitro compounds were obtained from military sources. Octahydro-1,3,5,7 - tetranitro - 1,3,5,7 - tetrazocine (HMX) and hexahydro-1,3,5-trinitro-*s*-triazine (RDX) were obtained in a purified form and have a minimum purity of 99.9%. The purity of the other nitro compounds was checked by thin layer chromatography. In several cases where further purification was indicated, the compounds were recrystallized until the desired purity was obtained.

Apparatus. Measurements were made with a modified Aminco-Bowman Freezing Point Depression instrument (No. 5-2050). Although the mechanical features were retained, the electrical circuit was considerably modified to permit recording of the thermistor bridge output rather than visual observation of an electric eye deflection. The new circuit consists of an unbalanced Wheatstone bridge whose output is fed to a 0–100 millivolt recording potentiometer. Provision has been made for coarse adjustments of one arm of the bridge so that the pen of the recorder may be kept on scale as the thermistor cools. A line operated, Zener diode regulated power supply was used to operate the bridge. With this arrangement, the thermistor provided a readability of 0.004 degrees centigrade. The modified circuit diagram is shown in Figure 1.

Procedure. The freezing point depression measurements could not be made reproducibly if the solutions were in contact with the atmosphere because of the highly hygroscopic nature of DMSO. Therefore, the molecular weight apparatus was enclosed in a dry box that was constantly purged with helium. The helium was monitored with a Consolidated Electrodynamics Corp. moisture monitor, and only helium tanks containing less than 10 p.p.m. water were used. It was not possible to monitor the dry box because the moisture monitor will also detect DMSO. All samples were placed in an entry port and purged overnight with helium before bringing them into the dry box. DMSO solutions should be handled cautiously as on contact DMSO is absorbed rapidly through the skin and can carry toxic materials with it.

No attempt was made to measure the freezing point temperature directly with this apparatus. Instead, the recorded thermistor bridge output in millivolts corresponding to the freezing point of the solution was used. The values obtained for standard solutions of known concentrations were used to construct a calibration curve from which concentrations of unknown solutions could be interpolated. The thermistor bridge values were obtained by slightly supercooling the solution and then initiating freezing by scratching the side of the test tube with the

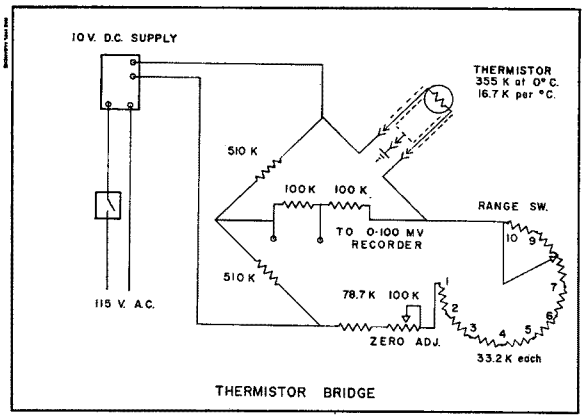

Figure 1. Circuit diagram of thermistor bridge

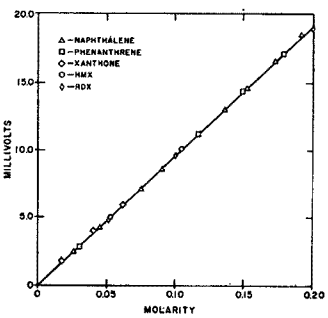

Figure 2. Calibration curve for freezing point depression in DMSO

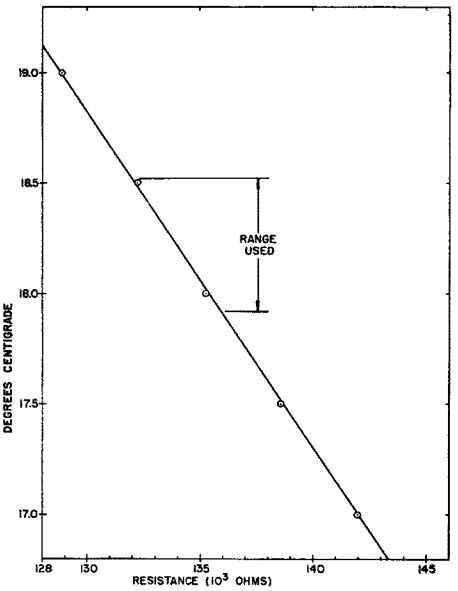

Figure 3. Calibration curve for 330K thermistor

thermistor. The partly frozen solution will exhibit a constant temperature until all of the frozen material has melted. This constant temperature represented the freezing point of the solution and was observed as a straight line on the recorder.

RDX and HMX, two commonly used explosives, and naphthalene, phenanthrene, and xanthone were used to construct the calibration curve.

RESULTS AND DISCUSSION

The calibration curve for freezing point depression using a 330K thermistor is shown in Figure 2. This curve represents a least squares fit of the data and has an average deviation of 0.1 millivolt. The differences between the reading for the pure solvent and the readings for the standard solutions were used for the ordinate of the calibration curve rather than the actual recorded values. In this way, small changes in the solvent due to slow decomposition and/or absorption of water were eliminated as the value for the pure solvent was determined immediately prior to dissolving the sample. It was found that the freezing point value of a freshly opened bottle of DMSO will decrease by 0.3 to 0.4 millivolts during several weeks storage in the dry box.

Albers and Müller (*1*) have determined the molal freezing point depression constant of DMSO and found it to be 4.4 ± 0.5° C./molal. By calibrating the resistance of the thermistor through the temperature range 17° to 19° C. (Figure 3), we obtained a value of 4.0 ± 0.1° C./molar from our data. The density of DMSO at 20° C. is 1.10 grams/ml. (*3*), so the two values are in excellent agreement. This value is lower than, or at best comparable to, the values for the common cryoscopic solvents.

The results of molecular weight determinations on several organic explosives are shown in Table I. The reported values are averages of at least four individual measurements.

The great advantage of DMSO is that HMX, RDX, and the first three compounds in Table I are too insoluble for molecular weight determinations in any of the common cryoscopic solvents, and the generally excellent solvent properties of DMSO suggest that this advantage also may be important with other classes of compounds. The disadvantages of using this solvent are the requirement of operating in a dry atmosphere and its relatively low cryoscopic constant. However, for routine molecular weight determinations on various classes of organic compounds, DMSO is a valuable addition to the list of useful solvents.

Table I. Molecular Weight Determination of Known Compounds

Compound	Molecular weight		
	Theoretical	Found	Error (%)
N-methyl-*N*,2,4,6-tetranitroaniline	287	285	−0.7
3,3′-Diamino-2,2′,4,4′,6,6′-hexanitrobiphenyl	454	440	−3.1
2,4-Diamino-1,3,5-trinitrobenzene	243	250	+2.9
1,3,5-Trinitrobenzene	213	211	−1.0
2,4-Dimethoxy-1,3,5-trinitrobenzene	273	277	+1.5
2,4,6-Trinitrotoluene	227	225	−0.9
Pentaerythritol tetranitrate	316	313	−1.0
2,2,2-Trinitroethyl-4,4,4-trinitrobutyrate	386	384	−0.5
N,*N*′-dinitro-1,4-diazacyclohexane	176	178	+1.1
N,*N*′-dinitro-1,3-diazacyclopentane	162	167	+3.1

LITERATURE CITED

(1) Albers, H., Müller, E., *Naturwissenschaften* 46, 75 (1959).
(2) "Dimethyl Sulfoxide," Technical Bulletin, p. 8, March 1963. Crown Zellerbach Corp., Chemical Products Division, Camas, Wash.
(3) *Ibid.*, p. 2.

WORK done under the auspices of the U. S. Atomic Energy Commission.

Selective Removal of Aldehydes from Complex Mixtures during Gas Chromatography

R. R. Allen, Anderson, Clayton & Co., Foods Division, Sherman, Texas

BECAUSE THE LIQUID PHASE FFAP (*3*) had been described as the "best general-purpose packing available" for gas–liquid chromatography, we tried it for separating a mixture of aldehydes, ketones, alcohols, and hydrocarbons. It gave excellent separation of the components in the mixture except that all of the aldehydes were missing from the chromatogram. Subsequent work showed a short column of FFAP could be used to subtract the aldehydes from a mixture by the same method alcohols are removed by a short boric acid column (*2*). This technique of "subtractive chromatography" should have considerable utility for the identification of peaks that result from the chromatography of a complex mixture.

The results using this technique are shown in Figure 1. The mixture was analyzed on a 12-foot column of 20% UCON Polar plus a 12-inch column of 20% Carbowax 20M at the head of the column. The upper chromatogram shows all the materials are well separated except heptanone and heptanal which are in one peak. The sample was again chromatographed on the same UCON column with a 12-inch 20% FFAP column replacing the short Carbowax column. The lower chromatogram shows all of the aldehydes have been removed without affecting the other classes of compounds. The heptanone peak is now revealed since the heptanal was removed. Although not shown, a 12-inch column of 2% boric acid in Carbowax (*2*) substituted for the FFAP column removed the alcohols. Thus chemical nature of the "missing" peaks can be assigned.

Aromatic aldehydes were also removed from the gas stream by FFAP. A mixture of benzaldehyde, anisaldehyde, isosafrole, eugenol, veratraldehyde, and vanillin were chromatographed first on a 3-foot × 1/4-inch 20% Carbowax 20M at 220° C., 60 ml. He per minute, then on a 3-foot, 20% FFAP under the same conditions. Comparison of the chromatograms showed only the isosafrole and eugenol peaks on the second chromatogram, and identified the other four peaks in the first chromatogram as aldehydes.

The material that is responsible for the removal of the aldehydes is unknown. However, when a thermal conductivity detector is used, a water peak can be observed when aldehydes are injected into an FFAP column. Also, the reaction must be comparatively slow; when a mixture of short- and long-chain aldehydes were injected into a 6-inch FFAP column only a small part of the short-chain, fast-moving, aldehydes came through the column whereas all of the longer-chain aldehydes were retained. Thus it is necessary to use a removal column long enough to allow complete reaction of the aldehydes.

Also, with continued use, the ability of the FFAP column to remove aldehydes is decreased (*1*). Thus a freshly prepared column should be used for the best effect.

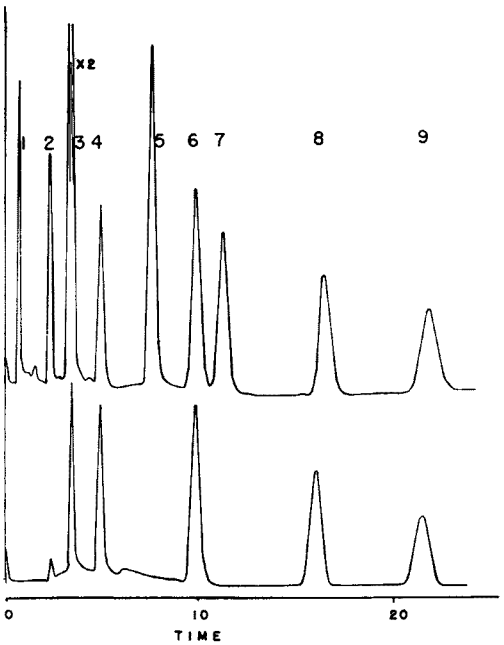

Figure 1. Gas chromatogram of mixture

Column: Upper- 12-foot × 1/4-inch 20% UCON Polar, 12-inch 20% Carbowax 20M, 210° C., 60 ml./min. He
Lower- Same as upper except 12-inch 20% FFAP instead of Carbowax

Peak identification:
1. Propanal
2. Hexanal
3. Heptanal + 2-heptanone
4. 2-Octanone
5. Nonanal
6. 1-Octanol
7. Decanal
8. Methyl caprate
9. 1-Decanol

LITERATURE CITED

(1) Hammarstrand, Kent, Varian Aerograph Co., private communication, January 1966.
(2) Ikeda, R. M., Simmons, D. E., Grossman, J. D., ANAL. CHEM. 36, 2188 (1964).
(3) Wilkens Instrument & Research, *Aerograph Research Notes*, p. 3, Fall 1964.

Near-Infrared Determination of Deuterium Oxide in Water

W. E. Keder and D. R. Kalkwarf, Battelle-Northwest,[1] Richland, Wash.

NUMEROUS PAPERS have been published on the determination of deuterium oxide in water by infrared spectrophotometry (*1–5*). Most workers have found it necessary to use especially constructed cells (which were usually very thin) and often their procedures were not applicable over wide concentration ranges. We report a technique that we have found convenient and rapid for measurements over the complete D_2O concentration range in cases where the highest precision is not required. This procedure uses an ordinary near-infrared spectrophotometer and commercially-available cells. It does not require exclusion of atmospheric moisture from the cells or from the samples after the solutions are prepared.

EXPERIMENTAL

A Beckman DK-2 spectrophotometer with a temperature-regulated cell holder and 1-cm. quartz cells with ground-glass stoppers were used to measure absorbances. Technical grade 1,4-dioxane was used as received from Allied Chemical and Dye Corp., after drying proved to be unnecessary. Deuterium oxide obtained from Abbott Laboratories was assumed to be 100% D_2O for this exercise. Five degree temperature variations were found to present no difficulty.

RESULTS AND DISCUSSION

The infrared spectrum of each isotopic water in the liquid phase consists of 3 fundamental modes plus a series of combination bands, the assignments of which are not yet completely certain (*1*). The band intensities decrease with decreasing wavelength and show a range in absorptivity of about 5 orders of magnitude.

Our original intent was to measure % D_2O in water samples not larger than 0.010 ml. (10 μl.) and our desire to use ordinary spectrophotometer cells suggested dilution to accommodate them.

[1] Battelle-Northwest is operated by the Battelle Memorial Institute for the U. S. Atomic Energy Commission under Contract No. AT(45-1)-1830.

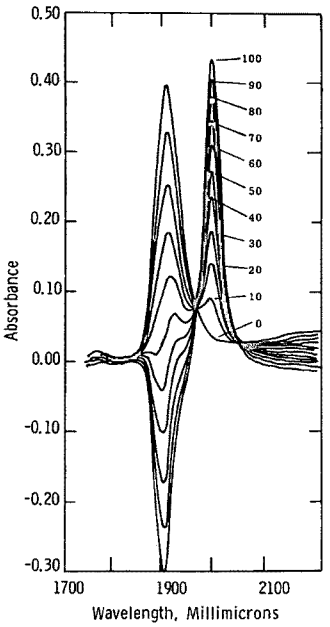

Figure 1. Absorption spectra of solutions of 10 μl. of D_2O–H_2O mixtures (0–100% D_2) in 2.50 ml. of 1% H_2O–99% dioxane *vs.* solvent

By surveying the spectra of H_2O, D_2O, and HDO in several organic solvents we found that the absorptivities of their combination bands near 2 microns were suitable for our purpose and that dioxane was transparent enough to be used in 1-cm. cells. Since commercial dioxane contains varying amounts of water, the 2.01-micron HDO band appeared at varying intensities when D_2O was dissolved in this material. Attempts to obtain reproducible D_2O spectra with solutions in carefully dried dioxane were discouraging, probably because of contamination of the solutions by water from the atmosphere and the glassware used. We found that we could obtain reproducible spectra of HDO, however, by introducing our D_2O-containing samples into a judiciously chosen water-dioxane mixture. The reaction $D_2O + H_2O \rightarrow 2HDO$ is rapid, and at large H_2O/D_2O ratios the HDO concentration is insensitive to H_2O concentration, thus eliminating the effect of contaminating water.

Figure 1 shows the spectra of solutions in which 10 μl. of each of a series of D_2O–H_2O mixtures was dissolved in 2.50 ml. of a solvent consisting of 1.0% H_2O and 99% dioxane. These spectra were measured in 1-cm. cells against 1 cm. of the solvent. This particular solvent composition was necessarily a compromise, chosen so that the reference was not impossibly dense at the 1.90-micron H_2O peak. The negative absorbances at this frequency in the spectra in Figure 1 are, of course, due to the H_2O that was removed from the solvent by the reaction with the D_2O of the samples. A plot of absorbances of the HDO peaks from Figure 1 *vs.* % D_2O in the water samples is a slightly curved line due to incomplete conversion of the D_2O to HDO at the higher concentrations.

When larger samples are available it is possible to work at higher concentrations and achieve higher sensitivity. We have found it convenient to use sample sizes from 10 to 100 μl. with a solvent composed of 1% H_2O–99% dioxane, but in these cases an extra amount of H_2O was added to the reference for each measurement, to make the reference H_2O concentration equal to the total water concentration in the sample solution.

Other variations of this technique can be suggested. With the procedure described here the precision is about 1% in D_2O over the entire concentration when 10 μl. samples are used and 0.1–0.2% with 100-μl. samples.

LITERATURE CITED

(1) Bayly, J. G., Kartha, V. B., Stevens, W. H., *Infrared Physics* **3**, 211 (1963).
(2) Crespi, H. L., Katz, J. J., *Anal. Biochem.* **2**, 274 (1961).
(3) Gaunt, J., *Spectrochim. Acta* **8**, 57 (1956); *Analyst* **79**, 580 (1954).
(4) Thornton, V., Condon, F. E., ANAL. CHEM. **22**, 690 (1950).
(5) Trenner, N. R., Walker, R. W., *Perkin-Elmer Instrument News*, **4** (No. 1), 1 (1952).

Conventional, fast sweep— for all polarographic applications

ONLY SARGENT MAKES 5 POLAROGRAPHS®

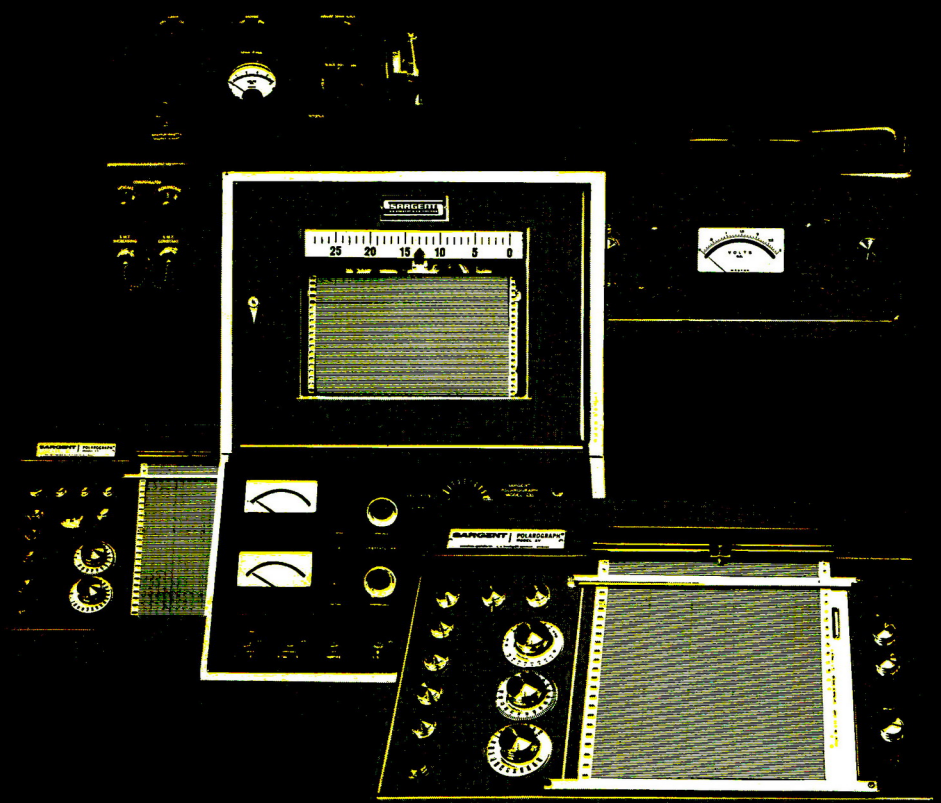

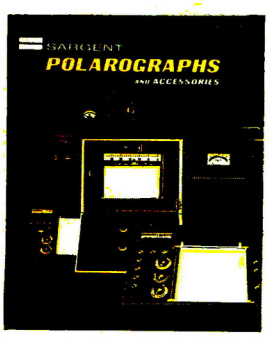

read all about all 5 models in this booklet—complete with illustrations, specifications, and recommended selections...plus a full line of polarographic accessories.

E. H. Sargent & Co., Dept. AC-86
4647 W. Foster Ave., Chicago, Ill. 60630

Yes, I would like a copy of your illustrated booklet (Bulletin P-5) about all five Sargent Polarographs.® Please send me my booklet.

Name_____
Title_____
Firm_____
Address_____
City_____ State_____ Zip_____

SARGENT® SCIENTIFIC LABORATORY INSTRUMENTS • APPARATUS • CHEMICALS

E. H. SARGENT & CO.
4647 West Foster Avenue
Chicago, Illinois 60630

Chicago • Anaheim, Calif. • Birmingham • Cincinnati • Cleveland
Dallas • Denver • Detroit • Springfield, N.J. • Toronto, Canada

Circle No. 65 on Readers' Service Card

conductivity meter, anyone?

Whatever your requirements, why not turn to the people who know most about conductivity measurement? Whether you need a general purpose, wide range meter with moderate accuracy, a precision laboratory bridge with 0.1% accuracy, a direct reading meter with output for a remote recorder, an electrodeless system for highly corrosive fluids, or almost anything else, we can probably supply what you require. Contact your local Beckman Sales Office or write direct.

Beckman INSTRUMENTS, INC.

CEDAR GROVE OPERATIONS
89 Commerce Road
Cedar Grove, New Jersey 07009

Formerly Industrial Instruments, Inc.

Circle No. 16 on Readers' Service Card

EQUIPMENT
APPARATUS
INSTRUMENTS

NEW PRODUCTS

Spectroradiometer, for use in applications requiring qualitative and quantitative measurement of radiance or irradiance of light sources, is available in both prism and grating monochromator versions. This instrument is capable of reproducing and directly plotting the spectral curve of a National Bureau of Standards source to ±2% of full scale. Prism versions provide linear readout from 0.25 to 2.5 microns; grating versions offer direct scanning from 320 to 920 mμ. Beckman Technical Information Section, 2500 Harbor Blvd., Fullerton, Calif. 92634 **401**

Organic Acid Analyzer

Automatic acid analyzer is for the routine quantitative analysis of organic acids such as the Krebs cycle intermediates and other carboxylic acids. The instrument is based on separation by silica gel chromatography and determination of concentration by indicator titration as plotted by a recording photometer. A typical analysis of 15 acids requires 5 hours. As little as 0.05 μequiv. of acid can be measured. The system may be applied to samples as small as 0.2 ml. of urine, 350 mg. of tissue, or 1 ml. of plasma. No preliminary deproteinization or extraction is required. Because of the simple sample preparation, there is no formation of artifacts. A series of calibration standards can be used so that an accuracy of ±3% can be obtained with this system. Waters Associates, Inc., 61 Fountain St., Framingham, Mass. **402**

Protein Separation

A new multimembrane electrodecanter is capable of separating pure protein from mixtures of proteins, processing up to 25 liters of protein solutions in a 24-hour period, or separating small quantities for analytical work. It can also be used for the concentration of protein solutions previously separated by electrodecantation or by column chromatography and for separation at low temperatures (0° to 5° C.). The apparatus contains three separation cells, each containing 22 membranes. These cells can be connected in series or in parallel for continuous and batch operation. The complete cell train contains four cooling cells and an electrode cell at each end of the train. Protein flow is regulated by two variable-speed, six-channel peristaltic pumps. Quickfit Reeve Angel, Inc., 1 Bridewell Pl., Clifton, N. J. 07014 **403**

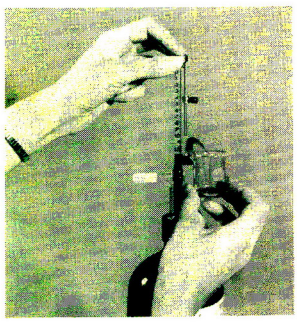

FOR DEPENDABLE LABORATORY DATA

Use L/I Automatic REPIPETS* and Automatic Dilutors to dispense, transfer, mix, aspirate and dilute. We guarantee 1% accuracy, 0.1% reproducibility. You'll speed up your research considerably, too. These two automatic L/I instruments complete any operation in a few seconds, enabling you to cut your analysis time 50–95%.

L/I's versatile instruments can handle any liquid, including those with viscosities as high as 45 centipoises. Even with viscous liquids you'll get 1% accuracy and 0.1% reproducibility because there's no drainage error.

L/I instruments give you complete freedom from contamination, require no change in your methods, and never need cleaning. Integral air filters keep reagents pure. Volumes? From microliters to deciliters.

Dilutors $89.50, including complete set of tips for highest precision in all ranges. REPIPETS $47.50. Immediate delivery in 1, 10, 20, and 50 ml sizes. Please write for details.

*Trademark
(Repetitive PIPETS)

LABINDUSTRIES

1802-A Second Street,
Berkeley, California 94710
TH 3-0220, Cable LABIND

Circle No. 45 on Readers' Service Card

NEW PRODUCTS

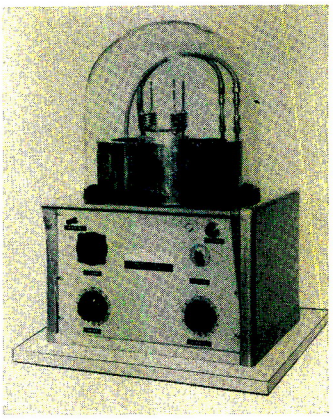

Comparative thermal conductivity measuring system determines the conductivity of materials between temperatures of −300° and +2000° F. by comparing the heat flow through standards of known conductivity with heat flow through materials of unknown conductivity. The test section of Model TCFCM-N4 consists of a stack containing a heater, a conductivity standard, a sample of unknown conductivity, a second standard, and a heat sink. An auxiliary heater is utilized for high-temperature operation. This model with silicone rubber heaters is also available for measuring conductivity between −300° and +400° F. Optional automatic controls and vacuum capabilities are available. Dynatech Corp., 17 Tudor St., Cambridge, Mass. 02139 **404**

Ion Exchanger Electrode

Direct measurement of total divalent cations in aqueous solution can be made with any expanded-scale pH meter using a new divalent ion electrode. Because the electrode is equally sensitive to calcium and magnesium, it is possible to determine water hardness directly even in the presence of large amounts of monovalent cations such as sodium or potassium. Two parts per million of calcium–magnesium (calculated as the carbonates) can be measured directly in the presence of 500 p.p.m. of sodium chloride. The new electrode is used in a similar manner to a conventional pH electrode; however, the glass sensing membrane in a pH electrode has been replaced by a thin porous membrane containing a water-soluble organic ion exchanger. The unit is constructed of an unbreakable, corrosion-resistant fluorocarbon plastic. Orion Research Inc., 11 Blackstone St., Cambridge, Mass. **405**

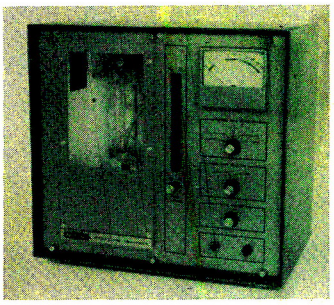

SO_2 analyzer for continuously detecting trace concentrations of sulfur dioxide in the atmosphere incorporates the technique of secondary coulometry with end point detection. Response time is less than 3 minutes, with accuracy to ±5%. Four operating ranges, from 0–0.5 to 0–4.0 p.p.m. full scale are manually selected. Direct readout in p.p.m. SO_2 is provided; a potentiometric recorder for continuous readout is optional. Model 906 can be panel-, van-, wall-, or bench-mounted and consists of a single unit housing three basic components: a sample and zero conditioner, a detector cell, and a pump to pull the sample through the detector. Beckman Technical Information Section, 2500 Harbor Blvd., Fullerton, Calif. 92634 **406**

Infrared Transmittance

Cortran Code 9753 glass transmits 82% of infrared energy at 4 microns. Transmittance at shorter wavelengths is essentially the same down to about 400 mμ. Sharp cutoffs occur at each end of the transmission band. The material is expected to find wide application as infrared transmitting filters and in other optical instrumentation systems. Corning Glass Works, Corning, N. Y. 14830 **407**

Particle Size Distribution

A new system for measuring particle size distribution by sedimentation is based on the company's RG Electrobalance. Other components of the system are a strip-chart recorder, a circulating constant-temperature bath, Model 1389 external filter, and Model 2030 time derivative computer. Particle size range is 1 to 100 microns diameter. Normal sample size is about 1 gram, but useful results can be obtained with less than 0.1 gram. Weight values are accurate to 0.01%. Cahn Instrument Co., 7500 Jefferson St., Paramount, Calif. **408**

ECONOMY!

Versatile, Value-priced x-y recorder ...just $895!

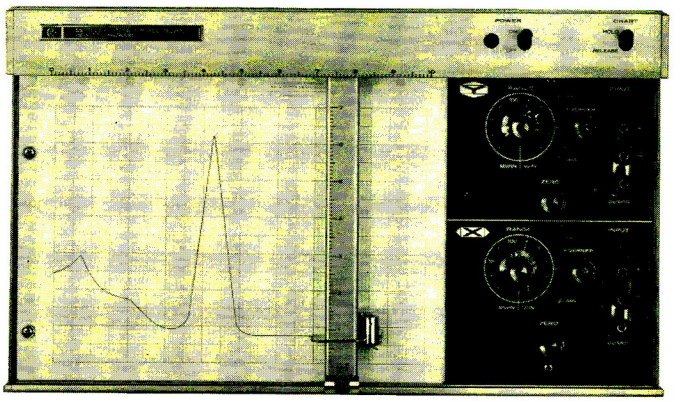

THE MOSELEY 7035A

This is a high-performance, low-cost solid-state recorder for everyday applications not requiring high dynamic performance. Five fixed calibrated ranges 1 mv/inch to 10 v/inch. High input impedance, floating guarded input, 0.2% accuracy at full scale. Adjustable zero set.

Each axis of the 7035A has an independent servo system with no interaction between channels. Maintenance-free AUTOGRIP* electric paper holddown and electric pen lift are standard. Options available include locks for zero and variable range controls, rear input, and retransmitting potentiometer for X axis.

For general-purpose applications, you can't beat the Moseley Division 7035A. Ask your Hewlett-Packard field engineer for a demonstration. Or write for complete specifications to Hewlett-Packard, Palo Alto, California 94304, Tel. (415) 326-7000; Europe: 54 Route des Acacias, Geneva.

Data subject to change without notice.
Price f.o.b. factory.

See New hp Instruments
Attend Measurement Seminars
WESCON–Hollywood Park

HEWLETT PACKARD hp MOSELEY DIVISION

An extra measure of quality

*Trade Mark Pat. pend.

947

Circle No. 156 on Readers' Service Card

cold plasma ashing preserves what you want

before ashing – urethane foam

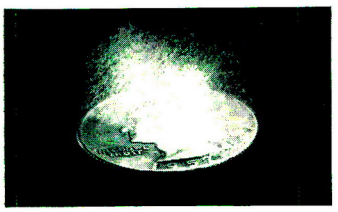

after ashing the delicate inorganic structure remains unaltered for precise quantitative analysis.

Tracerlab's new LTA-600 oxidizes samples with a cold plasma of atomic oxygen to leave inorganic constituents unaltered.

Permits more accurate quantitative elemental and structural analyses of plant and animal tissues, bones, coal, oil well cores, polymers, and radioactive materials. Prepares pure samples for atomic absorption spectrophotometry, mass spectrometry, emission spectroscopy, X-ray diffraction, and electron microscopy.

send for literature on equipment, techniques and services.

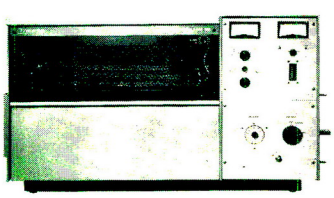

LFE | TRACERLAB
A Division of Laboratory for Electronics
2030 WRIGHT AVENUE, RICHMOND, CALIFORNIA
Circle No. 148 on Readers' Service Card

NEW PRODUCTS

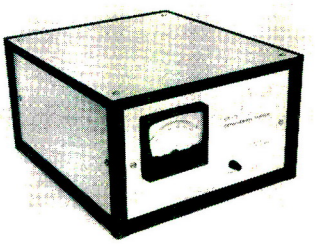

CT-75 cryothermal system extends the range in temperature programming, providing sub-ambient operation using either CO_2 or liquid N_2 with direct pyrometer readout from −180° to +400° C. This modular system is adaptable to most chromatographs. Micro-Tek Instruments, Inc., P. O. Box 15409, Baton Rouge, La. **409**

Neutron Activation Foils

Kit No. 1550 contains a variety of neutron activation foils and is designed to aid in choosing the most suitable foils for a particular application. The kit consists of 34 foils of 15 different foil types, a 50-page manual, forceps, and a special summary of reactions, cross-sections, and energies for each of the materials. Aluminum, cobalt, copper, dysprosium-aluminum, gold, indium, iron, magnesium, manganese-copper, nickel, silver, thorium, vanadium, sulfur pellets, and cadmium cover sets are included. Reactor Experiments, Inc., 140 Harbor Blvd., Belmont, Calif. 94002 **410**

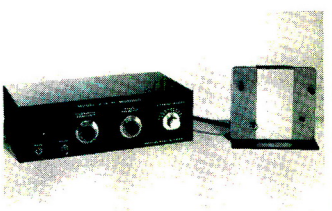

Refractive index flow monitor measures changes of sample components as they elute from a liquid column, reaction vessel, or distilling column. Model 404 provides a continuous readout (and strip-chart recording) of refractive index. Sensitivity is within 0.0005 refractive index unit full scale on a 1-mv. recorder. Two measurement ranges are offered: 1.30 to 1.45 units and 1.45 to 1.60 units. The detector is dual differential with measurement of two streams or one stream and a captive reference. Internal volume is 1.1 ml. Nester/Faust Mfg. Corp., 2401 Ogletown Rd., Newark, Del. 19711 **411**

YOU'RE NEVER IN DOUBT WHEN IT'S "Alconox-Clean!"

Where perfection depends on cleanliness, it is impossible to escape the fact that glassware, equipment, instruments and component parts—requiring absolute cleanliness—in Laboratories, Hospitals and Industries—must depend on the highest quality detergents.

ALCONOX
THE MASTER CLEANER

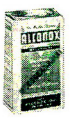

For manual cleaning. Meets highest government specifications! In 3 lb. boxes, and 25, 50, 100, 300 lb. drums.

3 lb. BOX—$2.12
Case of 12 Boxes—$20.00

ALCOJET

prevents water-spotting from final rinse, for scientifically-clean glass, metals, plastics, etc., in all mechanical washers. In 5 lb. boxes and drums as above.

5 lb. BOX—$3.00
Case of 6 Boxes—$15.00

ALCOTABS

For syphon-type pipette and test tube washers—one easy operation! In 100-tablet boxes.

Box of 100 Tablets—$5.00

LIQUI-NOX

THE PERFECT LIQUID DETERGENT!

For manual cleaning. Mild (neutral pH). Non-toxic. Contains no phosphates. Equally effective in hard or soft water. Outstanding blood and fat solvent. In quarts, gallons, & 15 gallon drums.

PER QUART—$2.15
Case of 12 Quarts—$19.92
PER GALLON—$7.00
Case of 4 Gallons—$24.00

All prices slightly higher West of Rockies.

E. H. SARGENT & CO.
Scientific Laboratory Instruments Apparatus • Chemicals
Chicago • Detroit • Dallas • Birmingham Anaheim • Springfield, N.J. Baltimore • Houston • Cleveland
Inquire about bulk prices for additional savings.

Circle No. 151 on Readers' Service Card

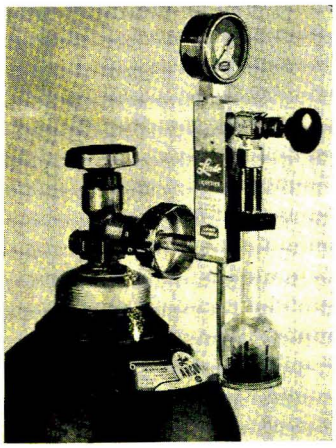

Gas liquefier produces small quantities of cryogenic fluids. The liquefier is a small counterflow heat exchanger which uses compressed gas from a conventional high-pressure cylinder. The amount of cryogenic fluid produced and the time required to produce it varies with the gas used and the pressure of the gas. With a cylinder of gaseous argon at 2600 p.s.i., 3 cc. of liquid argon can be produced in 5 minutes. Linde Division, Union Carbide Corp., 270 Park Ave., New York, N. Y. 10017 **412**

Germanium Detectors

Lithium drifted germanium detectors are available in this series in five standard sizes, complete with vacuum cryostat, liquid nitrogen chamber, and a 1-liter-per-second ion pump. Guaranteed resolution for these detectors is 4 k.e.v. A compatible series of low-noise preamplifiers and amplifier-coincidence modules is also available for high-resolution applications in nuclear spectrometry. Technical Measurement Corp., 441 Washington Ave., North Haven, Conn. 06473 **413**

Chromatography Column

New Sephadex laboratory columns for gel filtration and ion exchange chromatography with aqueous systems are designed to serve as one basic column system for both descending and ascending chromatography. The initial column is available as a descending system, either jacketed or unjacketed, but can be quickly converted to an ascending system by removing both end pieces of the column and replacing them with two upward flow adaptors. Pharmacia Fine Chemicals, Inc., 800 Centennial Ave., Piscataway, N. J. 08854 **414**

Current Detector

Streaming current detector is an alternating streaming current device in a rugged, portable form for determining the polarity and quantity related to the electrical charge density on colloidal particles. The instrument provides a measurement of streaming current rather than potential. A valveless positive displacement pump is the energy coupler of the system. Waters Associates Inc., 61 Fountain St., Framingham, Mass. **415**

Filter Membranes

New filter membranes permit filtration of any corrosive liquid or gas at temperatures as high as 550° F. or down to −450° F. These membranes are made of Zitex, a new physical form of Teflon/Halon. They are characterized by their chemical inertness, heat resistance, low temperature flexibility, and nonadhesive quality. Six grades are available in diameters ranging from 75 to 150 mm. Chemplast, Inc., 150 Dey Rd., Wayne, N. J. 07470 **416**

Read Number-Average Molecular Weight in Minutes

For speed and convenience in determining molecular weight (5,000 to 500,000 MW), you'll find it hard to steal a march on Hallikainen's Model 1361 Automatic Osmometer. Within 10 minutes of sample injection, osmotic pressure appears on a large digital counter within 0.01-cm accuracy over a 10-cm range. You can read four concentrations and calculate number-average molecular weight in less than an hour.

With a simple exchange of sample inlet funnels, Model 1361 can be used for both low (35°C) and high (135°C) temperature work. No need to invest in separate instruments.

The entire unit, including built-in chart recorder, occupies a trim 12x 15 x 13-inch cabinet. For further information, write today for the informative four-page brochure.

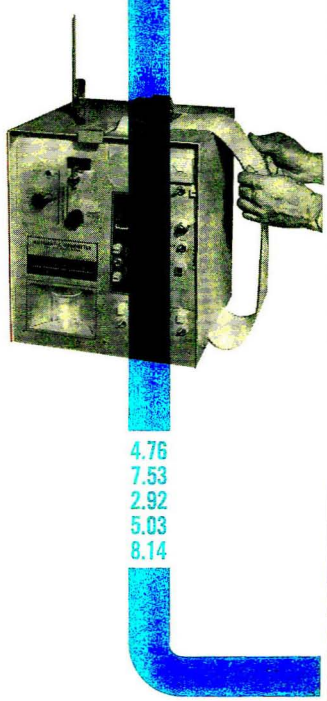

HALLIKAINEN *Instruments*

750 National Court, Richmond, Cal. 94804

Respondents living outside North America, South America, and Japan are invited to address their inquiries to: Hallikainen Instruments Ltd., Blackwall Lane, Greenwich, London SE10, England.

Circle No. 167 on Readers' Service Card

high-intensity mercury vapor arc lamps for halogenations, oxidations, hydrogenations, polymerizations, isomerizations, nitrogen and iron reduction, decompositions

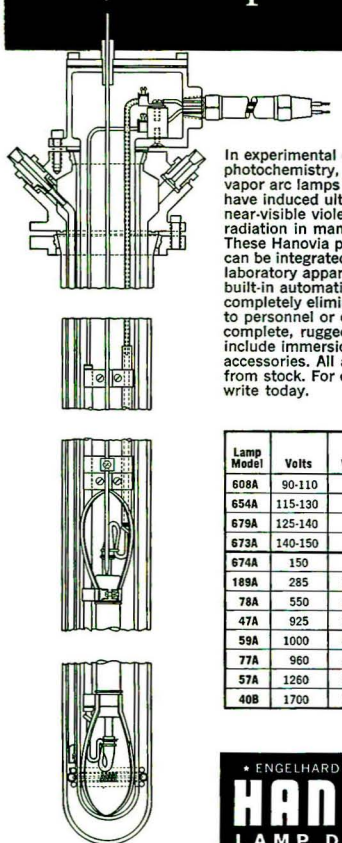

In experimental or commercial photochemistry, the Hanovia mercury vapor arc lamps listed below have induced ultraviolet radiation and near-visible violet and blue radiation in many photo-reactions. These Hanovia photochemical systems can be integrated easily into standard laboratory apparatus. And a built-in automatic protective system completely eliminates any hazard to personnel or equipment. The complete, ruggedly-built systems include immersion wells, lamps and accessories. All available immediately from stock. For complete details, write today.

Lamp Model	Volts	Watts	Arc Length In.	
608A	90-110	100	1.2	Laboratory Scale
654A	115-130	200	1.9	
679A	125-140	450	3.7	
673A	140-150	550	4.5	
674A	150	700	7.5	Pilot Plant and Commercial Scale
189A	285	1200	12.0	
78A	550	2000	21.0	
47A	925	3450	48.0	
59A	1000	4500	58.0	
77A	960	4500	42.0	
57A	1260	5000	46.5	
40B	1700	7500	59.0	

• ENGELHARD HANOVIA, INC. •
HANOVIA
LAMP DIVISION
100 Chestnut St., Newark, New Jersey 07105

355

Circle No. 172 on Readers' Service Card

NEW PRODUCTS

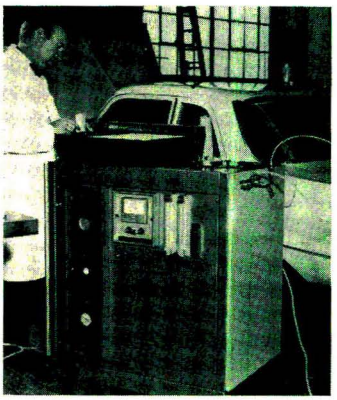

NO_x analyzer makes continuous, dynamic measurements of the concentration of total oxides of nitrogen in automobile exhaust as they leave the tail pipe. The instrument has a dual range of 0 to 1000 and 0 to 6000 p.p.m. and a response time of 3 seconds to 90% of scale. Dynamic analyses are performed by connecting a probe to the tail pipe. Integrated sample analyses can be made from bag samples of automobile exhaust. The analyzer consists of an oxidation system for sample preparation and the company's Model 255 ultraviolet dual-beam filter photometer sensitized to monitor concentrations of NO_2. Both utilize pressure techniques. The equipment is combined into one compact, semiportable, wheel-mounted unit. Beckman Technical Information Section, 2500 Harbor Blvd., Fullerton, Calif. 92634 **417**

Spectrum Stabilizer

Digital logic and integrated circuitry are employed in a new spectrum stabilizer. Two completely independent sections are used to correct for gain and baseline drift effects in a nuclear detector/analyzer system. The gain section is capable of correcting for system gain changes in steps as small as 1 part in 64,000 or as great as 1 part in 1000. Stabilization is unaffected by variations in input counting rate up to 50,000 repetitions per second. Gain and/or zero stabilization may be based either on a prominent peak in the input spectrum or on an externally generated reference signal. The channel selected for gain stabilization is adjustable from 0 to 9999 in single-channel increments, while the zero peak channel is switch-selectable from 0 to 99 in single-channel increments. Technical Measurement Corp., 441 Washington Ave., North Haven, Conn. 06473 **418**

A Fluid Handling Innovation!

Rugged, compact unit transfers, circulates and dispenses fluids dependably, safely!

Since no parts of this unique pump are ever in contact with the fluid, it may be used even with abrasive slurries or sterile solutions conducted through appropriate tubing.

The ingenious design employs an encapsulated electrical induction coil which imparts 7,200 vibrations per minute, through an adjustable pressure-pedal, to the wall of the fluid-conducting flexible tubing. The result is a controllable, peristaltic, unidirectional flow of the liquid.

The CRC Pump has only one moving part . . . requires no lubrication . . . operates on 115 volt A.C. current.

CATALOG NO. AC-37 . . Each $37.50

Available only from the manufacturer:

THE
CHEMICAL RUBBER
CO.
2310 Superior Ave.
Cleveland, Ohio 44114

A-5472

Circle No. 22 on Readers' Service Card

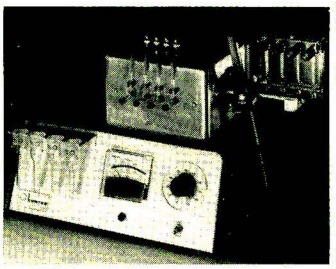

Sweep codistillation apparatus, designed for the rapid and efficient clean-up of samples from crude extracts in pesticide analysis, avoids column contamination in gas chromatographs while conserving solvents. Clean-up levels are reported as low as 0.025 p.p.m. Full proportionally controlled oven has a range of 100° to 400° C., accurate to ±0.5° C. The sample is in contact only with parts made of Teflon and borosilicate glass. Typical run times from introduction to clean sample are approximately 20 minutes with recoveries from 90 to 99% dependent on pesticide. Kontes Glass Co., Spruce St., Vineland, N. J. 08360 **419**

Amplifier

Model 301 is a d.c. differential operational amplifier. Its offset current and drift performance at 25° C. are 1 pa. (10^{-12} amp.) and 0.06 pa./° C. with offset doubling for every 10° C. temperature increase. Voltage drift is 30 μv./° C. maximum over the temperature range −25° to 85° C. Noise referred to the input is 0.01 pa. and 1 μv. peak-to-peak, in the frequency range d.c.-1 Hz. Common mode performance figures include ±300 volt common mode voltage rating, 160 db. (10^8) common mode rejection ratio at d.c., and one trillion ohms common mode input impedance. Differential input impedance is 10^{10} ohms. Analog Devices, 221 Fifth St., Cambridge, Mass. 02142 **420**

Voltmeter/Ratiometer

A new differential d.c. voltmeter and ratiometer carries a 0.002% accuracy spec, with stability of 1 p.p.m. per hour (of range) and 5 p.p.m. per day. Null meter resolution is 0.2 p.p.m. of range. The instrument comes in two versions: Model 3420A is for a.c. line operation only; Model 3420B is for line or self-contained battery-powered operation. The ratio of two applied d.c. voltages can be determined to six significant figures. Hewlett-Packard, 1501 Page Mill Rd., Palo Alto, Calif. 94304 **421**

TODAY ITS

BIODEGRADABLE

Sud'n

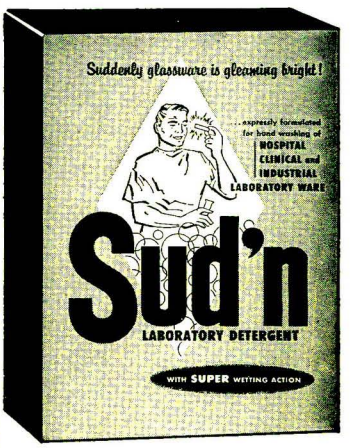

for BRUSH and ULTRA-SONIC Washing of all laboratory glassware, missile and outer space components. . .used wherever the ULTIMATE in cleaning is ESSENTIAL —where any thing less would be too EXPENSIVE!

CLEANS completely—
RINSES freely—

MONARCH QUALITY PRODUCTS

without film or residue even in **COLD WATER!**

SPECIFY SUD'N

See your laboratory supplier or mail coupon for sample.

SEP-KO CHEMICALS, INC.
3900 Jackson St., N.E.
Minneapolis, Minnesota

OK send free test package of
☐ SUD'N for hand washing
☐ LAB-GLO Mechanical cleaning

Name

Address

City State

Circle No. 68 on Readers' Service Card

If the heating system you want hasn't been built yet... build it!

It's simple—with Lindberg Hevi-Duty building blocks of heat. These flexible, low-cost elements can be assembled in countless ways.

They're perfect to heat piping systems where liquids must be kept at constant temperature. Or for special lab requirements that don't justify a furnace. Or where there isn't a furnace to do the job.

They have excellent capacity. High watt density. 1000° or 1200° C. Control them manually, or automatically.

They're available from leading lab dealers in sizes, shapes, and lengths to fit your projects.

Write for bulletin 50910, Lindberg Hevi-Duty, Watertown, Wis. 53094.

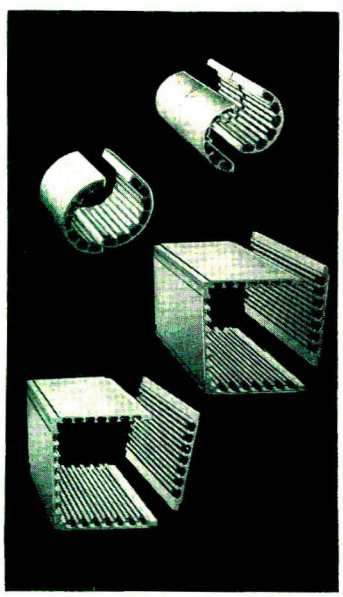

LINDBERG HEVI-DUTY SB

DIVISION OF SOLA BASIC INDUSTRIES

"See Laboratory Guide for all Products/Sales Offices"
Circle No. 131 on Readers' Service Card

NEW PRODUCTS

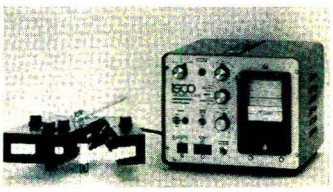

Model UA-2 ultraviolet analyzer is a new dual-beam flow stream monitor for column chromatography and similar applications, which operates at both 254 and 280 $m\mu$. A strip chart record of absorbance at either or both 254 and 280 $m\mu$ can be made at two sensitivity ranges. Dual-beam operation provides base line compensation for gradient elution; absorbance recording allows the chart record to be directly integrated for quantitative determinations. An automatic actuator causes an associated fraction collector to index in such a way that individual absorbance peaks are deposited in separate test tubes. Instrumentation Specialties Co., Inc., 5624 Seward Ave., Lincoln, Neb. 68507 **422**

UV Intensity Meters

Two new Blak-Ray ultraviolet intensity meters measure long-wave or short-wave ultraviolet intensities without interference from visible light. Accuracy is calibrated to ±5%, traceable to the National Bureau of Standards. Switch-controlled scales cover 0 to 1000 and 0 to 5000 microwatts per square centimeter. Sensor cells are detachable for remote measurements and for measuring as close as $1/4$ inch from an irradiated surface. Ultra-Violet Products, Inc., 5114 Walnut Grove Ave., San Gabriel, Calif. 91778 **423**

Optical Sample Holders

A new group of four basic variable-temperature optical sample holders permits long-term optical studies in continuum from 1.04° to 300° K. and above. The variable temperature design is optimized for use with most commercial spectrophotometers. A wide range of window materials permits studies in infrared and ultraviolet ranges. Various methods of positioning samples under examination are provided. Standard temperature control accessories and temperature sensors are available for manual or automatic temperature control to an accuracy (±1 millidegree) limited by the sensitivity of the sensor at the temperature set point. Andonian Associates, Inc., 26 Thayer Rd., Waltham, Mass. 02154 **424**

Now...a Water Hardness Monitor at a practical price!

New Milton Roy Chemalyzer,® Jr.

ONLY $293.00

Precision-built. And so economical you can afford one for constant, automatic check of feedwater hardness at every sampling point in your plant!

Here's long-needed, low-cost, dependable protection of high-priced equipment. Chemalyzer, Jr. gives continuous colorimetric analysis of industrial water hardness within the 0 to 3 parts per million range. Eliminates more sophisticated monitors where process doesn't require them. Ends human errors in manual analysis.

Chemalyzer, Jr. continuously blends a reagent with water sample, constantly checking color intensity of mix. If pre-set upper limit of 3 ppm is reached, alarm is triggered instantly and automatically, alerting operating personnel of impending hardness breakthrough. Signal can be panel lights, or remote audio-visual alarm.

Solid state circuitry throughout. Economical to operate and maintain. Just supply one liter of reagent about every four days and clean key components occasionally. Compact. Easily installed.

ORDER TODAY

Sold direct, F.O.B. St. Petersburg, Fla. Fully guaranteed. Money back if not satisfied after 30 days. Send order now. Or write for Data Bulletin 260.

mR TECHNOLOGY IN FLUIDS

MILTON ROY COMPANY
P.O. Box 12169, St. Petersburg, Florida 33733
Circle No. 82 on Readers' Service Card

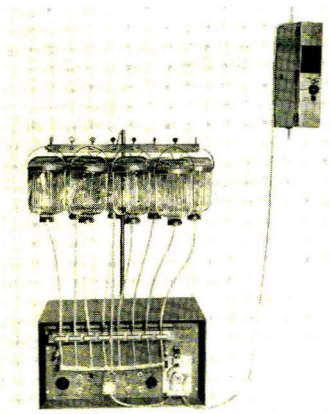

Sequential column eluter will run 1 to 8 samples of up to 1 liter each, continuously and automatically, until the last solution has been delivered. The liquid may be fed to the chromatography column by gravity or by means of the built-in peristaltic pump. The eluter is designed for step elutions, for upward or downward flowing columns. The instrument measures 17 × 11 × 9½ inches in height. Kraft Apparatus, Inc., 125–9 Liberty Ave., Richmond Hill, N. Y. 11419 **425**

Indicator Paper

Panpeha, developed in cooperation with Ridel-de Haen AG of West Germany, are indicator strips which provide visual determination of color values in the 0.1 to 14 pH range. From pH 0.1 to 10, values can be determined to within 0.5 of a pH unit. The color change is read by changes in shade of more than one indicator color. Carl Schleicher & Schuell Co., Keene, N. H. **426**

Programmer

Model 412 analog programmer is an all electronic programmer for system variables. Although the basic unit has one channel, up to four additional channels of program storage are available as modular supplements, without duplication of controls, and utilizing the same time base. Rates of change range from 1 volt per μsec. to 1 volt per 0.5 hour, or longer under external timing control. Time resolution is ±0.2% of full program. Additional features include automatic interpolation for continuity, provision for computer control, and either automatic or manual loading of program. Evans Associates, P. O. Box 5055, Berkeley, Calif. 94705 **427**

Digital Stabilizer

Model NS-401 digital stabilizer provides zero and gain stabilization of all pulse height analyzers currently in the field. An exclusive passive device, which does not degrade the system linearity, is used to control the gain of the input pulses. The conversion rate of the stabilizer is limited only by the pulse height analyzer duty cycle. A front panel control is provided to adjust the correction rate so that the stabilizer performance can be optimized for any system stability. A baseline sensing circuit eliminates count rate and pulse pile-up problems in zero stabilization and gives the incoming signal priority over the zero-stabilization pulses. All the correction devices for the zero and gain stabilization are electronic. The standard unit is designed to operate with pulse height analyzers up to 4096 channels with digitizing rates up to 16 Mc. Northern Scientific Inc., 303 Price Pl., P. O. Box 4247, Madison, Wis. 53711 **428**

Yes, our MR Recorder often seems like many instruments at work...and the specs tell you why.

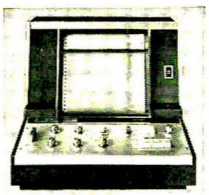

DESCRIPTION: SARGENT MODEL MR RECORDER—automatic, self-balancing, 10-inch potentiometer recorder. High gain amplifier; high stability solid state reference power supply needs no standardization. Line operated.

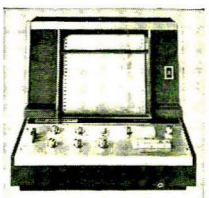

QUANTITY RECORDED: mV, V, μa and ma—selected by panel switch.
ZERO DISPLACEMENT: calibrated ranges of 10, 100, 1000 and 5000 of the selected units, upscale or downscale.

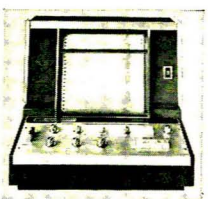

ELECTRICAL RANGE: twelve pre-calibrated ranges by switch selection—0.5, 1, 2, 5, 10, 20, 50, 100, 200, 500, 1000, 2000. Variable range expansion from 100% (off) to 40% of selected range.

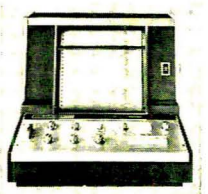

LIMIT OF ERROR: 0.1% or 5μV, whichever is greater.
SOURCE RESISTANCE TOLERANCE: 50,000 ohms in most sensitive range, increasing with increasing range.

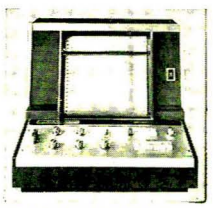

ELECTRICAL FILTERING: four position switch to reject transverse and common mode A.C. superimposed on the D.C. signal, without loss of sharp balancing characteristics.

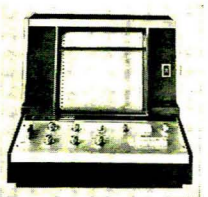

DAMPING GAIN ADJUSTMENT: automatic with range change; panel dial for fine adjustment—especially for low resistance systems like thermocouples.

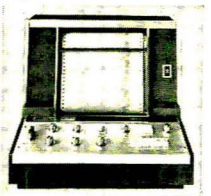

CHART DRIVE: twelve synchronous speeds—0.5, 1, 2, 4, 10, 20—by dial selection, inches per hour or per minute by panel switch. Rapid scanning in forward and reverse.

PEN SPEED: 1 second for full scale transverse.
CHART TAKE-UP: automatic, by motor with preset torque—or by-pass for free end chart tear off.

This gives you some idea why the SARGENT MODEL MR can do the work of several less versatile recorders, manual potentiometers or precision meters. To get the complete picture, write for Bulletin MR.

SARGENT® SCIENTIFIC LABORATORY INSTRUMENTS • APPARATUS • CHEMICALS

E. H. SARGENT & CO.
4647 West Foster Avenue
Chicago, Illinois 60630

Chicago • Anaheim, Calif. • Birmingham • Cincinnati • Cleveland
Dallas • Denver • Detroit • Springfield, N.J. • Toronto, Canada

Circle No. 138 on Readers' Service Card

Klett . . .

Photometers

Klett-Summerson *Photoelectric Glass Cell Colorimeter*

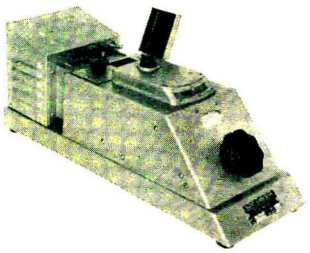

No. 900-3

●

The Klett Fluorimeter

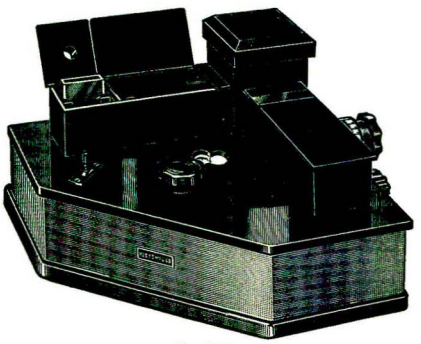

No. 2070

Designed for the rapid and accurate determination of thiamin, riboflavin, and other substances which fluoresce, in solution. The sensitivity and stability are such that it has been found particularly useful in determining very small amounts of these substances.

●

KLETT SCIENTIFIC PRODUCTS

PHOTOELECTRIC COLORIMETERS • BIO-COLORIMETERS
COLORIMETER-NEPHELOMETERS • COLONY MARKER
• KLETT REAGENTS • GLASS CELLS

■

Klett Manufacturing Co., Inc.

179 EAST 87TH STREET, NEW YORK, N. Y.

Circle No. 44 on Readers' Service Card

THE FLOW SHEET

One of a series devoted to enriching the Art of conveying & controlling fluids

Working With MASS SPECTROMETRY?

Let Hoke Help You...

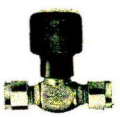

CALIBRATE LEAK DETECTOR SENSITIVITY.
This inexpensive, miniature bellows valve has low internal volume. Kel-F stem disc provides a vacuum-tight closure of Helium supply.

SHUT OFF BACK-FILL GAS INSTANTLY.
Hoke toggle valves operate with a flick of the finger. Buna "N" or Viton O-Ring and stem disc seal the valve.

METER & ANALYZE MINUTE GAS QUANTITIES.
"Milli-Mite" fine metering valve has low internal volume, 3° angle stem, and 3/64" orifice for extremely accurate and reproducible flow settings.

BAKE OUT TESTED COMPONENTS.
Use this all metal diaphragm sealed valve for vacuums to 10^{-10} TORR. Branch port permits leak-testing and closure without disturbing the straight-thru vacuum line.

And don't forget to hook-up the entire system with New, Hoke **Gyrolok** Tube Fittings. A catalog is available.

For complete information on how these Hoke products can help you, contact your local Hoke distributor or write to us directly.

HOKE

Hoke Incorporated • 1 Tenakill Park • Cresskill, N.J.

Circle No. 107 on Readers' Service Card

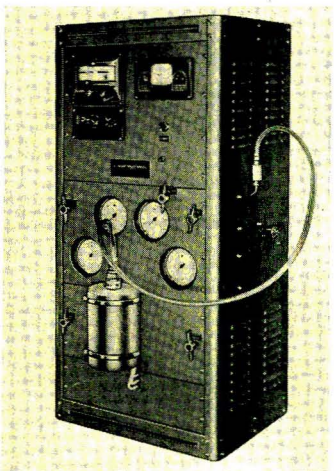

High shear rate, gas operated rheometer features improved temperature control and improved closure using an O-ring made of Teflon. The equipment is used for flow rate studies in the non-Newtonian ranges of high shear polymers and is suitable for research or quality control. The desired temperatures can be reached in less than 1 hour and controlled to within 0.5° C. Temperature recovery after loading a new sample takes 15 minutes. The rheometer is gas (nitrogen) pressurized to provide constant shear rates throughout the run. The carbide extrusion die (ASTM D-1238-57T, 1.048 mm. diameter × 8.00 mm. long) can be quickly removed and replaced. Carbide dies of other sizes can be furnished for the standard extruder body. Pressure Products Industries, Inc., Hatboro, Pa. **429**

Cryostat

The Cryojet is a variable temperature cryostat which provides an operating range of 4.2° to 400° K. and may be operated from any cryogenic storage container. The Cryojet features a high refrigeration capacity with efficient cryogen consumption. At 20° K. the apparatus will dissipate 3 watts with less than a 1-liquid-liter-per-hour helium consumption. A temperature of 4.2° K. can be obtained from ambient in less than 10 minutes using only 0.6 liquid liter of helium. The entire operating range can be covered with liquid nitrogen or helium; no flammable fluids are needed and the Cryojet may be vented directly to the laboratory atmosphere. A variety of special tails and accessories are available. Magnion, Inc., 144 Middlesex Turnpike, Burlington, Mass. **430**

FOR DTA EQUIPMENT TO MAKE THERMOGRAMS LIKE THIS, YOU CAN PAY UP TO $35,000

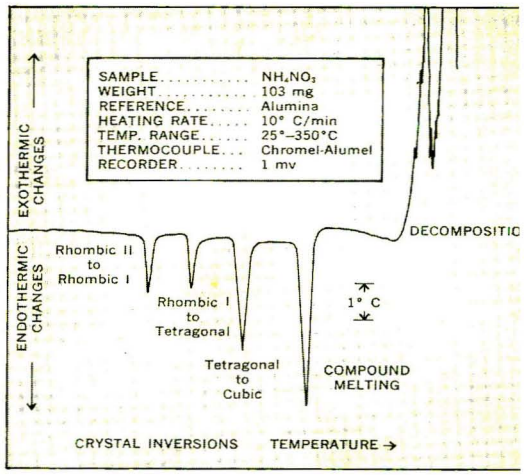

FISHER'S NEW AUTOMATIC DTA SYSTEM COSTS LESS THAN $1,000

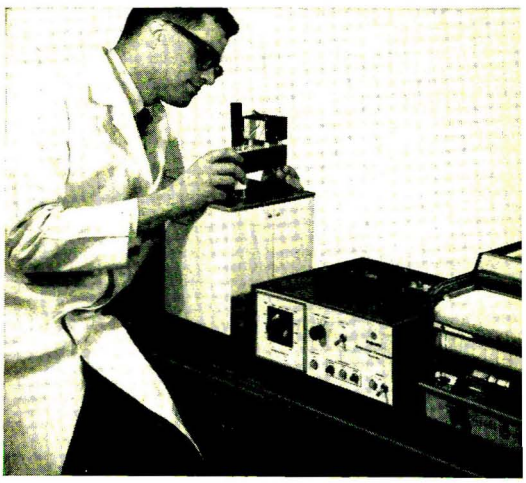

At $950, Fisher's new Model 260 Differential Thermalyzer™—programmer, furnace and sample holder—is priced far below the elaborate micro-DTA systems. Used with a 1-mv recorder, it can plot the thermal "fingerprints" that identify impurities in pharmaceuticals . . . analyze clays or ceramics . . . differentiate between different types of coal, soils or isomers . . . test polymer curing behavior. The programmer feeds power to the furnace, heating the samples at a uniform 5°, 10° or 25°C per minute, while differential thermocouples plot the thermogram. You can run two 50-200 mg samples simultaneously, heat them to 500° or 1200°C, record temperature changes as small as 0.25°C.

We'll be glad to send you a pair of bulletins that describe the Thermalyzer and illustrate what it can do. Just write Fisher Scientific Company, 100 Fisher Building, Pittsburgh, Pa. 15219. J-484

FISHER SCIENTIFIC CO.

Instruments, Apparatus, Furniture and Chemicals for Laboratories

Complete stocks in all these locations: Atlanta • Boston • Chicago • Cleveland • Houston • New York Philadelphia • Pittsburgh • St. Louis • Union, N. J. • Washington • Edmonton • Montreal • Toronto • Vancouver

"See Laboratory Guide for all Products/Sales Offices"

Circle No. 33 on Readers' Service Card

From Lysine To Phenylalanine In Less Than Four Hours

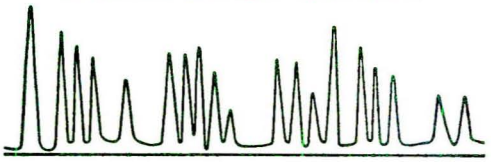

You can convert your 2 column, 24 hour analyzer system to Bio-Rad's new accelerated, low pressure system for under $230—and this includes the price of the new spherical resins: **Aminex A-4, Aminex A-5.**

Full details are in the new Aminex Technical Bulletin 115A4.

BIO-RAD *Laboratories* Dept. A-10

Bio-Rad Laboratories, 32 & Griffin Avenues, Richmond, California

Gentlemen: Please send my free copy of the new Aminex Technical Bulletin, 115A4.

NAME TITLE

ORGANIZATION

ADDRESS

CITY STATE

Circle No. 69 on Readers' Service Card

WOELM

Adsorbents for Column and Thin-Layer Chromatography and for purification of organic solvents

Plan to attend the

International Exhibit for Clinical Chhmistry

which will take place in Munich, West Germany, from July 26th–30th, 1966. See the latest techniques in Column and TL Chromatography at the WOELM Exhibit.

M. WOELM, Eschwege

Sole Distributor:

ALUPHARM CHEMICALS, New Orleans, La.
P.O. Box 30628 JA 5-3477

Circle No. 11 on Readers' Service Card

obviously

this is a 3 micron diameter particle

or is it ?

It all depends on how you measure it. The Coulter Counter® provides the most significant measurable dimension — volume. Particle volume is the single value parameter which, by means of the Coulter Counter, avoids confusion, is readily reproducible and is the best basis for particle size distribution data.

Write today for free literature.

See us in Booth 911, American Chemical Society National Meeting, New York City

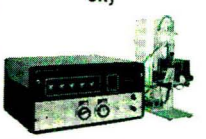

COULTER ELECTRONICS
INDUSTRIAL DIVISION

2601 Mannheim Rd., Franklin Park, Ill. 60131

Patented throughout the world

Circle No. 93 on Readers' Service Card

pH Measurement

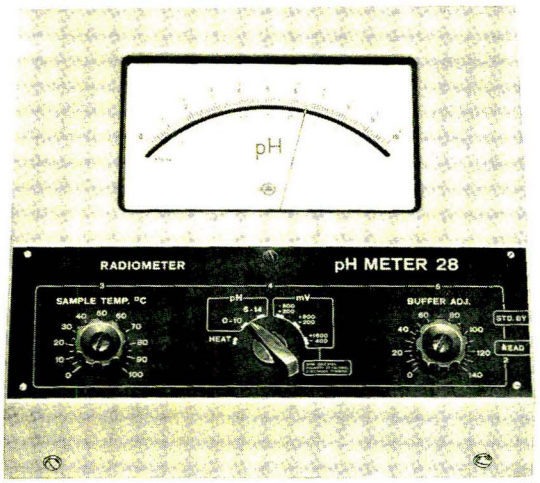

Teamwork: The basis of Radiometer systems for measuring and controlling pH.

The pH meter above is a Model 28, ready to measure pH accurately and dependably. It is typical of the several fine Radiometer models from which the one best meeting your particular requirements can be selected. The Titrators below are designed to team up with the pH meter either singly or in pairs.

One of these economically priced model 11s adds the facility to perform all types of end-point titrations automatically, or to control pH in one direction.

Two of them provide control to maintain a constant pH regardless of which way the pH is changing.

The variety of delivery systems and recording facilities available provides for even more potent combinations. Write for more detailed information on how to put a Radiometer team to work for you.

THE LONDON COMPANY

811 SHARON DRIVE, WESTLAKE, OHIO

RADIOMETER COPENHAGEN

In Canada: Bach-Simpson Limited, Box 2484, London

See this equipment in Booth No. 900 at the Chemical Exposition

pH Control

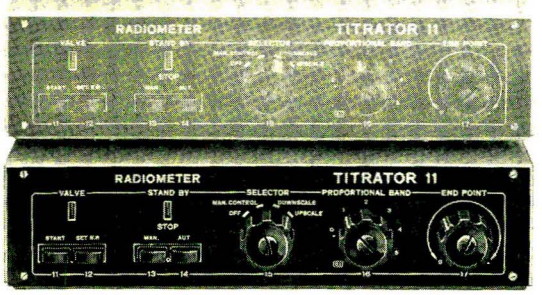

Circle No. 112 on Readers' Service Card

Why are so many analytical chemists switching to MC&B?

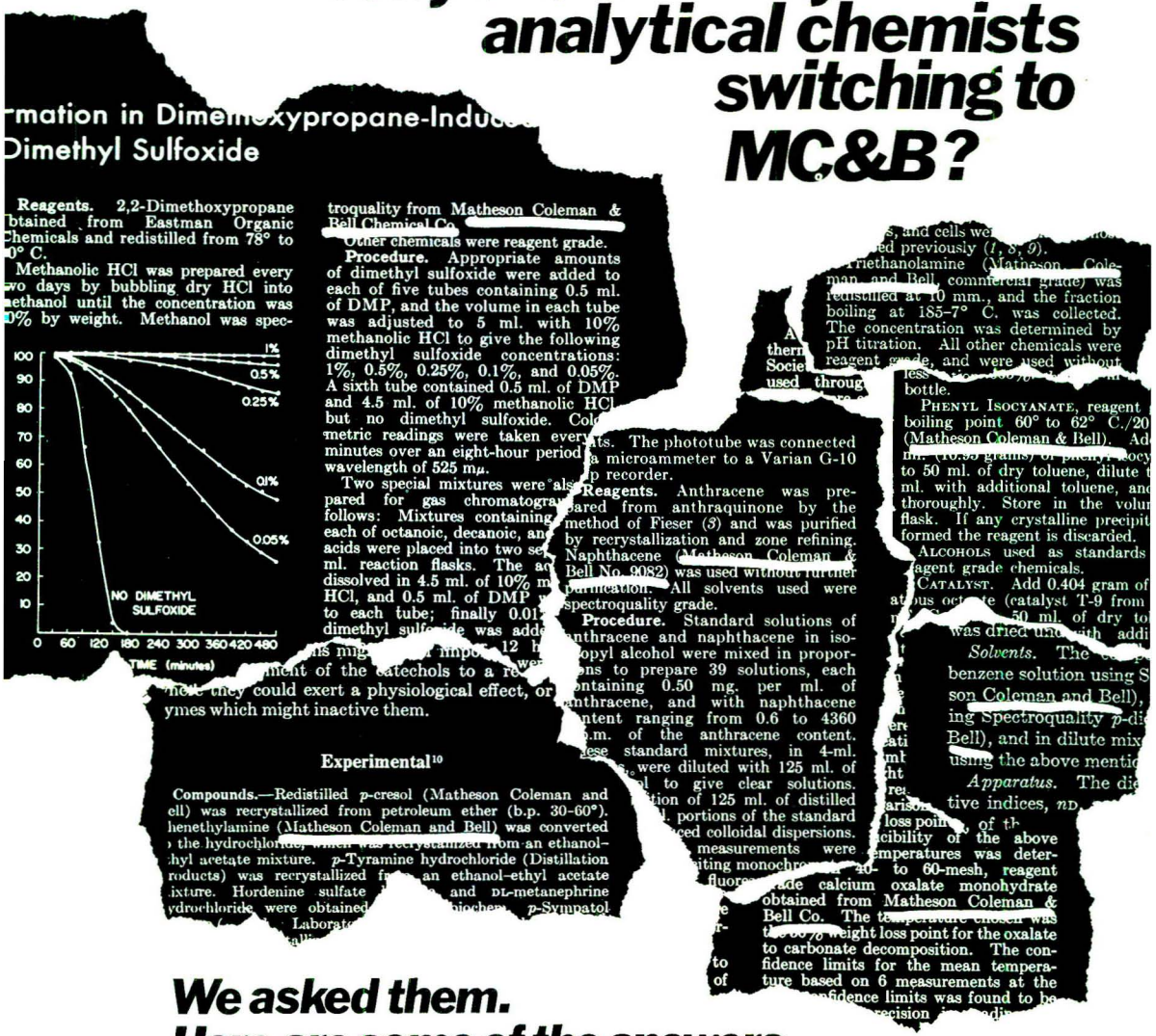
rmation in Dimethoxypropane-Induc
Dimethyl Sulfoxide

Reagents. 2,2-Dimethoxypropane btained from Eastman Organic hemicals and redistilled from 78° to 0° C.
Methanolic HCl was prepared every wo days by bubbling dry HCl into ethanol until the concentration was 0% by weight. Methanol was spec-

troquality from Matheson Coleman & Bell Chemical Co.
Other chemicals were reagent grade.
Procedure. Appropriate amounts of dimethyl sulfoxide were added to each of five tubes containing 0.5 ml. of DMP, and the volume in each tube was adjusted to 5 ml. with 10% methanolic HCl to give the following dimethyl sulfoxide concentrations: 1%, 0.5%, 0.25%, 0.1%, and 0.05%. A sixth tube contained 0.5 ml. of DMP and 4.5 ml. of 10% methanolic HCl but no dimethyl sulfoxide. Col metric readings were taken every minutes over an eight-hour period wavelength of 525 mμ.
Two special mixtures were als pared for gas chromatogra follows: Mixtures containing each of octanoic, decanoic, an acids were placed into two se ml. reaction flasks. The ac dissolved in 4.5 ml. of 10% m HCl, and 0.5 ml. of DMP to each tube; finally 0.01 dimethyl sulfoxide was add

ment of the catechols to a re
ment they could exert a physiological effect, or
ymes which might inactive them.

Experimental[10]

Compounds.—Redistilled p-cresol (Matheson Coleman and ell) was recrystallized from petroleum ether (b.p. 30-60°). henethylamine (Matheson Coleman and Bell) was converted the hydrochloride, which was recrystallized from an ethanol-hyl acetate mixture. p-Tyramine hydrochloride (Distillation roducts) was recrystallized fr an ethanol-ethyl acetate ixture. Hordenine sulfate and DL-metanephrine ydrochloride were obtained biochem. p-Sympatol

ts. The phototube was connected a microammeter to a Varian G-10 p recorder.
Reagents. Anthracene was prepared from anthraquinone by the method of Fieser (3) and was purified by recrystallization and zone refining. Naphthacene (Matheson Coleman & Bell No. 9082) was used without further purification. All solvents used were spectroquality grade.
Procedure. Standard solutions of anthracene and naphthacene in isopyl alcohol were mixed in proportions to prepare 39 solutions, each containing 0.50 mg. per ml. of anthracene, and with naphthacene content ranging from 0.6 to 4360 p.m. of the anthracene content. ese standard mixtures, in 4-ml. were diluted with 125 ml. of l to give clear solutions. tion of 125 ml. of distilled l. portions of the standard ced colloidal dispersions. measurements were iting monochr fluore

s, and cells we ed previously (1, 8, 9).
Triethanolamine (Matheson Coleman and Bell, commercial grade) was redistilled at 10 mm., and the fraction boiling at 185-7° C. was collected. The concentration was determined by pH titration. All other chemicals were reagent grade, and were used without less bottle.
Phenyl Isocyanate, reagent boiling point 60° to 62° C./20 (Matheson Coleman & Bell). Ad to 50 ml. of dry toluene, dilute ml. with additional toluene, and thoroughly. Store in the volu flask. If any crystalline precipit formed the reagent is discarded.
Alcohols used as standards agent grade chemicals.
Catalyst. Add 0.404 gram of at us octate (catalyst T-9 from 50 ml. of dry to was dried und with addi
Solvents. The benzene solution using S son Coleman and Bell), ing Spectroquality p-di Bell), and in dilute mix using the above mentio
Apparatus. The di tive indices, nD of th
cibility of the above mperatures was deter- 40- to 60-mesh, reagent ade calcium oxalate monohydrate obtained from Matheson Coleman & Bell Co. The temperature chosen was the 60% weight loss point for the oxalate to carbonate decomposition. The confidence limits for the mean temperature based on 6 measurements at the confidence limits was found to be

We asked them. Here are some of the answers.

"We found the purity of MC&B p-dimethylaminobenzaldehyde exceeds all other brands tested." "Extremely low residue, etc., of MC&B Spectroquality pentane makes it our first choice." "I've switched to MC&B Chromatoquality organics because I can rely on their 99+ mol % purity . . . saves me a lot of time and trouble." " . . . appreciate your remarkable help in obtaining high quality materials for my study of cationic detergents." " . . . no one gives us service like MC&B" . . . etc., etc., etc. Reliable purity and better service have made MC&B the fastest growing line. Have you switched yet?

MC&B

Norwood, Ohio East Rutherford, N. J. Los Angeles

Circle No. 121 on Readers' Service Card

NEW CHEMICALS

Permittivity Standards

The National Bureau of Standards Office of Standard Reference Materials has made available six permittivity standards. These standards are the result of cooperation among the National Bureau of Standards, the National Physical Laboratory of England, and the National Research Council of Canada. Two materials, 1723 glass and 7940 fused silica, have been certified for relative permittivity—i.e., dielectric constant—and both are available in three sizes as standard reference materials for $87.50 each. These standards are intended for use in checking and improving measurement systems for complex permittivity. The glass standards are certified for relative permittivity of approximately 6.3 in the range of 10^3 to 10^{10} hertz. NBS Standard No. 1501, 1723 glass, is a rough-cut blank, 2¼ by 2¼ by 3 in., for making a 2-inch disk for low-frequency, capacity-type holders. NBS Standard No. 1502, 1723 glass is a rough-cut blank, 1 by ½ by ½ in., for X-band waveguides. NBS Standard No. 1503, 1723 glass, is a rough-cut blank, 1¼ by 1¼ by ⅜ in., for making a nominally 1-inch cylindrical waveguide for dielectrometers.

The fused silica standards are certified for relative permittivity of about 3.83 in the range 10^3 to 10^{10} hertz. NBS Standard No. 1504, 7940 fused silica, is a rough-cut blank, 2¼ by 2¼ by 0.015 in., for making a 2-inch disk for low-frequency capacity-type holders. NBS Standard 1505, 7940 fused silica, is a rough-cut blank, 1 by ½ by ½ in., for X-band waveguides. NBS Standards No. 1506, 7940 fused silica, is a rough-cut blank, 1¼ by 1¼ by ⅜ in., for making a 1-inch cylindrical waveguide for dielectrometers.

For a complete list of NBS standard materials, see Standard Reference Materials: Catalog and Price List, NBS Misc. Publ. 260, available from the Superintendent of Documents, U. S. Government Printing Office, Washington, D. C. 20402, for 45 cents.

Laboratory Detergent

A new granular detergent, Washermix, is available for use in automatic laboratory washers. This new material is noncaustic, nontoxic, and foam-controlled. It contains only biodegradable surfactants. Chemical Rubber Co., Labwasher Division, 2310 Superior Ave., Cleveland, Ohio 44114 **501**

Analytical Standards

Four new kits contain collections of high purity standards. Each kit contains 15 analytical standards in quantities of 5 ml. per standard. All standards are of highest purity—99+% in nearly all cases. Cat. No. 260 contains high paraffinic hydrocarbons, C_{11} to C_{36}. Cat. No. 170 contains phenols, 13 pure standards and 2 calibrations mixtures. Cat. No. 710 consists of mercaptans and sulfides, 14 pure standards and 1 calibration mixture. Cat. No. 610 contains 15 methyl esters of fatty acids. Each kit contains a comprehensive manual giving general instructions for use of calibration mixtures, physical properties, analytical hints, retention data, chromatograms and composition of calibration mixtures (where applicable), and a bibliography of references on the subject covering the period 1952 to May 1966. PolyScience Corp., 909 Pitner Ave., Evanston, Ill. 60202. **502**

Lipophilic Derivative

The new Sephadex LH-20 is the first lipophilic derivative to extend the use of Sephadex gel filtration technique to organic solvents. The ability of LH-20 to swell in organic solvents has been obtained by the alkalinization of most of the hydroxyl groups of Sephadex G-25. Sephadex LH-20 is therefore quite stable in solvents where the pH is above 2 or strong oxidants are not present. The principle of fractionation according to molecular size is the same as for the Sephadex G types. Solvents that can be used include water and polar organic solvents as well as mixtures of these solvents with each other and with water. Pharmacia Fine Chemicals, Inc., 800 Centennial Ave., Piscataway, N. J. 08854 **503**

Ion Exchange Celluloses

New microgranular ion exchange celluloses offer controlled particle size and shape which lead to higher capacity, faster kinetics, and improved resolution in the separation of biologically active charged macromolecules. This material is available in two physical forms: dry, free flowing, fine white powders in both DEAE and CM variants, and wet, in a pre-swollen state in both DEAE and CM variants. Scientifica Division, H. Reeve Angel & Co., Inc., 9 Bridewell Place, Clifton, N. J. 07014 **504**

Are You Up On The Latest In Available ORGANIC ANALYTICAL REAGENTS?

Receive these free supplements to our 1966 catalog which already lists over 8000 chemicals!

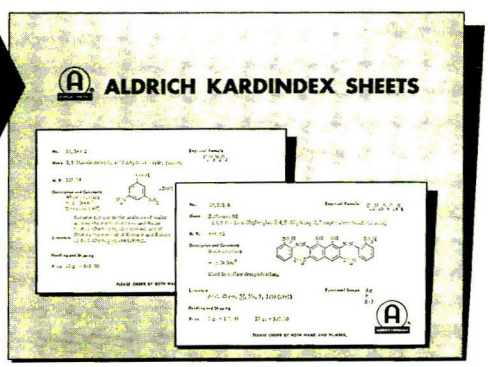

Detailed descriptions of exciting new additions to our rapidly expanding product line are sent to you quarterly, keeping you up-to-date on the latest in organic, analytical and biochemical tools.

Visit us in Booth 206 at the N.Y. A.C.S. Meeting
For your FREE subscription to our Kardindex Service, simply fill in the coupon and mail to us at one of our offices shown below.

KARDINDEX
NAME _____ POSITION _____
COMPANY _____
ADDRESS _____
CITY _____ STATE _____ ZIP _____

ALDRICH CHEMICAL CO., INC.

Main Offices and Labs
2363 North 30th Street
Milwaukee, Wis. 53210

Eastern Office
78 Clinton Road
Fairfield, N. J. 07006

West Coast Distributor
Wilshire Chemical Co., Inc.
15324 So. Broadway
Gardena, Calif. 90247

Circle No. 10 on Readers' Service Card

MODULINE

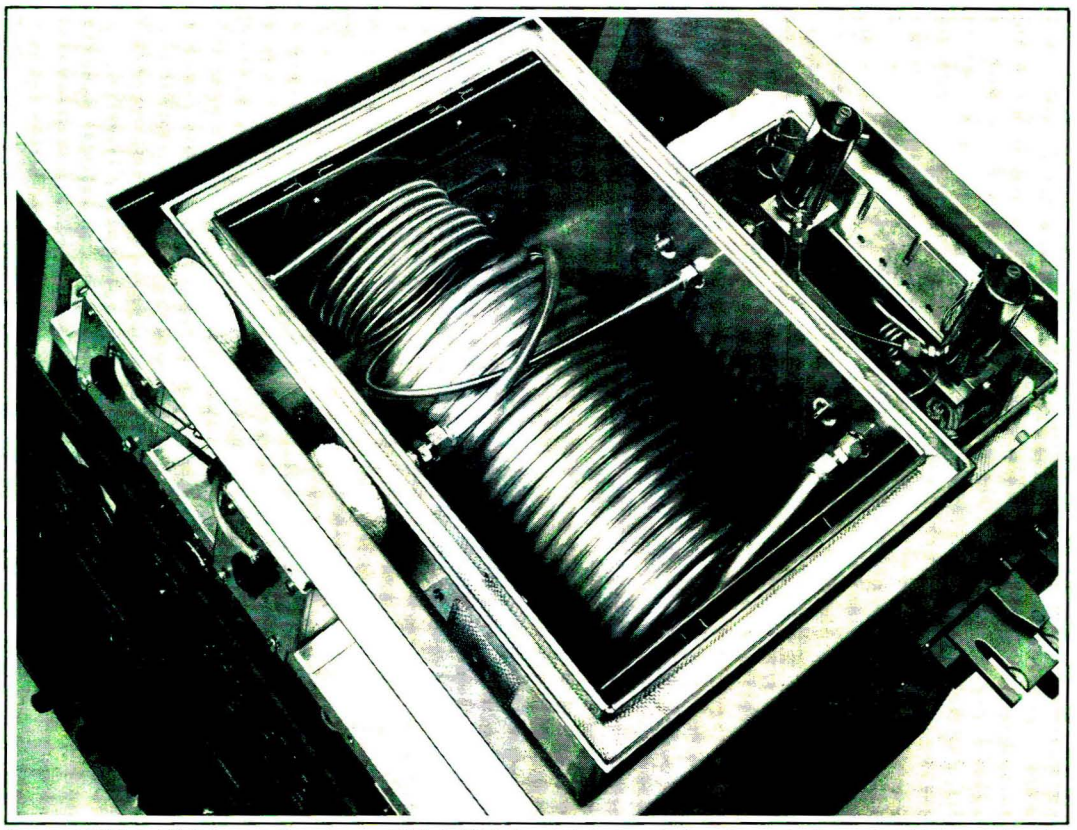

Shown are 150 feet of ⅜ inch preparative column and 10 feet of ¼ inch analytical column. Both can be run simultaneously and independently at the same temperature with the unique dual channel electrometer.

- LARGE OVEN
- PREPARATIVE CAPABILITY
- DUAL COLUMN
- INTERCHANGEABLE DETECTORS
- TWO-CHANNEL ELECTROMETER

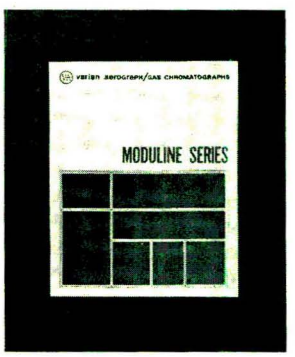

Write for new Moduline Product Bulletin

Specialists in Gas Chromatography

varian aerograph

formerly Wilkens Instrument & Research

WALNUT CREEK, CALIFORNIA • REXDALE, ONTARIO, CANADA • BASEL, SWITZERLAND

Circle No. 74 on Readers' Service Card

MANUFACTURERS' LITERATURE

Gel Filtration. A 10-page brochure describes the new Sephadex LH-20, a lipophilic derivative of Sephadex which extends the gel filtration technique to organic solvents. The booklet contains technical information on handling characteristics and lists some of the separations which can be accomplished. Pharmacia Fine Chemicals, Inc., 800 Centennial Ave., Piscataway, N. J. 08854 **601**

Analytical Chemicals. Deuterated solvents, solvents and internal standards for NMR and IR spectrometry, ultrapure reagents, and Titrisols (concentrated normal solutions in special ampoules) from E. Merck (Darmstadt) are included in a 15-page price list, P102, effective June 1, 1966. Brinkmann Instruments Inc., Westbury, N. Y. 11590 **602**

Filter Papers. Technical Bulletin F-3 is a compilation of data on Whatman filter papers for air sampling. It contains a general description of each type, physical characteristics, filtration characteristics, and other properties. Reeve Angel, 9 Bridewell Pl., Clifton, N. J. 07014 **603**

Gas Chromatograph. A gas chromatograph and a full line of accessories, designed primarily for the educational field, are described in Bulletins B5661 and B5662. Carle Instruments, Inc., 532 S. Rose St., Anaheim, Calif. 92805 **604**

Bibliography. A 24-page bibliography covers separations of proteins, enzymes, hemoglobins, hormones, serum proteins, viruses, miscellaneous proteins, nucleic acids and derivatives, and polysaccharides on ion exchange celluloses. Reeve Angel, 9 Bridewell Pl., Clifton, N. J. 07014 **605**

Metallographic Apparatus. A 4-page bulletin describes the Knuth system which comprises a complete range of metallographic equipment and is based on wetgrinding with water-resistant silicon carbide paper, electrolytic polishing, diamond polishing, and electrolytic lap-polishing. William J. Hacker & Co., Inc., P.O. Box 646, West Caldwell, N. J. 07006 **606**

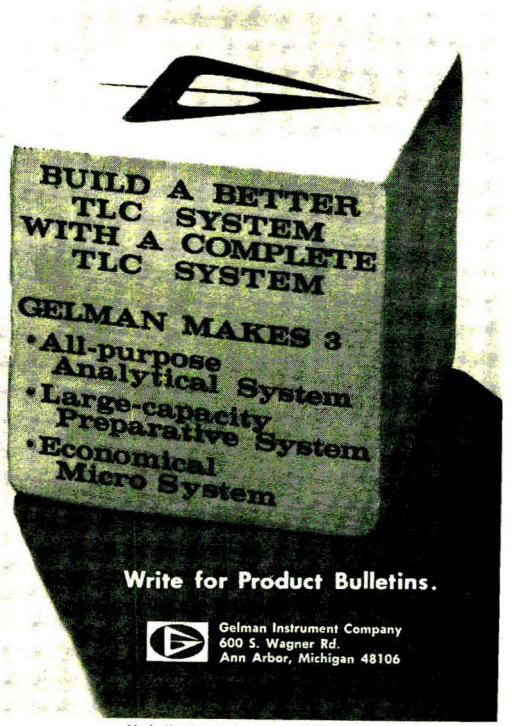

Circle No. 155 on Readers' Service Card

New Refractive Index Flow Monitor

Nester/Faust's Model 404 Refractive Index Flow Monitor provides continuous readout (and strip chart recording) of R.I. changes of sample components as they elute from a liquid column, reaction vessel or still. Refractive index is one of the most universally useful properties of materials since it affords high measurement sensitivity and is non-destructive to the sample. The versatile 404 is inexpensive, accurate, and has a wide measurement range capable of monitoring darkly colored materials. Send for technical literature today.

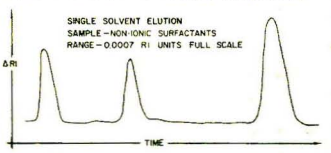

Specifications
Ranges—1.30 to 1.45 RI Units
1.45 to 1.60 RI Units
Sensitivity—0.0005 RI Units full scale
(One mv recorder)
Internal Volume—1.1 ml
Detector Type—Dual differential
Price—Under $800.00

NESTER/FAUST

Instrument Products Division
2401 Ogletown Road, Newark, Del. 19711

"See Laboratory Guide for all Products/Sales Offices"
Circle No. 50 on Readers' Service Card

Mix & Dispense
Two Gases
to ±0.05% Accuracy
with the

i/a CALI-GAS MIXING PUMP

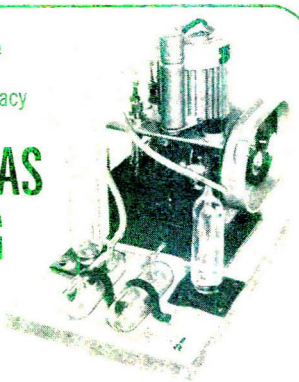

Ideal for
▪ Instrumentation Standardization ▪ Critical Mixing Requirements ▪ Metering Gases ▪ Gas Standards

Two pistons, timed to each other, enables the i/a Cali-Gas Mixing Pump to combine and dispense two pure gases to highly accurate calibration ranges. Complete with two pumps, bronze gears, oil bath housing and plastic case — $775.

For Complete Information, Write:
INSTRUMENTATION ASSOCIATES, INC.
17 West 60th St, New York, N.Y. 10023 (212) CI 5-0840
Scientific Instruments for Medicine & Industry

See us at Booth 605
Circle No. 7 on Readers' Service Card

INTEGRATE PREVIOUSLY RECORDED VARIABLES

Quickly and Easily with the

ROYSON Planimeter

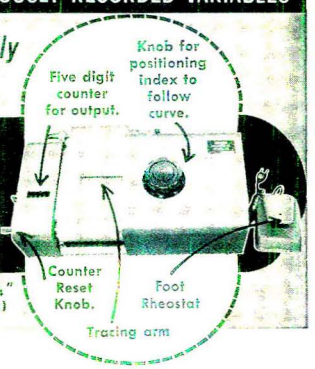

Size: 8" x 15" x 4¼" (for 4" charts)

▪ for linear or square root charts—easily convertible from one to the other ▪ accurate within 1% or better, even on short sections ▪ controllable chart feed speed using a foot operated rheostat ▪ portable, easy to operate on 110 volt AC current.

The ROYSON Planimeter provides a simple means for integrating strip chart records. It enables quick, easy integration of variables that have already been recorded and is widely used for charts of all widths as well as for integrating flow on the narrow strip charts of pneumatic control systems.

Send a sample of your chart for a quotation and additional data or, call for complete details.

ROYSON ENGINEERING COMPANY
Hatboro, Pennsylvania • Phone: (215) OSborne 5-2800
Circle No. 63 on Readers' Service Card

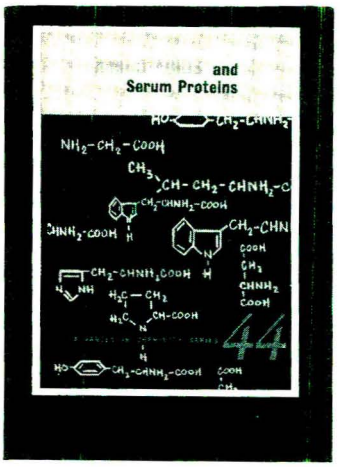

AMINO ACIDS AND SERUM PROTEINS

ADVANCES IN CHEMISTRY SERIES 44

Perhaps more individuals are concerned with amino acid and protein research than any other area of biochemistry, not only from the standpoint of nutrition and nutritional and physiological effects, but the growing evidence of a possible link to the genetic code.

AMINO ACIDS AND SERUM PROTEINS is based on the Richard J. Block Memorial Symposium, organized by the Division of Biological Chemistry of the American Chemical Society. The 10 papers by 20 contributors reflect work at the frontier of today's research activity in amino acids and protein chemistry. In the opening paper Julius Schultz discusses the nature and origin of serum proteins and suggests that undifferentiated proteins may be continuous systems rather than discrete molecular species.

Other papers on biosynthesis examine the role of the liver in the biosynthesis of plasma proteins, aminoacyl transfer in ribosomes, and the role of phosphates in the urea cycle. A paper by Nobel Laureate Vincent du Vigneaud reports the fate of cystathionine in a human cystinuric.

154 Pages, cloth bound $5.50 postpaid in U. S. and Canada; plus 20 cents foreign and PUAS

Order from:

Special Issues Sales/American Chemical Society
1155 Sixteenth St., N. W./Washington, D. C. 20036

MANUFACTURERS' LITERATURE

Column. A 7-page booklet describes and illustrates the new Sephadex solvent resistant column, a specially designed laboratory column for use with organic solvents. Pharmacia Fine Chemicals, Inc., 800 Centennial Ave., Piscataway, N. J. 08854 **607**

Bibliography. A 27-page bibliography on chromatography and related methods is available. M. Woelm, 344 Eschwege, Germany **608**

Counting System. Brochure 600, 4 pages, describes Model 2600 gas flow counting system, which has an efficiency of 62% for C^{14}, S^{35}, and P^{32}. Also described is a new 12-inch benchtop beta–gamma detector. Nuclear Supplies, Inc., P.O. Box 312, Encino, Calif. **609**

Chromatography Kit. A new chromatography dyes and reagents kit, Model 08101, contains seven of the most popular reagents for thin layer and paper chromatography and electrophoresis. Sheet 023T115 describes this kit and gives a table of applications for the reagents and price information. Warner-Chilcott Laboratories, Morris Plains, N. J. **610**

Ratemeter for Analog Data. A 2-page technical bulletin describes Model N-780 log/linear precision ratemeter designed to provide analog recovery of counting data in x-ray materials analysis and nuclear counting systems. Hamner Electronics Inc., Box 531, Princeton, N. J. 08540 **611**

Magnetic Susceptibility. A 4-page article by W. E. Hatfield discusses the company's equipment for the determination of magnetic susceptibilities by the Faraday method. Cahn Instrument Co., 7500 Jefferson St., Paramount, Calif. **612**

Syringes. Series 700 microliter syringes are discussed and illustrated in a 4-page brochure. Hamilton Co., P.O. Box 307, Whittier, Calif. 90608 **613**

Flame Photometric Detector. Product Bulletin 680, 2 pages, describes a flame photometric detector which will detect less than one billionth of a gram of phosphorus compounds and less than 1 p.p.m. of sulfur compounds. Micro Tek Instruments, Inc., P.O. Box 15409, Baton Rouge, La. **614**

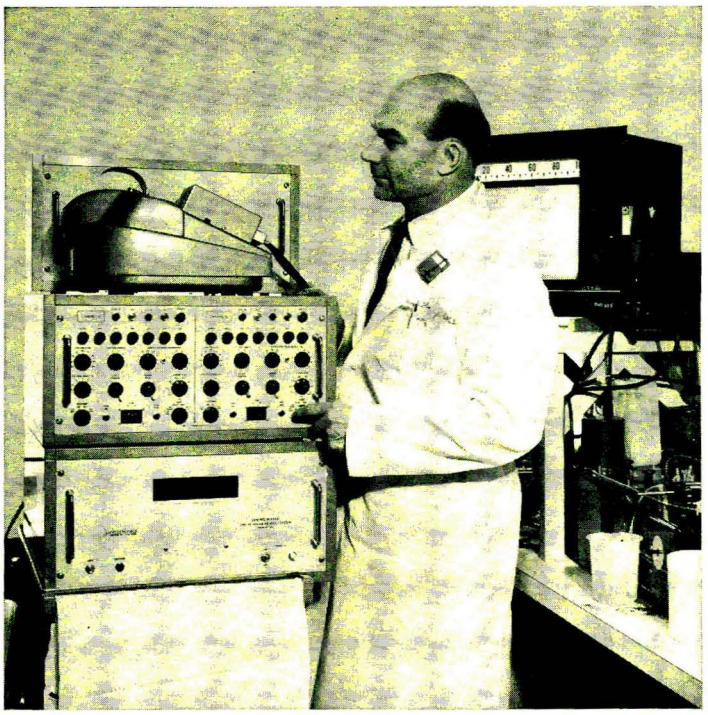

take the "labor" out of the clinical laboratory with Infotronics Digital Data Systems

Save manpower, eliminate fatigue, reduce human error, simplify reports! Infotronics CRS-70 completely automates calibration and detection of peak heights, digitizes and prints results from up to 12 colorimetric chemical analyzers. Output scaling controls enable printing of results for each patient in the normally used concentration units. With the addition of collating equipment, individual reports can be prepared to give a tabular summary of all tests for each patient.

The output of each analyzer is continuously monitored by a peak crest detector, memorized and held until ready for digitizing by an analog-to-digital converter. Digital values are transferred for readout on a variety of outputs such as: digital printer, computer-compatible tape perforator, electric typewriter, card punch coupler or combination page printer/tape perforator. Let Infotronics sales/service representatives assist in obtaining the best system for your requirements.

write for the CRS-70 bulletin

CRS DIGITAL SYSTEMS

INFOTRONICS CORP.

7800 Westglen Drive • Houston, Texas 77042

269

Circle No. 110 on Readers' Service Card

Technical Manual explains in detail how to use Millipore Filters for microchemical analysis by:

- Visible Light Microscopy
- Electron Microscopy
- Spot Tests
- Ring Oven Analysis
- Infrared Spectroscopy
- U. V. Spectroscopy
- Visible Light Colorimetry
- Flame Photometry
- Arc Emission Spectroscopy
- X-Ray Fluorescence
- X-Ray Diffraction
- Activation Analysis
- Gravimetric Analysis
- Autoradiography

76 pages of illustrated procedures in ADM-70 "Microchemical and Instrumental Analysis" available free of charge from

Millipore®
FILTER CORPORATION
115 Ashby Rd., Bedford, Mass. 01730

SEND FOR FREE COPY

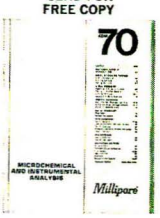

Circle No. 8 on Readers' Service Card

UNRAVEL that problem FAST!

Don't guess! Don't grope! Get the **facts** and your process problem will start **solving** itself. Just reach across your desk — grab your copy of CHEMICAL MATERIALS CATALOG. Quick—the 5-way index! And in a flash you're looking at the latest data on the chemicals and raw materials your problem calls for.

CMC works like a slave—digging up facts and fresh ideas to stimulate your thinking. It will help you unravel problems **fast.**

CHEMICAL MATERIALS CATALOG **CMC**

REINHOLD PUBLISHING CORPORATION

430 PARK AVENUE, NEW YORK, N.Y. 10022

Circle No. 21 on Readers' Service Card

HIGHEST PURITY FUSED QUARTZ

PRECISION FABRICATION • ENGINEERING CONSULTATION

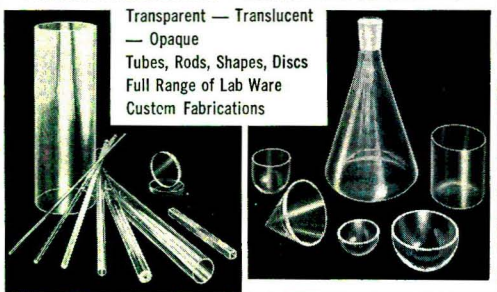

Transparent — Translucent
— Opaque
Tubes, Rods, Shapes, Discs
Full Range of Lab Ware
Custom Fabrications

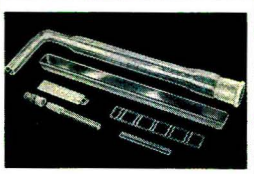

QUARTZ PRODUCTS CORP. can respond to the full range of INDUSTRIAL, DESIGN ENGINEERING or RESEARCH LAB requirements.

Precision Fabrication — we can work any geometric shape: spheres to ±0.000025". **From Stock** — a full range of Tubes, Rods and Laboratory Ware. **Design** — we can work directly with your engineers to meet any custom application. For complete details, write for free literature or call Code 201 - 757-4545.

Sales Representatives Located in Major Cities Throughout the World

QUARTZ PRODUCTS CORP.

681 Somerset Street
Plainfield, New Jersey

Circle No. 62 on Readers' Service Card

UNIVERSITY OF CANTERBURY
CHRISTCHURCH, NEW ZEALAND

Senior Lecturer or Lecturer in Chemistry

Applications are invited for the position of Senior Lecturer or Lecturer in the Department of Chemistry and it is likely that preference will be given to applicants with special interests in organic chemistry. The appointee will be required to take up the position on 1st February, 1967 or as soon as possible thereafter. The salary attached to the position is £NZ1,300 to £NZ2,500 per annum subject to a bar at £NZ2,000 per annum but these salaries are currently under review. Commencing salary is in accordance with qualifications and experience with annual increments normally of £NZ100. (The designation "Senior Lecturer" is used to denote members of staff who are at present above the £NZ2,000 bar.) Approved fares to Christchurch will be paid.

Further particulars and Conditions of Appointment may be obtained from the undersigned or from registrars of all other universities in New Zealand.

Applications close on 22nd August, 1966.

Private Bag
CHRISTCHURCH, NEW ZEALAND

G. G. Turbott,
REGISTRAR

MANUFACTURERS' LITERATURE

Quartz Products. A 32-page catalog contains illustrations, technical information, specifications, and prices of 32 product categories of fabricated quartz products. U. S. Fused Quartz Co., Inc., E. Garden Pl., Pompton Plains, N. J. 07444 **615**

Oils, Greases, and Waxes. An 8-page catalog gives technical and application data regarding Apiezon oils, greases, and waxes and their use in high vacuum work. James G. Biddle Co., Plymouth Meeting, Pa. 19462 **616**

Digital Integrator. The suitability of Model 125 digital integrator for work with the company's amino acid analyzers is discussed. Brochure SB-265, 4 pages, includes illustrations of the integrator's automatic response to proline and hydroxyproline, double peaks, plateaus, etc. Spinco Division of Beckman Instruments, Inc., 1117 California Ave., Palo Alto, Calif. 94304 **617**

Digital Readout. A 12-page brochure on the Cary digital readout systems which convert output data from the company's spectrophotometers and spectropolarimeters to punched tape, card, or magnetic tape output is available. Bulletin 200 describes 13 spectral and kinetic digital systems, as well as more than 25 individual system components. Illustrations and tape-and-punch formats are included. Applied Physics Corp., 2724 S. Peck Rd., Monrovia, Calif. **618**

Interference Filters. A 16-page brochure includes the company's latest additions to its line of interference filters. The brochure gives specifications and prices. Baird-Atomic, Inc., 33 University Rd., Cambridge, Mass. 02138 **619**

Fraction Collector. Brochure SB-226, 4 pages, describes the rectangular Model 132 fraction collector and the companion Model 133A mobile refrigeration unit. Spinco Division of Beckman Instruments, Inc., 1117 California Ave., Palo Alto, Calif. 94304 **620**

Liquid Scintillation Counting. The 200-sample, controlled temperature Model 3375 Tri-Carb spectrometer, an addition to the company's line of liquid scintillation counting systems, is described in Bulletin 1057P. Packard Instrument Co., Inc., 2200 Warrenville Rd., Downers Grove, Ill. **621**

PUMP
YOUR SAMPLES
Liquids or solids in solution

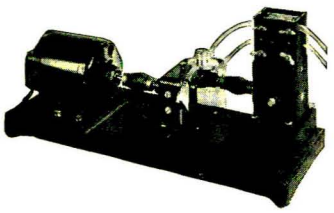

There is no contamination of samples, no corrosion of the pump mechanism, since material is forced through tubing by wave-like action of fingers in the Sigmamotor pump. The tubing is easily removed from the pump or replaced. The pumping units are available separately, with motor drive or with motor and variable speed control as shown above. Capacity from .005 c.c./min. to 4.5 gpm.

Write for complete information on sizes; capacities and tubing available.

SIGMAMOTOR, INC.
47 North Main Street • Middleport, New York

Circle No. 6 on Readers' Service Card

EEL

Evans Electroselenium Ltd., a leader in emission spectroscopy for over 20 years has devoted its analytical experience and skills to the development of a uniquely designed, completely self-contained atomic absorption spectrophotometer, the EEL 140. This compact, versatile instrument will meet the needs of the most discriminating users pursuing the latest analytical technique.

Fast and Versatile—Readout is in direct concentration on a large 8.4 inch scale eliminating conversion and plotting. The 140 contains a socket for use of 1, 5 or 10 mv recorders. The Universal tube mount accepts all makes of hollow cathode lamps without the necessity of adjustment, orientation, or clamping. One hundred twenty sample analyses per hour have been performed.

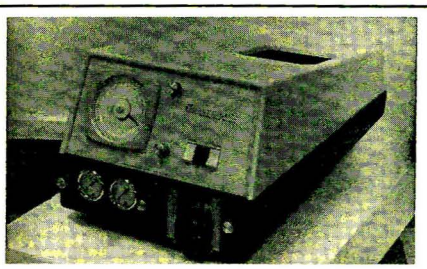

EEL 140 Atomic Absorption Spectrophotometer

Simple and compact—the unique design of the EEL 140 utilizes only 14-1/2 inches of bench front space so valuable in most laboratories. A single burner head, rotatable 180° burns both acetylene/air or acetylene/N_2O and is explosion proof. No changing of burners is required. The world famous EEL atomizer and premix burner are incorporated. The high transmission optical system provides excellent detection limits. Monochromater slit width is continuously variable over a wide range of 0 to 1.1 mm.

Parts and Information—complete stocks of instruments, parts, method sheets and technical bulletins are available from all Fisher Scientific and Van Waters & Rogers branches. Equipment service is also provided by these branches. Evans Electroselenium and its U.S. representatives provide additional back-up service.

For additional information on these and other EEL instruments, contact your nearest

FISHER SCIENTIFIC CO. or

VAN WATERS & ROGERS, INC.
sales offices

INTERNATIONAL SALES ASSOCIATES
115 EAST MAPLE AVE., LANGHORNE, PA. (215) SK7-9874

"See Laboratory Guide for all Products/Sales Offices"
Circle No. 111 on Readers' Service Card

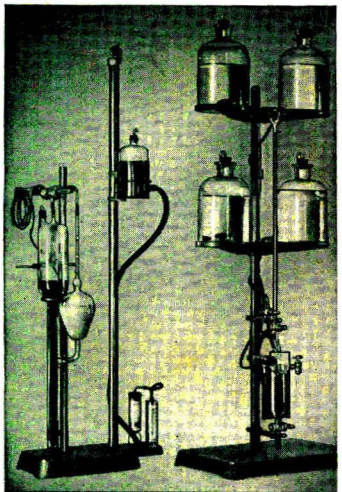
(Left) Carbon Determinator, (Right) Sulfur Determinator

CARBON & SULFUR DETERMINATORS

BY

DIETERT-DETROIT

ARE THE

MOST DEPENDABLE
EASIEST TO OPERATE
LEAST EXPENSIVE
MOST VERSATILE

Hot tube combustion is still the simple, fail-safe way to make carbon and sulfur tests in a hurry.
If you are interested in the analysis of–

IRON AND STEEL
PETROLEUM CATALYST
STAINLESS ALLOYS
ORGANICS
FOUNDRY SANDS

. . . let us send you detailed information on the Dietert-Detroit Two Minute Carbon Determinator and Three Minute Sulfur Determinator.

HARRY W. DIETERT CO.
9330 Roselawn • Detroit 4, Mich.
Area Code 313 • Phone: WEbster 3-9790

Send me free 16-page Sulfur-Carbon Bulletin

Name_____

Company_____

Address_____

City_____ State_____

Circle No. 26 on Readers' Service Card

MANUFACTURERS' LITERATURE

Instrumentation. Specification Index S66-2 is a guide to the company's literature for its complete line of instrumentation and controls. Fischer & Porter Co., 841 Jacksonville Rd., Warminster, Pa. 18974 **622**

Operational Amplifiers. A 1-page application note shows how to obtain both fast response and high impedance with operational amplifiers, using Model 102 as an illustration. Analog Devices, Inc., 221 Fifth St., Cambridge, Mass. 02142 **623**

Scintillation Flow Monitor. Details of the Scinti/Flow dual-channel, scintillation flow monitor are given in 4-page Bulletin N-6601. Picker Nuclear, White Plains, N. Y. **624**

Reference Chemicals. Bulletin 7085 describes three kits of purified reference chemicals. Calikit No. 1 contains 100 mg. each of 12 fatty acid methyl esters; Calikit No. 2, 5 grams each of 12 pesticides; and Calikit No. 3, 5 ml. each of 12 *n*-alkanes for general laboratory use. Beckman Technical Information Section, 2500 Harbor Blvd., Fullerton, Calif. 92634 **625**

Paper Chromatography. Properties, applications, techniques, and choice of paper for all Whatman paper Chromedia are covered in 35-page Technical Bulletin C-4. H. Reeve Angel & Co., Inc., 9 Bridewell Pl., Clifton, N. J. 07014 **626**

Residual Gas Analyer. Bulletin 21615, 7 pages, describes Type 21-615 residual gas analyzer which features a scan of the full mass range from 2 to 100 in a single sweep and automatic repetitive scanning of any portion of the range. Consolidated Electrodynamics Corp., 360 Sierra Madre Villa, Pasadena, Calif. 91109 **627**

Radioactivity Measurement. A complete selection of chemicals, standards, and accessories for radioactivity measurement is contained in a 16-page catalog, Bulletin 405AP. Packard Instrument Co., Inc., 2200 Warrenville Rd., Downers Grove, Ill. **628**

Flow Controller. Bulletin DS-8743 describes a flow controller designed to maintain small gas flows in analytical instrumentation applications. Emerson-Electric Co., Hatfield, Pa. **629**

Calcium Ion Activity. A calcium ion activity electrode for direct measurement of calcium ion activity is described in a 4-page bulletin. The electrode utilizes a liquid ion exchange membrane and permits measurement with an expanded scale pH meter. Orion Research Inc., 11 Blackstone St., Cambridge, Mass. 02139 **630**

Spectrophotometry. "An Introduction to Spectrophotometry," Bulletin 295-B, is a brochure designed specifically for lay readers and students, which gives an illustrated description of the principles of spectrophotometry. Beckman Technical Information Section, 2500 Harbor Blvd., Fullerton, Calif. 92634 **631**

Ultracentrifuge. Brochure SB-189A, 16 pages, contains a description of the features and applications of Model E analytical ultracentrifuge. Beckman Spinco Division, 1117 California Ave., Palo Alto, Calif. 94304 **632**

Company Periodicals

Requests for copies of the following publications, catalogs, etc., should be sent directly to the address shown. Business or professional letterheads are requested.

Spectrum Scanner, Vol. 21, No. 2. This periodical, formerly entitled "Newsletter," will be published under its new name bimonthly. Articles on a new laser microprobe with a neodymium tube, the Lang camera, and direct reading spectrometry are included among others. Jarrell-Ash Co., 590 Lincoln St., Waltham, Mass. 02154

The Analyzer, Vol. VII, No. 2. Articles included in this issue cover the Microspec infrared spectrophotometer, the design and performance of the DB-G filter-grating spectrophotometer, cryogenic storage of natural gas, and the pH values of beef. Beckman Scientific and Process Instruments Division, 2500 Harbor Blvd., Fullerton, Calif. 92634

Commentary, No. 10, 1966. Unusual applications of internal reflection spectrometry and silver bromide as a new material for MIR plates are among the articles. Wilks Scientific Corp., 140 Water St., South Norwalk, Conn.

Facts and Methods, Vol. 7, No. 3. Featured is the company's Model 185 CHN analyzer. The 5750 research gas chromatographs, Polypak columns, and behavior of solutions are other topics F & M Scientific, Rt. 41 and Starr Rd., Avondale, Pa. 19311

PARR *Automatic*
ADIABATIC CALORIMETRY

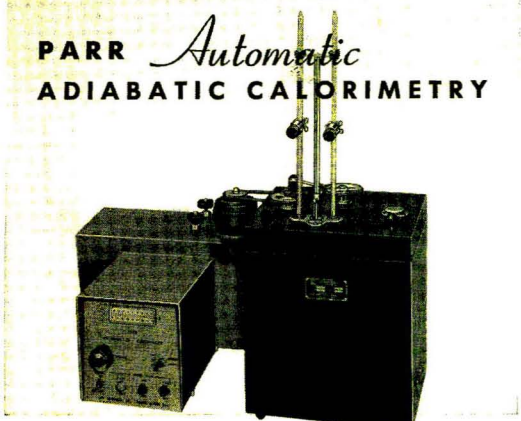

An automatic controller added to either an old or a new Parr adiabatic calorimeter eliminates all time-consuming manual temperature adjustments, doubles the output per operator and improves the repeatability in calorific tests.

Ask for Spec. 2600 or phone (309) 762-7716 for information explaining how you can up-date your present calorimeter to secure the advantages offered by this new thermistor-actuated automatic control system.

PARR INSTRUMENT COMPANY
211 Fifty-Third St. Moline, Illinois 61265

Circle No. 53 on Readers' Service Card

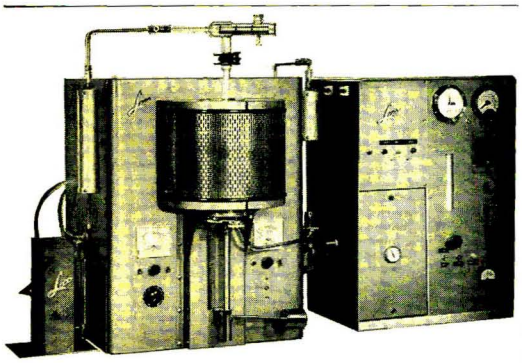

2 MINUTE
OXYGEN ANALYZER
NEW! FROM Leco®

One of the most significant developments in laboratory apparatus in recent years. A fast, accurate method for determining oxygen in steel. No solutions, no glass blower, no vacuum. For use in research laboratories, final analysis laboratories, and quality control laboratories.

Write for detailed information.

LABORATORY EQUIPMENT CORP. 243 Hilltop Road St. Joseph, Mich.

Circle No. 47 on Readers' Service Card

LABELING SYSTEMS for the laboratory

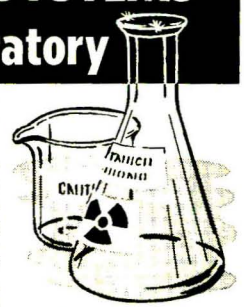

Time pressure-sensitive Tapes and Labels provide a versatile system of identification for laboratory procedures. May be printed with quality control labels, diagrams, radiation warning symbols or consecutive numbers. Custom imprints for every labeling program. High quality vinyl coated tape can be marked with pen or pencil. Tapes and Labels have strong holding adhesive that leaves no sticky residue. Withstand temperatures from —70°F. to +250°F. (High temperature tapes with range to +550°F. also available.) Oil-proof, water-proof, and acid-resistant. Write for new 32-page catalog listing more than 100 laboratory labeling aids.

AVAILABLE THROUGH LABORATORY DEALERS.

TIME® SELF STICKING LABELS VINYL COATED

PROFESSIONAL TAPE CO., INC.
363 EAST BURLINGTON ROAD
RIVERSIDE, ILLINOIS 60546

Circle No. 60 on Readers' Service Card

GALILEO SCIENTIFIC INSTRUMENTS

RESEARCH MICROSCOPE AT LABORATORY INSTRUMENT PRICE

The Model LN microscope has a pre-aligned 6V-15W illumination system built into the base. The inclined binocular head is an integral part of the arm assuring alignment at all times. A straight tube is provided for observation or photography and accepts cameras of different types.

Standard optics are: Achromatic objectives 3X, 10X, 40X and 100X corrected for flatness of field and high resolution. Paired Huyghenian compensated eyepieces 5X and 10X.

Optical accessories available for phase contact, dark field illumination, polarization, fluorescent microscopy and photomicroscopy.

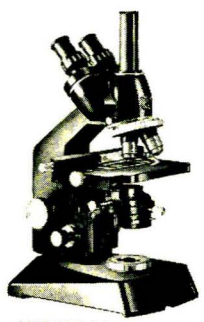

$680.00 F.O.B. New York

Write for A-6 illustrated catalog

Known world-wide since 1866 for precision scientific instruments

GALILEO CORPORATION OF AMERICA
18 East 53rd Street • New York, N.Y. 10022

Circle No. 34 on Readers' Service Card

Bendix Automatic Polarimeters are the most accurate available.

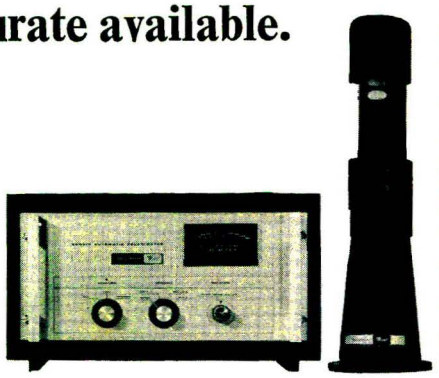

It figures. They're the most sensitive, too.

With a sensitivity of 0.0001° and accuracies to ±0.0002°, Bendix® polarimeters are powerful analytical tools. They often give more precise results than methods based on any other physical or chemical phenomena.

Three types are available, differing only in their readout: basic, recording and our four-place digital readout model. All are electronic throughout, so they'll operate a recorder directly.

Basic range is from −500 millidegrees to +500 millidegrees from any preset point. Completely accurate readings can be obtained in less than 30 seconds, visible in normal room light. Extreme sensitivity makes practical the use of very short sample cells. (All kinds are available as optional equipment.)

All features considered, Bendix automatic polarimeters are naturals for quality control, process control, reaction monitoring and for studying optical and physical properties. Like more information? Just contact us at 3625 Hauck Road, Cincinnati, Ohio.

Bendix Cincinnati builds mass spectrometers, polarimeters, polarographic systems, viscometers and other scientific instruments for over 100 areas of research and analysis.

Cincinnati Division THE Bendix CORPORATION

Circle No. 17 on Readers' Service Card

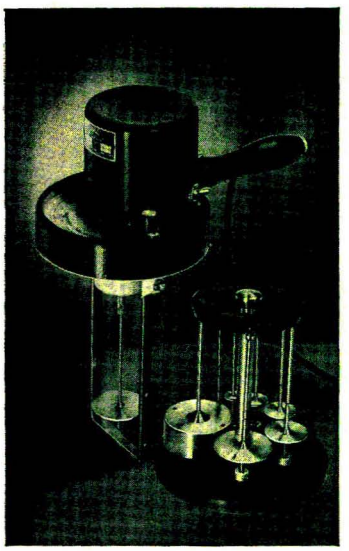

8 SPEEDS + 7 SPINDLES = 56 VISCOSITY MEASUREMENT RANGES!

BROOKFIELD

The most versatile viscometer in the world, at lowest price in its field!

Upgrade! Update! The 8-speed Brookfield Viscometer will give your lab a valuable capability dimension. Measure the viscosity or consistency of any fluid, at the flick of a switch. Extremes in viscosity, temperature or corrosion present no problem. You obtain accurate readings in seconds with materials having viscosity of from 1 to 64 million centipoises. Anyone can do it, in the laboratory or in the plant!

If you currently have a single-speed, or 4-speed Brookfield ask about converting it or trading it in for a new 8-speed model.

GET THE FACTS!

New catalog yours for the asking.

WORLD'S STANDARD FOR VISCOSITY MEASUREMENT-CONTROL

Brookfield

ENGINEERING LABORATORIES, INC.
Stoughton 29, Massachusetts

Circle No. 20 on Readers' Service Card

MANUFACTURERS' LITERATURE

Library Bulletin, Vol. 10, No. 6. Included is a listing of recent articles on analytical procedures for essential oils, aromatic chemicals, perfume, and flavor raw materials. Fritzsche Brothers, Inc., 76 Ninth Ave., New York, N. Y. 10011

Gas-Chrom Newsletter, Vol. 7, No. 3. Brief notes on 17-ketosteriods, OV-17 phenylmethylsilicone, Porapak columns, and equipment for thin layer chromatography are given. Applied Science Laboratories, Inc., State College, Pa. 16801

Atomic Absorption Newsletter, Vol. 5, No. 3. This issue contains articles on routine analyses of nonferrous alloys and plant intermediates, an automated determination of trace metals, cooled burner heads for biological analyses, and recent developments in the field. A bibliography for atomic absorption literature for 1965 is also included. Perkin-Elmer Corp., Main Ave., Norwalk, Conn. 06852

Engineering Note, Vol. 13, No. 7. Complete specifications and description of the Model 153 d.c. microvolt-ammeter and a block diagram and typical drift charts are contained in this issue. Keithley Instruments, Inc., 12415 Euclid Ave., Cleveland, Ohio 44106

LabLog, 2-66. This 12-page folder is a supplement to the company's Catalog No. 9 and contains detailed articles on thin layer chromatography supplies, general laboratory equipment, and spectrophotometers and metallographs. Will Scientific, Inc., Box No. 1050, Rochester, N. Y. 14603

Arcs and Sparks, Vol. 11, No. 2. This issue is dedicated to John R. Ferraro, outgoing president of the Society for Applied Spectroscopy. It includes summaries of the most recent Pittsburgh Conference and the dedication of the David Richardson Grating Laboratory and a brief biography of Dr. H. Kaiser. Ultra Carbon Corp., P. O. Box 747, Bay City, Mich.

Technical Bulletin, Vol. VI, No. 4. "Infrared Determination of Ethylene Oxide, Ethylene, Carbon Dioxide, and Ethylene Glycol" by Oscar Wolsky is one of the articles included. Abstracts of selected U. S. Patents (October–December 1965) are also given. Engelhard Industries, Inc., 497 Delancy St., Newark, N. J. 07105

The Laboratory, Vol. 34, No. 2. A summary of work at the Institute of Molecular Evolution is featured. Some of the company's latest instruments—semiautomatic dilutor, Vibratome, blood-pH system, and the Dynazoom II metallograph, and others—are also described. Fisher Scientific Co., 711 Forbes Ave., Pittsburgh, Pa. 15219

what price plastic pumps? . . . mighty low -- when you order them in quantity! And pump performance, reliability stays right up there with the all-metal centrifugal pumps. The new Eastern FK-FD-17, FK-FD-34 series offer pressures to 18 psi, flows to 17 gpm. Kralastic pumps are suited to temperatures up to 130° F., are inert to wide variety of dilute acids and alkalies. Penton pumps are resistant to all inorganic acids except fuming nitric and fuming sulfuric — and to temperatures as high as 220° F. Both types show excellent impact shock resistance, and are particularly suited for applications such as continuous duty pilot plants, laboratory and industrial applications like film processing, ultrasonic equipment, and filter cleaning systems.

Send for Bulletin 131

LFE

EASTERN INDUSTRIES

A DIVISION OF LABORATORY FOR ELECTRONICS, INC.
100 SKIFF STREET • HAMDEN 14, CONNECTICUT

BRANCH OFFICES: Massachusetts, Topsfield, 58 North Main Street **New Jersey,** Lyndhurst, 13 Orient Way **Delaware,** Wilmington, 2625 Concord Pike **Illinois,** Chicago, 612 North Michigan Avenue **California,** Torrance, 3011 W. Lomita Blvd.

"See Laboratory Guide for all Products/Sales Offices"
Circle No. 100 on Readers' Service Card

LABORATORY SUPPLY CENTER

Meets the test from East to West . . .
EASTERN Organics are the best!

1-Benzyl-4-Piperidone • 1-Bromooctane • 4-Chloropropiophenone
tert.-Butyl Bromide & Chloride • Citraconic Acid & Anhydride
Diacetyl Monoxime • 1,2-Dihydronaphthalene • o-Ethylphenol
Ethyl & Methyl Pyruvate • o-Ethylvanillin • p-Fluoroanisole
Hydroxy-L-Proline • 3-Methoxybenzaldehyde • 6-Methoxy-1-Tetralone
cis-& trans-Stilbene • Suberic Acid • Succinamide & Succinimide

Write for list K-66 of other chemicals

Tel.: 201 696-1700 TWX: 510 234-5831 Zip Code 07440

EASTERN CHEMICAL CORPORATION BOX K PEQUANNOCK, N. J.

Best for Fluoride

AMADAC-F™

Convenience-packaged mixture of lanthanum chelate of 3-aminomethylalizarin-NN-diacetic acid, buffers and stabilizers; affords accurate, sensitive and convenient quantitative colorimetric method for fluoride.

50 g. (for 100 detns.), with bibliography and complete instructions.....$15

BURDICK & JACKSON LABORATORIES

1953 S. HARVEY ST., MUSKEGON, MICHIGAN

CEC 21-103C
MASS SPECTROMETER SERVICE

Accepted Industry standard. Resolution to mass 600. Suitable for most organic gases, liquids, solids (min. vapor press. 1 mm. Hg. at 300° C.). Complete petroleum laboratory • Continuous and batch distillations • Pilot plant facilities include high temp.–high pressure continuous feed reactor.

Since 1955—EXPERIENCE COUNTS!

Petroleum Analytical Research Corporation
P. O. Box 12334 Houston, Texas 77017
Tel. MI 9-2753

1919—1966
LaMotte Chemical
Chestertown, Maryland U.S.A.
Specialists in
Colorimetric Techniques
Reagents—Standards—Comparator
Send for illustrated Controls Catalog
Dept. AC

GAS ANALYSES
Mass Spectrometry • Gas Chromatography
• Leak Detection
• Vacuum and Inert Gas Fusion

GOLLOB ANALYTICAL SERVICE INC.
47 Industrial Road, Berkeley Heights, N. J. 07922
201-464-3331

TRACE ELEMENT PROBLEMS?

Contact General Atomic Division of General Dynamics.
FOR FREE BROCHURE, write to: Activation Analysis Service, Dept. AA-39 General Atomic Division, General Dynamics, P.O. Box 608, San Diego, California 92112. Or, phone: Area Code 714, 453-1000, Ext. 618.

GENERAL DYNAMICS
General Atomic Division

YOUR ANNOUNCEMENT of Chemicals and Materials for Sale and/or Wanted can carry YOUR MESSAGE to the readers of the leading work magazine for instrumentation, control and analysis.

ANALYTICAL CHEMISTRY

Advertising Office:

430 Park Avenue New York, N. Y. 10022

LABORATORY SERVICE CENTER

(Equipment, Materials, Services)

Maximum space — 4 inches per advertisement. Agency commission and cash discount allowed. Column width $2\frac{3}{16}$"; two column width, $4\frac{9}{16}$". Flush mount cuts. No bulking of display and directory rates.

Inches per year	Rate per inch
1	$31.00
12	30.00
24	29.00
48	27.00

ANALYTICAL CHEMISTRY
Advertising Office
430 Park Avenue
New York, N. Y. 10022

SPECIAL **LIGHT** SOURCES

- Mercury Point Sources
- Raymaster Blacklight (long and short wave ultraviolet)
- Sodium Vapor
- Mercury Vapor
- Zirconium, Xenon, Deuterium and Hydrogen Arc Lamps
- Imported Spectral Lamps
- Photochemical or High Intensity "Uviarcs"
- Auxiliary Operating Equipment for above

WRITE FOR FREE CATALOG OR CONTACT YOUR LABORATORY SUPPLY DEALER

GATES
GEORGE W. GATES & CO.
LUCILLE AVE. FRANKLIN SQUARE, L.I., N.Y.

INDEX TO ADVERTISERS IN THIS ISSUE

Alberene Stone, A Div. of The Georgia Marble Co. 101
Basford, Inc.

Alconox, Inc. 108
Miller Advertising Agency, Inc.

Aldrich Chemical Co., Inc. 119
The Barry Agency

Alupharm Chemicals 116
M. Woelm

Applied Physics Corp. 21:78
The Bowes Co.

Applied Science Laboratories, Inc. 96
Barash Advertising

Barber-Colman Co. 91
E. R. Hollingsworth & Associates

Bausch & Lomb, Inc. 8-9
Wolff Associates, Inc.

Beckman Instruments, Inc.
Cedar Grove Operations 104
Lescarboura Advertising, Inc.
Scientific Instruments Div. 33:35:37:39:40:41
Hixson & Jorgensen, Inc.
Spinco Div. 1
Hixson & Jorgensen, Inc.

Bendix Corp., Cincinnati Div. 128
MacManus, John & Adams, Inc.

Bethlehem Apparatus Co., Inc. 54
Beaumont, Heller & Sperling, Inc.

James G. Biddle Co. 79
The Michener Co.

Bio-Rad Laboratories 116
Cappel, Pera & Reid, Inc.

Brinkmann Instruments, Inc. 25
The Shaller-Rubin Co., Inc.

Brookfield Enfiineering Laboratories, Inc. 128
Creamer, Trowbridge & Case, Inc.

Buchler Instruments, Inc. 52
Selvin & Jaffe

Burdick & Jackson Laboratories, Inc. 132
Studio 5 Advertising

Chemical Materials Catalog 124
Persons Advertising, Inc.

The Chemical Rubber Co. 111
Ad Enterprise Advertising Agency

Chromatronix, Inc. 75
Bonfield Associates, Inc.

Coleman Instruments, Inc. 102C
Winfield Advertising Agency, Inc.

Corning Glass Works 82-83
Rumrill-Hoyt, Inc.

Coulter Electronics 116
Leonard Primer Adv. Inc.

W. H. Curtin & Co. 134
Robinson-Gerrard, Inc.

Datex Div. of Giannini Controls Corp. 95
Faust/Day, Inc.

Harry W. Dietert Co. 126
Watkins-Rogers, Inc.

Dimco-Gray Co. 132
Weber, Geiger & Kalat, Inc.

Disc Instruments, Inc. 5
Leland Oliver Co., Inc.

Distillation Products Industries 20
Rumrill-Hoyt, Inc.

Eastern Industries, Div. of Laboratory for Electronics, Inc. 129
Hepler & Gibney, Inc.

Engelhard Hanovia, Inc., Hanovia Lamp Div. 110
Keyes, Martin & Co.

Carlo Erba 77
Publicitas

Farrand Optical Co., Inc. 70
Snow & Depew, Inc.

Fischer & Porter Co. 74
The Harry P. Bridge Co.

Fisher Scientific Co. 36:72:115
Fuller & Smith & Ross, Inc.

Galileo Corp. 127
Artley, Inc.

Gelman Instrument Co. 121
Active Advertising Associates

General Electric Co. 92
George R. Nelson, Inc.

Gilford Instrument Laboratories, Inc. ... 73
Garber-Evans Advertising, Inc.

Gow-Mac Instrument Co. 94
Kniep Associates

Hallikainen Instruments Corp. 109
Hal Lawrence, Inc.

Hamilton Co., Inc. 53
Swain Mealer, Inc.

Haws Drinking Faucet Co. 133
Pacific Advertising Staff

Hewlett-Packard, F & M Scientific Div. 98
Richardson, Thomas & Bushman, Inc.

Hewlett-Packard, Moseley Div. 107
Lennen & Newell, Inc.

Hewlett-Packard, Colorado Springs Div. 55
Tallant/Yates Advertising, Inc.

Hoffman Electronics Corp. 71
Jay Chiat Associates

Hoke Mfg. Co. 6:114
Tek-Mark, Inc.

Infotronics Corp. 123
Robinson-Gerrard, Inc.

Instrumentation Associates, Inc. 122
S. M. Sachs & Associates, Inc.

Instrumentation Laboratory, Inc. 80
Pazolt & Co.

Instrumentation Specialties Co., Inc. .. 19
Graham Printing & Advertising Service

Instruments, Inc. 47
Advertising Engineers, Inc.

Instruments for Research & Industry .. 61
Heller Creative Advertising

International Sales Associates 123
Edward J. Gulfoy

Jarrell-Ash Co. 68
Culver Advertising, Inc.

Johns-Manville Corp. 38
Cunningham & Walsh, Inc.

Kewaunee Manufacturing Co. 43
Phillipps Associates, Inc.

Klett Mfg. Co., Inc. 114

Labindustries 106
Bonfield Associates, Inc.

Laboratory Construction Co. ..... IFC
Valentine-Radford, Inc.

Laboratory Equipment Corp. 127
Creative Advertising, Inc.

Leeds & Northrup Co. 7
Gaynor & Ducas, Inc.

Lindberg/Hevi Duty, Div. of Sola Industries 30:75:112
Marsteller, Inc.

The London Co. 117
James Lovick, Ltd.

The Magna Corp. 32
Martin Wolfson Advertising

Mallinckrodt Chemical Works 22:40
Winfield Advertising Agency, Inc.

Manostat Corp. 54
Fairfax, Inc.

The Matheson Co., Inc. 90
Leonard M. Sive & Associates, Inc.

Matheson, Coleman & Bell 118
Leonard M. Sive & Associates, Inc.

McPherson Instrument Corp. 16
Briant Advertising

Melabs 84
Bonfield Associates, Inc.

Mettler Instrument Corp. 10:102B
Mort Barish Associates, Inc.

Midvale-Heppenstall 64
Sykes Advertising, Inc.

Millipore Filter Corp. 124
Culver Advertising, Inc.

Milton Roy Co. 112
The Harry P. Bridge Co.

The Nalge Co., Inc. 34:66
Wolff Associates, Inc.

Nester Faust Mfg. Co. 63:121
Allyn H. Jacobson

Nuclear-Chicago Corp., Texas Nuclear Corp., Subsidiary 51
Sidney Clayton & Associates, Inc.

Nuclear Products Co. ..... IBC
Falls Advertising Co.

Nuclear Science & Engineering Corp. .. 49
Bachman, Kelly & Trautman, Inc.

Ohaus Scale Corp. 70
Robert M. Baldwin Co.

Owens-Illinois, Inc. 65
Meldrum & Fewsmith, Inc.

Packard Instrument Co., Inc. 12
Ross Llewellyn, Inc.

Parr Instrument Co. 127
F. Willard Hills

Pennsylvania Industrial Chemical Corp. 56
Reeds and Farris

Perkin-Elmer Corp. 23:85
Gaynor & Ducas, Inc.

Philbrick Researches, Inc. 57
Culver Advertising, Inc.

Philips Electronic Instruments 44
Anders Advertising, Inc.

Phoenix Precision Instrument Co. 79
Product Promotions Agency, Inc.

Photovolt Corp. 64
The M. B. Pearlman Co.

Picker Nuclear 26:86
Dean L. Burdick Associates, Inc.

Precision Scientific Co. 58
Tri-State Advertising Co., Inc.

INDEX TO ADVERTISERS IN THIS ISSUE

Professional Tape Co., Inc. 127
Robert Peterson Advertising Agency

Puffer-Hubbard 56
Pippel-Patterson

Quartz Products Corp. 124
Raymond-Nicholas Advertising

Quickfit Reeve Angel 18
Eckstein-Stone, Inc.

Research Appliance Co. 76
The Albert P. Hill Co., Inc.

Royco Instruments, Inc. 100
Norton M. Jacobs

Royson Engineering Co. 122
John B. Ferguson, Jr.

Sadtler Research Laboratories, Inc. ... 14
Romer & Co., Inc.

E. H. Sargent & Co. 103:113
Sidney Clayton & Associates, Inc.

Carl Schleicher & Schuell Co. 29
Wildrick & Miller, Inc.

Scientific Glass Apparatus Co., Inc. ... 49

Scientific Industries, Inc. 60
Rick Marrus Associates, Inc.

Sep-Ko Chemicals, Inc. 111
Faber Advertising, Inc.

Sigmamotor, Inc. 125
Gelia and Wells, Inc.

Technical Measurement Corp. 81
Culver Advertising, Inc.

Texas Nuclear Corp., Subsidiary of Nuclear-Chicago Corp. 51
Sidney Clayton & Associates, Inc.

Thermolyne Corp. 62
E. R. Hollingsworth & Associates

Arthur H. Thomas Co. 102:102B

The Torsion Balance Co. 97
Michel-Cather, Inc.

Tracerlab, A Div. of Laboratory for Electronics, Inc. 42:43
Hepler & Gibney, Inc.

Tracerlab, A Division of Laboratory for Electronics, Inc. 108
Bonfield Associates, Inc.

Union Carbide Corp. 24
J. M. Mathes, Inc.

University of Canterbury 124
Spanjer, Murdoch & Co., Ltd.

Varian Aerograph 120
Bob Barriskill

The Victoreen Instrument Co. 59
Palm & Patterson, Inc.

Wang Laboratories 133
Larcom Randall Advertising, Inc.

Warner-Chilcott Laboratories, Instrument Div. 67
Lambert & Feasley, Inc.

Warner-Chilcott Laboratories, Instrument Div. 99
Bonfield Associates, Inc.

Waters Associates, Inc. ..... OBC
Studio D

Wilkens-Anderson Co. 89
Mandabach & Simms, Inc.

Wilks Scientific Corp. 31
Arthur B. W. Toft & Co.

Laboratory Supply Center 130

Burdick & Jackson Laboratories
Eastern Chemical Corp.
George W. Gates & Co.
General Atomic Div., General Dynamics
Collob Analytical Service, Inc.
LaMotte Chemical Products Co.
Petroleum Analytical Research Corp.

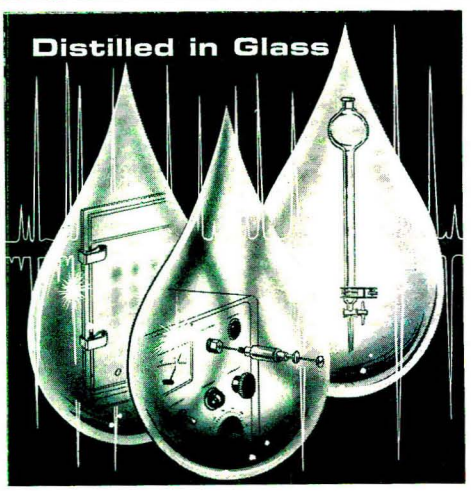

...to meet exacting solvent needs

Acetone • Acetonitrile • Benzene • Butanol-1 • Butanol-2 • Carbon Tetrachloride • Chloroform • Cyclohexane • Dimethyl Formamide • Dimethyl Sulfoxide • Dioxane • Ethyl Acetate • Ethyl Ether • "Heptane", 95-9° • Hexane, 68-69° • Methanol • 2-Methoxyethanol • Methylene Chloride • N-Methylpyrrolidone • Pentane • Petroleum Ether, 30-60° • Propanol-2 • Tetrahydrofuran • Toluene • Trimethylpentane • Others . . .

Ask for Bulletin BJ-13j U.S. Agencies use F.S.S.

BURDICK & JACKSON LABORATORIES, INC. 616 PA 2-2310
MUSKEGON, MICHIGAN 49442

Circle No. 133 on Readers' Service Card

TIME YOUR TESTS IN SPLIT-SECONDS!

GRA LAB

ALL PURPOSE LABORATORY TIMERS

MODELS AT $25.00 to $31.00

You can set the large 8" dial for any desired time period within an unusually wide range of 3600 possible settings, (ie., 1 sec. to 60 min., 1 min. to 60 hrs., etc.). At end of preset interval, alarm sounds and external load is automatically switched on or off.

GRA-LAB MICRO TIMERS, Electric Stop Clocks are available in 1/10 sec. or 1/1000 min. graduations for split-second measurements of elapsed time in laboratory or production operations. Price $39.50

WRITE FOR COMPLETE CATALOG!

DIMCO-GRAY COMPANY 210 E. Sixth St. DAYTON 2, OHIO

Circle No. 99 on Readers' Service Card

HAWS has a solution for accidents...

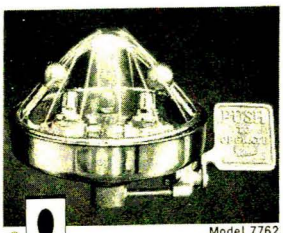

Model 7762

®

Instant Water

Contaminated eyes call for first aid in a hurry...and Haws provides water in abundance to flood away contaminating chemicals and irritants. Haws emergency drench showers and eye/face-wash fountains offer instant first aid...in the model to suit your safety requirements. Write for Haws "First Aid on Tap!" catalog today. **Haws Drinking Faucet Co., 1443 Fourth Street, Berkeley, California 94710.**

Model 8902 hose spray

Model 8550 spray shower

Since 1909 HAWS®

Emergency Equipment

Circle No. 106 on Readers' Service Card

REINHOLD PUBLISHING CORPORATION

Advertising Management for the American Chemical Society Publications

430 Park Ave., New York, N.Y. 10022

Cable Address: REINPUB NYK

Thomas N. J. Koerwer
Advertising Sales Director, ACS Publications

Arthur P. Watts
Advertising Sales Manager, AC

J. Barry Stanford
Assistant Advertising Sales Manager, AC

SALES REPRESENTATIVES

New York 10022 . . . **Arthur P. Watts, Clay S. Holden, J. Barry Stanford, Sam W. Percy, Robert N. Gillespie, William N. Wham, Reinhold Publishing Corp., 430 Park Ave., 212-688-8600**

Chicago 60603 . . . **Eugene P. Eldridge, Reinhold Publishing Corp., 10 So. La Salle St., 312-726-1282**

Cleveland 44114 . . . **Joseph C. Hoopes, Reinhold Publishing Corp., East Ohio Bldg., 1717 East 9th St., 216-771-4011**

San Francisco 94109 . . . **Denis A. Cardone, Reinhold Publishing Corp., 1255 Post St., 415-771-7044**

Los Angeles 90045 . . . **Clay S. Holden, Reinhold Publishing Corp., 8939 So. Sepulveda Blvd., 213-776-0552**

Portland 97221 . . . **Francis M. Eaton, Roy McDonald Associates, Inc., 2035 S.W. 58th Avenue, 503-292-8521**

Denver 90203 . . . **Robert H. Heidersbach, Roy McDonald Associates, Inc., 846 Lincoln St., 303-825-3325**

Houston 77006 . . . **Frank N. Vickrey, Roy McDonald Associates, Inc., 3130 Southwest Freeway, 713-529-6711**

Tulsa 74114 . . . **Max C. Nelson, Roy McDonald Associates, Inc., 570 South Harvard, 918-742-9961**

Great Britain and Western Europe . . . **Brayton Nichols, The American Magazine Group, 44 Conduit Street, London, W. 1, England**

Japan . . . **Bancho Koheki Co., Ltd., 8 Shinanomachi, Shinjuku-ku Tokyo, Japan**

PROMOTION DEPARTMENT

Robert Voepel
Promotion Manager

PRODUCTION DEPARTMENT

Alfred E. Gall
Advertising Production Director, ACS Publications

Anne Forrest
Advertising Production Manager, Analytical Chemistry

Now you can determine Copolymer Composition in a few minutes at your desk...

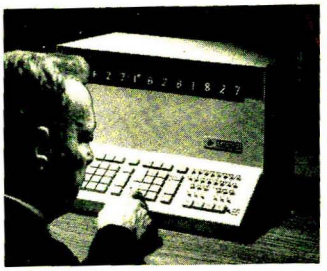

instead of days in the lab

The **WANG LOCI-2** is a programmable, desk-top computer with an extraordinary capacity for making life easier for the chemist.

Much more powerful and more flexible than any other desk-top computer system available, **LOCI-2** derives its unusual capabilities from its unique, logarithmic approach to data handling. It offers the chemist an immediate, simple means of solving complex expressions, without the usual delays and difficulties involved in having them run on a full-scale central computer.

For example:

The determination of Copolymer Composition at specified degrees of conversion has been accomplished traditionally by experimental methods. This has always been a time consuming and tedious procedure requiring several days to arrive at numerical results. By using numerical integration on Skeist Equations, we can arrive at the results much more quickly from theoretical grounds.

The basic equation is:

$$\frac{d\,[f_i\,(1-x)]}{dx} = -F_i$$

where

f_i = mole fraction of monomer i in the unreacted monomer,
F_i = mole fraction of monomer i in the instantaneous polymer,
X = degree of conversion.

In a few simple steps, the LOCI Program A106 integrates numerically for different values of X.

Find out how the **LOCI-2** can save you time and improve overall efficiency of your laboratory procedures. **LOCI-2** prices range from $2750 to $8450. Write today for complete details.

WANG LABORATORIES, INC.

DEPT. XX-8, 836 NORTH STREET
TEWKSBURY, MASSACHUSETTS 01876
TEL. (617) 851-7311

Circle No. 132 on Readers' Service Card

FUTURE ARTICLES

Listed below are papers to appear in forthcoming issues of Analytical Chemistry

Gas-Solid Chromatography of Hydrocarbons on Activated Alumina. Effect of Carrier Gas on Retention Time and Column Efficiency

R. L. Hoffmann and C. D. Evans

Spectrophotometric Determination of Thallium(III) with 3-Hydroxy-1,3-Diphenyltriazine in 70% Alcohol

S. C. Shome, H. R. Das, and B. Das

Chronopotentiometry with Current Reversal of the Hg/Hg_2^{+2} System at the Hanging Mercury Drop. Deviations from Semi-Infinite Diffusion Control

Stein Deron and H. A. Laitinen

Polarographic Kinetically Controlled Currents in Systems Containing Persulfate, Copper(II), and an Agent Which Reacts with Sulfate Free Radical

R. Woods and I. M. Kolthoff

Identification of Forty Cations and Nineteen Anions by Circular Thin Layer Chromatography

M. H. Hashmi, M. A. Shahid, F. R. Chughtai, A. A. Ayaz, Nasim Hassan, and A. S. Adil

Measurement of Specific Heat Functions by Differential Scanning Calorimetry

M. J. O'Neill

Identification and Determination of Nitrides in Steel. A DTA–EGA Method

W. R. Bandi, W. A. Straub, E. G. Buyok, and L. M. Melnick

Automated Anion Exchange Chromatography of Some Carboxylic Acids

R. C. Zerfing and Hans Veening

Specific Spectrophotometric Determination of Ozone in the Atmosphere Using 1,2-Di-(4-Pyridyl)Ethylene

T. R. Hauser and D. W. Bradley

Qualitative Analysis of Petroleum and Related Materials Using Linear Elution Adsorption Chromatography

L. R. Snyder

Determination of Metallic Impurities in Molybdenum by a Combined Ion Exchange–X-Ray Spectrographic Method

E. F. Spano and T. E. Green

Exchange Equilibrium through Ion Exchange Membranes. Analytical Applications

W. J. Blaedel and T. J. Haupert

Preparation, Stability, and Use of Preformed Solutions of Iodine Isocyanate

Samuel Rosen and Daniel Swern

from CURTIN...

Lab-Tool* Kit

- Convenient • Compact • High Quality
- For On-the-Spot Adjustments and Repairs

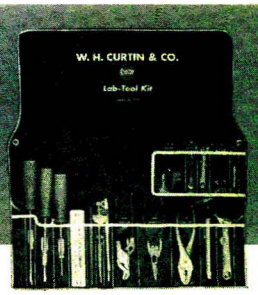

The Curtin LAB-TOOL Kit contains a selection of 17 high-quality tools recommended by our instrument engineers for routine repairs and adjustments to laboratory instruments. Tools are furnished in a sturdy vinyl roll-type case that may be hung on the wall or rolled up for storage in a drawer. Each tool has its separate compartment and each compartment is clearly identified to facilitate replacement of tools after use.

LAB-TOOL Kit provides five types of screwdrivers, two sizes of adjustable wrenches, three types of pliers, hex wrench set and other tools to perform a wide variety of mechanical operations.

*A tradename of W. H. Curtin & Co.

21719 LAB-TOOL Kit, Curtin, consisting of:

Wrench, Adjustable, 4"
Wrench, Adjustable, 6"
Pliers, Long Nose, with Side Cutters, 6"
Pliers, Utility, 6"
Pliers, Slip-Joint, 6"
Wrench Set, Hex, in handle
File, Triangular, 5"
Magnetic Pick-Up Tool
Inspection Light
Screwdriver, Phillips, #1
Screwdriver, 6" x 3/16"
Screwdriver, 4" x 1/4"
Screwdriver Set, Jewelers, with 5 blades
Screwdriver, Ratchet, Offset
Ruler, Plastic, 6" x 150 mm
Mirror, Inspection
Contact Burnishing Tool

Furnished complete in plastic tool roll with individual pocket for each tool ... 29.50

For more information, write: W. H. Curtin and Company, P. O. Box 1546, Houston, Texas 77001.

W. H. CURTIN & CO.

SCIENTIFIC APPARATUS AND CHEMICALS

HOUSTON • TULSA • BIRMINGHAM • NEW ORLEANS • MIAMI
DALLAS • JACKSONVILLE • ATLANTA • CORPUS CHRISTI
ALBUQUERQUE • MEMPHIS • SAN ANTONIO • MEXICO CITY

198

Circle No. 25 on Readers' Service Card

NUPRO®

VALVES FOR INSTRUMENTATION & RESEARCH: METERING VALVES / FILTERS / BELLOWS VALVES / CHECK VALVES

NUPRO Valves and fluid control products are particularly recommended for instrumentation, laboratory use and any other application which demands reliable performance.

NUPRO Valves are available with SWAGELOK® Tube Fitting Connections, male pipe and female pipe connections. All of these products can be ordered directly from your local NUPRO Sales and Service Representative.

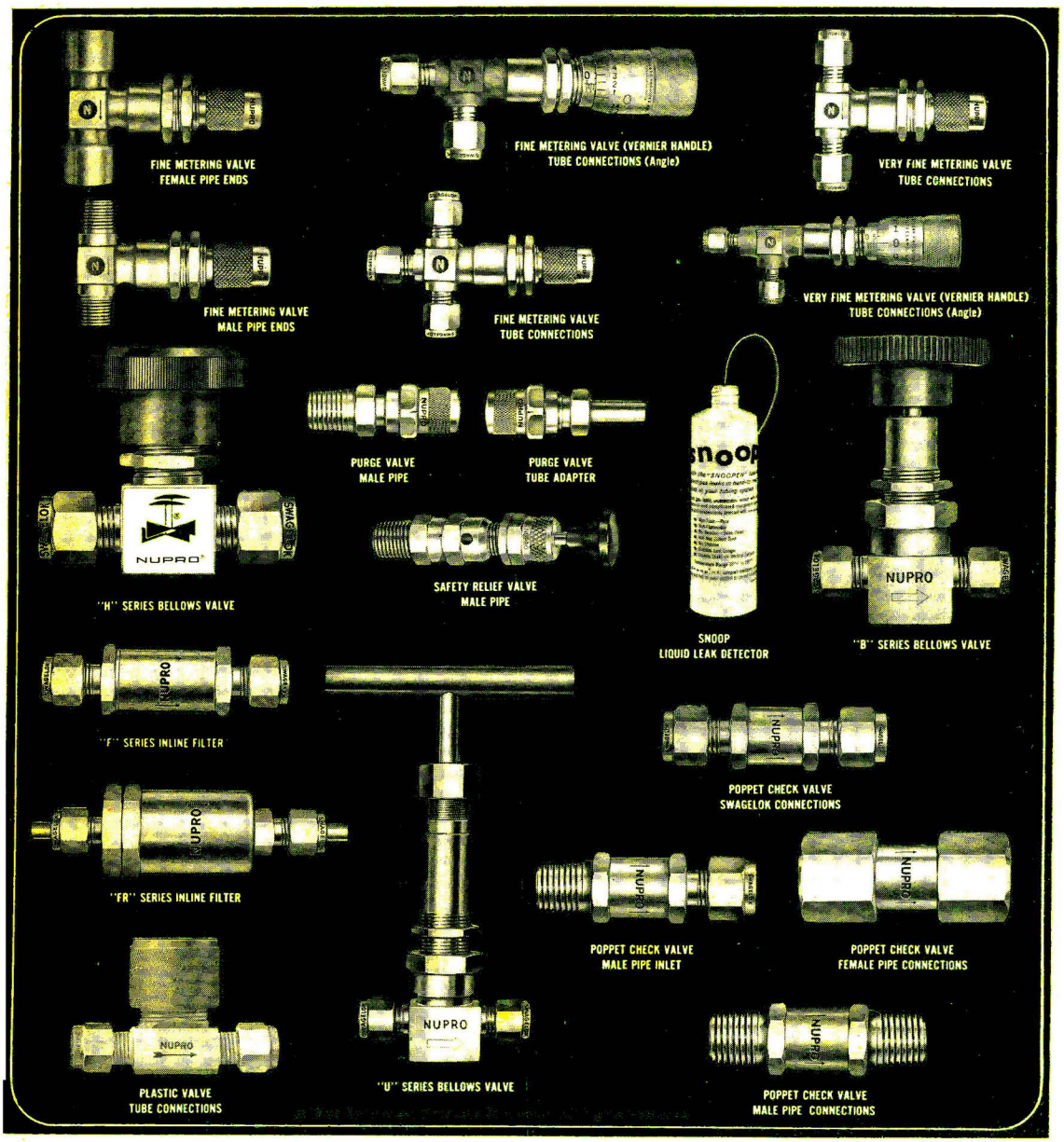

NUCLEAR PRODUCTS COMPANY / 15635 SARANAC ROAD / CLEVELAND, OHIO 44110

TWO NEW INSTRUMENTS FROM WATERS ASSOC. INC.

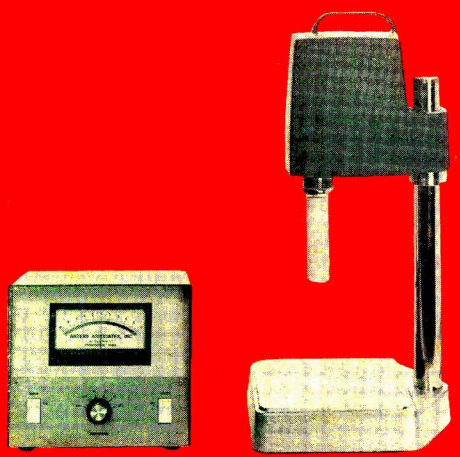

STREAMING CURRENT DETECTOR

The SCD is an alternating streaming current device packaged in a rugged portable form to provide a simple and convenient means for determining the polarity and a quantity related to the electrical charge density on colloidal particles. The SCD consists of two sections, the Measuring Head and the Electronic Indicator. Applications: Titrations / Continuous flocculation of water or sewage / Pulp and paper mills / Detergents / Paints, Latex, film, pharmaceuticals.

This instrument is manufactured under the license from The Dow Chemical Co.

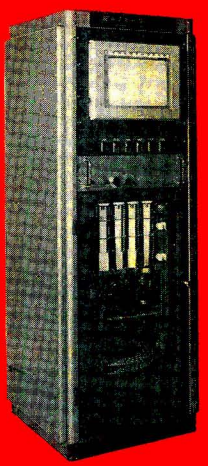

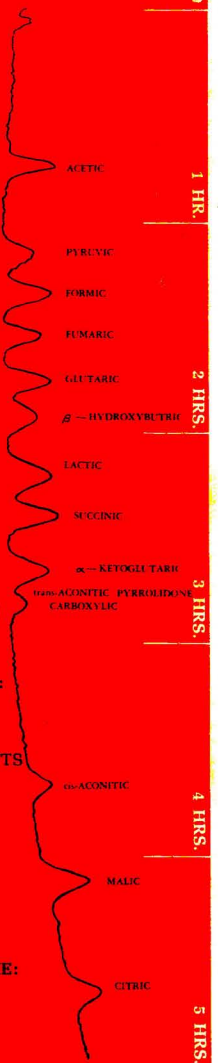

AUTOMATIC ORGANIC ACID ANALYZER

QUANTITATIVE ACCURACY:
BETTER THAN ±3%

SENSITIVITY:
.03 TO 3 MICRO EQUIVALENTS OF ACID

SAMPLE SIZE:
1/2 ml. OF URINE
1 ml. OF PLASMA
350 mg. OF TISSUE

ANALYSIS TIME:
< 5 HRS.

SAMPLE PREPARATION TIME:
< 15 MIN.

WATERS ASSOCIATES INC.
executive offices, 61 FOUNTAIN STREET, FRAMINGHAM, MASS. 01701, U.S.A. (617) 872-6528
overseas offices,
WATERS ASSOCIATES (INSTRUMENTS) LTD., 94 OFFERTON LANE, STOCKPORT, CHESHIRE, ENGLAND — STEPPING HILL 7551
WATERS MESSTECHNIK GmbH, FRANKFURT / MAIN, WEST GERMANY

Circle No. 84 on Readers' Service Card